

**ELUCIDATING THE ROLE OF RHT-1 PROTEIN
IN REGULATION OF GIBBERELLIN SIGNALLING
IN THE ALEURONE OF WHEAT**

PATRYCJA NINA SOKOŁOWSKA

**Thesis submitted to The University of Nottingham for the degree of Doctor
of Philosophy**

MARCH 2021

ABSTRACT

Germinating embryos release gibberellins (GAs), which act on aleurone cells to promote the expression of hydrolytic enzymes via the transcription factor (TF) GAMYB. GAs promote the degradation of DELLA proteins, which in the aleurone results in the upregulation of *GAMYB* expression. Although it is known that DELLAs negatively regulate *GAMYB* activity, the molecular mechanisms underlying this response are currently unclear. Recent studies have demonstrated that DELLAs do not contain a DNA-binding domain and they regulate transcription by acting as coactivators or corepressors of TFs. It was therefore hypothesised that the regulation of *GAMYB* by DELLA may be indirect, by working in a complex with other TF/TFs.

A yeast two-hybrid (Y2H) screen of the wheat aleurone cDNA library revealed that wheat DELLA protein, RHT-1, interacts with different classes of TFs. Two TFs were selected for further analysis: INDETERMINATE DOMAIN 11 (*TaIDD11*) and ETHYLENE RESPONSE FACTOR 5 (*TaERF5*). The interactions between RHT-1 and *TaIDD11* and *TaERF5* were confirmed in Y2H assays and *in planta*.

Reverse genetics approach was applied to understand the roles of identified TFs in the regulation of GA response. *TaIDD11* was found to be a positive regulator of GA-mediated growth and floral transition, as the *Taidd11* (triple knockout mutant) displayed reduced growth and delayed transition to flowering. The transcript levels of *GA3ox*, *GA20ox* and *GID1b*, the genes positively regulating GA biosynthesis and signalling, were enhanced in the mutant, which resulted in enhanced levels of bioactive GA₁.

The *TaERF5* has a close paralogue in wheat (*TaERF5a*), which shows high level of conservation and is hypothesized to have redundant function. Genome editing using CRISPR/Cas9 was applied to generate sextuple *Taerf5 Taerf5a* mutant, and the Cas9-free T3 seeds are now awaiting phenotypic analysis.

Together, this study identified a novel component of GA signalling that regulates GA-mediated growth and development, possibly via interaction with RHT-1.

ACKNOWLEDGMENTS

First and foremost, I would like to express my extreme gratitude to my supervisors, Dr Stephen Thomas, and Dr Alison Huttly, for their support, invaluable expertise, passion, and true involvement in this project throughout. I consider myself lucky to have had you as supervisors, as you are not only great scientific mentors but also extremely nice and understanding people. Thank you for always being there for me during this project.

I cannot even start to express how grateful I am to Dr Andy Phillips for his help with every bioinformatic aspect of this project, as well as the overall help and advice. You are truly an inspiration and it was an honour learning from you. Big thank you goes again to Dr Alison Huttly, whose molecular biology expertise, patience, and a rare talent for passing the knowledge helped me repeatedly. I would like to thank Professor Peter Hedden for his input throughout this project. His immense expertise was a valuable source of new ideas and is much appreciated.

I would like to thank the people in the office and in the lab who eventually became my true friends, especially Matthew Dale, Dr Megan Rafter and Dr Florian Hahn, who made me laugh and provided me with a shoulder to moan on when things didn't go well.

A big thank you to the whole Cereal Transformation team for always being enthusiastic and willing to help, Bioimaging for their support with microscopy, and glasshouse staff for taking care of my precious plants.

A huge thank you goes to my other half Darek, who is the most understanding partner one could ask for and always knows how to calm me down. You always being there for me makes everything I do in life less scary. Thank you.

I want to thank my family. My mum, who is more proud of my achievements than I will ever be. My sister, for everyday chats that kept me sane and for her contagious passion for work, that motivated me to work hard even when things were tough. My brother for the weekend visits and his support.

Finally, I would like to thank UKRI for funding the Covid-19 related additional period of my studies.

BRIEF CONTENTS

| | |
|--|------|
| ABSTRACT..... | i |
| ACKNOWLEDGMENTS..... | ii |
| BRIEF CONTENTS..... | iii |
| DETAILED CONTENTS | v |
| LIST OF FIGURES..... | xii |
| LIST OF TABLES..... | xv |
| LIST OF ABBREVIATIONS | xvii |
| Chapter 1: Introduction | 1 |
| 1.1 Wheat..... | 1 |
| 1.2 Gibberellins | 8 |
| 1.3 GA signalling in the aleurone of germinating seed..... | 22 |
| 1.4 The hormonal regulation of the aleurone is a cause of pre-harvest sprouting (PHS) and pre-maturity α -amylase (PMA) | 30 |
| 1.5 The role of ethylene in regulation of germination | 36 |
| 1.6 DELLA proteins, the master repressors of GA signalling..... | 41 |
| 1.7 Project outline and objectives | 57 |
| Chapter 2: General materials and methods | 59 |
| 2.1 General molecular biology methods..... | 59 |
| 2.2 Yeast two-hybrid (Y2H) assays..... | 69 |
| 2.3 Plant material and growing conditions..... | 71 |
| 2.4 Bioinformatics | 73 |
| 2.5 Statistical analysis | 75 |
| Chapter 3: Wheat RHT-1 protein interacts with INDETERMINATE DOMAIN 11 (TaIDD11) and ETHYLENE RESPONSIVE FACTOR 5 (TaERF5)..... | 76 |
| 3.1 Introduction | 76 |
| 3.2 Material and Methods | 83 |
| 3.3 Results..... | 88 |
| 3.4 Discussion | 123 |
| Chapter 4: The genetic characterisation of the <i>TaIDD11</i> genes..... | 131 |

| | |
|--|-----|
| 4.1 Introduction | 131 |
| 4.2 Material and Methods | 136 |
| 4.3 Results..... | 140 |
| 4.4 Discussion | 201 |
| Chapter 5: Generation of the <i>Taerf5 Taerf5a</i> mutant in wheat using CRISPR/Cas9 system..... | 221 |
| 5.1 Introduction | 221 |
| 5.2 Material and methods | 228 |
| 5.3 Results..... | 230 |
| 5.4 Discussion | 252 |
| Chapter 6: General discussion | 259 |
| 6.1 Project summary..... | 259 |
| 6.2 The roles of IDD proteins in plants | 260 |
| 6.3 IDD TFs interact with GRAS family protein members to regulate expression of genes involved in GA-regulated processes | 266 |
| 6.4 <i>TalIDD11</i> gene has the potential to uncouple pleiotropic effects of <i>Rht</i> semi-dwarfing alleles..... | 274 |
| References | 277 |
| APPENDIX..... | 331 |

DETAILED CONTENTS

| | |
|---|------|
| ABSTRACT..... | i |
| ACKNOWLEDGMENTS..... | ii |
| BRIEF CONTENTS..... | iii |
| DETAILED CONTENTS | v |
| LIST OF FIGURES..... | xii |
| LIST OF TABLES..... | xv |
| LIST OF ABBREVIATIONS | xvii |
| Chapter 1: Introduction | 1 |
| 1.1 Wheat..... | 1 |
| 1.1.1 Wheat value as a staple crop..... | 1 |
| 1.1.2 Wheat ploidy and domestication..... | 2 |
| 1.1.3 Wheat grain structure..... | 4 |
| 1.1.4 Aleurone development, structure, and function..... | 6 |
| 1.2 Gibberellins | 8 |
| 1.2.1 Gibberellin discovery | 8 |
| 1.2.2 The roles of gibberellins in plant development | 9 |
| 1.2.2.1 Stem elongation..... | 9 |
| 1.2.2.2 Leaf elongation | 10 |
| 1.2.2.3 Tillering | 11 |
| 1.2.2.4 Floral induction and development..... | 12 |
| 1.2.2.5 Pollen development..... | 13 |
| 1.2.2.6 Grain development..... | 14 |
| 1.2.3 Gibberellin biosynthesis..... | 15 |
| 1.2.3.1 Formation of <i>ent</i> -kaurene..... | 15 |
| 1.2.3.2 Synthesis of early precursor, GA ₁₂ | 16 |
| 1.2.3.3 Synthesis of the bioactive GAs..... | 17 |
| 1.2.3.4 Inactivation of bioactive GAs | 18 |
| 1.2.4 GA homeostasis is achieved by feedback regulation of the GA biosynthetic genes..... | 20 |
| 1.3 GA signalling in the aleurone of germinating seed..... | 22 |
| 1.3.1 Gibberellin signalling overview..... | 24 |
| 1.3.2 Gibberellin signalling in the aleurone cells | 24 |
| 1.3.3 Time course of molecular changes in the aleurone in response to GA | 26 |

| | |
|---|----|
| 1.3.4 α -amylase expression is regulated by GAMYB | 28 |
| 1.4 The hormonal regulation of the aleurone is a cause of pre-harvest sprouting (PHS) and pre-maturity α -amylase (PMA) | 30 |
| 1.4.1 PHS is controlled by grain sensitivity to ABA and GA | 30 |
| 1.4.2 PMA results from increased levels of GAs in the aleurone | 33 |
| 1.5 The role of ethylene in regulation of germination | 36 |
| 1.5.1 The effect of exogenous ethylene application on germination..... | 37 |
| 1.5.2 Ethylene signalling results in activation of genes that increase the rate of germination..... | 38 |
| 1.5.3 Transcriptome analysis of dormant and after-ripened imbibed wheat seed reveals upregulation of genes involved in ethylene metabolism..... | 39 |
| 1.5.4 Ethylene signalling pathway components, including ERF transcription factors, are involved in regulation of germination | 40 |
| 1.6 DELLA proteins, the master repressors of GA signalling..... | 41 |
| 1.6.1 The DELLA domain is required for GA-GID1-mediated degradation | 42 |
| 1.6.2 Structure and function of the GRAS domain in DELLAs..... | 43 |
| 1.6.3 Green Revolution alleles encode mutated DELLA proteins..... | 45 |
| 1.6.4 DELLAs interact with multiple transcription factors to regulate their activity | 47 |
| 1.6.4.1 DELLAs negatively regulates gene expression by sequestering <i>bona fide</i> TFs | 48 |
| 1.6.4.2 DELLA activates transcription by binding to transcriptional factors in the context of their promoters | 50 |
| 1.6.4.3 DELLAs interact with other transcriptional regulators to modulate gene expression | 54 |
| 1.6.5 Regulation of GAMYB by DELLAs | 56 |
| 1.7 Project outline and objectives | 57 |
| Chapter 2: General materials and methods | 59 |
| 2.1 General molecular biology methods..... | 59 |
| 2.1.1 PCR..... | 59 |
| 2.1.2 Quantitative PCR (qPCR) | 60 |
| 2.1.3 Gel electrophoresis | 61 |
| 2.1.4 PCR product purification and gel clean up..... | 62 |
| 2.1.5 Restriction digestion | 62 |

| | |
|---|----|
| 2.1.6 DNA ligation reactions | 63 |
| 2.1.7 Gateway cloning | 63 |
| 2.1.8 Bacterial transformation..... | 64 |
| 2.1.9 Agrobacterium tumefaciens transformation..... | 64 |
| 2.1.10 Bacterial cultures | 65 |
| 2.1.11 DNA isolation from the bacteria cells | 65 |
| 2.1.12 Genomic DNA extraction | 65 |
| 2.1.13 RNA extraction | 66 |
| 2.1.14 Complementary DNA (cDNA) synthesis..... | 67 |
| 2.1.15 DNA precipitation | 67 |
| 2.1.16 Long term storage of bacteria and yeast cells..... | 67 |
| 2.1.17 Genotyping by sequencing | 68 |
| 2.1.18 Kompetitive Allele Specific PCR (KASP) genotyping..... | 68 |
| 2.2 Yeast two-hybrid (Y2H) assays..... | 69 |
| 2.2.1 Yeast cultures..... | 69 |
| 2.2.2 Preparation of competent yeast cells..... | 69 |
| 2.2.3 Yeast transformation | 70 |
| 2.2.4 Replica plating..... | 70 |
| 2.2.5 Isolation and retransformation of prey plasmid..... | 70 |
| 2.3 Plant material and growing conditions..... | 71 |
| 2.3.1 Germinating the seeds..... | 71 |
| 2.3.2 Growing conditions..... | 72 |
| 2.3.3 Crossing wheat plants..... | 72 |
| 2.3.4 Aleurone isolation..... | 73 |
| 2.4 Bioinformatics..... | 73 |
| 2.4.1 RHT-1 interactors identification..... | 73 |
| 2.4.2 Phylogenetic analysis..... | 74 |
| 2.4.3 KnetMiner analysis..... | 74 |
| 2.4.4 TILLING mutations identification | 74 |
| 2.4.5 Primer design | 74 |
| 2.5 Statistical analysis | 75 |
| 2.5.1 Randomisation | 75 |
| 2.5.2 Analysis of variance (ANOVA) | 75 |

| | |
|--|-----|
| Chapter 3: Wheat RHT-1 protein interacts with INDETERMINATE DOMAIN 11 (TaIDD11) and ETHYLENE RESPONSIVE FACTOR 5 (TaERF5)..... | 76 |
| 3.1 Introduction | 76 |
| 3.1.1 Yeast two-hybrid screening as a tool to detect protein-protein interactions | 77 |
| 3.1.2 Y2H screens identified multiple TFs as DIPs | 79 |
| 3.1.3 Objectives | 81 |
| 3.2 Material and Methods | 83 |
| 3.2.1 Yeast two-hybrid screen | 83 |
| 3.2.2 Yeast two-hybrid interaction study | 84 |
| 3.2.2.1 His auxotrophy assay | 84 |
| 3.2.2.2 X-gal assay..... | 84 |
| 3.2.3 Identification of prey clones | 85 |
| 3.2.4 Generating the expression vectors for bimolecular fluorescence complementation (BiFC) | 85 |
| 3.2.5 Transient gene expression by <i>Agrobacterium tumefaciens</i> infiltration | 86 |
| 3.2.6 Microscopic observation..... | 87 |
| 3.3 Results..... | 88 |
| 3.3.1 Identification RHT-D1A interactors using Y2H screen | 88 |
| 3.3.1.1 Identification of prey cDNA clones | 92 |
| 3.3.1.2 Selection of the putative interactors for further analysis | 93 |
| 3.3.2 Confirmation of the interaction between RHT-D1A and TaERF-A5 and TaIDD-D11..... | 96 |
| 3.3.3 Phylogenetic analysis of the RHT-D1A interactors, TaERF5 and TaIDD11 | 100 |
| 3.3.3.1 Phylogenetic analysis of group IX of ERF transcription factors in wheat | 100 |
| 3.3.3.2 Phylogenetic analysis of the IDD transcription factor family in wheat | 103 |
| 3.3.4 RHT-D1A interacts with TaERF-A5A and TaIDD-A11A <i>in planta</i> | 115 |
| 3.4 Discussion | 123 |
| 3.4.1 RHT-1 interacts with different classes of TFs..... | 123 |
| 3.4.2 Multiple ethylene responsive factors (ERFs) identified as putative RHT-1 interactors..... | 125 |

| | |
|---|-----|
| 3.4.3 RHT-1 interacts with TaIDD11 transcription factors in wheat..... | 128 |
| 3.4.3.1 DELLAs interact with AtIDD1 and AtIDD2 to regulate growth and germination in Arabidopsis..... | 128 |
| 3.4.4 Summary..... | 130 |
| Chapter 4: The genetic characterisation of the <i>TaIDD11</i> genes..... | 131 |
| 4.1 Introduction..... | 131 |
| 4.1.1 TILLING as a reverse genetics approach to study wheat genetics..... | 132 |
| 4.1.2 DELLAs act as IDD protein coactivators to regulate GA-mediated gene expression..... | 133 |
| 4.2 Material and Methods..... | 136 |
| 4.2.1 GA dose response assays..... | 136 |
| 4.2.2 GA hormone extraction and analysis..... | 137 |
| 4.2.3 RNA-Seq..... | 137 |
| 4.2.4 qRT-PCR..... | 138 |
| 4.3 Results..... | 140 |
| 4.3.1 Tissue-specific expression patterns of <i>TaIDD11</i> in wheat..... | 140 |
| 4.3.2 Generation of a <i>Taidd11</i> knockout mutant in wheat using TILLING..... | 143 |
| 4.3.2.1 Identification of the EMS (ethyl methanesulfonate)-induced mutations in the <i>TaIDD11</i> genes..... | 143 |
| 4.3.2.2 Validating the LIB8437 mutation..... | 146 |
| 4.3.2.3 Stacking the EMS mutations to generate the <i>Taidd11</i> triple mutant..... | 148 |
| 4.3.3 Phenotypic characterisation of the <i>Taidd11</i> triple mutant..... | 151 |
| 4.3.3.1 Heading and anthesis date..... | 152 |
| 4.3.3.2 Flag leaf characteristics..... | 154 |
| 4.3.3.3 Stem and internodes length..... | 158 |
| 4.3.3.4 Tillering..... | 163 |
| 4.3.3.5 Ear length and spikelet number..... | 164 |
| 4.3.3.6 Grain characteristics..... | 167 |
| 4.3.3.7 GA dose response assays..... | 170 |
| 4.3.3.8 Gibberellin content in leaf sheaths of wheat seedlings..... | 180 |
| 4.3.3.9 The genes involved in GA biosynthesis and signalling are differentially expressed in <i>Taidd11</i> mutant..... | 189 |
| 4.3.3.10 <i>TaAMY1</i> expression levels..... | 198 |

| | |
|---|-----|
| 4.4 Discussion | 201 |
| 4.4.1 Proposed functional domains in IDD proteins and severity of the <i>Taidd11</i> mutant | 202 |
| 4.4.2 <i>Taidd11</i> displays a dwarf phenotype typical for GA mutants..... | 213 |
| 4.4.3 <i>Taidd11</i> is a GA-insensitive mutant that accumulates bioactive GA ₁ through increased expression of <i>GA20ox</i> and <i>GA3ox</i> | 216 |
| Chapter 5: Generation of the <i>Taerf5 Taerf5a</i> mutant in wheat using CRISPR/Cas9 system | 221 |
| 5.1 Introduction | 221 |
| 5.1.1 CRISPR/Cas as a method of genome editing..... | 222 |
| 5.1.2 CRISPR/Cas system has been successfully applied in wheat | 224 |
| 5.1.3 Objectives | 226 |
| 5.2 Material and methods | 228 |
| 5.2.1 Generation of transgenic plants | 228 |
| 5.2.2 Next-generation sequencing (NGS) results analysis | 228 |
| 5.2.3 Genotyping of T0, T1 and T2 plants | 229 |
| 5.3 Results..... | 230 |
| 5.3.1 The expression of the <i>TaERF5</i> and <i>TaERF5a</i> genes is seed-specific | 230 |
| 5.3.2 Selection of the gene target sites for generating sgRNAs | 233 |
| 5.3.3 Generation of the CRISPR vector used for genome editing of the <i>TaERF5</i> and <i>TaERF5a</i> genes | 236 |
| 5.3.4 INDELS identified in the T0 population..... | 239 |
| 5.3.5 Identification of INDELS in T1 and T2 plants..... | 246 |
| 5.4 Discussion | 252 |
| Chapter 6: General discussion | 259 |
| 6.1 Project summary | 259 |
| 6.2 The roles of IDD proteins in plants | 260 |
| 6.3 IDD TFs interact with GRAS family protein members to regulate expression of genes involved in GA-regulated processes | 266 |
| 6.3.1 <i>TaIDD11</i> interacts with RHT-1 and is a positive regulator of GA signalling | 272 |
| 6.4 <i>TaIDD11</i> gene has the potential to uncouple pleiotropic effects of <i>Rht</i> semi-dwarfing alleles..... | 274 |
| References | 277 |

APPENDIX..... 331

LIST OF FIGURES

| | |
|---|-----|
| Figure 1. 1 The evolution of modern wheat..... | 3 |
| Figure 1. 2 The structure of wheat grain..... | 6 |
| Figure 1. 3 Gibberellin signalling in the aleurone cells..... | 25 |
| Figure 1. 4 GA-induced responses in barley and wheat aleurone tissue expressed in percentage versus time..... | 27 |
| Figure 1. 5 Conserved domains in DELLA proteins..... | 44 |
| Figure 1. 6 Molecular mechanisms of DELLA action..... | 51 |
| | |
| Figure 3. 1 Alignment of the full length <i>Rht-D1a</i> CDS (yellow) and a CDS fragment used in the Y2H screen (red) compared with the model of the DELLA protein with all the functional domains annotated..... | 89 |
| Figure 3. 2 Results of the histidine auxotrophy and X-gal assays of the putative DIPs identified in the Y2H screen..... | 90 |
| Figure 3. 3 KnetMiner results tables..... | 94 |
| Figure 3. 4 KnetMiner networks for <i>TaERF5</i> and <i>TaIDD11</i> | 95 |
| Figure 3. 5 The cDNA fragments of <i>TaERF5</i> and <i>TaIDD11</i> genes cloned into pDEST22 prey vectors pulled out in the Y2H screen..... | 98 |
| Figure 3. 6 Interaction study between Δ RHT-D1A and the prey clones <i>TaERF-A5A</i> and <i>TaIDD-D11A</i> | 99 |
| Figure 3. 7 Phylogenetic tree of Arabidopsis ERF proteins..... | 101 |
| Figure 3. 8 Phylogenetic tree of group IX ERFs in wheat, Arabidopsis and rice..... | 107 |
| Figure 3. 9 The functional domains of the wheat <i>TaERF5</i> and <i>TaERF5a</i> proteins..... | 110 |
| Figure 3. 10 Phylogenetic tree for the IDD family of transcription factors in wheat, rice and Arabidopsis..... | 112 |
| Figure 3. 11 The functional domains of the wheat <i>TaIDD11</i> proteins..... | 113 |
| Figure 3. 12 Schematic representation of the Gateway cloning technology-compatible vectors used in the BiFC experiment..... | 118 |
| Figure 3. 13 Mutations introduced into the <i>Rht-D1a</i> gene and their effect on the protein sequence..... | 119 |
| Figure 3. 14 Detection of protein-protein interactions in tobacco leaves using bimolecular fluorescence complementation (BiFC)..... | 120 |
| Figure 3. 15 Alignment of all ERF proteins identified in the Y2H screen..... | 127 |

| | |
|--|-----|
| Figure 4. 1 10-days old wheat seedling variety Cadenza..... | 136 |
| Figure 4. 2 Relative expression of the three homoeologues of the <i>TaIDD11</i> gene in wheat variety Chinese Spring..... | 142 |
| Figure 4. 3 <i>TaIDD11</i> homoeologues gene models, with functional protein domains and EMS mutations used to generate the <i>Taidd11</i> mutant annotated..... | 144 |
| Figure 4. 4 A. The donor and acceptor splicing sites in the first intron of the <i>TaIDD-B11</i> gene..... | 147 |
| Figure 4. 5 Confirmation of <i>TaIDD11</i> TILLING mutations in M5 plants and crossing strategy to generate the triple mutant..... | 150 |
| Figure 4. 6 Heading and anthesis time data..... | 154 |
| Figure 4. 7 Graphs showing various flag leaf measurements taken for the four genotypes assessed..... | 157 |
| Figure 4. 8 Comparison of the final height of the four different genotypes used in the phenotypic assessment study..... | 161 |
| Figure 4. 9 Contribution of individual internodes to the final stem length..... | 162 |
| Figure 4. 10 Graph presenting the mean tiller number per plant for Cadenza, NS, <i>Taidd11</i> and <i>Rht-D1b</i> | 164 |
| Figure 4. 11 Graphs presenting the data for ear length and the number of spikelets per ear..... | 166 |
| Figure 4. 12 Characteristics of grains of four genotypes compared in the study..... | 169 |
| Figure 4. 13 GA3 dose response assay results..... | 179 |
| Figure 4. 14 Pathways of GAs biosynthesis and levels of GAs in leaf sheaths of the seedlings of Cadenza, NS, <i>Taidd11</i> and <i>Rht-D1b</i> | 185 |
| Figure 4. 15 The role of DELLA and GAs in regulation of GA homeostasis..... | 190 |
| Figure 4. 16 RNASeq experiment results..... | 194 |
| Figure 4. 17 <i>TaAMY1</i> relative expression levels in embryoless aleurones of Cadenza, NS, <i>Taidd11</i> and <i>Rht-B1c</i> | 199 |
| Figure 4. 18 Alignment of protein sequences of <i>TaIDD11</i> , its orthologues in barley, maize and rice, and the most structurally similar proteins in Arabidopsis..... | 205 |
| Figure 4. 19 Conserved domains in wheat IDD proteins..... | 211 |
| | |
| Figure 5. 1 Relative expression of the three homoeologues of <i>TaERF5</i> gene and its close paralogue <i>TaERF5a</i> in wheat variety Chinese Spring..... | 232 |

| | |
|---|-----|
| Figure 5. 2 Single guide RNA target sites (sgRNAs) for three homoeologues of <i>TaERF5</i> and <i>TaERF5a</i> genes..... | 235 |
| Figure 5. 3 Generation of the plasmid used in genome editing..... | 238 |
| Figure 5. 4 Screening for INDELS in T0 plants..... | 240 |
| Figure 5. 5 INDELS produced by various sgRNAs in the B3781 R5P1 plant..... | 248 |
| Figure 5. 6 Gel electrophoresis of PCR amplicons amplified from T1 and T2 plants..... | 249 |
| | |
| Figure 6. 1 IDD proteins interact with GRAS proteins to regulate expression of genes involved in regulating GA-responses..... | 270 |
| | |
| Supplementary Figure 3. 1 The gene models of the three homoeologues of <i>TaIDD11</i> gene | 331 |
| Supplementary Figure 3. 2 Validation of <i>TaIDD11</i> gene models by gene transcript data..... | 332 |
| Supplementary Figure 3. 3 The Y2H assays to test the interaction between mutated RHT-D1A proteins (M1 - M4) and transcription factors TaERF-A5 and TaIDD-D11.... | 334 |
| | |
| Supplementary Figure 5. 1 Maps of plasmids used in the genome editing study..... | 358 |
| | |
| Supplementary Figure 6. 1 Relative expression of the three homoeologues of <i>TaIDD12</i> gene..... | 364 |

LIST OF TABLES

| | |
|---|-----|
| Table 1. 1 Summary of DELLAs interacting partners (DIPs) grouped based on the mode of DELLA regulation..... | 52 |
| Table 3. 1 Identity of the prey cDNA clones identified as encoding strong RHT-D1A interactors in Y2H assays..... | 91 |
| Table 3. 2 ERF TFs identified as putative DIPs in the Y2H screen..... | 126 |
| Table 4. 1 Expression of three homoeologues of the <i>TaIDD11</i> gene in various parts of the grain 10, 20, and 30 days post anthesis..... | 142 |
| Table 4. 2 Wheat TILLING lines carrying the EMS mutations, their effect and zygosity..... | 145 |
| Table 4. 3 ANOVA output for heading date..... | 153 |
| Table 4. 4 ANOVA output for anthesis date..... | 153 |
| Table 4. 5 ANOVA output for flag leaf length..... | 156 |
| Table 4. 6 ANOVA output for flag leaf width..... | 156 |
| Table 4. 7 ANOVA output for flag leaf area..... | 156 |
| Table 4. 8 ANOVA output for individual internodes and the final stem length..... | 160 |
| Table 4. 9 ANOVA output for tiller number per plant..... | 164 |
| Table 4. 10 ANOVA output for ear length and number of spikelets per ear..... | 165 |
| Table 4. 11 ANOVA output for grain characteristics..... | 168 |
| Table 4. 12 Table summarising mean values \pm standard deviation and General ANOVA output for leaf sheath length [mm] for four genotypes in response to a range of GA ₃ treatments..... | 172 |
| Table 4. 13 Table summarising mean values \pm standard deviation and General ANOVA output for the L1 blade length [mm] of four genotypes in response to a range of GA ₃ treatments..... | 174 |
| Table 4. 14 Mean (\pm SD) GA content [pg/mg DW] in leaf sheaths of four genotypes with General ANOVA values for each GA measured..... | 182 |
| Table 4. 15 Fold change in GA levels in NS, <i>Taidd11</i> and <i>Rht-D1b</i> compared to Cadenza..... | 182 |
| Table 4. 16 GA biosynthesis and signaling genes that were found to be differentially expressed within the contrast groups..... | 195 |
| Table 4. 17 Mean expression of <i>TaAMY1</i> gene \pm SE and the ANOVA output data.... | 199 |

| | |
|--|-----|
| Table 5. 1 Expression of three homoeologues of <i>TaERF5</i> gene and <i>TaERF-A5a</i> gene in various parts of the grain 10, 20 and 30 days post anthesis..... | 232 |
| Table 5. 2 Summary of the selected sgRNAs..... | 234 |
| Table 5. 3 INDELS identified in R5P1 and R7P1 plants from B3781 transformation..... | 242 |
| Table 5. 4 INDELS identified on various alleles of <i>TaERF5</i> and <i>TaERF5a</i> genes present in R5P1 plant, and their effect on the encoded protein..... | 244 |
| Table 5. 5 INDELS identified on various alleles of <i>TaERF5</i> and <i>TaERF5a</i> genes present in R7P1 plant, and their effect on the encoded protein..... | 245 |
| Table 5. 6 INDELS found in each of the genes in the T1 population..... | 250 |
| Table 5. 7 INDELS identified in T2 plants..... | 250 |
| | |
| Supplementary Table 3. 1 Full list of identified interactors grouped into functional categories..... | 335 |
| Supplementary Table 3. 2 Members of subgroup IX of the ERF family in Arabidopsis and rice..... | 346 |
| Supplementary Table 3. 3 Members of the IDD family in Arabidopsis and rice..... | 347 |
| | |
| Supplementary Table 4. 1 Primers used in the experiments summarised in Chapter 4 | 348 |
| Supplementary Table 4. 2 Legend for the expression data taken from Ramírez-González et al., (2018)..... | 349 |
| Supplementary Table 4. 3 TPMs of DE genes involved in GA biosynthesis and signalling identified in the RNA-seq experiment..... | 351 |
| Supplementary Table 4. 4 Mean TPMs of DE genes involved in GA biosynthesis and signalling identified in the RNA-seq experiment..... | 352 |
| | |
| Supplementary Table 5. 1 Primers used in the experiments summarised in Chapter 5..... | 353 |
| Supplementary Table 5. 2 INDELS detected in B3792 T0 plants that were selected for NGS analysis..... | 354 |
| Supplementary Table 5. 3 Segregation of the INDELS in the T1 population..... | 355 |
| Supplementary Table 5. 4 Putative off-target sites for the sgRNAs used..... | 356 |
| | |
| SUPPLEMENTARY NOTES | |
| Supplementary Notes 5. 1 DNA sequences of the plasmids used in the genome editing study..... | 358 |

LIST OF ABBREVIATIONS

| | |
|--------|---|
| 2-ODDs | 2-oxoglutarate-dependent dioxygenases |
| 3-AT | 3-Amino-1,2,4-triazole |
| ABA | Abscisic acid |
| AD | Activation domain |
| ALC | ALCATRAZ |
| ANOVA | Analysis of variance |
| bHLH | Basic helix-loop-helix |
| BiFC | Bimolecular Fluorescence Complementation |
| BOI | Botrytis susceptible1 interactor |
| BR | Brassinosteroid |
| BRG | BOI related |
| bZIP | basic leucine zipper |
| BRZ1 | BRASSINAZOLE-RESISTANT1 |
| Cas | CRISPR-associated |
| cDNA | Complementary deoxyribonucleic acid |
| CE | Controlled environment |
| ChIP | Chromatin immunoprecipitation |
| cm | Centimetre |
| CPS | <i>ent</i> -copalyl diphosphate synthase |
| CRISPR | Clustered regularly interspaced short palindromic repeats |
| CT | Cytokinin |
| D8 | <i>Dwarf-8</i> |
| DE | Differentially expressed |
| DIP | DELLA-interacting protein |
| DNA | Deoxyribonucleic acid |
| DBD | DNA binding domain |
| EMS | Ethyl methanesulfonate |
| ER | Endoplasmic reticulum |
| ERF | Ethylene-responsive element binding factors |
| ET | Ethylene |
| FKPM | Fragments per kilobase per million reads mapped |
| GA | Gibberellin |
| GA20ox | Gibberellin-20 oxidase |
| GA2ox | Gibberellin-2 oxidase |
| GA3ox | Gibberellin-3 oxidase |
| GAF1 | GAI-ASSOCIATED FACTOR1 |
| GAI | Gibberellin insensitive |
| GAMYB | GA-induced Myb-like protein |
| gDNA | Genomic DNA |
| GFP | Green fluorescent protein |
| GGPP | Geranylgeranyl diphosphate |
| GID1 | GIBBERELLIN INSENSITIVE DWARF1 |
| GUS | Glucuronidase reporter gene |
| HFN | Hagberg falling number |
| ID1 | INDETERMINATE1 |
| IDD | ID1 domain protein |
| IWGSC | International Wheat Genome Sequencing Consortium |
| JA | Jasmonic acid |
| JAZ | Jasmonate-ZIM domain |

| | |
|---------|------------------------------------|
| KAO | <i>ent</i> -kaurenoic acid oxidase |
| KNOX1 | KNOTTED1-like homeobox |
| KO | <i>ent</i> -kaurene oxidase |
| KS | <i>ent</i> -kaurene synthase |
| LHR | Leucine heptad repeat |
| LM | Lemma primordia |
| L.S.D. | Least significant difference |
| miRNA | micro RNA |
| mm | Millimetre |
| mM | Millimolar |
| MOC1 | MONOCULM 1 |
| NGS | Next Generation Sequencing |
| NLS | Nuclear localisation signal |
| PAC | Paclitaxel |
| PCD | Programmed cell death |
| PCR | Polymerase chain reaction |
| PIF | PHYTOCHROME INTERACTING FACTORS |
| PKL | Pickle |
| PPI | Protein-protein interaction |
| RAP | Related to APETALA |
| RGA | Repressor of <i>ga1-3</i> |
| RGL | RGA-like |
| RHT | Reduced height |
| RNA | Ribonucleic acid |
| RNA-seq | RNA sequencing |
| SA | Salicylic acid |
| SAM | Shoot apical meristem |
| SCF | Skp1-cullin-F-box |
| SCL-3 | SCARECROW-LIKE 3 |
| SCR | Scarecrow |
| S.E.D. | Standard error of the mean |
| SLN1 | SLENDER 1 |
| SLR1 | SLENDER RICE 1 |
| SNP | Single Nucleotide Polymorphism |
| SPT | SPATULA |
| TF | Transcription factor |
| TILLING | Targeted Induced Lesions in Genome |
| TPR | TOPELESS-RELATED |
| UTR | Untranslated region |
| WT | Wild type |
| Y2H | Yeast two-hybrid |
| µg | Microgram |
| µl | Microlitre |
| µm | Micrometre |
| µM | Micromolar |

Chapter 1: Introduction

1.1 Wheat

1.1.1 Wheat value as a staple crop

Wheat (*Triticum aestivum*) is one of the three main cereals grown worldwide, the other two being rice and maize. These three crops supply more than half of the world's energy intake (IDRC, 2010). Whilst the cereals that are grown in developed countries are used predominantly for consumption and animal feed, people in developing countries rely on plants for about 90% of their daily needs; besides food, plants are used as a source for fuel, medicines and shelter. Wheat is the most widely grown cereal and occupies 17% of the world's total cultivated land. It is extensively grown across the temperate, Mediterranean, and subtropical climate zones on both hemispheres of the world. The worldwide cereal harvest in 2019/2020 was 2 761 million tonnes, with 764.39 million tonnes being wheat (FAO, 2021). In the UK, the 2020 wheat harvest was particularly bad due to extreme weather. It was 10.13 million tonnes (DEFRA, 2020), 37.5% lower than in 2019 and well below the five-year average of 15.1 million tonnes. Being the staple food for 35% of the world's population, wheat provides more calories and protein in the world's diet than any other crop; the wheat grain contains about 60 to 80% of starch and 8 to 15% of protein, with some varieties having a protein content of 23%. Whereas carbohydrate content of the three main cereals is roughly similar, wheat contains significantly more protein and fibre, and less fat per 100 g than maize and rice. The protein content in wheat varies depending on variety from around 10.4 g per 100 g in soft red winter wheat to 15.4 g per 100 g in hard red spring wheat. For comparison, brown, long-grain rice and yellow maize protein content per 100 g is 7.94 g and 9.42 g, respectively (Nutritional Qualities of Grains Comparison Chart, Einkorn.com). Dietary fiber content of wheat is around 12.5 g per 100 g, compared to 3.5 g per 100 g in rice and 2.4 g per 100 g in maize, and fat constitutes about 1.7 g per 100 g, whereas rice contains 2.9 g per 100 g and maize 4.7 g per 100 g of dry seed. Wheat is also

high in nutrients; it contains more calcium, iron, selenium and potassium compared to the other cereals. With wheat being a staple crop in many countries and becoming more popular in countries like China, India, Egypt, Indonesia and Pakistan, the global wheat consumption is expected to increase by 13% compared to the base period 2015-2017 by 2027 (OECD/FAO, 2018). No growth in wheat consumption per capita is expected, nevertheless the increase in population growth will cause further increase in demand for wheat. The food use is predicted to be the major driver behind the increase in overall wheat utilisation. Consequently, the global production of wheat needs to increase, and is projected to increase to 833 Mt by 2027 (OECD/FAO, 2018). As the area designated to farmland will not increase significantly, the majority of the production increase will need to be achieved through higher yields, thus devising higher-yielding wheat varieties is essential to ensure food security.

1.1.2 Wheat ploidy and domestication

Wheat occurs as six biological species at three ploidy levels: diploid *Triticum urartu* (genome AA) and *Triticum monococcum* (genome A^mA^m), tetraploid *Triticum turgidum* (genome BBAA) and *Triticum tmopheevii* (genome GGAA) and hexaploid *Triticum aestivum* (genome BBAADD) and *Triticum zhukovskyi* (genome GGAAA^mA^m). Genetic relationship studies showed that the principal wheat lineage is formed by *T. urartu*, *T. turgidum*, and *T. aestivum*. *T. aestivum*, the modern bread wheat, was developed through two hybridization events, first between *T. urartu* and *Aegilops speltoides* (genome SS from which genome BB was derived) giving rise to *T. turgidum*, and second between domesticated *T. turgidum* and *Aegilops tauschii*, donor of the DD genome (McFadden & Sears, 1946; Petersen *et al.*, 2006) (Figure 1.1). Hexaploid wheat resynthesized as an amphiploid of wild or domesticated emmer with *Ae. Tauschii* resembled spelt (*T. aestivum ssp spelta*), hence the conclusion that the free-threshing forms of modern bread wheat evolved from naturally hulled spelt (McFadden & Sears, 1946).

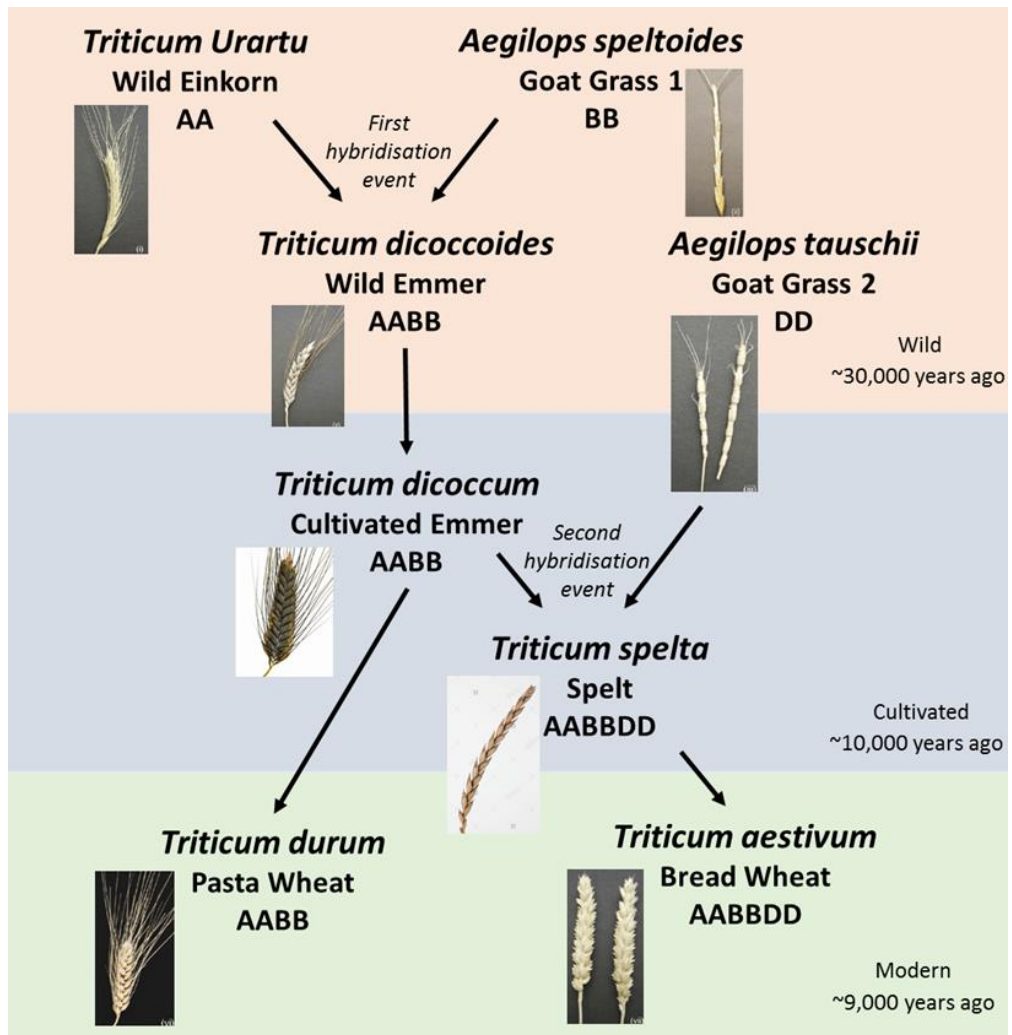


Figure 1. 1 The evolution of modern wheat. The wheat used for bread making nowadays is hexaploid (AABBDD) and arose through two processes of hybridisation: first between *Triticum urartu* (Wild Einkorn, donor of the A genome) and *Aegilops speltoides* (Goat grass 1, donor of the B genome) around 30,000 years ago giving rise to *Triticum dicoccoides* (Wild Emmer, AABB), and second between *Triticum dicoccum* (Cultivated Emmer, AABB) and *Aegilops tauschii* (GoatGrass 2, donor of the D genome), which occurred around 10,000 years ago and resulted in origin of *Triticum spelta* (Spelt, AABBDD). Domestication of Cultivated Emmer and Spelt gave rise to Pasta wheat and Bread wheat, respectively.

Wheat first started to be cultivated around 10,000 years ago, in the geographical region of today's Iraq, Syria, Lebanon, Jordan, Israel and northern Egypt, known as the Fertile Crescent. The earliest cultivated varieties were the

diploid variety einkorn (*T. monococcum*) and the tetraploid variety emmer (*T. dicoccum*) (reviewed in Shewry, 2009). Hexaploid bread wheat, *T. aestivum*, arose about 9,000 years ago. Domestication of wild varieties relied on selecting landraces with desirable characteristics from wild populations. The most crucial traits that allowed wheat domestication were loss of shattering of the spike at maturity and free threshing of the grain. Non-brittle rachis limited the natural seed dispersal mechanisms of the wild type varieties allowing the farmer to harvest more grain and were found to be caused by mutations at the *Br* (*brittle rachis*) locus (Nalam *et al.*, 2006). Free threshing allowed for easier stripping of the grain off the glumes, making it less labour intensive to harvest the naked grain, and arose through a dominant mutation at the *Q* locus, that pleiotropically affected the other characteristics, such as rachis fragility and glume tenacity (Simons *et al.*, 2006). Among other desirable traits in domesticated wheat were larger spikes and grain, more determinate growth and loss of dormancy (Harlan *et al.*, 1973). Modern wheat belongs primarily to two species: tetraploid durum wheat (*T. turgidum*) used for pasta and low-rising bread, and hexaploid bread wheat (*T. aestivum*).

1.1.3 Wheat grain structure

Wheat belongs to the *Poaceae* family and like all other grasses produce single seeded fruits, known as caryopses. The wheat caryopsis (Figure 1.2) consists mainly of endosperm, which constitutes 80 to 85% of the grain, and also bran (13 to 17%) and embryo (2 to 3%) (Belderok, 2000). The bran consists of seed coat and pericarp tissues, and its main purpose is to protect the embryo and endosperm. The embryo is the most important component of the grain as it develops into a plant and ensures survival of the species. At grain maturity, it is composed of shoot, mesocotyl and radicle, which together form the embryonic axis, and scutellum. The scutellum lies between the embryonic axis and endosperm and serves to absorb nutrients from endosperm during germination. The endosperm can be divided into two tissues which are morphologically and physiologically distinct: starchy endosperm and aleurone

layer. The aleurone in wheat is a single layer of cuboidal cells that surround the endosperm and embryo. The starchy endosperm is the storage tissue of the grain and accumulates mainly starch and proteins, while the aleurone cells are rich in proteins, lipids, vitamins and nutrients (Evers & Millar, 2002). The main role of the aleurone is to supply the enzymes necessary to break down resources stored in the starchy endosperm to facilitate grain germination.

The embryo and the endosperm are surrounded by a remnant of the nucellus called nucellar epidermis, which is regarded as a seed coat. The next protective layer of the seed is the true seed coat, or testa. The testa is composed of two layers, the inner being adjacent to the nucellar epidermis. It derives from the two integuments of the carpel surrounding the nucellus and its role is to keep the grain impermeable to water. During grain development, the testa is discontinuous in the crease region of the grain, and this opening facilitates transport of nutrients from the vascular strand to the nucellar projection. When the grain matures, the opening becomes sealed with impermeable tissue, connecting the borders of the integuments, and making the grain impermeable, called the pigment strand. The only opening through which water can enter the grain at maturity is the micropyle, a small pore situated close to the tip of the embryo. On the outside of the seed coat is the pericarp, which originates from the carpel wall, and can be subdivided into exocarp, mesocarp and endocarp. The endocarp is composed of tube and cross cells and constitute the photosynthetic tissue of the pericarp at the early developmental stages of the grain (Morrison, 1976). When the grain matures, the endocarp becomes closely linked to the seed coat (Xiong *et al.*, 2013). The central part of the pericarp is made up of a few layers of parenchyma cells and is known as the mesocarp. By around 15 days after anthesis (DAA) the mesocarp cells are mostly dead and only one cell layer persists (Xiong *et al.*, 2013). The outermost layer of the pericarp is the exocarp, whose sole function is to protect the seed. Taken together, the pericarp has a few functions, including photosynthesis, storage, transport, and breakdown of starch, as well as providing a protective layer for the seed.

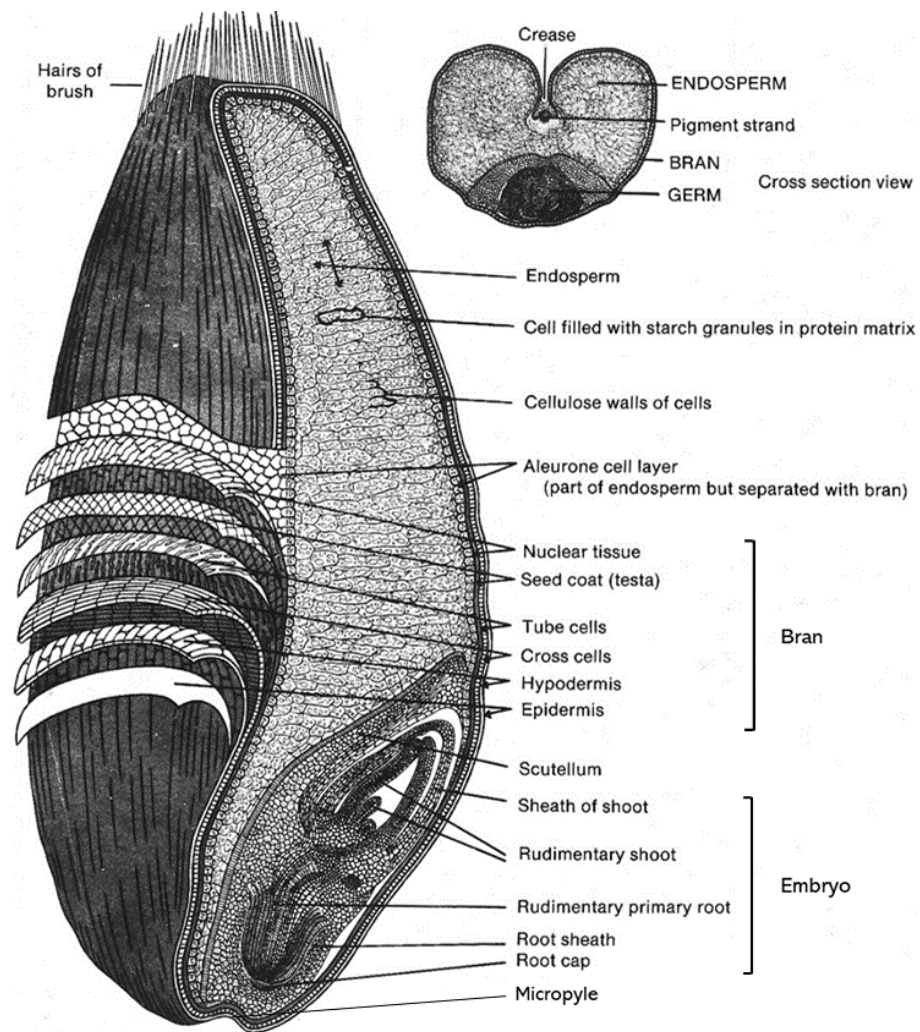


Figure 1. 2 The structure of wheat grain. Detailed specification of bran layers, endosperm, and embryo structure. Cross section view is also shown. Figure taken from Pomeranz (1982).

1.1.4 Aleurone development, structure, and function

The aleurone in wheat is a single cell layer surrounding the embryo and the endosperm. The aleurone layer envelops nearly the entire embryo and starchy endosperm, with the only exception being its absence at the micropyle. Cells of the aleurone are of three types: crease aleurone cells, embryo-surrounding

germ aleurone cells, and aleurone cells that envelop the starchy endosperm. In addition to other standard plant cell organelles, the aleurone cells are filled with amino acid-packed protein storage vacuoles (PSV), lipid-containing oleosomes, and glyoxysomes (Lonsdale *et al.*, 1999).

The aleurone differentiates from the surface cells of the endosperm, but cell morphology, biochemical composition and the transcription profiles are distinct between the two cell types (Becraft & Yi, 2011). The endosperm cells are triploid and develop in the process of double fertilisation, when one of the sperm nuclei undergoes syngamy with the two polar nuclei in the central cell. After cellularization, the internal and peripheral cells behave differently. The divisions in peripheral cells are highly ordered and occur almost exclusively in the anticlinal and periclinal planes; they show a typical plant cell division cycle with microtubules organised in a structure that will form a division plane in the pre-prophase. In internal cells, however, division of cells is unordered, with lack of the pre-prophase microtubule structure (reviewed in Becraft and Yi, 2010). In the mature cereal grain, the endosperm is made of two specialized tissues, the starchy endosperm and the aleurone layer. Both tissues undergo programmed cell death (PCD), but at different developmental stages. The starchy endosperm undergoes PCD after the grain filling has completed, and the dead starchy endosperm serves as a reserve of carbon and nitrogen for the germinating embryo. Aleurone cells are alive in the mature grain and die a few days after germination, once the enzymes needed for breakdown of the endosperm reserves have been produced. PCD is tightly regulated by gibberellins (GAs) and abscisic acid (ABA), with GA stimulating the onset of PCD in wheat aleurone (Kuo *et al.*, 1996), and ABA delaying it.

The main functions of the aleurone layer in the grain are accumulation of the storage compounds during seed development, and secretion of hydrolases to break down reserves stored in the starchy endosperm during seed germination. During the seed maturation process, when embryo growth ceases and storage products accumulate, ABA induces the aleurone cells to acquire desiccation tolerance, while the starchy endosperm dies (Young *et al.*,

1997; Young & Gallie, 2000). When the embryo undergoes imbibition, it releases GAs, which enter the aleurone cells and induce transcription of many genes, including amylases and proteases that break down starch and proteins stored in the endosperm. The released free sugars and amino acids are the nutrient source for germinating embryos. Additionally, the aleurone acts as a protective layer for endosperm, both as a mechanical protection, and also by expressing stress and pathogen-protective proteins, for example pathogenesis-related protein PR-4 also known as wheatwin1 (Jerkovic *et al.*, 2010).

1.2 Gibberellins

1.2.1 Gibberellin discovery

Gibberellins (GAs) are plant growth regulators (PGRs) that control many aspects of plant development. The effect of GAs was first observed in the late 19th century in Japan, where abnormal over-elongated rice seedlings were attributed to a fungal infection (Hedden & Sponsel, 2015). The fungus causing the altered development was *Gibberella fujikuroi*, and the rice seedlings that it infected, among other symptoms, showed excessive elongation and infertility. In the 1950s, the realisation of the potential of the active compounds secreted by *Gibberella fujikuroi* initiated active research programs in and outside of Japan that led to isolation and structural determination of the main active compound from the fungus, which was named gibberellic acid (GA₃).

Around 130 GAs have been identified in bacteria, fungi, and plants to date, but only a few of them are thought to function as bioactive hormones (Hedden & Phillips, 2000; Macmillan, 2002; Yamaguchi, 2008). The major bioactive forms are GA₁, GA₃, GA₄ and GA₇ and many non-bioactive GAs found in plants are either bioactive GAs' precursors or de-activated metabolites (Rademacher, 2015).

1.2.2 The roles of gibberellins in plant development

The identification and study of GA-deficient mutants revealed that GAs, apart from modulating growth, participate in most, if not all, stages of plant development. It is not then surprising that GAs can be found in all tissues of a plant, but their concentrations vary depending on the type of the tissue, its developmental stage, and the influence of the environment. The sections below briefly summarise the role of GAs in controlling various developmental processes.

1.2.2.1 Stem elongation

One of the most dramatic effects of GA application is accelerated stem growth. Most of the GA mutants deficient either in GA biosynthetic or GA signalling genes have a characteristic dwarf phenotype. On the contrary, mutants with constitutive GA responses are very tall (Sun, 2010). The effect of GA on stem elongation in wheat was found to be predominantly due to cell elongation rather than increased cell division (Tonkinson *et al.*, 1995). GAs stimulate cell elongation by altering the properties of the cell wall, which results in lower water potential of the cell, increased water uptake and therefore increased cell volume (Jones & Kaufman, 1983). GA signalling activates transcription of expansins and some of the genes encoding xyloglucan endotransglycosylases (XET), which increase the plasticity of the cell wall (Cho and Kende, 1997; Uozu *et al.*, 2000). Transcripts of genes encoding cyclin-dependent protein kinases have also been found to be elevated in the rice intercalary meristem after GA treatment (Fabian *et al.*, 2000), which shows the role of GAs in the cell division process. In wheat, application of GA₃ increases the length while decreasing the stem diameter of the basal second internode, whereas paclobutrazol has the opposite effect (Peng *et al.*, 2014). Reduced stature of *Rht-B1b* and *Rht-D1b* semi-dwarf mutants, encoding mutated DELLA proteins that repress GA signalling, is caused by a reduction in cell elongation, while the phenotype of the severe dwarf *Rht-B1c* mutant was the result of both reduced cell length

and cell proliferation (Hoogendoorn *et al.*, 1990). Taken together, GAs affect the stem elongation by regulating both cell elongation and cell division.

1.2.2.2 Leaf elongation

Gibberellins also have an important role controlling leaf elongation and expansion. In the base of a maize leaf, bioactive GAs were found at highest levels at the time of transition between the division and expansion zone (Nelissen *et al.*, 2012). Metabolic and transcriptomic profiling revealed that it is enhanced GA biosynthesis in the division zone and GA catabolism at the onset of expansion zone that establishes a GA maximum. Altering GA levels, therefore, specifically affects the size of the division zone resulting in changes in leaf growth rates. The leaf elongation rate (LER_{max}) increases in barley treated with exogenous GA, while in GA-insensitive dwarf mutants, no change in the LER_{max} is observed even at high GA_3 concentrations (Chandler & Robertson, 1999). The overgrowth alleles present in the GA biosynthesis, GA receptor (GID1), and DELLA (Sln1) dwarfs cause an increase in LER_{max} (Chandler & Harding, 2013). These alleles were shown to contain single nucleotide substitutions in *Slender1* or *Spindly1* genes, the negative regulators of GA signalling, that lead to increased GA signalling. In the tall cultivar of tall fescue (*Festuca arundinacea*), that shows higher accumulation of endogenous GA, LER is significantly higher (63%) than that of the dwarf cultivar, that accumulate GA to lesser extent (Xu *et al.*, 2016). Moreover, application of GA significantly increases LER while treatment with GA inhibitor inhibits leaf elongation. Again, the genes found to be upregulated in GA-stimulated elongating leaves were expansins and XET genes (Xu *et al.*, 2016). In wheat, the GA-insensitive alleles *Rht-B1b* and *Rht-B1c* reduce the rate of second leaf extension by 12% and 52%, respectively compared to *Rht-1* controls (Appleford & Lenton, 1991). The effect of *Rht-B1c* allele was confirmed in the study of Wen *et al.* (2013). Introduction of the allele resulted in significantly shorter and wider leaves at all positions. The loss of length however was not proportional to the width increase as the overall flag leaf area was reduced.

More recent study by Van De Velde *et al.* (2017) identified tall and semi-dwarf *Rht-B1c overgrowth (ovg)* alleles, that had differential effects on leaf length, with a general trend of tall alleles reducing and semi-dwarf increasing the flag leaf lamina length in the studied varieties. The width of the flag leaf lamina was found to be increased by both tall and semi-dwarf *ovg* alleles.

1.2.2.3 Tillering

Shoot branching is an important agronomic trait that determines crop yield and is primarily controlled by the auxin and cytokinin. However, GAs have a role too. Generally, increased tillering is associated with a reduction in stem elongation. In rice, lines overexpressing *GA2oxs*, a GA catabolic genes, exhibit early and increased tillering (Lo *et al.*, 2008). GA was shown to inhibit tillering by negatively regulating expression of *OSH1 (homeobox 1)* and *TB1 (TEOSINTE BRANCHED1)*, two transcription factors that control meristem initiation and axillary bud outgrowth, respectively (Hubbard *et al.*, 2002; Sato *et al.*, 1996). The GRAS protein MOC1 (MONOCULM1), which acts upstream of OSH1 and TB1 (Li *et al.*, 2003) is protected from degradation by binding to SLR1, and the degradation of SLR1 in response to GA causes degradation of MOC1, and hence a reduction in tiller number (Liao *et al.*, 2019). This model of regulation explains the coordinated control of plant height and tiller number by GA via SLR1. Consistently with these results, in wheat, a GA synthesis inhibitor, paclobutrazol (PBZ), positively affects tiller initiation and the percentage of tillered plants (Assuero *et al.*, 2012), while treatment with GA₃ can significantly inhibit the growth of tiller buds and the number of tillers (Cai *et al.*, 2013; Filho *et al.*, 2013). The GA were found to regulate tiller growth indirectly, by changing the endogenous ration of IAA to cytokinin zeatin (Z) and ABA to Z (Cai *et al.*, 2018). Recently, *NITROGEN-MEDIATED TILLER GROWTH RESPONSE 5 (NGR5)*, a nitrogen-induced TF that promotes repressive modification of branching-inhibitory genes, thereby increasing the number of tillers, was found to be a target of GA-GID1-mediated degradation. This degradation was

distorted in the DELLA-accumulating *sd1* and *Rht-B1b* mutants, due to competition between NGR5 and SLR1 for GID1 binding (Wu *et al.*, 2020). Therefore, enhanced DELLA function in *sd1* and *Rht-B1b* mutants increases tiller number in response to nitrogen by increasing the stability of NGR5, which in turn promotes tillering by inhibiting the expression of shoot branching inhibitor genes.

1.2.2.4 Floral induction and development

The timing of floral transition has a major effect on yield in cereal crops such as wheat and barley. In barley, GA was found to be necessary for flowering of the spring varieties (Boden *et al.*, 2014). The analysis of barley *elf3* mutant, that shows early flowering phenotype irrespective of the photoperiod, revealed increased expression levels of the GA biosynthetic *GA20ox2* gene and an increase in bioactive GA₁ compared to the wild type, indicating a positive effect of GAs on flowering. Under short days, inhibition of GA biosynthesis suppressed the early flowering of *elf3* independently of *FLOWERING LOCUS T1* (*FT1*) (Boden *et al.*, 2014), a central regulator of floral transition (Lv *et al.*, 2014). Instead, GA was shown to promote early flowering of *elf3* by enhancing expression of genes required for inflorescence development: *LEAFY* (*LFY1*), *SUPPRESSOR OF CONSTANS1* (*SOC1*), *FLORAL PROMOTING FACTOR3* (*FPF3*) and *PANICLE PHYTOMER2* (*PAP2*). In the same study, GA signalling loss-of-function mutant *sln1c* (constitutive GA response) flowered earlier than the WT plant, whereas gain-of-function *Sln1d* (GA insensitive), GID1 loss-of-function (*gse1a*) and *GA3ox* biosynthetic mutant (*grd2c*) flowered later (Boden *et al.*, 2014). Moreover, the delayed inflorescence development of *grd2c* was restored by GA₃ application (Boden *et al.*, 2014).

In wheat, a critical regulatory point in flowering requires activation of the meristem identity gene *VERNALIZATION1* (*VRN1*), a homolog of Arabidopsis *AP1* gene (Danyluk *et al.*, 2003). In wheat varieties that are photoperiod sensitive, *VRN1* is expressed under long days only, but an additional regulatory

mechanism of flowering, dependent on photoperiod duration, was also suggested. Exogenous GA application accelerates flowering in wheat only in the presence of *VRN1*, and the concurrent presence of GA and *VRN1* leads to increased expression of *SOC1-1* and *LFY*. Paclobutrazol treatment, on the other hand, inhibits expression of *SOC1-1* and *LFY* genes under long days (Pearce *et al.*, 2013). The involvement of GA in flowering in wheat is further supported by the enhanced expression of GA biosynthetic genes and decrease in GA catabolism genes in the apices of plants that were transferred from short days to long days. Interestingly, in the *Rht-B1b* and *Rht-D1b* lines, due to more favourable assimilate partitioning to the spike during pre-anthesis, a higher number of distal primordia progress to the stage of fertile floret at anthesis, and produce more grain (Miralles *et al.*, 1998).

1.2.2.5 Pollen development

Pollen develops from an undifferentiated mound of cells (anther primordium) within the anthers. During its development, the anther forms two general groups of cells. The reproductive or sporogenous cells give rise to the microspores, and the non-reproductive cells form discrete anther tissues layers: the endothelium, middle layer and tapetum (Wilson & Zhang, 2009). The tapetum, which is the innermost layer of the pollen sac, plays a dominant role during pollen development, especially during the microspore stage. The release of viable pollen depends upon the prior competence of the tapetum. During pollen mitotic division the tapetum undergoes programmed cell death (PCD), releasing components essential to pollen formation (Parish & Li, 2010). The PCD of tapetum is a highly regulated process which when interrupted, results in nonviable pollen formation (Aya *et al.*, 2009). GA signalling has been shown to regulate PCD and this regulation is dependent on a GA-regulated transcription factor GAMYB. In fact, GAMYB was found to be involved in regulation of almost all GA-regulated genes in anthers (Aya *et al.*, 2009). The *gamyb* mutants in rice are male sterile due to failure of the tapetum to initiate

PCD (Aya *et al.*, 2009; Liu *et al.*, 2010). GAMYB was also shown to directly regulate expression of two lipid metabolism genes, *cytochrome P450 hydroxylase (CYP703A3)* and *β -ketoacyl-reductase (KAR)*, which are involved in providing substrate for exine and Ubisch body formation, structures necessary for normal pollen grain development. Moreover, the GA biosynthesis and signalling mutants in rice, *Ososcp1-1* and *Osgid-2*, respectively, and another two mutants *Osgamyb-2* and *Oscyp703a* are either lacking or deficient in Ubisch bodies (Aya *et al.*, 2009). In wheat, *gamyb* mutant shows complete male sterility due to failure to produce viable pollen (Audley, 2016).

1.2.2.6 Grain development

GAs play a critical role in wheat grain development. Levels of endogenous GAs in the developing grains are very high and increase during grain expansion (Radley, 1976). Gene expression analysis in wheat revealed that the endosperm is the main site of GA biosynthesis in the developing grains, while GA signalling occurs mainly in the seed coat and pericarp layers (Pearce *et al.*, 2015). It was speculated that GA produced in the endosperm is transported into the outer layers, where it promotes cell expansion, allowing growth of the endosperm and hence increasing the grain size. This model would be supported by the decreased size of the grains in the GA-insensitive *Rht-1* lines (Flintham *et al.*, 1997). The grain size in wheat was also shown to be negatively regulated by *TaGW2-6A*, a RING E₃ ubiquitin-ligase (Li *et al.*, 2017). NIL31 line, which encodes nonviable *TaGW2-6A* allele, showed increased GA levels compared to WT line, and increased expression of *GA3-ox* and *GASA4* genes, which was suggested to increase the grain size by controlling endosperm elongation and division during grain filling (Li *et al.*, 2017). In the same study, GA₃ application three days after flowering resulted in an increase in grain length, width, and weight, whereas in the NIL31 lines the effects were opposite.

1.2.3 Gibberellin biosynthesis

The GA biosynthesis pathway in higher plants can be subdivided into three parts based on the cellular compartment and the class of enzymes involved in the synthesis (Yamaguchi *et al.*, 2001): first, the conversion of geranylgeranyl diphosphate (GGPP) to ent-kaurene by diterpene cyclases takes place in the plastids; second, the conversion of ent-kaurene to GA₁₂ and GA₅₃ by cytochrome P450 mono-oxygenases takes place in the endoplasmic reticulum (ER); and third, the conversion of precursors GA₁₂ and GA₅₃ to bioactive GA₄ and GA₁, respectively, by two 2-oxoglutarate-dependent dioxygenases (2-ODDs), GA3- and GA20-oxidases, in the non-13-hydroxylation pathway and early 13-hydroxylation pathway, respectively, that take place in the cytoplasm (reviewed in Hedden and Thomas, 2012; Hedden, 2020). The following subsections briefly describe the respective steps.

1.2.3.1 Formation of *ent*-kaurene

Early steps of gibberellin biosynthesis occur in plastids, where *trans*-geranylgeranyl diphosphate (GGDP) is converted into *ent*-kaurene by the action of *ent*-copalyl diphosphate synthase (CPS) and *ent*-kaurene synthase (KS) in two separate reactions, with *ent*-copalyl diphosphate (CPP) as the intermediate (Hedden & Kamiya, 1997). In plants, *ent*-kaurene formation occurs in the stroma of proplastids and developing, but not mature chloroplasts (Aach *et al.*, 1995, 1997). CPS, a type-II diterpene cyclase, catalyses cyclization of GGPP to CPP, and act as a proton donor to initiate cyclization. The second step, conversion of CPP to *ent*-kaurene by another cyclization is catalysed by type-I cyclase, KS, and is initiated by metal-dependent heterolytic cleavage of the C–O bond. In Arabidopsis overexpression of *AtCPS* and *AtKS* genes results in increased levels of *ent*-kaurene, but not bioactive GAs (Fleet *et al.*, 2003), whereas loss of function results in severe GA-deficient phenotypes (Koornneef & van der Veen, 1980). Wheat genome encodes three homoeologues of *TaCPS* and *TaKS* located on

chromosomes 7A, 7B and 7D, and 2A, 2B and 2D, respectively (Huang *et al.*, 2012; Spielmeier *et al.*, 2004). The genes are constitutively expressed, but the expression varies depending on the homoeologue and the tissue. The biggest expression was found in internodes 3 and 4, and the peduncle of the stems (Huang *et al.*, 2012). These genes were not found to be subject to feedback regulation.

1.2.3.2 Synthesis of early precursor, GA₁₂

The conversion of *ent*-kaurene to GA₁₂, the common precursor of all GAs in plants is catalysed by two cytochrome P450 mono-oxygenases (P450s), *ent*-kaurene oxidase (KO) and *ent*-kaurenoic acid oxidase (KAO) (Helliwell, 2001; Helliwell *et al.*, 1999). Studies in *Arabidopsis* showed that KO can be found in the outer chloroplast membrane and the ER, while KAO is located exclusively in the ER (Helliwell, 2001). KO catalyses the three-step oxidation of *ent*-kaurene to *ent*-kaurenoic acid by repeated hydroxylation of C₁₉, with the first hydroxylation to *ent*-kaurenol being the rate-limiting step (Morrone *et al.*, 2009). The oxidation of *ent*-kaurenoic acid to GA₁₂ is another three-step reaction catalysed by KAO, and requires successive oxidations at C-7β, C-6β and C-7 (Castellaro *et al.*, 1990). Loss-of-function mutations in *OsKO* and *OsKAO* genes in rice cause severe dwarf phenotype without flower or seed development, whereas an amino acid substitution caused by single nucleotide substitution in exon 5 of *OsKO2* gene in the *d35* mutant results in semi-dwarf phenotype with seed development, and lower GA levels (Sakamoto *et al.*, 2004). Recently, *OsKO1* was shown to catalyse the conversion of *ent*-kaurene to *ent*-kaurenoic acid mainly at seed germination and seedling stages, and the mutations in the gene decrease this activity and lead to delayed germination phenotype (Zhang *et al.*, 2020). Lack of KAO was also reported to cause GA deficiency and resulting phenotypes in barley *grd5* (Helliwell, 2001) and sunflower *dwarf2* (Fambrini *et al.*, 2011). In wheat, three *TaKO* homoeologues are located on chromosomes 7A, 7B and 7D, and three *TaKAO* genes are located on chromosomes 4A, 7A and 7D (Huang *et al.*, 2012; Spielmeier *et al.*,

2004). The expression analysis of various wheat tissues at heading stage show predominant *TaKO* expression in leaves, young spikes, and internode 3, whereas *TaKAO* is mainly expressed in internodes 3 and 4, but not in the peduncle (Huang *et al.*, 2012).

1.2.3.3 Synthesis of the bioactive GAs

After the synthesis of GA_{12} , the GA biosynthesis pathway splits into two parallel pathways: the non-13-hydroxylation pathway, in which GA_{12} is converted to bioactive GA_4 , and early 13-hydroxylation pathway, where GA_{12} is hydroxylated to GA_{53} , from which bioactive GA_1 is formed, in a series of reactions catalysed by 2-ODD enzymes. There are three classes of dioxygenases, GA-promoting GA 20-oxidase (*GA20ox*) and GA 3-oxidase (*GA3ox*) and GA-inactivating GA 2-oxidase (*GA2ox*). The majority of studies have revealed that indeed the dioxygenases are the main sites of regulation of the GA biosynthesis in response to the developmental and environmental signals, and *GA2ox* genes were found to be especially responsive to abiotic stress (Dubois *et al.*, 2013; Magome *et al.*, 2004, 2008). In wheat, the early 13-hydroxylation pathway is the predominant pathway of bioactive GA synthesis (Appleford & Lenton, 1991). *GA13ox* was found to be encoded by two genes in wheat, *TaGA13ox1* and *TaGA13ox2*, with the former being more highly expressed in the studied tissues, except the mature spikes (Pearce *et al.*, 2015). *GA20ox* catalyses a series of reactions converting GA_{53} to GA_{20} in the early 13-hydroxylation pathway, and GA_{12} to GA_9 in the non-13-hydroxylation pathway. Seed plants encode a family of *GA20ox* genes which display different tissue, developmental and environmental expression patterns. Grass *GA20ox* genes, including wheats', fall into four paralogous clades, each containing one of the four *GA20ox* genes (Pearce *et al.*, 2015). The biochemical function was first reported for all three homoeologues of *TaGA20ox1* (Appleford *et al.*, 2006) and validated for a single homoeologue of the other three genes *TaGA20ox2B*, *TaGA20ox3B* and *TaGA20ox4D* (Pearce *et al.*, 2015).

The final step in synthesis of biologically active GAs is 3 β -hydroxylation of GA₉ to GA₄, and GA₂₀ to GA₁, catalysed by GA3-oxidases. *GA3ox* genes make a very small family with four members in Arabidopsis and two in rice and barley. Only *GA3ox2* gene has a major role in the development of vegetative organs in cereal, whereas *GA3ox1* contributes mainly toward reproductive development (Hedden, 2020). In wheat, three *GA3ox* genes were identified: *TaGA3ox2* and *TaGA3ox3*, which are encoded by a single gene in all three genomes, and *TaGA1ox1*, which was initially assigned as *TaGA3ox4*, but unexpectedly was demonstrated to possess 1 β -hydroxylase activity, catalysing conversion of GA₉ to GA₆₁ (Pearce *et al.*, 2015), and is encoded by a single homoeologue on the B genome. Heterologous expression in *E.coli* confirmed that the predominant function of the *TaGA3ox2* gene product was conversion of GA₉ and GA₂₀ to GA₄ and GA₁, respectively (Appleford *et al.*, 2006), and the same activity was demonstrated for *TaGA3ox3* (Pearce *et al.*, 2015).

The *GA20ox* and *GA3ox* gene families showed tissue-specific expression profiles in wheat. *TaGA20ox1* and *TaGA20ox2* were the most highly expressed *GA20ox* genes in vegetative tissues, *TaGA20ox3* is almost completely restricted to the expanding grain, while *TaGA20ox4* was highest in the spike at anthesis. *TaGA3ox2* was most highly expressed in vegetative and floral organs, while *TaGA1ox-B1* and *TaGA3ox3* were expressed at a very high levels and almost exclusively at the mid-way stage of grain development (Pearce *et al.*, 2015).

1.2.3.4 Inactivation of bioactive GAs

Inactivation of bioactive GAs is achieved by introducing structural modifications that decrease affinity of the GA for its receptor. The most common inactivating reaction is 2 β -hydroxylation, catalysed by GA 2-oxidase enzymes, which can use the bioactive end products of the pathway or the C₁₉- and C₂₀-GA precursors as substrates, therefore preventing formation of the active GAs. The conversion to inactive forms is irreversible and thus prevents

accumulation of bioactive GAs, enabling their levels to be tuned appropriately for plant tissues or developmental stages. Recently, through X-ray crystallography, it was revealed that rice OsGA2ox3 forms a homotetramer, with the monomers linked by two disulfide bridges and hydrogen bonds bridged by the two GA₄ molecules between the monomers (Takehara *et al.*, 2020). This tetrameric form was shown to be more active than a monomer, thus the regulation mechanism was proposed in which elevated levels of GA₄ trigger OsGA2ox3 tetramerization and hence increased activity, resulting in active inactivation of GA₄. The overall molecular structure is similar for all 2ODD enzymes, and amino acids essential for binding the co-substrate 2OG and interacting with Fe(II) are located in the same manner as reported for other 2ODD enzymes.

GA 2-oxidases can be divided into two major groups based on the GA type they use as a substrate: C₁₉-GA-binding and C₂₀-GA-binding. These groups are not phylogenetically closely related, however, some functional overlap has been reported (Pearce *et al.*, 2015). A comprehensive expression analysis of *GA2ox* genes in *Arabidopsis* showed differential expression during growth, development as well as in response to abiotic stress, allowing for more specific targeting of genetic interventions aiming to improve specific traits in plants (Li *et al.*, 2019). Twelve *GA2ox* genes were found in wheat, nine of them are likely orthologs of rice *GA2ox* genes (*TaGA2ox1 – 10*; no *TaGA2ox5*), and three that did not have obvious orthologs in rice and showed sequence similarity to *TaGA2ox6* (*TaGA2ox11 - 13*) (Pearce *et al.*, 2015). Wheat *GA2ox* genes also show differential expression, depending on the homoeologue, tissue and time point. *TaGA2ox3, 4* and *9* are the most highly expressed *GA2ox* genes overall, contributing most to *GA2ox* levels in roots, leaves and stems, while *TaGA2ox3, 6, 7* and *8*, are the most abundant *GA2ox* transcripts in the spike at anthesis. *TaGA2ox7* is also most highly expressed *GA2ox* gene in developing grain. *TaGA2ox1* and *2* show very low or no expression, respectively, and only very low levels of *TaGA2ox-B12* transcripts can be found among the *TaGA2ox11 – 13* group. The activity of all GA 2-oxidases in wheat

assessed against C₁₉ and C₂₀ substrates, GA₉ and GA₁₂, respectively, identified that TaGA2ox-D1, -D2, -B3, -D4, -D7, -D8 and -D10 were all active against GA₉, while TaGA2ox-D6 and TaGA2ox-D9 were active against GA₁₂. In fact, GA-responsive semi-dwarf phenotype of *Rht18* was showed to be caused by overexpression of the *GA2oxA9* gene, which resulted in the increase in GA₁₂ to GA₁₁₀ inactivation, and lower levels of bioactive GA₁ (Ford *et al.*, 2018). No activity against either substrate was found for TaGA2ox11 – 13 (Pearce *et al.*, 2015).

1.2.4 GA homeostasis is achieved by feedback regulation of the GA biosynthetic genes

The levels of bioactive GAs in GA-responsive tissues is subject to strict regulation on the level of GA biosynthesis, inactivation and transport (Hedden, 2020). Regulation of the biosynthesis is only a part of the wider homeostatic mechanism that includes regulation of GA signalling components (reviewed in Hedden and Thomas, 2012; Hedden, 2020). It has been elucidated that the members of the 2-ODD gene families, particularly GA 20-oxidases, are major sites of feedback regulation (Fleet *et al.*, 2003; Middleton *et al.*, 2012). Many studies report that plants with reduced GA levels, regardless if the decrease is a result of a mutation in the GA biosynthesis or signalling pathway, or a result of GA biosynthesis inhibitor application, display elevated levels of *GA20ox* and *GA3ox* transcripts, while application of bioactive GAs results in lower *GA20ox* and *GA3ox* transcript levels (Hedden & Phillips, 2000). Transcriptional regulation of GA biosynthesis genes was shown in an *Arabidopsis* GA-deficient *ga1-2* mutant by exogenous application of GA₃ (Thomas *et al.*, 1999), where transcript levels of *AtGA20ox2* and *AtGA3ox1* genes were reduced, and transcript levels of *AtGA2ox1* and *AtGA2ox2* genes were elevated, compared to the WT plants. These results confirmed the existence of a feedback mechanism that maintains bioactive GA concentrations, but also indicated a presence of a feed-forward regulation that works to stabilise GAs levels by

deactivation of bioactive GAs and their immediate precursors (Thomas *et al.*, 1999). Another study showed the effects of overexpression of the *GA3ox1* and *GA20ox1* feedback-regulated genes in tobacco (Gallego-Giraldo *et al.*, 2008). In lines overexpressing *GA3ox1* (3ox-OE), the conversion of GA₂₀ to GA₁ was more efficient than in the WT plants, which resulted in relatively decreased levels of GA₂₀, but increased levels of GA₁ and GA₈ in 3ox-OE plants. Investigation of the 2-ODD genes transcript levels showed that overexpression of *GA3ox* results in enhanced expression of *GA2ox* genes, indicating that increase of bioactive GA triggers increases in bioactive GA-inactivating genes levels. Analysis of the 3ox/20ox-OE transgenic hybrid showed that simultaneous overexpression of *GA3ox* and *GA20ox* results in elevated levels of GAs belonging to non 13-hydroxylation pathway and significant increases in the net levels of bioactive GAs (GA₄ + GA₁). Overexpression of *GA20ox* alone resulted in a similar response. The levels of *NtGA3ox1* and *NtGA20ox1* genes in 3ox/20ox-OE lines were reduced indicating the negative feedback. Reciprocal effect of GA₁ application on the expression of *GA20ox* and *GA3ox*, and *GA2ox* genes was also shown, with the biosynthetic genes' expression being reduced, and inactivation genes expression being activated by GA₁ application (Gallego-Giraldo *et al.*, 2008). These results validated the existence of feedback and feed-forward mechanisms regulating GA levels in tobacco. GA₃ application was also shown to alter expression of the genes responsible for regulating GA homeostasis (Cheng *et al.*, 2015; Chiang *et al.*, 1995; Phillips *et al.*, 1995; Ribeiro *et al.*, 2012; Thomas *et al.*, 1999). The feedback and feedforward mechanisms also operate at the level of GA perception, as *GID1b* is down-regulated and a few different *DELLA* genes in Arabidopsis are up-regulated after GA₃ treatment, while the opposite can be observed after the treatment with PAC (Cheng *et al.*, 2015; Ribeiro *et al.*, 2012). In the study of Middleton *et al.* (2011) the mathematical model of GA signalling-modulating feedback loops was validated by data. GA-deficient *ga1-3* and *GA2ox1OE* (overexpression) lines showed downregulation of *GA20ox2*, *GA3ox1* and *GID1a*, and upregulation of *DELLA* genes, *RGA* and *GAI*, in response to GA₄ treatment. It was also shown that DELLA protein steady state concentration

decreases with the increasing GA₁₂ availability, and this response is affected by constitutive expression of *GA20ox* gene, indicating that *GA20ox* feedback is important for determining the levels of endogenous DELLA proteins levels (Middleton *et al.*, 2012).

DELLA proteins indeed were shown to play an important role in regulating GA levels. DELLAs upregulate the expression of genes involved in feedback *GA3ox1*, *GA20ox2* and *GID1b*, and DELLA gain-of-function mutants show reduced transcript levels of some of the *GA2ox* genes (reviewed in Hedden & Thomas, 2012). Semi-dominant dwarf DELLA mutants in barley and wheat show increased levels of *GA3ox* and *GA20ox* genes (Jung *et al.*, 2020; Rafter, 2019) which shows that enhanced expression of genes promoting GA biosynthesis is typical for DELLA gain-of-function mutants. The regulation of GA feedback genes by Arabidopsis DELLAs was identified to be mediated by their interaction with IDD TFs, ENHYDROUS (ENY) and GAI-ASSOCIATED FACTOR1 (GAF1) (Feurtado *et al.*, 2011; Fukazawa *et al.*, 2014). Both TFs were shown to regulate the core GA biosynthesis and signalling genes. The follow up study identified GAF1-DELLA complex as the main component of GA feedback regulation of *AtGA20ox2* (Fukazawa *et al.*, 2017).

The levels of bioactive GAs are controlled by the availability of GAs themselves in a DELLA-mediated manner. In the absence of GAs, DELLAs act to promote GAs synthesis by upregulating expression of *GA3ox*, *GA20ox*, and *GID1* genes. Increases in GAs levels lead to DELLAs degradation and hence inhibition of GAs synthesis. When GAs levels are low, DELLAs accumulate and promote GAs synthesis.

1.3 GA signalling in the aleurone of germinating seed

The main events taking place during grain germination have been well characterised (Bewley & Black, 1994). Germination of the grain starts with imbibition of the dry seed and ends when the radicle penetrates through the

seed coat. The process of germination can be subdivided into three phases: phase I, II and III. The rapid influx of water during phase I, called the imbibition, causes a rapid leakage of solutes and low molecular weight metabolites into the surrounding solution and leads to a series of intracellular processes, for example DNA repair and protein synthesis, which in the phase III of germination result in resumption of metabolic activity. Protein synthesis in phase I relies on extant mRNA (Bewley, 1997). During phase II, the water uptake is ceased, newly transcribed mRNA is translated, and mitochondria are synthesized. Phase III initiates post germination and during this phase massive mobilisation of storage products from the endosperm takes place (Tan-Wilson & Wilson, 2012). Seed maturation and germination are regulated mainly by two hormones, abscisic acid (ABA) and gibberellins (GAs) (Holdsworth *et al.*, 2008; Sun & Gubler, 2004). The ratio of these two hormones determines whether the grain remains dormant or commences germination. ABA is synthesized in the embryo and maternal tissues during seed maturation and its level decreases rapidly after imbibition (Millar *et al.*, 2006). GA synthesis occurs in the embryo and increases during germination and seedling growth. Following imbibition, sugars in the embryo become rapidly depleted which leads to activation of α -amylase synthesis in the scutellum and initiation of starch degradation. At the same time the embryo synthesizes GAs and releases them to the aleurone of the grain, where they regulate transcription of transactivating factors for various enzymes, mainly hydrolases and proteases (Bewley, 1997). Transcript profiling studies have demonstrated that GAs release into barley and rice aleurone results in upregulation of around 1300 genes, encoding hydrolases and functionally diverse proteins involved in general metabolism, transcription, nutrient transport, and programmed cell death (Chen & An, 2006; Tsuji *et al.*, 2006). These enzymes are then transported from the aleurone to the endosperm where they act to break down reserves, predominantly starch, but also other sugars and proteins. The simple sugars, reduced nitrogen and other nutrients are absorbed by the scutellum and transported to the embryonic axis, where they support

establishment of a viable seedling, capable of photosynthesizing and producing its own energy.

1.3.1 Gibberellin signalling overview

Gibberellins act through the degradation of a group of transcriptional regulators, the DELLA proteins (DELLAs). DELLAs are known to repress growth and they owe their name to the conserved domain within their N-terminus, which is unique to this group of proteins and is essential for GA-induced degradation (reviewed in Hedden and Sponsel, 2015). Upon binding of GA to its receptor, GID1, the GID1 protein undergoes a conformational change which promotes its association with the N-terminal domain of DELLA protein. Binding of GID1 to DELLAs allows for interaction between the DELLA protein and SCF^{SLY1/GID2} ubiquitin ligase complex, which then acts to add ubiquitin moieties onto DELLA protein leading to its recognition and degradation via the 26S proteasome. It was originally hypothesized that the GA is perceived by the plasma membrane bound GA receptor (reviewed in Ueguchi-Tanaka *et al.*, 2007). However, more recent study provides the evidence that GA signalling is mediated predominantly by a soluble GA receptor GID1 (Nakajima *et al.*, 2006; Ueguchi-Tanaka *et al.*, 2005; Yano *et al.*, 2015).

1.3.2 Gibberellin signalling in the aleurone cells

In the aleurone cells, GA activates transcription of many GA-responsive genes, mainly hydrolases, peptidases and other digestive enzymes that act to release protein reserves and to break down cell walls to aid their diffusion into the endosperm. Among these activated genes is a transcription factor *GAMYB*, which regulates expression of many GA-responsive genes, including α -*amylases*. The α -amylase released from the aleurone cells diffuse into the neighbouring endosperm cells where it hydrolyses the α -1,4 glycosidic bonds of starch, releasing simple sugars that feed the heterotrophic growth of the embryo until it is ready to photosynthesize itself (Figure 1.3).

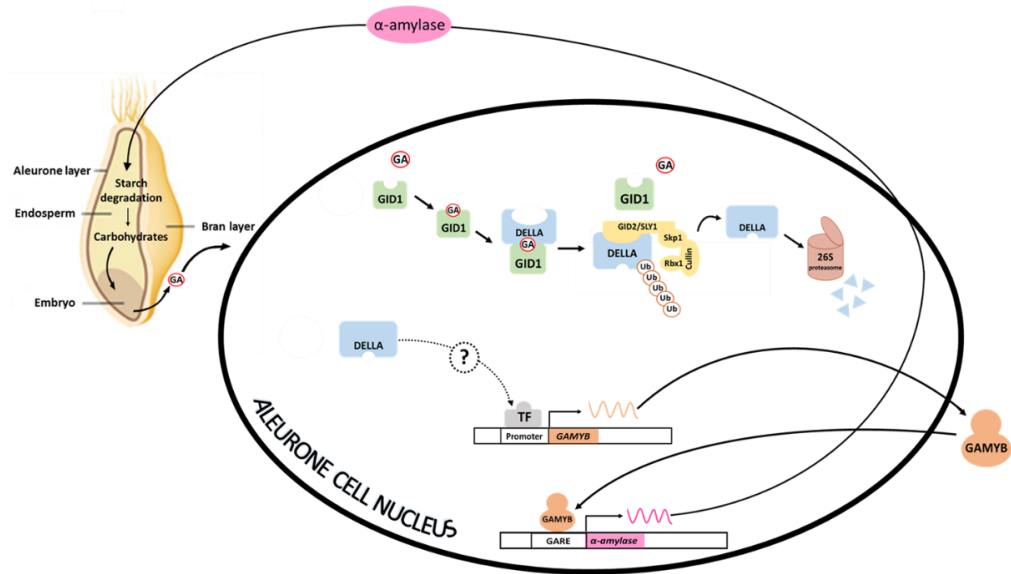


Figure 1. 3 Gibberellin signalling in the aleurone cells. Gibberellin (GA) is synthesized in the embryo scutellum, from where it diffuses into the aleurone layer. In the aleurone cell nucleus, GA binds to its receptor, GID1, and the GA-GID1 complex binds DELLA protein. This binding causes conformational change in DELLA that allows for binding of SCF^{SLY1/GID2} ubiquitin ligase complex, which ubiquitinates DELLA and therefore sends it for degradation by the 26S proteasome. GA signalling in the aleurone results in activation of GAMYB, and subsequent α -amylase expression. α -amylase is then released into the endosperm where it hydrolyses starch into simple sugars that are utilised by the embryo until it reaches photosynthetic capacity. GAMYB, a transcription factor that regulates transcription of α -amylase, is negatively regulated by DELLA, but the mechanism of this regulation remains to be elucidated.

GA signalling was shown to induce a rapid increase in *GAMYB* gene expression in the barley aleurone layer, which is followed by an increase in the expression of the *GAMYB* target gene, α -amylase (Gubler *et al.*, 1995). DELLA is a negative regulator of GA-induced responses in aleurone cells, and as results from Gubler and colleagues (2002) studying barley suggest, GA acts on *GAMYB* expression via DELLA. In fact, loss-of-function mutations in barley and rice DELLA genes *SLENDER1* (*SLN1*) and *SLR1*, respectively, result in constitutive expression of α -amylase genes (Chandler, 1988; Ikeda *et al.*, 2001). This indicates that DELLAs

are repressors of α -amylase expression and this negative regulation may occur through the repression of GAMYB. The levels of SLN1 protein fall rapidly in response to GA, before the increase in *GAMYB* levels, therefore it was suggested that SLN1 acts as a negative regulator of *GAMYB* gene expression. The mechanism underpinning this regulation, however, remains to be elucidated.

1.3.3 Time course of molecular changes in the aleurone in response to GA

Cereals aleurone layers have been extensively used to study GA signalling (Penson *et al.*, 1996; Bethke, Schuurink and Jones, 1997; Lovegrove and Hooley, 2000; Sun and Gubler, 2004). Isolated aleurones are a very convenient system for studying GA signalling due to the lack of endogenous GAs, ease of isolation and relatively easy assessment of the response gene, α -amylase. Aleurone layers from wheat and barley grains were used to study the accumulation of GA signalling intermediates over time of the GA application. The binding of the GA to its receptor initiates a sequence of events summarised in reviews by Bethke, Schuurink and Jones (1997) and Sun and Gubler (2004) (Figure 1.4). The earliest observed event in response to GAs is the degradation of SLN1 protein (the DELLA protein in barley) which occurs within 10 minutes of the GA treatment. This is closely followed by an almost simultaneous accumulation of the second messenger, Ca^{2+} cations. After about 50 minutes, an increase in calmodulin (CaM) expression can be observed. CaM is a Ca^{2+} -binding protein and is a part of calcium signalling transduction pathway. Activation of Ca^{2+} /calmodulin signalling pathway by GA plays an important role in the synthesis and secretion of hydrolases. Ca^{2+} /CaM targets include many proteins that through interaction with CaM and other Ca^{2+} binding proteins (CBPs) are involved in regulation of transcription, protein phosphorylation and

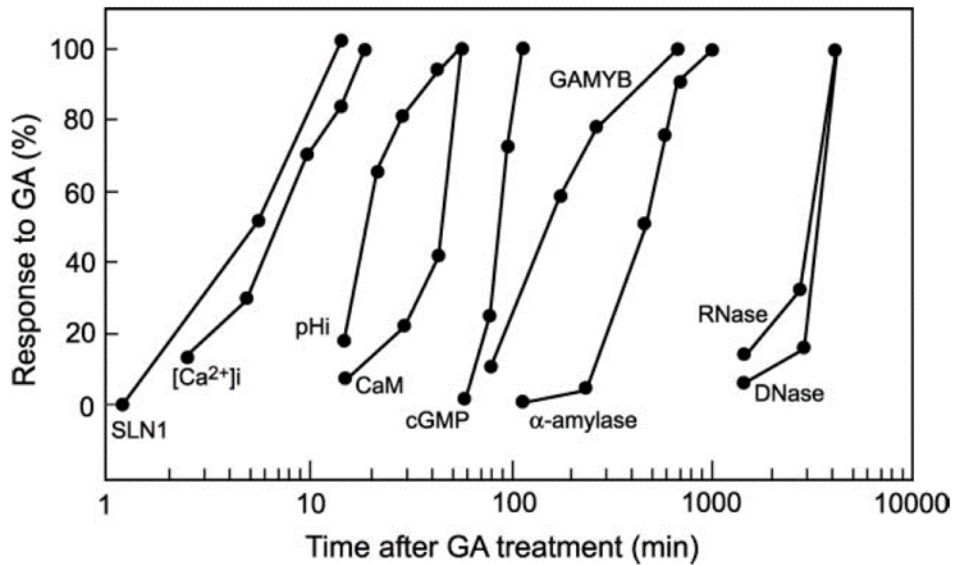


Figure 1. 4 GA-induced responses in barley and wheat aleurone tissue expressed in percentage versus time. The graph for SLN1 shows the protein degradation over time after the GA treatment, whereas for every other molecule, it shows accumulation over time after the GA treatment. Time is plotted on the logarithmic scale. The graph is taken from Sun and Gubler, 2004.

dephosphorylation, and metabolic shifts. Simultaneously, while accumulation of CaM takes place, the internal pH of the cell increases. This is essential in regulating gene expression, cell metabolism and indeed the Ca²⁺ homeostasis (Puc at, 1999). An increase in *GAMYB* transcript levels is preceded by the induction of cGMP, another second messenger that activates intracellular protein kinases, and which has an intermediary function between SLN1 and *GAMYB* (Penson *et al.*, 1996). *GAMYB* transcript accumulation starts around 80 minutes after GA application and takes about ten hours to reach maximum expression level. 20 minutes after the onset of *GAMYB* expression activation, the levels of *α-amylase* start accumulating which demonstrates that 20 minutes is enough time to synthesize the *GAMYB* protein and activate its target gene. The GA signalling in the aleurone completes with the programmed

cell death (PCD) of the aleurone cells, for which to happen, RNases and DNases are transcribed. The involvement of nucleases in the PCD is established and has been reviewed by Dominguez and Cejudo (Dominguez & Cejudo, 2014).

1.3.4 α -amylase expression is regulated by GAMYB

α -amylase plays a central role during germination and its activity determines the rate of germination and seedling growth. The storage reserves in wheat grains are mainly starch and the major enzyme involved in its breakdown during germination is α -amylase. α -amylase hydrolyses internal bonds of alpha-linked polysaccharides, including starch, yielding α -glucans that can be metabolized to provide energy to drive the germination process. Hormonal regulation of α -amylase gene expression is through trans-acting regulatory proteins which interact with cis-acting elements within GARC.

The α -amylase gene promoter contains a GA-responsive complex (GARC) which is a collection of *cis*-acting GA-responsive sequences that bind positive and negative regulators of gene transcription and is highly conserved among GA-regulated genes. Functional analysis of barley high-pI α -amylase promoters revealed that GARC consists of pyrimidine box (C/TCTTTT), GA-response element (GARE; TAACAAA) and TATCCAC/T box (Gubler & Jacobsen, 1992; Rogers *et al.*, 1994; Skriver *et al.*, 1991). An additional box, Opaque 2-binding (O2S) sequence is necessary for activation of GA-inducible low-pI α -amylase genes (Lanahan *et al.*, 1992). In wheat, the promoters of all *AMY1* genes contain GARE, pyrimidine and TATCCAT or TATCCAC boxes, and cAMP-like motif (TGAGCTC). The GARE is required for GA induction of *AMY1* expression, pyrimidine and TATCCAT/C boxes enhance the expression of *AMY1* and cAMP-like motif represses the GA action (Gubler & Jacobsen, 1992; Lanahan *et al.*, 1992). Promoters of *AMY2* genes are more diverse in structure between genes belonging to this subgroup and contain slightly different GARE (TAACAGAG), pyrimidine and TATCCAT boxes and O2S motif (Zhang & Li, 2017). Two highly conserved sequences in GARC, GARE and TATCCAC box, which occur in

promoters of all GA-regulated genes, act as positive control elements in GA regulation.

In 1995, Gubler and colleagues reported a Myb-related protein synthesized in barley aleurone cells that trans-activated expression of the α -amylase gene in response to GA (named GAMYB). GAMYB bound to the central GARC element, the TAACAAA box, of the α -amylase gene. Based on their results, Gubler and colleagues proposed a model, in which GA binds to the receptor on the plasma membrane of aleurone cell and activates a signal transduction pathway that leads to the *GAMYB* gene expression induction. The newly synthesized GAMYB protein then binds to the GARC of α -amylase gene promoter and activates its expression. GAMYB was found to be sufficient for α -amylase gene induction in the absence of GA, thus it was concluded that GAMYB is the sole GA-regulated transcription factor required for activation of α -amylase gene promoter. GAMYB binds specifically to GARE, which is present in promoters of all hydrolase genes (Gubler *et al.*, 1995). The TAACAAA motif plays a central role in GA activation of gene transcription (Gubler & Jacobsen, 1992) and mutations in this region result in a loss of GA responsiveness.

Two MYB transcription factors regulate gene expression in response to GA signalling or nutrient starvation in barley and rice. These transcription factors are GAMYB and MYBS₁ respectively (Hong *et al.*, 2012). GAMYB is induced by GA and it binds to the promoters of genes encoding α -amylase and other hydrolases, activating their expression (Gubler *et al.*, 1995; Tsuji *et al.*, 2006). MYBS₁ binds to the same promoters under sugar starvation (Lu *et al.*, 2007). These two signalling pathways have been regarded as independent, but it was found that GA response interferes with the sugar response in rice endosperm, indicating possible crosstalk between these pathways (Chen *et al.*, 2006). MYBS₁ forms homodimers and activates α -amylase gene promoters in response to GA and sugar starvation (Lu *et al.*, 2002). Later it was found that in response to the nutrient deprivation and GA signalling GAMYB and MYBS₁ interact, which results in their co-nuclear import and activation of target gene

promoters. Even deprivation of individual nutrients, like nitrogen, phosphate or carbon resulted in α -amylase gene expression (Hong *et al.*, 2012).

1.4 The hormonal regulation of the aleurone is a cause of pre-harvest sprouting (PHS) and pre-maturity α -amylase (PMA)

Seed dormancy is the inability of ripe and healthy seeds to germinate under the optimal water, light and temperature conditions (Bewley, 1997). It is an adaptive trait that plants acquired to ensure that germination occurs in the season appropriate for the successful seedling growth. Primary dormancy is initiated during seed maturation and is maintained to seed maturity; its maintenance is regulated by genetic and environmental factors (Bewley, 1997; Gubler *et al.*, 2005). Secondary dormancy can be initiated in non-dormant seeds by unfavourable environmental conditions and the loss of dormancy may occur naturally over time of dry storage in a process known as after-ripening or can be terminated by various environmental triggers. The induction, maintenance and release of dormancy is regulated mainly by two plant hormones, abscisic acid (ABA) and GA.

1.4.1 PHS is controlled by grain sensitivity to ABA and GA

Dormancy is the major genetic mechanism that provides resistance to PHS, a phenomenon that causes significant financial losses in the wheat market. PHS occurs when grain germinates before harvest, while still attached to the ear of the parent plant. The precocious germination is evoked by environmental conditions shortly before the harvest. High humidity, prolonged rainfalls and low temperatures favour the occurrence of PHS (Groos *et al.*, 2002; Yücel *et al.*, 2011). Germination of the grain is initiated by the transfer of rainwater from the vegetative structures of the wheat ear to the grain. Once grains

achieve the level of moisture required for germination to commence, the embryo synthesizes hormones that act on the aleurone layer and initiate a series of responses that in turn result in synthesis of multiple hydrolytic enzymes, including α -amylases. These enzymes work to break down starch and proteins stored in the grain, and this is a natural sequence of events that facilitate seedling growth during germination, however, when it takes place before harvest, this has a negative effect on grain yield and quality (Edwards *et al.*, 1989). Only a relatively small increase in total α -amylase activity is enough to substantially reduce the grain quality causing the end-products made from such grain of substandard quality. The grain is deemed unacceptable for human food production if it contains more than 4% sprouted grain. If the sprouted grain constitutes more than 4%, the whole yield is downgraded to use for livestock feed, for which prices can be 20 to 50% lower than those for grain for human consumption. This can in turn result in huge economic losses for the farmers from the regions prone to occurrence of PHS (Moot & Every, 1990; Wahl & O'Rourke, 1994). The extent of damage caused by PHS is measured using the Hagberg Falling Number (HFN) assay, a simple method of indirectly determining α -amylase activity using wheat meal as a substrate (Hagberg, 1960, 1961; Perten, 1964). Usually, to be classified as high-quality grain, the HFN must be above 250-350.

PHS resistance is a complex trait, influenced by developmental, physiological, and morphological features of wheat spike and seed. Seed coat colour and permeability, seed dormancy, α -amylase activity and hormones levels, all contribute to PHS resistance (Wahl and O'Rourke, 1994; Groos *et al.*, 2002; Liu *et al.*, 2013, 2015; Mares and Mrva, 2014; Tuttle *et al.*, 2015; Lin *et al.*, 2016; Shao *et al.*, 2018). Among them, seed dormancy seems to be the major genetic factor influencing plants' susceptibility to PHS. Grain dormancy and associated PHS resistance in wheat have been linked to the higher accumulation and sensitivity to the dormancy-promoting hormone ABA, and lower accumulation and sensitivity to the germination-promoting hormone GA (reviewed in Rodríguez *et al.*, 2015; Tuttle *et al.*, 2015). ABA accumulates during embryo

maturation, establishing seed dormancy and desiccation tolerance, and its levels decrease with dormancy loss. Conversely, the levels of bioactive GA are low in the dormant and after-ripened seed and only increase with the progress of germination, after the levels of ABA have decreased (Jacobsen *et al.*, 2002). Interestingly, comparative genomics studies of barley, rice and wheat revealed a QTL controlling both PHS and dormancy, and one of the GA biosynthesis gene, *GA20ox*, was identified as a candidate gene controlling the QTL (Li *et al.*, 2004). This notion was supported by the discovery that overexpression of *GA2ox*, the GA catabolic gene, renders wheat more dormant and PHS tolerant (Appleford *et al.*, 2007). In wheat, PHS resistance is controlled by multiple QTLs located on almost all 21 chromosomes (Ali *et al.*, 2019), with the major one being identified to reside on chromosome 4B (Wang *et al.*, 2019). A few candidate genes for PHS resistance were also characterised in wheat, including *TaSdr-1* on chromosome 2, *TaPHS1* and *TaMFT* on chromosome 3A, *TaVp-1* and *Tamyb10* on group 3 chromosomes, and *PM19-A1/A2* and *TaMKK3-A* on 4A chromosome (Ali *et al.*, 2019).

Nevertheless, it was suggested that reduction in ABA signalling is more crucial for the dormancy loss than increased GA signalling, as after-ripened seeds showed lower levels of ABA and ABA-responsive genes, but no change in GA-regulated gene expression (Barrero *et al.*, 2009). It was also suggested that hormone levels and signalling in specialised tissues of cereal grains have various roles in dormancy release. In barley, ABA levels in the coleorhiza was the key factor controlling dormancy and germination (Barrero *et al.*, 2009), whereas in *Arabidopsis* and *Lepidium* it was the aleurone that acted as a barrier to germination (Müller *et al.*, 2006). A recent study in wheat identified an ABA signalling gene, *TaMKK3-A*, as a loci responsible for increased dormancy and resulting reduced PHS susceptibility of *ENHANCED RESPONSE TO ABA8* (*ERA8*) lines (Martinez *et al.*, 2020).

Another aspect affecting the extent of PHS is the activity of α -amylase. The expression of the gene encoding α -amylase is strictly regulated by ABA and GA; it is inhibited by ABA during grain development and activated by GA during

germination (reviewed in Liu and Hou, 2018). The endogenous, high pI α -amylase, which is responsible for starch degradation in response to PHS, is *de novo* synthesized during germination in the scutellum and aleurone. The field study of three wheat landraces with different susceptibility to PHS reported that in the less resistant varieties, there was a 20- to 40-fold increase in α -amylase activity, whereas the α -amylase activity in the PHS resistant landrace was only 10 times higher (Olaerts *et al.*, 2016). Also, the main site of α -amylase activity was found to be located in the scutellum, whereas the aleurone cells played only a minor role during sprouting in the field (Olaerts *et al.*, 2017).

1.4.2 PMA results from increased levels of GAs in the aleurone

High pI α -amylase in the intact wheat grain is not normally synthesized until after maturity, and in the mature grain is only synthesized if germination has been initiated. In early stages of germination, high pI α -amylase is briefly produced in the scutellum and its production is independent of *de novo* GA biosynthesis (Lenton *et al.*, 1994). Concomitantly, the GA synthesised in the embryo acts on aleurone cells and activates high pI α -amylase synthesis in the aleurone layer. The enzyme then diffuses from proximal (embryo side) to distal (brush side) end of the grain forming a gradient of the enzyme activity. During grain development, another isoform of the enzyme is produced, the low pI α -amylase. Low pI α -amylase is synthesised in the pericarp shortly after anthesis and its levels peak between 10 and 20 days after anthesis (DAA), but this activity declines with ripening, leaving negligible amounts in the ripe grain (Mares & Gale, 1990). However, under certain environmental conditions, for example cold shock, some wheat genotypes may experience excessive synthesis of high pI α -amylase in the later stages of grain ripening, prior to germination, a phenomenon called pre-maturity α -amylase (PMA). Synthesis of the high pI α -amylase in the aleurone of PMA-susceptible grain occurs around 20 to 30 DAA and the enzyme is retained through harvest, causing a reduction in starch content. PMA transcription of the *Amy-1* genes, which

encode the high pI α -amylase, takes place in isolated cells or cell islands scattered around the aleurone layer, in contrast to during germination when α -amylase is expressed throughout the aleurone (Mrva *et al.*, 2006). Similarly, during germination, α -amylase accumulates exponentially, whereas in PMA the synthesis reaches a plateau at a relatively low level of activity. Tissue-specific α -amylase activity studies revealed that *AMY1* is predominantly synthesised in the aleurone cells, supporting the view that the aleurone is the main site of PMA induction (Mamytova *et al.*, 2014). Furthermore, no concomitant synthesis of low pI α -amylase, proteases or other hydrolytic enzymes takes place in the PMA-affected aleurone (Barrero *et al.*, 2013; Mares & Mrva, 2014) suggesting that PMA is caused solely by high pI α -amylase. Barrero and colleagues (2013) investigated the levels of several hormones, including ABA and GA, as well as transcriptional changes in the PMA-constitutive lines and those that do not express PMA. Very little difference in gene expression was found between the lines, and out of several GA- and ABA-responsive genes tested, only the *AMY1* genes were upregulated in PMA-constitutive lines. Interestingly, quite dramatic changes in hormone levels were seen; the ratio of GA to ABA was 10 times higher in lines expressing PMA. GA treatment was also identified to lower the expression of several selected PMA-activated genes. It was therefore concluded that PMA is a consequence of a transient peak of high pI α -amylase expression during grain development and that the PMA phenotype is an incomplete GA response (Barrero *et al.*, 2013).

PMA can be induced by many different environmental conditions if applied during the window of sensitivity (26 – 30 DAA) (summarised in Kondhare *et al.*, 2015), with cold shock being the most effective and consistent method. Premature drying of developing barley grains, 30 to 40 DAA, has been shown to enhance the sensitivity of aleurone cells to GA, resulting in higher levels of α -amylase (Jiang *et al.*, 1996). Wheat seems to display a similar response to that of barley (Armstrong *et al.*, 1982). Mrva and Mares (1996) found that approximately at 30 to 40 DAA, wheat aleurone tissue acquires GA sensitivity,

which coincides with the onset of PMA synthesis. Furthermore, when the grain is treated with an inhibitor of GA synthesis, no PMA induction is observed, even when a simultaneous cold treatment is applied (Kondhare *et al.*, 2014).

The occurrence of PMA in some wheat genotypes is constitutive and in others sporadic and unpredictable (Flintham *et al.*, 2011; Mares & Mrva, 2008), but an interesting observation was made linking *Reduced height-1 (Rht-1)* genes and PMA resistance. The wheat *Rht-1* homoeologous genes encode DELLA proteins, which are master negative regulators of GA signalling. Alleles conferring semi-dwarfism in wheat, *Rht-B1b (Rht1)* and *Rht-D1b (Rht2)*, when combined, almost completely inhibited PMA expression, and the strong dwarfing allele *Rht-B1c (Rht3)* alone was enough to block PMA expression (Mrva & Mares, 1996). What these alleles have in common is reduced sensitivity of the aleurone to GA; *Rht1* and *Rht2* are mildly insensitive to GA while *Rht3* is insensitive. In contrast, the GA-sensitive *Rht8* allele shows constitutive PMA expression (Mares & Mrva, 2008). These observations led to a conclusion that GA-sensitivity of the aleurone tissue may have a role in PMA formation. Moreover, PMA-susceptible genotypes showed higher GA sensitivity at mid-grain development than more resistant varieties confirming that GA-sensitivity has a role in regulating the susceptibility to PMA (Kondhare *et al.*, 2012, 2013). Recent work by Derkx *et al.* (2021) identified a locus on the long arm of the chromosome 7B that is responsible for variation in PMA, the *LATE MATURITY α -AMYLASE 1 (LMA-1)*. *LMA-1* encodes an *ent*-copalyl diphosphate synthase (CPS) and single mutations in its coding sequence that affect the protein viability results in resistance to PMA. Varieties resistant to PMA showed low levels of *LMA-1* transcripts, which was associated with a dramatic reduction in the levels of bioactive GA precursors, confirming CPS role in the GA biosynthesis pathway, and reinforcing the fact that low levels of GA in developing grain confer resistance to PMA (Derkx *et al.*, 2021).

Although PMA activity definitely affects the starch content of the grain and has been considered as a trait rendering the grain as unacceptable due to lower HFN, a recent study has shown that PMA, unlike PHS, does not negatively

affect bread baking properties of wheat (Newberry *et al.*, 2018). No negative, or positive correlation was identified between lower HFN in the PMA susceptible landraces and several standard quality traits of bread loaf. This is the first study on the subject that provides evidence that PMA is not as detrimental for the quality of the end-product as PHS. However, more research on the effects of PMA on the quality of end-products, together with affordable and easy means of testing to distinguish between PHS and PMA in place would be needed to reduce potential financial losses caused by the misconception that low HFN always means low quality grain.

To summarise, PHS and PMA are distinct phenomena that affect wheat grain quality and bring big financial losses annually to the wheat growers around the world. Undoubtedly, the hormonal regulation of the aleurone layer is the direct cause of the high pI α -amylase expression and starch degradation, which is an underlying problem for both PHS and PMA. However, the developmental stages at which the processes are established and the stimuli leading to PHS and PMA are different. Although considerable efforts have been made in order to understand these phenomena, the molecular mechanisms leading to PHS and PMA remain unknown.

1.5 The role of ethylene in regulation of germination

It has been known that regulation of seed germination and dormancy is achieved by the balance in ABA and GA levels. However, other hormones are also involved in regulation of these processes. Auxins, jasmonates, brassinosteroids and in particular ethylene play a role (Linkies & Leubner-Metzger, 2012; Miransari & Smith, 2014). The synthesis of ethylene in the seed begins immediately after the onset of imbibition, increases with time of germination, and reaches a peak at the time of radicle emergence (Fu & Yang, 1983). However, ethylene production by the seed is species dependent (Kepczynski and Kepczynska, 1997). In wheat, ethylene production increases 20 hours after initiation of imbibition and peaks after 35-40 hours,

corresponding to early elongation of the radicle. There is also another peak in ethylene production around hour 57, the time when the coleoptile elongates and starts upward growth (Petruzzelli *et al.*, 1994).

1.5.1 The effect of exogenous ethylene application on germination

Exogenous application of ethylene or ethephon, an ethylene releasing substance, improves germination in many species. It stimulates germination of non-dormant seeds under non-optimal environmental conditions such as high temperature (Gallardo *et al.*, 1991), salinity (Lin *et al.*, 2013), osmotic stress (Kepczynski, 1986b) and hypoxia (Esashi *et al.*, 1989), and can also break primary and secondary dormancy (Calvo *et al.*, 2004; Corbineau *et al.*, 1988). Moreover, it promotes the germination of seeds exhibiting a seed coat-imposed dormancy in various species, including *Arabidopsis* (Siriwitayawan *et al.*, 2003). In *Arabidopsis* and *Lepidium sativum* ethylene promotes endosperm cap weakening and endosperm rupture, counteracting the inhibitory effect that ABA has on these processes (Linkies *et al.*, 2009). The inhibition of seed germination imposed by gibberellin biosynthesis inhibitors, tetcyclacis and paclobutrazol, in tassel flower (*Amaranthus caudatus*) can be reversed not only by GA, but also by ethephon (Kepczynski, 1986; Kepczynski *et al.*, 1988). In *Arabidopsis*, GA-deficient mutant, *ga-1*, can complete germination in light when ethylene is applied (Karssen *et al.*, 1989). Ethylene was found to significantly increase the accumulation and activity of xylanase in the aleurone of barley in response to GA, and also to positively affect α -amylase synthesis (Eastwell & Spencer, 1982). In wheat, ethylene treatment combined with GA application causes 60% increase in the protease synthesis (Varty *et al.*, 1983), and the same protease *de novo* synthesis had been previously reported to parallel that of α -amylase. Moreover, ethylene has been reported to stimulate GA-induced α -amylase production in wheat aleurone cells (Varty *et al.*, 1983), and it was discovered that it acts synergistically with GA to reverse ABA inhibition of α -amylase synthesis in barley aleurone tissue (Jacobsen, 1973).

1.5.2 Ethylene signalling results in activation of genes that increase the rate of germination

Transcriptome studies of *Andrographis paniculata*, tracing changes in gene expression during germination, revealed upregulation of four genes related to ethylene signal transduction: *EIN2*, *EIN3*, *ETR1* and *ERF118*. The genes were activated during the first 48 hours after sowing, suggesting that ethylene plays a critical role in seed germination. The expression of *EIN2*, *EIN3* and *ERF118* peaked and then slightly decreased over the 48 hours period, which led to the conclusion that rapid ethylene signal transduction may be required for the initiation of seed germination (Tong *et al.*, 2019). The molecular mechanism by which ethylene activates the expression of genes, at least in some cases, has been elucidated by epigenetic studies. The studies of epigenetic changes during ethylene induced germination in soybean (*Glycine max* (L.)) revealed the role of ethylene as a DNA demethylating factor (Manoharlal *et al.*, 2019) and acetylating factor (Manoharlal and Saiprasad, 2020). Ethylene significantly enhance the cellular acetyl-CoA levels, histone acetyltransferase activity and subsequent histone H3 (H3ac) and H3 lysine 9 (H3K9ac) acetylation levels, which results in increased global *de novo* RNA synthesis and enhanced germination rates. Moreover, ethephon-primed soybean sprouts showed reduced starch content concomitant with a mRNA accumulation and enhanced transcriptional rate and proximal H3K9ac levels of α -amylase 1 (*GmaAMY1*) (Manoharlal and Saiprasad, 2020a; Manoharlal and Saiprasad, 2020b). In wheat, the treatment of seeds with aminoethoxyvinylglycine (AVG, a potent inhibitor of ethylene synthesis) significantly reduced the transcript levels of starch-degrading enzymes like α -amylases, especially *AMY1* and *AMY2*, and alpha-glucosidases *AGL1* and *AGL2*. This resulted in significantly reduced α -amylase and α -glucosidase activity and lower levels of glucose, fructose and maltose (Sun, 2018). It was concluded that specific starch-degrading genes play roles in mediating the effect of ethylene on starch degradation. Similar observations were recorded for barley. Ethylene treatment had a comparable effect on the starch levels decrease and concomitant reducing sugars increase

as GA treatment. Moreover, as GA inhibitor daminozide (B-nine) reduced α -amylase activity, the addition of ethylene with the B-nine treatment increased the enzyme activity, however, ethylene on its own had no effect. This suggests that ethylene stimulates amylase activity when GA synthesis is inhibited (Zanamwe, 2019).

1.5.3 Transcriptome analysis of dormant and after-ripened imbibed wheat seed reveals upregulation of genes involved in ethylene metabolism

Transcriptomics studies in wheat investigating the expression of 78 genes annotated as ethylene metabolism- and signalling-related showed that between dormant and after-ripened seeds there is 2-fold upregulation of *ACO* gene, aminocyclopropane-1-carboxylic acid oxidase, which catalyses the conversion of ACC (1-aminocyclopropane-1-carboxylic acid) to ethylene. *ETHYLENE RESPONSE SENSOR1 (ERS1)*, was also upregulated in imbibed after-ripened seeds, suggesting that transcriptional activation of ethylene signalling is one of the mechanisms to break dormancy by after-ripening (Chitnis *et al.*, 2014). A set of probes representing ethylene-regulated genes encoding endosperm weakening β -glucanase and chitinase enzymes were also found to be upregulated in after-ripened imbibed seeds. The ethylene pathway interacts with ABA and GA signalling pathways, hormones known to be essential in regulating germination and dormancy. Ethylene inhibits both ABA synthesis and signalling, and ABA inhibits biosynthesis of ethylene. Additionally, ethylene affects GAs biosynthesis and signalling and *vice versa* (Corbineau *et al.*, 2014). *ctr1*, a mutant lacking Raf-like kinase CTR1, a negative regulator of ethylene signalling, accumulates higher levels of *GA3ox1* and *GA20ox1* gene transcripts and DELLA protein, and is more resistant to destabilising effect of GA in presence of ethylene (Achard *et al.*, 2003; Achard *et al.*, 2007). Taken together, there is strong evidence for the involvement of ethylene in dormancy release and regulation of germination.

1.5.4 Ethylene signalling pathway components, including ERF transcription factors, are involved in regulation of germination

Understanding of the roles of various ethylene signalling pathway intermediates comes from studying Arabidopsis knockout lines. Many genes in the pathway have been characterised. For example, ethylene insensitive *etr1-1* (*ethylene receptor1*) and *ein2* (*ethylene insensitive2*) mutants show enhanced primary dormancy when compared to the wild type, whereas *ctr1* (*constitutive triple responses*) mutants have slightly enhanced rate of germination (Beaudoin *et al.*, 2000). EIN2 was found to play a key role in ethylene signalling, and loss of its function leads to hypersensitivity to salt and osmotic stress during germination and early seedling development. *ein2* accumulates ABA and displays reduced rate of germination during salt and osmotic stress (Wang *et al.*, 2007). ETR1 in turn, functions to reduce the inhibition of germination imposed by far-red light. It was suggested by Wilson and colleagues that *ETR1* genetically interacts with *PHYA* and *PHYB* to control germination (Wilson *et al.*, 2014). There is also evidence that ERFs may play a central role in response to ethylene and regulation of germination. *ERF1* expression in beechnut (*Fagus sylvatica*) and sunflower (*Helianthus annuus* L.) is increased in seeds that received a dormancy-breaking stimulus (Jimenez *et al.*, 2005; Oracz *et al.*, 2008). Furthermore, in sunflower, the levels of *ERF1* transcripts are fivefold higher in non-dormant seed. Germinating tomato (*Solanum lycopersicon*) seeds accumulate *ERF2* transcript levels, and its overexpression causes early germination (Pirrello *et al.*, 2006). The same was found in Arabidopsis; *ERF1*, *ERF2* and *ERF5* expression in Arabidopsis was significantly upregulated in stratified seeds (Narsai *et al.*, 2011). It was speculated in that publication that ethylene promotes endosperm cap weakening and endosperm rupture in Arabidopsis and cress (*Lepidium sativum*) and could contribute to the greater germination rates after stratification. Moreover, members of group VII of ERFs, RAP2.12, RAP2.2 and RAP2.3, were found to regulate the key germination repressor, ABI5.

Chromatin immunoprecipitation (ChIP) analysis showed that RAP2.3 binds specifically to the promoter of *ABI5* (Gibbs *et al.*, 2014). Interestingly, group VII of ERFs were also identified as DELLA partners in a yeast two-hybrid screen, but the significance of these interactions was linked with apical hook development (Marín-de la Rosa *et al.*, 2014).

1.6 DELLA proteins, the master repressors of GA signalling

Gibberellins act through the degradation of a group of transcriptional regulators, the DELLA proteins. DELLA proteins take part in two aspects of the GA signalling network, they help establish homeostasis by regulating the expression of GA-biosynthetic and signalling genes and they promote the expression of downstream putative negative components in GA signalling network (Zentella *et al.*, 2007).

DELLA proteins belong to the GRAS family of putative transcriptional regulators, named after the original members, identified in Arabidopsis: GIBBERELLIN-INSENSITIVE (GAI), REPRESSOR of *ga1-3* (RGA), and SCARECROW (SCR). The Arabidopsis genome contains 33 GRAS genes including five encoding DELLAs: *REPRESSOR OF ga1-3 (RGA)*, *GA-INSENSITIVE (GAI)*, *RGA-LIKE1 (RGL1)*, *RGL2*, and *RGL3* (Pysh *et al.*, 1999; Cenci and Rouard, 2017). Duplication events have contributed to the expansion of the GRAS genes in cereals with 57 members in rice, 84 in maize and 48 in Brachypodium (Guo *et al.*, 2017; Niu *et al.*, 2019; Tian *et al.*, 2004). However, cereals contain only a single *DELLA* gene (*SLR1* in rice, *SLN1* in barley and *RHT-1* in wheat), with maize being an exception and encoding two DELLA proteins, Dwarf plant8 (d8) and d9.

1.6.1 The DELLA domain is required for GA-GID1-mediated degradation

DELLA proteins were first identified to bind GID1 receptor in the yeast two hybrid (Y2H) study reported by Ueguchi-Tanaka *et al.* (2005). Not much later it was elucidated that it is the regulatory DELLA domain at the N terminus of DELLA proteins that is necessary for interacting with GID1. Three motifs that constitute the regulatory DELLA domain, the DELLA, LExLE and TVHYNP motifs (Figure 1.5 A, C), are highly conserved, and both DELLA and TVHYNP motifs were found to be necessary for the interaction with GID1 (Griffiths *et al.*, 2006). Their function is to bind to GID1-GA complex which results in enhanced DELLA-SLY1 interaction and initiate the SCF^{SLY1}-mediated proteolysis of DELLAs. X-ray crystallography allowed for resolving the crystal structure of GA-GID1-DELLA complex in *Arabidopsis* that contains bioactive GA₃ or GA₄, AtGID1A and the GAI protein (Murase *et al.*, 2008).

The DELLA domain of GAI forms four α -helices, α A, α B, α C and α D, and resembles a palm consisting of helices α B to α D, with helix α A sticking out like a thumb. The amino acid DELLA sequence is located within the α A helix, LExLE within the α B helix and the VHYNP motif within loop C-D. All three conserved motifs were found to be essential for direct contact with the GA receptor, GID1A. The DELLA palm interacts with the GID1A N-terminal extension helices, whereas the thumb interacts both with N-terminal extension helices and the core domain of GID1A. In fact, DELLA binding was found to enhance the binding of GA to GID1A. Conversely, the deletions of DELLA motif or the mutations in the key residues of the LExLE motif markedly reduced binding to the GA-GID1A complex and showed to confer a GA-insensitive phenotype (Murase *et al.*, 2008). Interestingly, the DELLA/TVHYNP domain also possesses transactivation activity, although the functional significance of this is still uncertain (Hirano *et al.*, 2012).

1.6.2 Structure and function of the GRAS domain in DELLAs

GRAS proteins contain a highly conserved functional GRAS domain at the C-terminus, that is responsible for binding to interacting proteins. The crystal structure of the GRAS domain of rice SCARECROW-LIKE7 (Os-SCL7) transcription factor was elucidated by Li and colleagues (2016). Their biochemical and structural studies revealed that the GRAS domain contains five conserved motifs: two leucine heptad repeats, LHR1 and LHR2 flanking the VHIID motif, PFYRE and SAW (Li *et al.*, 2016). The structure of the GRAS domain revealed the presence of a core subdomain and an additional cap subdomain. The cap subdomain is composed of a helical bundle formed by N-terminal α -helices A1, A2 and A3 of the LHR1 motif, and a helical bundle insert A9 and A10 from the PFYRE motif (Figure 1.5 B). The much larger core subunit forms a α - β - α three-layer sandwiched Rossmann fold-like structure made of central β -sheet flanked by two helical layers. Os-SCL7 forms a homodimer that is primarily formed by interaction of A12 with A7 and A6 through helix-helix hydrophobic interaction. Above the dimer interface is a large groove that is a site of binding of the minor groove of the DNA (Li *et al.*, 2016).

Work of Hirano *et al.* (2010) showed that the VHIID, PFYRE and SAW motifs have a role in stabilisation of the DELLA-GID1-GA complex in rice and mutations in these motifs lead to a decreased rate of SLR1 degradation in response to GA. The VHIID and LHR2 motifs were found to have a major role in binding to GID2, and the LHR1 motif appears to be responsible for the protein homodimerization (Bai *et al.*, 2012). Mutations that reduce the ability of DELLAs to repress downstream GA responses were found to cluster in LHR1, VHIID and PFYRE motifs (reviewed in Chandler and Harding, 2013; Thomas, Blázquez and Alabadí, 2016).

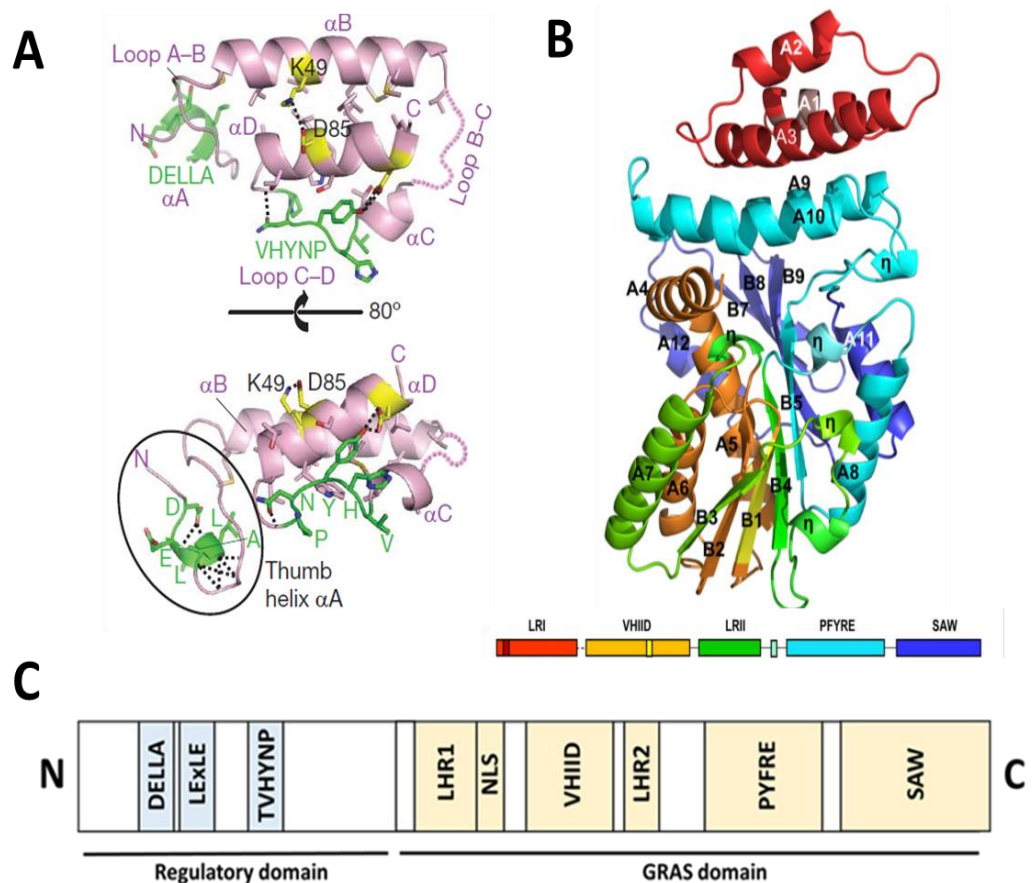


Figure 1. 5 Conserved domains in DELLA proteins. **A.** The crystal structure of GAI DELLA regulatory domain. DELLA domain of GAI consists of four α -helices: α A, α B, α C and α D. Motifs important for GID1 binding, DELLA and VHYNP, are highlighted in green. Black dotted lines represent intra-domain hydrogen bonds. The thumb-like part containing helix α A (circled) hooks onto the nonpolar crevice of GID1A. Adapted from Murase et al., (2008). **B.** The crystal structure of the GRAS domain. GRAS domain contains five distinct conserved motifs: LRI (red), VHIID (orange), LRII (green), PFYRE (cyan), and SAW (blue); α -helices and β -strands are labelled with A and B, respectively, and 3_{10} helices are labelled with η . Adapted from Li et al., (2016). **C.** Diagram showing domains of the DELLA proteins. Regulatory domain of the protein is positioned in the N terminal part of the protein and contains DELLA, LEXLE and TVHYNP motifs. The functional GRAS domain that allows DELLAs to bind their interacting proteins contains five motifs: LHR1 and 2, VHIID, PFYRE and SAW. NLS is a nuclear localization signal.

Of great interest is the work of Chandler and Harding (2013) who identified novel mutations in barley and wheat *DELLA* gene that caused 'overgrowth' phenotypes in gain-of-function *DELLA* mutant lines. The new alleles identified as single-nucleotide substitutions (SNPs) resulting in a single amino acid change were identified in the C-terminal part of *DELLA*, corresponding to the GRAS domain. The lines carrying the overgrowth alleles were found to have enhanced rate of leaf elongation and they produced larger grains. It was therefore concluded that the degree of GA signalling in the overgrowth mutants compared to the dwarf lines was enhanced (Chandler & Harding, 2013). In wheat, 19 new derivative alleles of *Rht-B1c* were identified. Four of these carried premature stop codon, and in barley they resulted in elongated slender phenotype and male sterility, clearly indicating loss of *DELLA* function. The other 15 alleles were identified as encoding amino acid substitutions and were associated with varying degrees of growth recovery. From comparison studies between barley and wheat overgrowth mutants, Chandler and Harding concluded that there is a limited set of amino acid substitutions that lead to an overgrowth phenotype, and that these mutations occur in the conserved motifs of GRAS domain: LHR1, VHIID and PFYRE. Therefore, it is likely that the mutated *DELLA* proteins have reduced affinity for interacting proteins and result in greater GA responses (Chandler & Harding, 2013).

1.6.3 Green Revolution alleles encode mutated *DELLA* proteins

The 'Green Revolution' was responsible for a great increase in crop grain yields, especially wheat and rice, during the 1960s and 1970s. This increase was possible partly due to improved farming techniques, including application of large amounts of pesticides and fertilizers, but mainly due to the introduction of high-yielding dwarf varieties that would not lodge even after application of increased amounts of nitrogen (Hedden, 2003; Peng *et al.*, 1999; Reynolds & Borlaug, 2006). In the 1940s and 1950s, the 'shuttle breeding' programme led by Norman Borlaug in Mexico to develop superior wheat cultivars resulted in identifying widely adapted, high-yielding, disease-resistant wheat varieties.

However, the height of these varieties limited yield due to lodging, as their long and thin stems were not strong enough to support the increased weight of grains and would eventually collapse causing grain losses (Reynolds & Borlaug, 2006). Around the same time, a dwarf wheat cultivar, Norin-10 Brevor, started to be extensively used in these breeding programmes, leading to identification of high-yielding, semi-dwarf wheat varieties. These semidwarfs had short, strong stems that did not lodge. Additionally, the increased partitioning of assimilates to grain resulted in further grain increases. The newly-developed, high-yielding, short varieties, thanks to Borlaug's initiative, were quickly distributed across Latin America and Southeast Asia, where they brought about immense yield increases, providing food security. For his efforts, Norman Borlaug was awarded the Nobel Peace Prize in 1970. Today, the Norin 10 dwarfing genes are estimated to be present in more than 70% of commercial wheat cultivars around the world (Evans, 1998).

The genes underlying the reduced stature and increased grain yield in 'Green Revolution' varieties have been identified, and in wheat these are *Rht-B1b* (formerly *Rht1*) and *Rht-D1b* (*Rht2*). These are the semi-dominant (gain-of-function) homoeologues of *Rht-1* gene, which encodes the wheat DELLA protein. The primary effect of these alleles is to reduce sensitivity to GAs (Gale & Youssefian, 1985), resulting in reduced stem elongation and increased grain yield. The molecular basis of the mutations present in the *Rht-B1b* and *Rht-D1b* dwarfing genes were elucidated in the study of Peng *et al.* (1999). In both alleles, they were found to be nucleotide substitutions that result in stop codons, T to C substitution that causes Q64* mutation and T to G substitution that leads to E61* mutation in *Rht-B1b* and *Rht-D1b*, respectively. Previous genetic analysis showed that both alleles produce active repressors of GA signalling (Gale & Marshall, 1976), hence it was hypothesized by Peng and colleagues that translation reinitiation following the stop codon may result in generation of N-terminally truncated DELLA protein, that lacks the DELLA motif, but contains a fully functional GRAS domain and hence can exert its

function. A recent study by Van De Velde *et al.* (2021) proved that this hypothesis was correct. This study revealed that the translation reinitiation of Δ N-RHT-B1 occurs only three amino acids downstream of the stop codon of *Rht-B1b*, at M67. Both Δ N-RHT-B1 and Δ N-RHT-D1 proteins were shown to be resistant to GA-activated degradation, and they were shown to be causative factors of the dwarfism of the *Rht-B1b* and *Rht-D1b* lines. On the other hand, the N-terminal 63 amino acid long peptide resulting from translation of full ORF of *Rht-B1b*, did not affect plant size (Van De Velde *et al.*, 2021). Sequence analysis shows that the truncated RHT-B1 and RHT-D1 proteins lack DELLA and LExLE motifs, and therefore cannot bind to the GA-GID1 complex, which results in RHT-1 protein accumulation and enhanced repression of GA responses. *Rht-B1b* and *Rht-D1b* semi-dwarfing varieties are known to reduce the stem length and increase grain yield without affecting the GA response in the aleurone (Gale & Marshall, 1973). Interestingly, no truncated RHT-1 proteins were identified in the aleurone (Van De Velde *et al.*, 2021), suggesting tissue specificity of translational reinitiation.

1.6.4 DELLAs interact with multiple transcription factors to regulate their activity

DELLAs are known to act as transcriptional regulators, however no DNA-binding domain has been identified in their structure (Hirano *et al.*, 2012; Zentella *et al.*, 2007). The regulation of transcription by DELLAs is through interactions with diverse classes of regulatory proteins, mainly *bona fide* transcription factors. DELLAs interact with TFs through their GRAS domain, and bound to them can associate with target genes promoters (Fukazawa *et al.*, 2014; Marín-De La Rosa *et al.*, 2015; Park *et al.*, 2013). A few different mechanisms were described thus far (Thomas, Blázquez and Alabadí, 2016; Van De Velde *et al.*, 2017). DELLAs may exert their transcriptional activity by inhibiting the DNA-binding ability of TFs, transcriptional regulators or repressors, or by acting as a co-regulator of TFs (Figure 1.6).

1.6.4.1 DELLAs negatively regulates gene expression by sequestering *bona fide* TFs

The first studies describing the molecular mechanism of DELLA transcriptional control were the studies performed by Feng *et al.* (2008) and de Lucas *et al.* (2008). They elucidated the mechanism of DELLA-mediated regulation of PHYTOCHROME INTERACTING FACTOR 3 (PIF3) and PIF4, bHLH TFs involved in integration of light and GA signal during light-mediated hypocotyl elongation (de Lucas *et al.*, 2008; Feng *et al.*, 2008). During seedling development, light and GA signalling interact to regulate hypocotyl elongation, cotyledon opening and light-induced gene expression. Inhibition of hypocotyl elongation during photomorphogenesis was found to be repressed by GA in the dark and promoted by DELLAs in the light (Alabadí *et al.*, 2004; Achard *et al.*, 2007). Interestingly, Arabidopsis plants that overexpressed mutated DELLA proteins resistant to GA-mediated degradation, displayed short hypocotyl phenotype, whereas in the *della* quintuple mutant, the hypocotyl was of comparable length to the one of WT treated with GA. This led to a hypothesis that GA controls hypocotyl growth mainly by regulating the levels of DELLA proteins (Feng *et al.*, 2008). Despite their efforts, the authors did not observe specific binding of DELLAs to any of the tested gene promoters, which inspired a hypothesis that DELLAs may repress GA-activated transcription by interacting with TFs. PIF3 was selected as a candidate TF to study the DELLA-mediated regulation of transcription, as it displayed opposite effect on hypocotyl elongation to DELLA, i.e. *pif3-1* has a short hypocotyl, whereas PIF3 overexpression lines show elongated hypocotyl. The physical interaction between RGA and PIF3 was confirmed in multiple *in vitro* and *in vivo* assays, and was shown to occur in the nuclei, confirming the role of the complex in regulating transcription. The interaction was dependent on RGA protein abundance and inhibited the effect of PIF3 on hypocotyl elongation. Further studies revealed that RGA binds to the DNA-binding domain of PIF3, thereby inhibiting PIF3 from binding to its target gene promoters. This was further confirmed by analysis of PIF3 target genes transcript levels, which were

elevated in low-DELLA, high-PIF3, and decreased in high-DELLA, low-PIF3 lines. Overall, it was concluded that DELLAs antagonise PIF3 function by direct interaction and sequestration, and that this is part of light and GA-coordinated hypocotyl growth regulation mechanism (Feng *et al.*, 2008). Interestingly, a separate study conducted by another group was published at the same time in the same journal by de Lucas *et al.* (2008), reporting the same DELLA mechanism in PIF4 regulation. Their findings were highly similar to those of Feng *et al.* (2008). They too found that interaction with RGA is mediated via bHLH DNA-binding domain of PIF4, the interaction with DELLA interferes with binding of PIF4 to its target genes promoters and is abolished by GA treatment. Additionally, they showed that del1RGA, a mutated RGA that does not bind PIF4, does not suppress the transcriptional activity of PIF4, confirming that it is indeed DELLA that suppresses the transcriptional activity of PIF4 (de Lucas *et al.*, 2008).

The seminal studies by Feng *et al.* and de Lucas *et al.*, demonstrated that the interaction of PIF3 and PIF4 with DELLA results in changes in gene expression, and is involved in regulation of GA-activated hypocotyl growth. These results led to the conclusion that DELLAs act to sequester the transcription factors, preventing them from binding to and activating their target genes promoters. The following mechanism was proposed: in the absence of GA, DELLA proteins accumulate and sequester PIFs and therefore abrogate PIF-mediated light control of hypocotyl elongation, however, when the GAs are present, DELLA degradation takes place, which leads to PIFs release, activation of the PIF-controlled genes and hypocotyl elongation (de Lucas *et al.*, 2008; Feng *et al.*, 2008).

In fact, the majority of studies reporting translational DELLA activity, describe the sequestration of the TFs as a mode of action (Table 1.1). Of all DELLA-interacting proteins (DIPs) identified to date, bHLH TFs are by far the most numerous, and it seems that sequestration is a typical mode of DELLA regulation of bHLH proteins. DELLA sequester ALCATRAZ (ALC) to regulate fruit patterning (Arnaud *et al.*, 2010), PIF5 in controlling apical hook development

(Gallego-Bartolomé *et al.*, 2011) or bHLH48 and bHLH60 to regulate flowering time (Li *et al.*, 2017).

1.6.4.2 DELLA activates transcription by binding to transcriptional factors in the context of their promoters

A different mode of action of DELLA transcriptional regulation is through their association with partner TFs in the context of the target genes promoters (Figure 1.6 C). In the study of Marin-de la Rosa *et al.* (2015) and Lantzouni *et al.* (2020), a genome wide binding site analysis performed using the RGA protein combined with *in silico* analysis of the identified binding sequences revealed multiple potential TF families as DELLA partners in regulating gene expression. These included bZIP and IDD TFs, previously identified to interact with DELLAs to activate transcription (Fukazawa *et al.*, 2014; Lim *et al.*, 2013; Yoshida & Ueguchi-Tanaka, 2014). The bZIP TFs ABA INSENSITIVE 3 (ABI3) and ABI5 were identified to physically interact with GAI, and all three proteins were found to bind to the promoter of high temperature-activated *SOMNUS* (*SOM*) gene (Lim *et al.*, 2013). *SOM* is a CCCH-type zinc finger protein that is known to inhibit light-dependent seed germination (Kim *et al.*, 2008). A complex of proteins including ABI3, ABI5 and DELLA regulate *SOM* expression in response to high temperature by binding directly to its promoter and activating its transcription, which results in inhibition of germination (Lim *et al.*, 2013). The same regulation by ABI3, ABI5 and DELLA was shown for three selected genes that were found to be highly expressed in response to high temperature, high levels of ABA and low levels of GAs (Lim *et al.*, 2013).

A few separate studies have demonstrated that DELLAs interact with members of the INDETERMINATE (IDD) family of TFs, and act as co-regulators of their target genes (Feurtado *et al.*, 2011; Fukazawa *et al.*, 2014; Lu *et al.*, 2020; Yoshida & Ueguchi-Tanaka, 2014). GAI-ASSOCIATED FACTOR1 (GAF1) belongs to the IDD family of transcription factors and is involved in regulation of GA homeostasis, as it regulates expression of *AtGA20ox2*, *AtGA3ox1* and *GID1b*

genes. In the study of Fukazawa *et al.* (2014), GAI was found to interact with GAF1 on the *AtGA20ox2* promoter and to be essential for GAF1-regulated transcription. Two other proteins, TOPLESS RELATED 1 (TPR1) and TPR4, were also found to be GAF1 binding partners, but they acted to inhibit GAF1-regulated transcription. GAF1 therefore acted as a transcriptional activator or repressor, depending on the presence of GAs. At low GA, DELLA protein GAI was stabilised and co-regulated GAF1-mediated gene expression, including the transcription of GA biosynthesis and signalling genes. However, when DELLAs

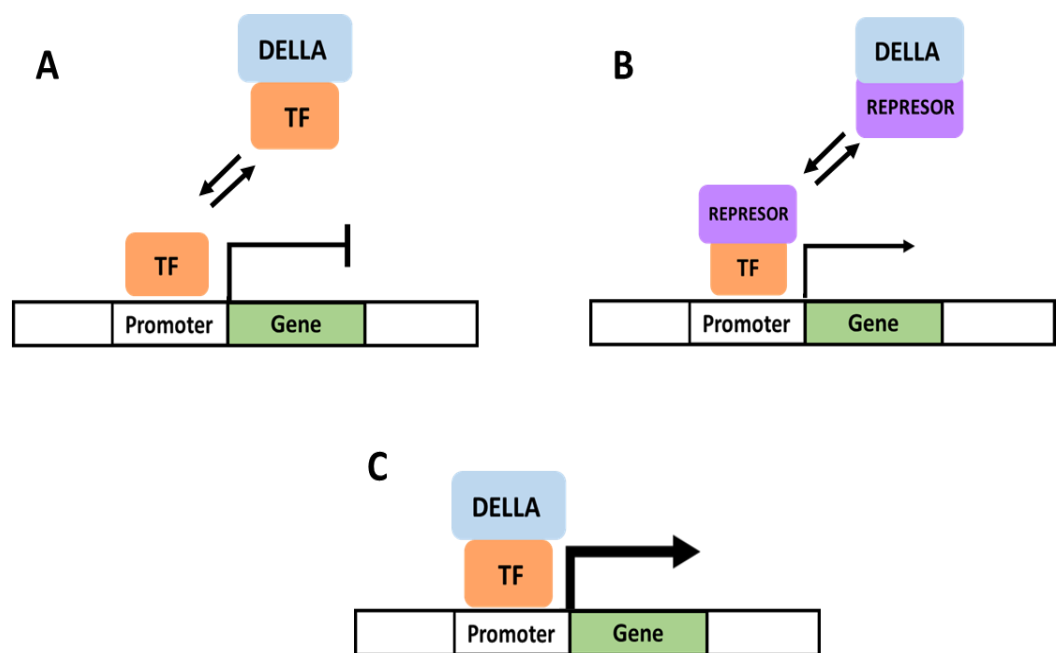


Figure 1. 6 Molecular mechanisms of DELLA action. A TF is sequestered by DELLA protein and the transcriptional activation is prevented. B. DELLA releases the negative regulation of a TF by interacting with the repressor (R), thereby allowing for gene transcription. C. DELLA promotes transcriptional activation of a TF.

Table 1. 1 Summary of DELLAs interacting partners (DIPs) grouped based on the mode of DELLA regulation.

| Mode of action | DIP name | Developmental significance | Reference |
|--|--|------------------------------|---|
| Sequestration of a transcription factor | PIF3 (PHYTOCHROME INTERACTING FACTOR 3) | Hypocotyl elongation | Feng <i>et al.</i> , 2008 |
| | PIF4 (PHYTOCHROME INTERACTING FACTOR 4) | Hypocotyl elongation | de Lucas <i>et al.</i> , 2008 |
| | ALC (ALCATRAZ) | Fruit patterning | Arnaud <i>et al.</i> , 2010 |
| | PIF1 (PHYTOCHROME INTERACTING FACTOR 1, also known as PIL5) | Unknown | Gallego-Bartolome <i>et al.</i> , 2010 |
| | PIF6 (PHYTOCHROME INTERACTING FACTOR 6, also known as PIL2) | | |
| | SPT (SPATULA) | | |
| | PIF5 (PHYTOCHROME INTERACTING FACTOR 5) | Apical hook development | Gallego-Bartolomé <i>et al.</i> , 2011 |
| | bHLH48 | Flowering time | Li <i>et al.</i> , 2017 |
| | bHLH60 | | |
| | MYC2 | Volatile biosynthesis | Hong <i>et al.</i> , 2012 |
| | GL1 (GALBARA 1) | Trichome initiation | Qi <i>et al.</i> , 2014 |
| | EGL3 (ENHANCER OF GL3) | | |
| | BZR1 (BRASSINAZOLE-RESISTANT 1) | Hypocotyl growth | Bai <i>et al.</i> , 2012; Li <i>et al.</i> , 2012 |
| | BES1 (BRASSINAZOLE-RESISTANT 2) | | |
| | EIN3 (ETHYLENE INSENSITIVE 3) | Apical hook development | An <i>et al.</i> , 2012 |
| | EIL1 (EIN3-LIKE 1) | | |
| | RAP2.3 (RELATED TO APETALA2.3) | | |
| TCP14 (TB1 (TEOSINTE BRANCHED 1), CYC (CYCLOIDEA), PCF (PROLIFERATING CELL FACTOR) 14) | Stem elongation, cell division in apical meristem (root and shoot) | Davière <i>et al.</i> , 2014 | |

| | | | |
|---|---|---|---------------------------------------|
| | CO (CONSTANS) | Flowering | Xu <i>et al.</i> , 2016 |
| | WRKY45 | Leaf senescence | Chen <i>et al.</i> , 2017 |
| | WRKY75 | Flowering | Zhang, Chen and Yu, 2018 |
| | ARF7 (AUXIN RESPONSE FACTOR 7) | Fruit initiation | Hu <i>et al.</i> , 2018 |
| | GRF4 (GROWTH-REGULATING FACTOR 4) | Nitrogen metabolism, carbon fixation, growth | Li <i>et al.</i> , 2018 |
| | MYB21 and MYB24 | Filament elongation | Huang <i>et al.</i> , 2020 |
| Co-activation of a transcription factor | ABI5 (ABA INSENSITIVE 5) | Seed germination | Lim <i>et al.</i> , 2013 |
| | ABI3 (ABA INSENSITIVE 3) | | |
| | GAF1 (GAI-ASSOCIATED FACTOR1, also known as IDD2) | GA homeostasis, GA-regulated growth, flowering | Fukazawa <i>et al.</i> , 2014 |
| | IDD3, -4, -5, -9 and -10 (INDETERMINATE 3, -4, -5, -9 and -10) | Unknown | Yoshida <i>et al.</i> , 2014 |
| | ARR1 (ARABIDOPSIS RESPONSE REGULATOR 1) | Root meristem maintenance and skotomorphogenesis | Marín-De La Rosa <i>et al.</i> , 2015 |
| | ARR2 and -14 (ARABIDOPSIS RESPONSE REGULATOR 2, and -14) | Unknown | |
| | OsIDD2 | Stem elongation | Lu <i>et al.</i> , 2020 |
| | FLC (FLOWERING LOCUS) | Flowering transition | Li <i>et al.</i> , 2016 |
| Sequestration of a transcriptional regulator | JAZ1 (JASMONATE-ZIM DOMAIN 1), JAZ3 and JAZ9 | Unknown | Hou <i>et al.</i> , 2010 |
| | JAZ1, -3, -4, -9 and -11 | Flowering | Yang <i>et al.</i> , 2012 |
| | BBX24 (B-BOX ZINC FINGER PROTEIN 24) | Shade avoidance | Crocco <i>et al.</i> , 2015 |
| Activation of a transcriptional regulator | BOI (BOTRYTIS SUSCEPTIBLE1 INTERACTOR), BRG1 (BOI-RELATED GENE1), BRG2 and BRG3 | Seed germination, juvenile to adult transition, flowering | Park <i>et al.</i> , 2013 |
| Other | ENY (ENHYDROUS, also known as IDD1) | Seed maturation and germination | Feurtado <i>et al.</i> , 2011 |
| | GRF1, 2, 3, 4, 5, 7 and 9 | Unknown | Lantzouni <i>et al.</i> , 2020 |
| | GRF5 | Cold stress, growth | |

were degraded in response to GA, GAF1 bound TPR corepressor, and the GAF1-regulated gene expression was inhibited. It was therefore concluded that DELLAs act as GAF1 coactivators, and TPR1 and TPR4 as GAF1 corepressors (Fukazawa *et al.*, 2014). In a follow-up study by Fukazawa *et al.* (2017), DELLA-GAF1 complex was identified as a main component regulating *AtGA20ox2* gene.

A similar mode of regulation was recently shown in rice, where SLR1 protein interacted with OsIDD2 to regulate expression of MiR396, a miRNA that regulates the transcript levels of GA-inducible *GRF* genes. GRF TFs regulate expression of cell-cycle-related genes, thus the DELLA-OsIDD2-mediated de-regulation of their activity negatively affects stem elongation (Lu *et al.*, 2020). Co-activation of target gene expression on binding DELLA was also shown for several other IDD proteins (Yoshida *et al.*, 2014), thus co-activation seems to be a common mechanism of IDD TFs regulation by DELLAs.

1.6.4.3 DELLAs interact with other transcriptional regulators to modulate gene expression

DELLAs can also interact with other transcriptional regulators that are not *bona fide* TFs. These interactions have been demonstrated to regulate transcription without the need to bind directly to the promoters of the target genes. An example of such a regulatory mechanism was demonstrated between DELLAs and JASMONATE-ZIM DOMAIN (JAZ) proteins by Hou *et al.* (2010) and Yang *et al.* (2012). JAZ proteins are negative regulators of JA signalling and they repress the activity of JA-induced TF MYC2. JA signalling results in degradation of JAZ proteins through the action of SCF^{CO11} E3 ubiquitin ligase, which in turn results in releasing the repression of MYC2 (Chini *et al.*, 2007). Hou and colleagues identified JAZ1 as an RGA-interacting partner in the Y2H screen, and confirmed that additional members of the JAZ family, JAZ3 and JAZ9 were also DELLA partners. It was demonstrated that DELLAs act downstream of JAZs, and that

RGA and MYC2 compete for binding to JAZs. They also found that the binding of MYC2 to its target genes, *LOX2* and *TAT1*, promoters was enhanced by increased levels of DELLA. It was therefore concluded that DELLA proteins modulate JA signalling by affecting the ability of MYC2 to regulate transcription of its target genes (Hou *et al.*, 2010). Interestingly, DELLA was found to interact with MYC2 and to compete with JAZ3 for its binding (Hong *et al.*, 2012). This indicates the existence of multiple mechanisms for the regulation of hormonal responses, and diverse roles for DELLAs as regulatory proteins. Interaction between DELLA and six other JAZ proteins: JAZ1, 3, 4, 9, 10 and 11 was confirmed by Yang *et al.* (2012), and overexpression of these JAZs conferred early flowering phenotype (Yang *et al.*, 2012). Strikingly, JAZ9 was found to inhibit RGA-PIF3 interaction without affecting RGA and PIF3 protein levels, which suggests that JAZ proteins compete for DELLA binding. It is an elegant example of DELLA regulation of GA and JA signalling. Under normal conditions, DELLAs bind to JAZ proteins, but when defence becomes a priority, JAZs are degraded in response to JA, and DELLAs can bind to and inactivate PIFs, which results in growth repression (Thomas *et al.*, 2016).

PIF4, which plays a crucial role in shade avoidance in Arabidopsis (Lorrain *et al.*, 2007), is negatively regulated by DELLA (de Lucas *et al.*, 2008; Feng *et al.*, 2008). It was observed that this repression is released in the presence of BBX24, a double B-Box (BBX) containing zinc finger TF (Crocco *et al.*, 2015). BBX24 physically interacts with GAI and RGA and was found to compete with PIF4 for DELLA binding. BBX24 was therefore identified as a DELLA negative regulator that binds DELLA away from the PIF4 promoter, thereby promoting transcription of PIF4-regulated genes (Crocco *et al.*, 2015).

The examples summarised in this section together give a good overview on the diverse roles that DELLA proteins have in regulating transcription. As described above and extensively reviewed in (Thomas *et al.*, 2016), DELLAs have different modes of regulating gene expression: they can directly interact with transcription factors and either sequestering them from target genes

promoters or enhancing their activation ability, or interact with other transcriptional regulators to promote or inhibit gene expression.

1.6.5 Regulation of GAMYB by DELLAs

The opposing effects of GA and ABA signalling on the aleurone has been established (Gómez-Cadenas *et al.*, 2001). GA signalling was shown to induce a rapid increase in *HvGAMYB* gene expression in barley aleurone layer (Gubler *et al.*, 1995), and ABA inhibits the GA-induced increase in *HvGAMYB* transcript synthesis (Gubler *et al.*, 2002). In barley, the inhibitory effect of ABA on GA-induced increase in *HvGAMYB* expression occurs downstream of SLN1 and upstream of *HvGAMYB* transcription, at least partly through the action of ABA-inducible kinase PKABA1 (Gómez-Cadenas *et al.*, 2001). PKABA1 was found to be sufficient to inhibit expression of *Amy32* and cysteine proteinase genes in GA-treated barley aleurone layers (Gomez-Cadenas *et al.*, 1999), and also to inhibit the constitutive expression of *GAMYB* and α -amylase in a *slender* mutant (Gómez-Cadenas *et al.*, 2001).

Studies from Gubler and colleagues (2002) in barley suggest that GA acts on *GAMYB* expression via DELLA. Both the *sln1* and *slr1* mutants showed increased levels of *GAMYB* in the aleurone and anthers, respectively (Aya *et al.*, 2009; Gubler *et al.*, 2002), and aleurone cells of *sln1* and *slr1* mutants constitutively express α -amylase with no requirement for GA (Chandler *et al.*, 2002; Fu *et al.*, 2002; Ikeda *et al.*, 2001). The levels of SLN1 protein fall rapidly in response to GA, before the increase in *HvGAMYB* transcript levels, therefore it is suggested that SLN1 acts as a negative regulator of *HvGAMYB* gene expression. However, the lag time observed between SLN1 degradation and the expression of *HvGAMYB* in aleurone cells of barley indicates that SLN1 is not directly repressing the *HvGAMYB* transcription, but rather may act through an intermediate molecule (Sun & Gubler, 2004).

These findings support the central role of the DELLA proteins in GA signalling pathway and suggest that they have a repressive effect on *GAMYB* expression.

However, as mentioned previously, GAMYB is unlikely to be a direct target of the DELLA proteins. Since DELLAs have been established as transcriptional regulators acting through interactions with *bona fide* transcription factors, it is hypothesized that the repression of *GAMYB* expression by DELLA in the aleurone might be achieved by DELLA binding and working in complex with another transcriptional factor, or factors.

1.7 Project outline and objectives

The overall objective of this study is to understand the role of the wheat DELLA protein, RHT-1, in regulating GA responses in the aleurone layer of wheat grain. Although GA biosynthesis and early signalling have been extensively researched, the understanding of the later steps of the GA pathway, including DELLA-interacting TFs that regulate GA-mediated gene expression, especially in cereals, is only just starting to emerge. The aim is to identify the downstream components of the GA-activated signalling in the aleurone of wheat and the physiological relevance of the interactions.

In this study, we aim to identify potential components that may act between DELLA and GAMYB, that are involved in the GA response in the germinating grain. Although the focus of this study is GA signalling in the aleurone which leads to germination, it needs to be emphasized that DELLAs are regulating GA signalling in all GA-responsive tissues in plants.

The aims will be achieved in three main steps: (1) identification of TFs that interact with RHT-1 in the aleurone of wheat, (2) generation of the null mutants for the identified TFs in wheat, and (3) phenotypic analysis of the null mutants.

Regarding the outline of the work, the initial step will be achieved by conducting the yeast two-hybrid (Y2H) screen of the cDNA library prepared from wheat's aleurone. *In silico* functional analysis of the putative interactors will help identify the potential targets for *in vivo* functional assessment. After determining the phylogenetic relationships between the putative interactors,

tailored reverse genetic methods will be applied to produce knock out (KO) lines. The null KO lines will be assessed phenotypically, with the focus on GA-regulated responses, to help understand the role of identified DIPs in regulating GA signalling in wheat.

Chapter 2: General materials and methods

Genotypes of the cells used in the project:

NEB® 10-beta Competent *E. coli* (High Efficiency): $\Delta(ara-leu)$ 7697 *araD139 fhuA* $\Delta lacX74 galK16 galE15 e14-\phi80\Delta lacZ\Delta M15 recA1 relA1 endA1 nupG rpsL$ (*Str^R*) *rph spoT1* $\Delta(mrrhsdRMS-mcrBC)$

NEB® 5-alpha Competent *E. coli* (High Efficiency): *fhuA2* $\Delta(argF-lacZ)U169$ *phoA glnV44* $\Phi80 \Delta(lacZ)M15 gyrA96 recA1 relA1 endA1 thi-1 hsdR17$

Invitrogen™ One Shot™ *ccdB Survival™ 2 T1R* Competent Cells: $F^-mcrA \Delta(mrrhsdRMS-mcrBC)$ $\Phi80lacZ\Delta M15$ $\Delta lacX74 recA1 ara\Delta139$ $\Delta(ara-leu)7697 galU galK rpsL$ (*Str^R*) *endA1 nupG fhuA::IS2*

Invitrogen™ MaV203 Competent Yeast Cells, Library Scale: *MAT*; *leu2-3,112; trp1-901; his3* $\otimes 200$; *ade2-101; cyh2^R; can1^R; gal4* \otimes ; *gal80* \otimes ; *GAL1::lacZ; HIS3_{UASGAL1}::HIS3@LYS2; SPAL10::URA3*

GV3101 *Agrobacterium tumefaciens* strain: C58 (*rif R*) Ti pMP90 (pTiC58DT-DNA) (*gentR*) Nopaline

2.1 General molecular biology methods

2.1.1 PCR

PCR reactions were carried out using a number of different Taq polymerases: GoTaq® DNA Polymerase (Promega, Madison, Wisconsin, USA), Phusion® or Q5® High-Fidelity DNA Polymerase (New England Biolabs, Ipswich, Massachusetts, USA), or HotShot Diamond PCR Master Mix (Clontech Life Science, Stourbridge, UK). All PCR reactions were carried out according to the manufacturer's protocol, on a BIO-RAD C1000™ Thermal Cycler (California, USA).

Annealing temperature was determined by the T_m of the primers used and the extension time was determined by the length of the PCR product. All primers were synthesised by SIGMA ALDRICH (Darmstadt, Germany).

2.1.2 Quantitative PCR (qPCR)

qPCR was carried out using the SYBR[®] Green JumpStart[™] *Taq* ReadyMix[™] (Sigma-Aldrich Company Ltd., Dorset, U.K.), according to the manufacturer's instructions. Two reference gene primer pairs were used to assess the relative abundance of a target gene. The reactions were set up as follows:

| Reagent | Volume (μ l) | Concentration |
|-------------------------|-------------------|---|
| SYBR | 9.8 | |
| ROX | 0.021 | |
| FOR primer | 0.5 | 0.25 μ M |
| REV primer | 0.5 | 0.25 μ M |
| cDNA | 2 | 1 in 15 dilution of cDNA synthesized from RNA |
| Sterile Distilled Water | 7.2 | |

The reactions were loaded onto a 96-well plate (4titude Ltd., Surrey, UK), and sealed with clear foil (4titude Ltd., Surrey, UK). The plate was centrifuged using Labnet MPS 1000 Mini plate spinner (Sigma-Aldrich Company Ltd., Dorset, UK), and the qPCR reaction was run on a 7500 Real Time PCR system (Applied Biosystems, California, USA), with the following PCR conditions:

| | | |
|-----------------------|---------------------|-----------|
| Initial denaturation | 95°C for 10 minutes | |
| Thermocycling | 95°C for 15 seconds | 40 cycles |
| | 60°C for 1 minute | |
| Dissociation analysis | 95°C for 15 seconds | |
| | 60°C for 1 minute | |
| | 95°C for 15 seconds | |
| | 60°C for 15 seconds | |

The analysis:

The melting curve was assessed to identify any secondary products or primer dimers, which were detected by the presence of more than one peak. If only one peak was present, further analysis was carried out.

Analysis was carried out by comparing the PCR efficiency (E) and threshold cycle (Ct) values for the target and reference genes in both control and treatment samples. The Ct and E values were calculated by the LinRegPCR software (Heart Failure Research Centre, Netherlands). The normalised relative quantity of the target gene (NRQ) was calculated using the equation:

$$NRQ = \frac{E_t^{-Ct,t}}{\sqrt[3]{E_{ref1}^{-Ct,ref1} \times E_{ref2}^{-Ct,ref2} \times E_{ref3}^{-Ct,ref3}}}$$

Where E_t and Ct,t are the efficiency and Ct values of the target gene, respectively, and E_{ref1} , E_{ref2} , E_{ref3} , $Ct,ref1$, $Ct,ref2$ and $Ct,ref3$ are the values for the three reference genes. The values fed into the equation were averaged across the biological replicates.

2.1.3 Gel electrophoresis

Prior to loading on the gel, samples were mixed with 6X DNA loading dye containing bromophenol blue and xylene cyanol FF (Thermo Fisher Scientific, Waltham, Massachusetts, USA), allowing for two-colour tracking of DNA migration. Separation was run on 1-2% w/v agarose-TBE gel matrix, depending on the size of separated fragments, containing 0.1 µg/ml ethidium bromide. A 1 kb or 100 bp DNA ladder (Invitrogen, Carlsbad, California, USA) was run alongside samples for size estimation. Electrophoresis was carried out at 70 V for 120 minutes. DNA fragments were visualised by ethidium bromide

fluorescence under UV light using the Gel Doc™ XR+ Gel Documentation System (BIO-RAD, Watford, UK).

2.1.4 PCR product purification and gel clean up

PCR products were purified either from the PCR mix or from the agarose gel using the Wizard® SV Gel and PCR Clean-Up System (Promega, Madison, Wisconsin, USA). Bands containing DNA fragments of interest were excised from the agarose gel using UV transilluminator and razor. Products were purified according to the respective protocol with minor alterations:

- in step 6 (the “Washing” section), the tubes were put on 65°C thermal block to evaporate residual ethanol,
- in step 8 (the “Elution” section), 55 µl of sterile water was added, incubated for 5 minutes at room temperature, and then centrifuged at top speed for 2 minutes.

Purified PCR products were quantified using the Nanodrop™ ND-1000 spectrophotometer (LabTech International Ltd., UK).

2.1.5 Restriction digestion

When restriction digest was performed for subsequent ligation purposes, the restriction digestion mix contained:

200-400 ng of plasmid DNA or 400-800 ng of insert DNA
3 µl of respective buffer
5 U of enzyme 1
5 U of enzyme 2
Sterile water up to 30 µl

All the enzymes used were purchased from New England Biolabs (New England Biolabs, Ipswich, Massachusetts, USA). Digestions were left on 37°C water bath overnight. After incubation, 1 µl of 1 U/µl New England Biolabs Shrimp Alkaline

Phosphatase was added to the tubes containing plasmid digest to avoid re-ligation.

2.1.6 DNA ligation reactions

Ligation reaction tubes were incubated at room temperature overnight.

Ligation reaction tubes contained:

- 1:3 molar ratio of vector to insert
- 2 µl of 5x reaction buffer
- 0.1-0.2 µl of Invitrogen Hi-T4™ DNA Ligase
- Sterile water up to 10 µl

Ligations were frozen prior to the bacterial transformation. The Hi-T4™ DNA Ligase was purchased from New England Biolabs (Ipswich, Massachusetts, USA).

2.1.7 Gateway cloning

To clone the gene of interest (GOI) into the destination vector, the GOI was amplified by PCR using sequence-specific primers with attB1 site attached to the 5' end and attB2 site attached to the 3' end of the coding sequence (CDS). The attB1-GOI-attB2 amplicon was then used in the Gateway BP reaction using pDONR221 vector and Gateway™ BP Clonase™ II Enzyme Mix (Invitrogen, Carlsbad, California, USA), following the supplied protocol. The reactions were incubated at 25°C overnight. 3 µl of the BP reaction mix was used to transform 20 µl of 10-beta Competent *E. coli* cells (New England Biolabs, Ipswich, Massachusetts, USA). The pENTR clones obtained in BP reactions were extracted from bacteria and their sequence validated by Sanger sequencing service provided by Eurofins Genomics service (Ebersberg, Germany).

The LR reactions were carried out using the Gateway™ LR Clonase™ II Enzyme Mix (Invitrogen, Carlsbad, California, USA), following the supplied protocol with two modifications: the volumes recommended to be used in the reactions

were halved and the incubation on 25°C extended from one hour to overnight. 2 µl of the LR reaction mix was used to transform 15 µl of 10-beta Competent *E. coli* cells (New England Biolabs, Ipswich, Massachusetts, USA).

2.1.8 Bacterial transformation

Competent *E. coli* cells were thawed on ice and used immediately. 10 to 30 µl of bacteria were mixed with 0.5 to 5 µl of DNA (15-300 ng) and left on ice for ~30 minutes. After incubation on ice, the bacteria were placed on a 42°C water bath for 35 seconds and put back on ice for 5 minutes. 250 µl of SOC medium was added to each transformation tube and the tubes incubated on the rotary shaker at 37°C and 220 rpm for 1 hour. Cultures were spread over 2X YT agar plates containing the appropriate antibiotic, sealed with Bemis™ Parafilm M™ Laboratory Wrapping Film (Fisher Scientific, Hampton, New Hampshire, USA) and left in a 37°C incubator overnight. The colonies were assessed the next morning and either used the same day or left in the 4°C fridge for future use.

2.1.9 *Agrobacterium tumefaciens* transformation

Tubes containing 200 µl of frozen chemocompetent *A. tumefaciens* cell aliquots were placed on ice and mixed with 500 – 1000 ng of plasmid DNA (while cells were still frozen). The mix was incubated on ice for 30 minutes after which the tubes were submerged in liquid nitrogen for 5 minutes, followed by 5 minutes incubation in a 37°C water bath. Subsequently, 800 µl of 2YT broth (FORMEDIUM LTD, Hunstanton, England) was added to the cell suspension and the mixture incubated at 28 °C and 160 rpm for 2 to 4 hours, and plated on the 2X YT solid growth medium containing 50 µg/ml Rifampicin, 25 µg/ml Gentamicin and selection antibiotic for the vectors. The plates were incubated at 28°C for 48 to 72 hours.

2.1.10 Bacterial cultures

Antibiotics were added to the sterile 2X YT Broth and 5 ml aliquots were distributed into sterile universal bottles. Single colonies of transformed bacteria were taken from the plates with a sterile toothpick and submerged in the medium with antibiotics. The bottles were left overnight (~16 hours) to incubate on a shaker at 37°C and 220 rpm. *Agrobacterium tumefaciens* cells were cultured like *E. coli* cells, but the incubation was performed at 28°C instead of 37°C.

2.1.11 DNA isolation from the bacteria cells

4 ml of overnight bacteria culture was centrifuged at 6,800 x g for 3 minutes to pellet the cells. Wizard® Plus SV Minipreps DNA Purification System (Promega, Madison, Wisconsin, USA) or Qiagen QIAprep Spin Miniprep Kit (Qiagen, Hilden, Germany) were used to isolate plasmid DNA from *E. coli* hosts according to the respective protocols with the following alterations:

- after the second ethanol wash the columns were additionally centrifuged at 16,000 x g for 5 minutes,
- 55 µl of Nuclease-Free Water was added to elute the DNA, incubated at room temperature for 5 minutes and centrifuged for 5 minutes.

Purified plasmid DNA was quantified using the Nanodrop™ ND-1000 spectrophotometer (LabTech International Ltd., UK).

2.1.12 Genomic DNA extraction

Genomic DNA (gDNA) was extracted from young leaves of wheat (*Triticum aestivum*) plants using the PVP DNA extraction method. Harvested leaf tissue was frozen in liquid nitrogen and lyophilised using the Edwards Modulyo RV8 Freeze Dryer (Burgess Hill, Sussex, UK). The samples were then homogenised using stainless steel ball-bearings and the 2010 GenoGrinder® (SPEX SamplePrep, New Jersey, USA) set to max speed for 5 minutes. The

homogenate was incubated in 1 ml of DNA extraction buffer (see below) at 65°C for 1 hour. Next, 333 µL of 5 M KAc was added and the reaction mix centrifuged at 17,900 x g for 10 minutes to bring down the cell debris. 1 ml of the supernatant was transferred into the fresh tube and mixed with 550 µl of chilled isopropanol, incubated at room temperature for 10 minutes and centrifuged (17,900 x g, 10 minutes) to pellet the DNA. The pelleted DNA was washed with 500 µl of 70 % ethanol and re-collected by centrifugation (17,900 x g, 10 minutes); the supernatant was discarded, and the DNA pellet air dried for at least 1 hour. The genomic DNA was resuspended in 200 µl of 10 mM tris buffer and incubated at 50°C for 60 minutes. DNA was quantified and stored at -20°C prior to use.

DNA Extraction Buffer final concentrations:

100 mM Trizma Base (Tris Base)

1 M KCl

10 mM EDTA pH 8.0

Adjust pH to 9.5 using 1 M NaOH

On the day of extraction, add:

0.18 mM PVP-40 (Polyvinylpyrrolidone)

34.6 mM Sodium bisulphite

2.1.13 RNA extraction

RNA was extracted from frozen tissue, homogenised either by hand using a mortar and pestle or using the 2010 Geno/Grinder® (SPEX SamplePrep, New Jersey, USA) and stainless-steel ball-bearings. For RNA extraction Monarch® Total RNA Miniprep Kit (New England Biolabs, Ipswich, Massachusetts, USA) was used following the protocol. The protocol includes the DNase treatment. RNA concentration and quality were assessed using Agilent 6000 Nano RNA Kit (Agilent, Santa Clara, California, USA) and Agilent 2100 Bioanalyzer (Agilent, Santa Clara, California, USA) as per the manufacturers' instructions and stored at -80°C freezer.

2.1.14 Complementary DNA (cDNA) synthesis

cDNA was synthesised from 1 µg total RNA using the SuperScript™ III First-Strand Synthesis System (incubation: 50°C, 50 min; inactivation 85°C, 10 min) or SuperScript™ IV First-Strand Synthesis System (incubation: 55°C, 10 min; inactivation 80°C, 10 min) with an Oligo dT(20) primer (Invitrogen, Carlsbad, California, USA) following the protocol. cDNA samples were stored at -20 °C.

2.1.15 DNA precipitation

1 volume of 3 M Sodium acetate (pH 5.2) was added to 9 volumes of DNA sample. Then 2.5 volumes of cold 100% ethanol was added, and the reaction mix left in -20°C overnight. The next day the tubes were centrifuged at 4°C at ~16,000 x g for 25 minutes, supernatant removed, pellet washed with 1 ml of cold 70% ethanol and centrifuged again for 10 minutes. After removing the supernatant and air drying, the pellet was resuspended in water to a final concentration.

2.1.16 Long term storage of bacteria and yeast cells

Bacteria:

500 µl of the overnight bacterial culture was mixed with 500 µl of 50% glycerol, gently mixed and frozen in the -80°C.

Yeast:

Using sterile toothpicks, a small number of cells originating from a single colony was scraped off and suspended by vortexing in 1 ml of a sterile 15% glycerol solution of YPD or selective medium.

Stocks were stored in a -80°C freezer and kept on dry ice when handling to avoid thawing. To recover a strain from the glycerol stock, a small amount of suspension was streaked on 2x YT medium with appropriate antibiotic (for bacteria) or YPD medium plate (for yeast) and incubated for 48-60 hours.

2.1.17 Genotyping by sequencing

Homoeologue-specific primers were designed to amplify the fragment of genomic DNA fragment. PCR products sequences were validated using Sanger sequencing service provided by Eurofins Genomics (Ebersberg, Germany) and aligned to the reference sequences of the genes in Geneious v.10.2.3 using ClustalW Alignment (Biomatters Ltd, Auckland, New Zealand) (Kearse *et al.* 2012), set to default settings.

2.1.18 Kompetitive Allele Specific PCR (KASP) genotyping

Low-ROX KASP Master mix (LGC, Teddington, UK) was used. Assay mix, per sample, contained:

- 0.14 μ l KASP primer mix
- 2.86 μ l water
- 5.00 μ l low-ROX KASP Master Mix

For each reaction, the primer mix was prepared:

- 12 μ l KASP WT SNP primer (100 μ M)
- 12 μ l KASP MUT SNP primer (100 μ M)
- 30 μ l KASP common primer (100 μ M)
- 46 μ l water

2 μ l of wheat genomic DNA (concentration ranging from 40 to 300 ng/ μ l) and 8 μ l of assay mix was loaded into each well of 96-well, semi-skirted q-PCR plates (4titude Ltd., Surrey, UK). The plates were sealed with clear foil (4titude Ltd., Surrey, UK) and spun down using Labnet MPS 1000 Mini plate spinner (Sigma-Aldrich Company Ltd., Dorset, UK). The KASP reactions were either carried out and analysed with the 7500 Real Time PCR system (Applied Biosystems, Foster City, California, USA) or carried out using a BIO-RAD C1000™ Thermal Cycler (Hercules, California, USA) and analysed with the 7500

Real Time PCR system using the allelic discrimination settings. Reaction conditions were as follows:

| | | |
|-------------------------|--|-------------------------------------|
| Initial denaturation | 95°C for 15 minutes | |
| Touchdown amplification | 95°C for 20 seconds 61°C for 60 seconds | 10 cycles, reducing 0.6°C per cycle |
| Amplification | 95°C for 20 seconds 55°C for 60 seconds | 27 cycles |

The plates were read with the 7500 Fast Software v2.3 (Applied Biosystems, Foster City, California, USA) and analysed using the KlusterCaller™ software (LGC, Teddington, UK).

2.2 Yeast two-hybrid (Y2H) assays

2.2.1 Yeast cultures

Yeast cells were cultured either in YPD liquid medium (Sigma-Aldrich, Saint Louis, Missouri, USA) or in SD Broth with 2% of glucose (FORMEDIUM LTD, Hunstanton, England) supplied with appropriate amino acid dropout mixes, obtained from Clontech Laboratories (Takara Bio Europe SAS, Saint-Germain-en-Laye, France) or from FORMEDIUM. Incubation was carried out at 30°C and 160 rpm.

2.2.2 Preparation of competent yeast cells

MaV203 yeast cells (Thermo Fisher Scientific, California, USA) were streaked onto YPD media (Sigma-Aldrich Company Ltd., Dorset, UK) with 2% agar (Scientific Laboratory Supplies, Nottingham, UK) plates and incubated at 30°C for 48 hours. 100 ml YPD liquid media was then inoculated with a single *MaV203* colony and incubated at 160 rpm, 30°C overnight. Once the OD₆₀₀ reached 1.0-1.5, the cells were harvested at room temperature, 1,505 x g for

5 minutes and washed twice with 20 ml of 0.1 M LiAc. The cells were then spun down at the same speed, resuspended in 2 ml of 0.1 M LiAc, and incubated at 30°C, 160 rpm for 1 hour. After the incubation the cells were used immediately.

2.2.3 Yeast transformation

Plasmids were introduced into yeast competent cells using a heat shock protocol. 150 µl of *MaV203* competent yeast cells were incubated with 1 µg of each plasmid DNA, 2 µl of 10 mg/ml sheared salmon sperm DNA (Thermo-fisher Scientific, California, USA) and 350 µl of 50% polyethylene glycol (PEG3350) at 30°C water bath for 30 minutes, mixed every 10 minutes. Reactions were transferred to 42°C for 5 minutes, followed by a 2-3-minute incubation on ice. Cells were harvested by centrifugation at 9,408 x g for 1 minute and cell pellet resuspended in 110 µl of sterile distilled water. Typically, 5 and 100 µl aliquots of cells were plated onto SD-Leu-Trp plates and incubated at 30°C for 48-72 hours.

2.2.4 Replica plating

Master plates were generated on the SD-Leu-Trp plates and incubated at 30°C for about 48 hours. After the incubation period, the master plates were gently pressed onto an autoclaved velvet; only a slight haze of cells was transferred. Then, the selection plates were gently pressed onto the velvet containing cells from the master plate to transfer the colonies. Single inoculated velvet was used to inoculate 3-5 selection plates. Inoculated plates were incubated at 30°C for 48-72 hours.

2.2.5 Isolation and retransformation of prey plasmid

Yeast colonies were grown on the SD-Leu-Trp solid medium for two days and a sterile toothpick was used to inoculate a single colony into the SD-Trp liquid medium. The culture was incubated at 30°C, 160 rpm overnight, and the prey

plasmid DNA isolated using Wizard® Plus SV Minipreps DNA Purification System (Promega, Madison, Wisconsin, USA). DNA was extracted according to the protocol, with the following alterations and additional steps:

- 4 ml of the culture was centrifuged in the 15 ml sterile conical tube (Greiner Bio-One, Kremsmünster, Austria), and the pellet resuspended in the Cell Resuspension Solution; after that the suspended pellet was transferred to the 2 ml microcentrifuge tube containing ~250 µl of acid-washed 425-600 µm glass beads (Sigma Aldrich, St. Louis, USA).
- After resuspension, the cells were frozen and thawed three times, either using liquid nitrogen or by placing the tubes in the -80°C freezer for a few minutes and placing them in the room temperature water bath to thaw.
- After the addition of the Cell Lysis Solution, the tubes were shaken vigorously at 1750 rpm for 5 minutes using GenoGrinder (SPEX SamplePrep, Metuchen, New Jersey, USA).

5 µl of the isolated plasmid DNA was used to transform bacteria as described in section 2.1.8.

2.3 Plant material and growing conditions

Wheat (*Triticum aestivum*) cv. Cadenza was used for all molecular, physiological, TILLING, genome editing and transformation experiments.

2.3.1 Germinating the seeds

The seeds were surface sterilised by soaking in 10% bleach with a drop of Tween20 (Sigma-Aldrich Company Ltd., Dorset, UK) for 10 minutes, rinsed in sterile water five times and distributed evenly on a wet filter paper in a Petri dish (crease side down). The plates were transferred to a dark, cold room (4°C) for about 3-4 days, after which they were moved into the controlled

environment (CE) growth room to germinate. CE growth conditions were 20°C during the day and 15°C during the night with a 16-hour photoperiod provided by tungsten fluorescent lamps providing 500 $\mu\text{molm}^{-2}\text{s}^{-1}$ PAR. The germinated seeds were planted the next day in a seed tray and kept in the Rothamsted Research glasshouse nursery until potting.

2.3.2 Growing conditions

Wheat plants were grown in 15 cm diameter plastic pots containing Rothamsted prescription mix compost (75% peat, 12% sterilised loam, 3% vermiculite, 10% grit) supplemented with fertiliser, in the standard glasshouse conditions. Temperature was maintained at 18-20°C (day) and 14-15°C (night) under a 16-hour photoperiod using natural light supplemented with 400-1000 $\mu\text{molm}^{-2}\text{s}^{-1}$ PAR from SON-T sodium lamps.

Tobacco (*Nicotiana benthamiana*) plants were grown in the square 9 cm x 9 cm plastic pots containing Rothamsted prescription mix compost in the glasshouse environment (23°C day/ 18°C night, 30% average humidity, 16-hour day length with supplementary lightning when sunlight radiation dropped below 175 W/m²).

2.3.3 Crossing wheat plants

The spikes to be pollen acceptors and pollen donors were selected based on the stage of development. Selected female parents were emasculated by excision of pale green/yellow immature anthers 1-3 days prior to anthesis. The bottom three and top two spikelets, and two innermost florets of all remaining spikelets were removed. Emasculated spikes were enclosed in transparent plastic crossing bags and labelled with the genotype and the date. When selected male parents entered anthesis, single pollen shedding spikes were excised, lemma and palea cut to ease the emergence of the anthers and placed upside-down inside the crossing bag with the emasculated spike. After

agitation to spread pollen around all available florets, pollen donor spikes were held in place upside-down against the female parent using paper clips. Pollen donor spikes were replaced as required. Grains were left to develop for 20-25 days before collection.

2.3.4 Aleurone isolation

Aleurone isolation was carried out in sterile conditions under the laminar flow cabinet. Mature wheat grains were de-embryonated and cut transversely using a sharp blade; grain brush was also removed. Grains were sterilised in 10% bleach solution containing a drop of Tween20 for 10 minutes on the roller shaker and rinsed generously with sterile water. To aid endosperm removal, half-grains were imbibed in sterile 20 mM CaCl₂ solution in the dark for three days. After three days, sterile spatula and tweezers were used to gently scrape off the endosperm; the pericarp, which at this developmental stage was dead, stayed attached to aleurone. Isolated aleurones were used immediately.

2.4 Bioinformatics

2.4.1 RHT-1 interactors identification

In order to identify the interactors, the BLAST tool in Ensembl Plant (Zerbino *et al.*, 2018) was used. Sequences of identified interactors were BLASTed against *Triticum aestivum* cv. Chinese spring, TGACv1 genome assembly (Clavijo *et al.*, 2017) and the best hit with the lowest e-value and highest sequence similarity chosen. Ensembl Plant (*Triticum aestivum*) was used to translate the full genomic sequence of the identified gene, and the protein sequence used to perform a BLAST search in Phytozome 12.1 (Goodstein *et al.*, 2012). The reference organisms chosen for the BLAST search were *Arabidopsis thaliana* (thale cress) genome assembly TAIR10 (Lamesch *et al.*, 2012), *Oryza sativa* (rice) genome assembly v7_JGI (Ouyang *et al.*, 2007) and *Zea mays*

(maize) genome assembly Ensembl-18 (Schnable *et al.*, 2009). Function of identified interactor was inferred based on similarity to the orthologous proteins.

2.4.2 Phylogenetic analysis

Phylogenetic analysis was conducted using PHMYL plugin in Geneious version 10.2.3 (Biomatters Ltd, Auckland, New Zealand), using substitution model Blosum62 and no bootstrapping. All phylogenetic trees were built using protein alignments calculated in Geneious using MUSCLE plugin (Edgar, 2004).

2.4.3 KnetMiner analysis

Wheat network (TGACv1) on KnetMiner website (Hassani-Pak *et al.*, 2016, 2020) (<https://knetminer.rothamsted.ac.uk/KnetMiner/>) was used to assess the involvement of the identified interactors in gibberellin signalling. The full list of the interactors, using the TGACv1 assembly gene accession numbers was pasted into the “Gene List” box, and the process of interest was defined in the “Query” box.

2.4.4 TILLING mutations identification

EMS (ethyl methanesulfonate) mutations used to produce the knockout line were identified comparing two sources: wheat TILLING website (<http://www.wheat-tilling.com/>) (Krasileva *et al.*, 2017) and genomic sequences from IWGSC_refseq_v1.1 assembly including mapped EMS mutations (Andy Phillips, personal communication).

2.4.5 Primer design

PCR primers were designed using the Primer3Plus (Untergasser *et al.*, 2007) plugin in Geneious version 10.2.3 (Biomatters Ltd, Auckland, New Zealand).

New England Biolabs Inc. Tm Calculator version 1.9.10 (<https://tmcalculator.neb.com/>) was used to determine the annealing temperature for the chosen pairs of primers depending on the polymerase used in the PCR reaction mix. The full list of primers used in this project is presented in the Appendix (Supplementary Tables 4.1 and 5.1).

2.5 Statistical analysis

2.5.1 Randomisation

For comparison experiments, plants, or plant tissues, i.e. units, were divided into blocks to reduce the variation of the design. Each block contained an equal number of units representing every genotype analysed. The units within blocks were randomized using the Genstat statistical package (20th edition, 2019, ©VSN International, Hemel Hempstead, UK).

2.5.2 Analysis of variance (ANOVA)

General analysis of variance (ANOVA) was applied to individual measurements for all the units used in the experiment, considering the variation due to replication, blocking and the difference between individual lines, in consecutive order using a nested treatment structure (Block/Unit). The least significant difference (LSD) was set at the 5% level of significance. To conduct the analysis, the GenStat statistical package (20th edition, 2019, ©VSN International, Hemel Hempstead, UK) was used. Residual plots and Mean plots calculated by the software were used to assess the normality of the data.

Chapter 3: Wheat RHT-1 protein interacts with INDETERMINATE DOMAIN 11 (TaIDD11) and ETHYLENE RESPONSIVE FACTOR 5 (TaERF5)

3.1 Introduction

DELLAs are the master regulators of GA responses and GA signalling leads to degradation of DELLA proteins. This degradation results in activation of many GA-regulated genes, allowing for GA-mediated processes to occur. However, DELLAs do not have a conserved DNA-binding domain and it has been established that they regulate GA-mediated gene expression by interacting with transcription factors (TFs) and either acting as their coregulators or sequestering them, hence rendering them inactive (reviewed in detail in Thomas *et al.*, (2016)). Much research has been done to understand GA biosynthesis and signalling that leads to DELLA degradation, but there are still significant gaps in our knowledge of GA signalling downstream of DELLAs. In this study, we aim to identify wheat DELLA, RHT-1, interactors that may have a potential role in regulating GA signalling in the aleurone of wheat. Cereals aleurone has been used as convenient tissue to study GA signalling as it is easy to isolate, it does not synthesize GAs and its GA-responsiveness can be easily measured by conducting α -amylase assays. *α -amylase* gene expression is directly regulated by the GAMYB TF (Gubler *et al.*, 1995). In the aleurone, GA has been shown to upregulate *GAMYB* expression via DELLA (Gubler *et al.*, 2002), however, this regulation is hypothesized to be regulated via another protein or proteins (Sun & Gubler, 2004). In order to identify the putative TFs that bind to wheat DELLA protein and may have a role in regulating the aleurone response, we conducted yeast two-hybrid (Y2H) screening of a cDNA library generated from wheat aleurone RNA, using RHT-1 as a bait.

3.1.1 Yeast two-hybrid screening as a tool to detect protein-protein interactions

Yeast two-hybrid (Y2H) is a genetic method of screening for protein-protein interactions (PPI) in living cells. It was developed by Fields and Song in 1989, following the discovery of the modular structure of Gal4 transcriptional activator in yeast (Keegan *et al.*, 1986). The modular structure of Gal4 was exploited to study PPI applying a very simple concept. The DNA-binding and transactivating domains of Gal4 are separated, linked to the two proteins whose interaction is being studied, and the functional Gal4 transcription factor is only reconstituted upon protein binding, which can be monitored by reporter gene expression. This method is a preferred method of studying protein-protein interactions because it is relatively simple, can be carried out in a lab using inexpensive reagents and its results are relatively easy to interpret. Other advantages are that it can be used to detect interaction between proteins originating from different organisms, there is no size limit (entire proteins or individual protein domains can be screened) and the assays are highly sensitive, allowing for even weak and transient interactions to be detected (reviewed in Brückner *et al.*, 2009).

The Y2H system is not only used to detect binary protein-protein interactions. It was modified so that it can be used for a genome-wide screen for interactors of a given bait. The classical Y2H cDNA library screen is used to search for pairwise interactions between defined protein of interest, the bait, and the proteins it interacts with, the preys, that are present in the pool of cDNA fragments cloned into the prey vectors. The fragments of cDNA in the prey clones from the library include whole ORFs (open reading frames) as well as random fragments of cDNA, and at the time of interaction identification, the nature of the interactor is unknown. Therefore, DNA isolation and a PCR amplification combined with sequencing and bioinformatics analysis is essential to identify the putative interactors.

However useful, Y2H has some limitations. In order for the system to work, the interaction must occur in the yeast nucleus and the bait protein must not be a potent transcriptional activator itself (Fields & Song, 1989). Additionally, there is also an issue of non-physiological level of protein expression and absence of necessary cofactors and chaperones needed for proper function and translocation of bacterial proteins into the yeast nucleus (Stellberger *et al.*, 2010). Membrane proteins, proteins that cannot enter the nucleus and protein fusions that are toxic or unstable in yeast cannot be studied using Y2H assay. Moreover, all interactions that depend on post-translational events that do not occur in yeast will not be detected. Also, all the interactions that rely on a free N terminus will be blocked if this end of a protein is fused to the transcription factor GAL4 functional domain (Mehla *et al.*, 2017).

One of the most common problems of Y2H are non-specific interactions which generate false positives. This problem can be mitigated by applying rigorous experimental conditions, like for example using 3-aminotriazole (3-AT), a competitive inhibitor of the *HIS3* reporter gene product. Selection for two reporter genes is also advised to correctly assess the interaction. Activating two reporter genes requires more solid transcriptional activation and increases the stringency of the assay. Another common problem with Y2H is self-activation of the bait construct which leads to activation of transcription of a reporter gene in the absence of interacting prey protein. This can often be resolved by using truncated versions of the bait protein that lack the transactivation domain.

Taken together, the Y2H screen is a relatively easy and inexpensive high-throughput method of detecting PPI *in vivo*. It is a preferred method of identifying binary PPI in the nucleus, and since our aim is to identify factors interacting with DELLA to activate transcription, it is the most convenient method to use in our study.

3.1.2 Y2H screens identified multiple TFs as DIPs

Although DELLAs are known to regulate gene expression, no DNA-binding domain has been identified in their structure (Hirano *et al.*, 2012; Zentella *et al.*, 2007). It has been demonstrated that DELLAs function through their physical association and regulation of multiple downstream proteins, including different classes of TFs. Y2H PPI assays have been extensively used to confirm the binary interaction between DELLAs and DIPs (reviewed in Chapter 1, Section 1.6.4). Y2H screens in turn have been used to screen cDNA libraries to reveal different classes of DELLAs interactors. One such study conducted by Marín-de la Rosa *et al.* (2014) determined the TF interactome of Arabidopsis DELLA protein GAI. A library containing approximately 1200 TFs, representing ~75% of all Arabidopsis TFs, was screened with the GRAS domain of GAI and led to the identification of 57 unique TFs belonging to 15 distinct families, with no strong bias for any particular family. Among them were bHLH, TCP (TEOSINTE BRANCHED 1 [TB1], CYCLOIDEA [CYC], and PROLIFERATING CELL FACTOR [PCF]), AP2 (APETALA2), MYB, NAC (NO APICAL MERISTEM [NAM], ATAF1–2, and CUP-SHAPED COTYLEDON [CUC2]), Zinc finger and bZIP TFs, that were categorised to be involved in many processes, including vegetative and reproductive development, germination, stress responses, light signalling, and hormone signalling. Their results showed that GAI interacts with many structurally diverse TFs, suggesting that DELLAs act as central signalling hubs connecting different signalling pathways. In the same study, to validate the functional significance of the screen results, the group decided to search for TFs involved in GA signalling and regulation of photomorphogenesis. RELATED TO APETALA2.3 (RAP2.3), a member of group VII of ERFs was identified as DIP (Marín-de la Rosa *et al.*, 2014) and DELLA-RAP2.3 interaction was shown to inhibit RAP2.3-mediated gene expression, suggesting the role of DELLA as a point of crosstalk between GA and ethylene signalling pathways in regulation of apical hook development.

Based on Y2H screen studies, an important mechanism regulating GA signalling in Arabidopsis root endodermis has been elucidated. Yoshida *et al.* (2014)

conducted a Y2H and Y1H screens using GRAS domain of RGA protein and cDNA library containing ~75% of Arabidopsis TFs, and identified five members of IDD TF family (AtIDD3, 4, 5, 9 and 10) as DIPs that bind to *SCARECROW-LIKE PROTEIN 3 (SCL3)* promoter. SCL3 is a tissue-specific positive regulator of the GA pathway in the root endodermis, and it acts by antagonising DELLA (Zhang *et al.*, 2011). SCL3 expression was shown to be positively regulated by DELLA (Heo *et al.*, 2011). Yoshida *et al.* (2014) showed that RGA and SCL3 use IDD proteins as transcriptional scaffolds to bind to DNA and activate and repress, respectively, the expression of SCL3. In fact, RGA and SCL3 were found to compete for IDD protein binding. Based on these results a model of gene expression regulation in the root endodermis was proposed in which DELLA, SCL3 and IDD proteins cooperate to control GA signalling during root development (Yoshida *et al.*, 2014).

A Y2H screen was used to understand the molecular mechanism through which GA signalling controls stem elongation in Arabidopsis (Davière *et al.*, 2014). cDNA library from inflorescence shoot apices was screened using N-terminally truncated RGA as bait, and TCP14 was identified as a potential DIP through which GA may regulate cell division. Further studies showed that DELLAs sequester TCP14 and by doing so inhibit expression of core cell-cycle genes such as *CYCA2;3*, *CYCB1;1*, *PCNA2*, and *RETINOBLASTOMA-RELATED 1 (RBR1)*. The results obtained in this study demonstrated that GAs regulate cell division in inflorescence shoot apices via suppression of DELLA and thus increased expression of genes controlling cell division (Davière *et al.*, 2014).

Recently, Y2H was used to obtain an overview of the spectrum of TFs that interact with two DELLA proteins in Arabidopsis, RGA and GAI (Lantzouni *et al.*, 2020). They screened a collection of 1956 Arabidopsis TFs (Pruneda-Paz *et al.*, 2014) and found that both DELLAs interact with 261 distinct TFs (86.6% of these were common for both DELLAs) belonging to 51 different TF families, which again shows the multitude of interactions, and possibly processes, that DELLAs mediate. To better understand the GA-mediate gene regulation in response to cold, the group searched for DELLA-interacting TFs whose

transcription is GA-regulated after a cold treatment. They identified GROWTH-REGULATING FACTORS (GRFs) as potential factors that mediate GA response to cold. Interestingly, the GRFs represented the TF family with the biggest number of members, proportionally, identified as DIPs. Using lines with low and high GRF levels, it was shown that DELLA and GA regulate cold-induced growth via GRF function. Moreover, GA biosynthesis and signalling genes: *GA20ox1*, *GA2ox1*, *GA2ox8*, *RGL1*, and *RGL2* were found to be differentially expressed in *GRF* over-expressor lines which further confirmed the involvement of GRFs in GA-regulated processes.

The examples cited here show that Y2H screening followed by functional studies is an established method of identifying novel components of signalling pathways.

3.1.3 Objectives

GA signalling in the aleurone results in activity of an α -amylase enzyme that breaks down starch to facilitate heterotrophic growth of the embryo. The *TaAMY1* gene, that encodes α -amylase, is regulated at transcriptional level by GAMYB, whose activity in turn is indirectly regulated by DELLA protein (Gubler *et al.*, 1995, 2002; Sun & Gubler, 2004). The hypothesis is that DELLA regulates GAMYB activity in a complex with a TF. The aim of this work was to identify DIPs that are potentially involved in GA signalling in the aleurone, acting downstream of DELLA. To achieve this aim, a Y2H screen using RHT-1 as bait, followed by identification and an *in silico* functional analysis of the putative interactors was performed. This Chapter reports screening the cDNA library constructed from wheat (cv. Cadenza) aleurone mRNA, with the wheat DELLA protein, RHT-1, in an attempt to elucidate downstream components of GA signalling in the aleurone cells. To aid establishing which putative DIPs may be involved in GA response, the KnetMiner online tool (Hassani-Pak *et al.*, 2020) combined with available literature searches was conducted.

Representatives of various protein classes were identified as putative RHT-1 binding partners. Among the TF classes that were identified in this study, two TFs were selected for further analysis: INDETERMINATE DOMAIN 11 (TaIDD11) and ETHYLENE RESPONSE FACTOR 5 (TaERF5). RHT-1 was found to interact with TaIDD11 and TaERF5 in both genetic and *in planta* studies. Our results provide further insight into the GA signalling in the aleurone of wheat and reinforce the findings that DELLA may potentially be a point of crosstalk between GA and ethylene signalling.

3.2 Material and Methods

3.2.1 Yeast two-hybrid screen

The bait plasmid containing truncated RTH-D1A (TraesCS4D02G040400) protein was tested for self-activation according to the Invitrogen ProQuest™ Two-Hybrid System Version A section “Testing Bait” by another student in the lab. Once the 3-AT concentration was established, the screen was performed.

The wheat aleurone prey cDNA library that was used in this study was generated from mature wheat (*Triticum aestivum*) cv. Cadenza grains. The mature grains were de-embryonated, and aleurone isolated from half-grains after three-day incubation in a 20 mM CaCl₂ buffer. Total RNA was extracted from the aleurone layers and the cDNA prey libraries constructed by Life Technologies Corporation (Dr Stephen Thomas, personal communication).

A 250 µl aliquot (over 1×10⁶ transformants) of Library scale *MaV203* competent cells (Thermo-fisher Scientific, California, USA) was mixed with 10 µg of the RHT-D1A bait plasmid, 10 µg of the wheat aleurone cDNA prey library and 1.5 ml of PEG/LiAc solution (supplied with the competent cells). The transformation mix was incubated at 30°C for 30 minutes, then mixed with 88 µl DMSO (Sigma-Aldrich, Darmstadt, Germany) and heat-shocked at 42°C for 20 minutes. Cells were then spun down at 400 x g for 5 minutes and resuspended in 8 ml of sterile 0.9% NaCl. Transformed cells were plated out onto 15-cm SD-Leu-Trp-His + 25 mM 3-AT (3-Amino-1,2,4-triazole) agar plates in 400 µl aliquots and incubated at 30°C for three days. After three days, single colonies were streaked onto SD-Leu-Trp plates and incubated at 30°C for 48 hours. Glycerol stocks of all colonies were made, and these glycerol stocks were subsequently plated in the same grid and the same order onto SD-Leu-Trp plates, generating the master plates.

3.2.2 Yeast two-hybrid interaction study

To confirm an interaction between two proteins, bait and prey plasmids were co-transformed into the *MaV203* yeast cells as described in Chapter 2, section 2.2.3, and His auxotrophy and X-gal assays were conducted.

3.2.2.1 His auxotrophy assay

Typically, a small proportion of a single colony of yeast was inoculated into 200 μ l of sterile distilled water, mixed, and 5 μ l of the mix spotted onto the plates. The colonies were grown on a SD-Leu-Trp-His medium supplemented with 10 mM, 25 mM, 50 mM, 75 mM or 100 mM of 3-AT. Three biological replicates for each strain were plated in a grid format. Once the cultures had dried onto the medium, the plates were incubated at 30°C for 48-72 hours, after which they were photographed and assessed for differences in growth levels. Assays were scored based on the levels of visible growth for each strain.

For the screen, the assay was set up in the same way as described above with 3-AT concentrations being: 25 mM, 37 mM, 50 mM and 75 mM. The master plates were generated containing 52 colonies per plate (nine colonies for the last plate), incubated at 30°C for 48 hours and replica-plated onto various selective plates. The interaction was assessed after three days of incubation.

3.2.2.2 X-gal assay

Colonies were streaked onto YPD plates with a 100 mm x 100 mm Amersham Protran supported 0.2 μ m nitrocellulose membrane (GE healthcare life sciences, Buckinghamshire, UK), and incubated at 30°C for 24 hours. After incubation, the nitrocellulose membranes were frozen in liquid nitrogen for 30 seconds and placed on foil to thaw. The membrane was then placed on 2-mm sterile filter paper soaked in 5 ml of Z buffer (60 mM Na₂HPO₄, 40 mM NaH₂PO₄, 10 mM KCl and 1 mM MgSO₄) mixed with 1 μ g/ml ortho-nitrophenyl- β -galactoside (ONPG) and 30 μ l 2-Mercaptoethanol, and incubated at 37°C for 24 hours. Colour of the colonies was assessed visually at 2, 6 and 24 hours of incubation.

3.2.3 Identification of prey clones

Prey clones were identified by PCR amplification from yeast plasmid preparations or by retransformation of the plasmid followed by amplification in *E.coli*. If the prey clone DNA was required for further studies, a retransformation assay was necessary, as plasmid DNA yields from yeast were very low. All sequencing and PCR reactions were performed using recommended pDEST22 forward (TATAACGCGTTTGGGAATCACT) and reverse (AGCCGACAACCTTGATTGGAGAC) primers.

The plasmid DNA was extracted from yeast colonies as described in Chapter 2, Section 2.2.5 and subjected to PCR amplification. The amplicons were separated by gel electrophoresis, and if one band was observed, indicating presence of one amplicon, this was sequenced directly without further purification. If additional fragments were visible on the gel, the bands were excised, purified and sequenced.

The plasmid DNA isolated from yeast colonies was retransformed to bacterial cells as described in ProQuest™ Two-Hybrid System Protocol. The plasmid isolated from *E.coli* was digested with the *Bsr*GI enzyme (NEB, Hitchin, UK), which has three recognition sites on the pDEST22 backbone, not including the fragment between the attR1 and attR2. Therefore, when the prey clone is digested with *Bsr*GI, it is expected to generate two fragments originating from the pDEST22 vector backbone (1094 bp and 6011 bp in size), and one or more bands resulting from the digest of the cDNA fragment cloned into the prey clone. The presence of a cDNA inserts containing additional *Bsr*GI sites can therefore be mapped by restriction mapping and then sequenced.

3.2.4 Generating the expression vectors for bimolecular fluorescence complementation (BiFC)

Full gene coding sequences (CDS) of *TaERF-A5a* (*TraesCS2A02G4171002*) was amplified from a prey vector extracted from yeast colony number 7. *TaIDD-*

A11 (*TraesCS2A02G188400*) gene was synthesized by GenScript (GenScript Biotech, Netherlands) and codon optimized for expression in tobacco (*Nicotiana benthamiana*). The *Rht-D1a* (*TraesCS4D02G040400*) sequence used in a study was a full CDS of a wheat gene, amplified from a plasmid generated previously by another member of the group. In order to clone genes into destination vectors, Gateway cloning was used. Destination vectors used in this study were previously reported in Kamigaki *et al.* (2016). Vectors AB830561 (pB5cRGW), AB830564 (pB5GWcR), AB830568 (pB5GWnR) and AB830572 (pB5nRGW), encoding split red fluorescent protein were used.

3.2.5 Transient gene expression by *Agrobacterium tumefaciens* infiltration

Tobacco (*Nicotiana benthamiana*) plants were grown in the glasshouse environment (23°C day/ 18°C night, 30% average humidity, 16-hour day length with supplementary lighting when sunlight radiation dropped below 175 W/m²) for about six weeks. At that stage, the plants containing at least three appropriate size, healthy leaves were chosen for inoculation. *Agrobacterium* cultures harbouring the fusion gene of interest were grown overnight in 2YT media containing 50 µg/ml Rifampicin, 25 µg/ml Gentamicin and 100 µg/ml Spectinomycin (in case of p19 plasmid 50 µg/ml Kanamycin instead of Spectinomycin). 1 ml of the culture was centrifuged at 1,505 x g for 5 minutes and the cell pellets were resuspended in infiltration medium (28 mM D-glucose, 50 mM MES, 2 mM Na₃PO₄·12H₂O and 100 µM Acetosyringone) to the OD₆₀₀ of 0.1. Appropriate pairs of cell suspensions, together with the suspension of cells transformed with the p19 plasmid were mixed in 1:1:1 ratio. The mixtures were infiltrated into the abaxial side of the tobacco leaves using 1 ml syringes (BD Plastipak Syringes 1ml, Medisave, Weymouth, UK) followed by a three-day incubation. After the incubation period, the infiltrated leaves were visualised using confocal microscopy.

3.2.6 Microscopic observation

Inoculated tobacco leaf explants were examined under Zeiss LSM 780 laser confocal microscope (Carl Zeiss Microscopy GmbH, Jena, Germany) using Leica Application Suite X (LAS X) software. To detect the reconstituted signals from YFP and mRFP1 emission eYFP and DsRed filters were used, respectively. To remove background fluorescence of the chloroplasts, the DsRed filter wavelength spectrum was shifted to 561 nm.

3.3 Results

3.3.1 Identification RHT-D1A interactors using Y2H screen

One of the main objectives of this project was to establish RHT-1 interactors in the aleurone of wheat grain and investigate their potential roles controlling GA responses. To identify RHT-1 interacting proteins in aleurone cells, a Y2H screen was conducted, using a truncated RHT-D1A (Δ RHT-D1A) as bait, as the presence of the N-terminal regulatory domain causes increased self-activation. The full-length CDS of *Rht-D1a* is 1872 bp, encoding a protein of 623 amino acids. The fragment cloned into the bait vector included nucleotides 652–1872 (Figure 3.1) and the encoded protein Δ RHT-D1A was lacking the self-activating N-terminal regulatory domain, but contained the intact functional GRAS domain, which is required for the interaction with downstream transcription factors (Van De Velde *et al.*, 2017). Therefore, it was assumed that this form of the RHT-D1A protein can interact with downstream GA signalling components. Another method for overcoming self-activation of bait proteins in the Y2H assays is to use higher concentrations of 3-Amino-1,2,4-triazole (3-AT), the competitive inhibitor of the *HIS3* gene product. The concentration of 3AT chosen for the screen was 25 mM. The Δ RHT-D1A, however, still showed some degree of self-activation on the 25 mM 3AT medium (Figure 3.6).

The screen was conducted as described in the Methods section (3.2.1). In total, 269 colonies were transferred onto 10 cm SD-Leu-Trp plates in a 52-cell grid (Figure 3.2 C). Master plates containing 52 colonies each (except for the sixth plate, onto which nine colonies were streaked; Figure 3.2 A, B) were generated for replica plating and used in histidine auxotrophy and X-gal assays.

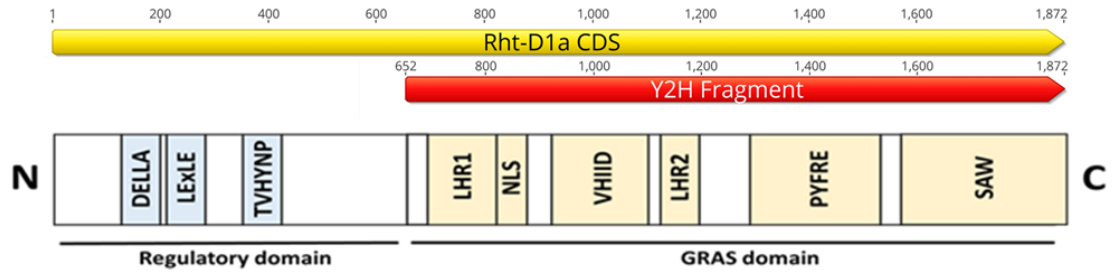


Figure 3. 1 Alignment of the full length *Rht-D1a* CDS (yellow) and a CDS fragment used in the Y2H screen (red) compared with the model of the DELLA protein with all the functional domains annotated. The fragment was cloned into the bait plasmid, *pDEST32*, and used in the cDNA library screen, because the regulatory domain that is contained in the N terminus of the protein causes self-activation of the Y2H system. The fragment cloned into the bait vector contains the functional GRAS domain that is sufficient for binding the interacting protein.

The strength of the interaction between Δ RHT-D1A bait and 269 potential interactors from the prey clones was assessed using two assays, histidine auxotrophy and X-gal. Both assays rely on the expression of the reporter genes, *HIS3* and *LacZ*, respectively. Replica plating was used to transfer all colonies from the master plates on SD-Leu-Trp-His + various concentrations of 3-AT (0, 25, 37, 50 and 75 mM), and on the YPD plates with nitrocellulose membrane, which were subsequently used in the X-gal assay. The results of the assays are presented in Figure 3.2 A and B. The growth on the medium supplemented with 75 mM 3-AT and colonies incubated with X-gal for 24 hours are shown.

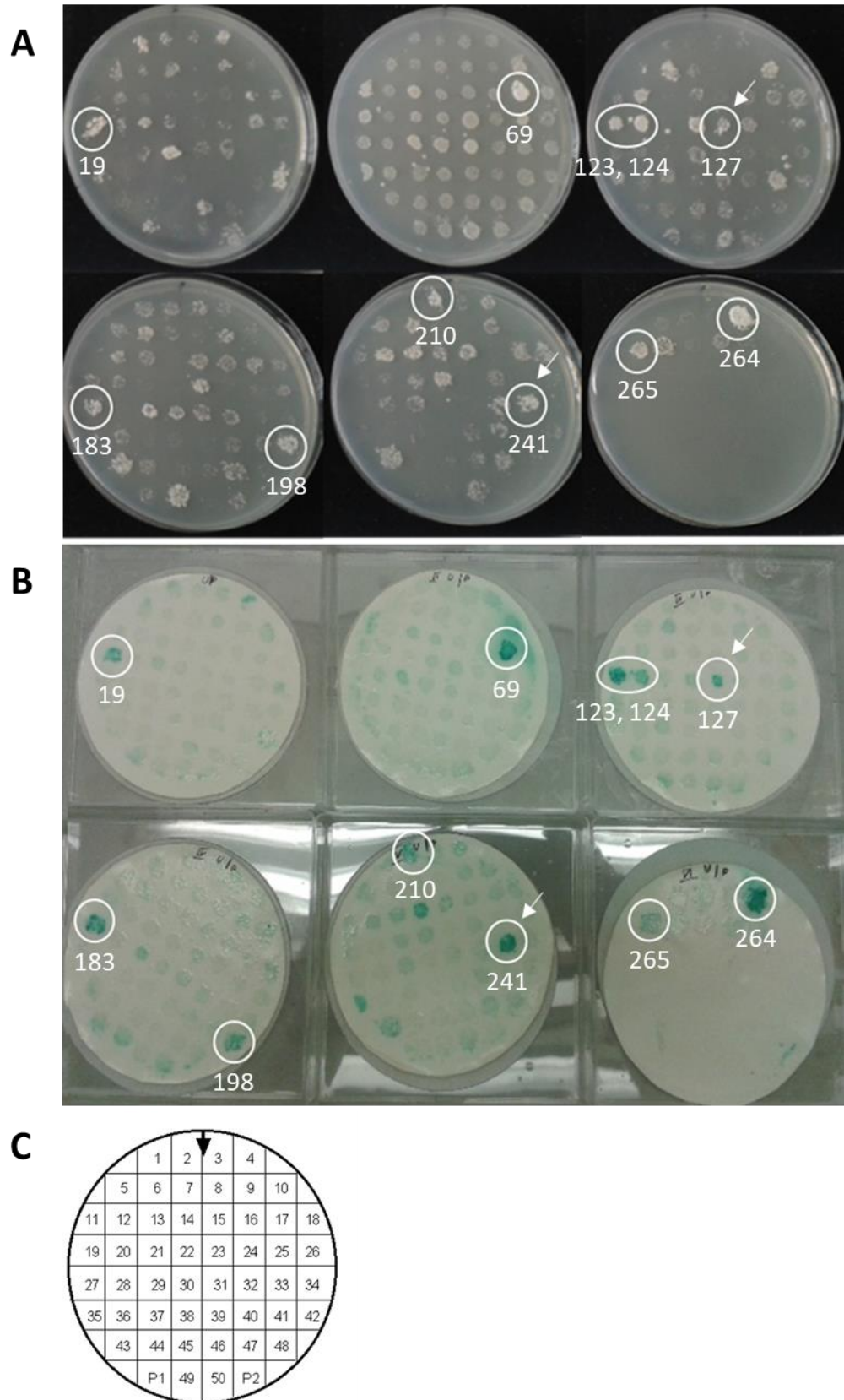


Figure 3. 2 Results of the histidine auxotrophy and X-gal assays of the putative DIPs identified in the Y2H screen. The colonies encircled in white are the strong interactors that were identified in both assays. Arrows indicate the homoeologues of interactor

TalIDD11. A. Histidine auxotrophy assay for all colonies identified in the cDNA library screen. Growth shown on SD-Leu-Trp-His + 75-mM 3-AT. The extent of growth indicates strength of the interaction. B. X-gal assay. The intensity of the blue colour indicates the strength of interaction between the Δ RHT-D1A protein and the potential interactor. C. The grid used when generating master plates. 52 yeast colonies containing prey clones were streaked onto one master plate (six in total) and used for replica plating. Plates one to five contain 52 colonies and sixth plate nine colonies.

Table 3. 1 Identity of the prey cDNA clones identified as encoding strong Δ RHT-D1A interactors in Y2H assays.

| Clone number | IWGSC RefSeq v1.0 gene accession number | Predicted gene product |
|--------------|---|---------------------------------------|
| 19 | TraesCS2B02G153800 | rho GTPase-activating 7-like |
| 69 | TraesCS3D02G115300 | heat-shock protein |
| 123 | TraesCS7B02G088600 | heat-shock protein |
| 124 | TraesCS6B02G028600 | component 3 of pyruvate dehydrogenase |
| 127 | TraesCS2B02G218900 | INDETERMINATE domain 11 (IDD11) |
| 183 | same as 123 | |
| 198 | TraesCS6B02G299800 | soluble inorganic pyrophosphatase |
| 210.1 | TraesCS3B02G529300 | beta-1,3-glucanase |
| 210.2 | TraesCS5B02G317000 | 6-phosphogluconolactonase |
| 210.3 | TraesCS2A02G291700 | aspartate kinase |
| 241 | TraesCS2A02G188400 | INDETERMINATE domain 11 (IDD11) |
| 264 | same as 69 | |
| 265 | TraesCS7B02G145800 | transcription factor bHLH130-like |

The extent of growth of the colonies on the SD-Leu-Trp-His +75 mM 3-AT medium provides an indication of the strength of interaction. Similarly, the intensity of the blue colour of the colony following the X-gal assay indicates increased expression of the *LacZ* gene, and hence the interaction between the two proteins. 11 putative interactors were identified to interact strongly with Δ RHT-D1A. Their gene accession numbers, and function based on *in silico*

analysis are summarised in Table 3.1. Among the 11 strong interactors, two TFs were identified: two IDD TFs, that are products of homoeologous genes (same gene encoded by separate genomes in wheat) and a bHLH TF.

The Y2H assays performed on putative DIPs pulled out in the Y2H screen revealed the strong interactors, nevertheless we decided to sequence all putative interactors identified in the screen, as weaker interactors may also play a role in regulating the GA response in the aleurone.

3.3.1.1 Identification of prey cDNA clones

Prey plasmids were isolated from yeast cells and either used in the PCR reaction to amplify the cDNA clone in the prey plasmid, or retransformed into *E.coli* cells, then purified and sequenced. Due to the substantial workload, bacterial retransformation was performed only for selected prey clones: for all the homoeologues of the genes that were selected for further analysis, and for the ones that either did not amplify during PCR, or showed multiple bands and could not be resolved by gel electrophoresis. PCR amplicons and prey plasmids containing putative DIP cDNA were sequenced and the sequence used to identify the corresponding wheat genes that they were derived from.

The identified prey clones were grouped based on the predicted function (Supplementary Table 3.1) and included TFs, enzymes, defence and heat shock proteins, and a collection of miscellaneous proteins and proteins of hypothetical or unknown function. As RHT-1 functions as a transcriptional regulator, the TFs were prioritised.

The largest TF group that was identified as potential Δ RHT-D1A interactors was the ethylene response factors (ERFs). Twelve different ERFs were identified, including homoeologues, and some of the interactors, as for example clone 4 or 7 were found multiple times. A second group of transcription factors that were represented in the screen were the zinc finger (ZF) proteins; 6 distinct ZF proteins were identified, including three IDD transcription factors, although in most cases the cDNAs from individual genes were only identified once.

Interestingly, all the identified IDD proteins were products of homoeologous genes in wheat. Other transcription factors groups identified included basic bHLH proteins (5 identified), MYB (3 identified), bZIP domain proteins (2 identified) and NAC (2 identified). A large proportion of identified DIPs were assigned as either hypothetical or unknown proteins. In total, 366 cDNA fragments extracted from 269 original individual yeast colonies were sequenced, and 248 distinct putative DIPs identified.

3.3.1.2 Selection of the putative interactors for further analysis

In order to determine if the identified interactors have a potential role in GA signalling during seed germination, the online tool KnetMiner (Hassani-Pak *et al.*, 2016, 2020) was used. KnetMiner is a simple and user-friendly online tool that gathers available published data about the plant model species *Arabidopsis* and a several staple crops, including wheat, rice, maize, and potato, and links them. It is then possible to identify the proteins of similar structures in *Arabidopsis*, the network of proteins they interact with, involvement in biological processes, known mutant phenotypes and the supporting publications. The tool identifies the genes that are involved in the process specified in the query and assigns a number in the “Evidence” column, the higher the collective number the stronger the evidence that the gene is involved in the process in question. In this search, the query phrase was “seed germination” and “gibberellin signalling during germination”, hence the genes that were assigned the highest score by the program were linked to these processes. The screenshots of the result tables (Figure 3.3) show only the first ten hits and for both queries they contain the same genes: NRPB5A (DNA-directed RNA polymerases II and IV subunit 5A), DPBF2 (also known as ABSCISIC ACID INSENSITIVE 5), SRK2G (serine/threonine-protein kinase), ERF5 and ERF1 (ethylene response factor 5 and 1) three bHLH proteins (87, 122 and 130), ELF3 (early-flowering 3) and RR21 (two-component response regulator).

“seed germination”

| ACCESSION | GENE NAME | SCORE | USER | EVIDENCE | Select |
|--|-----------|-------|------|-------------|--------------------------|
| TRIAE_CS42_2DL_TGACv1_161282_AA0557670 | NRPB5A | 91.19 | yes | 4 88 4 | <input type="checkbox"/> |
| TRIAE_CS42_3B_TGACv1_220594_AA0710320 | DPBF2 | 36.96 | yes | 2 4 67 4 | <input type="checkbox"/> |
| TRIAE_CS42_2DL_TGACv1_161348_AA0558130 | SRK2G | 25.17 | yes | 1 3 80 4 | <input type="checkbox"/> |
| TRIAE_CS42_2AL_TGACv1_093794_AA0286840 | ERF5 | 23.98 | yes | 2 75 5 | <input type="checkbox"/> |
| TRIAE_CS42_2DL_TGACv1_162279_AA0562340 | ERF1 | 23.74 | yes | 2 75 5 | <input type="checkbox"/> |
| TRIAE_CS42_7BS_TGACv1_591787_AA1921120 | BHLH130 | 23.48 | yes | 4 4 45 3 | <input type="checkbox"/> |
| TRIAE_CS42_7AS_TGACv1_569290_AA1812510 | BHLH122 | 23.43 | yes | 4 4 45 3 | <input type="checkbox"/> |
| TRIAE_CS42_1BL_TGACv1_030506_AA0092700 | BHLH87 | 22.71 | yes | 2 32 2 | <input type="checkbox"/> |
| TRIAE_CS42_1BL_TGACv1_030346_AA0087580 | ELF3 | 16.34 | yes | 8 9 95 10 | <input type="checkbox"/> |
| TRIAE_CS42_6BL_TGACv1_499730_AA1590220 | RR21 | 13.87 | yes | 8 10 59 5 1 | <input type="checkbox"/> |

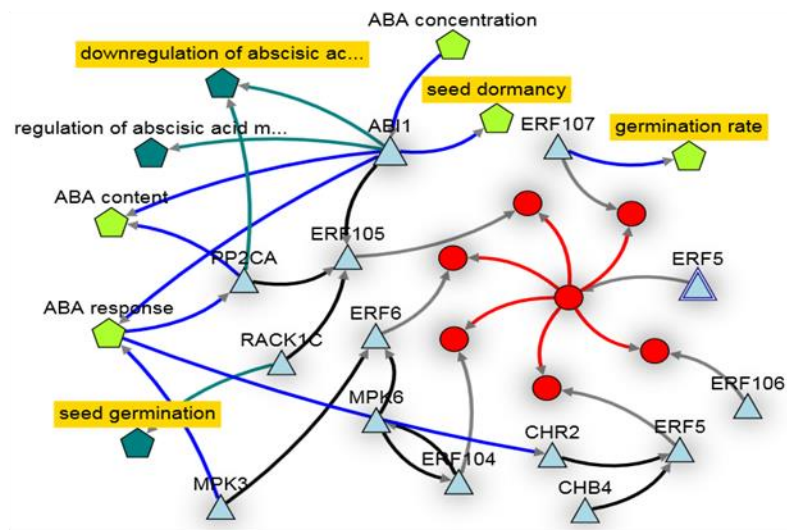
“gibberellin signalling during germination”

| ACCESSION | GENE NAME | SCORE | USER | EVIDENCE | Select |
|--|-----------|--------|------|---------------|--------------------------|
| TRIAE_CS42_1BL_TGACv1_030506_AA0092700 | BHLH87 | 0.00 | yes | 2 31 | <input type="checkbox"/> |
| TRIAE_CS42_3B_TGACv1_220594_AA0710320 | DPBF2 | 51.41 | yes | 4 9 97 2 2 | <input type="checkbox"/> |
| TRIAE_CS42_7BS_TGACv1_591787_AA1921120 | BHLH130 | 29.78 | yes | 6 76 1 | <input type="checkbox"/> |
| TRIAE_CS42_7AS_TGACv1_569290_AA1812510 | BHLH122 | 0.00 | yes | 6 76 1 | <input type="checkbox"/> |
| TRIAE_CS42_2DL_TGACv1_161282_AA0557670 | NRPB5A | 76.96 | yes | 3 96 2 | <input type="checkbox"/> |
| TRIAE_CS42_6BL_TGACv1_499730_AA1590220 | RR21 | 8.17 | yes | 7 2 22 1 80 1 | <input type="checkbox"/> |
| TRIAE_CS42_2AL_TGACv1_093794_AA0286840 | ERF5 | 106.81 | yes | 3 207 4 | <input type="checkbox"/> |
| TRIAE_CS42_2DL_TGACv1_162279_AA0562340 | ERF1 | 105.72 | yes | 3 207 4 | <input type="checkbox"/> |
| TRIAE_CS42_1BL_TGACv1_030346_AA0087580 | ELF3 | 12.59 | yes | 6 170 2 | <input type="checkbox"/> |
| TRIAE_CS42_2DL_TGACv1_161348_AA0558130 | SRK2G | 112.37 | yes | 3 191 3 | <input type="checkbox"/> |

| | | | | | | | | | | | | | | | |
|------|---------|---------|-----|--------|----------|-------------|---------------|-----------|------|---------------|-----------------|----------------|----------------|-----------------------|------|
| | | | | | | | | | | | | | | | |
| Gene | Protein | Pathway | SNP | Enzyme | Reaction | Publication | Mol. Function | Phenotype | DGES | Biol. Process | Cell. Component | Protein Domain | Trait Ontology | Enzyme Classification | GWAS |

Figure 3. 3 KnetMiner results tables. Top ten genes identified by KnetMiner as having a role in “seed germination” (top table) or “GA signalling during germination” (bottom table). Each gene is assigned a score and evidence. The explanation of the icons in the “Evidence” column is included in the legend below the tables. At the time of the analysis the wheat genome assembly available on Ensemble Plant was TGACv1, therefore the accession numbers for the genes shown in the table correspond to the TGACv1 assembly.

7 – ERF5



9.1– IDD11

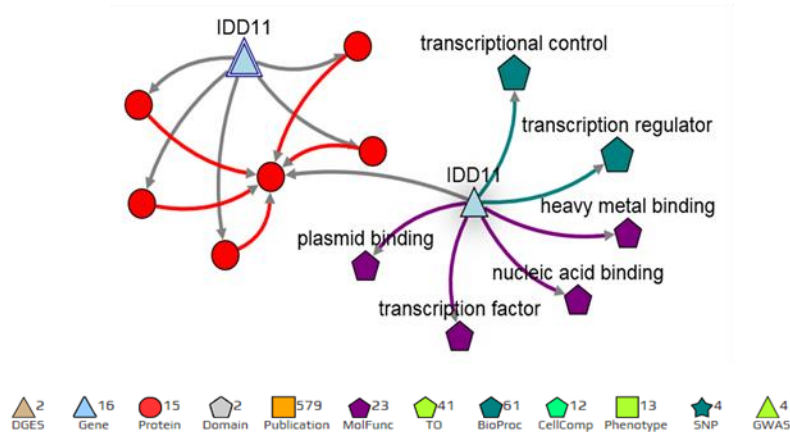


Figure 3. 4 KnetMiner networks for *TaERF5* and *TaIDD11*. The legend at the bottom explains the meaning of icons. Arrows colours meaning: grey = encodes, red = orthologue, black = has physical interaction, dark green = participates in, blue = co-occurs with, purple = has function in. Some icons were removed for a clearer depiction of interactions between genes and processes they are involved in. The maps were generated on 27th October 2017.

Networks for all putative interactors that were assigned any evidence were studied in detail. After more thorough analysis of the gene networks and the supporting literature, the interactors that were selected for further analysis

were TaERF5 (interactor 7) and TaIDD11 (interactor 9.1). The Knetminer networks for the chosen interactors are depicted in Figure 3.4. For TaERF5 wheat protein, there are six highly similar proteins in Arabidopsis: ERF5, ERF6, ERF104, ERF105, ERF106 and ERF107. ERF105 is shown to interact with ABI1 (abscisic acid (ABA)-INSENSITIVE1 protein phosphatase 2C) and PP2CA (protein phosphatase 2CA), which both regulate abscisic acid (ABA) content and ABA response, and with RACK1C (receptor for activated C kinase 1C) that has a function in seed germination. ERF6 interacts with MPK3 (mitogen-activated protein kinase 3), involved in ABA response, and MPK6. One of the proteins in Arabidopsis, ERF107, is shown to have a function in a biological process defined as “germination rate”. There is therefore little evidence linking structurally similar ERF proteins in Arabidopsis to GA and ABA signalling and to the process of germination. Little information was shown in the network for the interactor identified as TaIDD11. It was only assigned a function as a transcription factor having a role in transcriptional control.

TaERF5 was pulled out multiple times in the study, suggesting high abundance of its transcript in the aleurone. It was also listed in the top ten results returned by KnetMiner searches among genes linked to the process of GA signalling and germination (Figure 3.3). Putative DIP identified as TaIDD11, although not listed in the top KnetMiner results, was of interest due to recent reports suggesting that IDD TF family members regulate GA-mediated gene expression using DELLAs as coactivators (Fukazawa *et al.*, 2014; Yoshida *et al.*, 2014). Therefore, these two TFs were selected for further analysis.

3.3.2 Confirmation of the interaction between RHT-D1A and TaERF-A5 and TaIDD-D11

It is important to confirm that the prey cDNA clones identified in the Y2H library screen encode Δ RHT-D1A interactors in yeast to ensure that the interaction is occurring between Δ RHT-D1A and the DIP of interest, and not another clone that might have been present in the yeast strain. The

confirmation of interaction between the bait protein and the identified prey interactor was performed for TaERF5 and TaIDD11. Yeast cells were transformed with bait plasmid encoding truncated RHT-D1A protein and prey plasmids encoding *TaERF-A5a* (WT A homoeologue of *TaERF5*) or *TaIDD-D11a* (WT D homoeologue of *TaIDD11*) fragments identified in the screen (Figure 3.5), as described in Materials and Methods Section 2.2.3. For all interaction tests, the histidine auxotrophy and X-gal assays were performed (Figure 3.6).

The strong positive control exhibits growth at high concentrations of 3-AT (100 mM). In contrast, the negative controls' growth was inhibited on medium supplemented with 10 mM 3-AT. The Δ RHT-D1A bait alone resulted in quite a high level of self-activation; the strain being capable of growing at 25 mM 3-AT. The strain co-transformed with the bait and TaERF-A5A prey plasmids did not grow on 100 mM, but the growth was considerable on 75 mM (Figure 3.6 A). The blue colour developed in the X-gal assay was less intense than that of the strong control, but more intense than the weak positive control. Strains co-transformed with the bait and TaIDD-D11A prey plasmids displayed growth on the medium containing 100 mM 3-AT indicating a strong interaction (Figure 3.6 B), which was confirmed in the X-gal assay. Taken together, these results indicate that Δ RHT-D1A interacts with both TaERF-A5A and TaIDD-D11A in the yeast cells.

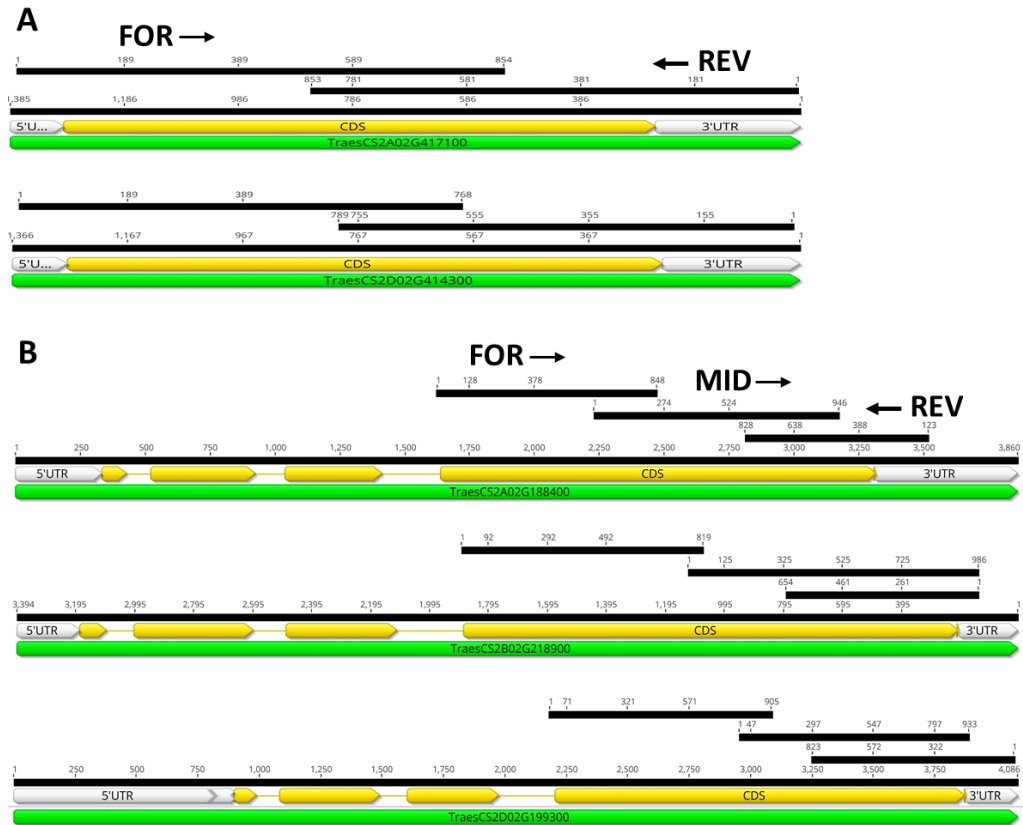


Figure 3.5 The cDNA fragments of *TaERF-A5* and *TaIDD-D11* genes cloned into *pDEST22* prey vectors pulled out in the Y2H screen. Prey clones were sequenced with the Invitrogen recommended sequencing primers (FOR and REV). All CDS sequences were in frame with GAL4 activation domain. A. *TaERF5* cDNA fragments sequenced from the prey clones 7 and 57.2. These interactors were identified as two homoeologues of the same gene, originating from the A and D genome, respectively. In both cases, the complete predicted CDS of the gene, along with the majority of the 5' and 3' untranslated regions (UTRs) were present in the cDNA clones. B. *TaIDD11* cDNA fragments sequenced from interactors 127.2, 241 and 9.1. The interactors are homoeologues of the same *TaIDD11* gene. In each of the three prey plasmids, the fragment encoding the last exon with a fragment of the 3' UTR was cloned. Prey clones were sequenced with the Invitrogen recommended sequencing primers (FOR and REV) and with sequence specific MID primers. Annotations: green - genomic sequences, yellow – CDSs, white – UTRs and black – nucleotide sequences and the fragments sequenced from the prey plasmids.

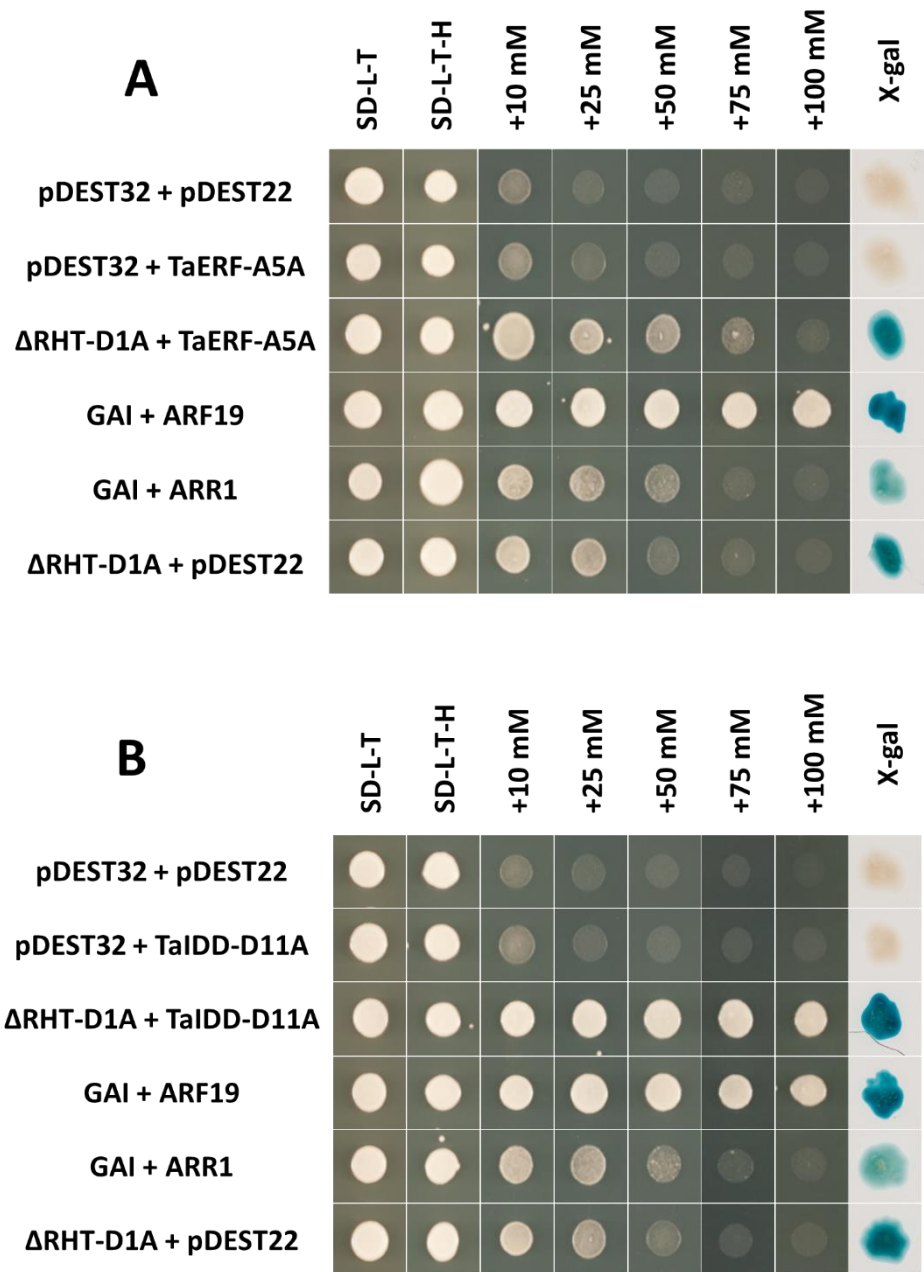


Figure 3. 6 Interaction study between Δ RHT-D1A and the prey clones TaERF-A5A and TaIDD-D11A. A. Y2H assays for Δ RHT-D1A-TaERF-A5A interaction. B. Y2H assays for Δ RHT-D1A-TaIDD-D11A interaction. Each panel shows results of the histidine auxotrophy and X-gal assays. Colonies were incubated on SD-Leu-Trp medium, supplemented with 10, 25, 50, 75 and 100 mM of 3-AT. Pictures were taken after three days of incubation. For X-gal assay, the intensity of the blue colour indicates presence of β -galactosidase, one of the reporter genes, and thus the interaction. Pictures were taken 24 hours after the incubation with ONPG.

3.3.3 Phylogenetic analysis of the RHT-D1A interactors, TaERF5 and TaIDD11

The gene phylogeny for both identified DIPs was investigated. First, the members of each of the AP2/ERF and IDD gene families in Arabidopsis and rice were identified (Colasanti *et al.*, 2006; Nakano *et al.*, 2006). Due to the size of the AP/ERF family (122 and 139 AP/ERF family members in Arabidopsis and rice respectively), the phylogenetic analysis was performed using only the members of the ERF family subgroup IXb, which TaERF5 homologs belong to. The protein sequence of each of the family, or family subgroup member (Supplementary Tables 3.2 and 3.3) was used to search the wheat proteome to identify the most similar proteins in wheat using BLAST option in Ensemble Plant (IWGSC) (Zerbino *et al.*, 2018). Arabidopsis, rice and the identified wheat sequences were then aligned using MUSCLE alignment plugin in Geneious v10.2 (Edgar, 2004) and the alignment used to calculate the phylogenetic tree using PhyML plugin (Guindon *et al.*, 2010) set to default settings.

3.3.3.1 Phylogenetic analysis of group IX of ERF transcription factors in wheat

The AP2/ERF superfamily in Arabidopsis can be subdivided into AP2, ERF and RAV families, and a standalone *At4g13040* gene. The ERF family contains 122 genes and can be further subdivided into CBF/DREB and ERF subfamilies (Figure 3.7) based on the domains and motifs they contain (Nakano *et al.*, 2006). The ERF subfamily of interest includes 65 members that are distributed between groups V to X. Where possible, orthologous proteins to the ERF wheat proteins in Arabidopsis were identified; where no orthologous proteins could be identified, BLAST tool was used to find the most structurally similar ERF proteins in Arabidopsis. Based on similarity to Arabidopsis protein, we assigned a subgroup number to each wheat protein identified as putative DIP. Twelve members of ERF subfamily were identified in the Y2H screen (indicated in Figure 3.7): two from group VII (interactors 50 and 61), one from group VIII (interactor 23), two from group IX (interactors 7 and 57) and seven from group

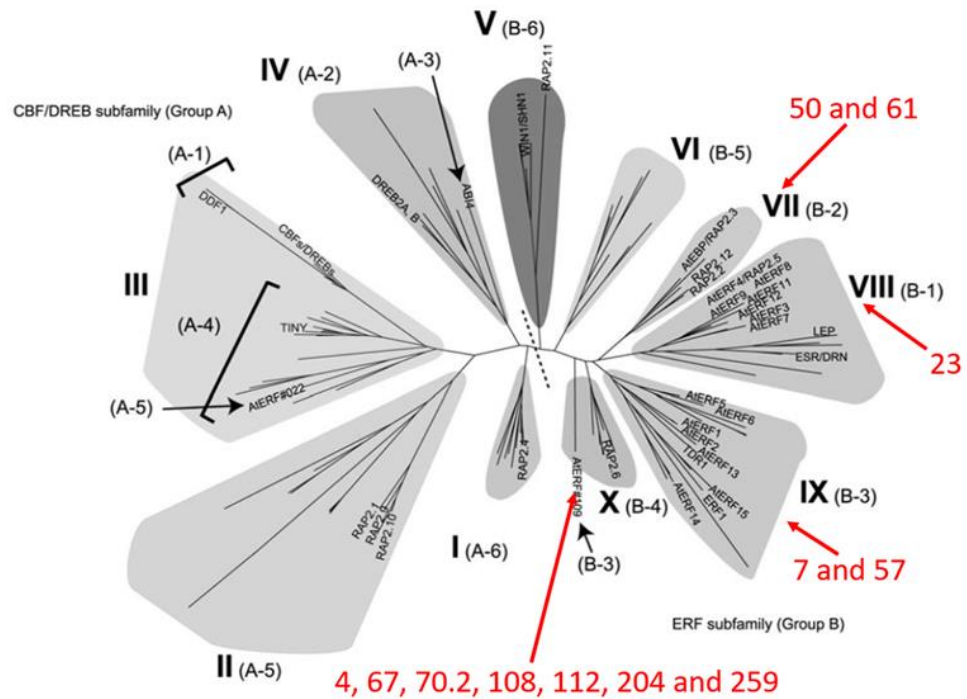


Figure 3. 7 Phylogenetic tree of Arabidopsis ERF proteins. The CBF/DREB and ERF subfamilies are divided with a dashed line. The interactors identified in the screen are indicated in red and the arrows identify the groups they belong to. The figure was taken from Nakano et al., 2006 and adjusted to show the interactors.

X (interactors 4, 67, 70.2, 108, 112, 204 and 259). Interactors 23, 50, 61, 67, 204 and 259 were pulled out only once, interactor 112 four times, interactor 108 five times, interactor 70.2 six times, interactor 7 seven times and interactors 4 and 57 ten times. The two homoeologues of *TaERF5* gene identified in the Y2H screen, *TraesCS2A02G417100* and *TraesCS2D02G414300*, have another homoeologue in the B genome, *TraesCS2B02G436100*, which was not identified in the screen. Each of the three homoeologues has two paralogues in wheat (Ensembl Plant; <http://plants.ensembl.org/index.html>). *TraesCS2A02G417100* shares 86.3% sequence identity with its close paralogue *TraesCS2A02G417200*, and 45.6% sequence identity with its other paralogue, *TraesCS6A02G243500*. *TraesCS2B02G436100* sequence identity with its paralogues *TraesCS2B02G436200* and *TraesCS6B02G280800* is 85.4% and

46.5%, respectively. *TraesCS2D02G414300* shares 83.6% sequence identity with *TraesCS2D02G414500* and 47.3% sequence identity with *TraesCS6D02G225700*. Neither of the genes, nor their paralogues have orthologues outside of the grass family.

As TaERF5 was the interactor of interest, and the most similar proteins identified through BLAST search in Phytozome 12.1 (Goodstein *et al.*, 2012) in Arabidopsis (AT5G47230, ERF5) and rice (LOC_Os04g46240 and LOC_Os04g46250) belong to subgroups IX of the ERF subfamilies, the analysis was conducted only for this subgroup of the subfamily. Wheat proteome search using the BLAST option on Ensemble Plant website yielded 72 distinct sequences, which along with the Arabidopsis and rice group IX ERFs protein sequences were used to calculate the phylogenetic tree (Figure 3.8).

The two TaERF5 proteins identified in the Y2H screen, TaERF-A5 (*TraesCS2A02G417100*) and TaERF-D5 (*TraesCS2D02G414300*) (highlighted in green in Figure 3.8), and the homoeologous protein TaERF-B5 (*TraesCS2B02G436100*) share the highest protein sequence similarity with the three proteins encoded by their close paralogues (hereafter called TaERF5a), TaERF-A5a (*TraesCS2A02G417200*), TaERF-B5a (*TraesCS2B02G436200*) and TaERF-D5a (*TraesCS2D02G414500*). A similar scenario is observed in the rice ERF subfamily; the most structurally similar proteins to ERF5 wheat proteins in rice, LOC_Os04g46240 and LOC_Os04g46250 (highlighted in red in Figure 3.8), show higher sequence similarity relative to each other than to wheat genes. The genes encoding these proteins, however, are not paralogues. There is no one gene in Arabidopsis that is the most similar in structure to the wheat and rice genes; the clade of six genes that are structurally most similar to the identified wheat genes is subgroup IXb of ERFs (Figure 3.8, highlighted in red).

The inferred functional domains of the TaERF5 and TaERF5a proteins in wheat (Figure 3.9 A) were based on the functional domains present in group IXb of ERFs in Arabidopsis and rice (Nakano *et al.*, 2006). All TaERF5 and TaERF5a proteins in wheat contain well-conserved AP2/ERF DNA-binding domain (Figure 3.9 B), CMIX-2 motif (Figure 3.9 C), which is a putative acidic region that

might function as transcriptional activation domain (Fujimoto *et al.*, 2000), and two putative MAP kinase phosphorylation sites, CMIX-6 and CMIX-5 (Nakano *et al.*, 2006) (Figure 3.9 D). The functional domains in wheat ERF proteins show high level of conservation, moreover, the TaERF5 and TaERF5a show a high degree of sequence similarity. The overall percent similarity between the proteins encoded by three homoeologues of the *TaERF5* and *TaERF5a* genes are 92.2% and 93.0%, respectively. The sequence identity between the proteins encoded by respective paralogues is 85.5%, 85.4% and 83.7% for genomes A, B and D, respectively. This level of sequence homology may indicate similar function in wheat and should be considered when generating a full knockout mutant for functional analysis of *TaERF5* gene effect, which is the further aim of this PhD project.

3.3.3.2 Phylogenetic analysis of the IDD transcription factor family in wheat

Despite the fact that TaIDD11 did not appear in the top ten genes identified to be connected to the process of GA signalling returned by KnetMiner, recent studies show that IDD transcription factors are interacting partners of DELLAs, and that they function together with DELLAs to control GA feedback regulation during plant growth and germination (Feurtado *et al.*, 2011; Fukazawa *et al.*, 2014; Yoshida *et al.*, 2014; Yoshida & Ueguchi-Tanaka, 2014). Therefore, TaIDD11 was selected for further analysis.

The IDD gene family in Arabidopsis and rice has 16 and 15 members respectively (Colasanti *et al.*, 2006). The protein sequences of all the Arabidopsis and rice members (Supplementary Table 3.3) were used to search the wheat proteome, yielding 41 sequences belonging to 14 distinct genes (one IDD gene lacks the A homoeologue). Protein sequences of all the members of the Arabidopsis and rice IDD family, and the 41 wheat IDD protein sequences identified through the BLAST search were used to build a phylogenetic tree (Figure 3.10). In the Y2H screen, three putative DIPs were

identified as IDD proteins: 9.1 (TraesCS2D02G199300), 127 (TraesCS2A02G188400) and 241 (TraesCS2B02G218900). These genes were identified as the homoeologues of the same IDD gene (Figure 3.10, highlighted in green). The proteins they encode share the biggest sequence homology with the rice IDD5 (LOC_Os07g39310) and with two Arabidopsis proteins, AtIDD1 (ENY, AT5G66730) and AtIDD2 (GAF1, AT3G50700). The rice *OsIDD5* is the wheat genes orthologue in rice, but no orthologous genes can be found in Arabidopsis. *OsIDD5* protein shares on average ~61.0% sequence homology with the wheat *TaIDD11* proteins.

The IDD gene family is a plant-specific class of zinc finger (ZF) transcription factors. The conserved domains of IDD proteins (Figure 3.11) were inferred based on similarity to Arabidopsis ENY and GAF1 proteins characterised in Colasanti *et al.* (2006), and on Fukazawa *et al.* (2014) report on the presence of an EAR domain in these Arabidopsis IDD proteins. All IDD proteins share conserved DNA-binding ID-domain (Figure 3.11 B), which in the *TaIDD11* proteins is a highly conserved region of 165 amino acids. It starts with a putative nuclear localization sequence consisting of three lysines (K) and one arginine (R) at N terminus and ends nine amino acids downstream of the last cysteine (C) of the last zinc finger motif. The ID-domain contains four ZF domains: C2H2-type ZF1 and ZF2, and two atypical C2HC domains, ZF3 and ZF4 (Figure 3.11 B). Apart from ID-domain, *TaIDD11* proteins have three short domains in the C-terminal region, M/ISATALLQKAA, EAR and the LDFLG domains, which are all highly conserved and were reported to be responsible for protein-protein interactions.

Alternative *TaIDD11* gene models for homoeologue A and D are suggested (Supplementary Figure 3.1; data taken from Ensembl Plant website). The gene structure of the identified *TaIDD11* genes in wheat variety Cadenza was revealed. The RNA-Seq reads from different tissue samples (crown, leaf and root) taken from wheat cv. Cadenza were mapped to the Chinese spring genomic sequences of *TaIDD11* genes (Supplementary Figure 3.2; sequences of genes from cv. Cadenza are missing parts of the sequence) and revealed that

the genes contain four exons: 91 bp, 403 bp and 374 bp in length for the first three in all genomes and 1670 bp for the A and D homoeologues and 1676 bp for the D homoeologue (Andy Phillips, personal communication). The coding sequences are 2538 bp for homoeologues A and D, and 2544 bp for homoeologue B, which encode predicted proteins of 845 and 847 amino acids from genomes A and D, and B, respectively.

The phylogenetic analysis revealed that *TaIDD11* is encoded by a single gene in each of the wheat genomes. Therefore, to generate null *Taidd11* mutant in wheat, three homoeologous genes need to be knocked out. *TaIDD11* is structurally most similar to Arabidopsis proteins ENY and GAF1, which were shown to interact with DELLAs to regulate GA-mediated processes, partly by regulating GA feedback mechanism (Feurtado *et al.*, 2011; Fukazawa *et al.*, 2014).

Figure 3. 8 *Phylogenetic tree of group IX ERFs in wheat, Arabidopsis and rice. Protein sequences of the genes belonging to this group in Arabidopsis and rice, and the sequences of the similar ERF proteins identified in wheat proteome were aligned using the MUSCLE alignment tool and the tree calculated using PhyML 3.0 plugin in Geneious v10.2.3. Wheat proteins identified in the screen are highlighted in green and the most structurally similar proteins in Arabidopsis and rice are highlighted in red.*

A

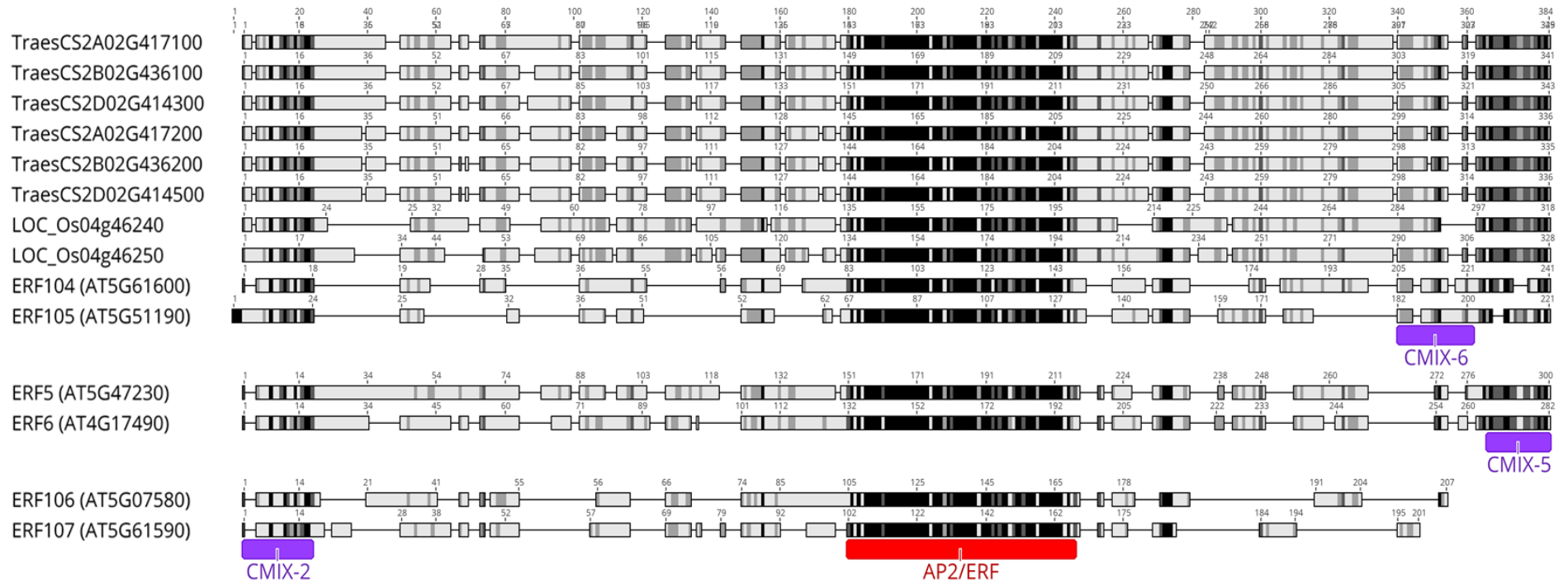
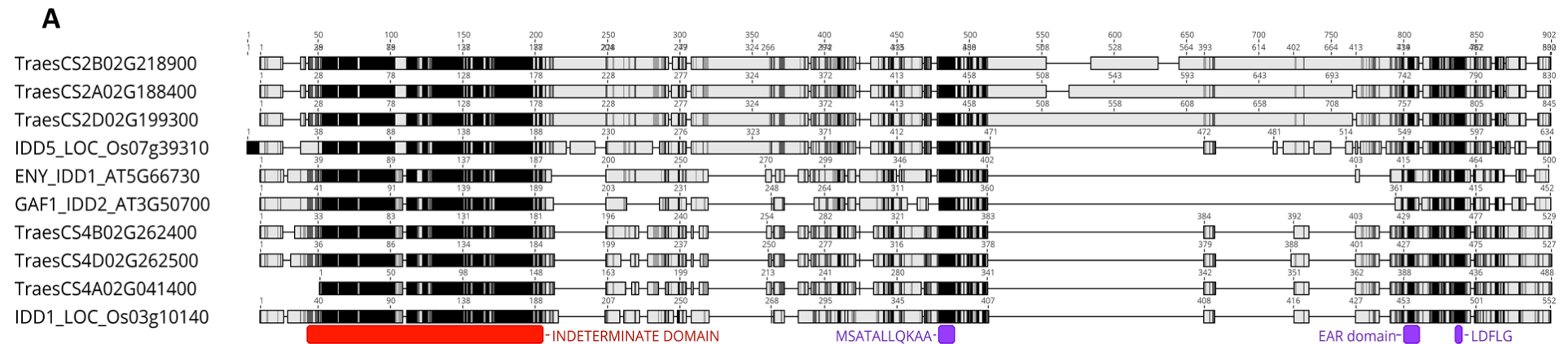


Figure 3. 9 *The functional domains of the wheat TaERF5 and TaERF5a proteins. The domains were inferred based on the similarity to the Arabidopsis and rice proteins that are the most structurally similar based on phylogenetic analysis. A. Alignment of three TaERF5 proteins and three TaERF5a proteins encoded by the close paralogue, the two rice proteins that are structurally most similar to the wheat proteins based on phylogenetic analysis, and the members of group IXb of Arabidopsis ERFs. The AP2/ERF DNA-binding domain is annotated in red and the other functional domains, CMIX-2, CMIX-6 and CMIX-5, are annotated in purple. All sequences over the domain annotation contain the domain. B, C and D. Alignment and sequence similarity of functional domains: AP2/ERF DNA-binding domain (B); asterisks represent amino acid residues that directly make contact with DNA (Allen et al., 1998), CMIX-2 (C) and CMIX-5 and CMIX-6 (D).*

Figure 3. 10 Phylogenetic tree for the IDD family of transcription factors in wheat, rice and Arabidopsis. Protein sequences of the genes belonging to the IDD family of transcription factors in Arabidopsis and rice, and the wheat IDD sequences identified through BLAST analysis were aligned using MUSCLE alignment tool and the tree calculated using PhyML 3.0 plugin in Geneious v10.2.3. Wheat proteins identified in the screen are highlighted in green and the most structurally similar proteins in Arabidopsis and rice are highlighted in red.



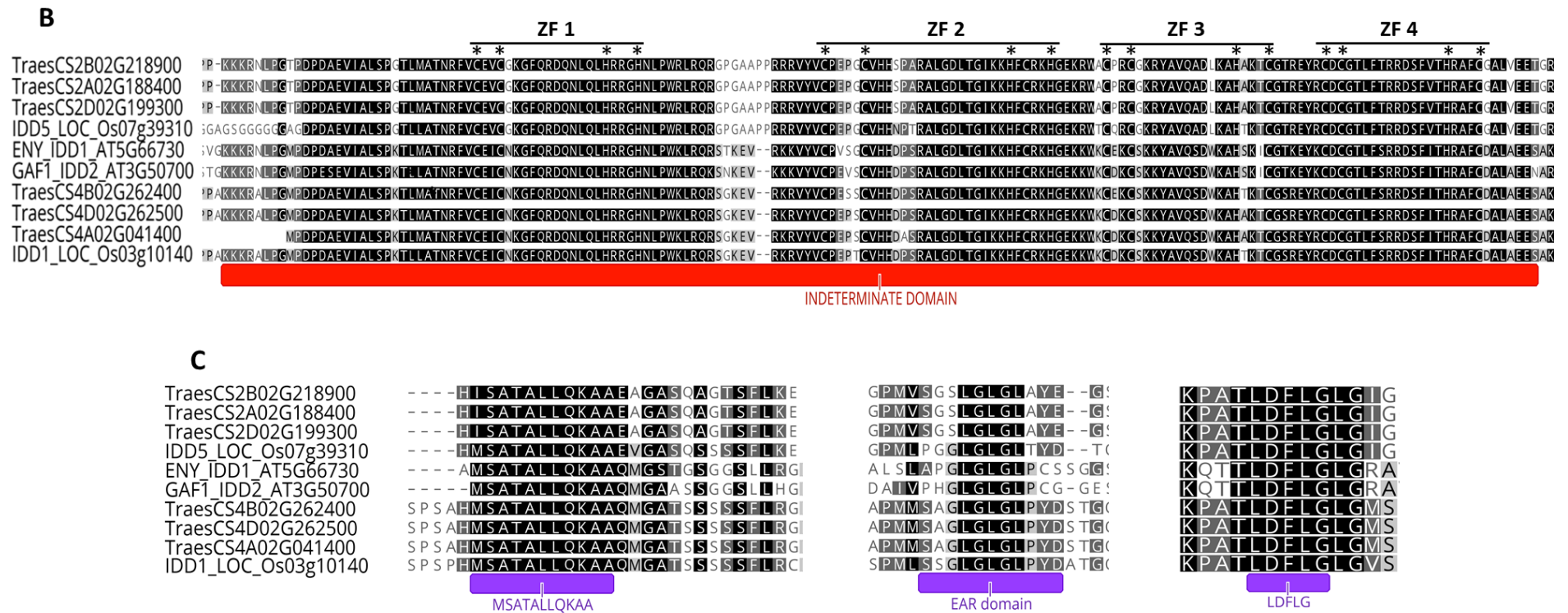


Figure 3. 11 The functional domains of the wheat *TaIDD11* proteins. The domains were inferred based on similarity to the *Arabidopsis* and rice proteins that are the most structurally similar to *TaIDD11* based on phylogenetic analysis. A. Alignment of three *TaIDD11* proteins identified as DIPs in Y2H screen and the other wheat, rice and *Arabidopsis* proteins found in the same clade of phylogenetic tree. All proteins contain the same functional domains: INDETERMINATE

(ID)-domain, which is a DNA-binding domain (annotated in red), and M/ISATALLQKAA, EAR and LDFLG domains (annotated in purple). B. Alignment of ID domain in the proteins aligned in A. The asterisks above the sequences indicate cysteine and histidine residues of zinc finger motifs (Colasanti et al., 2006). C. Alignment of functional domains hypothesized to be involved in protein binding. All the proteins contain the EAR domain, which can only be found in ENY and GAF in Arabidopsis, OsIDD1 and OsIDD5 in rice and the six wheat proteins included in the alignment, and was found to be responsible for repressor (TPR4) binding (Fukazawa et al., 2014).

3.3.4 RHT-D1A interacts with TaERF-A5A and TaIDD-A11A *in planta*

The interactions identified in yeast needed to be confirmed in an *in vivo* system, to ensure that they occur in plants. The method of choice to confirm the interactions between the selected transcription factors and the RHT-D1A protein was bimolecular fluorescence complementation (BiFC). BiFC was chosen thanks to its multiple advantages. The method is highly sensitive with minimum background fluorescence and allows for visualisation of the protein complexes in the live cells. The fluorescent signal reconstituted on protein interaction does not require any special treatments with exogenous reagents, no cell fixation or lysis, and therefore allows visualisation of subcellular locations of specific protein interactions with minimal disturbance of the normal cellular environment. Additionally, BiFC procedure is relatively simple, does not require synthesis of antibodies, like e.g. co-immunoprecipitation, or expensive equipment as rapid visualisation of the PPIs *in vivo* can be performed using a confocal microscope (Miller *et al.*, 2015).

The system that was used is described in Kamigaki *et al.*, (2016) and provides binary vectors that allow for generation of various fluorescent protein fusions for the BiFC assay using a simple Gateway cloning system (Figure 3.12). The vectors that were used in the experiment were pB5nRGW (AB830572), pB5cRGW (AB830561), pB5GWnR (AB830568) and pB5GWcR (AB830564), and they encoded N- or C-terminal fragment of the mRFP1 upstream or downstream of the Gateway cassette, containing chloramphenicol-resistance marker and *ccdB* gene (Figure 3.12 B). During the BP step of the Gateway cloning, that cassette is swapped for the gene of interest, generating a fusion between the gene and the N- or C- terminal fragment of the fluorescent protein. There are four different combinations in which a protein can be fused with a fragment of mRFP1:

nmRFP1 – Protein*

cmRFP1 – Protein*

Protein – nmRFP1*

Protein – cmRFP1*,

where '*' indicates a STOP codon, and eight combinations in which two given proteins can be tested for the interaction (X and Y are the tested proteins):

nmRFP1-Protein X* + cmRFP1-Protein Y*
nmRFP1-Protein X* + Protein Y-cmRFP1*
Protein X-nmRFP1* + Protein Y-cmRFP1*
Protein X-nmRFP1* + cmRFP1-Protein Y*
cmRFP1-Protein X* + nmRFP1-Protein Y*
cmRFP1-Protein X* + Protein Y-nmRFP1*
Protein X-cmRFP1* + Protein Y-nmRFP1*
Protein X-cmRFP1* + nmRFP1-Protein Y*.

All possible gene and fluorescent protein fusions were cloned, and all possible pairs tested to study the interaction between RHT-D1A and TaERF-A5A. Unfortunately, although attempted several times, generating an TaIDD-A11A-nmRFP1 fusion was unsuccessful, thus the interaction between RHT-D1A and TaIDD-A11A was tested using only six out of eight combinations. A homoeologue of *TaIDD11* was chosen as it is the only homoeologue for which the full CDS sequence in cv. Cadenza is known. As a positive control in the experiments, the interaction between PTS2 and PEX7 proteins, which reconstitutes yellow fluorescent protein (YFP) was used. The PTS2 interaction with PEX7 occurs in peroxisomes and these proteins were shown previously to interact strongly (Kamigaki *et al.*, 2016).

Negative controls need to be included in each BiFC experiment to establish whether the fluorescence observed is a result of a specific protein interaction. It is recommended to test the validity of the interaction observed in BiFC assay by examining fluorescence complementation of proteins in which the interaction interface has been mutated (Hu *et al.*, 2002; Kerppola, 2006, 2008), and the potential interaction of mutant protein with the protein of interest should be tested in the assay in the same combinations as the wild type protein. As the negative controls, the mutated versions of *Rht-D1* genes were used, named M1, M2, M3 and M4. Mutated *Rht-D1* genes were generated by Dr

Marek Szecowka (Palacký University Olomouc, Czechia), and they contained introduced missense mutations that affected residues in conserved motifs in the GRAS domain of RHT-1 protein, LHR1 and PFYRE (Figure 3.13). These mutations were based on the mutations found in the overgrowth mutants of DELLA dwarf lines identified in the suppressor screens in barley and wheat (Chandler & Harding, 2013; Rafter, 2019), and were hypothesized to cause reduced affinity of the DELLA in the overgrowth mutants to bind their interacting partners. All mutants were tested in Y2H assays for interaction with TaERF-A5A and TaIDD-D11A (the fragments pulled out in the Y2H screen) in the yeast system prior to the infiltration experiment. Based on the results from the Y2H experiments (Supplementary Figure 3.3), two mutated RHT-D1 proteins were selected, M1 (V235M) for testing the interaction with TaERF-A5A, and M2 (E427K) for testing the interaction with TaIDD-D11A. The mutation in M1 mutant is a G to A nucleotide substitution at nucleotide 703 of *Rht-D1a* CDS, which causes V235M substitution in the LHR1 motif. The M2 mutant contains another G to A nucleotide substitution, in this case at position 1414 of CDS, causing E472K substitution in the PFYRE motif. When sequenced, the M2 mutant also showed to contain three nucleotide deletions at positions 675, 678 and 680 causing one amino acid deletion, and one amino acid substitution at positions 225 to 227 (there is K instead of D and T at these positions). The results of the assays showed that the presence of the mutations in M1 and M2 mutants reduce the strength of interaction between RHT-D1A and TaERF-A5A, and RHT-D1A and TaIDD-D11A, respectively. Based on these results, M1 and M2 were selected as negative controls.

Leaves of five to six weeks old tobacco (*Nicotiana benthamiana*) plants were co-inoculated with *Agrobacterium GV3101* transformed with tested constructs encoding fusion genes. p19 plasmid was mixed with the plasmids in equal ratio to enhance the expression. On average three to four leaves per plant were inoculated and the plants left to incubate for three to four days. After the incubation time, the explant of the inoculated leaf was observed under the confocal microscope (Figure 3.14).

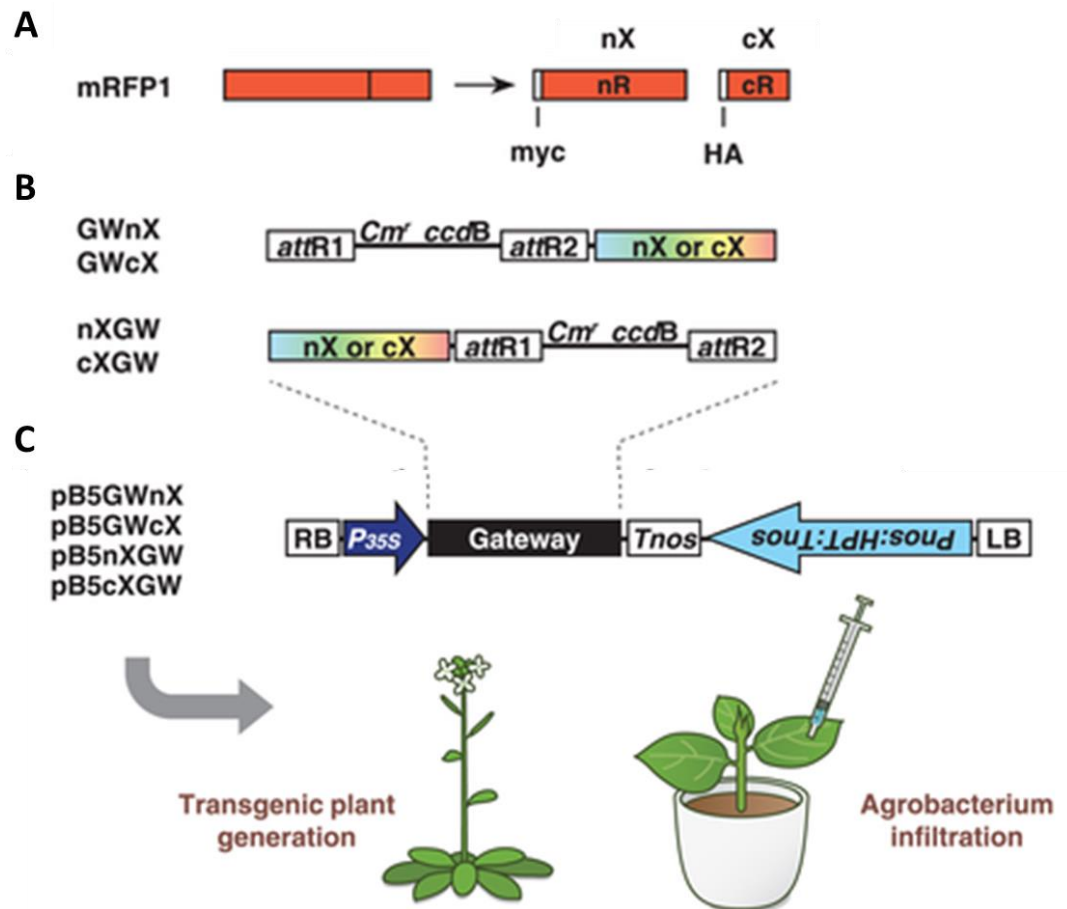


Figure 3. 12 Schematic representation of the Gateway cloning technology-compatible vectors used in the BiFC experiment. A. Fluorescent protein, mRFP1 can be divided into two fragments. The letters 'n' and 'c' represent N- and C-terminal fragments of a split fluorescent protein and the letter 'R' represent the type of fluorescent protein (mRFP1), 'myc' and 'HA' in the N- and C-terminal fragment of mRFP1 represent myc- and hemagglutinin-epitope tags, respectively. B. The structures of the region indicated as 'Gateway' in C. GWnX and GWcX contain N- or C-terminal split fluorescent protein downstream of the attR2 site, respectively, whereas nXGW and cXGW contain N- or C-terminal split fluorescent protein upstream of the attR1 site, respectively. C. Outline of the binary vector for BiFC. The pB5 vector contain Hygromycin marker (HPT), chloramphenicol-resistance marker (Cm^r), ccdB gene, Spectinomycin resistance, 35S promoter, nopaline synthase terminator (Tnos) and Gateway cassette. Figure adapted from Kamigaki et al., 2016.



M1 – G to A at nucleotide 703 of CDS, V235M

M2 – G to A at nucleotide 1414 of CDS, E472K

M3 – C to T at nucleotide 1466 of CDS, S489F

M4 – C to T at nucleotide 1484 of CDS, T495I

Figure 3. 13 Mutations introduced into the *Rht-D1a* gene and their effect on the protein sequence. All the mutations are missense mutations and they are located in the LHR1 and PFYRE domains, which are the main domains responsible for binding the proteins and are therefore hypothesized to affect protein binding. In yellow is *Rht-D1a* CDS, in orange are the functional domains of the RHT-1 protein, in red are the introduced mutations.

The positive control (Figure 3.14 A and B) transformation efficiency appeared to be higher compared to the other fusion genes' combinations. The signal originating from the positive control can be observed in the majority of the cells, whereas for the RHT-D1A interactions, the fluorescence could be seen only in a few single cells. The positive control interaction takes place in the peroxisomes, therefore the signal is expected to be seen in those cellular compartments. In the B panel of the figure, the small, roundish structures that show signals, follow the shape of the cell. Mature epidermal cells of tobacco plants contain large vacuoles that "push" all the other cell structures to the edge on the cell, hence the observed *Rht* pattern. The interaction of RHT-D1A with the transcription factors TaERF-A5A and TaIDD-A11A is expected to take place in the nucleus, hence one round fluorescing structure was expected per cell. This is what was observed for the investigated explants (Figure 3.14 C-S).

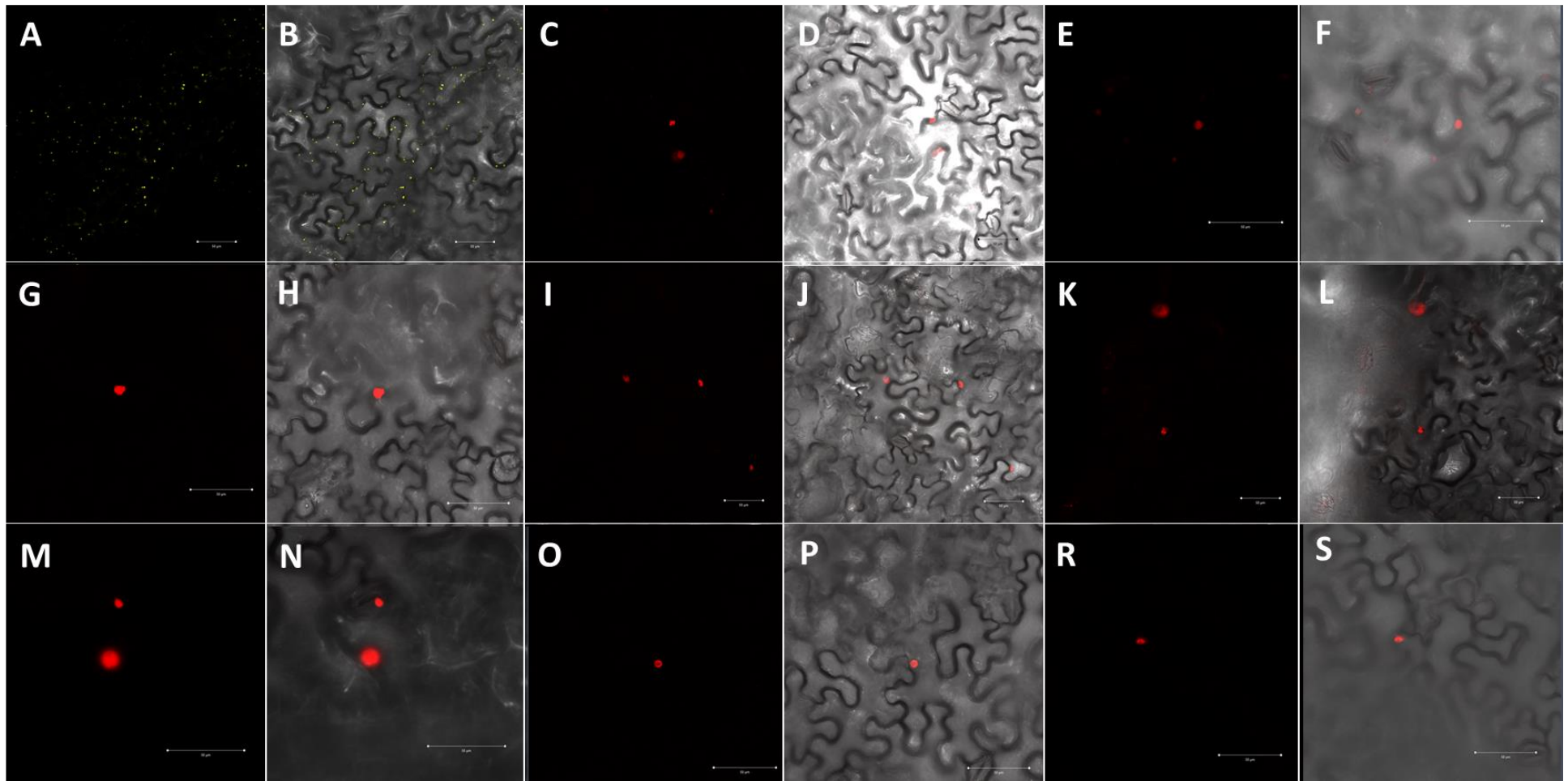


Figure 3. 14 Detection of protein-protein interactions in tobacco leaves using bimolecular fluorescence complementation (BiFC). Various combinations of fusion genes were introduced by *Agrobacterium* infiltration. For each co-infiltration the image of reconstituted fluorescent signal (A, C, E, G, I, K, M, O and R) and merged image of reconstituted fluorescent signal with bright field image (B, D, F, H, J, L, N, P and S) are presented. A and B. Positive control, PTS2-cYFP with nYFP-PEX7, which interact in peroxisomes and on interaction reconstitute YFP. C to J. RHT-D1A with TaERF-A5A various fusion genes combinations: C, D.

nmRFP1-TaERF-A5A + cmRFP1-RHT-D1A; E, F. TaERF-A5A-nmRFP1 + cmRFP1-RHT-D1A; G, H. TaERF-A5A-nmRFP1 + RHT-D1A-cmRFP1; I, J. TaERF-A5A-cmRFP1 + nmRFP1-RHT-D1A. K and L. Unexpectedly, a negative control (nmRFP1-M1 + cmRFP1-TaERF-A5A) also showed reconstitution of the mRFP1. M to P. RHT-D1A with TaIDD-A11A various fusion genes combinations: M, N. nmRFP1-TaIDD-A11A + cmRFP1-RHT-D1A; O, P. TaIDD-A11A-cmRFP1 + RHT-D1A-nmRFP1. R and S. The negative control, nmRFP1-M2 + cmRFP1-TaIDD-A11A, also showed reconstitution of the mRFP1. The tested interactions take place in the cell nucleus; hence the observed signal is expected to be nuclei. Pictures taken using Zeiss LSM 780 laser confocal microscope and Leica Application Suite X (LAS X) software.

Not all the tested combinations of fusion genes showed interaction, possibly due to the efficiency issue rather than the effect of linking the fragments of split fluorescent protein to N' or C' terminus of the transcription factors, as the positive samples were expressing proteins fused to N'- and C'-terminal mRFP1 fragments both at N'- and C' terminus. Most of the observed signal was originating from the epidermal cells, but occasionally the signal from the next cell layer, the mesophyll cells, was also detected. For the RHT-D1A-TaERF-A5A pair, the signal was observed in nmRFP1-TaERF-A5A + cmRFP1-RHT-D1A, TaERF-A5A-nmRFP1 + cmRFP1-RHT-D1A, TaERF-A5A-nmRFP1 + RHT-D1A-cmRFP1 and TaERF-A5A-cmRFP1 + nmRFP1-RHT-D1A co-infiltrations (Figure 3.14 C-J). Unexpectedly, some signal was also detected in the negative control, nmRFP1-M1 + cmRFP1-TaERF-A5A (Figure 3.14 K and L).

Co-infiltration with RHT-D1A and TaIDD-A11A was less efficient compared to RHT-D1A-TaERF-A5A co-infiltration, possibly due to the size of the plasmids containing the TaIDD-A11A CDS. The signal was detected in two out of six possible combinations (only six out of eight were tested, mentioned earlier), nmRFP1-TaIDD-A11A + cmRFP1-RHT-D1A and TaIDD-A11A-cmRFP1 + RHT-D1A-nmRFP1 (Figure 3.14 M-P). Again, some signal was detected for the negative control, nmRFP1-M2 + cmRFP1-TaIDD-A11A (Figure 3.14 R and S).

To conclude, the RHT-D1A was shown to interact with TaERF-A5A and TaIDD-A11A *in vivo*, but the efficiency of the transformation was relatively low compared to the transformation with the positive control, where the fluorescent signal was abundant. Based on the signal observed in the negative controls, it is conceivable that the mutations in RHT-D1A do not completely abolish the interaction between RHT-D1A and TaERF-A5A and TaIDD-A11A, but instead they may reduce the affinity of RHT-D1A for their binding, as results from the Y2H studies show (Supplementary Figure 3.3).

3.4 Discussion

DELLAs negatively regulate GA-mediated responses by indirectly regulating GA-controlled gene expression (Zentella *et al.*, 2007). Due to the lack of an established DNA-binding domain it is widely accepted that DELLAs modulate gene expression by binding and affecting the activity of TFs. The aim of this study was to identify TFs that interact with wheat's DELLA protein, RHT-1, in the wheat aleurone, with a view to establishing their potential roles in regulating GA responses. A Y2H screen of an aleurone cDNA prey library revealed multiple classes of putative DIPs, including various classes of TFs, enzymes, and defence proteins, however, the interactions between RHT-1 and all the putative interactors were not confirmed. Instead, *in silico* characterisation and literature search using KnetMiner was performed to enable selection of two DIPs with potential role in regulating GA signalling. Two transcription factors were selected: TaERF5 and TaIDD11. Genetic *in vivo* and *in planta* studies, confirmed the interaction between RHT-1 and TaERF5 and TaIDD11 TFs. Phylogenetic studies revealed that TaIDD11 is encoded by a single *TaIDD11* gene (Figure 3.10), whereas *TaERF5* gene, that encodes TaERF5, has a close paralogue in each of the three genomes, with a potentially redundant role in regulating gene expression in wheat (Figure 3.8).

3.4.1 RHT-1 interacts with different classes of TFs

The aim of the screen was to identify the TFs that potentially interact with RHT-1 to regulate GA signalling; thus, our focus was on this class of DIPs. 30 distinct interactors were identified as TFs, and among them were homoeologues of the same genes, lowering the number of distinct TFs to 24. The TFs belonged to six distinct families: AP2/ERF, Zinc finger, including IDD, bHLH, MYB, bZIP and NAC, which is much fewer than previously reported TF interactomes of DELLAs in *Arabidopsis* (Lantzouni *et al.*, 2020; Marín-de la Rosa *et al.*, 2014). The screen conducted by Marín-de la Rosa (2014) identified 57 unique GAI-interacting TFs representing 15 different TF families, including TCP, bHLH, AP2/EREB, MYB,

NAC, different subfamilies of Zinc finger, MADS, HD, SPB, GARP/ARR, EIN3-like and bZIP families. The difference between the results yielded by our study and the screen performed by Marin-de la Rosa (2014) is the studied tissue and plant species. Marin-de la Rosa and colleagues screened a cDNA library from three-day-old etiolated *Arabidopsis* seedlings while we used mature wheat aleurone. The stringency of the assays also differed as we used 25 mM 3-AT, while Marin-de la Rosa and colleagues used 5 mM 3-AT for the screen, possibly allowing for identification of more false positives. Another study identified 244 and 243 TF to interact with RGA and GAI, respectively, belonging to 51 TF families including, among others: GRF, TCP, ZIM, G2-like, bHLH, C2C2-DOF, HB, AP2-ERE BP, C2H2, MYB, ABI3-VP1, WRKY, bZIP, NAC and MADS (Lantzouni *et al.*, 2020). This more targeted study screened a collection of 1956 *Arabidopsis* TFs cloned into the Invitrogen pDEST22 prey vectors (Pruneda-Paz *et al.*, 2014) and used 2 and 3 mM 3-AT for the screen with RGA and GAI, respectively.

Despite the differences in the numbers of different TFs classes identified to interact with DELLA in our study compared to the studies in *Arabidopsis*, the members of the TF families that were identified in our study were previously reported to interact with DELLAs with a functional significance defined. DELLAs interactions with bHLH superfamily members, PIF3 (Feng *et al.*, 2008) and PIF4 (de Lucas *et al.*, 2008), identified to regulate hypocotyl elongation in response to GA and light, were the first to be ever reported. Since then, plenty more bHLH TFs were reported as DIPs (Arnaud *et al.*, 2010; Gallego-Bartolome *et al.*, 2010; Gallego-Bartolomé *et al.*, 2011; Li *et al.*, 2017a). The study by Marin-de la Rosa mentioned above, identified group VII of ERF TFs as DELLA binding partners, with RAP2.3, together with DELLA, being involved in regulation of apical hook development (Marín-de la Rosa *et al.*, 2014). Interestingly, AtERF11 was found to be a positive regulator of both GA biosynthesis and GA signalling during internode elongation by antagonising DELLA function on interaction (Zhou *et al.*, 2016). Many studies in the last few years reported IDD subfamily of the Zinc finger TFs and DIPs (Feurtado *et al.*, 2011; Fukazawa *et al.*, 2014; Huang *et al.*, 2018; Yoshida *et al.*, 2014) and identified DELLAs as IDDs

co-activators in regulating gene expression during processes including growth, germination or root patterning. The bZIP TFs, ABI5, and ABI3, interact with DELLA to form a complex that activates transcription of *SOMNUS* gene to regulate seed germination in response to high temperatures (Lim *et al.*, 2013). Recently, MYB TFs MYB21 and MYB24 were found to bind DELLAs, and these interactions were found to negatively affect filament elongation (Huang *et al.*, 2020) and in rice, DELLA interacts with a NAC TF to regulate cellulose synthesis (Huang *et al.*, 2015).

As can be observed from the cited examples, all the TF families identified as DIPs in our study have already been reported to interact with DELLAs in Arabidopsis or rice, and for some, the mechanism of regulation and physiological relevance have been revealed.

3.4.2 Multiple ethylene responsive factors (ERFs) identified as putative RHT-1 interactors

Y2H screen identified 12 ERFs encoding eight distinct *ERF* genes in wheat. Since little is known about the function of ERF TFs in cereals, the hypothetical function and organisation of protein functional domains were based on similarity to Arabidopsis ERF proteins. The most similar proteins in Arabidopsis to the identified wheat ERF proteins belong to the subgroups: group VII, VIII, IX and X of ERF family (Table 3.2). Four out of eight distinct ERF TFs identified as putative DIPs in the Y2H screen were most similar to Arabidopsis subgroup X members (Table 3.2). Subgroup X in Arabidopsis has eight members, thus, assuming similar division and subgroup sizes of ERF family in wheat, identifying half of them in the screen indicates the potential importance of this group as DELLA binding partners. Two identified interactors that were classified as most similar to subgroup VII encoded orthologs of Arabidopsis RAP2-2 and RAP2-12 (interactor 50) and rice OsEREBP (interactor 61), and group VII of ERF TFs was previously identified as DELLA interactors in Arabidopsis (Marín-de la Rosa *et al.*, 2014). One interactor (23) falls into subgroup VIII, whose members too

were shown to interact with DELLA (Zhou *et al.*, 2016), and one into subgroup IX (interactors 7 and 57, homoeologues of the same gene).

Table 3. 2 *ERF TFs identified as putative DIPs in the Y2H screen. The number in the superscript next to the gene accession number indicates that the genes are homoeologues of the same gene in wheat.*

| Colony # | IWGSC accession number | ERF subgroup in Arabidopsis | Putative function |
|----------|---------------------------------|-----------------------------|--------------------------------|
| 4 | TraesCS1B02G282300 ¹ | X | AtERF110-like |
| 7 | TraesCS2A02G417100 ² | IX | AtERF105-like |
| 23 | TraesCS6B02G199800 | VIII | AP2-EREBP-transcription factor |
| 50 | TraesCS5A02G314600 | VII | RAP2-2-like |
| 57 | TraesCS2D02G414300 ² | IX | AtERF105-like |
| 61 | TraesCS5A02G215900 | VII | OsEREBP-like |
| 67 | TraesCS6A02G097700 | X | EREBP transcription factor |
| 70.2 | TraesCS3A02G379900 ³ | X | AtABR1-like |
| 108 | TraesCS1D02G272600 ¹ | X | AtERF110-like |
| 112 | TraesCS3B02G412500 ³ | X | AtABR1-like |
| 204 | TraesCS2D02G286300 | X | Ethylene responsive factor 8 |
| 259 | TraesCS1A02G272300 ¹ | X | AtERF110-like |

Identifying numerous ERF TFs belonging to various subgroups of the ERF family as putative RHT-1 interactors sparked an interest to further analyse their protein structure and identify potential domains that may be responsible for the interaction with RHT-1. Alignment of protein sequences of all ERF TFs identified in the screen revealed that the only domain conserved among all the proteins is the AP2/ERF DNA-binding domain (Figure 3.15), and no other conserved motifs seem to be shared among the TFs. Thus far, one study identified that the highly conserved amino terminus and the AP2/ERF DNA-binding domain of group VII representatives, RAP2.3 and RAP2.12, are necessary for DELLA binding, and that the interaction may affect DNA binding ability of RAP2.3 (Marín-de la Rosa *et al.*, 2014). Another study identified that the DELLA protein RGA can only interact with group VIII-B-1a ERF TFs ERF11,

| |
|---------------------------|
| 7 - TraesCS2A02G417100 |
| 57 - TraesCS2D02G414300 |
| 23 - TraesCS6B02G199800 |
| 67 - TraesCS6A02G097700 |
| 204 - TraesCS2D02G286300 |
| 108 - TraesCS1D02G272600 |
| 259 - TraesCS1A02G272300 |
| 4 - TraesCS1B02G282300 |
| 70.2 - TraesCS3A02G379900 |
| 112 - TraesCS3B02G412500 |
| 50 - TraesCS5A02G314600 |
| 61 - TraesCS5A02G215900 |

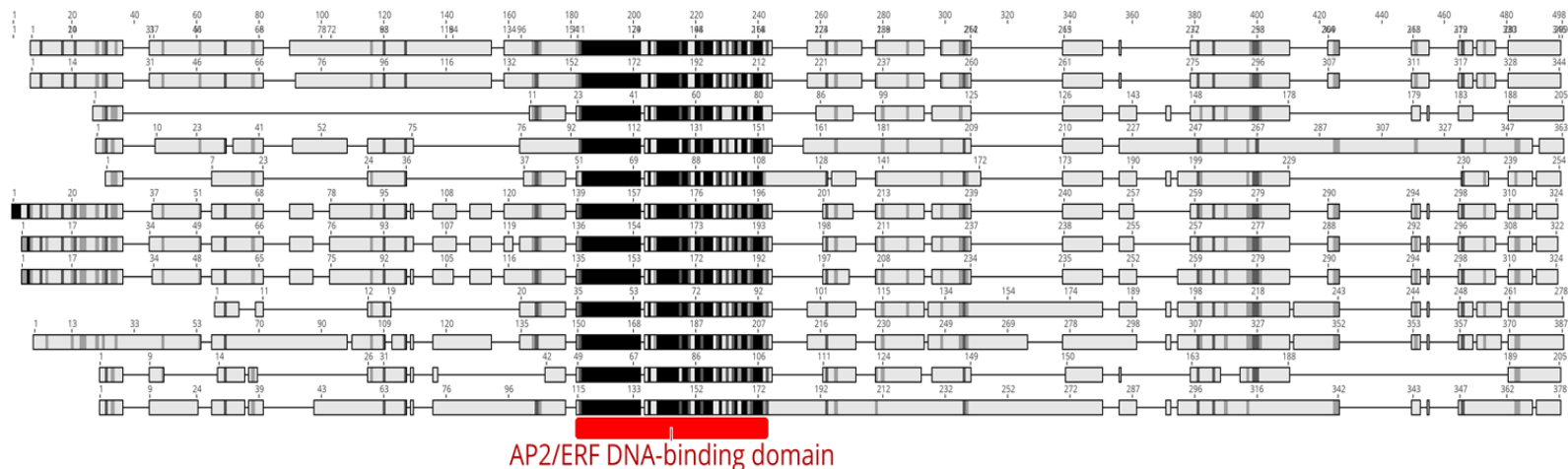


Figure 3. 15 Alignment of all ERF proteins identified in the Y2H screen. The proteins belong to four different groups of ERF subfamily: group IX (7 and 57; highlighted in green), group VIII (23; highlighted in grey), group X (4, 67, 70.2, 108, 112, 204 and 259; highlighted in yellow) and group VII (highlighted in orange). The only known functional domain conserved in all proteins is AP2/ERF DNA-binding domain (annotated in red).

ERF4, ERF8 and ERF10, whereas ERF88, which belongs to subgroup VIII-B-1b does not interact with RGA, suggesting that RGA specifically interacts with ERFs in the VIII-B-1a subfamily (Zhou *et al.*, 2016). Therefore, it seems that DELLAs may exclusively interact with only a subset of ERF TFs, and these interactions are potentially mediated via different protein motifs, depending on an ERF class.

3.4.3 RHT-1 interacts with TaIDD11 transcription factors in wheat

Two out of the 11 strongest interactors identified in the screen, interactors 127 (TraesCS2B02G218900) and 241 (TraesCS2A02G188400) (Figure 3.2, Table 3.1) are homoeologues of the same *TaIDD11* gene in wheat. The third homoeologue of the gene was also identified in the screen (interactor 9.1, TraesCS2D02G199300), but did not show such strong interaction in the Y2H assays. The interaction between TaIDD11 and RHT-1 was confirmed in Y2H assays and by BiFC. Interestingly, no other IDD protein was identified in the aleurone screen, although DELLAs have been shown to interact with almost all subgroups of IDD proteins, apart from the distinct subgroup formed by AtIDD14, AtIDD15 and AtIDD16 (Aoyanagi *et al.*, 2020).

The IDD family in Arabidopsis and rice has 16 and 15 members, respectively (Supplementary Table 3.3; Colasanti *et al.*, 2006). The IDD family of TFs in wheat has not yet been identified, but our phylogenetic analysis identified 14 distinct IDD proteins in wheat (Figure 3.10).

3.4.3.1 DELLAs interact with AtIDD1 and AtIDD2 to regulate growth and germination in Arabidopsis

Few studies in the last decade reported IDD TFs as DIPs (Aoyanagi *et al.*, 2020; Feurtado *et al.*, 2011; Fukazawa *et al.*, 2014; Yoshida *et al.*, 2014). Among these, two reports were especially interesting as they characterised the

function of the IDD TFs ENY (Feurtado *et al.*, 2011) and GAF1 (Fukazawa *et al.*, 2014), that were found in the same clade as TaIDD11. These two homologous Arabidopsis IDD proteins were found to interact with all DELLA proteins, and it was hypothesized that they may act redundantly, depending on the site of expression (Feurtado *et al.*, 2011; Fukazawa *et al.*, 2014). GAF1 was found to bind to GAI and use it as a cofactor to enhance the expression of *AtGA20ox2* gene, whereas binding of GAF1 to its corepressor, TPR4 (TOPLESS-RELATED 4), repressed the transcription. Furthermore, it was confirmed that GAF1 associates with GAI and TRP4 on the *AtGA20ox2* promoter. GAF1-GAI complex was also found to activate the promoters of *AtGA20ox2*, *AtGA3ox1* and *GID1b*, genes involved in GA biosynthesis and signal reception. Analysis of GAF1 overexpression lines and *gaf1 idd1* double mutant revealed that GAF1 is involved in GA-mediated cell elongation and transition to flowering. In turn ENY downregulates the top five genes identified as GA-downregulated and DELLA-upregulated (*GA4*, *GA20ox2*, *SCL3*, *AT4G19700*, and *GID1b*). In a study by Feurtado *et al.* (2011), ENY was found to strongly interact with all five DELLAs in Arabidopsis and affect the expression levels of *SCL3* and *DELLA* genes during seed development. *ENY* overexpression lines were hypersensitive to GA during photomorphogenesis and less sensitive to inhibition of germination by ABA, and mature seeds of overexpression lines accumulated lower amounts of endogenous ABA compared to the WT. What is more, ENY also represses the expression of *GATA TRANSCRIPTION FACTOR 21 (GNC)*, a protein that function to repress GA action and inhibit germination (Richter *et al.*, 2010) and reduces the modulation of GA positive feedback loop by downregulating *AT-HOOK PROTEIN OF GA FEEDBACK1 (AGF1)*, a transcription factor that promotes the GA positive feedback loop and counteracts the negative loop (Matsushita *et al.*, 2007).

The wheat protein TaIDD11 shares the most sequence homology with Arabidopsis ENY and GAF1. Phylogenetic analysis showed that TaIDD11 clusters with ENY, GAF1, OsIDD1, OsIDD5 and another wheat IDD protein (hereafter called TaIDD12) (Figure 3.10). Sequence analysis revealed that all

these IDD proteins contain the same functional domains in their structure (Figure 3.11), including the EAR motif, which can only be found in this clade of IDD proteins. This indicates similar roles for the IDD proteins in Arabidopsis, rice, and wheat. ENY and GAF1 were suggested to have redundant roles in Arabidopsis, and since OsIDD1, OsIDD5, TaIDD11 and TaIDD12 were all found in the same clade, it could be hypothesized that similar is true for rice and wheat. The functional studies of the rice IDD TFs have not yet been conducted, nevertheless, since both Arabidopsis proteins, ENY and GAF1, are involved in regulating GA-mediated growth and germination, it can be hypothesized that TaIDD11 may have a role in controlling similar developmental processes in wheat.

3.4.4 Summary

This Chapter reports the screening of wheat aleurone for binding partners of wheat DELLA protein, RHT-1. Such attempts have not yet been reported and the results provide prospective insights into the roles of RHT-1 in the aleurone of wheat, and potentially other cereals. RHT-1 was found to interact with various classes of proteins, including TFs, enzymes, defensins and heat shock proteins. Two selected TFs, TaIDD11 and TaERF5, were shown to interact with RHT-1 in yeast and in the plant system. Interactor identified as TaIDD11 showed the highest sequence similarity to Arabidopsis ENY and GAF1, which are involved in regulation of GA synthesis and signalling during growth and germination. This suggests that TaIDD11 may play a similar role controlling GA signalling in the aleurone. TaERF5 does not have a clear homolog in Arabidopsis, hence inferring its function and relevance of its interaction with RHT-1 remains to be established. In summary, Y2H screen was successfully used to identify two candidate TFs that may be involved in regulation of the GA response in the aleurone of wheat.

Chapter 4: The genetic characterisation of the *TaIDD11* genes

4.1 Introduction

Genetic analysis is a powerful tool that allows for establishing a direct link between the biochemical function of a gene product and its biological significance (Ben-Amar *et al.*, 2016; Jankowicz-Cieslak & Till, 2016). Recent advances in the sequencing technologies along with their increasing affordability sparked an increase in genome sequencing projects. In the last few decades, there has been a dramatic increase in the available genome sequence data for major crop species, and in 2018, after many years of collective efforts, a fully annotated reference genome for wheat was released (International Wheat Genome Sequencing Consortium (IWGSC) *et al.*, 2018). Genome sequencing projects have identified a multitude of plant genes, their genomic location and structure; however, for many of these genes, their function is yet to be elucidated. The growing use of bioinformatics helped understand the function of genetic components, for example the presence of known functional domains and the possible modes of genetic regulation, but the elucidation of gene physiological function must always be verified using genetic analysis *in vivo*.

Characterisation of the genes in plant systems is achieved by comparing the development, phenotype, and responses to given stimuli, as well as alterations to molecular mechanisms in knockout (KO) lines, i.e. lines in which the function of the gene of interest (GOI) has been removed, as well as in the lines overexpressing the respective gene. The function of the *TaIDD11* gene was decided to be studied in the wheat mutant line in which *TaIDD11* gene was inactivated in all three genomes, named *Taidd11* mutant. The mutant was generated using the Targeted Induced Lesions in Genomes (TILLING), an easy and relatively inexpensive reverse genetics method that has been widely used in Rothamsted.

4.1.1 TILLING as a reverse genetics approach to study wheat genetics

Reverse genetics aid the understanding of gene function by analysing the phenotypic traits acquired by genetically engineering specific sequences within the gene to generate loss- or gain-of-function, reduced function or overexpression mutants. This represents an opposite approach to the classically used forward genetics, where researchers seek to elucidate the genetic basis of an observed phenotypic abnormality. Understanding the gene function in staple crops is essential to achieve trait improvement by allowing targeted breeding approaches. Considerable reverse genetics-based studies have been conducted in *Arabidopsis* and other model species; however, this research does not necessarily translate directly into crops. Therefore, functional genetics studies in crop species are critical for crop improvement. With the emergence of functional genomics resources in wheat and other crop species, the discoveries from model species can be relatively easily tested in crops (Borrill, 2019).

Several reverse genetics approaches have been developed for studying plant genes, including TILLING. The TILLING approach combines chemical mutagenesis using ethyl methanesulfonate (EMS), which generates single nucleotide polymorphisms (SNPs), with high-throughput genome-wide screening for point mutations, to create novel mutant alleles in the GOI. These point mutations are generated at random locations, but knowing the sequence of the GOI, it is easy to infer the effect of each mutation. TILLING-based approaches do not involve the introduction of foreign DNA or RNA and are therefore subject to fewer regulatory restrictions and barriers to commercial application of resulting accession lines than other widely used transgenic-based reverse genetics techniques, such as RNAi and CRISPR-Cas.

TILLING was developed and successfully applied in *Arabidopsis* when, after the completion of genome sequencing, the emphasis in genomics shifted from sequence analysis to understanding gene function (Colbert *et al.*, 2001;

McCallum *et al.*, 2000). However, this method can be applied to any species and was shown to be a suitable method for generating null knockout mutants in wheat (Dong *et al.*, 2009; Slade *et al.*, 2005). The polyploid nature of the bread wheat genome limits the scope of classical phenotypic screens due to the presence of functionally redundant homoeologues. At the same time, the ploidy of wheat makes it a well-suited species for mutational approaches, as the functional genomic redundancy allows for higher tolerance of mutational load compared with diploid species (Uauy *et al.*, 2017). Among many advances in genomic resources for *in silico* studies of the wheat genome, a wheat TILLING resource has been developed (Krasileva *et al.*, 2017), allowing for rapid identification of mutations in the GOI. This data is now publicly available on Ensemble Plants website (<https://plants.ensembl.org>). The spring wheat cultivar Cadenza was used to generate this TILLING population in hexaploid wheat. This population was established at Rothamsted Research UK in 2004/05 and characterised in the field for agronomic traits in the M₃-M₆ generations (Rakszegi *et al.*, 2010). TILLING was used in the present study as a method to generate a null knockout *Taidd11* mutant in wheat.

4.1.2 DELLAs act as IDD protein coactivators to regulate GA-mediated gene expression

The *INDETERMINATE DOMAIN (IDD)* genes belong to a conserved family of transcription factors that regulate many diverse developmental and physiological processes in plants, including plant architecture, seed development, modulation of floral transition, sugar and ammonium metabolism and cold responses (reviewed in Kumar *et al.*, 2019). Some family members were also identified to take part in regulating hormonal signalling.

Several IDD proteins were demonstrated to interact with DELLAs to regulate gene expression (Aoyanagi *et al.*, 2020; Feurtado *et al.*, 2011; Fukazawa *et al.*, 2014; Lu *et al.*, 2020; Xuan *et al.*, 2013; Yoshida *et al.*, 2014; Yoshida & Ueguchi-Tanaka, 2014). Detailed studies of the mechanism of gene regulation revealed

that DELLAs act as IDD coactivators (Fukazawa *et al.*, 2014; Lu *et al.*, 2020). The GAI-ASSOCIATED FACTOR1 (GAF1; AtIDD2) transcription factor was identified to have dual action in regulating gene expression in response to GA (Fukazawa *et al.*, 2014). In the absence of GA, GAI acted as a GAF1 coactivator, promoting the transcription of GA-biosynthetic genes *AtGA20ox2* and *AtGA3ox1*, and the GA receptor *GID1b*. However, when GAI was degraded in response to GA signalling, the same genes were found to be repressed by GAF1 in complex with its corepressors, TOPLESS RELATED 1 (TPR1) and TPR4. Thus, GAF1 can either activate or inhibit gene expression, depending on the balance between its coactivator GAI and corepressor TPR. A similar mode of action in which DELLA acts as an IDD coactivator was established in rice (Lu *et al.*, 2020). In the absence of GA, SLR1 in complex with OsIDD2 promoted expression of MiR396, which in turn reduced the transcript levels of miR396-regulated *GRF* genes, resulting in decreased cell proliferation and a subsequent reduction in stem elongation. Conversely, GA-mediated SLR1 degradation and resulting lack of OsIDD2 coactivation inhibited miR396 activation, leading to higher expression of *GRF* genes and an increase in stem length (Lu *et al.*, 2020). These studies show that the typical mode of DELLA-IDD complex action is to positively affect gene expression with DELLA acting as an IDD coactivator.

The following Chapter describes the generation of the *Taidd11* mutant in wheat using TILLING technology and its subsequent phenotypic characterisation, with a particular emphasis on perturbations in GA signalling. BC₁F₂ and BC₁F₃ populations were subjected to phenotypic analysis. The *Taidd11* triple mutant was assessed at the physiological level (flowering time, plant and leaf size, components of the yield) as well as at the molecular level (gene expression in growing leaf sheaths). The sensitivity to applied GA was evaluated, along with the GA levels in the growing seedling leaf sheaths and the levels of *TaAMY1* gene in the aleurone in response to GA application. The *Taidd11* mutant was demonstrated to be a GA-insensitive semidwarf that produces shorter stems than WT lines in the same background, but does not

seem to affect the aleurone response, even though the original interaction between TaIDD11 and RHT-1 was identified in the aleurone.

4.2 Material and Methods

4.2.1 GA dose response assays

WT Cadenza, null segregant (NS; BC₁F₂ or BC₁F₃ segregating line that is WT at the *TalDD11* loci), *Taldd11* and *Rht-D1b* seeds were surface sterilised and germinated as described in Chapter 2, Section 2.3.1. Three days after imbibition, seeds were transplanted into moist vermiculite containing water or GA₃ solution. GA₃ concentrations used ranged from 10⁻⁹ M (1 nM) to 10⁻⁴ M (100 μM), in 10-fold increments. Eight seeds per genotype were planted in randomly distributed rows in the tray, and the trays distributed randomly on the shelf in the controlled environment (CE) room. CE growth conditions were a 16-hour photoperiod with 21°C/16°C day/night temperatures. Photoperiod was provided by tungsten fluorescent lamps providing 500 μmol/m²/s¹ PAR (photosynthetically active radiation). The trays were watered with 150 ml of water or the respective GA₃ solution every other day. On the tenth day, seedlings were removed from the vermiculite and the leaf sheaths (between the grain crown and ligule of the first leaf (L1)) and L1 blade lengths (Figure 4.1) were measured. GA dose response data was statistically analysed using GenStat (20th edition, 2019, ©VSN International, Hemel Hempstead, UK).

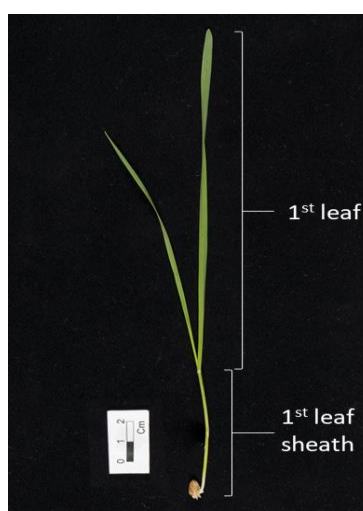


Figure 4. 1 10-days old wheat seedling variety Cadenza. Seedlings at this stage of development were measured in GA dose response assays. The parts of the seedling that were measured were leaf sheath and L1 blade.

4.2.2 GA hormone extraction and analysis

WT Cadenza, NS, *Taidd11* and *Rht-D1b* seeds were sterilised, germinated, and grown in vermiculite trays in the CE room (conditions as specified in Section 4.2.1). The seedlings were watered every other day. Four biological replicates per genotype per treatment were grown, and each biological replicate included ten samples. The leaf sheath fragments of 7-day old wheat seedlings were harvested between the grain crown and the top of the coleoptile, freeze dried for five days and sent for analysis of GAs levels.

The protocol used for extraction and analysis is described in Urbanová *et al.*, (2013) and was performed by Dr Danuše Tarkowská in the Laboratory of Growth Regulators at Palacký University Olomouc. GAs were extracted from the freeze-dried, ground leaf sheaths homogenate and purified using Oasis® MAX anion exchange column, providing selective enrichment and efficient clean-up. Ultra-performance liquid chromatography (UPLC) was used to separate different GAs which were quantified by ESI-M/MS, using multiple-reaction monitoring mode (MRM). Data was statistically assessed using general ANOVA in GenStat (20th edition, 2019, ©VSN International, Hemel Hempstead, UK).

4.2.3 RNA-Seq

WT Cadenza, *Taidd11* and *Rht-D1b* seeds were sterilised, germinated, and grown in trays containing vermiculite in the CE room (conditions as specified in Section 4.2.1). Four biological replicates per genotype per treatment were grown, and each biological replicate included ten samples. Seeds were sown in randomly distributed rows in randomly distributed trays and watered every other day with 150 ml of water. Seven days post-germination, half of the trays were treated with 100 µM GA₃ and the other half with water. 8 hours after the treatment the material (tissue between the grain crown and the top of the coleoptile) was harvested and flash-frozen in liquid nitrogen. The samples

were homogenized manually using mortar and pestle, and around 75 – 100 mg of the frozen homogenate used for RNA extraction. RNA was extracted using Monarch® Total RNA Miniprep Kit (New England Biolabs, Ipswich, Massachusetts, USA) according to the protocol, which included a DNase treatment. The quality of the RNA was assessed using the Agilent RNA 6000 Nano Chip and Agilent 2100 Bioanalyzer (Agilent, Santa Clara, USA). RNA samples were sent to Novogene Europe (Cambridge, UK) for further processing and sequencing to a depth of 30 million reads.

The raw files received from Novogene were processed using Galaxy (Afgan *et al.*, 2018) and the free online 3D RNA-seq App (Guo *et al.*, 2019). The raw FASTQ files were uploaded to Galaxy and mapped to the latest IWGSC RefSeq v1.0 assembly for *Triticum aestivum* using Kalisto quant function (Bray *et al.*, 2016). The resultant tabular files were uploaded to the 3D RNA-seq App and the data analysed using a CPM cut-off of 1, $p_{adj} < 0.01$ and no fold change settings. Comparisons were made between control and GA₃ treatment for the three genotypes, as well as for the genotypes with the same treatment. Heat maps were plotted using matrix visualization and analysis software, Morpheus (<https://software.broadinstitute.org/morpheus>).

4.2.4 qRT-PCR

Seeds of WT Cadenza, NS, *Taidd11* and *Rht-B1c* were used in the study. Embryoleless half-seeds were surface sterilised and imbibed in 20 mM CaCl₂ in the dark for 72 hours. After the incubation the aleurone layer was isolated by scraping off the endosperm, and either snap frozen (time zero, T₀) or further incubated in 20 mM CaCl₂ or 20 mM CaCl₂ supplemented with 10 µM GA₃ for 48 hours (48h -GA and 48h +GA, respectively) and then snap frozen in liquid nitrogen. Three biological replicates per genotype per treatment were analysed. Each biological replicate contained 5 half-aleurones. RNA was extracted using Monarch® Total RNA Miniprep Kit (New England Biolabs, Ipswich, Massachusetts, USA) according to the protocol, including the DNase

treatment. cDNA synthesis was performed according to SuperScript™ III Reverse Transcriptase protocol (Waltham, Massachusetts, USA) and transcript amplification using SYBR™ Green PCR Master Mix (Waltham, Massachusetts, USA). The data analysis workflow is described in Chapter 2, Section 2.1.2.

4.3 Results

4.3.1 Tissue-specific expression patterns of *TaIDD11* in wheat

Studying the expression pattern of the gene helps identify its potential developmental- and tissue-specific roles. In polyploid species it also establishes the potential contribution of individual homoeologous genes. Expression of the three homoeologues of *TaIDD11* was obtained from publicly available RNA-seq data generated from another spring wheat variety, Chinese Spring, by searching the Wheat Expression Browser (www.wheat-expression.com). The data available on the website include 82,567 high-confidence (HC) genes (74.5% of the genome) collected from 123 samples across 15 different tissues at various developmental stages (Supplementary Table 4.2) (Ramírez-González *et al.*, 2018).

The expression data for *TaIDD11* homoeologues in the 70 samples included in the study are presented on the graph in Figure 4.2. The *TaIDD11* gene is expressed in all investigated samples at each developmental stage, and all three homoeologues of the gene are expressed. *TaIDD-D11* is the most highly expressed homoeologue in most tissues, whereas *TaIDD-A11* is consistently the least highly expressed homoeologue. Homoeologues from the B and D genomes display more similar expression, with *TaIDD-D11* being the predominant transcript at all developmental stages in tissues including the ligule, leaf sheath and blade and peduncle, and *TaIDD-B11* in lemma, embryo proper (the part that will differentiate into the mature embryo) and grain.

Differential expression of distinct homoeoloci was studied in detail in wheat (Leach *et al.*, 2014). In that study, around 45% of genes on wheat chromosomes 1 and 5 were expressed as three distinct homoeoloci in both shoot and root tissues, with most of these genes displaying a bias towards a single dominating homoeolocus. No global bias towards preferential expression of particular homoeologue was observed, however, in cases when two homoeologues equally dominated total gene

Gene expression

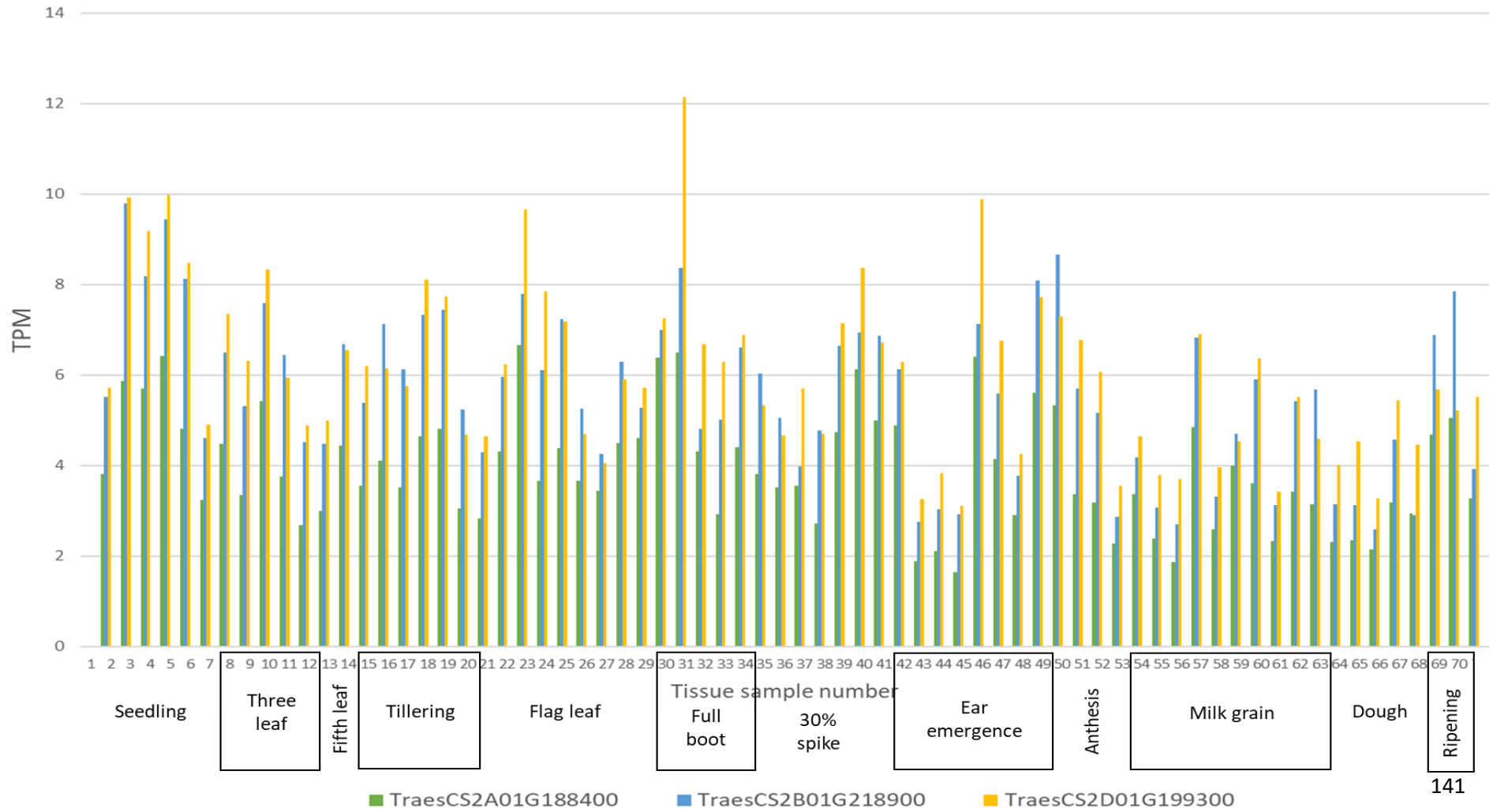


Figure 4. 2 Relative expression of the three homoeologues of the *TaIDD11* gene in wheat variety Chinese Spring. Data for 70 samples taken from various tissues at various developmental stages calculated in TPMs (transcripts per million) are presented. The developmental stage groups are: seedling (1-7), three leaf (8-12), fifth leaf (13-14), tillering (15-20), flag leaf (21-29), full boot (30-34), 30% spike (35-41), ear emergence (42-49), anthesis (50-53), milk grain (54-63), dough grain (64-68) and ripening (69-70) (refer to Appendix, Table 4 for full details). Data taken from Ramírez-González et al., (2018).

Table 4. 1 Expression of three homoeologues of the *TaIDD11* gene in various parts of the grain 10, 20, and 30 days post anthesis. Expression was measured in RPKMs (reads per kilobase per million). Data taken from Pfeifer et al., (2014). WE = whole endosperm, AL = aleurone layer, SE = starchy endosperm, TC = transfer cells, ALSE = aleurone contaminated with starchy endosperm.

| Gene | IWGSC RefSeq v1.0 | IWGSC | Expression in RPKM | | | | | | |
|------------------|---------------------------|----------------------------|--------------------|------|------|------|------|--------|------|
| | | | WE10 | AL20 | SE20 | TC20 | WE20 | ALSE30 | SE30 |
| <i>TaIDD-A11</i> | <i>TraesCS2A02G188400</i> | <i>Traes_2AS_9D9D66343</i> | 1.91 | 4.48 | 2.91 | 3.60 | 2.99 | 4.10 | 4.53 |
| <i>TaIDD-B11</i> | <i>TraesCS1B02G218900</i> | <i>Traes_2BS_C270C0C9F</i> | 1.26 | 2.81 | 1.06 | 1.85 | 1.55 | 1.96 | 2.39 |
| <i>TaIDD-D11</i> | <i>TraesCS2D02G199300</i> | <i>Traes_2DS_9A20BB46C</i> | 2.99 | 5.66 | 4.09 | 4.75 | 4.96 | 5.57 | 8.02 |

expression, A and D or B and D homoeoloci dominance was much more prevalent than that of homoeologues A and B. The expression of *TaIDD11* homoeologues displays a slight bias towards B and D homeoloci. Relative overall expression of *TaIDD11* is highest in stem and various leaf tissues at seedling, 3-leaf, tillering, flag leaf and full boot stages. At ear emergence, the expression in leaf sheath and blade decreases and higher expression is observed in the peduncle, glumes, and lemma. Relatively lowest expression of the gene is observed at later developmental stages (ear emergence, milk, and dough grain stages) in leaf sheaths, blades, and grains.

Since the aleurone was the tissue where RHT-1-TaIDD11 interaction was identified, grain tissue-specific *TaIDD11* expression was investigated (Table 4.1). Pfeifer *et al.*, (2014) data, collected from wheat cv. Chinese spring grain tissues during seed differentiation (10 and 20 DPA) and maturation (30 DPA) were used. *TaIDD-D11* is the most highly expressed, whereas *TaIDD-B11* is the least highly expressed homoeologue. The expression seems to increase slightly with the progressing development. While at 20 DPA the overall expression of *TaIDD11* is highest in the aleurone, at 30 DPA it is higher in the starchy endosperm.

To conclude, *TaIDD11* is expressed across all wheat tissues and could regulate many developmental processes.

4.3.2 Generation of a *Taidd11* knockout mutant in wheat using TILLING

4.3.2.1 Identification of the EMS (ethyl methanesulfonate)-induced mutations in the *TaIDD11* genes

Ethyl methanesulfonate (EMS) is a mutagenic organic compound that produces random G to A or C to T point mutations in DNA by nucleotide substitution. To identify the EMS-induced mutations in the *TaIDD11* homoeologues that would result in an inactive protein product, genomic

sequences from IWGSC_RefSeq_v1.1 assembly including mapped EMS mutations were used. Mutations were originally identified in M2 segregants using exome capture and subsequent sequencing. The mutations were annotated with the library number and the number of supporting variant reads found to be WT or mutated at the SNP position, e.g. LIB16234:28:32, which indicates that the mutation was identified in library 16234 and in M2 population, 28 reads sequenced from the fragment surrounding the mutation shown to be WT at the SNP position, and 32 reads contained the mutation. The library number was converted to a CAD4 identification code for the line number, and M4 seed used in the study. From all the identified mutations, those that were expected to cause a loss-of-gene function were selected. Figure 4.3 shows three *TaIDD11* homoeologues in wheat with the assumed gene models, known functional protein domains, and the position and predicted effect of the EMS mutations selected for generating the *Taidd11* mutant. The EMS mutation number, the number of the wheat line carrying the mutation, the effect of the mutation and its zygosity are summarised in Table 4.2.

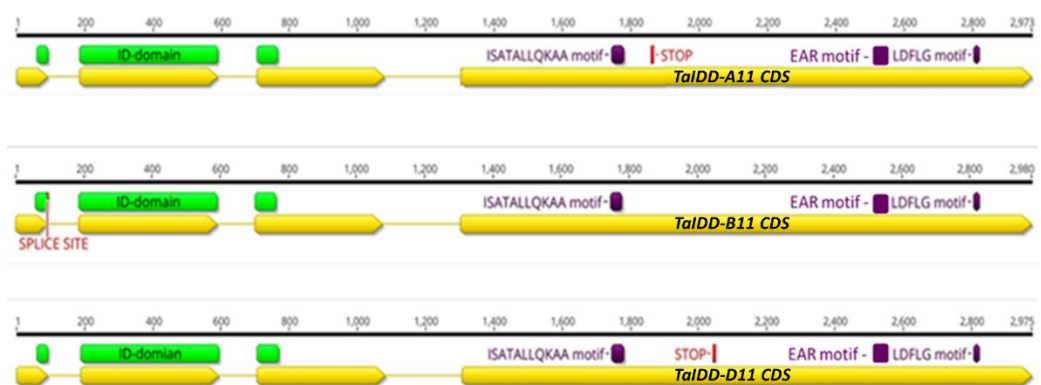


Figure 4. 3 *TaIDD11* homoeologues gene models, with functional protein domains and EMS mutations used to generate the *Taidd11* mutant annotated. Yellow arrowed lines are the exons, green box is the Indeterminate (ID) domain (DNA-binding domain), purple boxes are the other protein functional domains: ISATALLQKAA, EAR and LDFLG. On each homoeologue, the EMS mutations used to generate the null *Taidd11* mutant are mapped. No UTRs are shown.

Table 4. 2 Wheat TILLING lines carrying the EMS mutations, their effect and zygosity.

| Homoeologue | Mutation number | Line number | Effect | Zygosity |
|------------------|-----------------|-------------|-------------|--------------|
| <i>TaIDD-A11</i> | LIB16234 | CAD4-1185 | STOP gained | Heterozygous |
| <i>TaIDD-B11</i> | LIB8437 | CAD4-1415 | SPLICE SITE | Heterozygous |
| <i>TaIDD-D11</i> | LIB15477 | CAD4-0828 | STOP gained | Heterozygous |

A potential loss-of-function mutation in *TaIDD-A11* was identified in LIB16234. This conferred a C to T substitution at nucleotide 2244 of the genomic sequence of the gene, which was predicted to introduce a nonsense mutation at position 491 in the protein sequence (Q491*). The predicted protein length for the protein encoded by the A homoeologue is 845 amino acids and the selected mutation would result in a premature stop codon and a protein containing only 490 amino acids. The presence of nonsense mutations was not identified in the *TaIDD-B11* gene. However, a mutation that was expected to affect splicing was selected. The LIB8437 mutation is located directly after the first exon (Figure 4.3 and Figure 4.4 A) and causes a G to A substitution at the nucleotide 306 of the genomic sequence of the gene. The presence of this mutation is expected to result in the spliceosome not recognising the splicing site and therefore leaving the first intron as a part of the transcribed mRNA. If splicing does not occur due to this mutation and the intron is translated into a protein, the frameshift will result in a premature stop codon early in the second exon (Figure 4.4 B) and a truncated protein of only 67 amino acids in length, instead of the predicted 847 of the native protein. A mutation identified in LIB15477 was found to introduce a premature stop codon in gene *TaIDD-D11*. The mutation causes a C to T substitution at nucleotide 2943 of the genomic sequence of the gene generating a Q537* substitution in the protein sequence. The truncated protein resulting from this mutation would be expected to be 536 amino acids in length as opposed to 845 amino acids in the native protein. All the selected EMS mutations were heterozygous in the M2 population.

4.3.2.2 Validating the LIB8437 mutation

Pre-mRNA splicing occurs in the spliceosome, a large complex assembled from small nuclear RNAs (snRNAs) and various protein components that together make up the small nuclear ribonucleoprotein particles (snRNPs). This process is conserved across eukaryotes and involves the recognition of the junction between exon and intron and intron excision through a two-step transesterification reaction (Hastings & Krainer, 2001). The spliceosome recognizes three conserved sequences at or near the exon-intron junction boundaries: 5' splice site (5'ss), the branch point sequence (BPS) and the 3'ss. There are at least two classes of introns: U2 snRNP-dependent introns and U12 snRNP-dependent introns. U2 snRNP-dependent introns make up the majority of all introns (99.8% of all introns in Arabidopsis, Sheth *et al.*, 2006) and they consist of three subtypes according to the dinucleotides at the donor and acceptor sites: GT-AG, GC-AG and AT-AC. U12 snRNP-dependent introns are the minor class of introns (~0.17% in Arabidopsis, Sheth *et al.*, 2006), and consist mainly of two subtypes: AT-AC and GT-AG introns, however, a small fraction of the U12-type introns contain different nucleotides at the donor and acceptor sites.

The LIB8437 mutation is positioned at the splicing donor site of the first intron of the *TaIDD-B11* gene (Figure 4.3 and Figure 4.4 A). The first intron is the U2 snRNP-dependent GC-AG type, and mutation LIB8437, which is a G to A mutation, causes loss of the splicing donor site, hence the splicing is not expected to occur. The CAD4-1415 line carrying the LIB8437 mutation was selected for further analysis to establish whether splicing is affected. A fragment encoding 198 bp (39 bp of the first exon, 95 bp of the first intron and 64 bp of the second exon of *TaIDD11* homoeologues) was amplified from WT Cadenza and the CAD4-1415 line cDNA and sequenced using barcoded primers (Supplementary Table 4.1). Primers were designed to be generic for the three *TaIDD11* homoeologues. However, the SNP caused by EMS mutation within the amplicon allowed the unspliced B homoeologue to be distinguished from the other two homoeologues.

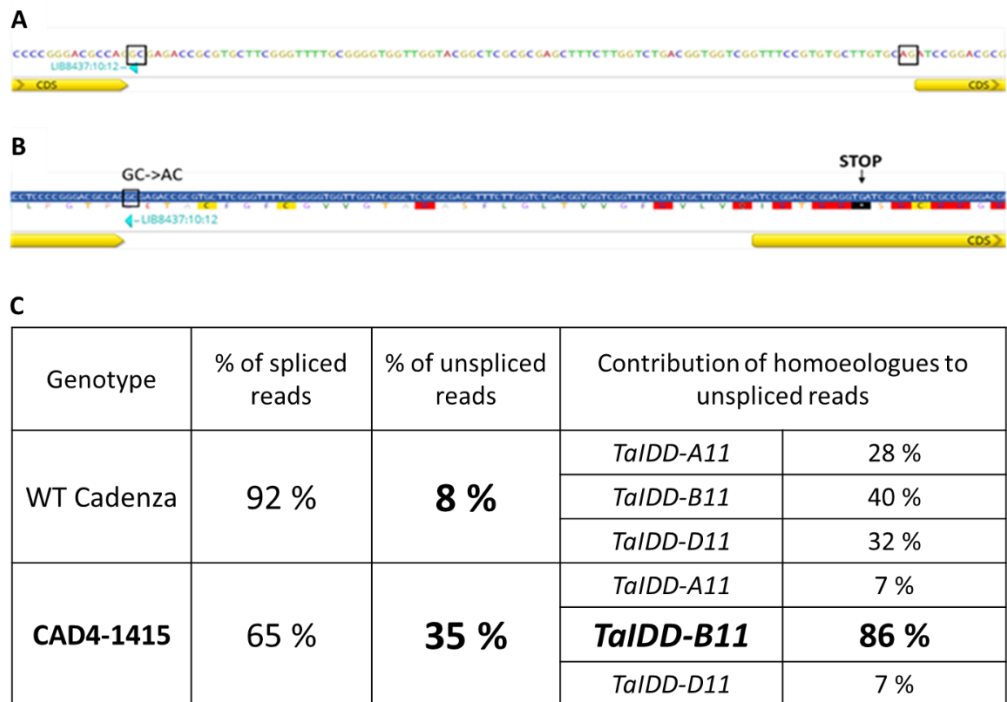


Figure 4.4 A. The donor and acceptor splicing sites in the first intron of the *TaIDD-B11* gene. The intron is the GC-AG (marked with black squares) subtype of the U2 snRNP-dependent intron. The mutation LIB8437, a G to A substitution, is annotated in blue. B. The effect of the splice site mutation on the translation. If the splicing does not occur due to mutation (G→A) and the intron is translated into a protein, the frameshift caused the STOP codon to appear early in the second exon (indicated as a black block with a white asterisk on it), and the translated protein is only 67 amino acids long. C. Table summarising the results of NGS analysis carried out on CAD4-1415 and WT Cadenza lines to investigate the effect of LIB8437 mutation on the splicing frequency.

Amplicons were sequenced using next-generation sequencing (NGS) that was performed by Dr Steve Hanley at Rothamsted Research, using Illumina sequencer. The reads were mapped to the genomic sequence of the *TaIDD-B11* gene using a splice-aware global aligner for DNA and RNA sequencing reads, BBMap (<https://jgi.doe.gov/data-and-tools/bbtools/bb-tools-user-guide/>), and analysed using Integrative Genomics Viewer (IVG, Thorvaldsdóttir *et al.*, 2013).

The table in Figure 4.4 C shows the percentage of spliced and unspliced reads in both samples, and the percentage contribution to the unspliced reads of

each homoeologue. The WT Cadenza sample contained 92% spliced and 8% unspliced reads compared to 65% and 35% of spliced and unspliced reads, respectively, in the CAD4-1415 line. The small percentage of unspliced reads in WT Cadenza sample originated relatively equally from all three homoeologues (28%, 40% and 32% from homoeologues A, B and D, respectively). In the CAD4-1415 sample, the big increase in the unspliced reads percentage (8% to 35%) was almost solely due to homoeologue B, which contributed 86% of the reads. The contribution of homoeologues to spliced reads could not be established due to lack of SNPs specific to each homoeologue in the CDS. The results confirm the deleterious impact of the LIB8437 mutation on the splicing efficiency of the CAD4-1415 line.

4.3.2.3 Stacking the EMS mutations to generate the *Taidd11* triple mutant

Generating a *Taidd11* triple mutant was essential to study the role of the *TaIDD11* gene in wheat as wheat is a hexaploid species and the presence of a gene copy in each of the three genomes introduces a high level of gene redundancy. To obtain this mutant, lines CAD4-1185, CAD4-1415 and CAD4-0828 were crossed to stack the mutations in the three homoeologues. The TILLING lines were obtained from Dr Andy Phillips at Rothamsted Research, UK, and the mutations confirmed in the M5 population (Figure 4.5 A, B). Primers used to amplify the respective genes' fragments (Supplementary Table 4.1) were designed to be homoeologue-specific. Amplicons were sequenced and then aligned to the genomic sequences of the respective homoeologues to establish the presence of the mutations and their zygosity (Figure 4.5).

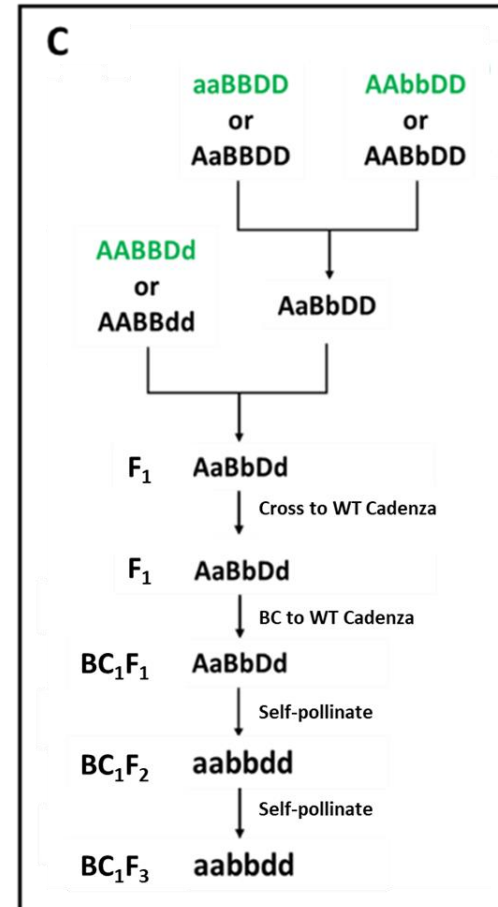
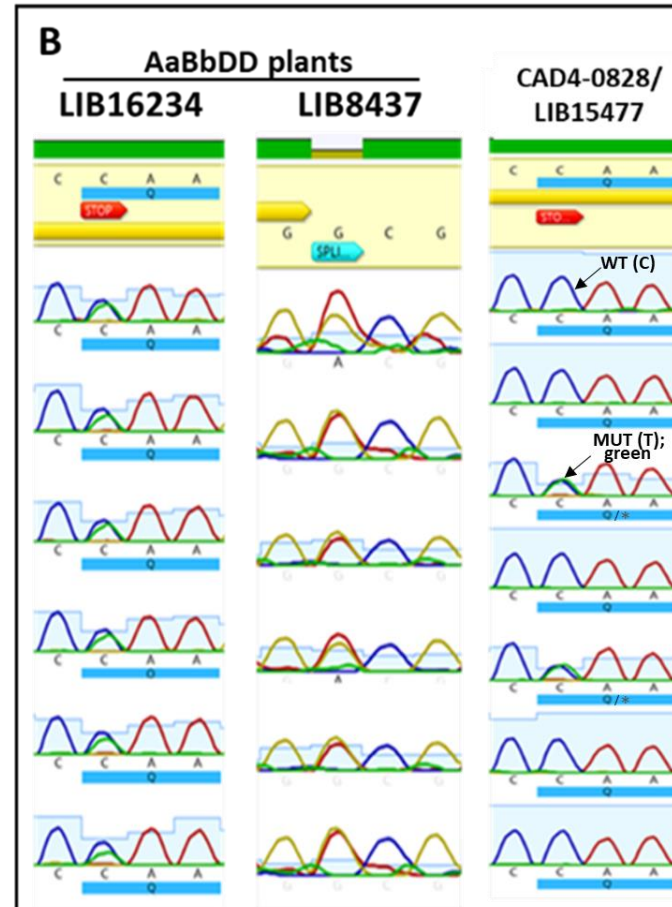
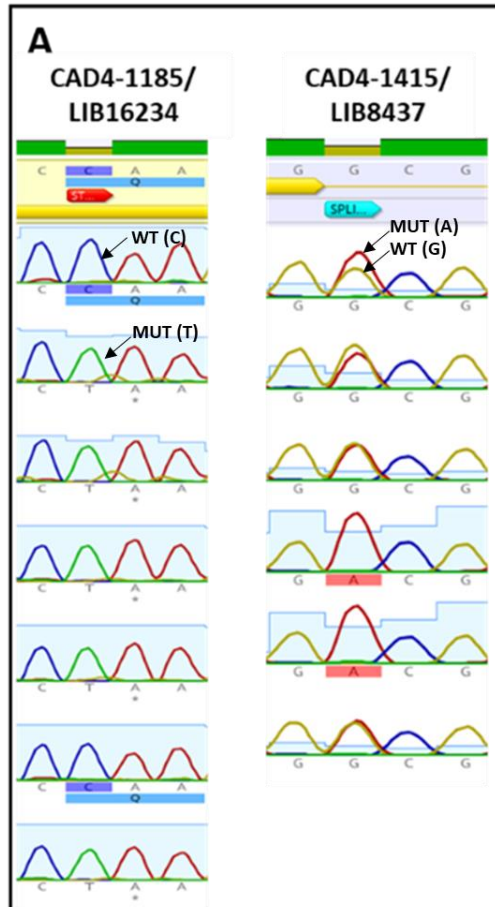


Figure 4. 5 Confirmation of *TaIDD11* TILLING mutations in M5 plants and crossing strategy to generate the triple mutant. A. Chromatograms of the CAD4-1185 and CAD4-1415 TILLING lines that contain LIB16234 and LIB8437 mutations, respectively. The sequences on the top of each panel are the WT sequences. Homozygous C (WT) to T (MUT) mutation is present in five out of seven screened CAD4-1185 plants. Majority of CAD4-1415 plants contained a heterozygous mutation (represented by double peak); the two with the homozygous G (WT) to A (MUT) mutation were used for crossing. B. All the progeny of CAD4-1185 and CAD4-1415 was heterozygous, and the AaBbDD double mutant was crossed with CAD4-0828 containing heterozygous LIB15477 mutation. Only two plants showed to contain heterozygous C (WT) to T (MUT) mutation. C. Standard crossing strategy when stacking the TILLING mutations in hexaploid wheat. A minimum of five generations are required to obtain a BC₁F₂ triple mutant for phenotypic characterisation. Highlighted in green are the genotypes of the plants crossed to generate the *Taidd11* knockout mutant.

Figure 4.5 C illustrates the crossing strategy used to obtain the triple homozygous mutant. Homozygous mutations in *TaIDD-A11* and *TaIDD-B11* genes were found in five CAD4-1185 plants and two CAD4-1415 plants, respectively (Figure 4.5 A). Homozygous plants were crossed as described in Chapter 2, Section 2.3.3, and the double heterozygous mutant (AaBbDD) was crossed with the CAD4-0828 line (AABBDD), containing the heterozygous LIB15477 mutation in *TaIDD-D11* gene (Figure 4.5 B) in the second round of crossing. The *Taidd11* triple mutant (aabbdd) was identified in the BC₁F₂ and BC₁F₃ population. The genotyping of homoeologue B and D was performed using KASP assays (for primers see Supplementary Table 4.1). The *TaIDD-A11* sequence around the mutation is highly repetitive and KASP assays were not feasible. Instead, genotyping by sequencing was performed.

4.3.3 Phenotypic characterisation of the *Taidd11* triple mutant

TaIDD11 gene was chosen as a candidate for functional analysis as it was shown to interact with RHT-1 and previous studies reported members of the IDD gene family as DIPs that together with DELLAs regulate gene expression (Aoyanagi *et al.*, 2020; Fukazawa *et al.*, 2014; Lu *et al.*, 2020; Yoshida *et al.*, 2014). Moreover, there is evidence of two IDD proteins in Arabidopsis being involved in regulating GA biosynthesis and signalling (Feurtado *et al.*, 2011; Fukazawa *et al.*, 2014). This section of the Chapter focuses on phenotypic analysis of the *Taidd11* triple mutant and its responsiveness to GA. As the *TaIDD11* gene product due to its interaction with RHT-1 is hypothesized to be involved in GA signalling, typical traits regulated by GAs in plants were assessed: heading (Suge & Yamada, 1965), stem elongation (Sun, 2010), tillering (Liao *et al.*, 2019) and grain yield (Wang *et al.*, 2019). All phenotypic measurements were taken from plants grown in one experiment including eight biological replicates of each of the four genotypes: WT Cadenza, NS (BC₁F₃), *Taidd11* (BC₁F₃) and *Rht-D1b* (BC₅F₅), grown in randomised block

design. Cadenza and NS were used as tall controls, additionally, NS served as a control to assess if the observed differences in *Taidd11* mutant are due to knocking out the *TaIDD11* gene, and not caused by background mutations. *Rht-D1b* was included in the experiment as another control, as the mutation in this line is known to confer a GA-insensitive semi-dwarf phenotype, with a yield advantage (Flintham *et al.*, 1997).

4.3.3.1 Heading and anthesis date

Heading and flowering dates are strongly correlated with the final grain yield in cereals (Snape *et al.*, 2001). GAs are known to regulate bolting and flowering in plants (Jung *et al.*, 2020; Pearce *et al.*, 2013; Suge & Yamada, 1965); moreover, a GA-biosynthetic mutant in barley, *Hvsdw1*, (caused by a mutation in the *GA20ox2* gene) displays a flowering time that is delayed by three to five days (Teplyakova *et al.*, 2017). A delay in flowering was also observed in some *Rht-1* NILs, with severe dwarfing mutations displaying much longer delays (13 to 18 days) than those conferring semi-dwarfing (9 days) (Addisu *et al.*, 2010). The *Rht-D1b* allele, in contrast, was shown to have no effect on flowering time (Langer *et al.*, 2014).

Heading date was taken for the first tiller at the time when it fully emerged from the flag leaf sheath, and the distance between the base of the ear and the flag leaf ligule was up to 1 cm. The number of days was calculated from the time when germinated seeds were planted. Anthesis date was taken when most anthers within the florets of the first ear had matured and shed pollen. Collected data were analysed using General ANOVA in Genstat. Residual plots for these data confirmed that the measurements were normally distributed and did not require transformation. The outputs of the ANOVAs for the heading and anthesis data are presented in Tables 4.3 and 4.4, and in Figure 4.6.

Table 4. 3 ANOVA output for heading date. The mean values with standard deviations are shown for all genotypes compared. P-value, standard error of differences of means (S.E.D.) and least significant difference of means at 5% (L.S.D. 5%) are included. Significant results (compared to Cadenza) are highlighted in bold.

| Line | Number of days from planting to heading | Difference compared to Cadenza/NS* | P-value (d.f.=31) | S.E.D. | L.S.D. 5% |
|----------------|---|------------------------------------|-------------------|--------|-----------|
| Cadenza | 63.1 ± 2.4 | N/A | 0.127 | 1.0 | 2.0 |
| NS | 63.1 ± 2.1 | 0.0 | | | |
| <i>Taidd11</i> | 65.3 ± 1.8 | 2.2 +2.2* | | | |
| <i>Rht-D1b</i> | 64.1 ± 1.6 | 1.0 | | | |

Table 4. 4 ANOVA output for anthesis date. The mean values with standard deviations are shown for all genotypes compared. P-value, standard error of differences of means (S.E.D.) and least significant difference of means at 5% (L.S.D. 5%) are included.

| Line | Number of days from heading to anthesis | Difference compared to Cadenza/NS* | P-value (d.f.=31) | S.E.D. | L.S.D. 5% |
|----------------|---|------------------------------------|-------------------|--------|-----------|
| Cadenza | 2.4 ± 0.5 | N/A | 0.979 | 0.3 | 0.7 |
| NS | 2.5 ± 0.5 | 0.1 | | | |
| <i>Taidd11</i> | 2.4 ± 0.7 | 0.0 -0.1* | | | |
| <i>Rht-D1b</i> | 2.4 ± 0.7 | 0.0 | | | |

The ANOVA confirmed no significant interactions, neither between genotype and the number of days taken to head ($P = 0.127$), nor between genotype and number of days taken from heading to anthesis ($P = 0.979$). The number of days from sowing to heading for both WT and NS was on average 63.1. The *Rht-D1b* took one day longer to head, which was not a significant difference, however, the *Taidd11* took 2.2 days longer, which was significant (L.S.D. at 5% = 2.0). The number of days from heading to anthesis was on average 2.5 days for all analysed genotypes and no difference was observed.

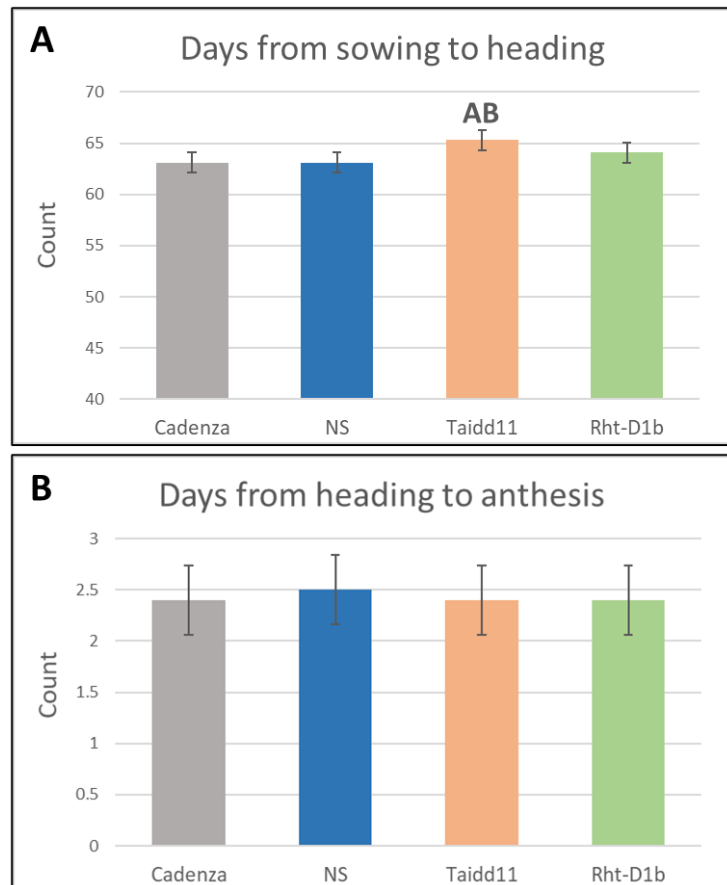


Figure 4. 6 Heading and anthesis time data. Graphs showing: A. Number of days from sowing to heading. $P = 0.127$. Error bars (S.E.D.) = 1.0. Taidd11 showed significantly delayed heading time compared to Cadenza (A) and NS (B). B. Number of days from heading to anthesis. $P = 0.979$. Error bars (S.E.D.) = 0.3. No significant difference was found. Four genotypes were assessed, and the data analysed using General ANOVA. Graphs were plotted using means calculated from eight biological replicates per genotype.

4.3.3.2 Flag leaf characteristics

Morphological traits of flag leaves are one of the most important determinants of plant architecture and yield potential. Flag leaves of wheat are regarded as the “functional leaves” as they are the main organs for photosynthesis and contribute 45–58% of photosynthetic performance during the grain-filling stage (Duncan, 1971; Khaliq *et al.*, 2008). The size of the flag leaf is estimated

by flag leaf length, width, and area, and is positively correlated with the thousand-grain weight, panicle weight, and other yield-related traits in cereals (Wang *et al.*, 2011, 2012; Yue *et al.*, 2006). *Rht-1* semi-dwarfing alleles were previously shown to negatively affect leaf blade area by their effect on reducing the length of cells (Flintham *et al.*, 1997; Keyes *et al.*, 1989; Miralles *et al.*, 1998). Interestingly, an IDD protein in barley, BLF1 (BROAD LEAF1), was identified as the regulator of cell proliferation causing a reduction in leaf width (Jöst *et al.*, 2016). As it was hypothesized that *TaIDD11* could be involved in GA signalling pathway, the phenotype of the *Taidd11* mutant flag leaves was assessed.

The measurements were taken for flag leaves of the first three tillers of each biological replicate at the time of anthesis. The length was measured from the flag leaf auricle to the tip of the leaf blade. The width was measured at half-length. The approximate area of the flag leaf blade was calculated using formula: length x width x 0.835 (Miralles *et al.*, 1998a).

Collected data were analysed using General ANOVA in Genstat. Residual plots for these data confirmed that the measurements were normally distributed and did not require transformation. The outputs of the ANOVAs for flag leaf blade length, width and area are presented in Tables 4.5, 4.6 and 4.7, respectively, and in Figure 4.7. L.S.D. at 5% was used to establish significant differences.

The General ANOVAs confirmed significant interaction between genotype and all flag leaf characteristics ($P < 0.001$). Interesting results were found for leaf blade length. NS (364.6 mm) was found to have significantly longer leaves than any other genotype, even Cadenza (341.6 mm), while *Rht-D1b* (330.0 mm) showed no significant differences compared to Cadenza (L.S.D. at 5% = 20.2; Figure 4.7 A). *Taidd11* mutant flag leaves (301.9 mm) were significantly shorter than flag leaves of all other genotypes.

Table 4. 5 ANOVA output for flag leaf length. The mean values with standard deviations are shown for all genotypes compared. P-value, standard error of differences of means (S.E.D.) and least significant difference of means at 5% (L.S.D. 5%) are included. Significant results (compared to Cadenza) are highlighted in bold.

| Line | Flag leaf length [mm] | Difference compared to Cadenza/NS* [mm] | | P-value (d.f.=31) | S.E.D. | L.S.D. 5% |
|----------------|-----------------------|---|---------------|-------------------|--------|-----------|
| Cadenza WT | 341.6 ± 38.3 | N/A | | <.001 | 9.8 | 20.2 |
| NS | 364.6 ± 46.6 | 23.0 | | | | |
| <i>Taidd11</i> | 301.9 ± 31.4 | -39.7 | -63.7* | | | |
| <i>Rht-D1b</i> | 330.0 ± 25.7 | -11.6 | | | | |

Table 4. 6 ANOVA output for flag leaf width. The mean values with standard deviations are shown for all genotypes compared. P-value, standard error of differences of means (S.E.D.) and least significant difference of means at 5% (L.S.D. 5%) are included. Significant results (compared to Cadenza) are highlighted in bold.

| Line | Flag leaf width [mm] | Difference compared to Cadenza/NS* [mm] | | P-value (d.f.=31) | S.E.D. | L.S.D. 5% |
|----------------|----------------------|---|--------------|-------------------|--------|-----------|
| Cadenza WT | 17.8 ± 1.4 | N/A | | <.001 | 0.4 | 0.9 |
| NS | 16.3 ± 0.9 | -1.5 | | | | |
| <i>Taidd11</i> | 15.9 ± 1.0 | -1.9 | -0.4* | | | |
| <i>Rht-D1b</i> | 16.3 ± 1.5 | -1.5 | | | | |

Table 4. 7 ANOVA output for flag leaf area. The mean values with standard deviations are shown for all genotypes compared. P-value, standard error of differences of means (S.E.D.) and least significant difference of means at 5% (L.S.D. 5%) are included. Significant results (compared to Cadenza) are highlighted in bold.

| Line | Flag leaf area [mm ²] | Difference compared to Cadenza/NS* [mm ²] | | P-value (d.f.=31) | S.E.D. | L.S.D. 5% |
|----------------|-----------------------------------|---|----------------|-------------------|--------|-----------|
| Cadenza WT | 5086.4 ± 767.6 | N/A | | <.001 | 194.7 | 400.9 |
| NS | 4971.6 ± 797.9 | -114.8 | | | | |
| <i>Taidd11</i> | 4013.5 ± 579.2 | -1072.9 | -958.1* | | | |
| <i>Rht-D1b</i> | 4523.7 ± 691.8 | -562.7 | | | | |

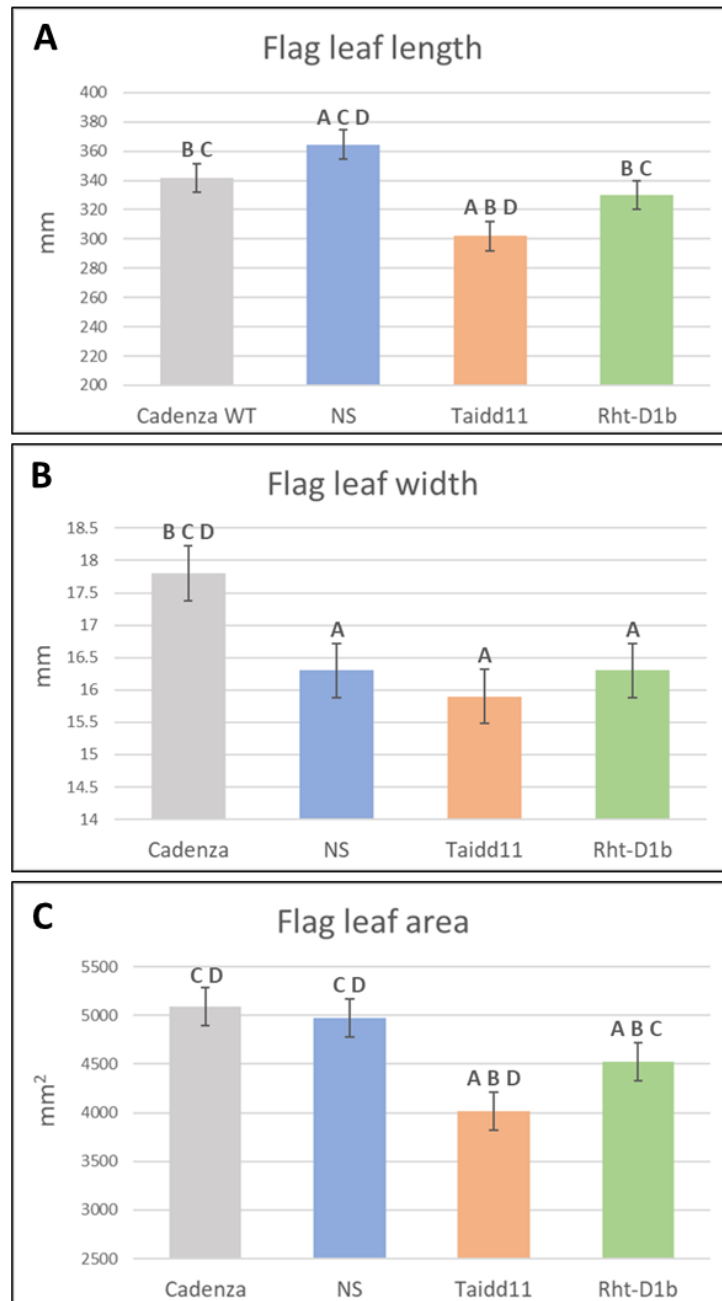


Figure 4. 7 Graphs showing various flag leaf measurements taken for the four genotypes assessed. A. Flag leaf length; measured from flag leaf auricle to the leaf tip. $P < 0.001$. Error bars (S.E.D.) = 9.790. B. Flag leaf width; measured at half-length of the flag leaf. $P < 0.001$. Error bars (S.E.D.) = 0.421. C. Flag leaf area; calculated from the formula length \times width \times 0.835. $P < 0.001$. Error bars (S.E.D.) = 194.7. Data were analysed using General ANOVA. Graphs were plotted using means calculated from eight biological replicates per genotype. The letters over the error bars indicate 'significantly different from': A = Cadenza, B = NS, C = Taidd11, D = Rht-D1b.

No significant difference in flag leaf width was found between NS (16.3 mm), *Taidd11* (15.9 mm) and *Rht-D1b* (16.3 mm), with L.S.D at 5% = 0.9; however, they were all significantly narrower than Cadenza flag leaves (17.8 mm). Regarding flag leaf area, there was no significant difference between the WT and NS. L.S.D. at 5% was 400.9 mm² and the average flag leaf area for Cadenza WT and NS was 5086.4 mm² and 4971.6 mm², respectively. The flag leaf area of the *Rht-D1b* (4523.7 mm²) was significantly smaller than the flag leaf area of the WT and NS, but significantly bigger than the flag leaf area of *Taidd11* mutant (4013.5 mm²). The results obtained for *Rht-D1b* differ slightly from the published data (Hoogendoorn *et al.*, 1990; Keyes *et al.*, 1989; Miralles *et al.*, 1998). The negative effect of the *Rht-D1b* mutation on the flag leaf length was not observed, although the flag leaf area was reduced (Figure 4.7). Leaf characteristics are highly affected by the environment, and in the cited studies, the leaf size was assessed in the field, whereas in this experiment, the plants were grown in the glasshouse. Perhaps this is the source of the observed differences. The flag leaf length and area were found to be significantly smaller than those of every other genotype. These results suggest that the *TaIDD11* gene is involved in regulation of flag leaf elongation and expansion, which together affect the flag leaf area.

4.3.3.3 Stem and internodes length

GA biosynthetic or signalling mutants have a characteristic semi-dwarf or dwarf phenotype. In contrast, mutants with constitutive GA responses are very tall (Sun, 2010). Previous studies characterising the classical *Rht-1* dwarfing mutations in various backgrounds have demonstrated that the severely GA insensitive *Rht-B1c* allele causes ~50% height reduction compared to the *Rht-1* tall control, whereas the *Rht-D1b* allele results in about a 17% height reduction (Flintham *et al.*, 1997). The reduced stature of the semi-dwarf mutants was found to be caused by reduced cell elongation whereas in the severe dwarf, the final height of the plant was the result of both reduced cell length and cell proliferation (Hoogendoorn *et al.*, 1990).

IDD transcription factors have also been identified to be involved in regulation of stem elongation. In Arabidopsis, the *gaf1 idd1* double mutant displays a semi-dwarf phenotype that cannot be rescued by GA₄ application (Fukazawa *et al.*, 2014). In rice, *Loose Plant Architecture1 (LPA1)* gene was identified as the functional ortholog of the *AtIDD15/SHOOT GRAVITROPISM5 (SGR5)* gene, and the *lpa1* mutant has shorter but thicker internodes, indicating a role of LPA1 in promoting stem elongation (Wu *et al.*, 2013). In contrast, the *OsIDD2* gene is a negative regulator of stem elongation in rice (Huang *et al.*, 2018).

To assess the role of the *TaIDD11* gene in controlling stem length, the *Taidd11* mutant was grown to maturity in a randomized block design in the glasshouse alongside the controls, Cadenza, NS, and *Rht-D1b*. Internode measurements were taken from the three tallest tillers of eight biological replicates per genotype. The individual internode measurements were then added to reveal the final stem length. The data was analysed using General ANOVA in Genstat. Residual plots for the data confirmed that the data follows normal distribution and did not require transformation. The output from ANOVA analyses are summarised in Table 4.8.

The phenotype of Cadenza, NS, *Taidd11* and *Rht-D1b* plants at maturity is illustrated in Figure 4.8 A. The *Taidd11* mutant was observed to display a notable semi-dwarf phenotype, similar to the one of *Rht-D1b* mutant. The average final length of the stem is summarised in Table 4.8 and in the graph presented in Figure 4.8 B. Statistically significant differences are highlighted in bold in the table and marked with an asterisk on the graph. A General ANOVA confirmed that there is a significant interaction between genotype and final stem length ($P < 0.001$). L.S.D. at 5% (15.7 mm) value was used to assess which genotypes stem lengths were significantly different from one another.

The average stem lengths for Cadenza and NS were 686.3 mm and 693.8 mm, respectively, whereas *Taidd11* and *Rht-D1b* lines final stem lengths averaged at 544.6 mm and 508.5 mm, respectively. Therefore, not only were the stems of the two mutant lines significantly shorter than the WT stems; *Rht-D1b* stem length was also significantly reduced compared to that of *Taidd11*.

Table 4. 8 ANOVA output for individual internodes and the final stem length. The mean values with standard deviations are shown for all genotypes compared as well as difference compared to Cadenza. P-value, standard error of differences of means (S.E.D.) and least significant difference of means at 5% (L.S.D. 5%) are included. Significant results (compared to Cadenza) are highlighted in bold.

| | Int. 4 length [mm] | Compared to Cadenza/NS* | | Int. 3 length [mm] | Compared to Cadenza/NS* | | Int. 2 length [mm] | Compared to Cadenza/NS* | | Peduncle length [mm] | Compared to Cadenza/NS* | | Stem length [mm] | Compared to Cadenza/NS* | |
|-------------------|--------------------|-------------------------|---------------|--------------------|-------------------------|---------------|---------------------|-------------------------|---------------|----------------------|-------------------------|---------------|---------------------|-------------------------|----------------|
| Cadenza | 62.4 ± 24.3 | N/A | | 112.0 ± 13.5 | N/A | | 171.8 ± 16.4 | N/A | | 330.2 ± 46.0 | N/A | | 686.3 ± 35.6 | N/A | |
| NS | 63.4 ± 21.6 | 1.0 | | 113.8 ± 12.1 | 1.8 | | 173.3 ± 13.6 | 1.5 | | 344.6 ± 34.5 | 14.4 | | 693.8 ± 38.6 | 7.5 | |
| <i>Taidd11</i> | 40.7 ± 15.3 | -21.7 | -22.7* | 81.4 ± 11.9 | -30.6 | -32.4* | 145.2 ± 14.7 | -26.6 | -28.1* | 275.6 ± 30.8 | -54.6 | -69.0* | 544.6 ± 29.1 | -141.7 | -149.2* |
| <i>Rht-D1b</i> | 22.0 ± 14.6 | -40.40 | | 66.2 ± 14.2 | -45.8 | | 133.2 ± 12.7 | -38.60 | | 287.0 ± 24.8 | -43.2 | | 508.5 ± 22.2 | -177.8 | |
| P-Value (d.f.=31) | <0.001 | | <0.001 | | <0.001 | | <0.001 | | <0.001 | | <0.001 | | <0.001 | | |
| S.E.D. | 5.7 | | 3.7 | | 4.0 | | 9.8 | | 7.9 | | | | | | |
| L.S.D. at 5% | 11.4 | | 7.3 | | 8.0 | | 19.5 | | 15.7 | | | | | | |

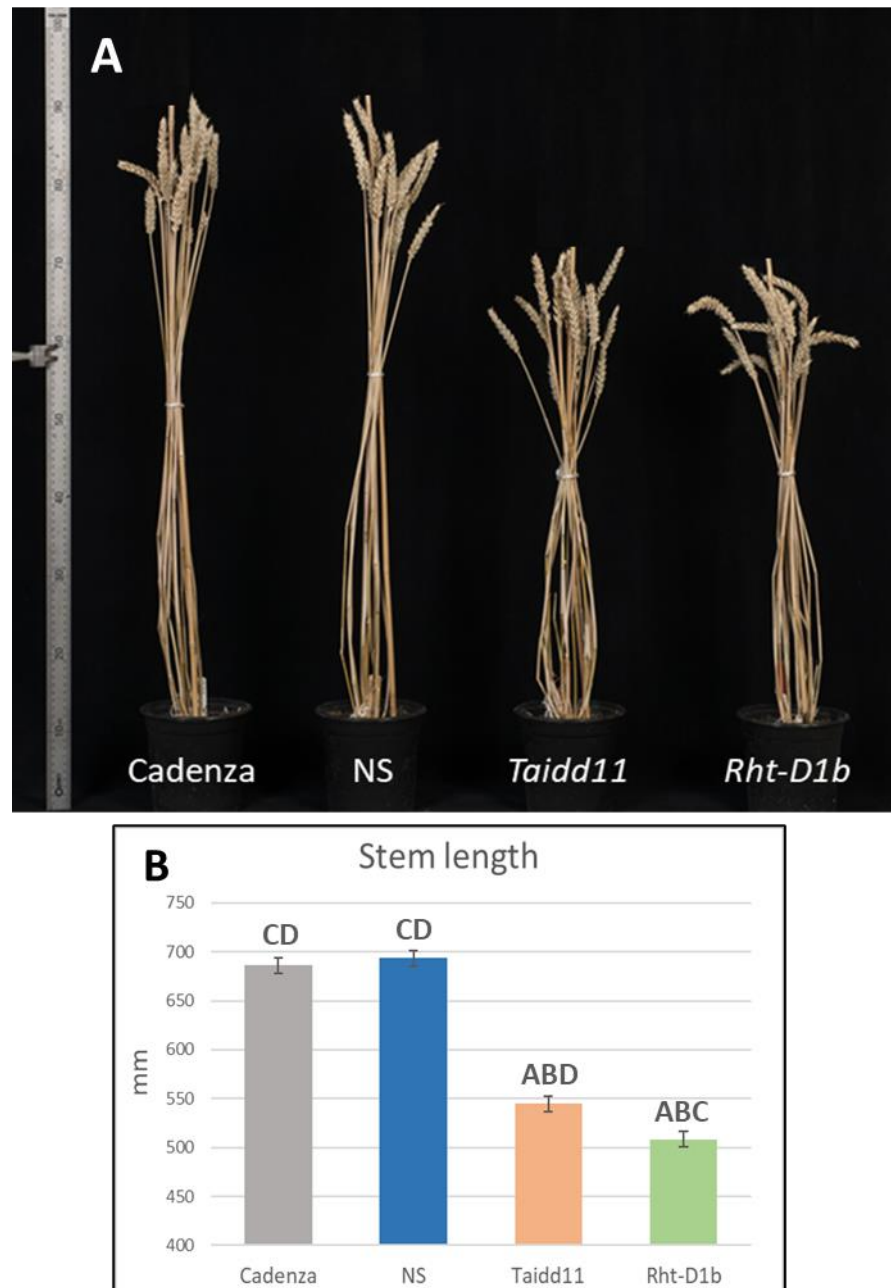


Figure 4. 8 Comparison of the final height of the four different genotypes used in the phenotypic assessment study. A. Photograph of the mature plants. The plants were grown in the same block in the glasshouse till maturity. B. Graph showing average final stem length of the four genotypes used in the study. The letters over the error bars indicate 'significantly different from' ($P < 0.001$): A = Cadenza, B = NS, C = Taidd11, D = Rht-D1b.

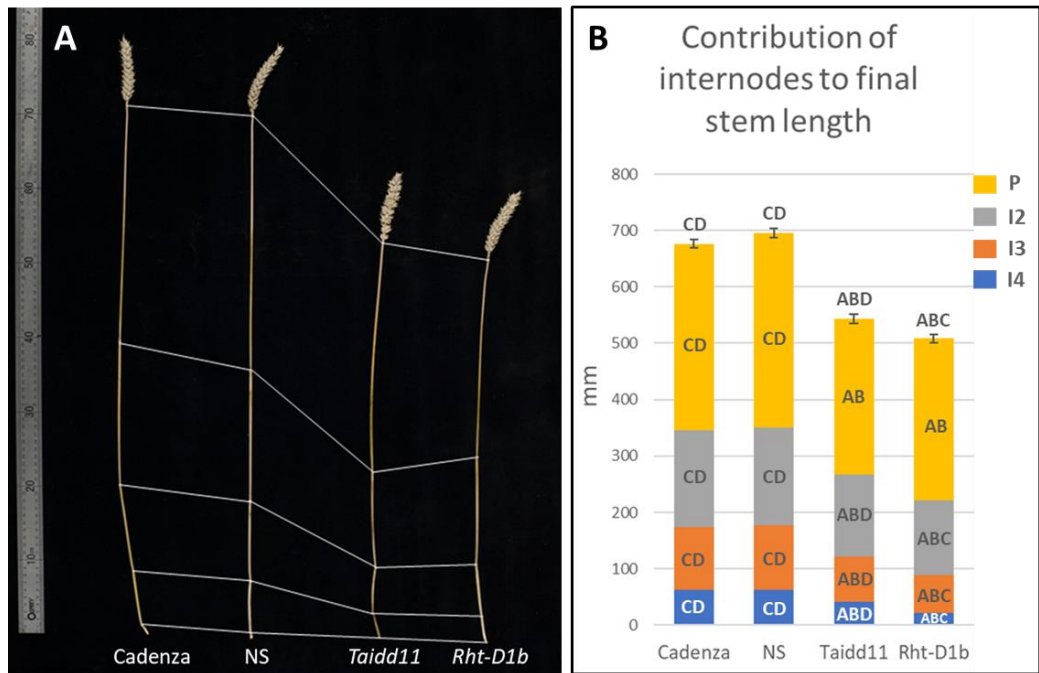


Figure 4.9 Contribution of individual internodes to the final stem length. A. Photograph of single mature tillers from Cadenza, NS, Taidd11 and Rht-D1b. Internode segments are shown: P = peduncle, I2, I3 and I4 = internode 2, 3 and 4, respectively. B. Graph summarising mean lengths of individual internodes for each genotype, averaged across three tallest tillers per eight biological replicates. The letters over the error bars indicate 'significantly different from' ($P < 0.001$): A = Cadenza, B = NS, C = Taidd11, D = Rht-D1b.

The contribution of individual internodes to the final stem length was investigated (Figure 4.9). It was observed that some tillers of both Cadenza and NS had relatively short fifth internodes that were never present in the mutant lines. Hence, only the contribution of the first four internodes were investigated. Figure 4.9 A depicts mature tillers of Cadenza, NS, Taidd11 and Rht-D1b and the lengths of individual internodes (peduncle and internodes 2, 3 and 4). The average lengths of individual internodes for each line are summarised in the Table 4.8 and shown graphically in Figure 4.9 B. A series of General ANOVAs confirmed significant interaction between genotype and each internode lengths ($P < 0.001$ for peduncle, I2, I3 and I4). L.S.D. at 5% values were used to assess which genotypes internodes differed in length significantly.

Internode 4 (L.S.D. at 5% = 11.4 mm), internode 3 (L.S.D. at 5% = 7.3 mm) and internode 2 (L.S.D. at 5% = 8.0 mm) were significantly shorter in *Taidd11* and *Rht-D1b* than in the two tall controls, which did not differ significantly in internodes 4, 3 and 2 length from one another. There was also a significant difference between the two mutants, with *Rht-D1b* having shorter internodes than *Taidd11*. In contrast, the peduncle (L.S.D. at 5% = 19.5 mm) was not significantly different in length in the two semidwarf mutants, yet peduncles of *Taidd11* and *Rht-D1b* were still significantly shorter than those of Cadenza and NS.

4.3.3.4 Tillering

Tillering is an important agronomic trait that determines final crop yield and there is some evidence that the process of tillering is at least partly regulated by GAs (Liao *et al.*, 2019; Lo *et al.*, 2008). Increased tillering was previously reported for *Rht-1* mutants, *Rht-B1b* and *Rht-D1b* (Kertesz *et al.*, 1991; Lanning *et al.*, 2012) compared to tall controls. However, in previous work using wheat cv. Cadenza, no effect of *Rht-A1b*, *Rht-D1b* or *Rht-B1c* on tillering was observed (Rafter, 2019). A recent study in rice has shown that overexpression of *OsIDD13* does not affect tillering (Sun *et al.*, 2020). No other links between IDD proteins and shoot branching have been reported to date. Increased tillering of *Taidd11* mutant was observed in the BC₁F₂ population (data not shown), hence it was expected to be seen in BC₁F₃ population too.

The effect of knocking out *TaIDD11* on plant tillering was assessed in the glasshouse experiment. Eight biological replicates of Cadenza, NS, *Taidd11* and *Rht-D1b* were grown to maturity in a randomised manner, and the total number of fertile tillers counted. The average number of tillers for each genotype is listed in Table 4.9 and presented graphically in Figure 4.10. General ANOVA was used to statistically assess the results. No significant interaction between genotype and number of tillers per plant was found (P = 0.284).

Table 4. 9 ANOVA output for tiller number per plant. The mean values with standard deviations are shown for all genotypes compared. P-value, standard error of differences of means (S.E.D.) and least significant difference of means at 5% (L.S.D. 5%) are included.

| Line | Number of tillers | Difference compared to Cadenza/NS* | | P-value (d.f.=31) | S.E.D. | L.S.D. at 5% |
|---------|-------------------|------------------------------------|-----|-------------------|--------|--------------|
| Cadenza | 12.6 ± 1.5 | N/A | | 0.284 | 1.1 | 2.2 |
| NS | 12.9 ± 2.0 | 0.3 | | | | |
| Taidd11 | 13.9 ± 2.2 | 1.3 | 1.0 | | | |
| Rht-D1b | 14.5 ± 2.4 | 1.9 | | | | |

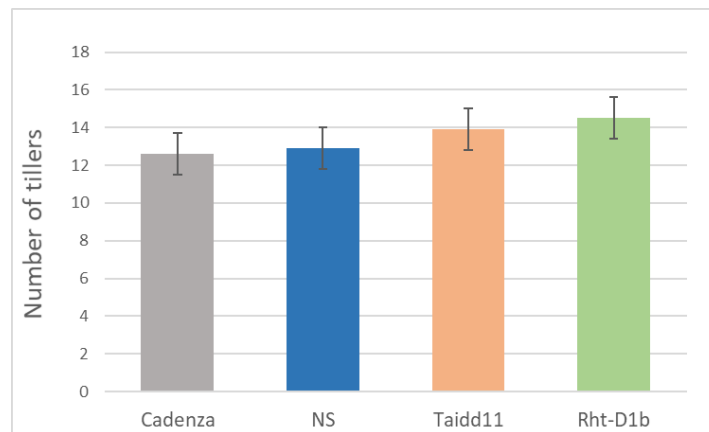


Figure 4. 10 Graph presenting the mean tiller number per plant for Cadenza, NS, Taidd11 and Rht-D1b. Measurements were taken from eight biological replicates per genotype and averaged. Error bars are S.E.D. (1.1) calculated by ANOVA.

4.3.3.5 Ear length and spikelet number

Although *Rht-1* dwarfing alleles result in preferential partitioning of assimilates to ear over stem (Borrell *et al.*, 1991), ear length in wheat dwarf lines has not been extensively studied. However, one study reports significant elongation of wheat ears in response to exogenous GAs (Islam *et al.*, 2014), which indicates that ear elongation may be a GA-regulated process. More attention has been focused on studying the spikelet number. In barley, the dwarf *Sln1d.5* mutant

has fewer spikelets than the WT, which is a result of reduced spikelet initiation (Serrano-Mislata *et al.*, 2017), whereas wheat *Rht-B1b* and *Rht-D1b* alleles do not confer increase in spikelet number (Borrell *et al.*, 1991; Li *et al.*, 2006). No evidence of IDD transcription factors being involved in regulation of spikelet number has yet been demonstrated, as overexpression of *IDD13* in rice did not affect the number of spikelets on the panicle (Sun *et al.*, 2020).

The length of the ear and the number of spikelets per ear were assessed for four genotypes compared in the phenotypic analysis, and the results analysed using General ANOVA in Genstat. The results of these analyses are presented in Table 4.10 and in the graphs in Figure 4.11. Significant interaction was found between the genotype and both ear length ($P < 0.001$) and number of spikelets per ear ($P < 0.001$). L.S.D.s at 5% were used to establish which genotypes differ significantly.

Table 4. 10 ANOVA output for ear length and number of spikelets per ear. The mean values with standard deviations are shown for all genotypes compared. *P*-value, standard error of differences of means (S.E.D.) and least significant difference of means at 5% (L.S.D. 5%) are included. Significant results (compared to Cadenza) are highlighted in bold.

| | Ear length [mm] | Difference compared to Cadenza/NS* | | Spikelet number | Difference compared to Cadenza/NS* | |
|-------------------|-------------------|------------------------------------|------|-------------------|------------------------------------|------|
| Cadenza | 88.3 ± 7.6 | N/A | | 19.1 ± 1.6 | N/A | |
| NS | 91.0 ± 7.2 | 2.7 | | 19.0 ± 1.5 | -0.1 | |
| <i>Taidd11</i> | 89.0 ± 4.0 | 0.7 | -2.0 | 18.3 ± 1.9 | -0.8 | -0.7 |
| <i>Rht-D1b</i> | 96.3 ± 6.7 | 8.0 | | 20.5 ± 1.4 | 1.4 | |
| P-Value (d.f.=31) | <0.001 | | | <0.001 | | |
| S.E.D. | 1.6 | | | 0.4 | | |
| L.S.D. at 5% | 3.2 | | | 0.8 | | |

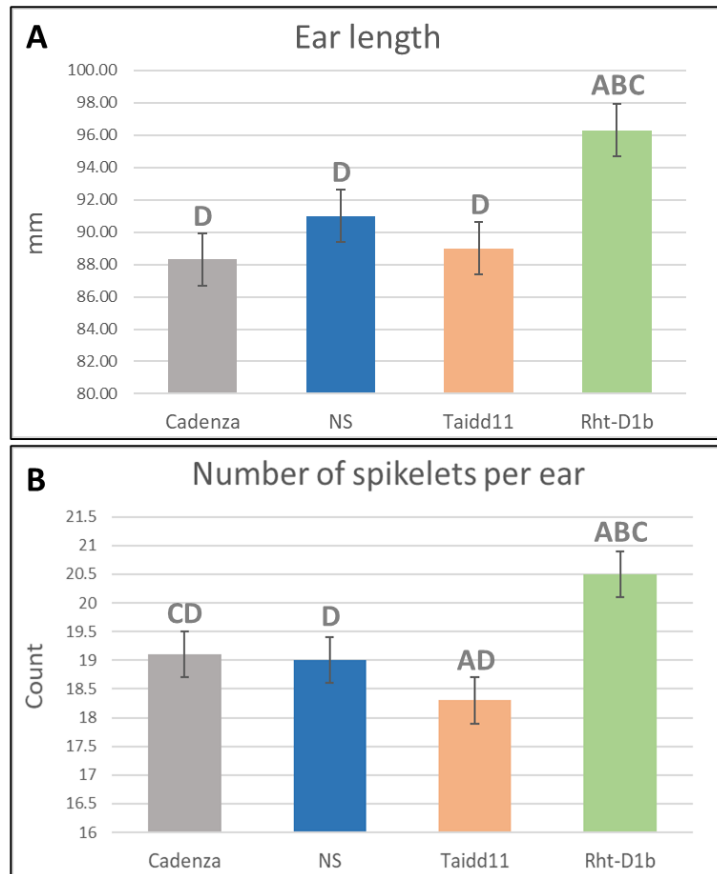


Figure 4. 11 Graphs presenting the data for ear length and the number of spikelets per ear. A. Ear length, B. Number of spikelets per ear. Measurements were taken from three tallest tillers from eight biological replicates of Cadenza, NS, Taidd11 and Rht-D1b. Error bars are S.E.D. values calculated by ANOVA ($A = 1.6$; $B = 0.4$). The letters over the error bars indicate 'significantly different from' ($P < 0.001$): A = Cadenza, B = NS, C = Taidd11, D = Rht-D1b.

Out of all compared genotypes, only *Rht-D1b* showed to have significantly different length of the ear, and it was on average 8.0 mm longer than that of Cadenza (L.S.D. at 5% = 3.2 mm). This genotype also produced on average 1.4 more spikelets per ear with L.S.D. = 0.8. *Taidd11* mutant ear did not differ in length from control, but it produced fewer spikelets per ear. The difference was on the border of being significant as it was equal to L.S.D. (0.8 mm).

4.3.3.6 Grain characteristics

Grain number, size and weight are important components of yield. While the Green Revolution allele *Rht-D1b* was shown to either positively (Flintham *et al.*, 1997) or not at all (Borrell *et al.*, 1991) affect the grain number per ear, it was established that it negatively affects seed weight (Borrell *et al.*, 1991; Casebow *et al.*, 2016). The cumulative negative effect of *Rht-1* alleles on seed area was also reported (Miralles *et al.*, 1998a). Three IDD proteins have been evaluated in the context of grain weight (Gontarek *et al.*, 2016; Sun *et al.*, 2020). In rice, overexpression of *IDD13* had no effect on thousand-grain weight (TGW) (Sun *et al.*, 2020). In maize, knocking out *naked endosperm1 (nkd1)* and *nkd2* results in reduced seed weight, which has been linked to decreased protein and starch content in the endosperm (Gontarek *et al.*, 2016).

To assess the effect of knocking out *TaIDD11* on the grain characteristics, Cadenza, NS, *Taidd11* and *Rht-D1b* were grown to maturity in a randomised glasshouse experiment. When plants were mature and dry, the ears from the three tallest tillers per plant were harvested and the grain characteristics assessed (Table 4.11) using Marvin Seed Analyser (INDOSAW, Haryana, India) Length (mm), width (mm) and area (mm²) of 20 grains per ear was assessed.

General ANOVA was used to statistically assess the differences between genotypes. Residual plots for these data were assessed in GenStat, which confirmed that the data was normally distributed and did not require transformation.

Significant interaction was found between genotype and every investigated characteristic: grain width (P < 0.001; L.S.D. at 5% = 0.06; S.E.D. = 0.03), grain length (P < 0.001; L.S.D. at 5% = 0.07; S.E.D. = 0.03), grain area (P < 0.001; L.S.D. at 5% = 0.38; S.E.D. = 0.19), number of grains per ear (P < 0.001; L.S.D. at 5% = 4.6; S.E.D. = 2.3) and average grain weight (P < 0.001; L.S.D. at 5% = 3.7; S.E.D. = 1.9) (Table 4.11 and Figure 4.12).

Table 4. 11 ANOVA output for grain characteristics. Grain number, grain weight [mg], grain area [mm²], grain length [mm] and grain width [mm] were measured. The mean values with standard deviations are shown for all genotypes compared. P-value, standard error of differences of means (S.E.D.) and least significant difference of means at 5% (L.S.D. 5%) are included. Significant results (compared to Cadenza) are highlighted in bold.

| | Grain number | Difference compared to Cadenza/NS* | | Grain weight [mg] | Difference compared to Cadenza/NS* | | Grain area [mm ²] | Difference compared to Cadenza/NS* | | Grain length [mm] | Difference compared to Cadenza/NS* | | Grain width [mm] | Difference compared to Cadenza/NS* | |
|-------------------|-------------------|------------------------------------|---------------|-------------------|------------------------------------|-------------|-------------------------------|------------------------------------|--------------|--------------------|------------------------------------|-------|--------------------|------------------------------------|--------------|
| Cadenza | 51.0 ± 8.4 | N/A | | 34.0 ± 6.1 | N/A | | 17.31 ± 3.13 | N/A | | 6.70 ± 0.51 | N/A | | 3.39 ± 0.48 | N/A | |
| NS | 50.3 ± 9.0 | -0.7 | | 32.6 ± 8.0 | -1.4 | | 16.79 ± 3.07 | -0.51 | | 6.70 ± 0.48 | 0.00 | | 3.30 ± 0.48 | -0.10 | |
| <i>Taidd11</i> | 36.5 ± 9.8 | 14.5 | -13.8* | 37.4 ± 8.7 | 3.4 | 4.8* | 17.35 ± 3.17 | 0.05 | 0.56* | 6.72 ± 0.61 | 0.02 | 0.02* | 3.42 ± 0.44 | 0.02 | 0.12* |
| <i>Rht-D1b</i> | 52.7 ± 7.6 | 1.7 | | 26.7 ± 5.9 | -7.3 | | 15.46 ± 2.76 | -1.84 | | 6.49 ± 0.50 | -0.21 | | 3.11 ± 0.47 | -0.29 | |
| P-Value (d.f.=31) | <0.001 | | | <0.001 | | | <0.001 | | | <0.001 | | | <0.001 | | |
| S.E.D. | 2.3 | | | 1.9 | | | 0.19 | | | 0.03 | | | 0.03 | | |
| L.S.D. at 5% | 4.6 | | | 3.7 | | | 0.38 | | | 0.07 | | | 0.06 | | |

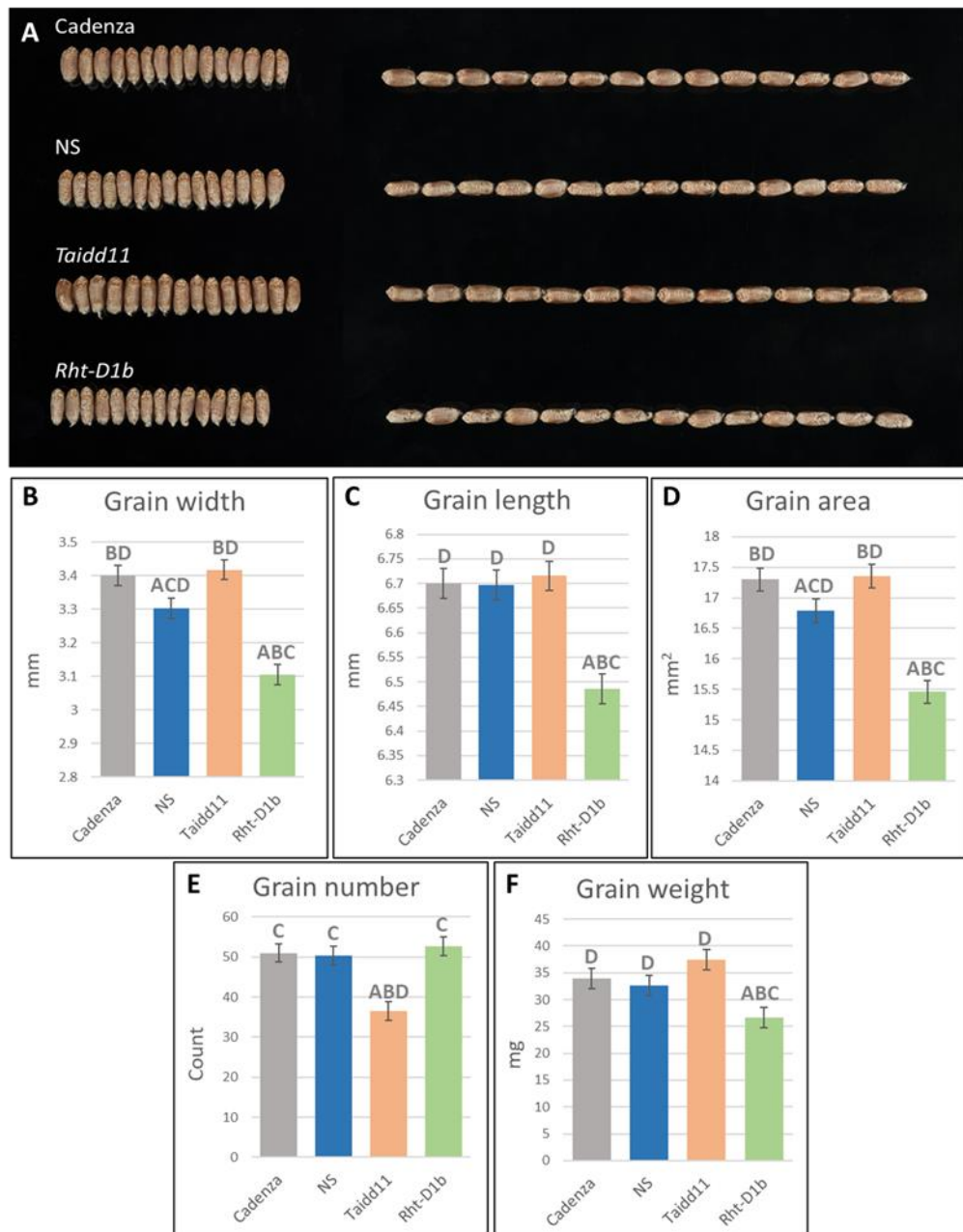


Figure 4. 12 Characteristics of grains of four genotypes compared in the study. A. Photograph of the same number of grains from each genotype aligned to show the difference in width and length between the genotypes. B. Graph showing mean grain width ($P < 0.001$; L.S.D. at 5% = 0.06; S.E.D. = 0.03). C. Graph showing mean grain length ($P < 0.001$; L.S.D. at 5% = 0.07; S.E.D. = 0.03). D. Graph showing mean grain area ($P < 0.001$; L.S.D. at 5% = 0.38; S.E.D. = 0.19). E. Graph showing mean grain number per ear ($P < 0.001$; L.S.D. at 5% = 4.6; S.E.D. = 2.3). F. Graph showing mean grain weight ($P < 0.001$; L.S.D. at 5% = 3.7; S.E.D. = 1.9). Error bars are the S.E.D. values. The letters over the error bars indicate 'significantly different from' ($P < 0.001$): A = Cadenza, B = NS, C = Taidd11, D = Rht-D1b.

The overall area of the *Rht-D1b* grains was significantly smaller compared to Cadenza control (on average by 1.84 mm²; Figure 4.12 D), and the decrease in total area was due to decrease in both width (-0.29 mm) and length (-0.21 mm) (Figure 4.12 A, B, C). The grains were also significantly lighter than those of other genotypes (-7.3 mg). Interestingly, NS also showed significantly smaller seed area (-0.51 mm²) due to decreased grain width (-0.10 mm) compared to Cadenza control. The grains of *Taidd11* mutant did not differ significantly in size or weight from Cadenza control, but this line produced significantly fewer seeds per ear (-14.5).

4.3.3.7 GA dose response assays

Elongation of the first leaf (L1) initially involves only the blade and it is between day 5 and 7 that leaf blade and leaf sheath both elongate. At later stages, the elongation of the leaf involves only the elongation of the sheath (Chandler & Robertson, 1999). GA response assays, measuring L1 elongation rates (LERs) were developed to define three classes of dwarf mutants in barley (Chandler & Robertson, 1999). In WT Himalaya barley, as well as in GA-synthesis mutants, increased LER was observed after treatment with between 10 nM and 1 μM of GA₃. Gibberellin signalling mutants that exhibited reduced GA sensitivity required 100-fold higher GA₃ concentration for comparable LERs and their response did not plateau even at highest concentrations tested. A third class of LER mutants were smaller than WT plants and were unresponsive to increasing GA₃ concentrations. In those mutants, GA signalling component, SLN1 was proposed to be affected and the lack of response to GA₃ was suggested to be observed because the leaves were already elongating at their maximal rate (Chandler & Robertson, 1999). One such mutant, M640 (*Slnd*), was shown to share 97% amino acid sequence identity with *Rht-D1a* and was identified as a mutant containing a nonconservative amino acid substitution (G46E) in a conserved region of the protein (Chandler *et al.*, 2002). This gain of function mutation conferred a phenotype similar to that of *Rht-D1b*, including reduced height, a lack of growth response to applied GA and accumulation of

bioactive GA. Similar GA dose response assays have also revealed the reduced rate of GA responsiveness in gain-of-function *Slr1-d* mutants in rice (Asano *et al.*, 2009).

Thus far, no robust GA response assay protocol was developed for wheat, as LER measurements are not as consistent in wheat as they are in barley, and growth responses in wheat can be easily affected by environmental changes. Therefore, the extent of L1 blade elongation, not elongation rate, of wheat seedlings was measured.

Seedling elongation in response to GA is a good method of assessing the GA-sensitivity of a given genotype because GAs affect both stem and leaf elongation rate. The severity of GA insensitivity is correlated with decreased seedling elongation and mature plant height; therefore, these studies provide a convenient measure of GA responsiveness. Gibberellin dose response assays were performed to compare the response to applied GA₃ between the four genotypes: Cadenza, NS, *Taidd11*, and *Rht-D1b*. Eight biological replicates were used for each genotype per treatment. They were sown in randomly distributed columns in trays and measured on the tenth day after sowing, when elongation of the first leaf was complete. The experiment was run in triplicate.

Figure 4.13 A shows the photographs of the seedlings with and without GA₃ treatment. The difference in response to applied GA₃ between genotypes is clearly visible; both the *Taidd11* and *Rht-D1b* mutants did not exhibit any obvious response to the treatment, whereas Cadenza and NS seedlings showed increased growth in response to GA₃. What is also interesting is the size of the seedlings grown without the treatment applied. Cadenza and NS seedling lengths were almost identical (232.7 mm and 232.6 mm, respectively), whereas *Rht-D1b* length was 176.6 mm and *Taidd11* was the shortest seedling with the length averaged at 158.3 mm. The lengths of leaf sheaths and L1 blades at every treatment were measured, averaged, and plotted to obtain the GA₃ dose response curves. Figure 4.13 B and C show the curves for leaf sheath and L1 blade, respectively.

The data were analysed using General ANOVA with combined treatments (Genotype*[GA₃]) in Genstat. The residual plots for both leaf sheath and L1 blade data confirmed normal distribution. The outputs of ANOVAs for leaf sheath and first leaf blade measurements comparisons are included in Table 4.12 and Table 4.13, respectively.

The General ANOVA conducted for leaf sheath data confirmed that both genotype (P < 0.001) and GA₃ treatment (P < 0.001) have a significant effect on leaf sheath elongation and that there is a significant interaction between genotype and GA₃ concentration (P < 0.001), which means that differences between treatments are not observed for all investigated genotypes.

Table 4. 12 Table summarising mean values ± standard deviation and General ANOVA output for leaf sheath length [mm] for four genotypes in response to a range of GA₃ treatments. P-value, standard error of differences of means (S.E.D.) and least significant difference of means at 5% (L.S.D. 5%) for genotype, treatment and interaction of both factors are included. The significant values (compared to Cadenza) are highlighted in bold.

| | [GA₃] (M) | | | | | | |
|-----------------------|---------------------------------------|-----------------------|-----------------------|------------------------|------------------------|------------------------|------------------------|
| | 0 | 10 ⁻⁹ | 10 ⁻⁸ | 10 ⁻⁷ | 10 ⁻⁶ | 10 ⁻⁵ | 10 ⁻⁴ |
| Cadenza | 62.5 ± 3.8 | 63.6 ± 4.8 | 67.0 ± 5.9 | 82.8 ± 7.7 | 103.5 ± 5.4 | 110.7 ± 6.7 | 106.1 ± 6.6 |
| NS | 62.4 ± 6.4 | 61.4 ± 6.3 | 65.9 ± 4.7 | 81.7 ± 5.9 | 99.8 ± 7.5 | 107.7 ± 8.6 | 103.5 ± 10.2 |
| <i>Taidd11</i> | 42.1 ± 4.7 | 41.7 ± 3.6 | 43.1 ± 2.6 | 44.1 ± 4.3 | 44.3 ± 5.9 | 47.2 ± 3.3 | 45.7 ± 2.9 |
| <i>Rht-D1b</i> | 40.0 ± 7.8 | 37.3 ± 6.4 | 42.7 ± 8.9 | 44.6 ± 10.9 | 43.7 ± 10.6 | 48.1 ± 11.8 | 40.8 ± 10.3 |
| P-value (d.f.=611) | Genotype < 0.001 | | | | | | |
| | [GA ₃] < 0.001 | | | | | | |
| | Genotype * [GA ₃] < 0.001 | | | | | | |
| S.E.D. | Genotype * [GA ₃] = 2.0 | | | | | | |
| L.S.D. at 5% | Genotype = 1.5 | | | | | | |
| | [GA ₃] = 1.9 | | | | | | |
| | Genotype * [GA ₃] = 3.9 | | | | | | |

The L.S.D. at 5% (3.9 mm) was used to assess whether there was a significant difference between the leaf sheath lengths of genotypes for the same GA treatment. The observed difference is depicted in the graph presented in Figure 4.13 B. Both Cadenza and NS response curves follow a very similar pattern and the lengths of their leaf sheaths are very similar (62.5 ± 3.8 mm and 62.4 ± 6.4 mm, respectively). The biggest increase in leaf sheath length occurred between 10 nM and 10 μ M, at which concentration it reached its maximum and was 48.2 mm for Cadenza and 45.3 mm for NS lines. Both *Taidd11* and *Rht-D1b* mutants showed a very different response in leaf sheath elongation to the applied GA₃ compared to Cadenza and NS. The average length of the water treated *Taidd11* and *Rht-D1b* control seedlings were 42.1 ± 4.7 mm and 40.0 ± 7.8 mm, respectively, and they did not show the concentration-dependent increase in leaf sheath length following GA₃ treatment. *Taidd11* showed a very small, but statistically significant increase (5.1 mm) at 10 μ M but the growth increase was not significant for any other GA concentration. The trend of the response curve for *Rht-D1b* mutant was overall very similar to the one of *Taidd11* mutant. There were slight, but statistically significant increases in *Rht-D1b* length at 100 nM (4.6 mm) and at 10 μ M (8.1 mm), but on the other hand the seedlings treated with 1 nM of GA₃ were 2.7 mm shorter than the controls and the seedlings treated with 1 μ M of GA₃ were 0.9 mm shorter than those treated with 100 nM of GA₃.

The final length of the L1 blade of the seedlings grown under various GA₃ regimes was measured after ten days from sowing. General ANOVA confirmed that both genotype ($P < 0.001$) and GA₃ treatment ($P < 0.001$) have a significant effect on L1 blade elongation and that there is a significant interaction between genotype and GA₃ concentration ($P < 0.001$).

The L.S.D. at 5% (6.3 mm) was used to assess whether there was a significant difference between the lengths of L1 blades of genotypes both within and between the GA treatments. The graph in Figure 4.13 C shows GA dose response curves plotted using L1 blade length measurements in mm versus molarity of applied GA₃. Both Cadenza and NS displayed a very similar response

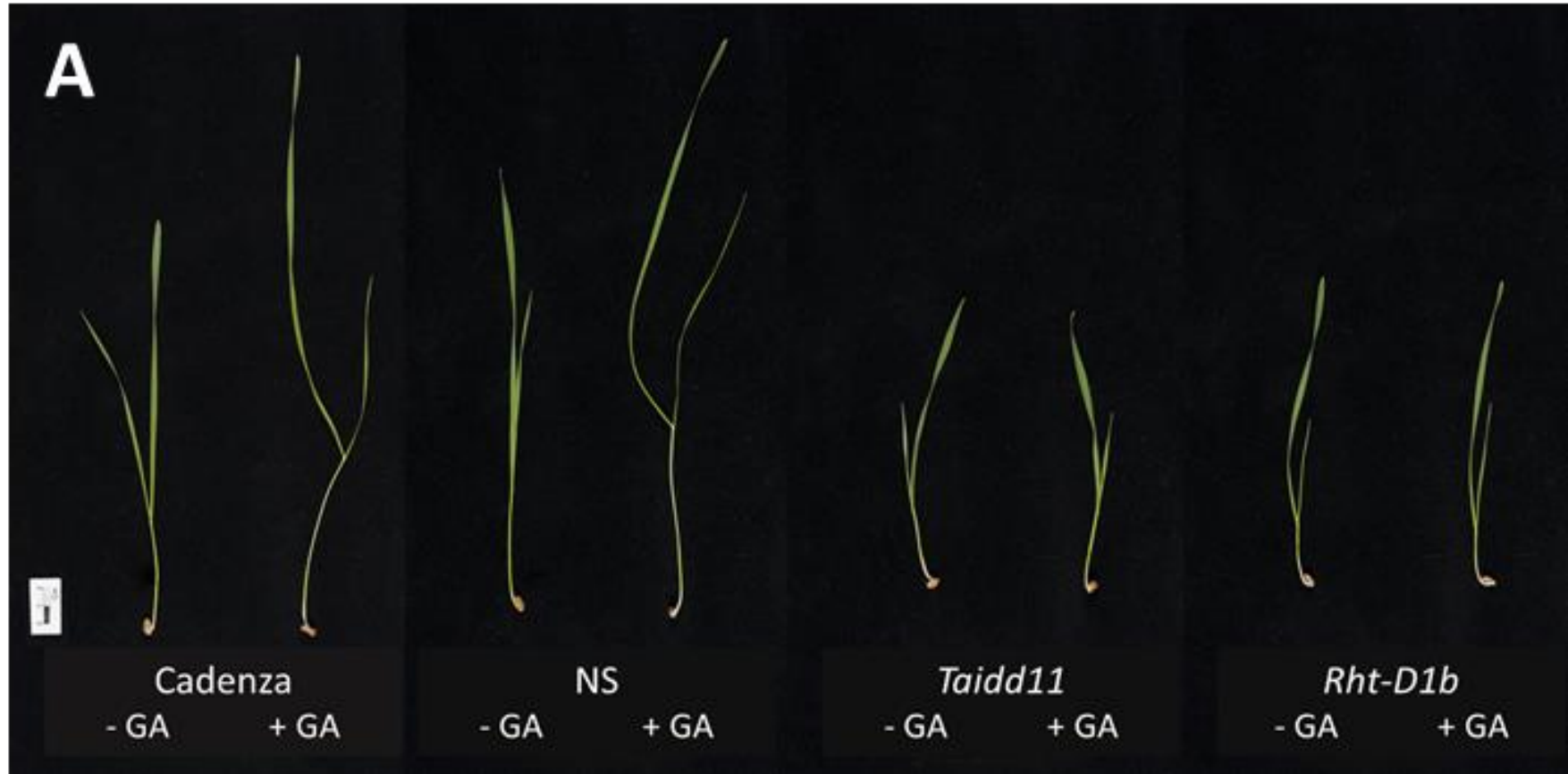
pattern and the lengths of their L1 blades at any GA treatment were very similar. Both seedlings measured on average 170.2 mm and the first significant differences in elongation were observed at 10 nM GA treatment. The increments in elongation with increasing GA concentrations were far from uniform. The biggest elongation (22.9 mm for Cadenza and 23.0 mm for NS) was recorded between 100 nM and 1 μ M of GA₃, and even at 100 μ M the response may not have been saturated.

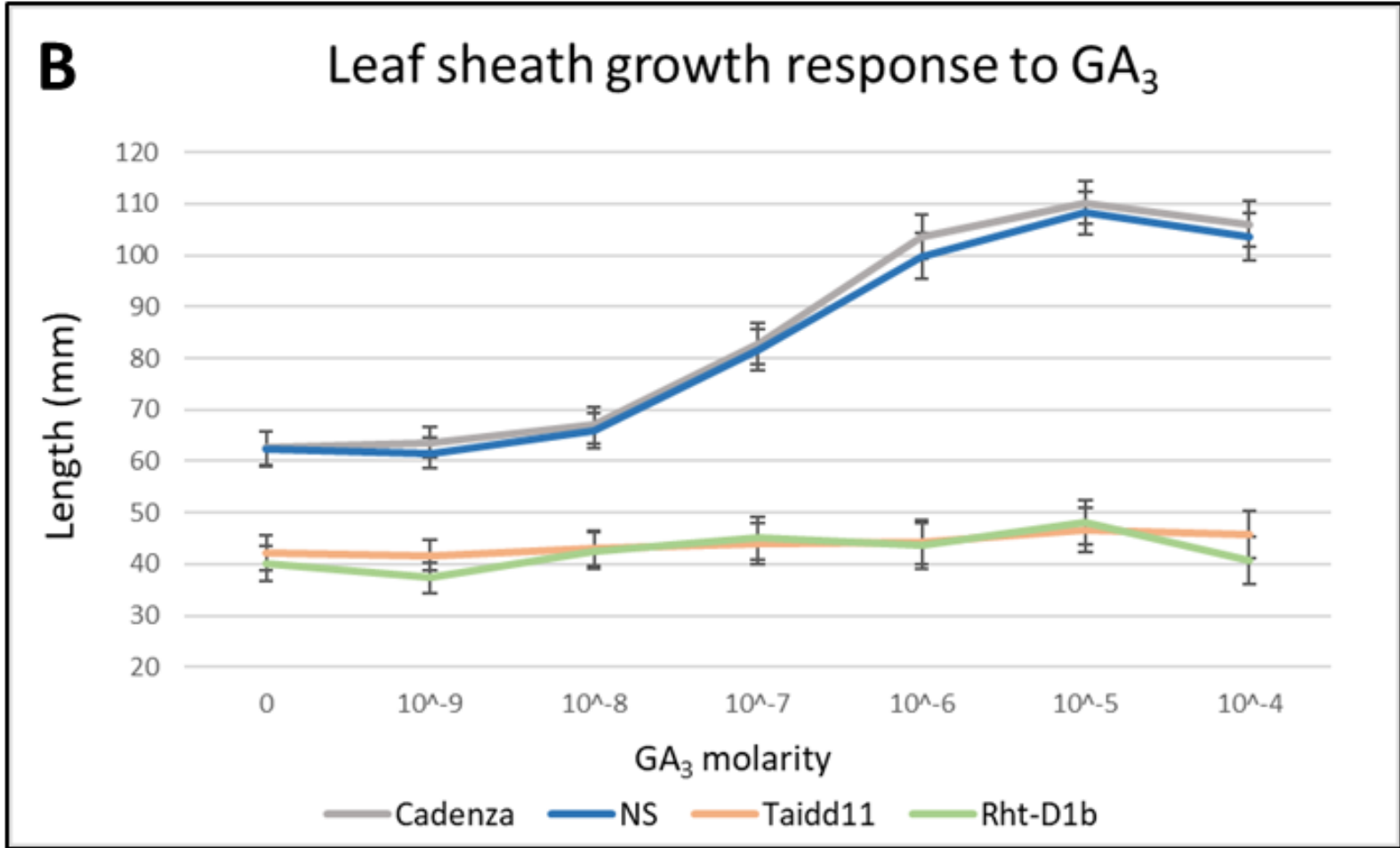
Table 4. 13 Table summarising mean values \pm standard deviation and General ANOVA output for the L1 blade length [mm] of four genotypes in response to a range of GA₃ treatments. P-value, standard error of differences of means (S.E.D.) and least significant difference of means at 5% (L.S.D. 5%) for genotype, treatment and interaction of both factors are included. Significant results (compared to Cadenza) are highlighted in bold.

| | [GA₃] (M) | | | | | | |
|-----------------------|---------------------------------------|--|---------------------------------------|--|--|--|--|
| | 0 | 10 ⁻⁹ | 10 ⁻⁸ | 10 ⁻⁷ | 10 ⁻⁶ | 10 ⁻⁵ | 10 ⁻⁴ |
| Cadenza | 170.2 \pm 15.6 | 171.9 \pm 7.8 | 179.7 \pm 11.4 | 189.1 \pm 10.0 | 212.0 \pm 9.9 | 213.8 \pm 10.8 | 221.9 \pm 8.8 |
| NS | 170.2 \pm 13.1 | 174.5 \pm 11.1 | 183.6 \pm 11.7 | 191.0 \pm 10.5 | 214.0 \pm 11.9 | 216.6 \pm 13.1 | 224.7 \pm 17.8 |
| <i>Taidd11</i> | 116.2 \pm 6.8 | 115.9 \pm 7.6 | 115.9 \pm 7.1 | 121.1 \pm 8.3 | 121.0 \pm 11.8 | 116.7 \pm 6.3 | 121.1 \pm 8.5 |
| <i>Rht-D1b</i> | 136.6 \pm 7.9 | 133.0 \pm 14.6 | 135.0 \pm 9.5 | 136.7 \pm 11.2 | 147.4 \pm 10.2 | 147.7 \pm 11.9 | 142.5 \pm 15.1 |
| P-value (d.f.=611) | Genotype < 0.001 | | | | | | |
| | [GA ₃] < 0.001 | | | | | | |
| | Genotype * [GA ₃] < 0.001 | | | | | | |
| S.E.D. | Genotype * [GA ₃] = 3.2 | | | | | | |
| L.S.D. | Genotype = 2.4 | | | | | | |
| | [GA ₃] = 3.1 | | | | | | |
| | Genotype * [GA ₃] = 6.3 | | | | | | |

Taidd11 and *Rht-D1b* mutants' GA dose response curves differed largely from the ones plotted for the GA-responsive controls. L1 blades of non-treated *Taidd11* and *Rht-D1b* seedlings were significantly shorter (116.2 ± 6.8 mm and 136.6 ± 7.9 mm, respectively) and their lengths did not show GA-dependent increases. In fact, at no GA concentration did *Taidd11* L1 show a significant change in length. *Rht-D1b* showed a significant increase in L1 blade length for 1 μ M and 10 μ M of GA₃ (by 10.8 mm and 11.1 mm, respectively), but then a decrease to non-significant level at the highest tested concentration. Another observation from this experiment was that *Taidd11* produces significantly shorter L1 blades than the semidwarf *Rht-D1b*. It is an interesting observation that the leaf sheaths lengths of the two mutants did not differ significantly, but the lengths of the L1 blades did. In barley, growth of the L1 blade precedes that of the sheath, and after seven days, the growth of the leaf is attributed solely to the sheath elongation (Chandler & Robertson, 1999). Therefore, it can be hypothesized that *TaIDD11* either has more impact on the regulation of the leaf blade rather than leaf sheath elongation, or its activity is more important in the first five days of the seedling growth.

Taken together these results show that like *Rht-D1b*, the *Taidd11* mutant is GA-insensitive and produces seedlings that are shorter than the WT in the same background. Compared to the *Rht-D1b* semidwarf, the *Taidd11* mutant displays further reduction in first leaf blade, but not sheath, elongation. Therefore, we suggest that *TaIDD11* encodes a novel positive regulator of GA-responsive leaf elongation processes.





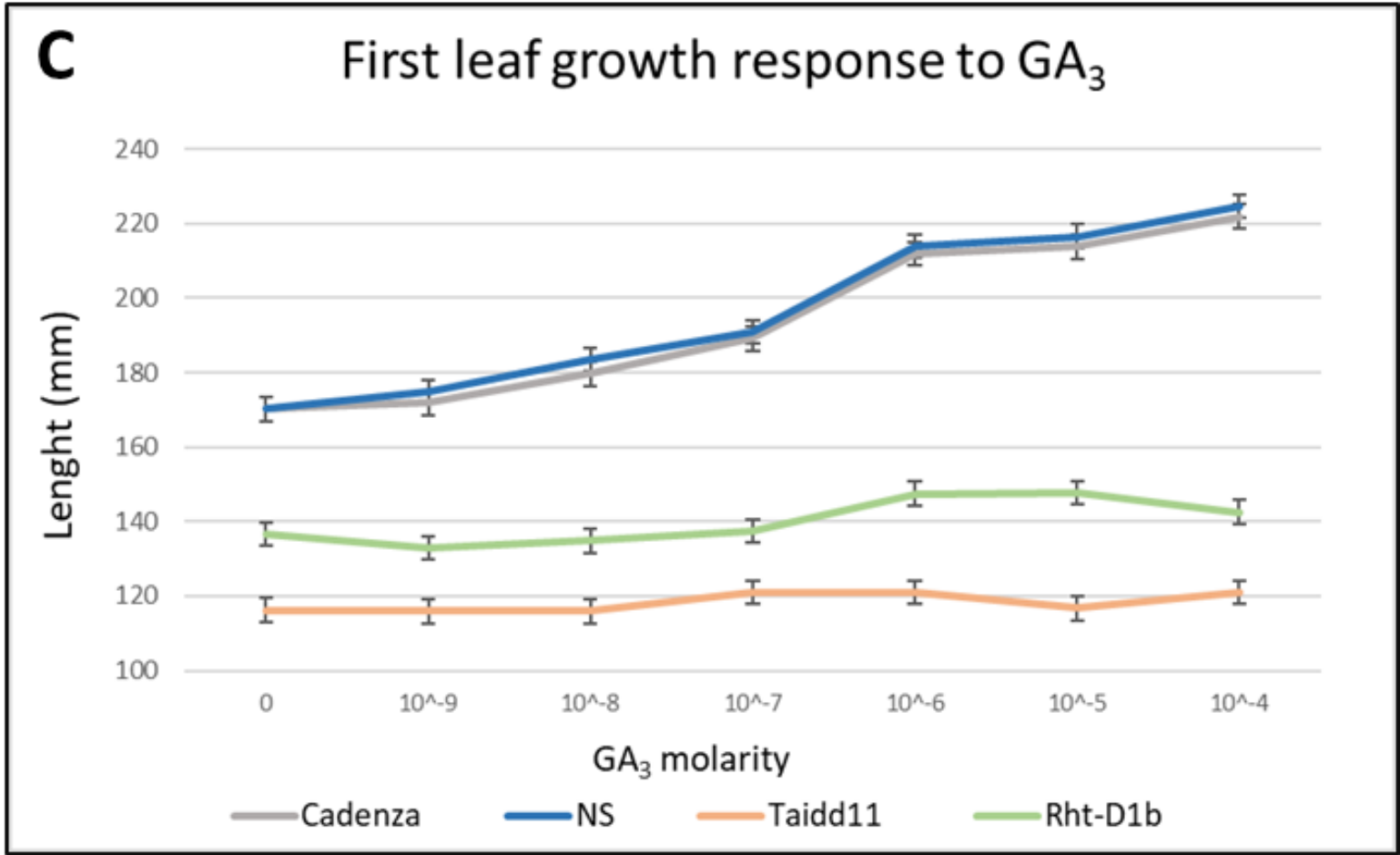


Figure 4. 13 GA₃ dose response assay results. Eight biological replicates per genotype per treatment were measured and the experiment repeated in triplicate. Data were assessed using General ANOVA. A. Photographs of untreated seedlings and seedlings treated with GA₃ harvested ten days after sowing. Four genotypes were compared: Cadenza, NS, Taidd11 mutant and GA-insensitive Rht-D1b mutant. The photos show the difference in growth response to applied GA₃ [10⁻⁴ M] and the physiological differences between genotypes. B. Graph showing the genotype response to applied GA₃, measured by the length of the first leaf sheath. $P < 0.001$. Error bars (S.E.D.) = 1.9. C. Graph showing the genotype response to applied GA₃, measured by the length of the first leaf. $P < 0.001$. Error bars (S.E.D.) = 3.2. Eight biological replicates per genotype per treatment were measured and the experiment repeated in triplicate.

4.3.3.8 Gibberellin content in leaf sheaths of wheat seedlings

Many GA-insensitive mutants have been demonstrated to accumulate bioactive GAs (Appleford & Lenton, 1991; Fujioka *et al.*, 1988; Talon *et al.*, 1990). The typical growth increase in response to GA application is due to cell elongation caused by enhanced expression of genes that alter properties of the cell wall, rendering it more plastic and susceptible to elongation (Tonkinson *et al.*, 1995). Consequently, many mutants deficient in GA biosynthetic or signalling genes display a dwarf phenotype. Analysis of GA levels in *Rht-1* mutants (cv. Maris Huntsman) showed 4- and 24-fold increase in GA₁ levels in the 12-day old seedling leaf expansion zone of *Rht-B1b* and *Rht-B1c*, respectively, compared to *Rht-1* tall seedlings (Appleford & Lenton, 1991). Very similar results were obtained by Webb *et al.*, (1998), who found that the very young uppermost expanding stem internodes of *Rht-B1c* and *Rht-B1b* (collected 46 days before anthesis) accumulated much more GA₁ than the WT (20- and 4-fold, respectively). The groups also analysed GA₁ precursors, GA₁₉ and GA₂₀, and GA₁ inactivation product GA₈, and based on the levels found in the *Rht-1* controls (GA₁₉ >>> GA₂₀ ≈ GA₁ <<GA₈) they concluded that GA₁₉ → GA₂₀ is a rate limiting step in GA biosynthesis. No such drop in GA₁₉ levels was observed in *Rht-B1c* suggesting a change in regulation at an earlier step in the GA biosynthesis (Webb *et al.*, 1998).

GAs are biosynthesized via complex pathways (Section 1.2.4, Figure 4.14 A) and their homeostasis is tightly regulated by several classes of enzymes. All GAs are synthesized from GA₁₂ through the action of dioxygenases that catalyse the final steps in the synthesis of bioactive GAs: GA-promoting GA20ox and GA3ox, and GA-inactivating GA2ox (reviewed in Lange & Pimenta Lange, 2020; Magome *et al.*, 2013; Pimenta Lange *et al.*, 2020). DELLAs, even though they are known repressors of GA-activated responses, play an important part in regulating GA homeostasis. In Arabidopsis, DELLA was shown to positively regulate expression of GA biosynthetic and signalling genes, namely *GA20ox2*, *GA3ox1*, *GID1a*, *GID1b* and *SCL3* (Zentella *et al.*, 2007). Fukazawa *et al.* (2014) discovered that the DELLA protein GAI regulates the

expression of *GA20ox2*, *GA3ox1* and *GID1b* by acting as a coactivator of an IDD transcription factor GAF1 (Fukazawa *et al.*, 2014). Therefore, it could be hypothesized that the TaIDD11 transcription factor may have a similar role in wheat. To assess whether TaIDD11 is involved in regulation of GA homeostasis, the levels of bioactive GAs, their precursors and inactivated products were analysed in the *Taidd11* mutant. *Rht-D1b* was assessed alongside as it is a known GA-insensitive semi-dwarf mutant, but more importantly to establish if knocking out *TaIDD11* gene has a similar effect on GAs homeostasis as mutation affecting the activity of RHT-1. If this were the case it would suggest that both RHT-1 and TaIDD11 have a role in regulating GA homeostasis. Analysis included quantification of 18 GAs (shown in Figure 4.14 A), 10 from non 13-hydroxylation pathway and 8 from early 13-hydroxylation pathway.

Seeds of Cadenza, NS, *Taidd11* and *Rht-D1b* were surfaced sterilised, imbibed at 4°C in the dark for three days and grown in vermiculite in CE room (16 h of light/ 8 h of dark) for seven days before harvesting. The tissue and time point were chosen based on the studies that showed that seven days after germination leaf sheaths of L1 are actively elongating (Appleford & Lenton, 1991; Chandler & Robertson, 1999) hence the GAs regulating leaf sheath elongation should be detected. GAs were extracted and quantified by colleagues at Palacký University Olomouc in Czechia following a modification of the method described in (Urbanová *et al.*, 2013).

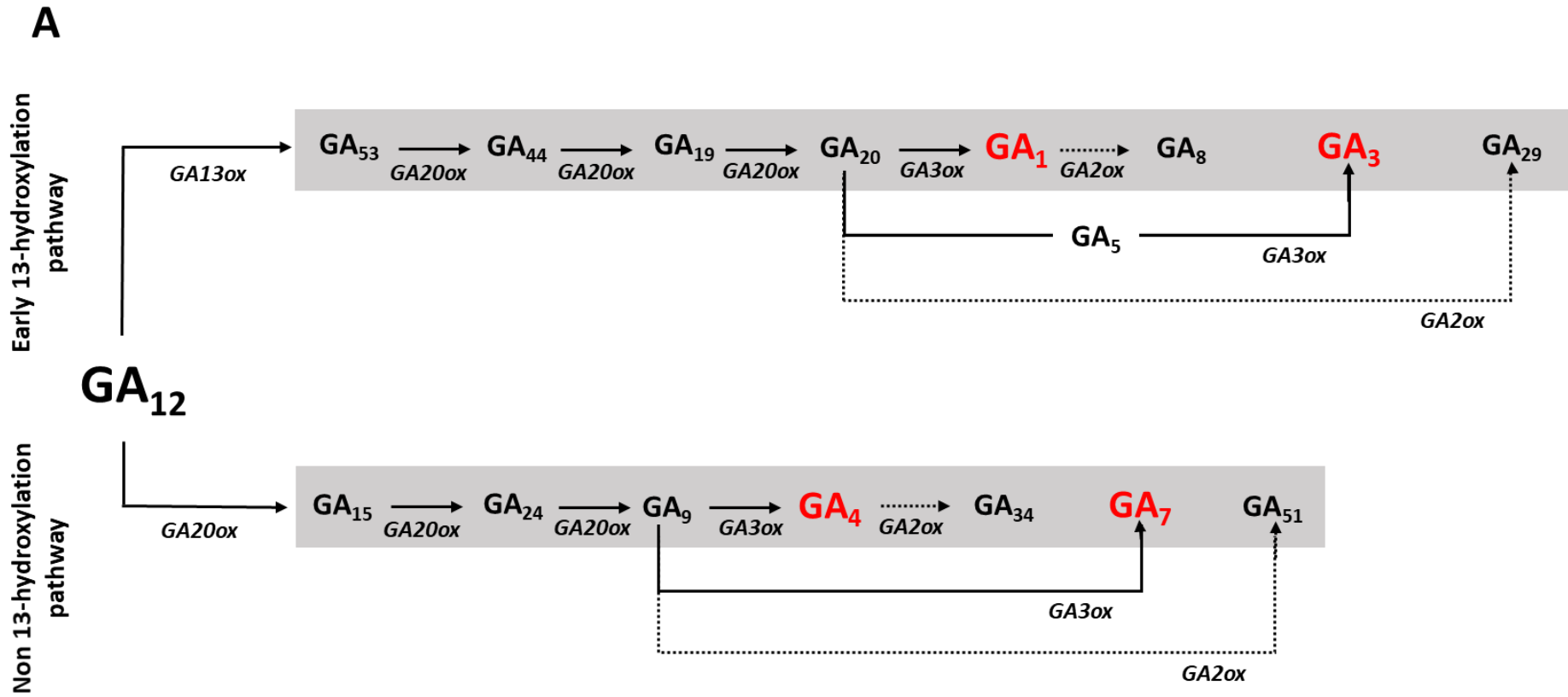
The results were provided as pg/mg of dry weight (DW) for three technical replicates for each biological replicate. The data were analysed in Genstat. A series of General ANOVAs were performed to assess significant differences in GAs levels between the genotypes (Table 4.14). Residual plots generated by Genstat confirmed normal distribution of the data. Fold changes in each line relative to Cadenza are summarised in Table 4.15.

Table 4. 14 Mean (\pm SD) GA content [$\mu\text{g}/\text{mg}$ DW] in leaf sheaths of four genotypes with General ANOVA values for each GA measured. Three significant figures are shown for every value. Significant values (compared to Cadenza) are highlighted in bold. ND = not detected.

| | Cadenza | NS | Taidd11 | Rht-D1b | P-value (d.f.=41) | S.E.D. | L.S.D. at 5% |
|------------------|----------------------|--------------------------------------|--------------------------------------|--------------------------------------|-------------------|---------|--------------|
| GA ₁ | 1.03 \pm 0.169 | 0.975 \pm 0.11 | 1.93 \pm 0.108 | 2.81 \pm 0.396 | <0.001 | 0.0741 | 0.15 |
| GA ₃ | 0.274 \pm 0.0791 | 0.33 \pm 0.168 | 0.305 \pm 0.0434 | 0.394 \pm 0.0542 | 0.019 | 0.0374 | 0.0756 |
| GA ₄ | ND | ND | ND | 0.261 \pm 0.218 | N/A | N/A | N/A |
| GA ₈ | 3.17 \pm 0.536 | 4.12 \pm 0.578 | 4.08 \pm 0.45 | 2.57 \pm 0.321 | <0.001 | 0.199 | 0.402 |
| GA ₁₉ | 1.08 \pm 0.166 | 1.14 \pm 0.0995 | 0.365 \pm 0.0521 | 0.506 \pm 0.132 | <0.001 | 0.0386 | 0.078 |
| GA ₂₀ | 0.612 \pm 0.0452 | 0.794 \pm 0.204 | 0.479 \pm 0.187 | 0.816 \pm 0.0926 | <0.001 | 0.0475 | 0.096 |
| GA ₂₉ | 0.408 \pm 0.0843 | 0.291 \pm 0.0607 | 0.148 \pm 0.0328 | 0.085 \pm 0.0348 | <0.001 | 0.0203 | 0.041 |
| GA ₃₄ | 0.0283 \pm 0.00718 | 0.0225 \pm 0.00622 | 0.0225 \pm 0.00452 | 0.0242 \pm 0.0116 | 0.116 | 0.00269 | 0.00544 |
| GA ₄₄ | 2.28 \pm 0.428 | 2.37 \pm 0.296 | 0.395 \pm 0.05 | 0.63 \pm 0.15 | <0.001 | 0.09 | 0.182 |
| GA ₅₃ | 0.015 \pm 0.00674 | 0.015 \pm 0.00674 | 0.0108 \pm 0.00289 | ND | 0.1 | 0.00216 | 0.00441 |

Table 4. 15 Fold change in GA levels in NS, Taidd11 and Rht-D1b compared to Cadenza. Highlighting in green and red represent decrease and increase relative to Cadenza, respectively. Significant values (compared to Cadenza) are highlighted in bold.

| | NS | Taidd11 | Rht-D1b |
|------------------|------------|------------|------------|
| GA ₁ | 1.1 | 1.9 | 2.7 |
| GA ₃ | 1.2 | 1.1 | 1.4 |
| GA ₈ | 1.3 | 1.3 | 1.2 |
| GA ₁₉ | 1.1 | 3.0 | 2.1 |
| GA ₂₀ | 1.3 | 1.3 | 1.3 |
| GA ₂₉ | 1.4 | 2.8 | 4.8 |
| GA ₃₄ | 1.3 | 1.3 | 1.2 |
| GA ₄₄ | 1.0 | 5.8 | 3.6 |
| GA ₅₃ | 1.0 | 1.4 | ND |



B

Gibberellin levels in leaf sheaths

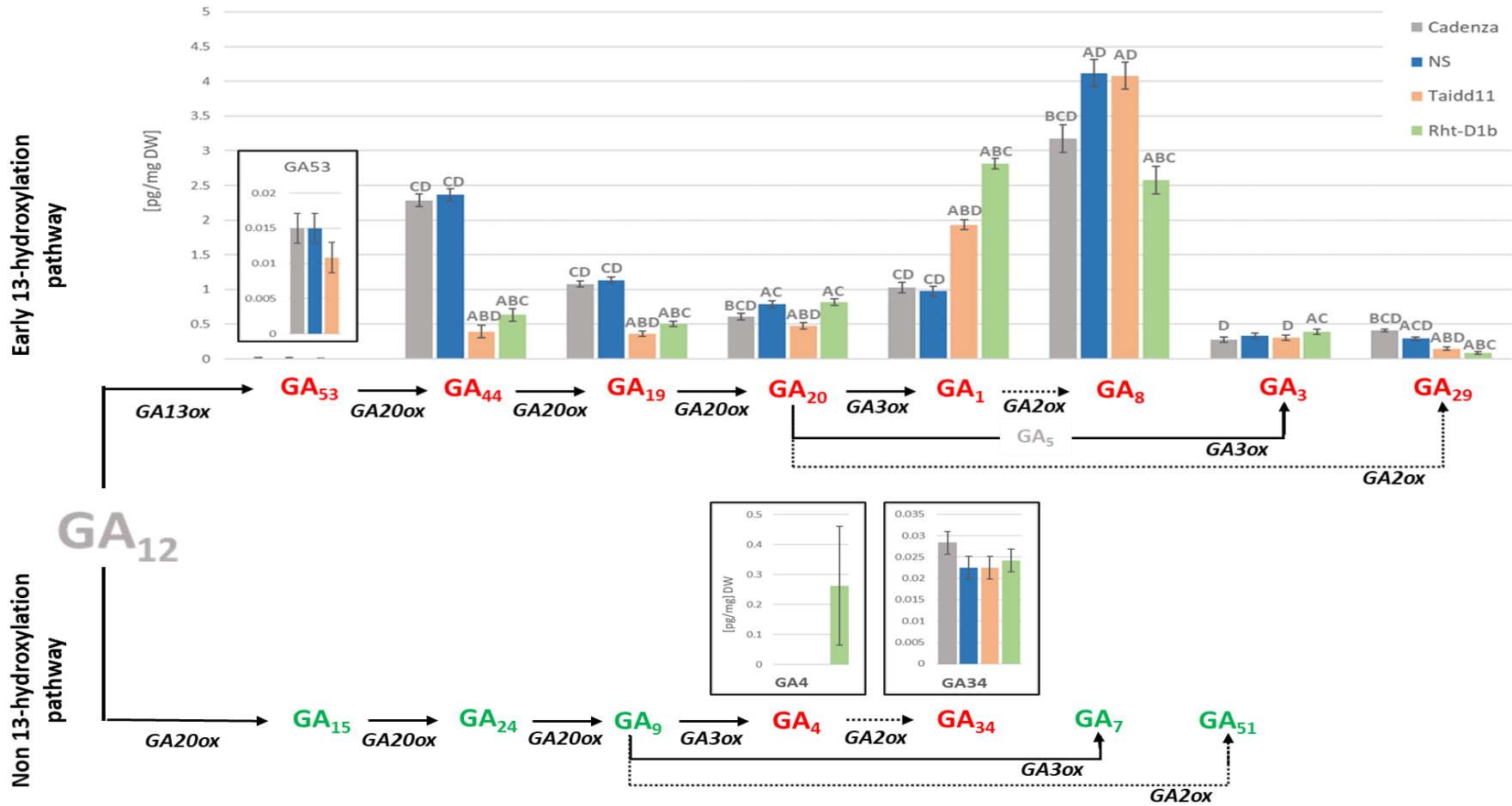


Figure 4. 14 Pathways of GAs biosynthesis and levels of GAs in leaf sheaths of the seedlings of Cadenza, NS, Taidd11 and Rht-D1b. A. Later steps of gibberellins' biosynthesis pathway. All GAs are synthesized from GA₁₂ by the action of oxidases (GA20ox, GA3ox, GA13ox, GA2ox). Two pathways exist: early 13-hydroxylation pathway and non 13-hydroxylation pathway, with the former predominant in wheat. The bioactive GAs are highlighted in red. The GAs which levels were assessed are boxed in grey. B. GA hormone analysis in four genotypes. Gibberellin content [$\mu\text{g}/\text{mg DW}$] was measured in freeze-dried leaf sheath tissue collected from the seedling seven days after germination. GA₅₃ was not detected in Rht-D1b leaf sheaths, but GA₄ was only detected in this genotype. Error bars are S.E.D.s (look Table 4.13), except for GA₄ where error bars represent standard deviation (0.198). The letters over the error bars indicate 'significantly different from' ($P < 0.001$): A = Cadenza, B = NS, C = Taidd11, D = Rht-D1b. GAs which levels were analysed in the experiment are shown: red = detected, green = not detected, grey = not analysed. Solid arrows represent synthesis and dotted arrows represent inactivation.

Figure 4.14 B shows both pathways of bioactive GA synthesis with a graphic representation of detected GAs levels (GA₁, GA₃, GA₄, GA₈, GA₁₉, GA₂₀, GA₂₉, GA₃₄, GA₄₄ and GA₅₃) found in analysed wheat seedlings. Highlighted in red are the GAs that were detected; the ones highlighted in green were measured, but not detected. The majority of the detected GAs belong to the early 13-hydroxylation pathway, which is a dominant pathway in wheat (Appleford & Lenton, 1991). Even though all the other precursors of GA₁ were present, no GA₅₃ was detected in *Rht-D1b*. On the other hand, it was the only genotype in which GA₄, the main bioactive GA of non 13-hydroxylation pathway, was detected. Relatively small amounts of GA₄ were previously found in wheat shoots (Appleford & Lenton, 1991; Webb *et al.*, 1998). A 15.9-, 8.2- and 6.5-fold increase in GA₄ compared to WT Cadenza in wheat seedlings was also reported in *Rht-B1c*, *Rht-A1b* and *Rht-D1b*, respectively (Rafter, 2019). However, we did not detect any GA₄ in any of the tall controls, nor in the *Taidd11* mutant. GA₅₃ was detected in these three lines in very small quantities, and the levels did not differ significantly between genotypes (L.S.D. at 5% = 0.100).

The steps of GA biosynthesis catalysed by GA 20-oxidase (GA20ox) in the early 13-hydroxylation pathway are as follows: GA₅₃ → GA₄₄ → GA₁₉ → GA₂₀, (Figure 4.14 A). The bioactive GA₁ and GA₃ are synthesized from GA₂₀ by the action of GA 3-oxidase (GA3ox), and GA₈ and GA₂₉ arise through inactivating action of GA 2-oxidase (GA2ox) on GA₁ and GA₂₀, respectively. The early 13-hydroxylation pathway is a dominant GA synthesis pathway in wheat as GA13ox converts GA₁₂ to GA₅₃ more efficiently than GA20ox converts GA₁₂ to GA₁₅ (Appleford & Lenton, 1991). GA₁ accumulates in wheat vegetative tissues perhaps due to high levels of *GA13ox* expression in these tissues (Webb *et al.*, 1998). Previous studies showed 4- and around 20-fold accumulation of bioactive GA₁ in leaves and internodes of *Rht-B1b* and *Rht-B1c* seedlings, respectively, compared with tall (*rht*) lines (Appleford & Lenton, 1991; Webb *et al.*, 1998). In our study *Rht-D1b* showed a significant 2.7-fold increase in GA₁ levels compared to Cadenza control (P < 0.001). Similarly, the *Taidd11* mutant

also had significantly elevated GA₁ levels compared to the control (1.9-fold increase; $P < 0.001$). The levels in Cadenza and NS lines did not differ significantly (L.S.D. at 5% = 0.150) (Figure 4.14 B). GA₁ synthesis from GA₂₀ is catalysed by GA3ox, hence the increased levels of GA₁ suggest that the activity of GA3ox may be increased in the mutants.

In both studies by Appleford & Lenton (1991) and Webb *et al.* (1998), *Rht-B1b* accumulated relatively high levels of GA₁₉, whereas the same was not observed in *Rht-B1c*. Neither of the lines analysed in our experiment showed high levels of GA₁₉, moreover, its levels were significantly reduced ($P < 0.001$) in *Rht-D1b* (by 2.1-fold) and *Taidd11* (by 3.0-fold) lines compared to the Cadenza control (Table 4.15). Relatively to Cadenza, the levels of GA₁₉ precursor, GA₄₄, were also significantly decreased in *Rht-D1b* (3.6-fold; $P < 0.001$) and *Taidd11* (5.8-fold; $P < 0.001$). These results suggest that the activity of GA20ox is increased in the mutants as a higher rate of conversion of GA₅₃ to GA₂₀ would result in lower levels of the GA₂₀ precursors. Interestingly, the levels of GA₂₀, which is the last GA synthesized by GA20ox, in Cadenza and NS did not differ greatly from levels of GA₁₉ (1.8- and 1.4-fold lower in Cadenza and NS, respectively) which is not in line with previous observation that GA₁₉ to GA₂₀ is a limiting step in GA biosynthesis (Appleford & Lenton, 1991; Webb *et al.*, 1998). Conversely to the GA-responsive lines, the analysed mutants accumulated slightly more GA₂₀ than GA₁₉. *Taidd11* accumulated 1.3-fold and *Rht-D1b* 1.6-fold more GA₂₀ than GA₁₉ which again supports the hypothesis that GA20ox activity is enhanced in the mutants. It is also worth noting that while *Rht-D1b* accumulated significantly more GA₂₀ than Cadenza (1.3-fold; $P < 0.001$), the levels of GA₂₀ in *Taidd11* were significantly (1.3-fold; $P < 0.001$) lower compared to Cadenza.

In previous studies, both *Rht-B1b* and *Rht-B1c* mutants accumulated relatively high levels of GA₈ in the studied tissues compared to tall wild types (Appleford & Lenton, 1991; Webb *et al.*, 1998). The exception was in 12-days old seedling leaf expansion zone of the *Rht-B1c* mutant where the levels of two GAs were comparable. GA₈ is a product of GA₁ inactivation, hence the relative levels of

these two GAs may indicate the relative activity of GA2ox. However, GA2ox enzymes also catalyse the inactivation of the immediate precursors of bioactive GAs, e.g. GA₂₀ to GA₂₉, and may oxidise the 2 β -hydroxylated inactive products further to the so-called GA catabolites. In *Rht-D1b* GA₈ levels were significantly reduced (by 1.2-fold; P < 0.001) compared to Cadenza, which would suggest reduced activity of GA2ox in the mutant. A different scenario was observed for *Taidd11* line, which accumulated significantly more GA₈ than the control (1.3-fold; P < 0.001). The ratio of GA₁ to GA₈ in *Rht-D1b* was 1.1, whereas that in the *Taidd11* mutant was 0.5. One possible explanation for the observed differences in the mutant lines is the activity of GA2ox. Lower activity in *Rht-D1b* might be the cause of slower rate of inactivation, and hence lower levels of GA₈ and increased levels of GA₁. Conversely, higher activity of the enzyme in *Taidd11* may explain higher levels of GA₈ compared to GA₁. Different activity of GA2ox in the mutants would also explain the observed differences in GA₂₀ levels between the mutants.

DELLAs play an important role in regulating GA levels; they were shown to upregulate expression of genes involved in feedback (*GA3ox1*, *GA20ox2* and *GID1b*) and, although probably independently of DELLA, the transcript levels of some of the *GA2ox* genes in DELLA gain-of-function mutants are downregulated (reviewed in Hedden & Thomas, 2012). Assuming that elevated transcript levels of the enzyme-encoding genes translate to increase in respective enzyme activities, the levels of GAs identified in *Rht-D1b* mutant, are consistent with the reported effect of DELLA on GA feedback genes. GA levels in the *Taidd11* mutant are very similar to those in *Rht-D1b*, suggesting that the *Taidd11* is too involved in GA feedback regulation, whereas the differences in bioactive GA catabolite levels implies that the regulation of *GA2ox* genes might be controlled by a distinct mechanism.

4.3.3.9 The genes involved in GA biosynthesis and signalling are differentially expressed in *Taidd11* mutant

GA₃ application was previously shown to alter expression of the genes responsible for regulating GA homeostasis (Figure 4.15) (Cheng *et al.*, 2015; Chiang *et al.*, 1995; Phillips *et al.*, 1995; Ribeiro *et al.*, 2012; Thomas *et al.*, 1999). *AtGA20ox1*, *AtGA20ox2*, *AtGA20ox3*, and *AtGA3ox1* were found to be highly up-regulated in GA-deficient mutants, whereas they were down-regulated after the application of GAs (Chiang *et al.*, 1995; Phillips *et al.*, 1995). Conversely, the expression of *AtGA2ox1* and *AtGA2ox2* genes was up-regulated after the GA treatment (Thomas *et al.*, 1999). More recent studies show that in grapevine and Arabidopsis the majority of *GA20ox* and *GA3ox* genes are down-regulated following application of GA₃. In contrast, the genes encoding *GA2ox* genes are up-regulated following GA treatment. In Arabidopsis, early GA biosynthesis genes, *KO*, *KAO1* and *KAO2* were also found to be negatively regulated by GA (Ribeiro *et al.*, 2012). These results indicate negative GA feedback regulation that controls the concentration of active GAs after exogenous GA₃ application. The feedback and feedforward mechanisms also operate at the level of GA perception, as *GID1B* is down-regulated and a few different *DELLA* genes are up-regulated after GA₃ treatment (Cheng *et al.*, 2015; Ribeiro *et al.*, 2012). Paclobutrazol (PAC), a GA biosynthesis inhibitor, had an opposite effect from GA on expression of GA-regulated genes (Ribeiro *et al.*, 2012), further reinforcing the effect of GA on expression of genes involved in GA metabolism and signal transduction.

The observed differences in response to applied GA and accumulation of GAs in *Rht-D1b* and *Taidd11* compared to Cadenza suggests that the genes involved in the GA biosynthesis and/or signalling may be differentially expressed in these mutants. To compare the expression of multiple genes in these genotypes under control conditions as well as in response to GA₃ treatment, an RNA-Seq experiment was conducted. Seeds of Cadenza, *Taidd11* and *Rht-D1b* were surface-sterilised, germinated and grown in vermiculite for seven days. On the eighth day, half of the plants were treated with 100 µM GA₃ and

the leaf sheaths (between the seed crown and the coleoptile tip) harvested and flash frozen eight hours after GA application. The time point was chosen based on previous studies in wheat cv. Cadenza, which identified that the 4 – 8 hours' time point after GA₃ application is when wheat seedlings show significant elongation response (Rafter, 2019). Sequencing and raw data quality service was provided by Novogene (<https://en.novogene.com/>) and data analysis conducted using Galaxy (Afgan *et al.*, 2018) and the 3D RNA-seq App (Guo *et al.*, 2019) by Dr Andy Phillips (Rothamsted Research, UK).

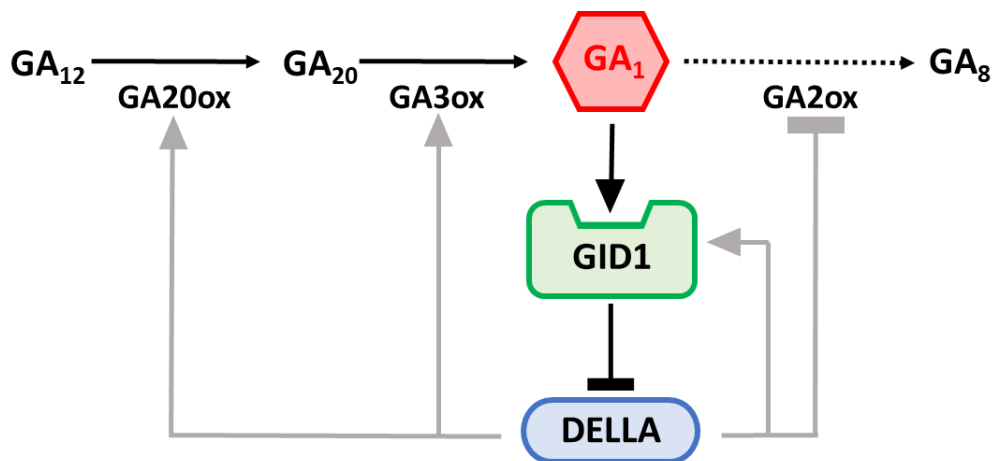


Figure 4. 15 The role of DELLA and GAs in regulation of GA homeostasis. In the absence of GAs, DELLA up-regulates the expression of GA biosynthesis feedback regulation genes GA20ox and GA3ox, and downregulates the expression of GA2ox, a biosynthetic feedforward gene. DELLA is also involved in transcriptional regulation of GA signalling gene, GID1. GAs initiate GID1-mediated degradation of DELLA and thus indirectly regulate the expression of feedback and feedforward genes. Grey lines indicate transcriptional regulation.

Figure 4.16 summarizes the results of the RNA-seq experiment. The transcriptome analysis was conducted to reveal the differences in gene expression between the genotypes. Additionally, the changes induced in the transcriptome of the three genotypes in response to GA₃ application were

compared. The plot in Figure 4.16 A shows the number of up- and down-regulated genes in every one of the nine contrast groups. As three genotypes were used: Cadenza (Cad), *Taidd11* (idd) and *Rht-D1b* (Rht), and two treatments applied (treated with GA₃ [GA] and non-treated [NT]), nine contrast groups were compared: all genotypes with and without GA₃ treatment (Cad.GA-Cad.NT, idd.GA-idd.NT, Rht.GA-Rht.NT), pairwise comparison between genotypes treated with GA₃ (Cad.GA-idd.GA, Cad.GA-Rht.GA, idd.GA-Rht.GA) and pairwise comparison between genotypes without the treatment (Cad.NT-idd.NT, Cad.NT-Rht.NT and idd.NT-Rht.NT).

120 DE genes were found in Cad.GA-Cad.NT contrast group; 100 were up-regulated and 20 were down-regulated in response to GA treatment. No change in gene expression in response to GA₃ treatment was noted in *Taidd11* and *Rht-D1b* mutants, which reinforced the notion that these mutants are GA-insensitive. Another striking observation from this plot is that the difference in gene expression, i.e. the number of DE genes, is much smaller when comparing the two GA-insensitive mutants than either of the mutants with Cadenza, and this is true for both untreated and GA-treated plants. With no treatment, 3061 and 2275 DE genes were found between Cadenza and *Taidd11* and *Rht-D1b*, respectively, whereas only 289 DE genes were found between the mutants. The numbers of DE genes roughly doubled in the GA-treated plants and were 6272 between Cadenza and *Taidd11*, 5211 between Cadenza and *Rht-D1b*, and 541 between *Taidd11* and *Rht-D1b*. This shows that *Taidd11* and *Rht-D1b* mutants share similar gene regulation mechanisms as around ten times fewer genes are differentially expressed between *Taidd11* and *Rht-D1b* mutants than between any of the mutants and Cadenza. Also, GA application causes 2-fold increase in the number of DE genes, and its effect is predominantly up-regulation; GA treatment results in about 12% more up-regulated genes in the same contrast groups. Of all DE genes in contrast groups Cad.NT-idd.NT, Cad.NT-Rht.NT and idd.NT-Rht.NT, upregulated genes constitute 32.3%, 38.5% and 38%, respectively, whereas in contrast groups Cad.GA-idd.GA, Cad.GA-

Rht.GA and idd.GA-Rht.GA, up-regulated genes are 44.6%, 51% and 49.1% of all DE genes, respectively.

Figure 4.16 B shows Venn diagrams of DE genes in all three genotypes treated with GA₃ (top) and without the treatment (bottom). There is a big overlap of genes that are differentially expressed between contrast groups Cad.GA-idd.GA and Cad.GA-Rht.GA. No such big overlap can be observed comparing the two contrast groups with idd.GA-Rht.GA contrast group, and only 65 genes are differentially expressed across all contrast groups. Similar pattern is observed for DE genes in three contrast groups that were not treated with GA₃. The biggest number of commonly DE genes is between contrast groups Cad.NT-idd.NT and Cad.NT-Rht.NT, the number of shared DE genes with idd.NT-Rht.NT contrast group is 10- and 20-fold smaller, respectively, and only 12 DE genes are shared between all three genotypes. These results show that the regulation of gene expression, as well as the effect of GA on the transcriptome is more similar when comparing the two mutants, *Taidd11* and *Rht-D1b*, than when comparing any of them individually to Cadenza.

Among DE genes, the genes that are involved in GA biosynthesis and signaling were identified and their expression between the contrast groups is summarized in Table 4.16. The mean TPM values for these genes were used to generate the heatmap that shows relative levels of expression between the samples (Figure 4.16 C). In Cadenza, after application of GA₃, increase in expression of various GA 2-oxidases (*GA2ox10-A*, *GA2ox10-B*, *GA2ox10-D*, *GA2ox3-A*, *GA2ox3-D* and *GA2ox7-D*) and all three *Rht-1* homoeologues was observed (Figure 4.16 C), however, only *GA2ox3-A*, *GA2ox10-B* and *Rht1-D* expression was statistically significant (Table 4.16).

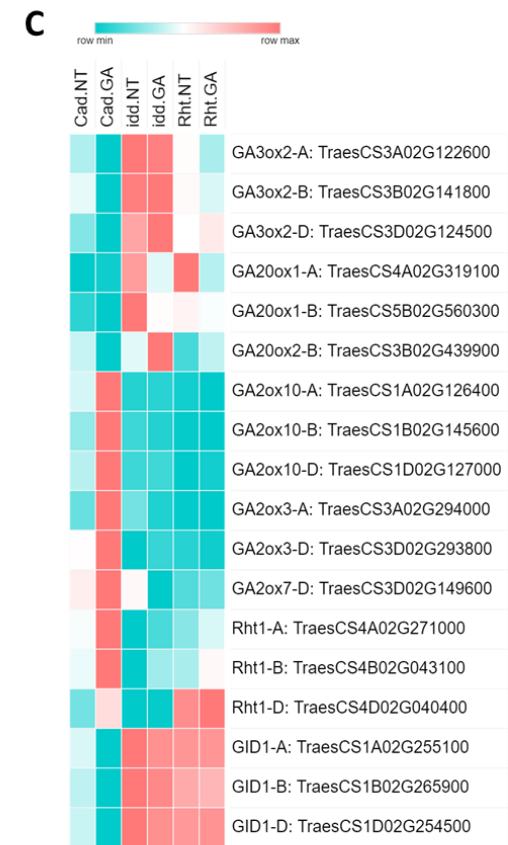
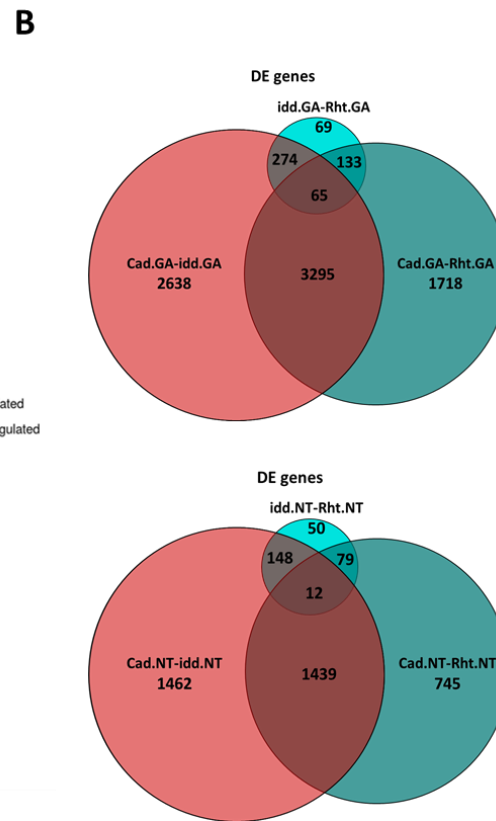
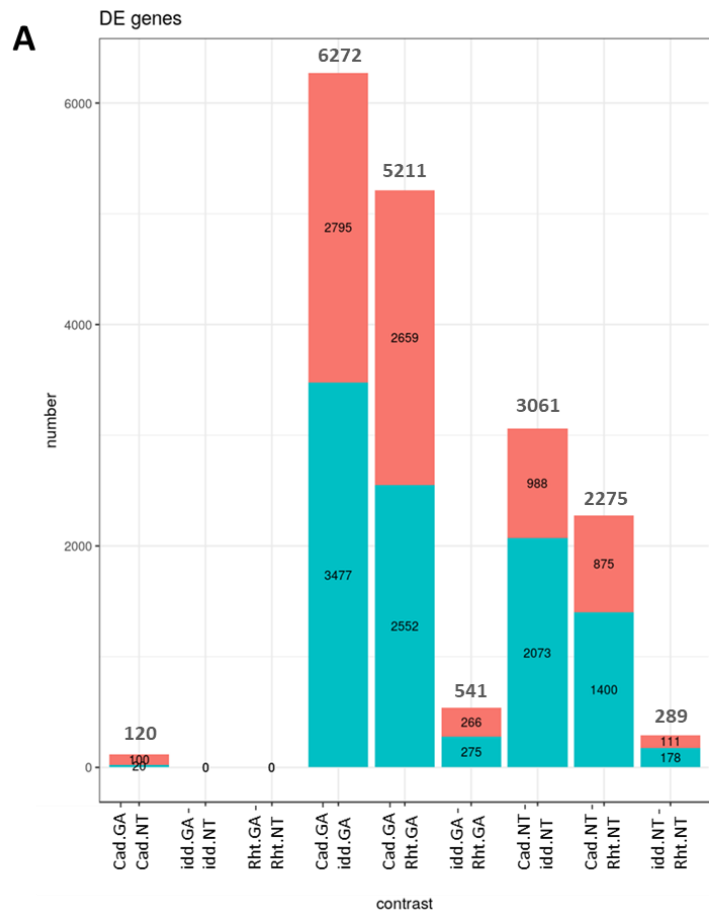


Figure 4. 16 RNASeq experiment results. A. The number of differentially expressed (DE) genes in nine contrast groups: Cad.GA - Cad.NT, idd.GA - idd.NT, Rht.GA - Rht.NT, Cad.GA - idd.GA, Cad.GA - Rht.GA, idd.GA - Rht.GA, Cad.NT - idd.NT, Cad.NT - Rht.NT and idd.NT - Rht.NT. The DE genes are divided into up- (orange) and down- (blue) regulated genes, and they are up- or down-regulated in the first of the two samples in the contrast group. The plot was generated in the 3D RNA-seq App. B. Venn diagrams showing DE genes between three genotypes for the two treatments. Diagrams were generated by 3D RNA-seq App. C. Heatmap showing relative expression of selected GA biosynthesis and signalling genes, showed to be differentially expressed in at least one contrast group. Heatmap generated using versatile matrix visualization and analysis software MORPHEUS (<https://software.broadinstitute.org/morpheus/>).

Table 4. 16 GA biosynthesis and signalling genes that were found to be differentially expressed within the contrast groups. Up-regulated genes are highlighted in red and down-regulated genes are highlighted in blue.

| Gene ID | Contrast | P value _{Adj} | log ₂ FC | Fold change | Effect | Gene description |
|--|---------------|------------------------|---------------------|-------------|----------------|------------------|
| Cadenza in response to GA | | | | | | |
| TraesCS4D02G040400 | Cad.NT-Cad.GA | 1.65E-03 | 0.45 | 1.37 | up-regulated | Rht-D1 |
| TraesCS3A02G294000 | Cad.NT-Cad.GA | 3.19E-03 | 1.45 | 2.73 | up-regulated | GA2ox3-A |
| TraesCS1B02G145600 | Cad.NT-Cad.GA | 8.37E-03 | 1.20 | 2.30 | up-regulated | GA2ox10-B |
| Taidd11 in response to GA | | | | | | |
| NO | | | | | | |
| Rht-D1b in response to GA | | | | | | |
| NO | | | | | | |
| Up- or down-regulated in Cadenza in Cad.GA-idd.GA group | | | | | | |
| TraesCS1A02G255100 | Cad.GA-idd.GA | 3.15E-06 | -1.72 | 3.29 | down-regulated | GID1-A |
| TraesCS1B02G265900 | Cad.GA-idd.GA | 9.31E-09 | -1.76 | 3.39 | down-regulated | GID1-B |
| TraesCS1D02G254500 | Cad.GA-idd.GA | 3.55E-08 | -1.76 | 3.39 | down-regulated | GID1-D |
| TraesCS3A02G122600 | Cad.GA-idd.GA | 2.62E-05 | -3.50 | 11.33 | down-regulated | GA3ox2-A |
| TraesCS3B02G141800 | Cad.GA-idd.GA | 1.01E-07 | -1.71 | 3.27 | down-regulated | GA3ox2-B |
| TraesCS3D02G124500 | Cad.GA-idd.GA | 4.60E-08 | -2.69 | 6.45 | down-regulated | GA3ox2-D |
| TraesCS3B02G439900 | Cad.GA-idd.GA | 9.74E-03 | -1.33 | 2.51 | down-regulated | GA20ox2-B |
| TraesCS4A02G271000 | Cad.GA-idd.GA | 5.03E-06 | 0.52 | 1.43 | up-regulated | Rht-A1 |
| TraesCS4B02G043100 | Cad.GA-idd.GA | 2.72E-03 | 0.32 | 1.25 | up-regulated | Rht-B1 |
| TraesCS4D02G040400 | Cad.GA-idd.GA | 2.31E-07 | 0.65 | 1.57 | up-regulated | Rht-D1 |
| TraesCS3A02G294000 | Cad.GA-idd.GA | 5.45E-06 | 1.88 | 3.67 | up-regulated | GA2ox3-A |
| TraesCS3D02G293800 | Cad.GA-idd.GA | 2.72E-04 | 1.97 | 3.91 | up-regulated | GA2ox3-D |
| TraesCS3D02G149600 | Cad.GA-idd.GA | 2.14E-03 | 2.10 | 4.30 | up-regulated | GA2ox7-D |
| TraesCS1A02G126400 | Cad.GA-idd.GA | 6.38E-07 | 1.59 | 3.02 | up-regulated | GA2ox10-A |
| TraesCS1B02G145600 | Cad.GA-idd.GA | 2.80E-06 | 1.85 | 3.62 | up-regulated | GA2ox10-B |
| TraesCS1D02G127000 | Cad.GA-idd.GA | 1.55E-04 | 1.12 | 2.17 | up-regulated | GA2ox10-D |
| Up- or down-regulated in Cadenza in Cad.GA-Rht.GA group | | | | | | |
| TraesCS1A02G255100 | Cad.GA-Rht.GA | 7.67E-06 | -1.67 | 3.19 | down-regulated | GID1-A |
| TraesCS1B02G265900 | Cad.GA-Rht.GA | 1.28E-07 | -1.55 | 2.94 | down-regulated | GID1-B |
| TraesCS1D02G254500 | Cad.GA-Rht.GA | 8.23E-08 | -1.71 | 3.27 | down-regulated | GID1-D |
| TraesCS3B02G141800 | Cad.GA-Rht.GA | 1.03E-03 | -0.95 | 1.94 | down-regulated | GA3ox2-B |
| TraesCS3D02G124500 | Cad.GA-Rht.GA | 8.42E-06 | -2.03 | 4.08 | down-regulated | GA3ox2-D |
| TraesCS1A02G126400 | Cad.GA-Rht.GA | 1.56E-06 | 1.67 | 3.18 | up-regulated | GA2ox10-A |
| TraesCS1B02G145600 | Cad.GA-Rht.GA | 4.89E-06 | 2.09 | 4.25 | up-regulated | GA2ox10-B |
| TraesCS1D02G127000 | Cad.GA-Rht.GA | 4.21E-05 | 1.42 | 2.67 | up-regulated | GA2ox10-D |
| TraesCS3A02G294000 | Cad.GA-Rht.GA | 7.28E-06 | 2.09 | 4.25 | up-regulated | GA2ox3-A |
| TraesCS3D02G293800 | Cad.GA-Rht.GA | 1.12E-04 | 2.71 | 6.53 | up-regulated | GA2ox3-D |

| Up- or down-regulated in idd.GA-Rht.GA group | | | | | | |
|--|---------------|----------|-------|------|--------------------------------|-----------|
| TraesCS4D02G040400 | idd.GA-Rht.GA | 4.73E-10 | -1.01 | 2.02 | up regulated in <i>Rht-D1b</i> | Rht-D1 |
| TraesCS3B02G141800 | idd.GA-Rht.GA | 3.13E-03 | 0.76 | 1.69 | up-regulated in <i>Taidd11</i> | GA3ox2-B |
| Up- or down-regulated in <i>Taidd11</i> compared to Cadenza | | | | | | |
| TraesCS1A02G255100 | Cad.NT-idd.NT | 6.46E-03 | -0.81 | 1.75 | up-regulated | GID1-A |
| TraesCS1B02G265900 | Cad.NT-idd.NT | 3.77E-05 | -0.92 | 1.89 | up-regulated | GID1-B |
| TraesCS1D02G254500 | Cad.NT-idd.NT | 1.51E-04 | -0.92 | 1.89 | up-regulated | GID1-D |
| TraesCS3A02G122600 | Cad.NT-idd.NT | 7.29E-03 | -1.58 | 2.98 | up-regulated | GA3ox2-A |
| TraesCS3B02G141800 | Cad.NT-idd.NT | 1.86E-03 | -0.73 | 1.66 | up-regulated | GA3ox2-B |
| TraesCS3D02G124500 | Cad.NT-idd.NT | 1.63E-04 | -1.25 | 2.39 | up-regulated | GA3ox2-D |
| TraesCS5B02G560300 | Cad.NT-idd.NT | 1.84E-03 | -2.22 | 4.67 | up-regulated | GA20ox1-B |
| Up- or down-regulated in <i>Rht-D1b</i> compared to Cadenza | | | | | | |
| TraesCS2D02G146300 | Cad.NT-Rht.NT | 5.37E-03 | -0.68 | 1.60 | up-regulated | GID1-A |
| TraesCS1B02G265900 | Cad.NT-Rht.NT | 1.26E-03 | -0.72 | 1.65 | up-regulated | GID1-B |
| TraesCS1D02G254500 | Cad.NT-Rht.NT | 1.38E-03 | -0.78 | 1.72 | up-regulated | GID1-D |
| TraesCS4A02G319100 | Cad.NT-Rht.NT | 9.48E-03 | -2.04 | 4.12 | up-regulated | GA20ox1-A |
| Up- or down-regulated in <i>Rht-D1b</i> compared to <i>Taidd11</i> | | | | | | |
| TraesCS4D02G040400 | idd.NT-Rht.NT | 1.70E-09 | -0.98 | 1.98 | up-regulated | Rht-D1 |

More DE genes were found between the same contrast groups (e.g. Cad.NT-idd.NT vs Cad.GA-idd.GA) after GA treatment than without, which was caused by the effect of GA₃ on transcription in Cadenza. When no treatment was applied, GA biosynthetic genes *GA3ox2-A*, *GA3ox2-B*, *GA3ox2-D* and *GA20ox1-B*, as well as the three homoeologues of *GID1* gene were up-regulated in the *Taidd11* mutant compared to Cadenza. In response to GA treatment, the set of up-regulated genes in *Taidd11* mutant relatively to Cadenza remained almost unchanged; instead of *GA20ox1-B*, *GA20ox2-B* was differentially expressed. In Cadenza, GA treatment elicited up-regulation of three homoeologues of *Rht-1* and *GA2ox10* genes, as well as *GA2ox3-A*, *GA2ox3-D* and *GA2ox7-D* genes. In control samples (no GA₃), DE genes that were up-regulated in *Rht-D1b* when compared to Cadenza were the three homoeologues of *GID1*, and *GA20ox1-A*. After application of GA₃, several *GA2ox* genes (*GA2ox10-A*, *GA2ox10-B*, *GA2ox10-D*, *GA2ox3-A* and *GA2ox3-D*) were up-regulated and *GA3ox2-B*, *GA3ox2-D* and three homoeologues of *GID1*

were down-regulated in Cadenza, whereas no DE genes were identified in *Rht-D1b*. The only GA-related DE gene between *Taidd11* and *Rht-D1b* was *Rht-D1*, which was up-regulated in the *Rht-D1b* mutant regardless if the treatment was applied or not. GA application also resulted in higher levels of *GA3ox2-B* in *Taidd11* compared to *Rht-D1b*.

In summary these results show that both *Taidd11* and *Rht-D1b* mutants are completely GA-insensitive, and that at the transcriptional level, the two mutants are more similar to one another than they are to Cadenza. The effect of GA on Cadenza was activation of genes that are known to negatively regulate GA signalling, *Rht1* and a few different *GA2ox* genes, and is consistent with previously reported observations (Cheng *et al.*, 2015; Ribeiro *et al.*, 2012; Thomas *et al.*, 1999). The genes up-regulated as a result of *TaIDD11* gene knockout were those encoding the two types of GA oxidases known to catalyse essential reactions in bioactive GA biosynthesis, *GA20ox* and *GA3ox*, and the GA receptor *GID1*. They are all part of a negative GA-feedback regulation (Figure 4.15). A similar set of GA homeostasis genes were up-regulated in *Rht-D1b*. Even though the genes were not classified as differentially expressed, some *GA2ox* genes were downregulated in the mutants (Figure 4.16 C, Supplementary Tables 4.3 and 4.4). The settings applied when analysing the RNA-Seq results were quite stringent (adjusted p-value < 0.01 and $L_2FC \geq 0$) and the fact that a gene was not classified as a DE gene, does not necessarily mean that its expression was not up- or down-regulated. These results suggest that *TaIDD11* regulates the same steps of GAs biosynthesis and signalling as *RHT-1* and is involved in controlling the feedback regulation. However, its function seems to be suppression of feedback regulation, which is opposite to the role of *RHT-1*.

4.3.3.10 *TaAMY1* expression levels

Evaluating *TaAMY1* expression levels in the aleurones treated with GAs is a convenient method of determining GA-responsiveness. *TaIDD11* was identified as an RHT-1 interacting partner, therefore, it was hypothesized that *TaIDD11* may be involved in controlling GA-mediated aleurone responses, including regulating the expression level of the *TaAMY1* gene. This was assessed by analysing expression of *TaAMY1* genes in the *Taidd11* mutant.

Four genotypes were compared in the experiment: Cadenza, NS, *Taidd11*, and the severe GA-insensitive mutant, *Rht-B1c*, in which GA-mediated induction of α -amylase activity in the aleurone is reduced (Van De Velde *et al.*, 2021). The qRT-PCR reactions to measure *TaAMY1* transcript abundance were set up and carried out as described in Section 4.2.4 of this Chapter, and Chapter 2, Section 2.1.2. The results were analysed using the LinRegPCR software (Heart Failure Research Centre, Netherlands) and the normalised expression was calculated relative to the expression of two reference genes: *Ta2526* (*TraesCS3A02G186600*, *TraesCS3B02G216100*, *TraesCS3D02G190500*) and *Ta2643* (*TraesCS4A02G147200*, *TraesCS4B02G166200*, *TraesCS4D02G160800*) (reference genes recommended by Dr Alison Huttly, Rothamsted Research). The primers used in the study (Supplementary Table 4.1) share 100% identity with four *TaAMY1* genes in wheat (*TraesCS6A02G334100*, *TraesCS6A02G319300*, *TraesCS6A02G334200* and *TraesCS6B02G364800*), and hence are expected to amplify all four genes.

The expression of *TaAMY1* in Cadenza, NS, *Taidd11* and *Rht-B1c* lines under no treatment at time 0 (T0) and after 48 hours of incubation (48h, -GA₃), as well as in response to the applied GA₃ 48 hours after application (48h, +GA₃) is presented in Table 4.17 and Figure 4.17. A General ANOVA with crossed treatment was performed to statistically evaluate the results.

Table 4. 17 Mean expression of *TaAMY1* gene \pm SE and the ANOVA output data. The expression was assessed at time zero (T0) and after 48 hours of incubation with and without applied GAs (48h, -GA and 48h, +GA, respectively) in four analysed genotypes. The significant values (compared to Cadenza) are highlighted in bold.

| | T0 | 48h, -GA ₃ | 48h, +GA ₃ |
|----------------------|----------------------------|-----------------------|--|
| Cadenza | 0.27 \pm 0.12 | 0.08 \pm 0.04 | 542 \pm 165 |
| NS | 0.57 \pm 0.46 | 0.14 \pm 0.05 | 613 \pm 133 |
| <i>Taidd11</i> | 0.39 \pm 0.14 | 0.09 \pm 0.03 | 427 \pm 167 |
| <i>Rht-B1c</i> | 0.93 \pm 0.57 | 0.06 \pm 0.03 | 163 \pm 74.5 |
| P-value (d.f.=35) | Genotype = 0.142 | | |
| | Treatment < 0.001 | | |
| | Genotype*Treatment = 0.106 | | |
| S.E.D. | Genotype*Treatment = 114 | | |
| L.S.D. at 5% | Genotype = 136 | | |
| | Treatment = 118 | | |
| | Genotype*Treatment = 236 | | |

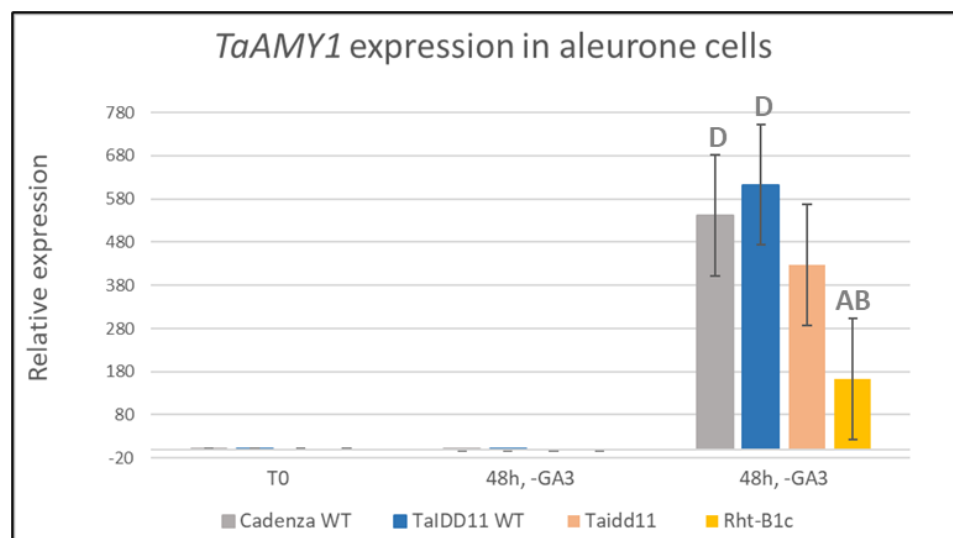


Figure 4. 17 *TaAMY1* relative expression levels in embryoless aleurones of Cadenza, NS, *Taidd11* and *Rht-B1c*. The expression was measured at time zero (T0), and at 48 hours of incubation with and without 10 μ M GA₃ (48h, -GA and 48h, +GA, respectively). The expression was averaged across three biological replicates. Error bars are \pm S.E.D.s reported in ANOVA. The letters over the error bars indicate 'significantly different from' ($P < 0.001$): A = Cadenza, B = NS, D = *Rht-D1b*.

The levels of *TaAMY1* expression at T0 and after 48 hours with no applied GA₃ were close to zero, and no difference in expression between genotypes were recorded. A significant increase in *TaAMY1* expression in all genotypes was observed 48 hours after GA₃ treatment ($P < 0.001$; L.S.D. = 118). The effect of the genotype alone was not significant ($P = 0.142$; L.S.D. = 136). Combined effect of genotype and treatment was also not statistically significant ($P = 0.106$; L.S.D. at 5% = 236), however, *Rht-B1c* mutant showed significantly lower expression of *TaAMY1* compared with the Cadenza and NS, but not compared with *Taidd11*.

These results suggest that TaIDD11 does not take part in regulating the GA-response in the aleurone, however, a more comprehensive study using a range of GA concentrations and timepoints measuring α -amylase enzyme activity would need to be performed to establish conclusively whether this is the case.

4.4 Discussion

The objective of the work presented in this Chapter was to generate the *Taidd11* knockout mutant in hexaploid wheat and assess the phenotype of the mutant, with a view to understanding the role of the *TaIDD11* gene in controlling GA-responsive growth and development. *TaIDD11* was identified as an interacting partner of RHT-1 in the Y2H screen, screening the cDNA library prepared from the aleurone of wheat. Therefore, it was initially hypothesized that *TaIDD11* might have a role in controlling GA-responses in the aleurone. However, the analysis of *TaIDD11* expression profiles revealed that the gene is expressed relatively uniformly across various wheat tissue types and throughout development, indicating that *TaIDD11* might have a more general role in regulating GA responses. In early generations (F₁) it was noticed that the *Taidd11* triple mutant displayed reduced elongation growth; even at the seedling stage reduced leaf sheath and leaf blade elongation were observed. A reduced stature, reminiscent of the semidwarf *Rht-B1b* or *Rht-D1b* mutants, was also observed at maturity. These exciting observations meant a shift in focus from the grain to studying effects on the overall architecture of the plant.

The *Taidd11* mutant has significantly reduced stature when compared to the WT, producing shorter stems and smaller leaves. In addition to having a similar reduction in stature to the GA-insensitive *Rht-1* mutants, *Taidd11* also displayed similar perturbations in the GA signalling pathway. It accumulated bioactive GAs through enhanced expression of genes known to be involved in the GA-feedback pathway including *GA3ox*, *GA20ox* and *GID1B*. Moreover, the *Taidd11* mutant was shown to display a striking GA-insensitive phenotype during seedling growth. This potentially explains the reduced height phenotype of the mutant and accumulation of bioactive GA₁. These results indicate that *TaIDD11* is a novel component of the GA signalling pathway regulating elongation growth and GA homeostasis in wheat.

4.4.1 Proposed functional domains in IDD proteins and severity of the *Taidd11* mutant

The *Taidd11* triple mutant was generated using TILLING. One of the main constraints of this approach is the availability of mutations that will result in a non-functional protein. When generating loss-of-function lines, the most desirable mutations are nonsense mutations that result in premature termination of translation and a truncated protein product. Nonsense mutations were identified in *TaIDD-A11* and *TaIDD-D11*; however, the position of the mutation is also an important factor when generating the loss-of-function. Ideally, the position of the nonsense mutation would be such that the resulting protein lacks an essential functional domain or domains. The conserved domains in IDD proteins were elucidated by studying protein sequences of IDD family members in Arabidopsis, rice and maize, and thus far three domains were identified: INDETERMINATE (IDD) domain, which is a DNA-binding domain, and M/V/L/ISATALLQKAA and Q/R/LDFLG domains, which are the domains responsible for protein-protein interactions (Colasanti *et al.*, 2006). The Q/R/LDFLG domain is highly conserved exclusively among IDD proteins, but some of the IDDs in Arabidopsis and rice do not contain this sequence; some lack the M/V/L/ISATALLQKAA domain. The clearly divergent subgroup in Arabidopsis (*AtIDD14*, *AtIDD15* and *AtIDD16*), rice (*OdIDD12*, *OsIDD13* and *OsIDD14*) and maize (*ZmIDD14*, *ZmIDD15* and *ZmIDD16*) lack both domains which may indicate different and distinct function of these IDDs (Colasanti *et al.*, 2006). The M/V/L/ISATALLQKAA and Q/R/LDFLG domains were found to be sufficient for interaction with DELLA protein (Yoshida & Ueguchi-Tanaka, 2014). Yoshida and colleagues found that both full-length and truncated *AtIDD3* proteins containing MSATALLQKAA and LDFLG domains, or the LDFLG domain on its own interact with RGA, whereas the truncated *AtIDD3* containing only the DNA-binding domain does not. Another study showed that the MSATALLQKAA domain is essential for DELLA binding and LDFLG significantly strengthens the binding activity (Fukazawa *et al.*, 2014). This is consistent with our findings, as the three *TaIDD11* homoeologues identified as

RHT-D1A partners in Y2H screen were fragments encoding the last exon, which encodes both domains (see Chapter 3, Section 3.3.2, Figure 3.5). Another conserved domain that seems to be specific to the clade of IDD proteins in which *TaIDD11* was identified is the EAR domain, through which GAF1 was shown to regulate GA homeostasis, using TPR4 as corepressor (Fukazawa *et al.*, 2014).

Most functional studies on IDD proteins come from Arabidopsis. The identified *TaIDD11* gene has no orthologues in Arabidopsis; hence no prediction of its function could be assumed. According to the Ensemble Plant website [Accessed on 14th November 2020] there are orthologous genes present in other crop grasses: barley (*Hordeum vulgare* variety Golden Promise, *HORVU.MOREX.r2.2HG0108280.1*), maize (*Zea mays*, *Zm00001d006682* and *Zm00001d021932*) and rice (*Oryza sativa* Japonica Group, *OsIDD5*, *Os07t0581366*). Phylogenetic studies by Huang *et al.* (2018) reported that *OsIDD5*, along with *OsIDD1*, cluster with ENY and GAF1, which reinforces our results. Another study reported a close phylogenetic relationship between *OsIDD5* and two maize proteins: *ZmIDD8* (GRMZM2G022213) and *ZmIDD10* (GRMZM2G058197), which are *Zm00001d006682* and *Zm00001d021932*, respectively.

Figure 4.18 A shows alignment of protein sequences of all transcript variants of three *TaIDD11* homoeologues in wheat and its orthologues in barley, maize and rice, and the two most structurally similar proteins in Arabidopsis, ENY and GAF1. The position of the EMS mutation used to generate the mutant in each homoeologue is also annotated. The conserved domains of IDD proteins, as well as EAR motif are present in all the presented proteins except for *TraesCS2D02G199300.1* and *Zm00001d006682_T002* which lack the IDD domain, and *Zm00001d021932_T002* and *Zm00001d021932_T003* which lack the MSATALLQKAT and LDFLG domains, respectively (Figure 4.18 A).

A

Identity

1. TraesCS4B02G230800
2. TraesCS4A02G074700
3. TraesCS4D02G232000
4. TraesCS5B02G232200
5. TraesCS5A02G233700
6. TraesCS5D02G240600
7. TraesCS4B02G296200
8. TraesCS4A02G008900
9. TraesCS4D02G294900
10. TraesCS2D02G287500
11. TraesCS2A02G289500
12. TraesCS2B02G306100
13. TraesCS3B02G497200
14. TraesCS3D02G449900
15. TraesCS5D02G364900
16. TraesCS5A02G356100
17. TraesCS5B02G358600
18. TraesCS2B02G421100
19. TraesCS2A02G403200
20. TraesCS2D02G400300
21. TraesCS6A02G254500
22. TraesCS6D02G235800
23. TraesCS6B02G271000
24. TraesCS2B02G218900
25. TraesCS2A02G188400
26. TraesCS2D02G199300
27. TraesCS6B02G154000
28. TraesCS6A02G126000
29. TraesCS6D02G116300
30. TraesCS3A02G105100
31. TraesCS3B02G123600
32. TraesCS3D02G107300
33. TraesCS3A02G205800
34. TraesCS3B02G237700
35. TraesCS3D02G209800
36. TraesCS3D02G171300
37. TraesCS3A02G170700
38. TraesCS3B02G195900
39. TraesCS4B02G262400
40. TraesCS4D02G262500
41. TraesCS4A02G041400

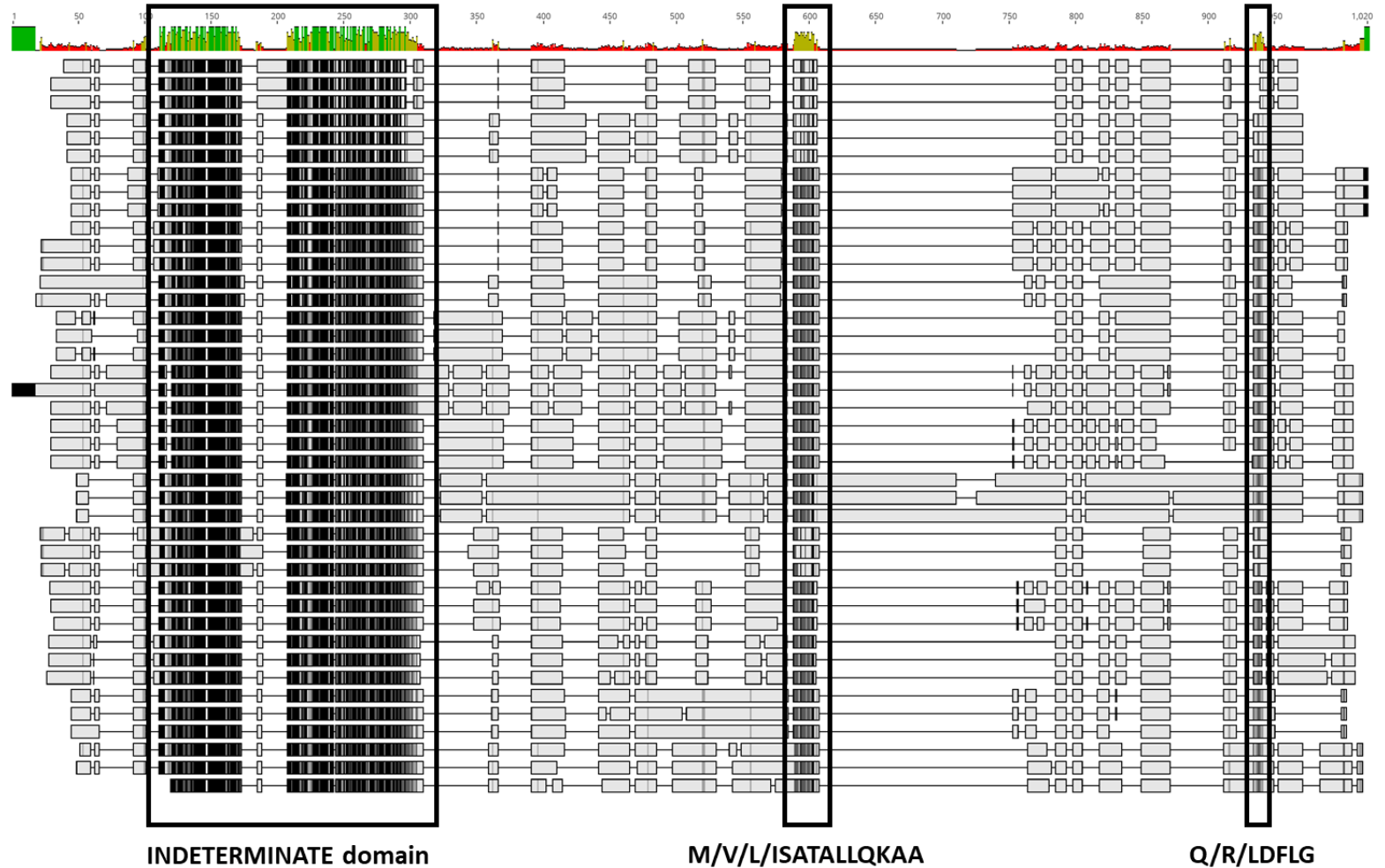


Figure 4. 19 Conserved domains in wheat IDD proteins. MUSCLE Alignment of all IDD proteins identified in wheat. IWGSC wheat proteome database (Ensemble Plant) was searched for IDD proteins using BLAST function. Protein sequences of all family members of IDD family in Arabidopsis and rice were used to identify most similar proteins in wheat, yielding 41 separate sequences encoding 14 distinct genes. Amino acids are highlighted based on similarity, the darker the colour, the more sequences share the same amino acid. Known functional domains are boxed and annotated. Boxed in red are the three homoeologues of TaIDD11 gene. B. INDETERMINATE domain in wheat IDD proteins. Marked with asterisks are the conserved amino acids of the zinc finger domains. C. M/V/L/ISATALLQKAA domain. D. Q/R/LDFLG domain. Some of the proteins do not contain all conserved domains. E. EAR motif (LxLxL type) is only present in TaIDD11 and TaIDD12 proteins in wheat (boxed in red; sequence of EAR motif is based on Fukazawa et al. (2014) studies and is boxed in black in TaIDD11; in TaIDD12, only the LxLxL motif is boxed).

The EAR motif is present in all orthologues except for Zm00001d021932_T002 and Zm00001d021932_T003 (Figure 4.18 B). All sequences of IDD proteins identified in wheat were searched for the presence of conserved domains and motifs, characteristic for IDD transcription factors. The only functional domain that was present in all identified IDD proteins was the INDETERMINATE domain (Figure 4.19 A, B), which is well conserved between the proteins. Two IDD proteins (TraesCS4A02G074700, TraesCS4B02G230800, TraesCS4D02G232000 and TraesCS5A02G233700, TraesCS5B02G232200, TraesCS5D02G240600) lacked M/V/L/ISATALLQKAA and Q/R/LDFLG domains, and these were found to belong to one clade with Arabidopsis IDD14, IDD15 and IDD16 and rice IDD12, IDD13 and IDD14 (Chapter 3, Figure 3.10), thus they may have a distinct function among the IDD family (Colasanti *et al.*, 2006). Interestingly, only two IDD proteins, TaIDD11 and TaIDD12 contain the EAR motif (Figure 4.19 E). This suggests that they could have a dual mode of regulating gene expression in a complex with a coactivator and corepressor (Fukazawa *et al.*, 2014).

The nonsense mutations in homoeologues A and D are positioned respectively 44 and 74 amino acids downstream of the ISATALLQKAA domain and therefore the TaIDD-A11 and TaIDD-D11 proteins lack both the EAR motif and LDFLG domain. As mentioned, lack of the LDFLG domain significantly reduces coactivator (DELLA) binding activity, and the EAR motif is essential for repressor (TPR4) binding. Thus, it is likely that the functionality of the proteins lacking these domains would be significantly reduced. The splice site mutation used to generate the mutant *TaIDD-B11* gene resulted in a frameshift and premature translation termination. The resultant predicted protein has 67 amino acids and only the first 30 belong to TaIDD-B11. The mutated version of the protein lacks all three functional domains and is therefore expected to be non-functional. It is therefore likely that in the *Taidd11* triple mutant, the activity of the TaIDD11 protein is significantly reduced if not completely abolished.

4.4.2 *Taidd11* displays a dwarf phenotype typical for GA mutants

The phenotype of the *Taidd11* mutant was assessed by comparison with the tall controls (cv. Cadenza and the NS line) and the GA insensitive semi-dwarf *Rht-D1b* mutant (Peng *et al.*, 1999). Cadenza shows the typical GA response of the variety as it carries no mutations affecting GA signalling. Another line expected to show a WT response was the NS line that segregated during backcrossing of the triple *Taidd11* mutant and contained only WT alleles (AABBDD) at the *TaIDD11* loci, along with a proportion of the same background mutations. As both the mutant and the NS originate from the same backcrossed plant, it is assumed that the observed phenotypic differences between the two lines are caused by the mutation in the gene of interest (Parry *et al.*, 2009; Slade *et al.*, 2012).

The striking difference in phenotype of the *Taidd11* mutant when compared to the WT Cadenza is a reduction in plant height (Figure 4.8 A). Detailed measurements of the stems revealed that knocking out *TaIDD11* genes results in 21% reduction in stem length compared to Cadenza (54.4 cm vs 68.6 cm). In this study the *Rht-D1b* allele resulted in a 26% decrease in stem length (50.8 cm vs 68.6 cm), which is in line with previous reports demonstrating about a 20% height reduction (Borrell *et al.*, 1991; Flintham *et al.*, 1997). In both mutants, the reduced height was due to the cumulative effects of individual internode length reductions. Both mutants showed reduced lengths of all internodes (peduncle, internode 2, 3 and 4) when compared to the WT; moreover, significant differences between internodes 2, 3 and 4, but not the peduncle were observed between the mutants. These findings demonstrate that *TaIDD11* is involved in regulating stem elongation and the effect of knocking it out is less severe than that of *Rht-D1b* allele.

Another noticeable difference in *Taidd11* physiology, that could be observed both at the young seedling and anthesis stage was reduced leaf elongation. When conducting GA dose response assays the length of L1 of a ten-day old seedling was measured (Table 4.13), and at anthesis, flag leaf area was assessed (Table 4.7). Both the length of L1 of the seedling and flag leaf area

were significantly reduced in *Taidd11* compared to all control genotypes. Reduced leaf size, including that of the flag leaf in *Rht-1* dwarfing alleles were reported previously, and were linked to reduced cell extensibility rather than reduced cell numbers (Keyes *et al.*, 1989; Miralles *et al.*, 1998). In this study, L1 of *Taidd11* seedling was 32% shorter than that of Cadenza, while *Rht-D1b* seedling displayed a 20% length decrease compared to Cadenza. At anthesis, the flag leaf of *Rht-D1b* showed a 11% reduction in surface area compared to Cadenza, and this difference was due to reduced leaf width rather than length. The effect of dwarfing *Rht-1* alleles on flag leaf characteristics reported in previous studies suggests that it varies between the cultivars and is environment-dependent (Jobson *et al.*, 2019; Li *et al.*, 2006; Miralles *et al.*, 1998). No effect of single *Rht-B1b* or double *Rht-B1b Rht-D1b* alleles on flag leaf length was found in wheat cv. Maringa (Miralles *et al.*, 1998). In three separate field trials run in different years, *Rht-B1b* was found to cause a slight increase in flag leaf area compared with *Rht-B1a* in cv. Maris Huntsman, but only in one year, whereas *Rht-D1b* flag leaf area was slightly smaller than the tall line in one of the trials (Li *et al.*, 2006). On the other hand, in another study, the progeny of cv. Hi-Line and Fortuna, carrying the *Rht-B1b* allele, showed 14% decrease in flag leaf length and 12% decrease in flag leaf width relative to *Rht-B1a* (Jobson *et al.*, 2019). The flag leaf of *Taidd11* was reduced by 21% compared to Cadenza, and the reduction was caused by both decreased length and width. These results show that both at early seedling stage and at anthesis, *Taidd11* produces significantly smaller leaves than Cadenza and *Rht-D1b*. *TaIDD11* is therefore involved in regulation of leaf size.

Taidd11 was also the only genotype that showed slightly delayed heading (by 2.2 days with L.S.D. at 5% = 2 days), indicating possible involvement in this GA-regulated process. IDD proteins in cereals have been identified to be involved in regulating flowering time (Colasanti *et al.*, 2006; Matsubara *et al.*, 2008) and the *gaf1 idd1* double mutant in *Arabidopsis* displays slightly delayed flowering, whereas the GAF1 overexpressor flowers earlier (Fukazawa *et al.*, 2014). *Rht-*

D1b did not influence flowering time which is in line with previous findings (Langer *et al.*, 2014).

No effect on tillering was found in any of the genotypes despite increased tillering being previously reported for *Rht-B1b* and *Rht-D1b* (Kertesz *et al.*, 1991; Lanning *et al.*, 2012). *Rht-D1b* produced slightly longer ears (by 8.0 mm) and more spikelets per ear (1.4), but this did not translate to increased seed number, which reinforces previous findings (Borrell *et al.*, 1991). *Rht-D1b* seeds were, however, significantly lighter (-7.3 mg) and smaller (-1.84 mm²), and the reduced area was a result of reduction in both seed length and width. Production of smaller and lighter seeds was previously observed for *Rht-B1b* and *Rht-D1b* (Casebow *et al.*, 2016; Miralles *et al.*, 1998) and our results are in line with this. Ears of *Taidd11* did not differ in length from the WT but produced fewer spikelets (-0.8). Fertility of the *Taidd11* spikelets might have also been compromised as the mutant produced significantly fewer grains per ear (-14.5). However, the grain weight and size did not differ from the WT accessions.

There is some evidence for IDD transcription factors having a role in the regulation of stem elongation (Fukazawa *et al.*, 2014; Huang *et al.*, 2018; Lu *et al.*, 2020). The *gaf1 idd1* double mutant line in *Arabidopsis* displays a dwarfed phenotype and the *GAF1* overexpressor plants are much taller than the WT in *Arabidopsis* (Fukazawa *et al.*, 2014). Fukazawa *et al.* (2014) found that GAF1 regulates growth-related gene expression in complexes, either in GAF1-DELLA activating complex or GAF1-TPR repressor complex. GAF1 was found to bind to the DELLA SAW domain, which is necessary for the repression of GA responses, suggesting that GAF1 is involved in DELLA-mediated growth repression. A recent study by Lu *et al.* (2020) identified that SLR1-OsIDD2 complex indeed promotes expression of miR396, a miRNA which post-transcriptionally reduces the transcript levels of *GRF* genes. GRFs are transcription factors that regulate many plant developmental processes, including GA-regulated stem and leaf growth (reviewed in Liebsch & Palatnik, 2020). Both miR396OE (overexpression) and OsIDD2OE lines display 50%

height reduction due to decreased cell proliferation. OsmiR396OE lines also displayed a reduction in leaf size. Reduced stem length of the over-expressors is caused by post-transcriptional repression of *GRF* genes and subsequent downregulation of cell-cycle-regulating genes *cycOs1* and *cycOs2*. Conversely, the OsIDD2 RNAi lines show a *slr1*-like phenotype, and the expression of miR396 in these lines is inhibited (Lu *et al.*, 2020).

TaIDD11 transcription factor is structurally more similar to Arabidopsis GAF1 than to rice OsIDD2, which lacks the EAR motif for corepressor binding. TaIDD11 binds RHT-1, is one of the two IDD proteins in wheat that include the EAR motif, and the *Taidd11* phenotype (plant height, leaf size, heading date) is similar to that of the *gaf1 idd1* mutant. It is therefore tempting to hypothesize that TaIDD11, like GAF1, regulates gene expression utilising RHT-1 as a coactivator and another protein, possibly TPR, as a corepressor. However, further studies are needed to elucidate the mechanism of TaIDD11 action.

4.4.3 *Taidd11* is a GA-insensitive mutant that accumulates bioactive GA₁ through increased expression of *GA20ox* and *GA3ox*

The *Taidd11* triple mutant displays pleiotropic phenotypic differences compared to cv. Cadenza, even at the seedling stage (Figure 4.1 A). The reduced elongation of the leaf sheath and blade is characteristic of GA biosynthesis or signalling mutants (Ross, 1994), and led us to hypothesize that *TaIDD11* may be involved in GA signalling. Therefore, it was investigated whether the *Taidd11* mutations may render the plant insensitive to applied GA. To test this, GA dose response assays were conducted, and the response compared to two GA-sensitive lines (Cadenza and NS) and the GA-insensitive *Rht-D1b* mutant. The *Taidd11* mutant, like *Rht-D1b*, did not show significant elongation of either leaf sheath or L1 blade even at high GA₃ concentrations. Based on these results it was concluded that the *Taidd11* mutant is insensitive to applied GA. It also displayed a similar phenotype to the *Rht-D1b* mutant (Figure 4.13 A). It has previously been shown that *Rht-D1b* seedlings produce

shorter leaves and leaf sheaths than the wild type (Botwright *et al.*, 2001; Ellis *et al.*, 2004; Rebetzke & Richards, 1999), and the reduced length of the leaf and coleoptile is due to GA-insensitivity-related reduction in cell wall extensibility that results in decrease in the length of the leaf extension zone (Keyes *et al.*, 1990; Keyes *et al.*, 1989; Tonkinson *et al.*, 1995). The leaf sheath lengths were comparable between the mutants (Figure 14.3 B). Interestingly, *Taidd11* mutant L1 blade length was significantly shorter than that of *Rht-D1b* (Figure 4.13 C). The basis for this difference at this point, however, remains unknown. Detailed analysis of cell dimensions and cell number would reveal what causes the reduced length of the L1 leaf. A recently developed imaging approach called Laser Ablation Tomography (LAT) allows for quick and accurate screening of multiple samples and is easier and more precise than traditional sectioning and imaging methods. It could be employed to study the reduced growth of the *Taidd11* mutant.

Many GA-insensitive mutants in different plant species have been demonstrated to accumulate bioactive GAs (Appleford & Lenton, 1991; Fujioka *et al.*, 1988; Talon *et al.*, 1990). These mutants accumulate DELLA protein, which is not degraded in response to GA, leading to enhanced expression of feedback-regulated GA biosynthetic genes and reduced expression of bioactive GA-inactivating genes (Figure 4.15). Consequently, GA homeostasis is disrupted, and biosynthesis predominates. As the *Taidd11* displayed a GA-insensitive semi-dwarf phenotype, we analysed the GA levels in the leaf sheaths of the seedlings.

Typically, the lines containing gain-of-function *DELLA* alleles accumulate bioactive GA₁ and their immediate precursor GA₂₀, but have lower levels of GA₁₉ (Appleford & Lenton, 1991; Fujioka *et al.*, 1988). Conversely, the tall *della* mutant, *sln1*, accumulates GA₁₉ whereas levels of bioactive GA₁ are depleted (Crocker *et al.*, 1990). It was therefore concluded that in tall, GA-responsive lines GA₁₉ to GA₂₀ is a rate-limiting step in GA₁ biosynthesis, and that bioactive GA acts to down-regulate the activity of GA₁₉ oxidase. In the GA-insensitive lines however, the activity of this enzyme would be repressed less effectively,

thus the levels of GA₁₉ would decrease and more GA₁ would accumulate as a result. In our study the observed relative levels of GAs in WT accession Cadenza were GA₄₄ > GA₁₉ > GA₂₀ < GA₁ << GA₈ which is different to GA₁₉ >>> GA₂₀ ≈ GA₁ <<< GA₈ reported by Webb *et al.* (1998) or GA₁₉ >> GA₂₀ = GA₁ reported by Appleford and Lenton (1991) for the tall *Rht* lines, and indicate that the alterations in GA signalling affect the balance of GAs levels. The relative levels of GAs in the early 13-hydroxylation pathway in the analysed mutants were different from WT and were GA₄₄ ≈ GA₁₉ ≈ GA₂₀ << GA₁ ≈ GA₈, in *Rht-D1b* and GA₄₄ ≈ GA₁₉ ≈ GA₂₀ << GA₁ << GA₈ in *Taidd11*. The mutants showed a similar pattern of GAs levels, with the only difference being the ratio of GA₁ to GA₈ levels. This indicates that the mechanism of synthesis of the bioactive GA₁ might be under similar mode of regulation in both *Rht-D1b* and *Taidd11*, with differences at the inactivation steps.

Upregulation of GA biosynthetic genes in response to reduced GA signalling in the GA-signalling mutants is a likely cause for the increased levels of endogenous C₁₉-GAs (Nelson & Steber, 2016). Since GA₄₄ and GA₁₉ levels were significantly reduced, and GA₁ levels were significantly increased in *Taidd11* and *Rht-D1b*, it was hypothesized that *GA20ox* and *GA3ox* genes might be differentially expressed in the mutants., and the conducted RNA-seq experiment indeed revealed the differences in GA-homeostasis related gene expression between the GA-insensitive mutants and Cadenza.

GA metabolism and signal transduction genes found to be differentially expressed in this study were the signal promoting *GA3ox2*, *GA20ox1*, *GA20ox2*, and *GID1* and suppressing *GA2ox3*, *GA2ox7*, *GA2ox10* and *Rht-1*. All these genes were previously found to be highly expressed in wheat vegetative tissues (Pearce *et al.*, 2015). The differentially expressed *GA2ox* genes belong to class I of 2-oxidases which almost exclusively use C₁₉-GAs (GA₂₀, GA₁, GA₉, GA₄) as substrates, but in wheat were found to have broader substrate specificities, as *GA2ox3* and *GA2ox10* also converted the C₂₀-GA GA₁₂ to GA₁₁₀, although less efficiently (Pearce *et al.*, 2015). Transcript levels of all *GA2ox* and *Rht-1* genes were lower in the mutants in comparison to Cadenza, except *Rht-*

D1, whose transcript levels were significantly higher in the *Rht-D1b* mutant. The basis for this remains unknown, although one possible explanation is that the mutation in *Rht-D1b* affects the translation efficiency so the transcript turnover may be negatively affected. The slightly higher levels of *GA2ox* transcripts in Cadenza may explain the relatively high level of GA_8 compared with GA_1 in this genotype. However, the difference in GA_8/GA_1 ratio between the mutants suggests a difference in GA inactivation regulation although no difference in *GA2ox* gene expression was observed between the mutants. This indicates that *GA2ox* enzymes may be regulated at the post-transcriptional level.

Analysis of gene expression in response to applied GA revealed that both *Rht-D1b* and *Taidd11* are completely GA-insensitive (Figure 4.16 A), while in Cadenza, GA_3 application results in upregulation of 120 genes. Among these genes were a few different *GA2ox* genes and the three homoeologues of the *Rht-1* gene, which all negatively affect GA levels and signalling. The genes involved in promoting biosynthesis of bioactive GAs, although not identified as DE genes, were slightly downregulated in GA-treated Cadenza (Figure 4.15 C). These are typical GA-induced responses in WT accessions (Cheng *et al.*, 2015; Ribeiro *et al.*, 2012; Zentella *et al.*, 2007). Both *Taidd11* and *Rht-D1b* mutants showed similar expression of genes involved in GA homeostasis, which indicates that *RHT-1* and *TaIDD11* may be involved in the same regulatory pathway but have opposite effects. In both mutants, *GID1*, *GA3ox2* and *GA20ox1* transcript levels were higher compared to Cadenza. Enhanced expression of *GA20ox* in the mutants would explain the differences in GA_{44} and GA_{19} levels between the mutants and Cadenza, as they are substrates for *GA20ox* and will be depleted with increased activity of the enzyme. The difference in bioactive GA_1 in turn can be explained by increased expression of *GA3ox* genes and resulting higher levels of *GA3ox* enzyme.

Recently, *GA3ox* and *GA20ox* genes were identified to be up-regulated in a series of semi-dominant dwarf DELLA mutants in barley (Jung *et al.*, 2020), which shows that enhanced expression of genes promoting GA biosynthesis is

typical for DELLA gain-of-function mutants. Moreover, ENY, one of the two Arabidopsis IDD1s that clustered with TaIDD11, was shown to be involved in regulation of GA homeostasis, as in *ENY* overexpression lines *GA3ox1*, *GA20ox2*, *SCL3* and *GID1b* genes were downregulated (Feurtado *et al.*, 2011). Although the mechanism of ENY-DELLA-mediated gene expression regulation was not elucidated, it was proposed that ENY has a repressive effect on DELLA and promotes GA-associated downstream signalling events, and the perceived increases in GA signalling trigger activation of feedback regulation. As mentioned previously, in Arabidopsis, GAF1 in complex with DELLA act as transcriptional activators of *GA20ox2*, *GA3ox1* and *GID1b* genes (Fukazawa *et al.*, 2014). The follow up study by Fukazawa *et al.* (2017) identified four GAF1-binding sites in the promoter of the *AtGA20ox2* promoter. Mutations in these sites abolished the negative feedback of *AtGA20ox2* in transgenic plants, suggesting that GAF1-DELLA complex is the main component of GA feedback regulation of *AtGA20ox2*. Since TaIDD11, GAF1 and ENY show high protein sequence homology and contain the same functional domains (Figure 4.18 A), and they all seem to be involved in GA-feedback regulation, it is tempting to hypothesize that TaIDD11 plays a similar role in regulating GA-feedback regulating gene expression in wheat as ENY and GAF1 in Arabidopsis. TaIDD11 shows similar effect on regulation of genes involved in GA homeostasis as ENY. On the other hand, *Taidd11* mutant shows similar characteristics to *gaf1 idd1* double mutant (i.e. effect on phenotype, GA-insensitivity). Therefore, more studies need to be performed to fully understand the role of TaIDD11 in regulation of GA signalling in wheat.

To conclude, in this study, we identified a novel component of GA signalling in wheat. TaIDD11 seems to be involved in many aspects of GA-regulated developmental responses, e.g. stem and leaf elongation, heading date and grain number and we propose that it acts by working in a complex with DELLA to regulate GA homeostasis.

Chapter 5: Generation of the *Taerf5 Taerf5a* mutant in wheat using CRISPR/Cas9 system

5.1 Introduction

Reverse genetics approaches have been widely used to elucidate the roles of genes in regulating crop development and physiology (Anai, 2016; Ben-Amar *et al.*, 2016). Until recently studying gene function in wheat posed challenges that in many cases could not be overcome. The development of genome editing techniques and the availability of the fully annotated wheat reference genome (International Wheat Genome Sequencing Consortium (IWGSC) *et al.*, 2018) made functional genetic studies in wheat more feasible and now being rapidly adopted (Borrill, 2019). The reverse genetics-based approach was adopted here to study the function of *TaERF5* gene in wheat. *TaERF5* has a close paralogue in wheat (named *TaERF5a*; Chapter 3, Section 3.3.3.1), and both genes, although not to the same extent, are expressed (Section 5.3.1). The sequence identity between the TaERF5 and TaERF5a proteins indicates a similar function. It was therefore necessary to knock out both *TaERF5* and *TaERF5a* genes. As both genes are encoded by each of the three wheat genomes, to generate the null mutant, six genes needed to be inactivated to investigate the function of the gene. The most suitable method to relatively easily and quickly generate knock outs in six genes is genome editing using the recently developed and perfected method CRISPR/Cas (clustered regularly interspaced palindromic repeat-associated protein nuclease). This approach is superior to RNAi, the method used to generate knock down lines, as RNAi rarely results in a complete suppression of transcripts (Smith *et al.*, 2017). Another method used routinely to generate knockout mutants in wheat, TILLING, would not be practical due to the number of crossing needed to generate backcrossed sextuple mutant.

CRISPR/Cas is an adaptive phage immunity system in archaea and bacteria that rely on DNA-RNA recognition and binding for sequence-specific nucleic acid cleavage and thus can be easily programmed to introduce double strand breaks (DSBs) at desired locations. Since its first application in plants (Li *et al.*, 2013; Nekrasov *et al.*, 2013; Shan *et al.*, 2013), CRISPR/Cas has been used as a genome editing method in a variety of crops (Zhang *et al.*, 2020). Owing to its capacity to introduce specific, targeted mutations, the method has the potential to have a major impact on agriculture.

5.1.1 CRISPR/Cas as a method of genome editing

Genome editing refers to the technologies that enable creating modifications in the genome, e.g. deletions, insertions, or substitutions (Zhang *et al.*, 2018). Until the discovery and development of CRISPR/Cas system, genome editing tools relied on engineered endonucleases, such as zinc finger nucleases (ZNFs) and transcription activator-like effector nucleases (TALENs). Both ZNFs and TALENs are composed of customised sequence-specific DNA-recognition domains fused to FokI DNA-cleavage domain, and therefore require complicated processes of protein design. Moreover, FokI requires dimerization to achieve its nucleolytic activity, thus ZNFs and TALENs must be engineered in pairs to generate double strand breaks (DSBs). Therefore, CRISPR/Cas system, thanks to its simplicity in target design, efficiency and possibility of target sites multiplexing, which is not achievable for neither ZFNs nor TALENs, has been a preferred method for genome editing in crops (Jaganathan *et al.*, 2018).

The CRISPR/Cas system consists of a Cas endonuclease and a small guide RNA (sgRNA) that directs the Cas protein to a specific genomic location. Each sgRNA contains variable 20 nucleotides at 5' end that are complementary to the targeted site. The ribonucleoprotein Cas-sgRNA complex recognizes all genomic locations that contain a protospacer adjacent motif (PAM) sequence and hence can be directed to any genomic location followed by a PAM domain. This requirement for a PAM domain somewhat limits the genomic locations

that can be targeted, however, alternative PAM sequences are also available (Kleinstiver *et al.*, 2015; Nishimasu *et al.*, 2018; Zetsche *et al.*, 2015) which largely expands the pool of putative target sites. Once at its target site, the Cas protein cleaves double-stranded DNA at a fixed position, usually between the third and fourth nucleotide upstream of PAM (Jinek *et al.*, 2012), resulting in the activation of the DSB repair machinery (Garneau *et al.*, 2010). The DSBs can be repaired through two mechanisms: non-homologous end joining (NHEJ) and the homology-directed repair (HDR) (Takata *et al.*, 1998). The error-prone NHEJ pathway is dominant in plants and results in insertions and/or deletions (INDELS) at the target sites, which may disrupt the targeted gene locus. In the HDR pathway, a donor template with homology to the targeted locus is supplied, and during the DNA repair, the specific mutations can be introduced. Due to its higher complexity, this pathway is less efficient.

The constantly expanding CRISPR toolbox comprises a choice of Cas proteins (Cas9, Cas12, Cas13) originating from various species and engineered for better expression (Zhang *et al.*, 2019), however, the most commonly used Cas protein is the *Streptococcus pyogenes* Cas9 (SpCas9). SpCas9 is a large multidomain and multifunctional DNA endonuclease which cleaves double-stranded DNA (dsDNA) through its two distinct nuclease domains: an HNH-like nuclease domain that cleaves the DNA strand complementary to the guide RNA sequence (target strand), and an RuvC-like nuclease domain responsible for cleaving the DNA strand opposite the complementary strand (nontarget strand). The PAM domain recognised by SpCas9 is NGG, thus the SpCas9-sgRNA ribonucleoprotein complex can target any DNA sequence of 5'-N20-NGG-3', where 'N' represents any nucleotide.

Originally, targeting more than one genomic location simultaneously was achieved by co-expressing Cas plasmid with vector, or vectors, containing stacked, customised cassettes, each with a promoter, sgRNA designed for singular target, and terminator (Li *et al.*, 2013; Ma *et al.*, 2015; Shan *et al.*, 2013; Zhou *et al.*, 2014). However, many limitations, i.e. delivery methods, vector capacity, and fewer putative targetable sites due to the requirement of

a specific nucleotide at the start of the Pol III-transcribed RNA, makes this approach inefficient. Recently developed technology allows for cloning multiple sgRNAs into one vector to produce a single polycistronic gene (PTG), whose expression is driven by a single promoter (Xie *et al.*, 2015). Xie *et al.*, (2015), engineered an endogenous RNA-processing system that allows for producing multiple sgRNAs from a single transcript. They used tRNA-sgRNA gene architecture for precise excision of transcripts *in vivo* by endogenous RNase P and RNase Z, which remove extra sequences at 5' and 3' end of the tRNA, respectively. The PTG consisted of tandem repeats of tRNA-sgRNA, and after transcription, the endogenous tRNA-processing RNases released the individual sgRNAs that would target Cas protein to the respective target sites for genome editing. Additionally, the system takes advantage of the fact that tRNA genes contain internal promoter elements that recruit the Pol III complex, and the abundance of the tRNA-processing system in the cell, which makes it very efficient. Moreover, due to a high conservation of the tRNA-processing mechanism across species, the system is applicable to virtually any organism.

5.1.2 CRISPR/Cas system has been successfully applied in wheat

To date, there have been many proof-of-concept studies reporting successful single and multiple homoeologues editing, and even editing multiple genes in a single transformation event (Kumar *et al.*, 2019).

Various methods of CRISPR/Cas delivery have been used for wheat transformation. Many studies report gene editions in wheat protoplast (Kim *et al.*, 2018; Shan *et al.*, 2014; Wang *et al.*, 2018; Wang *et al.*, 2014), whereas stable plant transformation is achieved either using biolistic methods (Liang *et al.*, 2017; Sánchez-León *et al.*, 2018; Zhang *et al.*, 2016; Zhang *et al.*, 2017) or *Agrobacterium tumefaciens* (Howells *et al.*, 2018; Upadhyay *et al.*, 2013; Zhang *et al.*, 2019). Particle bombardment of immature embryos or scutella have been a preferred method of wheat transformation due to its increased

efficiency, however, in recent years some progress in *Agrobacterium*-mediated transformation efficiency of wheat was reported (Ishida *et al.*, 2015; Richardson *et al.*, 2014), which makes it more promising delivery method for wheat genome editing in the future. Transformation efficiency can be further improved by using virus-based vectors to deliver genome-editing reagents to plant cells. Indeed, a 12-fold increase in gene targeting frequencies was observed using a deconstructed version of the wheat dwarf virus (WDV) compared to non-viral methods (Gil-Humanes *et al.*, 2017). An additional advantage of the virus-based vectors is lack of RNA integration in the plant genome, which makes such plants non-transgenic.

Most proof-of-concept CRISPR/Cas studies in wheat used single sgRNA to target single gene of interest, nevertheless the studies reporting editing a gene using two sgRNAs (Upadhyay *et al.*, 2013) and even sgRNA multiplexing to target multiple genes (Wang *et al.*, 2018) had also been conducted. The first published reports using CRISPR/Cas in wheat were studies silencing the *TaMLO* gene in wheat protoplasts (Shan *et al.*, 2013), and *TaPDS* and *TaINOX* genes in wheat plants (Upadhyay *et al.*, 2013). The method was applied in a separate study to induce mutations in a single *TaMLO* (A) homoeologue in wheat plants (Wang *et al.*, 2014). Since then stable, heritable INDELS in all three copies of targeted genes have been reported (Wang *et al.*, 2018; Zhang *et al.*, 2016; Zhang *et al.*, 2019; Zhang *et al.*, 2017). Zhang *et al.* (2016) was first to report all three homoeologues of a gene knocked out. Editing all copies of the *TaGASR7* gene resulted in increased TGW in both tested varieties Bobwhite and Kenong199, and the heritability of the edits was validated both by PCR and by characterisation of the phenotype of T2 plants. Resistance to powdery mildew was achieved by editing all copies of *TaEDR1* gene, and the transgenerational inheritance was validated by the lack of susceptibility to *Blumeria graminis* f. sp. *tritici* of the T2 plants (Zhang *et al.*, 2017). Zhang *et al.* (2019), in separate transformation events, targeted four grain-regulatory genes and were able to stably knock out all homoeologues of the *TaCKX2-1* gene. And finally the most ambitious study reported thus far, using target gene

multiplexing developed by Xie *et al.* (2015) to edit three distinct genes: *TaGW2*, *TaLpx-1*, and *TaMLO*, and successfully editing all three homoeologues of *TaGW2* gene (Wang *et al.*, 2018). Knocking out of *TaGW2* gene, which was previously shown to be negatively associated with TGW, grain area, grain width, and grain length, showed to affect all these characteristics and was heritable, which again was validated by phenotypic data.

The summarised examples illustrate that genome editing using CRISPR/Cas has already been applied to generate full gene knockout mutants in wheat. The advances of CRISPR/Cas technology are not limited to study gene function; the additive effect of the individual homoeologues on the phenotypic traits can be examined, or even the conserved motifs in genes promoters' sequences. Not surprisingly, considering the novelty of the method and bottlenecks of molecular biology in wheat, the majority of studies reported thus far are proof-of-concept studies. However, CRISPR/Cas technology is starting to be applied to study functional genetics and generate germplasm for better quality wheat. Studies reporting generation of low gluten wheat (Sánchez-León *et al.*, 2018) and low acrylamide wheat (Raffan, 2020) are most definitely a good start and will be followed with many more to come in the future.

5.1.3 Objectives

The following Chapter describes the approach adopted to generate null *Taerf5* *Taerf5a* mutant in wheat. The TaERF5 protein was identified to interact with RHT-1 to activate expression of reporter genes in Y2H studies (Chapter 3, Section 3.3.2) and to reconstitute fluorescent signal in BiFC studies in tobacco (Chapter 3, Section 3.3.4). These observations, together with suggested links to the process of GA signalling during germination (Chapter 3, Section 3.3.1.2) led us to believe that TaERF5 may be involved in GA response in the aleurone of wheat.

As described in Chapter 3 section 3.3.3.1, wheat genome encodes a close paralogue of *TaERF5* gene, *TaERF5a*, which shares around 87% sequence

similarity at gene, and 85% sequence similarity at protein level. The conserved domains in the proteins encoded by the homoeologues of two genes show 90 to 100% sequence homology, hence it may be hypothesized that the two genes have redundant functions in wheat. Therefore, generating the null mutant requires knocking out six copies, instead of three, and the most feasible approach was to use the CRISPR/Cas system. This Chapter describes the process from sgRNAs design, through cloning of the expression vector, to the analysis of the INDELS in T0, T1 and T2 populations. The system applied to generate the mutant takes advantage of gene multiplexing and the tRNA-processing system developed by Xie *et al.* (2015) to target all six copies using one construct, and to date is the first study reporting successful knocking out of six genes in wheat.

5.2 Material and methods

5.2.1 Generation of transgenic plants

pCRISPR-TaERF5 plasmid was supplied to the Rothamsted Research Cereal Transformation Group for stable wheat transformation. The transformation of immature wheat embryos (12 – 16 days post anthesis) was performed using the biolistic system PDS-1000/He particle delivery system (Bio-Rad Laboratories Ltd., UK) as described in (Sparks & Doherty, 2020). The *Streptococcus pyogenes* Cas9 (SpCas9) protein and Basta selection were encoded on two separate plasmids and were introduced by co-bombardment. The variant of SpCas9 that was used in this experiment (Appendix, Notes) was additionally codon-optimised for expression in wheat by Dr Alison Huttly (Rothamsted Research).

The Cereal Transformation Group transformed wheat cv. Cadenza embryos with pCRISPR-TaERF5 plasmid in two separate bombardments, designated B3781 and B3792. After regeneration and selection of the transgenic plantlets, which took six weeks, the plantlets with established shoot and root system were transferred to soil. Approximately two weeks after potting, leaf explants were taken for extraction of genomic DNA. The PCR analysis was carried out to ensure the presence of the PTG and Cas9 protein (for primers see Supplementary Table 5.1). The positive plants, along with extracted genomic DNA were supplied for further analysis.

5.2.2 Next-generation sequencing (NGS) results analysis

Next-generation sequencing (NGS) was performed on PCR fragment amplified from genomic DNA using either GENEWIZ Amplicon-EZ service (<https://www.genewiz.com/>) or in-house sequencing service (Dr Stephen Hanley, Rothamsted Research). GENEWIZ Amplicon-EZ service utilises Illumina 2x250 bp sequencing configuration and the results are supplied as two FASTQ files per sample (forward and reverse, respectively). In-house Single-read

sequencing Illumina service sequenced only in forward direction. The quality check for the raw data was performed, the reads trimmed to the quality of 20, paired and merged (where necessary), and mapped to the Cadenza genome using BBMap aligner (sourceforge.net/projects/bbmap/).

5.2.3 Genotyping of T0, T1 and T2 plants

Amplification of fragments encompassing all sgRNA sites in T0 plants was performed by PCR using primers listed in Supplementary Table 5.1 and Q5[®] High-Fidelity 2X Master Mix (New England Biolabs, Ipswich, Massachusetts, USA). Amplicons from selected T0 plants were genotyped by NGS using GENEWIZ Amplicon-EZ service. T1 plants were genotyped by NGS using Illumina single-read sequencing service provided by Rothamsted Research. T2 plants' amplicons were genotyped using KASP (*TaERF5* gene) and NGS using Illumina single-read sequencing service provided by Rothamsted Research.

5.3 Results

5.3.1 The expression of the *TaERF5* and *TaERF5a* genes is seed-specific

Studying the expression pattern of a gene provides possible clues to the developmental and tissue-specific roles that it performs. In polyploid species, such as wheat, it can also provide an indication of homoeologue specificity. It was established that the *TaERF5* gene has a close paralogue in wheat and the proteins encoded by the *TaERF5* and *TaERF5a* genes show high similarity. Therefore, the expression of the three homoeologues encoding *TaERF5* (*TraesCS2A02G417100*, *TraesCS2B02G436100*, *TraesCS2D02G414300*) and *TaERF5a* (*TraesCS2A02G417200*, *TraesCS2B02G436200*, *TraesCS2D02G414500*) genes was investigated. Expression data for the genes were obtained from existing data for another spring wheat variety, Chinese Spring, by searching the Wheat Expression Browser (www.wheat-expression.com; already described in Chapter 4, Section 4.3.1).

The expression data are presented on the graph in Figure 5.1. Both *TaERF5* and *TaERF5a* are expressed exclusively in the grain (samples 66 – 69) and predominantly at the ripening stage (sample 69). All homoeologues of two genes are expressed, with homoeologues B being the most highly expressed genes. Expression of *TaERF-B5* and *TaERF-D5* genes is 4.1- and 3.4-fold higher than the expression of *TaERF-B5a* and *TaERF-D5a*, respectively, whereas the expression of *TaERF-A5* is 22.9-fold higher than that of *TaERF-A5a*. At least 45% of genes in wheat were found to be expressed unequivocally from all three homoeoloci and when two homoeologues equally dominate total gene expression, A and D or B and D homoeologues dominance is much more common (Leach *et al.*, 2014). This appears to be the case as for *TaERF5* all three homoeologues contribute to the transcript levels, whereas for *TaERF5a*, *TaERF-B5a* and *TaERF-D5a* dominance is observed.

Gene expression

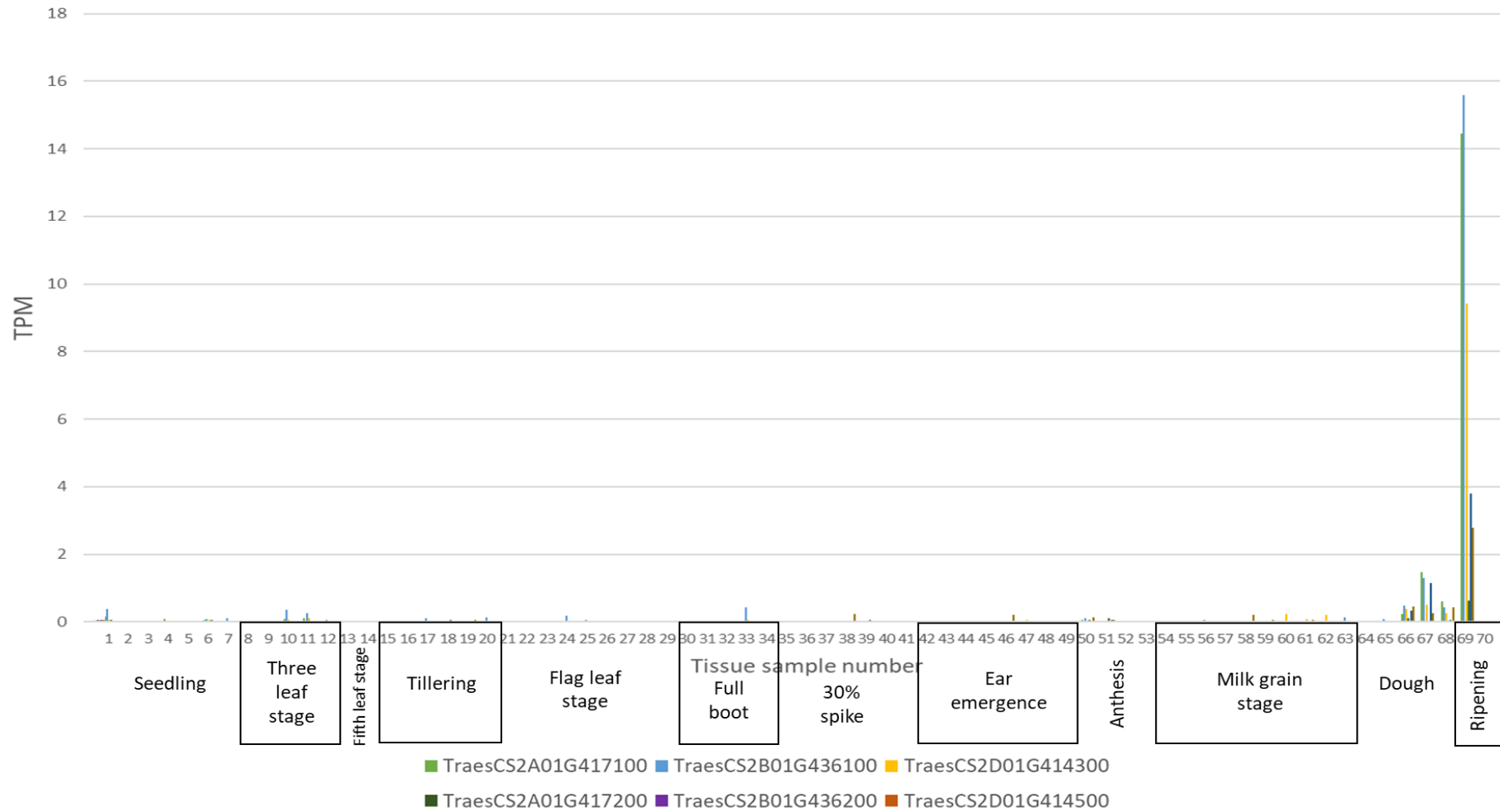


Figure 5. 1 Relative expression of the three homoeologues of TaERF5 gene and its close paralogue TaERF5a in wheat variety Chinese Spring. The expression is calculated in TPMs (transcripts per million). Data for 70 samples taken from various tissues at various developmental stages are presented. The developmental stages groups are: seedling (1-7), three leaf (8-12), fifth leaf (13-14), tillering (15-20), flag leaf (21-29), full boot (30-34), 30% spike (35-41), ear emergence (42-49), anthesis (50-53), milk grain (54-63), dough grain (64-68) and ripening (69-70) (refer to Appendix, Table 4 for full details). Data taken from Ramírez-González et al., 2018.

Table 5. 1 Expression of three homoeologues of TaERF5 gene and TaERF5a-A gene in various parts of the grain 10, 20 and 30 days post anthesis. Expression was measured in RPKMs (reads per kilobase per million). Data taken from Pfeifer et al., (2014). WE = whole endosperm, AL = aleurone layer, SE = starchy endosperm, TC = transfer cells, ALSE = aleurone contaminated with starchy endosperm.

| Gene | IWGSC RefSeq v1.0 | IWGSC | Expression in RPKM | | | | | | |
|-----------|--------------------|---------------------|--------------------|-------|-------|-------|-------|--------|-------|
| | | | WE10 | AL20 | SE20 | TC20 | WE20 | ALSE30 | SE30 |
| TaERF-A5 | TraesCS2A02G417100 | Traes_2AL_E5A9615E2 | 0.012 | 0.713 | 0.019 | 0.279 | 1.906 | 1.542 | 1.437 |
| TaERF-B5 | TraesCS2B02G436100 | Traes_2BL_859E9B1DA | 0.121 | 0.637 | 0.217 | 2.172 | 3.246 | 4.356 | 1.966 |
| TaERF-D5 | TraesCS2D02G414300 | Traes_2DL_81E326F1A | 0.000 | 0.480 | 0.000 | 0.148 | 0.466 | 0.218 | 0.103 |
| TaERF-A5a | TraesCS2A02G417200 | Traes_2AL_FC6DD1383 | 0.000 | 0.211 | 0.000 | 0.128 | 0.492 | 0.322 | 0.199 |

As the genes are expressed exclusively in the grain, the expression in the grain tissues were more closely investigated using publicly available RNAseq data. Expression data generated by Pfeifer *et al.*, (2014) was collected from wheat cv. Chinese spring during seed differentiation (10 and 20 DPA) and maturation (30 DPA) either from whole endosperm (WE) or from three layers of the endosperm: starchy endosperm (SE), aleurone layer (AL) and transfer cells (TC). They reported expression of 46,487 out of 85,173 high-confidence genes (IWGSC) during endosperm development. Expression of all three homoeologues of the *TaERF5* gene and only the A homoeologue of the *TaERF5a* gene was confirmed in this data. Based on the Pfeifer *et al.*, (2014) data (Table 5.1), it can be concluded that the expression of the genes increases with progressing development of the endosperm and is at its highest during maturation. A and B homoeologues contribute the majority of the *TaERF5* transcript and the levels of all four genes are highest in aleurone cells, both at 20 and 30 DPA, except for *TaERF-B5*, which is most highly expressed in transfer cells.

In summary, the expression of *TaERF5* and its close paralogue *TaERF5a* is seed-specific and is at its highest at later stages of seed development, i.e. maturation and ripening.

5.3.2 Selection of the gene target sites for generating sgRNAs

Target sites for the guide RNA constructs were designed by screening *TaERF5* and *TaERF5a* CDS gene sequences (cv. Cadenza) in Geneious (version 10.2.3, Biomatters Ltd, Auckland, New Zealand) to identify 20-nucleotide fragments followed by NGG Pam domain (N20-NGG), as well as using the CRISPOR site version 4.4, (Haeussler *et al.*, 2016). Searching for the off-target sites was performed using BLAST tool in Geneious, screening the Cadenza_EI_v1_arm-classified genome, available to download at the Earlham Institute Grassroots Data Repository (https://opendata.earlham.ac.uk/opendata/data/Triticum_aestivum/EI/v1/).

The approach was to target all genes at two or more positions using as few

sgRNAs as possible. It was therefore necessary to identify regions of the gene sequences that are identical to each other. To identify sgRNA target sites, the coding sequences of three homoeologues of *TaERF5* and *TaERF5a* genes were aligned and screened for 20 bp of identical sequence fragments directly followed by NGG (PAM domain). To produce non-functional transcription factors, target sites upstream of AP2/ERF DNA-binding domain (Figure 5.2 A, annotated in red) were prioritised, as out-of-frame INDELS would result in proteins lacking the DNA-binding domain and therefore unable to function properly.

Table 5. 2 Summary of the selected sgRNAs. Genes targeted by the sgRNA with nucleotide positions they target are listed along with cleavage efficiencies calculated using two different algorithms, out-of-frame prediction (all on the scale 0 to 100) and off-targets. CRISPOR website (Haeussler et al., 2016) was used to assess cleavage efficiency and out-of-frame outcome.

| Guide | Genes targeted | Nucleotides of the CDS spanned | Efficiency (Doench et al., 2016) | Efficiency (Moreno-Mateos et al., 2015) | Out-of-frame outcome | Off-targets |
|---------------|------------------|--------------------------------|----------------------------------|---|----------------------|-------------|
| sgRNA1 | <i>TaERF-A5</i> | 111 - 130 | 54 | 63 | 69 | NO |
| | <i>TaERF-B5</i> | 111 - 130 | 54 | 63 | 79 | |
| | <i>TaERF-D5</i> | 111 - 130 | 54 | 63 | 77 | |
| | <i>TaERF-A5a</i> | 108 - 127 | 54 | 63 | 72 | |
| sgRNA2 | <i>TaERF-A5a</i> | 243 - 262 | 60 | 54 | 60 | NO |
| | <i>TaERF-B5a</i> | 240 - 259 | 59 | 62 | 75 | |
| | <i>TaERF-D5a</i> | 240 - 259 | 59 | 67 | 80 | |
| sgRNA3 | <i>TaERF-A5</i> | 386 - 405 | 55 | 68 | 49 | NO |
| | <i>TaERF-B5</i> | 380 - 399 | 57 | 68 | 48 | |
| | <i>TaERF-D5</i> | 374 - 393 | 57 | 68 | 47 | |
| sgRNA4 | <i>TaERF-A5a</i> | 430 - 449 | 54 | 64 | 91 | NO |
| | <i>TaERF-B5a</i> | 427 - 446 | 54 | 64 | 94 | |
| | <i>TaERF-D5a</i> | 427 - 446 | 57 | 67 | 93 | |

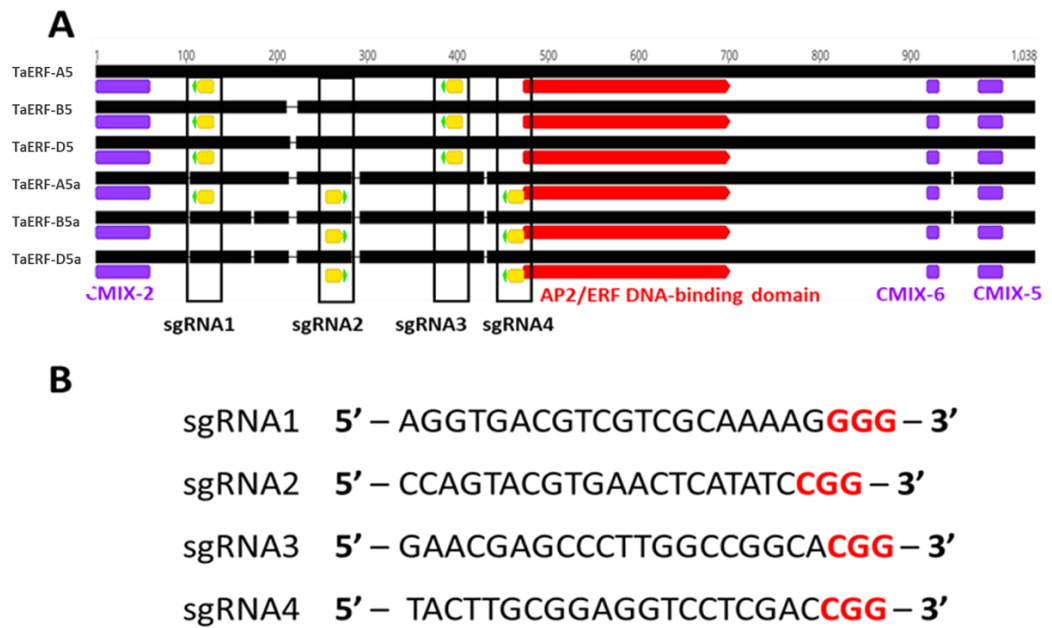


Figure 5. 2 Single guide RNA target sites (sgRNAs) for three homoeologues of *TaERF5* and *TaERF5a* genes. A. Alignment of the coding sequences of A, B and D homoeologues of *TaERF5* and *TaERF5a*. Annotations: red - DNA-binding domain; purple - CMIX-2 motif, which is a putative acidic region that might function as transcriptional activation domain, and CMIX-6 and CMIX-5, two putative MAP kinase phosphorylation sites; yellow – sgRNAs; green - PAM domains. B. Sequences of all sgRNAs chosen to edit the *TaERF5* genes, with PAM domain highlighted in red.

These selected 20 bp fragments were compared with the results returned for each gene individually by CRISPOR website (Haeussler *et al.*, 2016), and corresponding sgRNAs identified to assess the predicted cleavage efficiencies (Doench *et al.*, 2016; Moreno-Mateos *et al.*, 2015) and out-of-frame effect (Bae *et al.*, 2014). All selected sgRNAs (the 20 nucleotides) were screened for putative off-target sites using BLAST option in Geneious v10.2, using Cadenza_EI_v1_arm genomic as BLAST reference sequence, and no 100% identical off-target sites were found for any of the selected sgRNA. Finally, four sgRNAs were selected (Figure 5.2 B), that target all genes upstream of the DNA-binding domain (Figure 5.2 A). The sgRNAs target genes, nucleotide positions that they span along with cleavage efficiencies, out-of-frame generating potential (based on CRISPOR website results, Haeussler *et al.*, 2016) and off-targets are summarised in Table

5.2. In summary, four sgRNAs were selected to target six distinct genes. The predicted cleavage efficiency and out-of-frame outcome indicated that the selected sites had the potential to produce INDELS resulting in frameshifts in all *TaERF5* and *TaERF5a* genes.

5.3.3 Generation of the CRISPR vector used for genome editing of the *TaERF5* and *TaERF5a* genes

The cloning strategy was based on the method described in Xie *et al.* (2015) (Figure 5.3 A), which was proven to be efficient in rice and wheat (Wang *et al.*, 2018; Xie *et al.*, 2015). This method involves Golden Gate cloning, using the *Bsal* restriction enzyme, which cuts outside of its GGTCTC recognition site (cuts GGTCTCN|NN...). This feature was used to generate custom discriminatory overhangs that when ligated would reconstitute guide RNA target sites. Five sets of primers (Supplementary Table 5.1) were designed as in Xie *et al.* (2015) and used to amplify gRNA scaffold and tRNA from pUC57-R504 template vector (Supplementary Figure 5.1 A). The primers were designed to amplify five fragments: *Bsal*-tRNA-first half of sgRNA1-*Bsal* (110 bp), *Bsal*-second half of sgRNA1-gRNA scaffold-tRNA-first half of sgRNA2-*Bsal* (205 bp), *Bsal*-second half of sgRNA2-gRNA scaffold-tRNA-first half of sgRNA3-*Bsal* (205 bp), *Bsal*-second half of sgRNA3-gRNA scaffold-tRNA-first half of sgRNA4-*Bsal* (205 bp), and *Bsal*-second half of sgRNA4-gRNA scaffold-*Bsal* (130 bp) (Figure 5.3 B). After restriction digestion and ligation, the fragments would ligate into one polycistronic gene (PTG) with reconstituted sgRNA sites linking the tRNA and gRNA scaffold (Figure 5.3 C). The polycistronic gene was subsequently cloned into the destination vector pUC57-R504 (Supplementary Figure 5.1 B). pUC57-R504 and pUC57-R504 vectors were obtained from Dr Alison Huttly, Rothamsted Research.

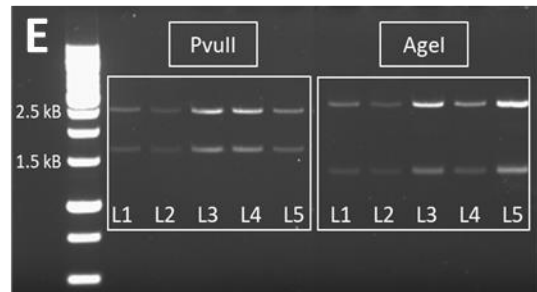
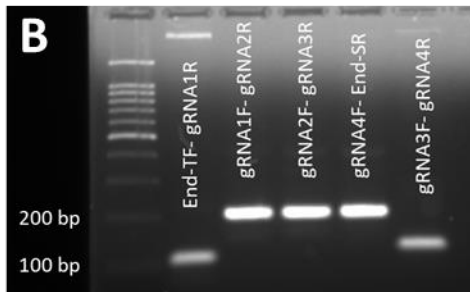
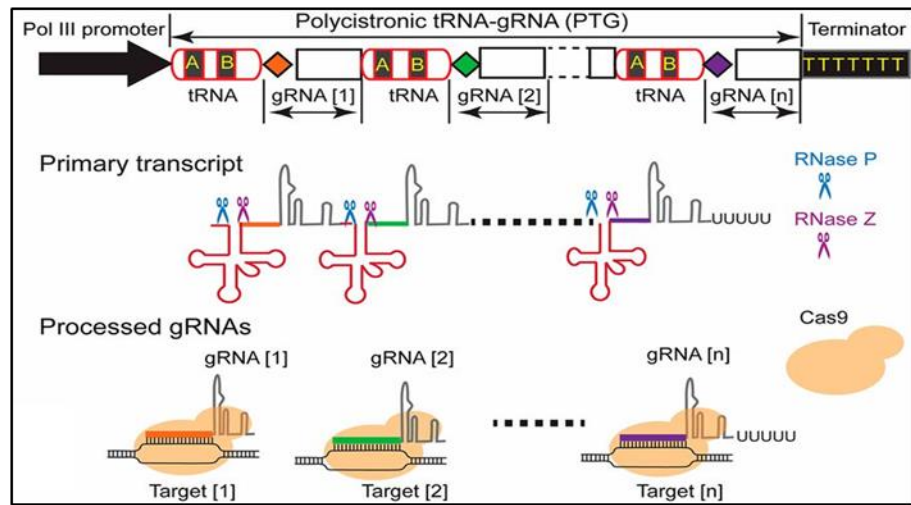
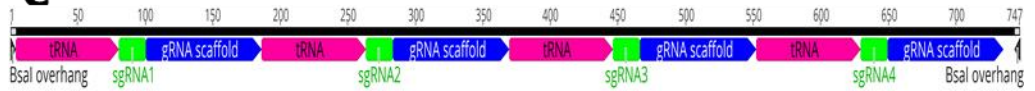
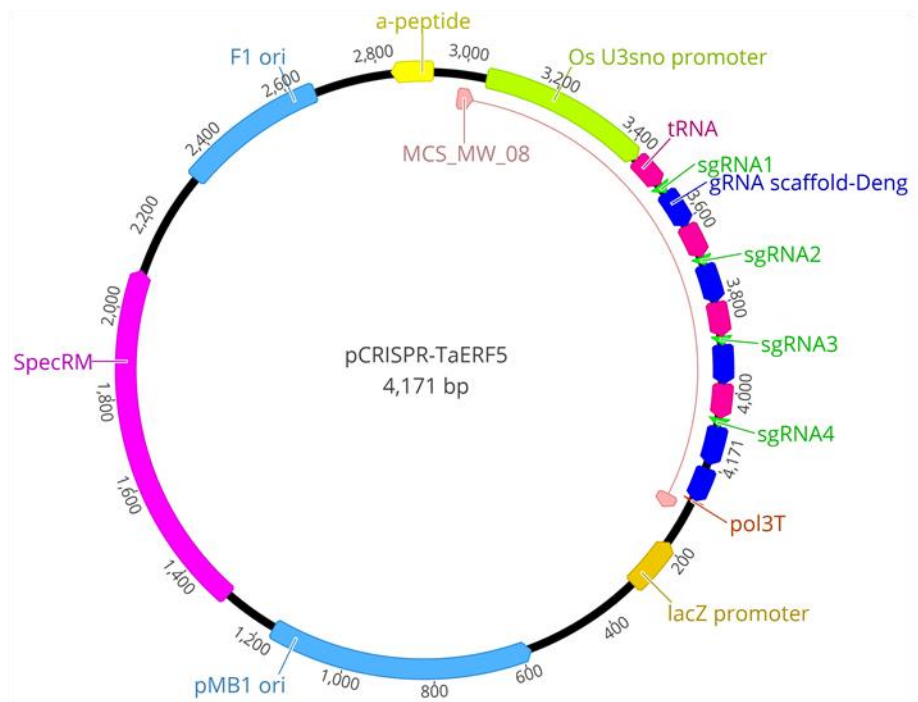
A**C****D**

Figure 5. 3 Generation of the plasmid used in genome editing. A. Cloning was based on the Golden Gate strategy described in Xie *et al.*, (2015), which allows targeting multiple genomic locations using one vector. Once the polycistronic gene (PTG) is transcribed, intrinsic cleaving machinery (represented by scissors) of the cell releases mature gRNAs and tRNA. The PTG consists of tandemly arrayed tRNA-gRNA units, with each gRNA containing a target-specific spacer (different coloured diamonds) and conserved gRNA scaffold (rectangle). The tRNA is shown as round rectangles. The excised mature gRNAs direct Cas9 to multiple targets. The Figure is adapted from Xie *et al.* (2015). B. Picture of agarose gel showing products of PTG fragments amplification. Fragments were amplified from the pUC57-R504 template vector using primers listed in Supplementary Table 5.1. C. Diagram showing the PTG generated in this study. Four sgRNAs were reconstituted in the ligation reaction, so that after cleaving with RNase P and RNase Z, Cas9 protein will be directed to four distinct target sites. D. Final pCRISPR-TaERF5 vector. PTG and the pRRes208.482 destination vector were digested with *BsaI* and the purified fragments used in a single ligation reaction. The final pCRISPR-TaERF5 vector contains the PTG with a chain of tRNA-sgRNA1-gRNA scaffold-tRNA-sgRNA2-gRNA scaffold-tRNA-sgRNA3-gRNA scaffold-tRNA-gRNA4-gRNA scaffold, where only the sgRNAs are unique.

The gRNA scaffold that is present in the pUC57-R504 vector is the same as in Dang *et al.* (2015). Deng and colleagues found that extending the gRNA scaffold by ~5 nucleotides and mutating the fifth nucleotide of the scaffold, which is fourth of the continuous sequence of Ts, to C or G, significantly increases CRISPR/Cas9 gene knockout efficiency (Dang *et al.*, 2015). In the gRNA sequence in the pUC57-R504 vector, another mutation was introduced by mistake. A was mutated to G at position 19, which is the second nucleotide of the tetraloop that links crRNA with tracrRNA, and therefore should not influence the gRNA binding ability. Once the fragments were amplified, a *BsaI* restriction enzyme was used to cut all the amplicons and the destination vector pRRes208.482. Digested fragments were used in a single ligation reaction, and the ligation mix transformed into *E.coli* cells. DNA isolated from the transformed colonies had been sequenced and subjected to restriction digest with *PvuII* and *AgeI*, which when digested with either enzyme should yield two DNA fragments: 2,505 and

1,666 bp for *PvuII* and 2,794 and 1,385 bp for *AgeI*. The restriction digest (Figure 5.3 E) and the sequencing showed that all fragments had ligated correctly. The complete pCRISPR-TaERF5 vector (Figure 5.3 D) contained the final construct with the PTG encoding a chain of tRNA-sgRNA1-gRNA scaffold-tRNA-sgRNA2-gRNA scaffold-tRNA-sgRNA3-gRNA scaffold-tRNA-gRNA4-gRNA scaffold, where only the sgRNAs were unique.

5.3.4 INDELS identified in the T0 population

Genotyping of T0 plants was performed using the genomic DNA supplied by the Cereal Transformation Group. Initially, PCR was performed on the DNA to reveal larger or smaller than expected bands caused by INDELS. The primers used for this amplification were generic for the six genes (will amplify three homoeologues of *TaERF5* and *TaERF5a*), and in WT plants should amplify fragments of 713 to 740 bp (Figure 5.4 A, Amplicon 1), depending on the gene. Any bands of different sizes would have been a result of editing causing a deletion or insertion in the gene sequence. The primers used for the initial PCR and NGS of T0, T1 and T2 plants are listed in Supplementary Table 5.1, and their positions on the genes shown in Figure 5.4 A.

Seven and 16 plants were found to contain both PTG and Cas9 plasmids from the respective transformations, B3781 and B3792. PCR amplification of the target genes in these plants had revealed clear additional bands in two plants from B3781 transformation (R5P1 and R7P1) and five plants from B3792 transformation (R2P1, R3P1, R5P2, R7P1 and R7P2) (marked with red asterisks in Figure 5.4 B). These plants, along with the R1P1 control (no PTG or Cas9 plasmid used) were selected for NGS analysis. The service used for NGS utilises Illumina 2x250 bp sequencing configuration and the maximum length of the amplicon that could be supplied was 500 bp. Therefore, another reverse primer (PR2) was designed to amplify a shorter fragment (see Figure 5.4 A, Amplicon 2). The reverse primer was designed to bind in the highly conserved AP2/ERF coding domain, and the expected size of the amplicons in the unedited controls

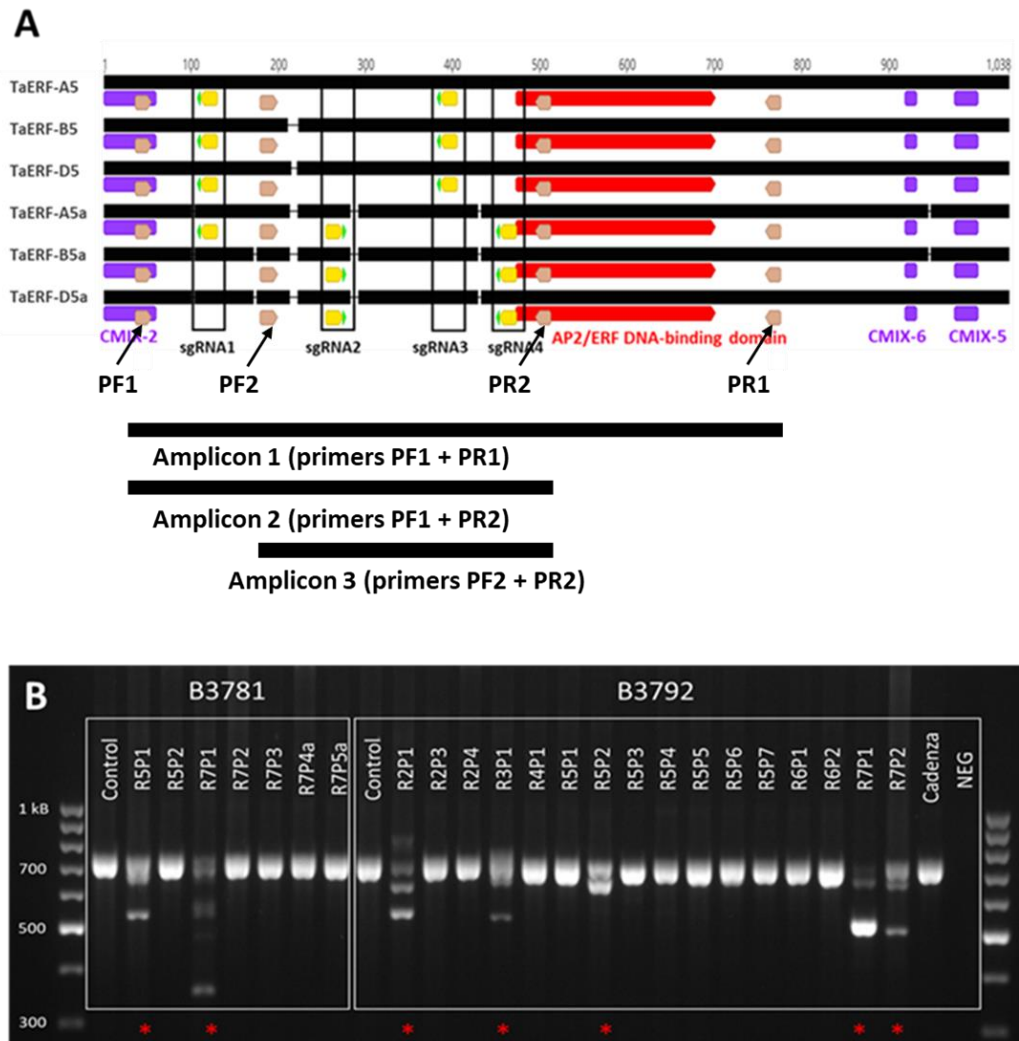


Figure 5. 4 Screening for INDELS in T0 plants. **A.** Alignment of the genes encoding TaERF5 and TaERF5a in wheat with the functional domains and sgRNAs annotated. The positions of the primers (PF1, PF2, PR1 and PR2; PF = primer forward; PR = primer reverse) used to amplify the amplicons 1, 2 and 3, are annotated in brown. **B.** Agarose gel electrophoresis of PCR products amplified from two batches of T0 plants: B3781 and B3792. Band shifts indicate the presence of INDELS in the genes. Plants marked with red asterisks were selected for NGS analysis. The control is a plant that went through a transformation process, but no plasmid DNA was being used, hence no editing is expected. Cadenza indicates the untransformed WT Cadenza plant and NEG is the no template negative control for the PCR. The letters and numbers following the batch number indicate the repeat (R) and plant (P) number; a = some calli broke during the regeneration process, hence more than one plant regenerated from the same original callus.

is 449 to 476 bp long, depending on the gene. The fragments for NGS analysis were amplified using primers with barcodes required by the sequencing provider (Supplementary Table 5.1) and purified on the column. The obtained reads were trimmed to the quality score over 20 (representing an error rate of 1 in 100, with a corresponding call accuracy of 99%), paired and merged, and mapped to the Cadenza genome using BMap aligner, discarding the reads with more than three mismatches. Each sample contained fragments amplified from the six genes, and three additional fragments amplified as a result of nonspecific primer binding: 266 bp fragment of non-coding DNA, and fragments of *TraesCS1A02G218100* (261 bp) and *TraesCS1B02G231500* (262 bp), genes containing AP2/ERF domain. No editing was observed in these amplicons.

The proportion of reads originating from different homoeologues of each gene varied from sample to sample, and in some cases no reads mapped to some of the homoeologues. Such plants were automatically discarded from further analysis, as the editing in at least one out of six genes targeted would be unknown. Out of 83 possible mutation sites (seven plants, 13 sites per plant = 91 – 8 that return no reads) the INDELS were identified at 51 sites (61.5% efficiency). Various INDELS were observed: 16 monoallelic (present on only one allele of the gene), 27 biallelic (present on both alleles of the gene), with the biallelic mutations being of the same (homozygous; 13 found) or different type (heterozygous; 14 found). In eight cases, there were more than two edits per sgRNA site, which is a clear indication of a chimeric plant. Eight mutation sites were undetermined as no reads mapped to these fragments (Supplementary Table 5.2). Deletions (DELs) were much more frequently observed than insertions (INSs), as only three instances of 1 bp INS in one allele of *TaERF-B5a* and *TaERF-D5a* genes were identified. Deletions varied in size from as small as 1 bp to as large as 387 bp. Quite a big disproportion of generated INDELS at each sgRNA site was observed, as from 19 possible edition sites (21 possible – 2 that did not map), and in case of sgRNA1 22 possible sites (24 possible – 2 that did not map), at sgRNA2, sgRNA3 and sgRNA4, 16, 11 and 18 genomic sequences were edited, respectively, whereas only six edited sequences were found at sgRNA1 site.

Table 5. 3 INDELS identified in R5P1 and R7P1 plants from B3781 transformation. The plants showed edits in all six genes targeted. PCR was used to amplify fragments encompassing all four target sites in three *TaERF5* and three *TaERF5a* genes. Amplicons with barcodes for NGS were sequenced using GENEWIZ Amplicon-EZ service, and the reads mapped to wheat (cv. Cadenza) genome using BMap aligner. A, B and D stand for the genome, and 1 and 2 are the two alleles. In case of more than two different edits from the same sgRNA site, number 3 was added

| | <i>TaERF5</i> | | <i>TaERF5a</i> | | |
|------|---------------|---------------|----------------|------------|------------|
| | sgRNA1 | sgRNA3 | sgRNA1 | sgRNA2 | sgRNA4 |
| R5P1 | | | | | |
| A1 | NO | 1 bp DEL | NO | NO | 2 bp DEL |
| A2 | NO | NO | NO | NO | 176 bp DEL |
| B1 | NO | 1 bp DEL | N/A | 40 bp DEL | 7 bp DEL |
| B2 | NO | 1 bp DEL | | NO | 1 bp INS |
| B3 | N/A | N/A | | 176 bp DEL | N/A |
| D1 | NO | 1 bp DEL | | 6 bp DEL | 17 bp DEL |
| D2 | NO | 1 bp DEL | | NO | 1 bp DEL |
| D3 | N/A | N/A | | 176 bp DEL | N/A |
| D3 | N/A | N/A | | 176 bp DEL | N/A |
| R7P1 | | | | | |
| A1 | 387 bp DEL | 1 + 53 bp DEL | NO | 27 bp DEL | 3 bp DEL |
| A2 | 387 bp DEL | 1 + 53 bp DEL | NO | 175 bp DEL | NO |
| A3 | N/A | N/A | 370 bp DEL | N/A | N/A |
| B1 | 372 bp DEL | NO | N/A | 51 bp DEL | 2 bp DEL |
| B2 | 372 bp DEL | NO | | 175 bp DEL | NO |
| D1 | 378 bp DEL | NO | | 6 bp DEL | 1 bp DEL |
| D2 | NO | 1 bp DEL | | 175 bp DEL | NO |
| D3 | NO | 1 + 53 bp DEL | | N/A | N/A |
| D3 | NO | 1 + 53 bp DEL | | N/A | N/A |
| D3 | NO | 1 + 53 bp DEL | | N/A | N/A |

INDELS in all homoeologues of *TaERF5* and *TaERF5a* genes were identified in two plants: R5P1 and R7P1 from B3781 transformation (summarised in Table 5.3). The INDELS identified in other plants analysed are shown in Supplementary Table 5.2. Since each gene was targeted at two (three in the case of *TaERF-A5a*) positions and each gene has two alleles, the maximum number of edits present on one gene should be four (six in *TaERF-A5a*; distributed over two alleles). Hence, two differently edited alleles with a maximum of four (or six in case of

TaERF-A5a) different INDELS should be identified. However, this was not what was observed.

All possible allele edition variants for the homoeologues of *TaERF5* and *TaERF5a* genes found in B3781 R5P1 and B3781 R7P1 plants, along with the predicted effect on the encoding protein sequence are summarised in Tables 5.4 and 5.5, respectively. In the B3781 R5P1 plant, B and D homoeologues of the *TaERF5a* gene, show five different alleles instead of two. In plant B3781 R7P1 *TaERF-A5a* gene, three differently edited alleles were identified. This would indicate that the leaf tissue analysed contained a mixture of differently edited cells, hence, the analysed T0 plants were most likely chimeras. Interestingly, in both B and D homoeologues of the *TaERF5a* gene in B3781 R5P1 plant, four different alleles contain the mixture of the same INDELS (40 bp DEL at sgRNA2 with either 7 bp DEL or 1 bp INS at sgRNA4 for *TaERF-B5a* and 6 bp DEL at sgRNA2 with either 17 bp DEL or 1 bp DEL at sgRNA4 for *TaERF-D5a*). When considering the percentage of reads that each of the possible alleles contribute to the total number of reads (Table 5.4), a similar scenario for both genes can be observed. For *TaERF-B5a*, 40 + 7 bp DELs and 1 bp INS are predominant alleles (81.42% of reads), whereas 40 bp DEL + 1 bp INS and 7 bp DEL contribute only a small percentage (9.01%). Similar ratios are observed for reads mapped to *TaERF-D5a*, where 6 + 17 bp DEL and 1 bp DEL alleles are much more abundant (86.29%) than 6 + 1 bp DEL and 17 bp DEL (7.86%). The same issue persisted during T1 and T2 plants genotyping. Another aspect, which will be described in the next section, is that in T1 and T2 population, only 40 + 7 bp DEL and 1 bp INS alleles for *TaERF-B5a* and 6 + 17 bp DEL and 1 bp DEL alleles for *TaERF-D5a* are seen, in different combinations (biallelic homozygous and biallelic heterozygous). One of the possible explanations of the observed phenomenon is interallelic gene conversion during PCR reaction, possibly due to 3'→5' proofreading activity of the polymerase or incomplete PCR product during extension step (Andy Phillips, personal communication). It can be therefore assumed with high probability that editions in *TaERF-B5a* and *TaERF-D5a* genes were biallelic heterozygous in one cell and biallelic homozygous in another cell (source of 176 bp deletion), and only three differently edited alleles were present, not five.

The aim of genome editing was to generate a complete knockout in *TaERF5* and *TaERF5a*, therefore only the INDELS that would encode a predicted non-functional transcription factor were selected for further analysis. The effects of identified INDELS on encoded proteins structures are summarised in Tables 5.4 and 5.5. All three homoeologues of the *TaERF5* gene in the B3781 R5P1 plant contain 1 bp DEL causing a frameshift and premature STOP codon. The resulting proteins are significantly shorter than the WT proteins and all lack the DNA-binding domain and the two putative MAP kinase phosphorylation sites, CMIX-5 and CMIX-6. Deletions in the B and D homoeologues are biallelic homozygous while the deletion in the A homoeologue is monoallelic.

Table 5. 4 INDELS identified on various alleles of *TaERF5* and *TaERF5a* genes present in R5P1 plant, and their effect on the encoded protein. Alleles marked with asterisks have been classified as resulting from interallelic gene conversion.

| Gene | INDELS identified in the alleles | Effect on the encoded protein |
|------------------|---|--|
| <i>TaERF-A5</i> | 1 bp (nt 388) DEL (51.84%); WT (48.16%) | frameshift from aa 129, STOP codon at aa 256 |
| <i>TaERF-B5</i> | 1 bp (nt 376) DEL (100%) | frameshift from aa 125, STOP codon at aa 252 |
| <i>TaERF-D5</i> | 1 bp (nt 382) DEL (100%) | frameshift from aa 127, STOP codon at aa 210 |
| <i>TaERF-A5a</i> | 1) 176 bp (nt 259 to 435) DEL (81.24%) 2) 2 bp (nt 432 - 433) DEL (15.63%) | 1) frameshift from aa 144, STOP codon at aa 163 2) STOP codon at aa 87 |
| <i>TaERF-B5a</i> | 1) 40 bp (nt 251 to 291) and 7 bp (nt 429 to 436) deletion (53.53%) 2) 1 bp (nt 430) insertion (27.89%) 3) 176 bp (nt 258 to 433) DEL (10.57%) 4) 40 bp (nt 251 to 291) deletion with 1 bp (nt 430) insertion (6.61%) * 5) 7 bp (429 to 436) deletion (2.40%) * | 1) frameshift from aa 85, STOP codon at aa 86 2) STOP codon at aa 144 3) STOP codon at aa 86 4) frameshift from aa 85, STOP codon at aa 86 5) frameshift from aa 143, STOP codon at aa 244 |
| <i>TaERF-D5a</i> | 1) 6 bp (nt 253 to 259) with 17 bp (nt 413 to 430) DEL (52.27%) 2) 1 bp (nt 430) DEL (34.02%) 3) 176 bp (nt 258 to 433) DEL (4.02%) 4) 17 bp (nt 413 to 430) DEL (4.01%) * 5) 6 bp (nt 253 to 259) with 1 bp (nt 430) DEL (3.85%) * | 1) frameshift from aa 136, STOP codon at aa 196 2) frameshift from aa 143, STOP codon at aa 247 3) STOP codon at aa 86 4) frameshift from aa 138, STOP codon at aa 198 5) frameshift from aa 143, STOP codon at aa 245 |

Table 5. 5 INDELS identified on various alleles of *TaERF5* and *TaERF5a* genes present in R7P1 plant, and their effect on the encoded protein.

| Gene | INDELS identified in the alleles | Effect on the encoded protein |
|------------------|--|---|
| <i>TaERF-A5</i> | 1) 1 bp (nt 388) and 53 bp (nt 429 to 482) DEL (36.14%) 2) 384 bp (nt 106 to 490) DEL (62.65%) | 1) frameshift from aa 127, back to frame at aa 161, 328 aa instead of 346; 3 aa of DNA binding domain missing 2) 128 aa missing, no frameshift; 6 aa of DNA binding domain missing |
| <i>TaERF-B5</i> | 1) 372 bp (nt 107 to 478) DEL (100%) | 1) 218 aa instead of 342, no frameshift, 6 aa of DNA binding domain missing |
| <i>TaERF-D5</i> | 1) 1 bp (nt 382) DEL (50.13%) 2) 378 bp (nt 109 to 486) DEL (45.38%) | 1) frameshift from aa 128, 210 aa instead of 344 2) 126 aa missing, 218 aa instead of 344, no frameshift, 7 aa of DNA binding domain missing |
| <i>TaERF-A5a</i> | 1) 27 bp (nt 250 to 276) and 3 bp (nt 433 to 435) DEL (16.57%) 2) 175 bp (nt 261 to 434) DEL (46.00%) 3) 363 bp (nt 109 to 471) DEL (23.43%) | 1) 10 aa missing, no frameshift, intact DNA binding domain 2) frameshift from aa 87, STOP codon at aa 190 3) 121 aa missing, 216 aa instead of 337, no frameshift, 8 aa of the DNA binding domain missing |
| <i>TaERF-B5a</i> | 1) 51 bp (nt 232 to 282) with 2 bp (nt 430 to 431) DEL (69.22%) 2) 175 bp (nt 258 to 431) DEL (21.33%) | 1) frameshift from aa 127, STOP codon at aa 186 2) frameshift from aa 86, STOP codon at aa 189 |
| <i>TaERF-D5a</i> | 1) 6 bp (nt 251 to 256) with 1 bp (nt 430) DEL (13.29%) 2) 175 bp (nt 257 to 431) DEL (79.66%) | 1) 2 aa missing (84 and 85) and frameshift from aa 144, STOP codon at aa 247 2) 58 aa missing, frameshift from aa 144, STOP codon at aa 189 |

More complex editing occurred in the three homoeologues of the *TaERF5a* gene. *TaERF-A5a* gene showed biallelic heterozygous editing at the sgRNA4 site, containing a two nucleotides deletion on one allele and a 176 bp deletion on the second allele. Both deletions cause a frameshift that would result in premature STOP codons and a loss of DNA-binding, CMIX-6 and CMIX-5 domain in the encoded proteins. No edits at sgRNA2 were detected. *TaERF-B5a* and *TaERF-D5a* genes showed three, rather than two differently edited alleles, which is typical for chimeras. All differently edited alleles of *TaERF-B5a* and *TaERF-D5a* genes are predicted to encode proteins with a frameshift affecting proper translation of the DNA-binding and CMIX-5 and CMIX-6 domains, and are therefore likely to confer loss-of-function (Table 5.4).

The edits of the *TaERF5* and *TaERF5a* genes in the B3781 R7P1 plant, albeit present on both alleles of all six genes, would not have such detrimental effects on the proteins as mutations in B3781 R5P1 plant (Table 5.5). It is important to

keep in mind that *TaERF5* gene is more highly expressed than *TaERF5a* (Figure 5.1, Table 5.1), therefore INDELS affecting the functionality of the proteins encoded by *TaERF5* should be prioritised when generating a non-functional mutant, if not present in all six genes. In the B3781 R7P1 plant, only *TaERF-B5a* and *TaERF-D5a* genes contain biallelic edits that would encode invalid TaERF5a protein (Table 5.5). The deletions found in A and B homoeologues of the *TaERF5* gene are all in-frame deletions that might only partially affect functionality. *TaERF-D5* and *TaERF-A5a* were demonstrated to contain both in-frame deletions that are unlikely to affect the functional domains of the protein and frame-shifting edits that would result in invalid proteins.

To summarise, the NGS analysis of the T0 plants revealed that the B3781 R5P1 plant was the only plant showing INDELS that are likely to have detrimental effect on the encoded proteins in all six genes targeted. Therefore, the B3781 R5P1 plant was chosen to be propagated to the T1 generation.

5.3.5 Identification of INDELS in T1 and T2 plants

To genotype T1 and T2 plants Illumina single-read sequencing service provided by Rothamsted Research was used. T1 and T2 plants were propagated from the B3781 R5P1 plant. As no INDELS were identified at sgRNA1 site in the T0 individual (Figure 5.5), a shorter region was amplified and sequenced to genotype the T1 and T2 plants (Figure 5.4; Amplicon 3). This was beneficial, as high-throughput, single-read sequencing service of raw PCR reaction mix without having to go through the column purification step allowed for inexpensive genotyping of multiple plants.

44 T1 plants were planted and genotyped. Amplicons for the NGS service were amplified using ERF5_NGS2-FOR and ERF5_NGS2-REV primers (Supplementary Table 5.1) that anneal to all six genes and in WT plants should result in 353 bp to 374 bp amplicons in the same sample, depending on the gene. Gel electrophoresis was performed to ensure successful amplification before sequencing the samples.

The mutations found at sgRNA sites in B3781 R5P1 plant (summarised in Figure 5.5 B, C, D), cause 40 bp and 176 bp deletions that would be clearly separated on the gel, but also small 1 – 7 bp INDELS, which would not be separated. Separation of the PCR amplicons by the agarose gel electrophoresis revealed the presence of bigger deletions in some, but not all T1 plants (Figure 5.6 A), which indicates clear segregation of the alleles in T1 population. Table 5.6 summarises the edits identified in all homoeologues of *TaERF5* and *TaERF5a* genes in T1 plants. In most analysed plants, majority of the analysed genes contained no edits (for detailed list of edits refer to Supplementary Table 5.3). A previously unobserved 175 bp deletion was identified in *TaERF-D5a* gene in 11 plants, indicating that Cas9 activity was still present.

Often only a small percentage of a certain type of INDEL was identified, especially the 176 bp DEL in *TaERF-A5a* gene and 175 bp DEL in *TaERF-D5a* gene, whereas no other genes were edited in the same plants. Eight plants did not contain any edits in any of the targeted genes. 20 plants showed editing only in one or two homoeologues of *TaERF5a* gene, but none in any of the homoeologues of the *TaERF5* gene. In five plants, all but one (*TaERF-A5*) genes were edited, and finally, all six genes were found to be edited in 12 plants. No plants were found to contain only homozygous biallelic mutations in all six genes. Again, due to higher expression of the *TaERF5* gene, which would indicate that its function may be more vital for the plants' physiology, plants containing homozygous biallelic INDELS in *TaERF5* gene were prioritised, while less emphasis was put on the zygosity of the edits in *TaERF5a* homoeologues. Homozygous biallelic mutations in all homoeologues of the *TaERF5* gene were identified in T1 plants number 6, 21, 32 and 40, and these plants were selected to be propagated into the T2 generation.

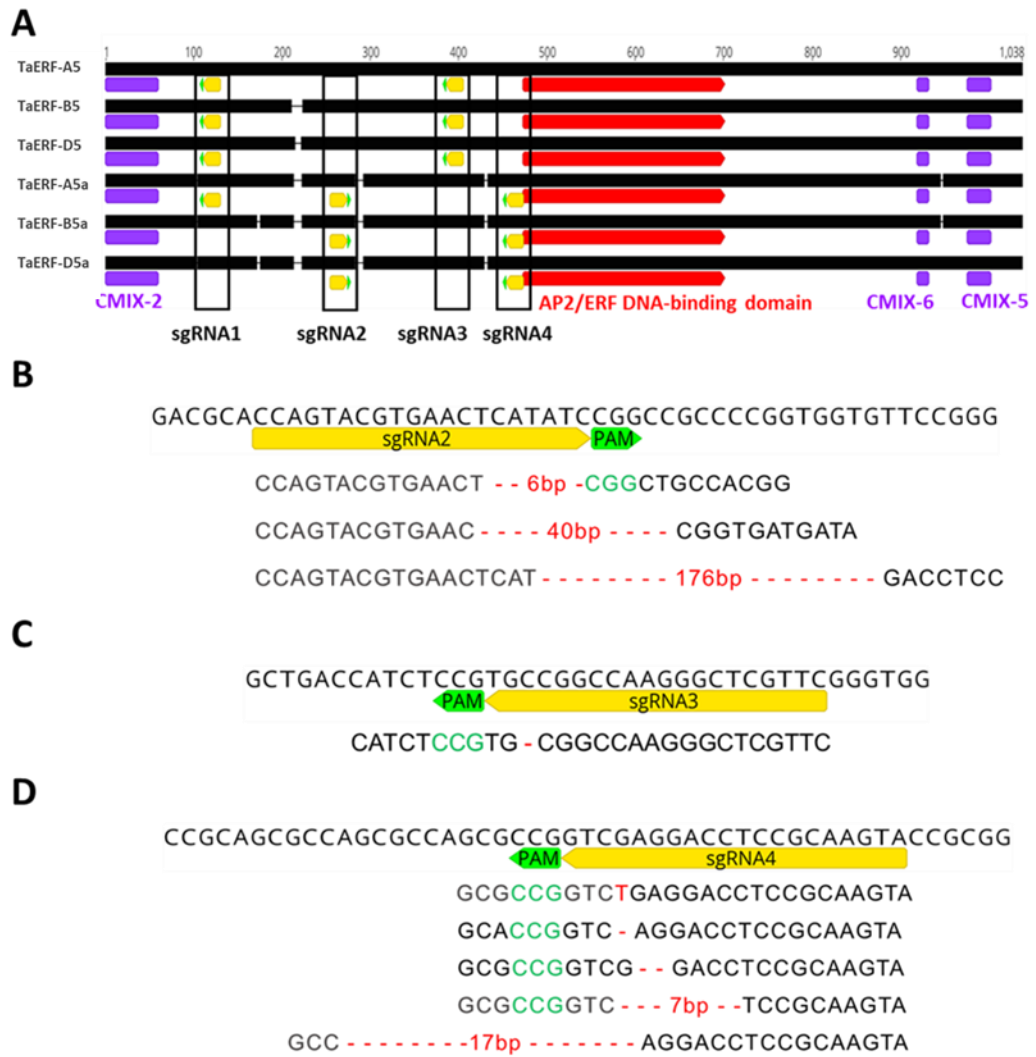


Figure 5. 5 INDELS produced by various sgRNAs in B3781 R5P1 plant. No edits were detected at sgRNA1 site. A. Alignment of all homoeologues of TaERF5 and TaERF5a genes with functional domains and sgRNA sites annotated. sgRNA sites were designed to generate mutations upstream of DNA-binding domain to ensure inactive transcription factors. B. 6 bp, 40 bp and 175 bp deletions were observed at sgRNA2 in TaERF-D5a, TaERF-B5a and TaERF-A5a, respectively. C. At sgRNA3 site 1 bp deletion was identified in all three homoeologues of TaERF5 gene. D. A large variety of generated INDELS was seen at sgRNA4: 2 bp deletion in TaERF-A5a, 1 bp insertion or 7 bp deletion in TaERF-B5a and 1 bp or 17 bp deletion in TaERF-D5a gene.

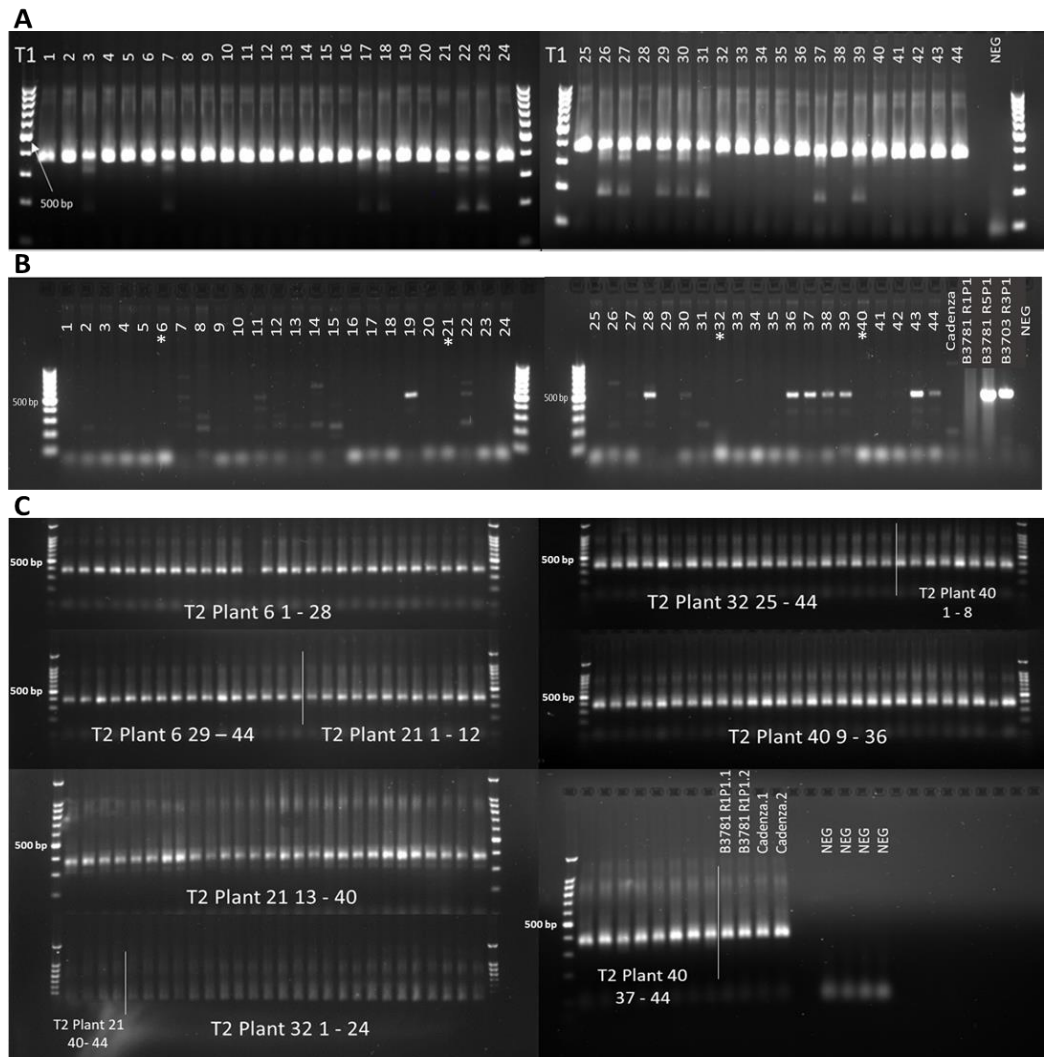


Figure 5. 6 Gel electrophoresis of PCR amplicons amplified from T1 and T2 plants. A. PCR product separation after amplification of *TaERF5* and *TaERF5a* genes fragments from T1 plants for NGS analysis. Primers used amplified a shorter fragment, not including *sgRNA1* site. The amplicons with NGS barcodes in WT plants should be 353 bp to 374 bp long, depending on the gene. Other bands indicate edited alleles containing INDELS. B. Diagnostic Cas9 PCR. All T1 plants were investigated for integration of the Cas9 protein. The expected amplicon size should be 559 bp. Marked with asterisks are the plants chosen to be propagated into the T2 population. C. PCR product separation after amplification of *TaERF5* and *TaERF5a* genes fragments from T2 plants for NGS analysis. The same primers were used as for T1 plants genotyping. Different bands indicate edited alleles containing INDELS. T2 Plant 21 40-44 and T2 Plant 32 1-24 – the electrophoresis was run for too long and the PCR amplicon migrated out of the gel, but NGS analysis proved that the amplicons were present, at least in samples T2 Plant 21 40-44. The marker is a Promega 100 bp DNA ladder.

Table 5. 6 INDELS found in each of the genes in the T1 population. The number of plants that showed respective mutation zygosity on that gene are shown. BI (HOM) = biallelic homozygous; MON = monoallelic; BI (HET) = biallelic heterozygous. New type of deletion was found in TaERF-D5a gene (175 bp DEL).

| | TaERF5 | | | TaERF5a | | |
|----------|---------------|----|----|----------------|-----------------|-----------------|
| | A | B | D | A | B | D |
| BI (HOM) | 4 | 17 | 17 | 4 (2 bp DEL) | 4 (40+7 bp DEL) | 8 (6+17 bp DEL) |
| | | | | 4 (176 bp DEL) | 5 (1 bp INS) | 4 (1 bp DEL) |
| MON | 8 | NO | NO | 15 | NO | NO |
| BI (HET) | NO | NO | NO | 9 | 8 | 5 |
| NEW | NO | NO | NO | NO | NO | 11 |
| NO EDIT | 32 | 27 | 27 | 12 | 27 | 16 |

Table 5. 7 INDELS identified in T2 plants. Types of mutations and their zygosity are shown. When not all the T2 plants showed the same edit for the respective gene, the number of plants showing each type of INDELS are shown. BI (HOM) = biallelic homozygous; MON = monoallelic; BI (HET) = biallelic heterozygous.

| T2 plant | TaERF5 | | | TaERF5a | | |
|----------|--|------------------------|------------------------|------------------------|-----------------------------|-----------------------------|
| | A | B | D | A | B | D |
| 6 | BI (HOM) (1 bp DEL) | BI (HOM) (1 bp DEL) | BI (HOM) (1 bp DEL) | BI (HOM) (2 bp DEL) | BI (HOM) (1 bp INS) | BI (HOM) (6+17 bp DEL) |
| 21 | BI (HOM) (1 bp DEL) | BI (HOM) (1 bp DEL) | BI (HOM) (1 bp DEL) | BI (HOM) (2 bp DEL) | HOM (40+7 bp DEL) | 8 BI (HOM) (6+17 bp DEL) |
| | | | | | | 16 BI (HOM) (1 bp DEL) |
| | | | | | | 20 BI (HET) |
| 32 | No reads returned by the provider of the NGS service | | | | | |
| 40 | BI (HOM) (1 bp DEL) | BI (HOM) (1 bp DEL) | BI (HOM) (1 bp DEL) | BI (HOM) (2 bp DEL) | 11 BI (HOM) (1 bp INS) | BI (HOM) (6+17 bp DEL) |
| | | | | | 8 BI (HOM) (40+7 bp DEL) | |
| | | | | | 25 BI (HET) | |

T1 plants were also screened for integration of the Cas9 protein by PCR, using Ubipr-SF2 and Cas9-SR1 primers (Supplementary Table 5.1). The expected amplicon size was 559 bp, and two Cas9-positive (B3781 R5P1 and B3703 R3P1) and Cas9-negative (Cadenza and B3781 R1P1) plants were used as positive and negative controls, respectively. The results of the Cas9 screen are shown in Figure 5.6 B. None of the plants selected to be propagated into the T2 population showed Cas9 integration.

Illumina single-read sequencing service provided by Rothamsted Research was used to genotype T2 plants. 44 T2 plants derived from each T1 plant were sequenced (176 plants in total) and the results are summarised in Table 5.7. No large band shifts were observed after gel electrophoresis for any of the samples (Figure 5.6 C). Very few, and of not sufficient quality reads were mapped for the T2 population of T1 Plant 32, thus the genotype of that plant was not resolved. All INDELS identified in T1 generation plants 6, 21 and 40 were propagated in the T2, following a 1:2:1 Mendelian inheritance pattern. For biallelic INDELS that were not homozygous, the segregation ratio was confirmed by Chi square test (*TaERF-B5a*: $\chi^2(\text{df}=2, N=44) = 0.195, P=0.05$; *TaERF-D5a*: $\chi^2(\text{df}=2, N=44) = 3.27, P=0.05$).

Taken together, the wheat genome was targeted at four distinct genomic locations to generate knockout mutations in six genes: three homoeologues of the *TaERF5* and *TaERF5a* genes. Cas9-free plants containing deleterious mutations in all six genes were identified in the T2 population. The mutations are stably transmitted to the next generations and follow Mendelian inheritance pattern. The PTG-based technology was proven to be an effective method of generating mutations at multiple genomic sites in wheat in one transformation event. In the future, the *Taerf5 Taerf5a* mutant should be used to evaluate the role of *TaERF5* and *TaERF5a* genes in regulating GA response in the aleurone of wheat.

5.4 Discussion

This Chapter describes generation of the *Taerf5 Taerf5a* null mutant that will be used to investigate the role of TaERF5 transcription factor in regulating GA signalling in the aleurone of wheat. TaERF5 was identified as an RHT-1 interactor in the aleurone and the expression of the *TaERF5* and *TaERF5a* genes is grain-specific (Figure 5.1). Due to the presence of a close paralogue and the possible redundancy between the genes, generation of the mutant required knocking out six genes in total, and the method of choice was genome editing using CRISPR/Cas9 system.

CRISPR/Cas9 target gene multiplexing using tRNA-sgRNA PTG and intrinsic tRNA-processing system was used. The system developed by Xie *et al.* (2015) has already been successfully applied to edit multiple gene targets in cereals, e.g. rice (Xie *et al.*, 2015), maize (Qi *et al.*, 2016) and wheat (Hahn *et al.*, 2020; Wang *et al.*, 2018), but thus far, no studies have reported successful, simultaneous knocking out of as many as six genes. To maximise the editing success rate in our study, each gene was targeted at at least two different sites (Figure 5.2 A). Targeting a gene at more than one location was already shown to greatly increase the gene knock-out capability as it enhances the edit probability (Shan *et al.*, 2014). Moreover, sgRNAs multiplexing using tRNA-sgRNA PTG system was shown to greatly increase the efficiency of gene knock-out compared to parallel simplex editing system (Qi *et al.*, 2016). The cloning of four tRNA-sgRNA units into one expression cassette under maize U6 snRNA promoter was previously shown to work well in maize (Qi *et al.*, 2016) and our results prove that multiplexing up to four tRNA-sgRNA units under rice U3 snRNA promoter is also an efficient method of gene editing in wheat.

The dominant type of edits observed in this study were deletions, while the insertions constituted only 3.53% of all INDELS in T0 plants. All the insertions identified were 1 bp A or T insertions. The deletions ranged in size from small, 1 bp, to as large as 175 – 176 bp, which is roughly the distance between the two sgRNAs in the genes where such deletions were found, and even over-380

bp deletions. Our results are similar to those previously reported for wheat (Liang *et al.*, 2017; Sánchez-León *et al.*, 2018; Wang *et al.*, 2018; Wang *et al.*, 2014; Zhang *et al.*, 2018; Zhang *et al.*, 2019). Not all sgRNA sites showed comparable numbers of INDELS generated. While at sgRNA2, 3 and 4, 58.0%, 84.2% and 94.7% of putative sites contained INDELS, only 23.1% of sites at sgRNA1 were edited. It has been speculated that high GC content (50 – 70%) of the CRISPR/Cas target site enhances the interaction between sgRNA and the DNA and may positively affect targeting efficiency (Ma *et al.*, 2015). However, the GC content of sgRNA1 (55% GC) was higher than that of sgRNA3 (45% GC) and comparable to the most efficient sgRNA4 (60% GC). Moreover, sgRNA2, which has the highest GC content (70%), did not show the highest editing efficiency, which is similar to results reported by Zhang *et al.*, (2018), where sgRNAs that were more GC-rich, did not show enhanced target editing efficiency. Thus, there must be other factors that affect the efficiency of generating INDELS. One possibility is the state of chromatin at the specific genomic location which may either favour or oppose the availability of DNA to Cas9 (Daer *et al.*, 2017; Liu *et al.*, 2019).

The GC content of sgRNA sites may also affect the off-target editing risk (Tsai *et al.*, 2015). In this study, the presence of off-target mutations was not validated by any experimental means, however, during the sgRNA sites selection, each 20 nucleotide-long fragment selected as a putative sgRNA site was used to search wheat (cv. Chinese spring and Cadenza) genome for identical sequences using the BLAST program. The 20 nucleotides of the selected sgRNAs shared 100% sequence homology only with the genes they were designed for (Supplementary Table 5.4). Previous studies have shown that 6 – 12 nucleotides immediately upstream 5' end of PAM domain, so called “seed sequence”, are critical in determining the target specificity and even single SNPs within that region abolish the Cas9 activity, while SNPs in more distal parts of sgRNA do not affect off-targeting as much (Hsu *et al.*, 2013; Jiang *et al.*, 2013). However, when tested, 1 bp mismatch outside of the “seed sequence” resulted in off-target INDELS, whereas four or five SNPs completely

abolished the off-target editing (Zhang *et al.*, 2014). In another study, no off-target editing was observed even though the putative off-target sites investigated were selected using the “seed sequence” with up to two mismatches (Sánchez-León *et al.*, 2018). Furthermore, Zhang *et al.*, (2018) hypothesized that observed lack of editing in the D homoeologue of *DA1* gene was due to a 1 bp mismatch in sgRNA sequence compared to A and B homoeologues, which indicates that as little as 1 SNP is enough to abolish DNA binding. The results from these reports indicate that there is no 100% accurate method that allows for prediction of target sites editing and it should always be validated experimentally. When the BLAST search against wheat genome was repeated using the seed sequences of all sgRNAs used in the study followed by all possible PAM domains recognised by Cas9 (AGG, CGG, GGG, TGG), 30 genes containing putative off-target sites were identified (Supplementary Table 5.4). Therefore, the *Taerf5 Taerf5a* plants should be screened for off-target activity before undertaking the physiological analysis to ensure that the observed phenotype is a result of knocking out *TaERF5* and *TaERF5a*, and not off-target genes. Whole genome sequencing would be a preferred method as it would pick up all edited off-target sites and ensure no integration of the Cas9 and PTG constructs.

Most of the genome editing events identified in T0 population were somatic in nature, and it is often found that T0 plants are genetic chimeras, i.e. contain cells with differently edited targets in different part of the plant (Feng *et al.*, 2014; Howells *et al.*, 2018; Michno *et al.*, 2020; Wang *et al.*, 2014; Xu *et al.*, 2015). More than two differently edited alleles, non-Mendelian segregation ratio or loss of mutations in subsequent generations, all indicate that mutations were restricted to somatic cells and did not participate in production of gametes. On the other hand, an abundance of biallelic INDELS, specifically homozygous in nature, that are stably transmitted to the next generations in expected segregation ratios, indicate that the mutations were generated during early development (Zhang *et al.*, 2014). Wheat embryos that were transformed with the CRISPR/Cas9 editing vectors were 12 to 16 DPA,

the stage of embryonic relative autonomy when scutellum, shoot apical meristem (SAM), coleoptile and epiblast are already differentiated (Kruglova *et al.*, 2020; Xiang *et al.*, 2019). In wheat, the cell lineages giving rise to developing shoot and floral structures, respectively, were traced to two or three cells in L1 and L2 cell layers at the apex of SAM (Simmonds, 1997). The L1 and L2 cells are the two, single-layer, outermost cell layers of SAM and are a good target for transformation as they can lead to modified germ lines. As the same genome editing event is very unlikely to happen in two separate cells independently, transformed tissues, in this case embryos, will often give rise to chimeric T0 plants. Moreover, the regeneration of transgenic plants after transformation using the biolistic method requires weeks, giving sgRNA-Cas9 complex ample time to generate more somatic mutations (Xu *et al.*, 2015). The presence of three differently edited alleles of *TaERF-B5a* and *TaERF-D5a* genes in T0 population, as well as lack of 175 bp deletion in T1 plants, indicated that B3781 R5P1 plant was a chimera. Two deletions identified in the *TaERF5* homoeologues in the T0 plant were biallelic homozygous in nature and one was biallelic heterozygous. Thus, all plants in the T1 population would expect to be biallelic if the mutation was present in germline cells. However, there was a high proportion of plants in the T1 population that showed no editing at all (15.9%), or only some of the targeted genes edited (45.5%). There was also a new INDEL identified in *TaERF-D5a* gene in some of the plants, which was most probably due to traces of Cas9 activity, either later in T0 plants or in T1 plants. The 17 plants that showed edits in either five or all six genes, showed segregation of alleles in accordance with Mendelian inheritance pattern, which would suggest that they were germline mutations. The question then arose: “how is it possible to see both Mendelian inheritance, typical for germline mutations and no, or atypical mutations in the offspring of the same plant?”. One possible explanation is that what was a somatic mutation to begin with, later in plant development differentiated to constitute the germline cells. It has been a widely accepted view that plants, in contrast to animals, do not set aside a specialized cell lineage early in embryogenesis and the germline of plants is established *de novo* from somatic cells in flowers (Schmidt *et al.*,

2015). A recent review (Lanfear, 2018) argues that as indeed, the differentiation of germline cells occurs later in development, its segregation, i.e. physical isolation from other cell lineages, may occur at any developmental point. Thus, even though the germline differentiates late in plant life, it could be segregated from somatic cell lineages early in development, or very late, in which case it is possible for somatic mutations to be incorporated into the germline cell lineage and subsequently passed on to the next generations (Lanfear, 2018). Moreover, germline segregation timing may vary between species, individuals of the same species, and even between flowers on the same plant. It is therefore possible that in some florets of the T0 B3781 R5P1 plant, the somatic mutations were incorporated and differentiated into germline cells, whereas in others they did not. Similar observation, of passing different mutations on to the subsequent generation through different flowers on the same plant has been also reported by Feng *et al.*, (2014). His suggestion to overcome the problem of somatic mutations in T0 populations and the lack of their inheritance, was either screening for heritable mutations in T2 generations, or using germline-specific promoters to drive Cas protein expression. The segregation of alleles in the T2 generation in our study was as predicted, and followed Mendelian segregation pattern, which showed that the introduced mutations were stably inherited.

The targeted mutations were introduced to generate a null knockout *Taerf5 Taerf5a* mutant in wheat. All ERF5 proteins encoded by the genes targeted in this study contain CMIX-2 motif at the very N' terminal, AP2/ERF DNA-binding domain and CMIX-6 and CMIX-5 at the C' terminal (Nakano *et al.*, 2006). The CMIX-2 is a putative transcriptional domain (Fujimoto *et al.*, 2000) and CMIX-5 and CMIX-6 are putative MAP kinase phosphorylation sites and may serve as protein regulation points. As the transcriptional domain was a difficult editing target due to its position, the aim was to target the genes such that the DNA-binding domain is affected. The generated INDELS in all six genes in the B3781 R5P1 plant resulted in frameshift upstream of the AP2/ERF domain and premature termination of the protein. Hence the translated proteins would be

significantly shorter and contain only the CMIX-2 motif. It can be therefore assumed that the activities of the TaERF5 proteins in *Taerf5 Taerf5a* mutant were eradicated.

As there are no orthologous *ERF5* genes identified in Arabidopsis, and no orthologues in cereals have been functionally characterised, the only inferred function may be based on functional protein domain homology to Arabidopsis ERF proteins of subgroup IXb. Subgroup IXb of ERFs includes six members: *AtERF102* (*At5g47230*), also known as *ERF5*, *AtERF103* (*At4g17490*), also known as *ERF6*, *AtERF104* (*At5g61600*), *AtERF105* (*At5g51190*), *AtERF106* (*At5g07580*), known as *DEWAX2* and *AtERF107* (*At5g61590*), also known as *DEWAX* (Nakano *et al.*, 2006), and they have been mostly linked with responses to abiotic and biotic stresses. Among these, *ERF6* was shown to be involved in regulating leaf growth during drought by inhibiting cell division and expansion and did that by stabilising DELLA protein through activation of *GA2ox6* expression (Dubois *et al.*, 2013). TaERF5-RHT-1 interaction and grain-specific expression of *TaERF5* and *TaERF5a* genes leads us to believe that the genes may have a role in GA response in the aleurone. A few experiments can be performed to test if this hypothesis is true. As GA signalling in the aleurone leads to enhanced *TaAMY1* expression, α -amylase protein levels are an indication of tissue sensitivity to GA signalling. The comparison of α -amylase levels between untreated aleurones and aleurones treated with GA in the *Taerf5 Taerf5a* mutant would establish the GA sensitivity of the tissue and show if TaERF5 transcription factor is involved in regulation of GA response. The activity of α -amylase enzyme can also be relatively easily measured performing HFN assays. An RNA-Seq experiment comparing the transcriptome of WT plant and the mutant plant in response to applied GA would reveal the biological processes that are regulated by the *TaERF5/5a* genes. The phenotype of the *Taerf5 Taerf5a* grain could also be assessed, to establish whether they have a role in controlling grain development.

In summary, the CRISPR/Cas9 system using sgRNA multiplexing was successfully used to introduce out-of-frame mutations in six genes in wheat.

Deletions were the predominant INDELS found, and biallelic mutations more frequently observed than monoallelic. Somatic mutations in T0 were incorporated into germplines and stably passed on to T1 and T2 generations. Our results show that the tRNA-processing system-based strategy is a robust and efficient tool for multiple targeted genome modification in wheat. Although using CRISPR/Cas9 in wheat genome editing has now been reported for several years, this is the first study describing successful editing of six genes simultaneously.

Chapter 6: General discussion

6.1 Project summary

DELLA proteins are master negative regulators of GA-induced responses. They act by activating or inhibiting the expression of target genes, through physical association and regulation of many proteins, including different classes of transcription factors (Davière & Achard, 2016; Thomas *et al.*, 2016). Although much research in the field of GA synthesis and early signalling has been validated in cereals (Hedden, 2020; Hedden & Sponsel, 2015), the majority of studies reporting functional genetic studies of DELLA interacting partners have been undertaken in Arabidopsis, and only some in rice. Wheat is a hexaploid monocot thus the research from dicot or diploid species are not always fully applicable to wheat. Recent advances in reverse genetics techniques allowing for efficient generation of knockout lines in polyploid plants, like CRISPR/Cas genome editing, and the release of the fully annotated wheat genome (International Wheat Genome Sequencing Consortium (IWGSC) *et al.*, 2018) make genetic studies in wheat more feasible, and therefore more common.

The aim of this study was to identify novel components of GA signalling interacting with RHT-1 in the wheat aleurone and elucidate their role in regulating the GA response. Among many putative DIPs, transcription factors were of special focus. Few different transcription factor families were identified as putative RHT-D1 interactors. ERFs and zinc finger TFs, including IDD TFs, were the largest groups, but a few bHLH, MYB, NAC and bZIP TFs were too identified as putative DIPs. PPI studies were validated *in planta* and revealed that RHT-D1 interacts with proteins identified as TaERF5 and TaIDD11.

Phylogenetic analysis revealed that a close paralogue of *TaERF5*, *TaERF5a*, is encoded in wheat genome. *TaIDD11* is present as a single copy gene in each genome. Reverse genetics approaches were used to generate knockout mutants in wheat that would serve to analyse the role of the identified DIPs in regulating GA responses. CRISPR/Cas9 was applied to generate *Taerf5* *Taerf5a*

line, and stable, heritable, out-of-frame mutations were introduced in all six genes targeted. The lines were shown to be Cas9-free and are awaiting phenotypic analysis. *Taidd11* mutant was generated using TILLING. Protein sequence analysis of the TaIDD11 proteins showed that the EMS mutations selected to be crossed in triple knockout mutant are positioned such that the truncated proteins will lack domains necessary for gene activation and repression and are therefore considered invalid.

Phenotypic analysis of the *Taidd11* mutant was performed on BC₁F₃ plants. Compared to WT Cadenza plants, mutant plants showed decrease in stem and leaf elongation, delayed flowering, and decreased seed number. The mutant showed to be completely GA-insensitive, which was validated by GA-dose response assays and analysis of transcriptome change between the untreated and GA₃-treated seedlings. Moreover, like another GA-insensitive semi-dwarf line, *Rht-D1b*, the *Taidd11* mutant was shown to accumulate bioactive GA₁ through increased regulation of GA homeostasis feedback genes *TaGA20ox2*, *TaGA3ox1* and *TaGID1b*.

6.2 The roles of IDD proteins in plants

The IDD gene family is a plant-specific class of zinc finger (ZF) transcription factors. All IDD genes share a conserved DNA-binding ID domain that was first characterised in maize (*Zea mays*) *INDETERMINATE1* gene, *ID1* (Kozaki *et al.*, 2004). The IDD gene families have been identified in species like Arabidopsis, rice, maize, cotton and apple (Ali *et al.*, 2019; Colasanti *et al.*, 2006; Fan *et al.*, 2017; Kozaki *et al.*, 2004). Majority of functional studies on IDD proteins come from studies conducted in Arabidopsis (reviewed in Coelho *et al.*, (2018) and Kumar *et al.*, (2019)). When it comes to cereal crop species, the biggest number of IDD proteins have been characterised in rice (Deng *et al.*, 2017; Dou *et al.*, 2016; Huang *et al.*, 2018; Wu *et al.*, 2008; Wu *et al.*, 2013; Xuan *et al.*, 2013, 2018), some in maize (Colasanti *et al.*, 1998, 2006; Gontarek *et al.*, 2016),

and one in barley (Jöst *et al.*, 2016). No IDD protein has been characterised in wheat so far.

The IDD family of transcription factors include 16 members in Arabidopsis and 15 in rice (Colasanti *et al.*, 2006) (Supplementary Table 3.2) while in our study, 14 distinct *IDD* genes were identified in wheat (Chapter 3 Section 3.3.3.2). Due to the divergence times between dicots and monocots, one-to-one orthologous relationships between Arabidopsis and cereal *IDD* genes cannot be determined, however, given the similar number of members in *IDD* families in Arabidopsis and grasses, it is possible that many of *IDD* genes control similar developmental processes in both (Coelho *et al.*, 2018). Based on phylogenetic evidence, Colasanti *et al.* (2006) identified four groups in Arabidopsis *IDD* family: group A (*AtIDD14*, *15*, and *16*), group B (*AtIDD1* and *2*), group C (*AtIDD9*, *10*, *12*, and *13*), and group D (*AtIDD4*, *5*, *6*, *7*, and *11*). *AtIDD3* and *AtIDD8* were not included in any of these groups. In our study, the TaIDD11 identified as the RHT-1 interactor, and TaIDD12 protein clustered with the B group of Arabidopsis *IDDs* (Chapter 3, Figure 3.10).

The originally identified *ID1* gene in maize was identified as a regulator of flowering time. Maize *id1* plants cannot undergo a normal transition to flowering; they continue to produce leaves long after the WT plants have flowered, and when they eventually do flower, the floral structures are aberrant with vegetative characteristics (Colasanti & Sundaresan, 2000; Singleton, 1946). In rice, the *ZmID1* ortholog, *OsID1* (*EARLY HEADING DATE2*, *EHD2*), also show extremely late flowering under both short and long-day conditions, suggesting a pivotal role for *EHD2* in floral transition (Matsubara *et al.*, 2008). It was found that overexpression of *OsIDD1*, *OsIDD6* or *SID1* (*Suppressor of rid1*), another *IDD* gene, is sufficient to partially rescue the late-flowering phenotype of *rid1* (*Rice Indeterminate 1*), implying functional redundancy between the *IDD* family members (Deng *et al.*, 2017). Another *IDD* transcription factor, *AtIDD8* (*NUTCRACKER*, *NUC*) seems to be involved in flowering. *AtIDD8* regulates photoperiodic flowering by modulating sugar transport and metabolism, as it was shown to regulate expression of sucrose

transporter genes *SUC2* and *SUC6*, and sucrose synthase genes *SUC7*, *SUC8*, *SUS1* and *SUS4*. Vegetative-to-reproductive phase transition is significantly delayed in *idd8*, but AtIDD8 regulates flowering primarily by modulating the reproductive phase change, which is distinct from ID1, which affects both vegetative and reproductive phase changes (Seo *et al.*, 2011).

Rice OsIDD2 is also involved in sugar metabolism. OsIDD2 negatively regulates the expression of genes involved in lignin biosynthesis, *cinnamyl alcohol dehydrogenase 2* and *3* (*CAD2* and *3*) and sucrose synthesis, *sucrose synthase 5* (*SUS5*). This regulation results in defects in secondary cell wall formation and subsequent dwarf phenotype (Huang *et al.*, 2018). In a separate study, OsIDD2 was identified to physically interact with SLR1, the rice DELLA, as a complex bind to the promoter, and regulating the expression of OsmiR396a (Lu *et al.*, 2020). The OsIDD2 overexpression lines displayed dwarfism, and the RNA interference lines, OsIDD2RNAi, in which the function of the OsIDD2 has been knocked down, showed a phenotype resembling *slr1*. There are therefore two separate studies reporting OsIDD2 involvement in stem elongation.

ZmID1 paralogs in maize, *ZmIDDveg9* (*NKD1*) and *ZmIDD9* (*NKD2*) are involved in regulating cell decision controlling aleurone cell layer number. The *nkd* mutants have multiple layers of peripheral endosperm cells that lack starch granules, or any other characteristic features of starchy endosperm. Interestingly, they only sporadically show the characteristics of the aleurone cells, which led to the conclusion that both NKDs are required for proper endosperm periphery cell fate specification and cell differentiation (Yi *et al.*, 2015). Another evidence supporting the involvement of *NKD1* and *NKD2* in cell division and differentiation is differential expression of genes involved in cell cycle processes, like *tubulin1*, *cell division cycle2-like*, *actin-1*, and *proliferating cell nuclear antigen2* in the aleurone layer of the double mutant (Gontarek *et al.*, 2016). The *nkd1* and *nkd2* mutants also have decreased total grain weight and germination rates, delayed anthesis, and tendency for vivipary (Gontarek *et al.*, 2016; Yi *et al.*, 2015).

AtIDD10 (JACKDAW) is required for correct expression of *GLABARA 2* (*GL2*), *CAPRICE* (*CPC*) and *WEREWOLF* (*WER*), transcription factors that interact to specify hair cell and non-hair cell identity of the epidermal layer in Arabidopsis. JACKDAW (JKD) has been proposed to act upstream of root hair network TFs and prevent the non-hair cell fate in the hair cell position (Hassan *et al.*, 2010). JKD also promotes *SCARECROW* (*SCR*) transcription and SHORT-ROOT (*SHR*) nuclear localisation in the quiescent centre and prevents excessive SHR-SCR-mediated asymmetric cell division to regulate cell type specification. In the ground tissue, JKD restricts SHR action by counteracting MAGPIE (*MGP*)-dependent cell division-promoting activity (Welch *et al.*, 2007). MAGPIE is another member of the IDD family, and together with JKD it regulates tissue boundaries and asymmetric cell division. It was also hypothesized that IDD proteins might mediate the activity of SHR/SCR in C4 bundle-sheath differentiation (Slewinski, 2013). Recently, the putative binding sequence in the *SCR* promoter to which JKD binds to was identified (Kobayashi *et al.*, 2017). Another function of IDD TFs in roots is ammonium uptake and nitrogen metabolism. OsIDD10 in rice, *Os04g47860*, was found to activate transcription of ammonium transporter *ATM1;2*, and to induce several genes involved in nitrogen-linked cellular and metabolic responses, including *glutamine synthetase 2*, nitrite reductases and *trehalose-6-phosphate synthase* (Xuan *et al.*, 2013).

Arabidopsis *AtIDD14*, *AtIDD15* and *AtIDD16*, and rice *OsIDD12*, *OsIDD13* and *OsIDD14*, are clearly divergent from the other *IDD* genes and form a distinct group relative to other sequences. This subfamily of the *IDD* family regulates auxin signalling by activating expression of some auxin biosynthesis and transport genes, such as *YUCCA5* (*YUC5*), *TRYPTOPHAN AMINOTRANSFERASE of ARABIDOPSIS1* (*TAA1*) and *PIN1*, and thus regulate aerial organ morphogenesis and gravitropic responses (Cui *et al.*, 2013). *IDD14* and *IDD16* act redundantly to regulate the morphology of aerial organs and fertility, and *IDD15* with *IDD16* control the gravitropic responses and plant architecture. *AtIDD15/SHOOT GRAVITROPISM5* (*SGR5*) gene function in gravity sensing and

amyloplasts in the shoot endodermis of *sgr5* sediment more slowly than in WT plants (Tanimoto *et al.*, 2008). These results suggest that this subfamily of IDD proteins may act as intermediates in hormone signalling that regulate starch metabolism to coordinate gravitropism and morphogenesis. Closely related gene in barley, *BROAD LEAF1 (BLF1)*, also acts to affect leaf morphogenesis by restricting cell proliferation in the width direction (Jöst *et al.*, 2016). *BLF1* is also expressed in the inflorescence meristem, indicating a similar function for the gene in floral development. Five Arabidopsis IDD genes, including *IDD15* and *IDD16*, have been found to be upregulated during flower differentiation, and in maize, *ZmIDD-p1* and *ZmIDD16/LOOSE PLANT ARCHITECTURE 1 (LPA1)* are the targets of the inflorescence regulatory genes *RAMOSA1 (RA1)* and *KNOTTED1 (KN1)* (Eveland *et al.*, 2014; Mantegazza *et al.*, 2014). These findings suggest that IDD proteins are involved in regulation of inflorescence and leaf boundary decisions.

IDD proteins have also been found to have a role in seed maturation and germination. *AtIDD1 (ENY)* positively regulates GA responses. Feurtado and colleagues (2011) found that overexpression of *ENY* affected many developmental processes, including fertility, seed development, germination and seedling establishment (Feurtado *et al.*, 2011). A delay in senescence of the seed coat and depletion of the endosperm, which resulted in enlarged endosperm and thus bigger grain was observed in the *ENY* overexpression lines. The increase in endosperm size was shown to result from increase in a cell number, which was caused by increased rate of cell division, a process regulated by GAs. *ENY* also positively regulates germination. *ENY* was found to regulate a high proportion of genes regulated also by red light and PIFs, and the overexpression lines were less sensitive to germination inhibition by FR light (Feurtado *et al.*, 2011). A close homolog of *AtIDD1* in Arabidopsis, *AtIDD2 (GAF1)*, was too found to be involved in the process of germination. The expression of the mutant version of *GAF1*, which cannot bind to *GAI*, rescues the germination phenotype of *ga1-3* (Fukazawa *et al.*, 2014). *GAF1* was also

found to be regulating flowering, hypocotyl length, and growth (Fukazawa *et al.*, 2014).

Recently, the IDD proteins have been linked to biotic stress responses (Sun *et al.*, 2020; Völz *et al.*, 2019). AtIDD4 was identified to have a role in plant growth and resistance to the pathogen *Pseudomonas syringae*, as the *idd4* mutant showed increased growth and reduced susceptibility to the pathogen. The *idd4* mutant expression levels of genes involved in salicylic acid biosynthesis, immunity response, and early-defence marker genes *FLG22-INDUCED RECEPTOR-LIKE KINASE 1* and *WRK22* were significantly higher. In contrast, the overexpression of IDD4 caused reduction of the defence-related genes like *WRKY38*, *PR5*, *ERF4* and *ERF5*. In addition, due to the lower levels of H₂O₂-scavenging enzymes and enhanced expression of H₂O₂ metabolism genes, the *idd4* mutant accumulated the H₂O₂, which resulted in enhanced resistance to biotrophic pathogens (Völz *et al.*, 2019). In the same study the comparison of the CHIP-SEQ data with the differentially expressed genes (DEGs) identified in the transcriptome analysis of the *idd4* and *IDD4ox* plants, yielded many genes, including *AP2C1*, *CPK28*, *CAF1* and *SERK1*, indicating IDD4 as a direct regulator of immunity-related genes. Another study identified differential expression of several IDD genes, including *IDD3*, *IDD5*, *IDD10* and *IDD13*, upon *Rhizoctonia solani* infection in rice. *R. solani* causes sheath blight disease (ShB) in rice, which can account for up to 50% yield reduction. *IDD5* was downregulated whereas the other three IDD genes were upregulated. Of these, *IDD3* and *IDD13* were found to interact with another IDD protein, LOOSE PLANT ARCHITECTURE 1 (LPA1), which was previously shown to promote the resistance to ShB by activating the *PIN1a* gene (Sun *et al.*, 2019). After detailed analysis, *IDD3* and *IDD13* were both found to bind to the *PIN1a* promoter and negatively and positively regulate resistance to ShB, respectively (Sun *et al.*, 2020).

In summary, IDD proteins are involved in many developmental processes in plants and they seem to act through regulation of hormonal pathways. So far, their involvement has been proven in GA, ABA and auxin hormonal signalling

controlling processes like flowering, cell differentiation and proliferation, gravitropism, starch metabolism and seed germination.

6.3 IDD TFs interact with GRAS family protein members to regulate expression of genes involved in GA-regulated processes

TFs regulate gene expression by recognising and binding to specific sequences in the target genes promoters. They often work in complexes with other TFs or proteins acting as transcriptional regulators, and may regulate many distinct target genes, depending on the interacting partner (Aoyanagi *et al.*, 2020). Often, members of the same TF family interact with common interacting partners to regulate the same target genes, thus showing functional redundancy (Wray, 2003). In recent years multiple IDD proteins were identified to interact with GRAS proteins to regulate gene expression (Aoyanagi *et al.*, 2020; Feurtado *et al.*, 2011; Fukazawa *et al.*, 2014, 2017; Lu *et al.*, 2020; Welch *et al.*, 2007; Yoshida *et al.*, 2014; Yoshida & Ueguchi-Tanaka, 2014). As GRAS proteins are known transcriptional regulators and no known DNA-binding motifs have been identified in their structures, IDDs provide the links between GRAS proteins and GRAS-regulated genes promoters.

One such example was identified by Welch *et al.* (2007) in *Arabidopsis*. JKD (AtIDD10) was shown to be required for radial patterning and stem cell niche maintenance, and its activity was counteracted by MGP (AtIDD3). The two IDD proteins were found to interact and form complexes with SHR and SCR, GRAS proteins known to regulate specification of the quiescent centre (QC) and ground tissue identity in the root. Interestingly, the interactions of JKD and MGP with SHR and SCR were identified to occur via the ZF domains of the INDETERMINATE domain. JKD and MGP were shown to regulate a range of SHR action in the cells where they are transcribed. JKD was also found to promote SCR transcription and control nuclear localisation of SHR in the QC mostly by

maintaining *SCR* expression. In QC it acted to regulate cell type specification and stable boundary formation by counteracting the occurrence of supernumerary SHR-*SCR*-mediated asymmetric cell divisions. In ground tissue, *JKD* restricted SHR action by counteracting MGP-mediated cell-division activity. The model was proposed where MGP, which was shown to act redundantly probably with some other IDD protein, is a part of the SHR-*SCR* complex and facilitates the asymmetric cell division-promoting activity. *JKD* was proposed to inhibit this activity by either competing for binding on the SHR-*SCR* complex or by interactions within the complex already containing MGP (Welch *et al.*, 2007). Organising tissues during root development has been shown to be synergistically regulated by GA and ABA hormones (reviewed in Choi & Lim, 2016). What is more, in the meristem zone, *SCL3*, a positive regulator of GA signalling (Zhang *et al.*, 2011), was shown to work in conjunction with SHR-*SCR* to control GA-modulated ground tissue maturation (Heo *et al.*, 2011). It is therefore possible that *JKD* and MGP regulation of SHR-*SCR* complex might be a part of DELLA-*SCL3* regulated GA signalling during the root development.

Another example of IDD-GRAS protein-regulated gene expression comes from the Y2H screen performed by Yoshida *et al.* (2014). Screen for TFs through which DELLA regulates transcription of *SCL3* gene revealed five different IDD proteins to be DIPs. Interestingly *AtIDD3*, 4, 5, 9 and 10 were identified to bind to GRAS domains of not only RGA, but also their target gene product, *SCL3*. More detailed interaction studies using *AtIDD3* as a representative showed that the interaction with both RGA and *SCL3* was mediated by MSATALLQKAA and TRDFLG motifs, with only the latter being sufficient for the interaction. In the GRAS domain, LRI domain was essential, but not sufficient for the interaction with *AtIDD3*. Yeast three-hybrid studies revealed competitive nature of DELLA and *SCL3* binding to *AtIDD3*. Based on these results a feedback-loop model was proposed (Figure 6.1 A) in which DELLA and *SCL3* compete for IDD TF binding to regulate GA signalling, e.g. expression of *SCL3*.

One of the group B IDD TFs, ENY, studied in the context of seed maturation and germination, was identified to interact with all five DELLAs in Arabidopsis (Feurtado *et al.*, 2011). ENY protein was shown to negatively affect expression of GA homeostasis feedback genes and upregulate the expression of feedforward genes. Given its interaction with DELLAs, and opposing regulatory effects of ENY compared to DELLA, it was proposed that the ENY-DELLA relationship resembles the antagonistic relationship of DELLA-SCL3. A model of ENY-DELLA interaction was proposed (Figure 6.1 B). ENY function was hypothesized to be promotion of GA-associated responses and repression of a subset of ABA responses through modulation of DELLA activity. The second representative of Arabidopsis IDD TFs group B, GAF1, was shown to interact with GRAS proteins to regulate GA homeostasis (Fukazawa *et al.*, 2014). In this study, GAF1 interacted with all Arabidopsis DELLAs and the motif responsible for GAF1 binding was elucidated to be the SAW motif of the GRAS domain. The domain of GAF1 that was responsible for DELLA binding was established to be the so-called PAM domain, 16 amino acids that include the MSATALLQKAA motif. Fukazawa *et al.* (2014) noticed that both intact GAF1 and Δ PAM (GAF1 including internal deletion of 16 amino acids containing MSATALLQKAA domain; Δ PAM cannot bind to DELLA) suppress the dwarf phenotypes of *ga1-3* and *gai-1*. Based on these results they hypothesized that GAF1 may play a role in promoting plant growth after DELLAs are degraded. Indeed, they identified TPR1 and TPR4 transcriptional corepressors as GAF1 interacting partners that in complex with GAF1 play opposite roles to the one of GAF1-GAI complex upon the GA treatment. The interaction between GAF1 and TPR4 was found to be mediated by the EAR motif. Δ EAR (GAF1 missing the EAR motif) was not able to interact with TPR4 but did not affect GAI binding. Similarly, Δ PAM could not bind GAI, but did bind TPR4, which showed that GAF1 uses different domains for interaction with its coactivator and corepressor. GAF1 together with GAI, but not on their own, greatly affected the expression of *AtGA20ox2* gene, a putative GAF1 target. Δ PAM together with GAI did not activate the gene, suggesting that GAF1-GAI interaction is essential for gene activation. The activation was also disrupted under GA treatment. Similar scenario was

observed with TPR4, which together with GAF1 repressed the expression of the target gene, but when Δ EAR affected the interaction with TPR4, no repression was observed. All GAF1, GAI and TPR4 were found to bind to *AtGA20ox2* promoter, indicating that GAI and TPR4 act as coactivator and corepressor of GAF1-regulated gene activation, respectively. Besides *AtGA20ox2* gene, GAF1-GAI complex activated promoters of *AtGA3ox1* and *GID1b* genes, which are involved in feedback regulation of GA biosynthesis. The model was therefore proposed (Figure 6.1 C) in which DELLAs act as coactivators of GAF1 to positively regulate expression of GA biosynthetic and signalling genes. Upon GA perception, DELLAs are degraded and the target genes are repressed by GAF1-TPR complex. Recently, SCL3 was identified to inhibit transcriptional activity of GAF1-RGA complex (Ito & Fukazawa, 2021). Although GAF1 was shown to bind to SCL3 and enhance its repressive activity, the inhibition of GAF1-RGA activity by SCL3 was not by inhibiting the interaction between GAF1 and RGA. Instead GAF1, RGA and SCL3 were found to form ternary complex, which was hypothesized to affect the activity of GAF1-RGA complex (Ito & Fukazawa, 2021).

In his study, Fukazawa *et al.* (2014) hypothesized that GAF1-DELLA complex role in growth inhibition might be via regulation of growth repressor expression. Recent study in rice has identified OsIDD2-SLR1 complex that activates expression of OsmiR396 (Lu *et al.*, 2020), microRNA that post-transcriptionally regulates transcript levels of *OsGRF* genes, GA-responsive TFs involved in stem elongation. The region of OsIDD2 elucidated to be responsible for SLR1 binding was located between ID-domain and MSATALLQKAA motif and contained no apparent conserved motifs required for interaction. Thus, the relatively conserved regions of MSTALLQKAA and TRDFLG were shown not to be necessary for the interaction with SLR1. Another example of GA-activated genes transcript levels by miRNA is regulation of *GAMYB* by miRNA159 (Tsuji *et al.*, 2006). The transcript levels of miR159, however, were not found to be controlled by GAs, which shows the variety of mechanisms that exist to regulate hormonal signalling pathways in plants.

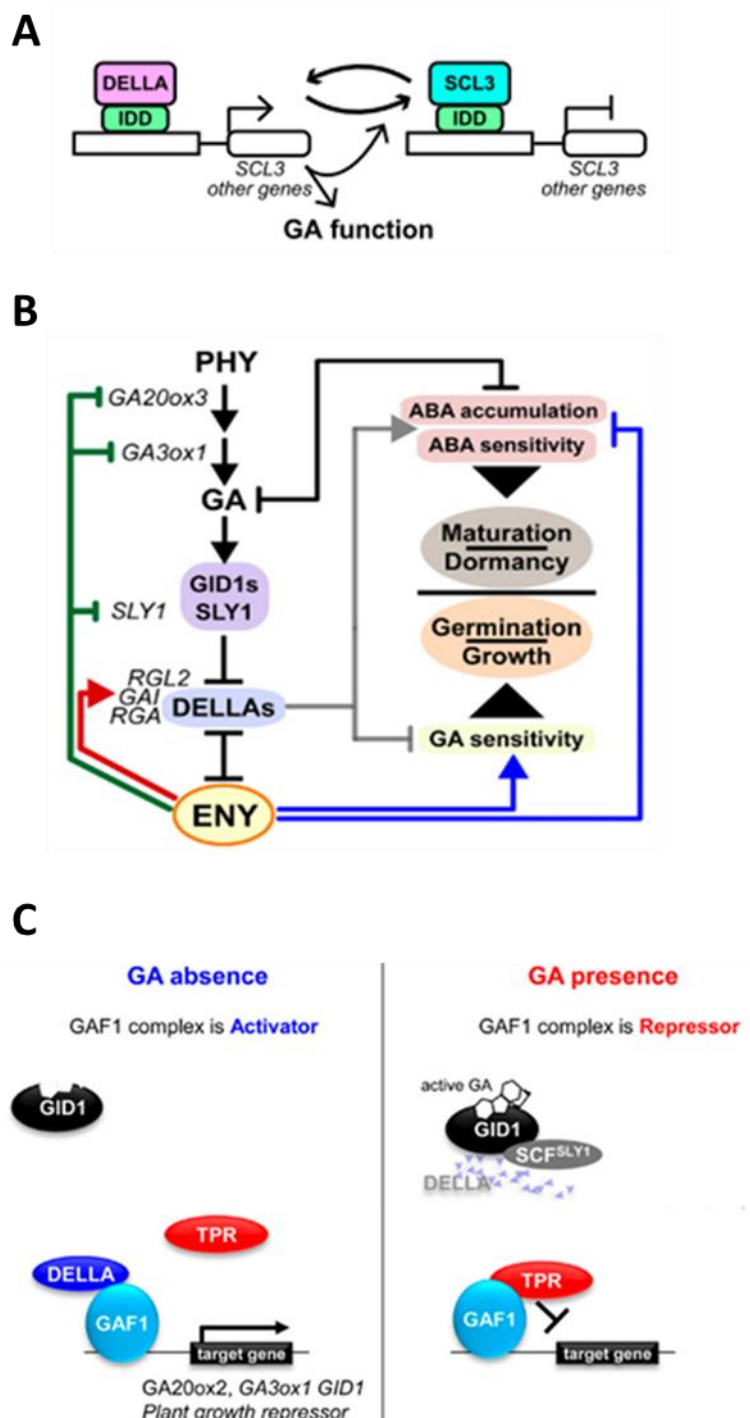


Figure 6. 1 IDD proteins interact with GRAS proteins to regulate expression of genes involved in regulating GA-responses. A. GA feedback regulation mediated by DELLA, SCL3 and IDD TFs. DELLA activates the expression of target genes, including SCL3, through IDD-mediated interaction with the target genes promoters. The subsequent increase in SCL3 protein level favours IDD-SCL3 complex formation and consequent suppression of SCL3 expression. Adapted from Yoshida et al. (2014). B. ENY increases

GA sensitivity while decreasing ABA sensitivity and accumulation to promote germination, partially through modulation of DELLA activity. ENY also regulates GA feedback genes, which result in downregulation of GA synthesis and signalling and upregulation of DELLAs transcripts. The blue lines indicate that ENY may also directly regulate the GA and ABA response. Adapted from Feurtado et al. (2011). C. GAF1 regulates gene expression by working with DELLA as a coactivator or TPR proteins as corepressors. Under GA-deficient conditions, DELLA proteins are stable and show high transcriptional activity with GAF1. In the presence of GA, DELLAs are degraded via the 26S proteasome pathway and GAF1-TPR complex is formed. TPR acts as GAF1 corepressor and thus GAF1 exhibits transcriptional repression activity. Adapted from Fukazawa et al. (2014).

Although IDD-GRAS-mediated gene regulation has been a subject of interest in recent years there has been a lack of studies on the properties of IDD proteins as TFs. Recent study by Aoyanagi *et al.* (2020) focused on elucidating the biochemical properties of the IDD family of TFs. Representatives of all four groups were chosen for the analysis: AtIDD15 and 16 (group A), AtIDD1 (group B), AtIDD10 (group C) and AtIDD6 (group D), and their ability to bind to GRAS proteins: SHR, SCL3, the five Arabidopsis DELLAs and rice SLR1, was investigated. The IDD proteins were additionally assessed for the potential of forming homo- or heterodimers. The results revealed the distinct PPI characteristics of different IDD clades. IDDs from group A were the only ones that showed no interaction with any of the GRAS proteins; at the same time only these IDDs showed evidence of dimerization, which was not seen for any other group members. AtIDD6 did not show to bind SCL3, RGL3 and SLR1 while AtIDD10 showed no interaction with RGL2 and RGL3. AtIDD1 interacted with all GRAS proteins, even with rice SLR1. The study also investigated transcriptional activities of different IDD-GRAS protein complexes on activation of target gene promoters. In brief, RGA and SHR-SCR acted as coactivators for AtIDD1- and AtIDD10-mediated activation of *SCR*, *SCL* and *GA3ox1* promoters, but had no additional effect on activation of the promoters

of *PIN1* and *YUC5*, genes regulated by group A of IDD s (Cui *et al.*, 2013). AtIDD6, 15 and 16 did not seem to use GRAS proteins as coactivators which is in line with the observation that they do not interact. AtIDD6 however, did interact with both RGA and SHR, but did not utilise them as coactivators, which was suggested to be caused by lack of PAM motif in AtIDD6 structure (Aoyanagi *et al.*, 2020).

In summary, there is enough evidence to link IDD TFs to DELLA- and SCL3-mediated regulation of GA signalling. The IDD family is not a big one; it has only 16 members in Arabidopsis, 15 in rice and 14 putative members in wheat. However, the multitude of PPI motifs in IDD s structure, different modes of regulation, and numerous target genes allow IDD TFs to regulate many responses in plants.

6.3.1 TaIDD11 interacts with RHT-1 and is a positive regulator of GA signalling

The TaIDD11 wheat proteins show highest sequence homology to Arabidopsis ENY and GAF1. Even though the wheat and Arabidopsis IDD proteins differ much in length and overall structure, they contain the same conserved functional domains, INDETERMINATE DNA-binding domain, M/ISTALLQKAA and TRDFLG, and also the EAR motif, which is known to be responsible for transcriptional repression (Kagale & Rozwadowski, 2010) and is present only in these two IDD proteins within the Arabidopsis IDD family (Fukazawa *et al.*, 2014). Based on the sequence homology, altered GA-homeostasis gene expression in *RAB18:ENY* (*ENY* overexpression lines) and *Taidd11* mutants, and phenotypes of the *gaf1 idd1* and *Taidd11* mutants (delayed flowering, reduction in stem length, GA-insensitivity) it can be hypothesized that TaIDD11 role in wheat is similar to the one of the two IDD s in Arabidopsis.

ENY and GAF1 were proposed to play redundant roles (Fukazawa *et al.*, 2014). In Arabidopsis, *ENY* is expressed mainly in seeds and its expression increases with maturation, while *GAF1* is expressed mainly in the vegetative tissues

(Feurtado *et al.*, 2011; Fukazawa *et al.*, 2014). *ENY* was shown to regulate GA and ABA sensitivity during maturation and germination, and hence promote germination (Feurtado *et al.*, 2011). Assessing the phenotype of *gaf1 idd1* and *GAF1* overexpressor lines revealed that *GAF1* positively regulates plant size, transition to flowering and GA response (Fukazawa *et al.*, 2014). Phylogenetic analysis showed presence of another wheat IDD protein in the same clade as *TaIDD11*, *TaIDD12*, that may act redundantly, depending on the tissue. *TaIDD11*, like *GAF1*, shows slightly higher expression in vegetative tissues (Chapter 4, Figure 4.2), whereas the *TaIDD12* is, like *ENY*, expressed slightly higher in the mature grains (Supplementary Figure 6.1). Few observations in our study show that *TaIDD11* is a positive regulator of GA responses (Chapter 4, Section 4.3.3). Firstly, the lack of GA responsiveness in the *Taidd11* clearly indicates that it is involved in GA signalling. Secondly, the phenotype of the knockout mutant shows characteristics of GA-deficient or GA-insensitive plant, i.e. reduced growth, delayed flowering, reduced seed number. Thirdly, enhanced expression of GA biosynthetic genes and resulting bioactive GA accumulation clearly indicates that the mutant is deficient in GA signalling. And finally, *TaIDD11* interacts with *RHT-1*, the master regulator of GA signalling, which indicates that the effect of *RHT-1* on gene expression is mediated via *TaIDD11*.

Similar phenotype and expression of GA homeostasis-regulating genes between *Taidd11* and *Rht-D1b*, a mutant that accumulates viable DELLA protein, suggests that *TaIDD11* and *RHT-1* have opposite effects on GA signalling. The fact that the proteins interact directly might suggest that either *TaIDD11* acts as *RHT-1* suppressor or *RHT-1* acts as *TaIDD11* suppressor. Both would support similar phenotypes and gene expression patterns observed in *Taidd11* and *Rht-D1b* mutants. *IDDs*, however, have been described as TFs through which *DELLAs* bind to target gene promoters to activate expression (Fukazawa *et al.*, 2014; Lu *et al.*, 2020; Yoshida *et al.*, 2014). Thus, alternatively, *RHT-1* might act as a *TaIDD11* coactivator, but the significance of this coactivation would be expression of genes that negatively regulate GA

responses. If this model was true, the observed upregulation of GA biosynthesis genes in the *Taidd11* mutant might be an indirect effect to compensate for reduction in perceived GA signalling. TaIDD11 also has a motif for binding a repressor, and assuming it does bind one, the TaIDD11-corepressor complex would inhibit expression of genes having a negative effect on GA-regulated processes. Thus, the gene regulation mediated by TaIDD11 may rely on the corepressor/coactivator status. Upon GA perception, RHT-1 would be degraded, favouring TaIDD11-corepressor activity.

This study is a first attempt to analyse the function of IDD family members in wheat. The results gathered here show that TaIDD11 is involved in GA signalling and controls GA-regulated processes by directly binding to RHT-1. In order to elucidate the mechanism of action of the TaIDD11 transcription factor in regulating gene expression, more studies need to be done. Revealing the target genes of TaIDD11 would show if the TF is involved in activation of the genes responsible for repression of GA responses. It is essential to reveal if the TaIDD11-RHT-1 complex assembles on target gene promoters and activates them directly. Studying a corepressor (possibly TPR) binding ability of TaIDD11 and determining the effect on target genes promoters would shed more light on the mechanism of action. It would also be beneficial to analyse *Taidd11* mutant produced by a “cleaner” method, e.g. CRISPR/Cas, which would be free of background mutations and in which no conserved domains are present, as well as to analyse the *Taidd11 Rht-D1b* mutant and establish the redundancy between TaIDD11 and TaIDD12 proteins.

6.4 *TaIDD11* gene has the potential to uncouple pleiotropic effects of *Rht* semi-dwarfing alleles

The yield increases in wheat during the Green Revolution are partly attributed to intensification of agronomic practices, i.e. applying large amounts of fertilizers and pesticides, but could not be achieved without introduction of varieties containing *Rht* dwarfing genes (Hedden, 2003). *Rht* semi-dwarfing

alleles that have been most widely utilized in wheat breeding programmes ever since are *Rht-B1b* and *Rht-D1b*, and are estimated to be present in approximately 70% of all modern wheat varieties (Evans, 1998). In standard varieties, high nitrogen regimes result in excessive stem elongation which makes the crop susceptible to lodging under environmental conditions. *Rht-1* alleles have been successful because the plants into which they are introduced have shorter stems that do not excessively elongate and are resistant to lodging even when fertilisers are applied. Additionally, the reduced stature allows for increased partitioning of photosynthates to the grain, which reduces pre-anthesis abortion of distal florets, increasing the total number of viable florets at anthesis, which results in increased grain number (Youssefian *et al.*, 1992). Altogether, the effects of these alleles allow for big increases in wheat grain yield. However, the alleles also carry pleiotropic effects, which in some cases may have a negative influence on plant development (summarized in Rafter, 2019). The reduced cell elongation in *Rht-1* lines negatively impacts seedling emergence when deep-sowing practices are in use (Rebetzke & Richards, 1999), delayed sowing time reduces grain yield (Balyan & Singh, 1994), the seeds, even though increased in numbers, are smaller and their weight is reduced (Flintham *et al.*, 1997). With the ever-growing population to feed and the climate change predicted to cause more frequent outbreaks of increased heat and drought in the UK (<https://www.metoffice.gov.uk>), it would be beneficial if these negative pleiotropic effects could be uncoupled so only the specific subset of DELLA-mediated responses are regulated.

Different functional domains within the GRAS domain are responsible for binding different DIPs and hence specific amino acid substitutions in the GRAS domain would provide one means to uncouple some of the individual effects and possibly limit the pleiotropic effects of DELLA (Van De Velde *et al.*, 2017). Substantial amount of work has been done trying to identify novel *Rht-1* alleles, so called 'overgrowth' (ovg) alleles in the *Rht-B1c* background (Chandler & Harding, 2013; Derkx *et al.*, 2017; Van De Velde *et al.*, 2017). In these studies, some ovg mutants were identified to increase the severe dwarf

phenotype of the *Rht-B1c* mutant but retain the yield increase and concomitantly improve the dormancy, which was speculated to have potential to reduce susceptibility to PHS. Screening for the novel mutations revealed that these ovg mutants had additional mutations within the GRAS domain that were hypothesized to alter the putative binding sites of RHT-1, which would result in reduction or inability to bind the interacting partners. However, knowing the plethora of DELLA interactions, it is more likely that the mutation in GRAS domain would modify a subset of DELLA-regulated processes rather than one or the few specific ones, and it is suggested that altering a specific DELLA-DIP interaction through targeted modification of the DIP can more effectively modify a single DELLA-regulated response (Van De Velde *et al.*, 2017). TaIDD11 is one potential DIP that could be altered to uncouple some of the DELLA pleiotropic effects. This study is the initial functional characterisation of the TaIDD11 protein, and more studies need to be performed to reveal the full potential of the gene as a novel dwarfing allele that potentially increases wheat yield.

References

- Aach, H., Bode, H., Robinson, D. G., & Graebe, J. E. (1997). *ent*-Kaurene synthase is located in proplastids of meristematic shoot tissues. *Planta*, *202*(2), 211–219. <https://doi.org/10.1007/s004250050121>
- Aach, H., Böse, G., & Graebe, J. E. (1995). *ent*-Kaurene biosynthesis in a cell-free system from wheat (*Triticum aestivum* L.) seedlings and the localisation of *ent*-kaurene synthetase in plastids of three species. *Planta*, *197*(2), 333–342. <https://doi.org/10.1007/BF00202655>
- Achard, P., Baghour, M., Chapple, A., Hedden, P., Van Der Straeten, D., Genschik, P., Moritz, T., & Harberd, N. P. (2007). The plant stress hormone ethylene controls floral transition via DELLA-dependent regulation of floral meristem-identity genes. *Proceedings of the National Academy of Sciences of the United States of America*, *104*(15), 6484–6489. <https://doi.org/10.1073/pnas.0610717104>
- Achard, P., Liao, L., Jiang, C., Desnos, T., Bartlett, J., Fu, X., & Harberd, N. P. (2007). DELLAs contribute to plant photomorphogenesis. *Plant Physiology*, *143*(3), 1163–1172. <https://doi.org/10.1104/pp.106.092254>
- Achard, P., Vriezen, W. H., Van Der Straeten, D., & Harberd, N. P. (2003). Ethylene regulates arabidopsis development via the modulation of DELLA protein growth repressor function. *The Plant Cell*, *15*(12), 2816–2825. <https://doi.org/10.1105/tpc.015685>
- Addisu, M., Snape, J. W., Simmonds, J. R., & Gooding, M. J. (2010). Effects of reduced height (*Rht*) and photoperiod insensitivity (*Ppd*) alleles on yield of wheat in contrasting production systems. *Euphytica*, *172*(2), 169–181. <https://doi.org/10.1007/s10681-009-0025-2>
- Afgan, E., Baker, D., Batut, B., Van Den Beek, M., Bouvier, D., Ech, M., Chilton, J., Clements, D., Coraor, N., Grüning, B. A., Guerler, A., Hillman-Jackson, J., Hiltemann, S., Jalili, V., Rasche, H., Soranzo, N., Goecks, J., Taylor, J., Nekrutenko, A., & Blankenberg, D. (2018). The Galaxy platform for accessible, reproducible and collaborative biomedical analyses: 2018 update. *Nucleic Acids Research*, *46*(W1), W537–W544. <https://doi.org/10.1093/nar/gky379>
- Alabadí, D., Gil, J., Blázquez, M. A., & García-Martínez, J. L. (2004). Gibberellins repress photomorphogenesis in darkness. *Plant Physiology*, *134*(3), 1050–1057.

<https://doi.org/10.1104/pp.103.035451>

- Ali, A., Cao, J., Jiang, H., Chang, C., Zhang, H.-P., Sheikh, S. W., Shah, L., & Ma, C. (2019). Unraveling molecular and genetic studies of wheat (*Triticum aestivum* L.) resistance against factors causing pre-harvest sprouting. *Agronomy*, *9*(3). <https://doi.org/10.3390/agronomy9030117>
- Ali, F., Qanmber, G., Li, Y., Ma, S., Lu, L., Yang, Z., Wang, Z., & Li, F. (2019). Genome-wide identification of Gossypium *INDETERMINATE DOMAIN* genes and their expression profiles in ovule development and abiotic stress responses. *Journal of Cotton Research*, *2*(1), 1–16. <https://doi.org/10.1186/s42397-019-0021-6>
- Allen, M. D., Yamasaki, K., Ohme-Takagi, M., Tatenno, M., & Suzuki, M. (1998). A novel mode of DNA recognition by a β -sheet revealed by the solution structure of the GCC-box binding domain in complex with DNA. *EMBO Journal*, *17*(18), 5484–5496. <https://doi.org/10.1093/emboj/17.18.5484>
- An, F., Zhang, X., Zhu, Z., Ji, Y., He, W., Jiang, Z., Li, M., & Guo, H. (2012). Coordinated regulation of apical hook development by gibberellins and ethylene in etiolated *Arabidopsis* seedlings. *Cell Research*, *22*(5), 915–927. <https://doi.org/10.1038/cr.2012.29>
- Anai, T. (2016). Mutant-based reverse genetics for functional genomics of non-model crops. *Advances in Plant Breeding Strategies: Breeding, Biotechnology and Molecular Tools*, *1*, 473–487. https://doi.org/10.1007/978-3-319-22521-0_16
- Aoyanagi, T., Ikeya, S., Kobayashi, A., & Kozaki, A. (2020). Gene regulation via the combination of transcription factors in the *INDETERMINATE DOMAIN* and *GRAS* families. *Genes*, *11*(6), 1–18. <https://doi.org/10.3390/genes11060613>
- Appleford, N. E. J., Evans, D. J., Lenton, J. R., Gaskin, P., Croker, S. J., Devos, K. M., Phillips, A. L., & Hedden, P. (2006). Function and transcript analysis of gibberellin-biosynthetic enzymes in wheat. *Planta*, *223*(3), 568–582. <https://doi.org/10.1007/s00425-005-0104-0>
- Appleford, N. E. J., & Lenton, J. R. (1991). Gibberellins and leaf expansion in near-isogenic wheat lines containing *Rht1* and *Rht3* dwarfing alleles. *Planta*, *183*(2), 229–236. <https://doi.org/10.1007/BF00197793>
- Appleford, N. E. J., Wilkinson, M. D., Ma, Q., Evans, D. J., Stone, M. C., Pearce, S. P., Powers, S. J., Thomas, S. G., Jones, H. D., Phillips, A. L., Hedden, P., & Lenton, J.

- R. (2007). Decreased shoot stature and grain α -amylase activity following ectopic expression of a gibberellin 2-oxidase gene in transgenic wheat. *Journal of Experimental Botany*, *58*(12), 3213–3226. <https://doi.org/10.1093/jxb/erm166>
- Armstrong, C., Black, M., Chapman, J. M., Norman, H. A., & Angold, R. (1982). The induction of sensitivity to gibberellin in aleurone tissue of developing wheat grains: The effect of dehydration. *Planta*, *154*(6), 573–577. <https://doi.org/10.1007/BF00403003>
- Arnaud, N., Girin, T., Sorefan, K., Fuentes, S., Wood, T. A., Lawrenson, T., Sablowski, R., & Østergaard, L. (2010). Gibberellins control fruit patterning in *Arabidopsis thaliana*. *Genes & Development*, *24*, 2127–2132. <https://doi.org/10.1101/gad.593410>
- Asano, K., Hirano, K., Ueguchi-Tanaka, M., Angeles-Shim, R. B., Komura, T., Satoh, H., Kitano, H., Matsuoka, M., & Ashikari, M. (2009). Isolation and characterization of dominant dwarf mutants, *Slr1-d*, in rice. *Molecular Genetics and Genomics*, *281*(2), 223–231. <https://doi.org/10.1007/s00438-008-0406-6>
- Assuero, S., Lorenzo, M., Pérez Ramírez, N., Velázquez, L., & Tognetti, J. (2012). Tillering promotion by paclobutrazol in wheat and its relationship with plant carbohydrate status. *New Zealand Journal of Agricultural Research*, *55*(4), 347–358. <https://doi.org/10.1080/00288233.2012.706223>
- Audley, M. (2016). Understanding the role of gibberellin signalling in wheat anther development during heat stress. PhD Thesis, University of Nottingham. <http://eprints.nottingham.ac.uk/id/eprint/39335>
- Aya, K., Tanaka, M. U., Kondo, M., Hamada, K., Yano, K., Nishimura, M., & Matsuoka, M. (2009). Gibberellin modulates anther development in rice via the transcriptional regulation of GAMYB. *The Plant Cell*, *21*(5), 1453–1472. <https://doi.org/10.1105/tpc.108.062935>
- Bae, S., Kweon, J., Kim, H. S., & Kim, J. S. (2014). Microhomology-based choice of Cas9 nuclease target sites. *Nature Methods*, *11*(7), 705–706. <https://doi.org/10.1038/nmeth.3015>
- Bai, M.-Y., Shang, J.-X., Oh, E., Fan, M., Bai, Y., Zentella, R., Sun, T.-P., & Wang, Z.-Y. (2012). Brassinosteroid, gibberellin and phytochrome impinge on a common transcription module in *Arabidopsis*. *Nature Cell Biology*, *14*(8), 810–817.

<https://doi.org/10.1038/ncb2546>

- Balyan, H. S., & Singh, O. (1994). Pleiotropic effects of GA-insensitive *Rht* genes on grain yield and its component characters in wheat. *Cereal Research Communications*, 22(3), 195–200.
- Barrero, Jose M., Mrva, K., Talbot, M. J., White, R. G., Taylor, J., Gubler, F., & Mares, D. J. (2013). Genetic, hormonal, and physiological analysis of late maturity α -amylase in wheat. *Plant Physiology*, 161(3), 1265–1277. <https://doi.org/10.1104/pp.112.209502>
- Barrero, José M., Talbot, M. J., White, R. G., Jacobsen, J. V., & Gubler, F. (2009). Anatomical and transcriptomic studies of the coleorhiza reveal the importance of this tissue in regulating dormancy in barley. *Plant Physiology*, 150(2), 1006–1021. <https://doi.org/10.1104/pp.109.137901>
- Beaudoin, N., Serizet, C., Gosti, F., & Giraudat, J. (2000). Interactions between abscisic acid and ethylene signaling cascades. *The Plant Cell*, 12(7), 1103–1115. <https://doi.org/10.1105/tpc.12.7.1103>
- Becraft, P. W., & Yi, G. (2011). Regulation of aleurone development in cereal grains. *Journal of Experimental Botany*, 62(5), 1669–1675. <https://doi.org/10.1093/jxb/erq372>
- Belderok, B. (2000). Developments in bread-making processes. *Plant Foods for Human Nutrition*, 55(1), 1–14. <https://doi.org/10.1023/A:1008199314267>
- Ben-Amar, A., Daldoul, S., M. Reustle, G., Krczal, G., & Mliki, A. (2016). Reverse genetics and high throughput sequencing methodologies for plant functional genomics. *Current Genomics*, 17(6), 460–475. <https://doi.org/10.2174/1389202917666160520102827>
- Bethke, P. C., Schuurink, R., & Jones, R. L. (1997). Hormonal signalling in cereal aleurone. *Journal of Experimental Botany*, 48(7), 1337–1356. <https://doi.org/10.1093/jxb/48.7.1337>
- Bewley, J. (1997). Seed germination and dormancy. *The Plant Cell*, 9(7), 1055–1066. <https://doi.org/10.1105/tpc.9.7.1055>
- Bewley, J. D., & Black, M. (1994). Seeds: germination, structure and composition. In *Seeds: Physiology of Development and Germination*.

- Boden, S. A., Weiss, D., Ross, J. J., Davies, N. W., Trevaskis, B., Chandler, P. M., & Swain, S. M. (2014). *EARLY FLOWERING3* regulates flowering in spring barley by mediating gibberellin production and *FLOWERING LOCUS T* expression. *Plant Cell*, *26*(4), 1557–1569. <https://doi.org/10.1105/tpc.114.123794>
- Borrell, A. K., Incoll, L. D., & Dalling, M. J. (1991). The influence of the *Rht1* and *Rht2* alleles on the growth of wheat stems and ears. *Annals of Botany*, *67*(2), 103–110. <https://doi.org/10.1093/oxfordjournals.aob.a088108>
- Borrill, P. (2019). Blurring the boundaries between cereal crops and model plants. *New Phytologist*, *228*, 1721–1727. <https://doi.org/10.1111/nph.16229>
- Botwright, T., Rebetzke, G., Condon, T., & Richards, R. (2001). The effect of *rht* genotype and temperature on coleoptile growth and dry matter partitioning in young wheat seedlings. *Australian Journal of Plant Physiology*, *28*(5), 417–423. <https://doi.org/10.1071/pp01010>
- Bray, N. L., Pimentel, H., Melsted, P., & Pachter, L. (2016). Near-optimal probabilistic RNA-seq quantification. *Nature Biotechnology*, *34*(5), 525–527. <https://doi.org/10.1038/nbt.3519>
- Brückner, A., Polge, C., Lentze, N., Auerbach, D., & Schlattner, U. (2009). Yeast two-hybrid, a powerful tool for systems biology. *International Journal of Molecular Sciences*, *10*(6), 2763–2788. <https://doi.org/10.3390/ijms10062763>
- Cai, T., Meng, X., Liu, X., Liu, T., Wang, H., Jia, Z., Yang, D., & Ren, X. (2018). Exogenous hormonal application regulates the occurrence of wheat tillers by changing endogenous hormones. *Frontiers in Plant Science*, *9*:1886. <https://doi.org/10.3389/fpls.2018.01886>
- Cai, T., Xu, H.-C., Yin, Y.-P., Yang, W.-B., Peng, D.-L., Ni, Y.-L., Xu, C.-L., Yang, D.-Q., & Wang, Z.-L. (2013). Mechanisms of tiller occurrence affected by exogenous IAA, GA3, and ABA in wheat with different spike-types. *Acta Agronomica Sinica*, *39*(10), 1835. <https://doi.org/10.3724/sp.j.1006.2013.01835>
- Calvo, A., Nicolas, C., Lorenzo, O., Nicolas, G., & Rodriguez, D. (2004). Evidence for positive regulation by gibberellins and ethylene of *ACC oxidase* expression and activity during transition from dormancy to germination in *Fagus sylvatica* L. seeds. *Journal of Plant Growth Regulation*, *23*(1), 44–53. <https://doi.org/10.1007/s00344-004-0074-7>

- Casebow, R., Hadley, C., Uppal, R., Addisu, M., Loddo, S., Kowalski, A., Griffiths, S., & Gooding, M. (2016). *Reduced height (Rht) alleles affect wheat grain quality. PLoS ONE, 11(5)*. <https://doi.org/10.1371/journal.pone.0156056>
- Castellaro, S. J., Dolan, S. C., Hedden, P., Gaskin, P., & MacMillan, J. (1990). Stereochemistry of the metabolic steps from kaurenoic acids to kaurenolides and gibberellins. *Phytochemistry, 29(6)*, 1833–1839. [https://doi.org/10.1016/0031-9422\(90\)85024-A](https://doi.org/10.1016/0031-9422(90)85024-A)
- Cenci, A., & Rouard, M. (2017). Evolutionary analyses of GRAS transcription factors in angiosperms. *Frontiers in Plant Science, 8*:273. <https://doi.org/10.3389/fpls.2017.00273>
- Chandler, Peter M. (1988). Hormonal regulation of gene expression in the “slender” mutant of barley (*Hordeum vulgare* L.). *Planta, 175(1)*, 115–120. <https://doi.org/10.1007/BF00402888>
- Chandler, Peter M., & Robertson, M. (1999). Gibberellin dose-response curves and the characterization of dwarf mutants of barley. *Plant Physiology, 120(2)*, 623–632. <https://doi.org/10.1104/pp.120.2.623>
- Chandler, Peter Michael, & Harding, C. A. (2013). “Overgrowth” mutants in barley and wheat: new alleles and phenotypes of the “Green Revolution” DELLA gene. *Journal of Experimental Botany, 64(6)*, 1603–1613. <https://doi.org/10.1093/jxb/ert022>
- Chandler, Peter Michael, Marion-Poll, A., Ellis, M., & Gubler, F. (2002). Mutants at the *Slender1* locus of barley cv Himalaya. Molecular and physiological characterization. *Plant Physiology, 129*, 181–190. <https://doi.org/10.1104/pp.010917>
- Chen, K., & An, Y. Q. C. (2006). Transcriptional responses to gibberellin and abscisic acid in barley aleurone. *Journal of Integrative Plant Biology, 48(5)*, 591–612. <https://doi.org/10.1111/j.1744-7909.2006.00270.x>
- Chen, L., Xiang, S., Chen, Y., Li, D., & Yu, D. (2017). Arabidopsis WRKY45 interacts with the DELLA protein RGL1 to positively regulate age-triggered leaf senescence. *Molecular Plant, 10(9)*, 1174–1189. <https://doi.org/10.1016/J.MOLP.2017.07.008>
- Chen, P.-W., Chiang, C.-M., Tseng, T.-H., & Yu, S.-M. (2006). Interaction between rice

MYBGA and the gibberellin response element controls tissue-specific sugar sensitivity of α -amylase genes. *The Plant Cell*, 18(9), 2326–2340. <https://doi.org/10.1105/tpc.105.038844>

Cheng, C., Jiao, C., Singer, S. D., Gao, M., Xu, X., Zhou, Y., Li, Z., Fei, Z., Wang, Y., & Wang, X. (2015). Gibberellin-induced changes in the transcriptome of grapevine (*Vitis labrusca* \times *V. vinifera*) cv. Kyoho flowers. *BMC Genomics*, 16(128). <https://doi.org/10.1186/s12864-015-1324-8>

Chiang, H.-H., Hwang, L., & Goodman, H. M. (1995). Isolation of the Arabidopsis GA4 Locus. *The Plant Cell*, 7(2), 195–201. <https://doi.org/10.1105/tpc.7.2.195>

Chini, A., Fonseca, S., Fernández, G., Adie, B., Chico, J. M., Lorenzo, O., García-Casado, G., López-Vidriero, I., Lozano, F. M., Ponce, M. R., Micol, J. L., & Solano, R. (2007). The JAZ family of repressors is the missing link in jasmonate signalling. *Nature*, 448(7154), 666–671. <https://doi.org/10.1038/nature06006>

Chitnis, V. R., Gao, F., Yao, Z., Jordan, M. C., Park, S., & Ayele, B. T. (2014). After-ripening induced transcriptional changes of hormonal genes in wheat seeds: the cases of brassinosteroids, ethylene, cytokinin and salicylic acid. *PLOS ONE*, 9(1). <https://doi.org/10.1371/journal.pone.0087543>

Cho, H. T., & Kende, H. (1997). Expression of expansin genes is correlated with growth in deepwater rice. *Plant Cell*, 9(9), 1661–1671. <https://doi.org/10.1105/tpc.9.9.1661>

Choi, J. W., & Lim, J. (2016). Control of asymmetric cell divisions during root ground tissue maturation. *Molecules and Cells*, 39(7), 524–529. <https://doi.org/10.14348/molcells.2016.0105>

Clavijo, B. J., Venturini, L., Schudoma, C., Accinelli, G. G., Kaithakottil, G., Wright, J., Borrill, P., Kettleborough, G., Heavens, D., Chapman, H., Lipscombe, J., Barker, T., Lu, F. H., McKenzie, N., Raats, D., Ramirez-Gonzalez, R. H., Counce, A., Peel, N., Percival-Alwyn, L., ... Clark, M. D. (2017). An improved assembly and annotation of the allohexaploid wheat genome identifies complete families of agronomic genes and provides genomic evidence for chromosomal translocations. *Genome Research*, 27(5), 885–896. <https://doi.org/10.1101/gr.217117.116>

Coelho, C. P., Huang, P., Lee, D.-Y., & Brutnell, T. P. (2018). Making roots, shoots, and seeds: IDD gene family diversification in plants. *Trends in Plant Science*, 23(1),

66–78. <https://doi.org/10.1016/j.tplants.2017.09.008>

- Coelho Filho, M. A., Colebrook, E. H., Lloyd, D. P. A., Webster, C. P., Mooney, S. J., Phillips, A. L., Hedden, P., & Whalley, W. R. (2013). The involvement of gibberellin signalling in the effect of soil resistance to root penetration on leaf elongation and tiller number in wheat. *Plant and Soil*, *371*(1–2), 81–94. <https://doi.org/10.1007/s11104-013-1662-8>
- Colasanti, J., & Sundaresan, V. (2000). ‘Florigen’ enters the molecular age: long-distance signals that cause plants to flower. *Trends in Biochemical Sciences*, *25*(5), 236–240. [https://doi.org/10.1016/S0968-0004\(00\)01542-5](https://doi.org/10.1016/S0968-0004(00)01542-5)
- Colasanti, J., Tremblay, R., Wong, A. Y. M., Coneva, V., Kozaki, A., & Mable, B. K. (2006). The maize *INDETERMINATE1* flowering time regulator defines a highly conserved zinc finger protein family in higher plants. *BMC Genomics*, *7*, 158. <https://doi.org/10.1186/1471-2164-7-158>
- Colasanti, J., Yuan, Z., & Sundaresan, V. (1998). The *indeterminate* gene encodes a zinc finger protein and regulates a leaf-generated signal required for the transition to flowering in maize. *Cell*, *93*(4), 593–603. [https://doi.org/10.1016/S0092-8674\(00\)81188-5](https://doi.org/10.1016/S0092-8674(00)81188-5)
- Colbert, T., Till, B. J., Tompa, R., Reynolds, S., Steine, M. N., Yeung, A. T., McCallum, C. M., Comai, L., & Henikoff, S. (2001). High-throughput screening for induced point mutations. *Plant Physiology*, *126*(2), 480–484. <https://doi.org/10.1104/pp.126.2.480>
- Corbineau, F., Rudnicki, R. M., & Come, D. (1988). Induction of secondary dormancy in sunflower seeds by high temperature. Possible involvement of ethylene biosynthesis. *Physiologia Plantarum*, *73*(3), 368–373. <https://doi.org/10.1111/j.1399-3054.1988.tb00612.x>
- Corbineau, Françoise, Xia, Q., Bailly, C., & El-Maarouf-Bouteau, H. (2014). Ethylene, a key factor in the regulation of seed dormancy. *Frontiers in Plant Science*, *5*:539. <https://doi.org/10.3389/fpls.2014.00539>
- Crocco, C. D., Locascio, A., Escudero, C. M., Alabadí, D., Blázquez, M. A., & Botto, J. F. (2015). The transcriptional regulator BBX24 impairs DELLA activity to promote shade avoidance in *Arabidopsis thaliana*. *Nature Communications*, *6*:6202. <https://doi.org/10.1038/ncomms7202>

- Crocker, S. J., Hedden, P., Lenton, J. R., & Stoddart, J. L. (1990). Comparison of gibberellins in normal and *slender* barley seedlings. *Plant Physiology*, *94*(1), 194–200. <https://doi.org/10.1104/pp.94.1.194>
- Cui, D., Zhao, J., Jing, Y., Fan, M., Liu, J., Wang, Z., Xin, W., & Hu, Y. (2013). The arabidopsis IDD14, IDD15, and IDD16 cooperatively regulate lateral organ morphogenesis and gravitropism by promoting auxin biosynthesis and transport. *PLoS Genetics*, *9*(9). <https://doi.org/10.1371/journal.pgen.1003759>
- Daer, R. M., Cutts, J. P., Brafman, D. A., & Haynes, K. A. (2017). The impact of chromatin dynamics on Cas9-mediated genome editing in human cells. *ACS Synthetic Biology*, *6*(3), 428–438. <https://doi.org/10.1021/acssynbio.5b00299>
- Dang, Y., Jia, G., Choi, J., Ma, H., Anaya, E., Ye, C., Shankar, P., & Wu, H. (2015). Optimizing sgRNA structure to improve CRISPR-Cas9 knockout efficiency. *Genome Biology*, *16*(280). <https://doi.org/10.1186/s13059-015-0846-3>
- Danyluk, J., Kane, N. A., Breton, G., Limin, A. E., Fowler, D. B., & Sarhan, F. (2003). TaVRT-1, a putative transcription factor associated with vegetative to reproductive transition in cereals. *Plant Physiology*, *132*(4), 1849–1860. <https://doi.org/10.1104/pp.103.023523>
- Davière, J.-M., & Achard, P. (2016). A pivotal role of DELLAs in regulating multiple hormone signals. *Molecular Plant*, *9*(1), 10–20. <https://doi.org/10.1016/J.MOLP.2015.09.011>
- Davière, J.-M., Wild, M., Regnault, T., Baumberger, N., Eisler, H., Genschik, P., & Achard, P. (2014). Class I TCP-DELLA interactions in inflorescence shoot apex determine plant height. *Current Biology*, *24*(16), 1923–1928. <https://doi.org/10.1016/J.CUB.2014.07.012>
- de Lucas, M., Davière, J.-M., Rodríguez-Falcón, M., Pontin, M., Iglesias-Pedraz, J. M., Lorrain, S., Fankhauser, C., Blázquez, M. A., Titarenko, E., & Prat, S. (2008). A molecular framework for light and gibberellin control of cell elongation. *Nature*, *451*(7177), 480–484. <https://doi.org/10.1038/nature06520>
- Deng, L., Li, L., Zhang, S., Shen, J., Li, S., Hu, S., Peng, Q., Xiao, J., & Wu, C. (2017). Suppressor of *rid1* (SID1) shares common targets with RID1 on florigen genes to initiate floral transition in rice. *PLOS Genetics*, *13*(2). <https://doi.org/10.1371/journal.pgen.1006642>

- Derkx, A., Baumann, U., Cheong, J., Mrva, K., Sharma, N., Pallotta, M., & Mares, D. (2021). A major locus on wheat chromosome 7B associated with Late-Maturity α -Amylase encodes a putative *ent*-copalyl diphosphate synthase. *Frontiers in Plant Science*, *12*:637685. <https://doi.org/10.3389/fpls.2021.637685>
- Derkx, A. P., Harding, C. A., Miraghazadeh, A., & Chandler, P. M. (2017). Overgrowth (*Della*) mutants of wheat: development, growth and yield of intragenic suppressors of the *Rht-B1c* dwarfing gene. *Functional Plant Biology*, *44*(5), 525–537. <https://doi.org/10.1071/FP16262>
- Doench, J. G., Fusi, N., Sullender, M., Hegde, M., Vaimberg, E. W., Donovan, K. F., Smith, I., Tothova, Z., Wilen, C., Orchard, R., Virgin, H. W., Listgarten, J., & Root, D. E. (2016). Optimized sgRNA design to maximize activity and minimize off-target effects of CRISPR-Cas9. *Nature Biotechnology*, *34*(2), 184–191. <https://doi.org/10.1038/nbt.3437>
- Dominguez, F., & Cejudo, F. J. (2014). Programmed cell death (PCD): an essential process of cereal seed development and germination. *Frontiers in Plant Science*, *5*:366. <https://doi.org/10.3389/fpls.2014.00366>
- Dong, C., Dalton-Morgan, J., Vincent, K., & Sharp, P. (2009). A modified TILLING method for wheat breeding. *The Plant Genome*, *2*(1), 39–47. <https://doi.org/10.3835/plantgenome2008.10.0012>
- Dou, M., Cheng, S., Zhao, B., Xuan, Y., & Shao, M. (2016). The indeterminate domain protein ROC1 regulates chilling tolerance via activation of *DREB1B/CBF1* in rice. *International Journal of Molecular Sciences*, *17*(3):233. <https://doi.org/10.3390/ijms17030233>
- Dubois, M., Skirycz, A., Claeys, H., Maleux, K., Dhondt, S., De Bodt, S., Vanden Bossche, R., De Milde, L., Yoshizumi, T., Matsui, M., & Inzé, D. (2013). The ETHYLENE RESPONSE FACTOR 6 acts as central regulator of leaf growth under water limiting conditions in *Arabidopsis thaliana*. *Plant Physiology*, *162*(1), 319–332. <https://doi.org/10.1104/pp.113.216341>
- Duncan, W. G. (1971). Leaf angles, leaf area, and canopy photosynthesis. *Crop Science*, *11*(4), 482–485. <https://doi.org/10.2135/cropsci1971.0011183x001100040006x>
- Eastwell, K. C., & Spencer, M. S. (1982). Modes of ethylene action in the release of amylase from barley aleurone layers. *Plant Physiology*, *69*(3), 563–567.

<https://doi.org/10.1104/pp.69.3.563>

- Edgar, R. C. (2004). MUSCLE: Multiple sequence alignment with high accuracy and high throughput. *Nucleic Acids Research*, *32*(5), 1792–1797. <https://doi.org/10.1093/nar/gkh340>
- Edwards, R. A., Ross, A. S., Mares, D. J., Ellison, F. W., & Tomlinson, J. D. (1989). Enzymes from rain-damaged and laboratory-germinated wheat. Effects on product quality. *Journal of Cereal Science*, *10*(2), 157–167. [https://doi.org/10.1016/S0733-5210\(89\)80044-X](https://doi.org/10.1016/S0733-5210(89)80044-X)
- Ellis, M. H., Rebetzke, G. J., Chandler, P., Bonnett, D., Spielmeier, W., & Richards, R. A. (2004). The effect of different height reducing genes on the early growth of wheat. *Functional Plant Biology*, *31*, 583–589. <https://doi.org/10.1071/FP03207>
- Esashi, Y., Abe, Y., Ashino, H., Ishizawa, K., & Saitoh, K. (1989). Germination of cocklebur seed and growth of their axial and cotyledonary tissues in response to C₂H₄, CO₂ and/or O₂ under water stress. *Plant, Cell and Environment*, *12*(2), 183–190. <https://doi.org/10.1111/j.1365-3040.1989.tb01931.x>
- Evans, L. T. (1998). *Feeding the ten billion: Plants and population growth*. Cambridge University Press.
- Eveland, A. L., Goldshmidt, A., Pautler, M., Morohashi, K., Liseron-Monfils, C., Lewis, M. W., Kumari, S., Hiraga, S., Yang, F., Unger-Wallace, E., Olson, A., Hake, S., Vollbrecht, E., Grotewold, E., Ware, D., & Jackson, D. (2014). Regulatory modules controlling maize inflorescence architecture. *Genome Research*, *24*(3), 431–443. <https://doi.org/10.1101/gr.166397.113>
- Evers, T., & Millar, S. (2002). Cereal grain structure and development: Some implications for quality. *Journal of Cereal Science*, *36*, 261–284. <https://doi.org/10.1006>
- Fabian, T., Lorbiecke, R., Umeda, M., & Sauter, M. (2000). The cell cycle genes *cycA1;1* and *cdc2Os-3* are coordinately regulated by gibberellin in planta. *Planta*, *211*(3), 376–383. <https://doi.org/10.1007/s004250000295>
- Fambrini, M., Mariotti, L., Parlanti, S., Picciarelli, P., Salvini, M., Ceccarelli, N., & Pugliesi, C. (2011). The extreme dwarf phenotype of the GA-sensitive mutant of sunflower, *dwarf2*, is generated by a deletion in the *ent-kaurenoic acid oxidase1 (HaKAO1)* gene sequence. *Plant Molecular Biology*, *75*(4–5), 431–450.

<https://doi.org/10.1007/s11103-011-9740-x>

- Fan, S., Zhang, D., Xing, L., Qi, S., Du, L., Wu, H., Shao, H., Li, Y., Ma, J., & Han, M. (2017). Phylogenetic analysis of IDD gene family and characterization of its expression in response to flower induction in *Malus*. *Molecular Genetics and Genomics*, *292*(4), 755–771. <https://doi.org/10.1007/s00438-017-1306-4>
- Feng, S., Martinez, C., Gusmaroli, G., Wang, Y., Zhou, J., Wang, F., Chen, L., Yu, L., Iglesias-Pedraz, J. M., Kircher, S., Schäfer, E., Fu, X., Fan, L. M., & Deng, X. W. (2008). Coordinated regulation of *Arabidopsis thaliana* development by light and gibberellins. *Nature*, *451*(7177), 475–479. <https://doi.org/10.1038/nature06448>
- Feng, Z., Mao, Y., Xu, N., Zhang, B., Wei, P., Yang, D. L., Wang, Z., Zhang, Z., Zheng, R., Yang, L., Zeng, L., Liu, X., & Zhu, J. K. (2014). Multigeneration analysis reveals the inheritance, specificity, and patterns of CRISPR/Cas-induced gene modifications in *Arabidopsis*. *Proceedings of the National Academy of Sciences of the United States of America*, *111*(12), 4632–4637. <https://doi.org/10.1073/pnas.1400822111>
- Feurtado, J. A., Huang, D., Wicki-Stordeur, L., Hemstock, L. E., Potentier, M. S., Tsang, E. W. T., & Cutler, A. J. (2011). The *Arabidopsis* C2H2 zinc finger INDETERMINATE DOMAIN1/ENHYDROUS promotes the transition to germination by regulating light and hormonal signaling during seed maturation. *The Plant Cell*, *23*(5), 1772–1794. <https://doi.org/10.1105/tpc.111.085134>
- Fields, S., & Song, O. (1989). A novel genetic system to detect protein–protein interactions. *Nature*, *340*(6230), 245–246. <https://doi.org/10.1038/340245a0>
- Fleet, C. M., Yamaguchi, S., Hanada, A., Kawaide, H., David, C. J., Kamiya, Y., & Sun, T. P. (2003). Overexpression of *AtCPS* and *AtKS* in *Arabidopsis* confers increased *ent*-kaurene production but no increase in bioactive gibberellins. *Plant Physiology*, *132*(2), 830–839. <https://doi.org/10.1104/pp.103.021725>
- Flintham, J. E., Borner, A., Worland, A. J., & Gale, M. D. (1997). Optimizing wheat grain yield: effects of *Rht* (giberellin-insensitive) dwarfing genes. *Journal of Agricultural Science*, *128*, 11–25. <https://doi.org/10.1017/S0021859696003942>
- Flintham, J. E., Holdsworth, M. J., Jack, P. L., Kettlewell, P. S., & Phillips, A. L. (2011). An integrated approach to stabilising Hagberg Falling Number in wheat: screens, genes and understanding. *HGCA Project Report, No.480*.

- Ford, B. A., Foo, E., Sharwood, R., Karafiatova, M., Vrána, J., MacMillan, C., Nichols, D. S., Steuernagel, B., Uauy, C., Doležel, J., Chandler, P. M., & Spielmeier, W. (2018). *Rht18* semidwarfism in wheat is due to increased *GA 2-oxidaseA9* expression and reduced GA content. *Plant Physiology*, *177*(1), 168–180. <https://doi.org/10.1104/pp.18.00023>
- Fu, J. R., & Yang, S. F. (1983). Release of heat pretreatment-induced dormancy in lettuce seeds by ethylene or cytokinin in relation to the production of ethylene and the synthesis of 1-aminocyclopropane-1-carboxylic acid during germination. *Journal of Plant Growth Regulation*, *2*:185. <https://doi.org/10.1007/BF02042247>
- Fu, X., Richards, D. E., Ait-ali, T., Hynes, L. W., Ougham, H., Peng, J., & Harberd, N. P. (2002). Gibberellin-mediated proteasome-dependent degradation of the Barley DELLA protein SLN1 repressor. *The Plant Cell*, *14*(12), 3191–3200. <https://doi.org/10.1105/tpc.006197>
- Fujimoto, S. Y., Ohta, M., Usui, A., Shinshi, H., & Ohme-Takagi, M. (2000). Arabidopsis ethylene-responsive element binding factors act as transcriptional activators or repressors of GCC box-mediated gene expression. *The Plant Cell*, *12*(3), 393–404. <https://doi.org/10.1105/tpc.12.3.393>
- Fujioka, S., Yamane, H., Spray, C. R., Katsumi, M., Phinney, B. O., Gaskin, P., MacMillan, J., & Takahashi, N. (1988). The dominant non-gibberellin-responding dwarf mutant (D8) of maize accumulates native gibberellins. *Proceedings of the National Academy of Sciences*, *85*(23), 9031–9035. <https://doi.org/10.1073/pnas.85.23.9031>
- Fukazawa, J., Mori, M., Watanabe, S., Miyamoto, C., Ito, T., & Takahashi, Y. (2017). DELLA-GAF1 complex is a main component in gibberellin feedback regulation of GA20 oxidase 2. *Plant Physiology*, *175*(3), 1395–1406. <https://doi.org/10.1104/pp.17.00282>
- Fukazawa, J., Teramura, H., Murakoshi, S., Nasuno, K., Nishida, N., Ito, T., Yoshida, M., Kamiya, Y., Yamaguchi, S., & Takahashi, Y. (2014). DELLAs function as coactivators of GAI-ASSOCIATED FACTOR1 in regulation of gibberellin homeostasis and signaling in Arabidopsis. *The Plant Cell*, *26*(7), 2920–2938. <https://doi.org/10.1105/tpc.114.125690>
- Gale, M. D., & Marshall, G. A. (1976). The chromosomal location of *gai 1* and *rht 1*,

genes for gibberellin insensitivity and semidwarfism, in a derivative of norin 10 wheat. *Heredity*, 37(2), 283–289. <https://doi.org/10.1038/hdy.1976.88>

Gale, M.D., & Youssefian, S. (1985). Dwarfing genes in wheat. In G. E. Russell (Ed.), *Progress in Plant Breeding* (pp. 1–35). Butterworths.

Gale, Michael D., & Marshall, G. A. (1973). Insensitivity to gibberellin in dwarf wheats. *Annals of Botany*, 37(4), 729–735. <https://doi.org/10.1093/oxfordjournals.aob.a084741>

Gallardo, M., Delgado, M. del M., Sánchez-Calle, I. M., & Matilla, A. J. (1991). Ethylene production and 1-aminocyclopropane-1-carboxylic acid conjugation in thermoinhibited *Cicer arietinum* L. seeds. *Plant Physiology*, 97(1), 122–127. <https://doi.org/10.1104/pp.97.1.122>

Gallego-Bartolomé, J., Arana, M. V., Vandebussche, F., Žádníková, P., Minguet, E. G., Guardiola, V., Van Der Straeten, D., Benkova, E., Alabadí, D., & Blázquez, M. A. (2011). Hierarchy of hormone action controlling apical hook development in Arabidopsis. *The Plant Journal*, 67(4), 622–634. <https://doi.org/10.1111/j.1365-3113.2011.04621.x>

Gallego-Bartolome, J., Minguet, E. G., Marin, J. A., Prat, S., Blazquez, M. A., & Alabadi, D. (2010). Transcriptional diversification and functional conservation between DELLA proteins in Arabidopsis. *Molecular Biology and Evolution*, 27(6), 1247–1256. <https://doi.org/10.1093/molbev/msq012>

Gallego-Giraldo, L., Ubeda-Tomás, S., Gisbert, C., García-Martínez, J. L., Moritz, T., & López-Díaz, I. (2008). Gibberellin homeostasis in tobacco is regulated by gibberellin metabolism genes with different gibberellin sensitivity. *Plant and Cell Physiology*, 49(5), 679–690. <https://doi.org/10.1093/pcp/pcn042>

Garneau, J. E., Dupuis, M.-È., Villion, M., Romero, D. A., Barrangou, R., Boyaval, P., Fremaux, C., Horvath, P., Magadán, A. H., & Moineau, S. (2010). The CRISPR/Cas bacterial immune system cleaves bacteriophage and plasmid DNA. *Nature*, 468(7320), 67–71. <https://doi.org/10.1038/nature09523>

Gibbs, D. J., Md Isa, N., Movahedi, M., Lozano-Juste, J., Mendiondo, G. M., Berckhan, S., Marín-de la Rosa, N., Vicente Conde, J., Sousa Correia, C., Pearce, S. P., Bassel, G. W., Hamali, B., Talloji, P., Tomé, D. F. A., Coego, A., Beynon, J., Alabadí, D., Bachmair, A., León, J., ... Holdsworth, M. J. (2014). Nitric oxide sensing in plants

- is mediated by proteolytic control of group VII ERF transcription factors. *Molecular Cell*, 53(3), 369–379. <https://doi.org/10.1016/J.MOLCEL.2013.12.020>
- Gil-Humanes, J., Wang, Y., Liang, Z., Shan, Q., Ozuna, C. V., Sánchez-León, S., Baltes, N. J., Starker, C., Barro, F., Gao, C., & Voytas, D. F. (2017). High-efficiency gene targeting in hexaploid wheat using DNA replicons and CRISPR/Cas9. *Plant Journal*, 89(6), 1251–1262. <https://doi.org/10.1111/tpj.13446>
- Gomez-Cadenas, A., Verhey, S. D., Holappa, L. D., Shen, Q., Ho, T. D., & Walker-simmons, M. K. (1999). An abscisic acid-induced protein kinase, PKABA1, mediates abscisic acid-suppressed gene expression in barley aleurone layers. *Proceedings of the National Academy of Science of the United States of America*, 96(4), 1767-1772. <https://doi.org/10.1073/pnas.96.4.1767>
- Gómez-Cadenas, A., Zentella, R., Walker-Simmons, M. K., & Ho, T. H. (2001). Gibberellin/abscisic acid antagonism in barley aleurone cells: site of action of the protein kinase PKABA1 in relation to gibberellin signaling molecules. *The Plant Cell*, 13(3), 667–679. <https://doi.org/10.1105/tpc.13.3.667>
- Gontarek, B. C., Neelakandan, A. K., Wu, H., & Becraft, P. W. (2016). NKD transcription factors are central regulators of maize endosperm development. *The Plant Cell*, 28(12), 2916–2936. <https://doi.org/10.1105/tpc.16.00609>
- Goodstein, D. M., Shu, S., Howson, R., Neupane, R., Hayes, R. D., Fazo, J., Mitros, T., Dirks, W., Hellsten, U., Putnam, N., & Rokhsar, D. S. (2012). Phytozome: A comparative platform for green plant genomics. *Nucleic Acids Research*, 40(D1), 1178–1186. <https://doi.org/10.1093/nar/gkr944>
- Griffiths, J., Murase, K., Rieu, I., Zentella, R., Zhang, Z. L., Powers, S. J., Gong, F., Phillips, A. L., Hedden, P., Sun, T. P., & Thomas, S. G. (2006). Genetic characterization and functional analysis of the GID1 gibberellin receptors in Arabidopsis. *Plant Cell*, 18(12), 3399–3414. <https://doi.org/10.1105/tpc.106.047415>
- Groos, C., Gay, G., Perretant, M. R., Gervais, L., Bernard, M., Dedryver, F., & Charmet, G. (2002). Study of the relationship between pre-harvest sprouting and grain color by quantitative trait loci analysis in a whitexred grain bread-wheat cross. *Theoretical and Applied Genetics*, 104(1), 39–47. <https://doi.org/10.1007/s001220200004>
- Gubler, F., & Jacobsen, J. V. (1992). Gibberellin-responsive elements in the promoter

- of a barley high-pl alpha-amylase gene. *The Plant Cell*, 4(11), 1435–1441. <https://doi.org/10.2307/3869514>
- Gubler, Frank, Chandler, P. M., White, R. G., Llewellyn, D. J., & Jacobsen, J. V. (2002). Gibberellin signaling in barley aleurone cells. Control of *SLN1* and *GAMYB* expression. *Plant Physiology*, 129, 191–200. <https://doi.org/10.1104/pp.010918>
- Gubler, Frank, Kalla, R., Roberts, J. K., & Jacobsen, J. V. (1995). Gibberellin-regulated expression of a myb gene in barley aleurone cells: evidence for Myb transactivation of a high-pl alpha-amylase gene promoter. *The Plant Cell*, 7(11), 1879–1891. <https://doi.org/10.1105/tpc.7.11.1879>
- Gubler, Frank, Millar, A. A., & Jacobsen, J. V. (2005). Dormancy release, ABA and pre-harvest sprouting. *Current Opinion in Plant Biology*, 8(2), 183–187. <https://doi.org/10.1016/j.pbi.2005.01.011>
- Guindon, S., Dufayard, J.-F., Lefort, V., Anisimova, M., Hordijk, W., & Gascuel, O. (2010). New algorithms and methods to estimate maximum-likelihood phylogenies: assessing the performance of PhyML 3.0. *Systematic Biology*, 59(3), 307–321. <https://doi.org/10.1093/sysbio/syq010>
- Guo, W., Tzioutziou, N., Stephen, G., Milne, I., Calixto, C., Waugh, R., Brown, J., & Zhang, R. (2019). 3D RNA-seq - a powerful and flexible tool for rapid and accurate differential expression and alternative splicing analysis of RNA-seq data for biologists. *BioRxiv*, 656686. <https://doi.org/10.1101/656686>
- Guo, Y., Wu, H., Li, X., Li, Q., Zhao, X., Duan, X., An, Y., Lv, W., & An, H. (2017). Identification and expression of GRAS family genes in maize (*Zea mays* L.). *PLOS ONE*, 12(9), e0185418. <https://doi.org/10.1371/journal.pone.0185418>
- Haeussler, M., Schönig, K., Eckert, H., Eschstruth, A., Mianné, J., Renaud, J.-B., Schneider-Maunoury, S., Shkumatava, A., Teboul, L., Kent, J., Joly, J.-S., & Concordet, J.-P. (2016). Evaluation of off-target and on-target scoring algorithms and integration into the guide RNA selection tool CRISPOR. *Genome Biology*, 17(1), 148. <https://doi.org/10.1186/s13059-016-1012-2>
- Hagberg, S. (1960). A rapid method for determining alpha-amylase activity. *Cereal Chemistry*, 37, 218.
- Hagberg, S. (1961). Simplified method for determining a-amylase activity. *Cereal Chemistry*, 37, 202–203.

- Hahn, F., Korolev, A., Sanjurjo Loures, L., & Nekrasov, V. (2020). A modular cloning toolkit for genome editing in plants. *BMC Plant Biology*, *20*(1):179. <https://doi.org/10.1186/s12870-020-02388-2>
- Harlan, J. R., DeWet, J. M. J., & Price, G. E. (1973). Comparative evolution of cereals. *Evolution*, *27*(2), 311–325. <https://doi.org/10.2307/2406971>
- Hassan, H., Scheres, B., & Blilou, I. (2010). JACKDAW controls epidermal patterning in the Arabidopsis root meristem through a non-cell-autonomous mechanism. *Development*, *137*(9), 1523–1529. <https://doi.org/10.1242/dev.048777>
- Hassani-Pak, K., Castellote, M., Esch, M., Hindle, M., Lysenko, A., Taubert, J., & Rawlings, C. (2016). Developing integrated crop knowledge networks to advance candidate gene discovery. *Applied and Translational Genomics*, *11*, 18–26. <https://doi.org/10.1016/j.atg.2016.10.003>
- Hassani-Pak, K., Singh, A., Brandizi, M., Hearnshaw, J., Amberkar, S., Phillips, A. L., Doonan, J. H., & Rawlings, C. (2020). KnetMiner: A comprehensive approach for supporting evidence-based gene discovery and complex trait analysis across species. In *bioRxiv*. bioRxiv. <https://doi.org/10.1101/2020.04.02.017004>
- Hastings, M. L., & Krainer, A. R. (2001). Pre-mRNA splicing in the new millennium. *Current Opinion in Cell Biology*, *13*(3), 302–309. [https://doi.org/10.1016/S0955-0674\(00\)00212-X](https://doi.org/10.1016/S0955-0674(00)00212-X)
- Hedden, P. (2003). The genes of the Green Revolution. *Trends in Genetics*, *19*(1), 5–9. [https://doi.org/10.1016/S0168-9525\(02\)00009-4](https://doi.org/10.1016/S0168-9525(02)00009-4)
- Hedden, P. (2020). The current status of research on gibberellin biosynthesis. *Plant and Cell Physiology*, *61*(11), 1832–1849. <https://doi.org/10.1093/pcp/pcaa092>
- Hedden, P., & Kamiya, Y. (1997). Gibberellin biosynthesis: enzymes, genes and their regulation. *Annual Review of Plant Biology*, *48*, 431–460. <https://doi.org/10.1146/annurev.arplant.48.1.431>
- Hedden, P., & Phillips, A. L. (2000). Gibberellin metabolism: New insights revealed by the genes. *Trends in Plant Science*, *5*(12), 523–530. [https://doi.org/10.1016/S1360-1385\(00\)01790-8](https://doi.org/10.1016/S1360-1385(00)01790-8)
- Hedden, P., & Sponsel, V. (2015). A century of gibberellin research. In *Journal of Plant Growth Regulation*, *34*(4), 740–760. <https://doi.org/10.1007/s00344-015-9546-1>

- Hedden, P., & Thomas, S. G. (2012). Gibberellin biosynthesis and its regulation. *Biochemical Journal*, *444*(1), 11–25. <https://doi.org/10.1042/BJ20120245>
- Helliwell, C. A. (2001). The CYP88A cytochrome P450, *ent*-kaurenoic acid oxidase, catalyzes three steps of the gibberellin biosynthesis pathway. *Proceedings of the National Academy of Sciences*, *98*(4), 2065–2070. <https://doi.org/10.1073/pnas.041588998>
- Helliwell, Chris A., Poole, A., Peacock, W. J., & Dennis, E. S. (1999). Arabidopsis *ent*-kaurene oxidase catalyzes three steps of gibberellin biosynthesis. *Plant Physiology*, *119*(2), 507–510. <https://doi.org/10.1104/pp.119.2.507>
- Heo, J. O., Chang, K. S., Kim, I. A., Lee, M. H., Lee, S. A., Song, S. K., Lee, M. M., & Lim, J. (2011). Funneling of gibberellin signaling by the GRAS transcription regulator SCARECROW-LIKE 3 in the Arabidopsis root. *Proceedings of the National Academy of Sciences of the United States of America*, *108*(5), 2166–2171. <https://doi.org/10.1073/pnas.1012215108>
- Hirano, K., Asano, K., Tsuji, H., Kawamura, M., Mori, H., Kitano, H., Ueguchi-Tanaka, M., & Matsuoka, M. (2010). Characterization of the molecular mechanism underlying gibberellin perception complex formation in rice. *The Plant Cell*, *22*(8), 2680–2696. <https://doi.org/10.1105/tpc.110.075549>
- Hirano, K., Kouketu, E., Katoh, H., Aya, K., Ueguchi-Tanaka, M., & Matsuoka, M. (2012). The suppressive function of the rice DELLA protein SLR1 is dependent on its transcriptional activation activity. *Plant Journal*, *71*(3), 443–453. <https://doi.org/10.1111/j.1365-313X.2012.05000.x>
- Holdsworth, M. J., Bentsink, L., & Soppe, W. J. J. (2008). Molecular networks regulating Arabidopsis seed maturation, after-ripening, dormancy and germination. *New Phytologist*, *179*(1), 33–54. <https://doi.org/10.1111/j.1469-8137.2008.02437.x>
- Hong, G.-J., Xue, X.-Y., Mao, Y.-B., Wang, L.-J., & Chen, X.-Y. (2012). Arabidopsis MYC2 interacts with DELLA proteins in regulating sesquiterpene synthase gene expression. *The Plant Cell*, *24*(6), 2635–2648. <https://doi.org/10.1105/tpc.112.098749>
- Hong, Y. F., Ho, T. H., Wu, C. F., Ho, S. L., Yeh, R. H., Lu, C. a, Chen, P. W., Yu, L. C., Chao, a, & Yu, S. M. (2012). Convergent starvation signals and hormone crosstalk in regulating nutrient mobilization upon germination in cereals. *Plant Cell*, *24*(7),

2857–2873. <https://doi.org/10.1105/tpc.112.097741>

- Hoogendoorn, J., Rickson, J. M., & Gale, M. D. (1990). Differences in leaf and stem anatomy related to plant height of tall and dwarf wheat (*Triticum aestivum* L.). *Journal of Plant Physiology*, *136*(1), 72–77. [https://doi.org/10.1016/S0176-1617\(11\)81618-4](https://doi.org/10.1016/S0176-1617(11)81618-4)
- Hou, X., Lee, L. Y. C., Xia, K., Yan, Y., & Yu, H. (2010). DELLAs modulate jasmonate signaling via competitive binding to JAZs. *Developmental Cell*, *19*(6), 884–894. <https://doi.org/10.1016/j.devcel.2010.10.024>
- Howells, R. M., Craze, M., Bowden, S., & Wallington, E. J. (2018). Efficient generation of stable, heritable gene edits in wheat using CRISPR/Cas9. *BMC Plant Biology*, *18*(1), 215. <https://doi.org/10.1186/s12870-018-1433-z>
- Hsu, P. D., Scott, D. A., Weinstein, J. A., Ran, F. A., Konermann, S., Agarwala, V., Li, Y., Fine, E. J., Wu, X., Shalem, O., Cradick, T. J., Marraffini, L. A., Bao, G., & Zhang, F. (2013). DNA targeting specificity of RNA-guided Cas9 nucleases. *Nature Biotechnology*, *31*(9), 827–832. <https://doi.org/10.1038/nbt.2647>
- Hu, C. D., Chinenov, Y., & Kerppola, T. K. (2002). Visualization of interactions among bZIP and Rel family proteins in living cells using bimolecular fluorescence complementation. *Molecular Cell*, *9*(4), 789–798. [https://doi.org/10.1016/S1097-2765\(02\)00496-3](https://doi.org/10.1016/S1097-2765(02)00496-3)
- Hu, J., Israeli, A., Ori, N., & Sun, T.-P. (2018). The interaction between DELLA and ARF/IAA mediates crosstalk between gibberellin and auxin signaling to control fruit initiation in tomato. *The Plant Cell*, *30*(8), 1710–1728. <https://doi.org/10.1105/tpc.18.00363>
- Huang, D., Wang, S., Zhang, B., Shang-Guan, K., Shi, Y., Zhang, D., Liu, X., Wu, K., Xu, Z., Fu, X., & Zhou, Y. (2015). A gibberellin-mediated DELLA-NAC signaling cascade regulates cellulose synthesis in rice. *Plant Cell*, *27*(6), 1681–1696. <https://doi.org/10.1105/tpc.15.00015>
- Huang, H., Gong, Y., Liu, B., Wu, D., Zhang, M., Xie, D., & Song, S. (2020). The DELLA proteins interact with MYB21 and MYB24 to regulate filament elongation in Arabidopsis. *BMC Plant Biology*, *20*(1), 64. <https://doi.org/10.1186/s12870-020-2274-0>
- Huang, P., Yoshida, H., Yano, K., Kinoshita, S., Kawai, K., Koketsu, E., Hattori, M.,

- Takehara, S., Huang, J., Hirano, K., Ordonio, R. L., Matsuoka, M., & Ueguchi-Tanaka, M. (2018). OsIDD2, a zinc finger and INDETERMINATE DOMAIN protein, regulates secondary cell wall formation. *Journal of Integrative Plant Biology*, *60*(2), 130–143. <https://doi.org/10.1111/jipb.12557>
- Huang, Y., Yang, W., Pei, Z., Guo, X., Liu, D., Sun, J., & Zhang, A. (2012). The genes for gibberellin biosynthesis in wheat. *Functional and Integrative Genomics*, *12*(1), 199–206. <https://doi.org/10.1007/s10142-011-0243-2>
- Hubbard, L., Mcsteen, P., Doebley, J., & Hake, S. (2002). Expression patterns and mutant phenotype of teosinte branched1 correlate with growth suppression in maize and teosinte. *Genetics*, *162*, 1927–1935.
- Ikeda, A., Ueguchi-Tanaka, M., Sonoda, Y., Kitano, H., Koshioka, M., Futsuhara, Y., Matsuoka, M., & Yamaguchi, J. (2001). *slender rice*, a constitutive gibberellin response mutant, is caused by a null mutation of the *SLR1* gene, an ortholog of the height-regulating gene *GAI/RGA/RHT/D8*. *The Plant Cell*, *13*(5), 999–1010. <https://doi.org/10.1105/tpc.13.5.999>
- International Wheat Genome Sequencing Consortium (IWGSC), Appels, R., Eversole, K., Feuillet, C., Keller, B., Rogers, J., Stein, N., Pozniak, C. J., Stein, N., Choulet, F., Distelfeld, A., Eversole, K., Poland, J., Rogers, J., Ronen, G., Sharpe, A. G., Uauy, C., ..., Wang, L. (2018). Shifting the limits in wheat research and breeding using a fully annotated reference genome. *Science*, *361*:6403, eaar7191. <https://doi.org/10.1126/science.aar7191>
- Ishida, Y., Tsunashima, M., Hiei, Y., & Komari, T. (2015). Wheat (*Triticum aestivum* L.) transformation using immature embryos. *Methods in Molecular Biology*, *1223*, 189–198. https://doi.org/10.1007/978-1-4939-1695-5_15
- Islam, S., Chakraborty, S., Uddin, M. J., Mehraj, H., & Jamal Uddin, A. F. M. (2014). Growth and yield of wheat as influenced by GA3 concentrations. *International Journal of Business, Social and Scientific Research*, *2*(1), 74–78.
- Ito, T., & Fukazawa, J. (2021). SCARECROW-LIKE3 regulates the transcription of gibberellin-related genes by acting as a transcriptional co-repressor of GAI-ASSOCIATED FACTOR1. *Plant Molecular Biology*, *105*(4), 463–482. <https://doi.org/10.1007/s11103-020-01101-z>
- Jacobsen, John V., Pearce, D. W., Poole, A. T., Pharis, R. P., & Mander, L. N. (2002).

- Abscisic acid, phaseic acid and gibberellin contents associated with dormancy and germination in barley. *Physiologia Plantarum*, 115(3), 428–441. <https://doi.org/10.1034/j.1399-3054.2002.1150313.x>
- Jacobsen, J. V. (1973). Interactions between gibberellic acid, ethylene, and abscisic acid in control of amylase synthesis in barley aleurone layers. *Plant Physiology*, 51(1), 198–202. <https://doi.org/10.1104/pp.51.1.198>
- Jaganathan, D., Ramasamy, K., Sellamuthu, G., Jayabalan, S., & Venkataraman, G. (2018). CRISPR for crop improvement: An update review. *Frontiers in Plant Science*, 9:985. <https://doi.org/10.3389/fpls.2018.00985>
- Jakoby, M., Weisshaar, B., Dröge-Laser, W., Vicente-Carbajosa, J., Tiedemann, J., Kroj, T., & Parcy, F. (2002). bZIP transcription factors in Arabidopsis. *Trends in Plant Science*, 7(3), 106–111. [https://doi.org/10.1016/S1360-1385\(01\)02223-3](https://doi.org/10.1016/S1360-1385(01)02223-3)
- Jankowicz-Cieslak, J., & Till, B. J. (2016). Forward and reverse genetics in crop breeding. *Advances in Plant Breeding Strategies: Breeding, Biotechnology and Molecular Tools*, (pp. 215–240). Springer Publishing. https://doi.org/10.1007/978-3-319-22521-0_8
- Jerkovic, A., Kriegel, A. M., Bradner, J. R., Atwell, B. J., Roberts, T. H., & Willows, R. D. (2010). Strategic distribution of protective proteins within bran layers of wheat protects the nutrient-rich endosperm. *Plant Physiology*, 152(3), 1459–1470. <https://doi.org/10.1104/pp.109.149864>
- Jiang, L., Kermod, A. R., & Jones, R. L. (1996). Premature drying increases the GA-responsiveness of developing aleurone layers of barley (*Hordeum vulgare* L.) grain. *Plant and Cell Physiology*, 37(8), 1116–1125. <https://doi.org/10.1093/oxfordjournals.pcp.a029062>
- Jiang, W., Bikard, D., Cox, D., Zhang, F., & Marraffini, L. A. (2013). RNA-guided editing of bacterial genomes using CRISPR-Cas systems. *Nature Biotechnology*, 31(3), 233–239. <https://doi.org/10.1038/nbt.2508>
- Jimenez, J. A., Rodriguez, D., Calvo, A. P., Mortensen, L. C., Nicolas, G., & Nicolas, C. (2005). Expression of a transcription factor (FsERF1) involved in ethylene signalling during the breaking of dormancy in *Fagus sylvatica* seeds. *Physiologia Plantarum*, 125(3), 373–380. <https://doi.org/10.1111/j.1399-3054.2005.00571.x>

- Jinek, M., Chylinski, K., Fonfara, I., Hauer, M., Doudna, J. A., & Charpentier, E. (2012). A programmable dual-RNA-guided DNA endonuclease in adaptive bacterial immunity. *Science*, 337(6096), 816–821. <https://doi.org/10.1126/science.1225829>
- Jobson, E. M., Johnston, R. E., Oiestad, A. J., Martin, J. M., & Giroux, M. J. (2019). The impact of the wheat *Rht-B1b* semi-dwarfing allele on photosynthesis and seed development under field conditions. *Frontiers in Plant Science*, 10:51. <https://doi.org/10.3389/fpls.2019.00051>
- Jones, R. L., & Kaufman, P. B. (1983). The role of gibberellins in plant cell elongation. *Critical Reviews in Plant Sciences*, 1(1), 23–47. <https://doi.org/10.1080/07352688309382170>
- Jöst, M., Hensel, G., Kappel, C., Druka, A., Sicard, A., Hohmann, U., Beier, S., Himmelbach, A., Waugh, R., Kumlehn, J., Stein, N., & Lenhard, M. (2016). The INDETERMINATE DOMAIN protein BROAD LEAF1 limits barley leaf width by restricting lateral proliferation. *Current Biology*, 26(7), 903–909. <https://doi.org/10.1016/j.cub.2016.01.047>
- Jung, H., Jo, S. H., Jung, W. Y., Park, H. J., Lee, A., Moon, J. S., Seong, S. Y., Kim, J. K., Kim, Y. S., & Cho, H. S. (2020). Gibberellin promotes bolting and flowering via the floral integrators *RsFT* and *RsSOC1-1* under marginal vernalization in radish. *Plants*, 9(5):594. <https://doi.org/10.3390/plants9050594>
- Jung, Y. J., Kim, J. H., Lee, H. J., Kim, D. H., Yu, J., Bae, S., Cho, Y. G., & Kang, K. K. (2020). Generation and transcriptome profiling of *Slr1-d7* and *Slr1-d8* mutant lines with a new semi-dominant dwarf allele of *SLR1* using the CRISPR/cas9 system in rice. *International Journal of Molecular Sciences*, 21(15), 1–11. <https://doi.org/10.3390/ijms21155492>
- Kagale, S., & Rozwadowski, K. (2010). Small yet effective: The Ethylene-responsive element binding factor-associated Amphiphilic Repression (EAR) motif. *Plant Signaling and Behavior*, 5(6), 691–694. <https://doi.org/10.4161/psb.5.6.11576>
- Kamigaki, A., Nito, K., Hikino, K., Goto-Yamada, S., Nishimura, M., & Nakagawa, T. (2016). Gateway vectors for simultaneous detection of multiple protein–protein interactions in plant cells using bimolecular fluorescence complementation. *PLoS ONE*, 11(8): e0160717. <https://doi.org/10.1371/journal.pone.0160717>

- Karssen, C. M., Zagorski, S., Kepczynski, J., & Groot, S. P. C. (1989). Key role for endogenous gibberellins in the control of seed germination. *Annals of Botany*, *63*(1), 71–80. <https://doi.org/10.1093/oxfordjournals.aob.a087730>
- Keegan, L., Gill, G., & Ptashne, M. (1986). Separation of DNA binding from the transcription-activating function of a eukaryotic regulatory protein. *Science*, *231*(4739), 699–704. DOI: 10.1126/science.3080805
- Kepczynski, J. (1986a). Ethylene-dependent action of gibberellin in seed germination of *Amaranthus caudatus*. *Physiologia Plantarum*, *67*(4), 584–587. <https://doi.org/10.1111/j.1399-3054.1986.tb05059.x>
- Kepczynski, J. (1986b). Inhibition of *Amaranthus caudatus* seed germination by polyethylene glycol-6000 and abscisic acid and its reversal by ethephon or 1-aminocyclopropane-1-carboxylic acid. *Physiologia Plantarum*, *67*(4), 588–591. <https://doi.org/10.1111/j.1399-3054.1986.tb05060.x>
- Kepczynski, J., & Kepczynska, E. (1997). Ethylene in seed dormancy and germination. *Physiologia Plantarum*, *101*(4), 120–126. <https://doi.org/10.1111/j.1399-3054.1997.tb01056.x>
- Kepczyński, J., Kepczyńska, E., & Knypl, J. S. (1988). Effects of gibberellic acid, ethephon, and 1-aminocyclopropane-1-carboxylic acid on germination of *Amaranthus caudatus* seeds inhibited by paclobutrazol. *Journal of Plant Growth Regulation*, *7*(1), 59–66. <https://doi.org/10.1007/BF02054162>
- Kerppola, T. K. (2006). Design and implementation of bimolecular fluorescence complementation (BiFC) assays for the visualization of protein interactions in living cells. *Nature Protocols*, *1*(3), 1278–1286. <https://doi.org/10.1038/nprot.2006.201>
- Kerppola, T. K. (2008). Bimolecular fluorescence complementation (BiFC) analysis as a probe of protein interactions in living cells. *Annual Review of Biophysics*, *37*, 465–487. <https://doi.org/10.1146/annurev.biophys.37.032807.125842>
- Kertesz, Z., Flintham, J. E., & Gale, M. D. (1991). Effects of *Rht* dwarfing genes on wheat grain yield and its components under Eastern European conditions. *Cereal Research Communications*, *19*(3), 297–304. <https://www.jstor.org/stable/23783715>
- Keyes, G. J., Paolillo, D. J., & Sorrells, M. E. (1989). The effects of dwarfing genes *Rht1*

- and *Rht2* on cellular dimensions and rate of leaf elongation in wheat. *Annals of Botany*, 64(6), 683–690. <https://doi.org/10.1093/oxfordjournals.aob.a087894>
- Keyes, G., Sorrells, M. E., & Setter, T. L. (1990). Gibberellic acid regulates cell wall extensibility in wheat (*Triticum aestivum* L.). *Plant Physiology*, 92(1), 242–245. <https://doi.org/10.1104/pp.92.1.242>
- Khaliq, I., Irshad, A., & Ahsan, M. (2008). Awns and flag leaf contribution towards grain yield in spring wheat (*Triticum aestivum* L.). *Cereal Research Communications*, 36(1), 65–76. <https://doi.org/10.1556/CRC.36.2008.1.7>
- Kim, D., Alptekin, B., & Budak, H. (2018). CRISPR/Cas9 genome editing in wheat. *Functional and Integrative Genomics*, 18(1), 31–41. <https://doi.org/10.1007/s10142-017-0572-x>
- Kim, D. H., Yamaguchi, S., Lim, S., Oh, E., Park, J., Hanada, A., Kamiya, Y., & Choi, G. (2008). SOMNUS, a CCCH-type zinc finger protein in Arabidopsis, negatively regulates light-dependent seed germination downstream of PIL5. *The Plant Cell*, 20(5), 1260–1277. <https://doi.org/10.1105/tpc.108.058859>
- Kleinstiver, B. P., Prew, M. S., Tsai, S. Q., Topkar, V. V., Nguyen, N. T., Zheng, Z., Gonzales, A. P. W., Li, Z., Peterson, R. T., Yeh, J. R. J., Aryee, M. J., & Joung, J. K. (2015). Engineered CRISPR-Cas9 nucleases with altered PAM specificities. *Nature*, 523(7561), 481–485. <https://doi.org/10.1038/nature14592>
- Kobayashi, A., Miura, S., & Kozaki, A. (2017). INDETERMINATE DOMAIN PROTEIN binding sequences in the 5'-untranslated region and promoter of the *SCARECROW* gene play crucial and distinct roles in regulating *SCARECROW* expression in roots and leaves. *Plant Molecular Biology*, 94(1–2), 1–13. <https://doi.org/10.1007/s11103-016-0578-0>
- Kobayashi, M., Yamaguchi, I., Murofushi, N., Ota, Y., & Takahashi, N. (1988). Fluctuation and Localization of Endogenous Gibberellins in Rice. *Agricultural and Biological Chemistry*, 52(5), 1189–1194. <https://doi.org/10.1080/00021369.1988.10868799>
- Kondhare, K. R., Farrell, a. D., Kettlewell, P. S., Hedden, P., & Monaghan, J. M. (2015). Pre-maturity alpha-amylase in wheat: The role of abscisic acid and gibberellins. *Journal of Cereal Science*, 63, 95–108. <https://doi.org/10.1016/j.jcs.2015.03.004>
- Kondhare, K. R., Hedden, P., Kettlewell, P. S., Farrell, A. D., & Monaghan, J. M. (2014).

Use of the hormone-biosynthesis inhibitors fluridone and paclobutrazol to determine the effects of altered abscisic acid and gibberellin levels on pre-maturity α -amylase formation in wheat grains. *Journal of Cereal Science*, *60*(1), 210–216. <https://doi.org/10.1016/j.jcs.2014.03.001>

Kondhare, K. R., Kettlewell, P. S., Farrell, A. D., Hedden, P., & Monaghan, J. M. (2012). Effects of exogenous abscisic acid and gibberellic acid on pre-maturity α -amylase formation in wheat grains. *Euphytica*, *188*(1), 51–60. <https://doi.org/10.1007/s10681-012-0706-0>

Kondhare, K. R., Kettlewell, P. S., Farrell, A. D., Hedden, P., & Monaghan, J. M. (2013). The role of sensitivity to abscisic acid and gibberellin in pre-maturity α -amylase formation in wheat grains. *Journal of Cereal Science*, *58*(3), 472–478. <https://doi.org/10.1016/j.jcs.2013.09.009>

Koornneef, M., & van der Veen, J. H. (1980). Induction and analysis of gibberellin sensitive mutants in *Arabidopsis thaliana* (L.) heynh. *Theoretical and Applied Genetics*, *58*(6), 257–263. <https://doi.org/10.1007/BF00265176>

Kozaki, A., Hake, S., & Colasanti, J. (2004). The maize ID1 flowering time regulator is a zinc finger protein with novel DNA binding properties. *Nucleic Acids Research*, *32*(5), 1710–1720. <https://doi.org/10.1093/nar/gkh337>

Krasileva, K. V., Vasquez-Gross, H. A., Howell, T., Bailey, P., Paraiso, F., Clissold, L., Simmonds, J., Ramirez-Gonzalez, R. H., Wang, X., Borrill, P., Fosker, C., Ayling, S., Phillips, A. L., Uauy, C., & Dubcovsky, J. (2017). Uncovering hidden variation in polyploid wheat. *Proceedings of the National Academy of Sciences of the United States of America*, *114*(6), E913–E921. <https://doi.org/10.1073/pnas.1619268114>

Kruglova, N. N., Titova, G. E., Seldimirova, O. A., Zinatullina, A. E., & Veselov, D. S. (2020). Embryo of flowering plants at the critical stage of embryogenesis relative autonomy (by example of cereals). *Russian Journal of Developmental Biology*, *51*(1), 1–15. <https://doi.org/10.1134/s1062360420010026>

Kumar, M., Le, D. T., Hwang, S., Seo, P. J., & Kim, H. U. (2019). Role of the INDETERMINATE DOMAIN genes in plants. In *International Journal of Molecular Sciences*, *20*(9), 2286. <https://doi.org/10.3390/ijms20092286>

Kumar, R., Kaur, A., Pandey, A., Mamrutha, H. M., & Singh, G. P. (2019). CRISPR-based

genome editing in wheat: a comprehensive review and future prospects. *Molecular Biology Reports*, 46(3), 3557–3569. <https://doi.org/10.1007/s11033-019-04761-3>

Kuo, A., Cappelluti, S., Cervantes-Cervantes, M., Rodriguez, M., & Bush, D. S. (1996). Okadaic acid, a protein phosphatase inhibitor, blocks calcium changes, gene expression, and cell death induced by gibberellin in wheat aleurone cells. *The Plant Cell*, 8(2), 259–269. <https://doi.org/10.1105/tpc.8.2.259>

Lamesch, P., Berardini, T. Z., Li, D., Swarbreck, D., Wilks, C., Sasidharan, R., Muller, R., Dreher, K., Alexander, D. L., Garcia-Hernandez, M., Karthikeyan, A. S., Lee, C. H., Nelson, W. D., Ploetz, L., Singh, S., Wensel, A., & Huala, E. (2012). The Arabidopsis Information Resource (TAIR): Improved gene annotation and new tools. *Nucleic Acids Research*, 40(D1), 1202–1210. <https://doi.org/10.1093/nar/gkr1090>

Lanahan, M. B., Ho, T.-H. D., Rogers, S. W., & Rogers, J. C. (1992). A gibberellin response complex in cereal α -amylase gene promoters. *The Plant Cell*, 4(2), 203–211. <https://doi.org/10.1105/tpc.4.2.203>

Lanfear, R. (2018). Do plants have a segregated germline? *PLOS Biology*, 16(5), e2005439. <https://doi.org/10.1371/journal.pbio.2005439>

Lange, T., & Pimenta Lange, M. J. (2020). The multifunctional dioxygenases of gibberellin synthesis. *Plant and Cell Physiology*, 61(11), 1869–1879. <https://doi.org/10.1093/pcp/pcaa051>

Langer, S. M., Longin, C. F. H., & Würschum, T. (2014). Flowering time control in European winter wheat. *Frontiers in Plant Science*, 5:537. <https://doi.org/10.3389/fpls.2014.00537>

Lanning, S. P., Martin, J. M., Stougaard, R. N., Guillen-Portal, F. R., Blake, N. K., Sherman, J. D., Robbins, A. M., Kephart, K. D., Lamb, P., Carlson, G. R., Pumphrey, M., & Talbert, L. E. (2012). Evaluation of near-isogenic lines for three height-reducing genes in hard red spring wheat. *Crop Science*, 52(3), 1145–1152. <https://doi.org/10.2135/cropsci2011.11.0625>

Lantzouni, O., Alkofer, A., Falter-Braun, P., & Schwechheimer, C. (2020). GROWTH-REGULATING FACTORS interact with dellas and regulate growth in cold stress. *Plant Cell*, 32(4), 1018–1034. <https://doi.org/10.1105/TPC.19.00784>

- Leach, L. J., Belfield, E. J., Jiang, C., Brown, C., Mithani, A., & Harberd, N. P. (2014). Patterns of homoeologous gene expression shown by RNA sequencing in hexaploid bread wheat. *BMC Genomics*, *15*(1):276. <https://doi.org/10.1186/1471-2164-15-276>
- Lenton, J. R., Appleford, N. E. J., & Croker, S. J. (1994). Gibberellins and α -amylase gene expression in germinating wheat grains. *Plant Growth Regulation*, *15*(3), 261–270. <https://doi.org/10.1007/BF00029899>
- Li, Chen, Zheng, L., Wang, X., Hu, Z., Zheng, Y., Chen, Q., Hao, X., Xiao, X., Wang, X., Wang, G., & Zhang, Y. (2019). Comprehensive expression analysis of Arabidopsis *GA2-oxidase* genes and their functional insights. *Plant Science*, *285*, 1–13. <https://doi.org/10.1016/j.plantsci.2019.04.023>
- Li, Chengdao, Ni, P., Francki, M., Hunter, A., Zhang, Y., Schibeci, D., Li, H., Tarr, A., Wang, J., Cakir, M., Yu, J., Bellgard, M., Lance, R., & Appels, R. (2004). Genes controlling seed dormancy and pre-harvest sprouting in a rice-wheat-barley comparison. *Functional and Integrative Genomics*, *4*(2), 84–93. <https://doi.org/10.1007/s10142-004-0104-3>
- Li, J. F., Norville, J. E., Aach, J., McCormack, M., Zhang, D., Bush, J., Church, G. M., & Sheen, J. (2013). Multiplex and homologous recombination-mediated genome editing in Arabidopsis and *Nicotiana benthamiana* using guide RNA and Cas9. In *Nature Biotechnology*, *31*(8), 688–691. <https://doi.org/10.1038/nbt.2654>
- Li, M., An, F., Li, W., Ma, M., Feng, Y., Zhang, X., & Guo, H. (2016). DELLA proteins interact with FLC to repress flowering transition. *Journal of Integrative Plant Biology*, *58*(7), 642–655. <https://doi.org/10.1111/jipb.12451>
- Li, Q.-F., Wang, C., Jiang, L., Li, S., Sun, S. S. M., & He, J.-X. (2012). An interaction between BZR1 and DELLAs mediates direct signaling crosstalk between brassinosteroids and gibberellins in Arabidopsis. *Science Signaling*, *5*(244), ra72. <https://doi.org/10.1126/scisignal.2002908>
- Li, Q., Li, L., Liu, Y., Lv, Q., Zhang, H., Zhu, J., & Li, X. (2017). Influence of *TaGW2-6A* on seed development in wheat by negatively regulating gibberellin synthesis. *Plant Science*, *263*, 226–235. <https://doi.org/10.1016/j.plantsci.2017.07.019>
- Li, Shan, Tian, Y., Wu, K., Ye, Y., Yu, J., Zhang, J., Liu, Q., Hu, M., Li, H., Tong, Y., Harberd, N. P., & Fu, X. (2018). Modulating plant growth–metabolism coordination for

sustainable agriculture. *Nature*, 560(7720), 595–600.
<https://doi.org/10.1038/s41586-018-0415-5>

Li, Shengping, Zhao, Y., Zhao, Z., Wu, X., Sun, L., Liu, Q., & Wu, Y. (2016). Crystal structure of the GRAS domain of SCARECROW-LIKE7 in *Oryza sativa*. *The Plant Cell*, 28(5), 1025–1034. <https://doi.org/10.1105/tpc.16.00018>

Li, X. P., Lan, S. Q., Liu, Y. P., Gale, M. D., & Worland, T. J. (2006). Effects of different *Rht-B1b*, *Rht-D1b* and *Rht-B1c* dwarfing genes on agronomic characteristics in wheat. *Cereal Research Communications*, 34(2), 919–924. <https://doi.org/10.1556/CRC.34.2006.2-3.220>

Li, X., Qian, Q., Fu, Z., Wang, Y., Xiong, G., Zeng, D., Wang, X., Liu, X., Teng, S., Hiroshi, F., Yuan, M., Luo, D., Han, B., & Li, J. (2003). Control of tillering in rice. *Nature*, 422(6932), 618–621. <https://doi.org/10.1038/nature01518>

Li, Y., Wang, H., Li, X., Liang, G., & Yu, D. (2017). Two DELLA-interacting proteins bHLH48 and bHLH60 regulate flowering under long-day conditions in *Arabidopsis thaliana*. *Journal of Experimental Botany*, 68(11), 2757–2767. <https://doi.org/10.1093/jxb/erx143>

Liang, Z., Chen, K., Li, T., Zhang, Y., Wang, Y., Zhao, Q., Liu, J., Zhang, H., Liu, C., Ran, Y., & Gao, C. (2017). Efficient DNA-free genome editing of bread wheat using CRISPR/Cas9 ribonucleoprotein complexes. *Nature Communications*, 8(1), 1–5. <https://doi.org/10.1038/ncomms14261>

Liao, Z., Yu, H., Duan, J., Yuan, K., Yu, C., Meng, X., Kou, L., Chen, M., Jing, Y., Liu, G., Smith, S. M., & Li, J. (2019). SLR1 inhibits MOC1 degradation to coordinate tiller number and plant height in rice. *Nature Communications*, 10(1), 1–9. <https://doi.org/10.1038/s41467-019-10667-2>

Liebsch, D., & Palatnik, J. F. (2020). MicroRNA miR396, GRF transcription factors and GIF co-regulators: a conserved plant growth regulatory module with potential for breeding and biotechnology. *Current Opinion in Plant Biology*, 53, 31–42. <https://doi.org/10.1016/j.pbi.2019.09.008>

Lim, S., Park, J., Lee, N., Jeong, J., Toh, S., Watanabe, A., Kim, J., Kang, H., Kim, D. H., Kawakami, N., & Choi, G. (2013). ABA-insensitive3, ABA-insensitive5, and DELLAs interact to activate the expression of *SOMNUS* and other high-temperature-inducible genes in imbibed seeds in *Arabidopsis*. *The Plant Cell*, 25(12), 4863–

4878. <https://doi.org/10.1105/tpc.113.118604>

- Lin, M., Zhang, D., Liu, S., Zhang, G., Yu, J., Fritz, A. K., & Bai, G. (2016). Genome-wide association analysis on pre-harvest sprouting resistance and grain color in U.S. winter wheat. *BMC Genomics*, *17*(1). <https://doi.org/10.1186/s12864-016-3148-6>
- Lin, Y., Yang, L., Paul, M., Zu, Y., & Tang, Z. (2013). Ethylene promotes germination of Arabidopsis seed under salinity by decreasing reactive oxygen species: Evidence for the involvement of nitric oxide simulated by sodium nitroprusside. *Plant Physiology and Biochemistry*, *73*, 211–218. <https://doi.org/10.1016/j.plaphy.2013.10.003>
- Linkies, A., & Leubner-Metzger, G. (2012). Beyond gibberellins and abscisic acid: how ethylene and jasmonates control seed germination. *Plant Cell Reports*, *31*(2), 253–270. <https://doi.org/10.1007/s00299-011-1180-1>
- Linkies, A., Müller, K., Morris, K., Turečková, V., Wenk, M., Cadman, C. S. C., Corbineau, F., Strnad, M., Lynn, J. R., Finch-Savage, W. E., & Leubner-Metzger, G. (2009). Ethylene interacts with abscisic acid to regulate endosperm rupture during germination: A comparative approach using *Lepidium sativum* and *Arabidopsis thaliana*. *Plant Cell*, *21*(12), 3803–3822. <https://doi.org/10.1105/tpc.109.070201>
- Liu, G., Yin, K., Zhang, Q., Gao, C., & Qiu, J. L. (2019). Modulating chromatin accessibility by transactivation and targeting proximal dsRNAs enhances Cas9 editing efficiency in vivo. *Genome Biology*, *20*(1), 145. <https://doi.org/10.1186/s13059-019-1762-8>
- Liu, S., Sehgal, S. K., Li, J., Lin, M., Trick, H. N., Yu, J., Gill, B. S., & Bai, G. (2013). Cloning and characterization of a critical regulator for preharvest sprouting in wheat. *Genetics*, *195*(1), 263–273. <https://doi.org/10.1534/genetics.113.152330>
- Liu, S., Sehgal, S. K., Lin, M., Li, J., Trick, H. N., Gill, B. S., & Bai, G. (2015). Independent mis-splicing mutations in *TaPHS1* causing loss of preharvest sprouting (PHS) resistance during wheat domestication. *New Phytologist*, *208*(3), 928–935. <https://doi.org/10.1111/nph.13489>
- Liu, X., & Hou, X. (2018). Antagonistic regulation of ABA and GA in metabolism and signaling pathways. *Frontiers in Plant Science*, *9*:251.

<https://doi.org/10.3389/fpls.2018.00251>

- Liu, Z., Bao, W., Liang, W., Yin, J., & Zhang, D. (2010). Identification of gamyb-4 and analysis of the regulatory role of GAMYB in rice anther development. *Journal of Integrative Plant Biology*, *52*(7), 670–678. <https://doi.org/10.1111/j.1744-7909.2010.00959.x>
- Lo, S. F., Yang, S. Y., Chen, K. T., Hsing, Y. I., Zeevaart, J. A. D., Chen, L. J., & Yu, S. M. (2008). A novel class of gibberellin 2-oxidases control semidwarfism, tillering, and root development in rice. *Plant Cell*, *20*(10), 2603–2618. <https://doi.org/10.1105/tpc.108.060913>
- Lonsdale, J. E., Mcdonald, K. L., & Jones, R. L. (1999). High pressure freezing and freeze substitution reveal new aspects of fine structure and maintain protein antigenicity in barley aleurone cells. *The Plant Journal*, *17*(2), 221–229. <https://doi.org/10.1046/j.1365-313X.1999.00362.x>
- Lorrain, S., Allen, T., Duek, P. D., Whitelam, G. C., & Fankhauser, C. (2007). Phytochrome-mediated inhibition of shade avoidance involves degradation of growth-promoting bHLH transcription factors. *The Plant Journal*, *53*(2), 312–323. <https://doi.org/10.1111/j.1365-313X.2007.03341.x>
- Lovergrove, a, & Hooley, R. (2000). Gibberellin and abscisic acid in aleurone. *Trends in Plant Science*, *5*(3), 102–110. [https://doi.org/10.1016/S1360-1385\(00\)01571-5](https://doi.org/10.1016/S1360-1385(00)01571-5)
- Lu, C.-A., Ho, T. D., Ho, S.-L., & Yu, S.-M. (2002). Three novel MYB proteins with one DNA binding repeat mediate sugar and hormone regulation of alpha-amylase gene expression. *The Plant Cell*, *14*(8), 1963–1980. <https://doi.org/10.1105/tpc.001735>
- Lu, C.-A., Lin, C.-C., Lee, K.-W., Chen, J.-L., Huang, L.-F., Ho, S.-L., Liu, H.-J., Hsing, Y.-I., & Yu, S.-M. (2007). The SnRK1A protein kinase plays a key role in sugar signaling during germination and seedling growth of rice. *The Plant Cell*, *19*(8), 2484–2499. <https://doi.org/10.1105/tpc.105.037887>
- Lu, Y., Feng, Z., Meng, Y., Bian, L., Xie, H., Mysore, K. S., & Liang, J.-S. (2020). SLENDER RICE1 and *Oryza sativa* INDETERMINATE DOMAIN2 regulating OsmiR396 are involved in stem elongation. *Plant Physiology*, *182*(4), 2213–2227. <https://doi.org/10.1104/pp.19.01008>

- Lv, B., Nitcher, R., Han, X., Wang, S., Ni, F., Li, K., Pearce, S., Wu, J., Dubcovsky, J., & Fu, D. (2014). Characterization of *FLOWERING LOCUS T1 (FT1)* gene in *Brachypodium* and wheat. *PLoS ONE*, *9*(4), e94171. <https://doi.org/10.1371/journal.pone.0094171>
- Ma, X., Zhang, Q., Zhu, Q., Liu, W., Chen, Y., Qiu, R., Wang, B., Yang, Z., Li, H., Lin, Y., Xie, Y., Shen, R., Chen, S., Wang, Z., Chen, Y., Guo, J., Chen, L., Zhao, X., Dong, Z., & Liu, Y. G. (2015). A robust CRISPR/Cas9 system for convenient, high-efficiency multiplex genome editing in monocot and dicot plants. *Molecular Plant*, *8*(8), 1274–1284. <https://doi.org/10.1016/j.molp.2015.04.007>
- Macmillan, J. (2002). Occurrence of gibberellins in vascular plants, fungi, and bacteria. *Journal of Plant Growth Regulation*, *20*, 387–442. <https://doi.org/10.1007/s003440010038>
- Magome, H., Nomura, T., Hanada, A., Takeda-Kamiya, N., Ohnishi, T., Shinma, Y., Katsumata, T., Kawaide, H., Kamiya, Y., & Yamaguchi, S. (2013). *CYP714B1* and *CYP714B2* encode gibberellin 13-oxidases that reduce gibberellin activity in rice. *Proceedings of the National Academy of Sciences of the United States of America*, *110*(5), 1947–1952. <https://doi.org/10.1073/pnas.1215788110>
- Magome, H., Yamaguchi, S., Hanada, A., Kamiya, Y., & Oda, K. (2004). *dwarf* and *delayed-flowering 1*, a novel Arabidopsis mutant deficient in gibberellin biosynthesis because of overexpression of a putative AP2 transcription factor. *Plant Journal*, *37*(5), 720–729. <https://doi.org/10.1111/j.1365-313X.2003.01998.x>
- Magome, H., Yamaguchi, S., Hanada, A., Kamiya, Y., & Oda, K. (2008). The DDF1 transcriptional activator upregulates expression of a gibberellin-deactivating gene, *GA2ox7*, under high-salinity stress in Arabidopsis. *Plant Journal*, *56*(4), 613–626. <https://doi.org/10.1111/j.1365-313X.2008.03627.x>
- Mamytova, N. S., Kuzovlev, V. A., Khakimzhanov, A. A., & Fursov, O. V. (2014). The contribution of different alpha-amylase isoenzymes of the commodity grain spring wheat in the formation of falling number values. *Prikladnaia Biokhimiia i Mikrobiologiia*, *50*(5), 533–540. <https://doi.org/10.7868/S0555109914040242>
- Manoharlal, R., & Saiprasad, G. V. S. (2020a). Global histone H3 hyperacetylation-associated epigenetic changes induced in ethephon-primed sprouts of soybean

[*Glycine max* (L.) Merrill]. *Acta Physiologiae Plantarum*, 42(2), 1–14.
<https://doi.org/10.1007/s11738-020-3015-6>

Manoharlal, R., & Saiprasad, G. V. S. (2020b). Gene-specific chromatin architecture changes associates with ethylene induced germination of soybean [*Glycine max* (L.) Merrill]. *Plant Physiology Reports*, 25(1), 163–170.
<https://doi.org/10.1007/s40502-020-00502-y>

Manoharlal, R., Saiprasad, G. V. S., & Kovařík, A. (2019). Gene-specific DNA demethylation changes associates with ethylene induced germination of soybean [*Glycine max* (L.) Merrill]. *Plant Physiology Reports*, 24(2), 272–277.
<https://doi.org/10.1007/s40502-019-00449-9>

Mantegazza, O., Gregis, V., Chiara, M., Selva, C., Leo, G., Horner, D. S., & Kater, M. M. (2014). Gene coexpression patterns during early development of the native *Arabidopsis* reproductive meristem: novel candidate developmental regulators and patterns of functional redundancy. *The Plant Journal*, 79(5), 861–877.
<https://doi.org/10.1111/tpj.12585>

Mares, D., & Mrva, K. (2008). Late-maturity α -amylase: Low falling number in wheat in the absence of preharvest sprouting. *Journal of Cereal Science*, 47(1), 6–17.
<https://doi.org/10.1016/j.jcs.2007.01.005>

Mares, D.J., & Gale, M. D. (1990). Control of α -amylase synthesis in wheat grains. In K. Ringlund, E. Mosleth, & D. J. Mares (Eds.), *Fifth International Symposium on Pre-Harvest Sprouting in Cereals*. Westview Press, Boulder, Co, USA, (pp. 183–194).

Mares, Daryl J., & Mrva, K. (2014). Wheat grain preharvest sprouting and late maturity α -amylase. *Planta*, 240(6), 1167–1178. <https://doi.org/10.1007/s00425-014-2172-5>

Marín-De La Rosa, N., Pfeiffer, A., Hill, K., Locascio, A., Bhalerao, R. P., Miskolczi, P., Grønlund, A. L., Wanchoo-Kohli, A., Thomas, S. G., Bennett, M. J., Lohmann, J. U., Blázquez, M. A., Alabadí, D., & Yu, H. (2015). Genome wide binding site analysis reveals transcriptional coactivation of cytokinin-responsive genes by DELLA proteins. *PLoS Genet*, 11(7), e1005337.
<https://doi.org/10.1371/journal.pgen.1005337>

Marín-de la Rosa, N., Sotillo, B., Miskolczi, P., Gibbs, D. J., Vicente, J., Carbonero, P., Oñate-Sánchez, L., Holdsworth, M. J., Bhalerao, R., Alabadí, D., & Blázquez, M. a.

- (2014). Large-scale identification of gibberellin-related transcription factors defines group VII ETHYLENE RESPONSE FACTORS as functional DELLA partners. *Plant Physiology*, *166*(2), 1022–1032. <https://doi.org/10.1104/pp.114.244723>
- Martinez, S. A., Shorinola, O., Conselman, S., See, D., Skinner, D. Z., Uauy, C., & Steber, C. M. (2020). Exome sequencing of bulked segregants identified a novel *TaMKK3-A* allele linked to the wheat ERA8 ABA-hypersensitive germination phenotype. *Theoretical and Applied Genetics*, *133*(3), 719–736. <https://doi.org/10.1007/s00122-019-03503-0>
- Matsubara, K., Yamanouchi, U., Wang, Z.-X., Minobe, Y., Izawa, T., & Yano, M. (2008). *Ehd2*, a rice ortholog of the maize *INDETERMINATE1* gene, promotes flowering by up-regulating *Ehd1*. *Plant Physiology*, *148*, 1425–1435. <https://doi.org/10.1104/pp.108.125542>
- Matsushita, A., Furumoto, T., Ishida, S., & Takahashi, Y. (2007). AGF1, an AT-hook protein, is necessary for the negative feedback of *AtGA3ox1* encoding GA 3-oxidase. *Plant Physiology*, *143*(3), 1152–1162. <https://doi.org/10.1104/pp.106.093542>
- McCallum, C. M., Comai, L., Greene, E. A., & Henikoff, S. (2000). Targeted screening for induced mutations. *Nature Biotechnology*, *18*(4), 455–457. <https://doi.org/10.1038/74542>
- McFadden, E. S., & Sears, E. R. (1946). The origin of *Triticum spelta* and its free-threshing hexaploid relatives. *The Journal of Heredity*, *37*(949), 81–107. <https://doi.org/10.1093/oxfordjournals.jhered.a105594>
- Mehla, J., Caufield, J. H., Sakhawalkar, N., & Uetz, P. (2017). A comparison of two-hybrid approaches for detecting protein-protein interactions. *Methods in Enzymology*, *586*, 333–358. <https://doi.org/10.1016/bs.mie.2016.10.020>
- Michno, J. M., Viridi, K., Stec, A. O., Liu, J., Wang, X., Xiong, Y., & Stupar, R. M. (2020). Integration, abundance, and transmission of mutations and transgenes in a series of CRISPR/Cas9 soybean lines. *BMC Biotechnology*, *20*(1):10. <https://doi.org/10.1186/s12896-020-00604-3>
- Middleton, A. M., Úbeda-Tomás, S., Griffiths, J., Holman, T., Hedden, P., Thomas, S. G., Phillips, A. L., Holdsworth, M. J., Bennett, M. J., King, J. R., & Owen, M. R. (2012). Mathematical modeling elucidates the role of transcriptional feedback

in gibberellin signaling. *Proceedings of the National Academy of Sciences of the United States of America*, 109(19), 7571–7576. <https://doi.org/10.1073/pnas.1113666109>

Millar, A. a., Jacobsen, J. V., Ross, J. J., Helliwell, C. a., Poole, A. T., Scofield, G., Reid, J. B., & Gubler, F. (2006). Seed dormancy and ABA metabolism in Arabidopsis and barley: The role of ABA 8'-hydroxylase. *Plant Journal*, 45(6), 942–954. <https://doi.org/10.1111/j.1365-313X.2006.02659.x>

Miller, K. E., Kim, Y., Huh, W. K., & Park, H. O. (2015). Bimolecular fluorescence complementation (BiFC) analysis: Advances and recent applications for Genome-Wide interaction studies. *Journal of Molecular Biology*, 427(11), 2039–2055. <https://doi.org/10.1016/j.jmb.2015.03.005>

Miralles, D. J., Calderini, D. F., Pomar, K. P., & D'Ambrogio, A. (1998). Dwarfing genes and cell dimensions in different organs of wheat. *Journal of Experimental Botany*, 49(324), 1119–1127. <https://doi.org/10.1093/jxb/49.324.1119>

Miralles, Daniel J., Katz, S. D., Colloca, A., & Slafer, G. A. (1998). Floret development in near isogenic wheat lines differing in plant height. *Field Crops Research*, 59(1), 21–30. [https://doi.org/10.1016/S0378-4290\(98\)00103-8](https://doi.org/10.1016/S0378-4290(98)00103-8)

Miransari, M., & Smith, D. L. (2014). Plant hormones and seed germination. *Environmental and Experimental Botany*, 99, 110–121. <https://doi.org/10.1016/J.ENVEXPBOT.2013.11.005>

Moot, D. J., & Every, D. (1990). A comparison of bread baking, falling number, α -amylase assay and visual method for the assessment of pre-harvest sprouting in wheat. *Journal of Cereal Science*, 11(3), 225–234. [https://doi.org/10.1016/S0733-5210\(09\)80166-5](https://doi.org/10.1016/S0733-5210(09)80166-5)

Moreno-Mateos, M. A., Vejnar, C. E., Beaudoin, J. D., Fernandez, J. P., Mis, E. K., Khokha, M. K., & Giraldez, A. J. (2015). CRISPRscan: Designing highly efficient sgRNAs for CRISPR-Cas9 targeting in vivo. *Nature Methods*, 12(10), 982–988. <https://doi.org/10.1038/nmeth.3543>

Morrison, I. N. (1976). The structure of the chlorophyll-containing cross cells and tube cells of the inner pericarp of wheat during grain development. *Botanical Gazette*, 137(1), 85–93. <https://doi.org/10.1086/336845>

Morrone, D., Chambers, J., Lowry, L., Kim, G., Anterola, A., Bender, K., & Peters, R. J.

- (2009). Gibberellin biosynthesis in bacteria: Separate *ent*-copalyl diphosphate and *ent*-kaurene synthases in *Bradyrhizobium japonicum*. *FEBS Letters*, *583*(2), 475–480. <https://doi.org/10.1016/j.febslet.2008.12.052>
- Mrva, K., & Mares, D. J. (1996). Expression of late maturity alpha-amylase in wheat containing gibberellic acid insensitivity genes. *Euphytica*, *88*(1), 69–76. <https://doi.org/10.1007/BF00029267>
- Mrva, Kolumbina, Wallwork, M., & Mares, D. J. (2006). A-amylase and programmed cell death in aleurone of ripening wheat grains. *Journal of Experimental Botany*, *57*(4), 877–885. <https://doi.org/10.1093/jxb/erj072>
- Müller, K., Tintelnot, S., & Leubner-Metzger, G. (2006). Endosperm-limited Brassicaceae seed germination: abscisic acid inhibits embryo-induced endosperm weakening of *Lepidium sativum* (cress) and endosperm rupture of cress and *Arabidopsis thaliana*. *Plant and Cell Physiology*, *47*(7), 864–877.
- Murase, K., Hirano, Y., Sun, T., & Hakoshima, T. (2008). Gibberellin-induced DELLA recognition by the gibberellin receptor GID1. *Nature*, *456*(7221), 459–U15. <https://doi.org/10.1038/nature07519>
- Nakajima, M., Shimada, A., Takashi, Y., Kim, Y. C., Park, S. H., Ueguchi-Tanaka, M., Suzuki, H., Katoh, E., Iuchi, S., Kobayashi, M., Maeda, T., Matsuoka, M., & Yamaguchi, I. (2006). Identification and characterization of Arabidopsis gibberellin receptors. *Plant Journal*, *46*(5), 880–889. <https://doi.org/10.1111/j.1365-3113X.2006.02748.x>
- Nakano, T., Suzuki, K., Fujimura, T., & Shinshi, H. (2006). Genome-wide analysis of the ERF gene family in Arabidopsis and rice. *Plant Physiology*, *140*(2), 411–432. <https://doi.org/10.1104/pp.105.073783>
- Nalam, V. J., Vales, M. I., Watson, C. J. W., Kianian, S. F., & Riera-Lizarazu, O. (2006). Map-based analysis of genes affecting the brittle rachis character in tetraploid wheat (*Triticum turgidum* L.). *Theoretical and Applied Genetics*, *112*(2), 373–381. <https://doi.org/10.1007/s00122-005-0140-y>
- Narsai, R., Law, S. R., Carrie, C., Xu, L., & Whelan, J. (2011). In-depth temporal transcriptome profiling reveals a crucial developmental switch with roles for RNA processing and organelle metabolism that are essential for germination in Arabidopsis. *Plant Physiology*, *157*(3), 1342–1362.

<https://doi.org/10.1104/pp.111.183129>

- Nekrasov, V., Staskawicz, B., Weigel, D., Jones, J. D. G., & Kamoun, S. (2013). Targeted mutagenesis in the model plant *Nicotiana benthamiana* using Cas9 RNA-guided endonuclease. *Nature Biotechnology*, *31*(8), 691–693. <https://doi.org/10.1038/nbt.2655>
- Nelissen, H., Rymen, B., Jikumaru, Y., Demuyne, K., Van Lijsebettens, M., Kamiya, Y., Inzé, D., & Beemster, G. T. S. (2012). A local maximum in gibberellin levels regulates maize leaf growth by spatial control of cell division. *Current Biology*, *22*(13), 1183–1187. <https://doi.org/10.1016/j.cub.2012.04.065>
- Nelson, S. K., & Steber, C. M. (2016). Gibberellin hormone signal perception: Down-regulating DELLA repressors of plant growth and development. *Annual Plant Reviews*, *49*, 153–188. <https://doi.org/10.1002/9781119210436.ch6>
- Newberry, M., Zwart, A. B., Whan, A., Mieog, J. C., Sun, M., Leyne, E., Pritchard, J., Daneri-Castro, S. N., Ibrahim, K., Diepeveen, D., Howitt, C. A., & Ral, J. P. F. (2018). Does late maturity alpha-amylase impact wheat baking quality? *Frontiers in Plant Science*, *9*. <https://doi.org/10.3389/fpls.2018.01356>
- Nijhawan, A., Jain, M., Tyagi, A. K., & Khurana, J. P. (2008). Genomic survey and gene expression analysis of the basic leucine zipper transcription factor family in rice. *Plant Physiology*, *146*(2), 333–350. <https://doi.org/10.1104/pp.107.112821>
- Nishimasu, H., Shi, X., Ishiguro, S., Gao, L., Hirano, S., Okazaki, S., Noda, T., Abudayyeh, O. O., Gootenberg, J. S., Mori, H., Oura, S., Holmes, B., Tanaka, M., Seki, M., Hirano, H., Aburatani, H., Ishitani, R., Ikawa, M., Yachie, N., ... Nureki, O. (2018). Engineered CRISPR-Cas9 nuclease with expanded targeting space. *Science*, *361*(6408), 1259–1262. <https://doi.org/10.1126/science.aas9129>
- Niu, X., Chen, S., Li, J., Liu, Y., Ji, W., & Li, H. (2019). Genome-wide identification of GRAS genes in *Brachypodium distachyon* and functional characterization of *BdSLR1* and *BdSLRL1*. *BMC Genomics*, *20*(1). <https://doi.org/10.1186/s12864-019-5985-6>
- Olaerts, H., De Bondt, Y., & Courtin, C. M. (2017). The heterogeneous distribution of α -amylase and endoxylanase activity over a population of preharvest sprouted wheat kernels and their localization in individual kernels. *Journal of Cereal Science*, *74*, 200–209. <https://doi.org/10.1016/j.jcs.2017.02.010>

- Olaerts, H., Roye, C., Derde, L. J., Sinnaeve, G., Meza, W. R., Bodson, B., & Courtin, C. M. (2016). Evolution and distribution of hydrolytic enzyme activities during preharvest sprouting of wheat (*Triticum aestivum*) in the field. *Journal of Agricultural and Food Chemistry*, 64(28), 5644-5652. <https://doi.org/10.1021/acs.jafc.6b01711>
- Oracz, K., El-Maarouf-Bouteau, H., Bogatek, R., Corbineau, F., & Bailly, C. (2008). Release of sunflower seed dormancy by cyanide: cross-talk with ethylene signalling pathway. *Journal of Experimental Botany*, 59(8), 2241-2251. <https://doi.org/10.1093/jxb/ern089>
- Ouyang, S., Zhu, W., Hamilton, J., Lin, H., Campbell, M., Childs, K., Thibaud-Nissen, F., Malek, R. L., Lee, Y., Zheng, L., Orvis, J., Haas, B., Wortman, J., & Buell, R. C. (2007). The TIGR Rice Genome Annotation Resource: Improvements and new features. *Nucleic Acids Research*, 35(1), 8-11. <https://doi.org/10.1093/nar/gkl976>
- Parish, R. W., & Li, S. F. (2010). Death of a tapetum: A programme of developmental altruism. *Plant Science*, 178(2), 73-89. <https://doi.org/10.1016/j.plantsci.2009.11.001>
- Park, J., Nguyen, K. T., Park, E., Jeon, J.-S., & Choi, G. (2013). DELLA proteins and their interacting RING Finger proteins repress gibberellin responses by binding to the promoters of a subset of gibberellin-responsive genes in Arabidopsis. *The Plant Cell*, 25(3), 927-943. <https://doi.org/10.1105/tpc.112.108951>
- Parry, M. A. J., Madgwick, P. J., Bayon, C., Tearall, K., Hernandez-Lopez, A., Baudo, M., Rakszegi, M., Hamada, W., Al-Yassin, A., Ouabbou, H., Labhili, M., & Phillips, A. L. (2009). Mutation discovery for crop improvement. *Journal of Experimental Botany*, 60(10), 2817-2825. <https://doi.org/10.1093/jxb/erp189>
- Pearce, S., Huttly, A. K., Prosser, I. M., Li, Y. D., Vaughan, S. P., Gallova, B., Patil, A., Coghill, J. A., Dubcovsky, J., Hedden, P., & Phillips, A. L. (2015). Heterologous expression and transcript analysis of gibberellin biosynthetic genes of grasses reveals novel functionality in the GA3ox family. *BMC Plant Biology*, 15(1). <https://doi.org/10.1186/s12870-015-0520-7>
- Pearce, S., Vanzetti, L. S., & Dubcovsky, J. (2013). Exogenous gibberellins induce wheat spike development under short days only in the presence of *VERNALIZATION1*.

Plant Physiology, 163(3), 1433–1445. <https://doi.org/10.1104/pp.113.225854>

- Peng, D., Chen, X., Yin, Y., Lu, K., Yang, W., Tang, Y., & Wang, Z. (2014). Lodging resistance of winter wheat (*Triticum aestivum* L.): Lignin accumulation and its related enzymes activities due to the application of paclobutrazol or gibberellin acid. *Field Crops Research*, 157, 1–7. <https://doi.org/10.1016/j.fcr.2013.11.015>
- Peng, J. R., Richards, D. E., Hartley, N. M., Murphy, G. P., Devos, K. M., Flintham, J. E., Beales, J., Fish, L. J., Worland, a J., Pelica, F., Sudhakar, D., Christou, P., Snape, J. W., Gale, M. D., & Harberd, N. P. (1999). “Green revolution” genes encode mutant gibberellin response modulators. *Nature*, 400(6741), 256–261. <https://doi.org/10.1038/22307>
- Penson, S. P., Schuurink, R. C., Fath, A., Gubler, F., Jacobsen, J. V., & Jones, R. L. (1996). cGMP Is required for gibberellic acid-induced gene expression in barley aleurone. *The Plant Cell*, 8(12), 2325–2333. <https://doi.org/10.1105/tpc.8.12.2325>
- Perten, H. (1964). Application of the falling number method for evaluating a-amylase activity. *Cereal Chemistry*, 41, 127–140.
- Petersen, G., Seberg, O., Yde, M., & Berthelsen, K. (2006). Phylogenetic relationships of *Triticum* and *Aegilops* and evidence for the origin of the A, B, and D genomes of common wheat (*Triticum aestivum*). *Molecular Phylogenetics and Evolution*, 39(1), 70–82. <https://doi.org/10.1016/j.ympev.2006.01.023>
- Petruzzelli, L., Harren, F., Reuss, J., & Patterns, Re. J. (1994). Patterns of C2H4 production during germination and seedling growth of pea and wheat as indicated by a laser-driven photoacoustic system. In *Environmental and Experimental Botany*, 34(1), 55-61. [https://doi.org/10.1016/0098-8472\(94\)90009-4](https://doi.org/10.1016/0098-8472(94)90009-4)
- Pfeifer, M., Kugler, K. G., Sandve, S. R., Zhan, B., Rudi, H., Hvidsten, T. R., International Wheat Genome Sequencing Consortium, I. W. G. S., Mayer, K. F. X., & Olsen, O.-A. (2014). Genome interplay in the grain transcriptome of hexaploid bread wheat. *Science*, 345(6194), 1250091. <https://doi.org/10.1126/science.1250091>
- Phillips, A. L., Ward, D. A., Uknes, S., Appleford, N. E. J., Lange, T., Huttly, A. K., Gaskin, P., Graebe, J. E., & Hedden, P. (1995). Isolation and expression of three gibberellin 20-oxidase cDNA clones from *Arabidopsis*. *Plant Physiology*, 108(3),

1049–1057. <https://doi.org/10.1104/pp.108.3.1049>

Pimenta Lange, M. J., Szperlinski, M., Kalix, L., & Lange, T. (2020). Cucumber gibberellin 1-oxidase/desaturase initiates novel gibberellin catabolic pathways. *The Journal of Biological Chemistry*, *295*(25), 8442–8448. <https://doi.org/10.1074/jbc.RA120.013708>

Pirrello, J., Jaimes-Miranda, F., Sanchez-Ballesta, M. T., Tournier, B., Khalil-Ahmad, Q., Regad, F., Latché, A., Pech, J. C., & Bouzayen, M. (2006). Sl-ERF2, a tomato ethylene response factor involved in ethylene response and seed germination. *Plant and Cell Physiology*, *47*(9), 1195–1205. <https://doi.org/10.1093/pcp/pcj084>

Pruneda-Paz, J. L., Breton, G., Nagel, D. H., Kang, S. E., Bonaldi, K., Doherty, C. J., Ravelo, S., Galli, M., Ecker, J. R., & Kay, S. A. (2014). A genome-scale resource for the functional characterization of Arabidopsis transcription factors. *Cell Reports*, *8*(2), 622–632. <https://doi.org/10.1016/j.celrep.2014.06.033>

Pucéat, M. (1999). pHi regulatory ion transporters: an update on structure, regulation and cell function. *Cellular and Molecular Life Sciences*, *55*(10), 1216–1229. <https://doi.org/10.1007/s000180050368>.

Pysh, L. D., Wysocka-Diller, J. W., Camilleri, C., Bouchez, D., & Benfey, P. N. (1999). The GRAS gene family in Arabidopsis: Sequence characterization and basic expression analysis of the SCARECROW-LIKE genes. *Plant Journal*, *18*(1), 111–119. <https://doi.org/10.1046/j.1365-313X.1999.00431.x>

Qi, T., Huang, H., Wu, D., Yan, J., Qi, Y., Song, S., & Xie, D. (2014). Arabidopsis DELLA and JAZ proteins bind the WD-repeat/bHLH/MYB complex to modulate gibberellin and jasmonate signaling synergy. *The Plant Cell*, *26*(3), 1118–1133. <https://doi.org/10.1105/tpc.113.121731>

Qi, W., Zhu, T., Tian, Z., Li, C., Zhang, W., & Song, R. (2016). High-efficiency CRISPR/Cas9 multiplex gene editing using the glycine tRNA-processing system-based strategy in maize. *BMC Biotechnology*, *16*(1), 1–8. <https://doi.org/10.1186/s12896-016-0289-2>

Rademacher, W. (2015). Plant Growth Regulators: backgrounds and uses in plant production. *Journal of Plant Growth Regulation*, *34*(4), 845–872. <https://doi.org/10.1007/s00344-015-9541-6>

- Radley, M. (1976). The development of wheat grain in relation to endogenous growth substances. *Journal of Experimental Botany*, 27(5), 1009–1021. <https://doi.org/10.1093/jxb/27.5.1009>
- Rafter, M. (2019). Targeting Rht-A1 for the generation of novel semi-dwarfing alleles in wheat. PhD Thesis, University of Nottingham.
- Rakszegi, M., Kisgyorgy, B. N., Tearall, K., Shewry, P. R., Lang, L., Phillips, A. L., & Bedo, Z. (2010). Diversity of agronomic and morphological traits in a mutant population of bread wheat studied in the Healthgrain program. *Euphytica*, 174(3), 409–421. <https://doi.org/10.1007/s10681-010-0149-4>
- Ramírez-González, R. H., Borrill, P., Lang, D., Harrington, S. A., Brinton, J., Venturini, L., Davey, M., Jacobs, J., van Ex, F., Pasha, A., Khedikar, Y., Robinson, S. J., Cory, A. T., Florio, T., Concia, L., Juery, C., Schoonbeek, H., Steuernagel, B., Xiang, D., ... Uauy, C. (2018). The transcriptional landscape of polyploid wheat. *Science*, 361(6403), eaar6089. <https://doi.org/10.1126/science.aar6089>
- Rebetzke, G. J., & Richards, R. A. (1999). Genetic improvement of early vigour in wheat. *Australian Journal of Agricultural Research*, 50(3), 291–301. <https://doi.org/10.1071/A98125>
- Reynolds, M. P., & Borlaug, N. E. (2006). Impacts of breeding on international collaborative wheat improvement. *The Journal of Agricultural Science*, 144(01), 3. <https://doi.org/10.1017/S0021859606005867>
- Ribeiro, D. M., Araújo, W. L., Fernie, A. R., Schippers, J. H. M., & Mueller-Roeber, B. (2012). Translatome and metabolome effects triggered by gibberellins during rosette growth in Arabidopsis. *Journal of Experimental Botany*, 63(7), 2769–2786. <https://doi.org/10.1093/jxb/err463>
- Richardson, T., Thistleton, J., Higgins, T. J., Howitt, C., & Ayliffe, M. (2014). Efficient *Agrobacterium* transformation of elite wheat germplasm without selection. *Plant Cell, Tissue and Organ Culture*, 119(3), 647–659. <https://doi.org/10.1007/s11240-014-0564-7>
- Richter, R., Behringer, C., Müller, I. K., & Schwechheimer, C. (2010). The GATA-type transcription factors GNC and GNL/CGA1 repress gibberellin signaling downstream from DELLA proteins and PHYTOCHROME-INTERACTING FACTORS. *Genes & Development*, 24(18), 2093–2104. <https://doi.org/10.1101/gad.594910>

- Rodríguez, M. V., Barrero, J. M., Corbineau, F., Gubler, F., & Benech-Arnold, R. L. (2015). Dormancy in cereals (not too much, not so little): About the mechanisms behind this trait. *Seed Science Research*, 25(2), 99–119. <https://doi.org/10.1017/S0960258515000021>
- Rogers, J. C., Lanahan, M. B., & Rogers, S. W. (1994). The cis-acting gibberellin response complex in high-pl a-amylase gene promoters. Requirement of a coupling element for high-level transcription. *Plant Physiology*, 105(1), 151-158. <https://doi.org/10.1104/pp.105.1.151>
- Ross, J. J. (1994). Recent advances in the study of gibberellin mutants. *Plant Growth Regulation*, 15(3), 193–206. <https://doi.org/10.1007/BF00029892>
- Sakamoto, T., Miura, K., Itoh, H., Tatsumi, T., Ueguchi-Tanaka, M., Ishiyama, K., Kobayashi, M., Agrawal, G. K., Takeda, S., Abe, K., Miyao, A., Hirochika, H., Kitano, H., Ashikari, M., & Matsuoka, M. (2004). An overview of gibberellin metabolism enzyme genes and their related mutants in rice. *Plant Physiology*, 134(4), 1642–1653. <https://doi.org/10.1104/pp.103.033696>
- Sánchez-León, S., Gil-Humanes, J., Ozuna, C. V., Giménez, M. J., Sousa, C., Voytas, D. F., & Barro, F. (2018). Low-gluten, nontransgenic wheat engineered with CRISPR/Cas9. *Plant Biotechnology Journal*, 16(4), 902–910. <https://doi.org/10.1111/pbi.12837>
- Sato, Y., Hong, S. K., Tagiri, A., Kitano, H., Yamamoto, N., Nagato, Y., & Matsuoka, M. (1996). A rice homeobox gene, *OSH1*, is expressed before organ differentiation in a specific region during early embryogenesis. *Proceedings of the National Academy of Sciences of the United States of America*, 93(15), 8117–8122. <https://doi.org/10.1073/pnas.93.15.8117>
- Schmidt, A., Schmid, M. W., & Grossniklaus, U. (2015). Plant germline formation: common concepts and developmental flexibility in sexual and asexual reproduction. *Development*, 142(2), 229–241. <https://doi.org/10.1242/dev.102103>
- Schnable, P. S., Ware, D., Fulton, R. S., Stein, J. C., Wei, F., Pasternak, S., Liang, C., Zhang, J., Fulton, L., Graves, T. A., Minx, P., Reily, A. D., Courtney, L., Kruchowski, S. S., Tomlinson, C., Strong, C., Delehaunty, K., Fronick, C., Courtney, B., ... Wilson, R. K. (2009). The B73 maize genome: complexity, diversity, and

- dynamics. *Science*, 326(5956), 1112–1115.
<https://doi.org/10.1126/science.1178534>
- Seo, P. J., Ryu, J., Kang, S. K., & Park, C.-M. (2011). Modulation of sugar metabolism by an INDETERMINATE DOMAIN transcription factor contributes to photoperiodic flowering in Arabidopsis. *The Plant Journal*, 65(3), 418–429.
<https://doi.org/10.1111/j.1365-313X.2010.04432.x>
- Serrano-Mislata, A., Bencivenga, S., Bush, M., Schiessl, K., Boden, S., & Sablowski, R. (2017). DELLA genes restrict inflorescence meristem function independently of plant height. *Nature Plants*, 3(9), 749–754. <https://doi.org/10.1038/s41477-017-0003-y>
- Shan, Q., Wang, Y., Li, J., & Gao, C. (2014). Genome editing in rice and wheat using the CRISPR/Cas system. *Nature Protocols*, 9(10), 2395–2410.
<https://doi.org/10.1038/nprot.2014.157>
- Shan, Q., Wang, Y., Li, J., Zhang, Y., Chen, K., Liang, Z., Zhang, K., Liu, J., Xi, J. J., Qiu, J. L., & Gao, C. (2013). Targeted genome modification of crop plants using a CRISPR-Cas system. *Nature Biotechnology*, 31(8), 686–688.
<https://doi.org/10.1038/nbt.2650>
- Shao, M., Bai, G., Rife, T. W., Poland, J., Lin, M., Liu, S., Chen, H., Kumssa, T., Fritz, A., Trick, H., Li, Y., & Zhang, G. (2018). QTL mapping of pre-harvest sprouting resistance in a white wheat cultivar Danby. *Theoretical and Applied Genetics*, 131(8), 1683–1697. <https://doi.org/10.1007/s00122-018-3107-5>
- Sheth, N., Roca, X., Hastings, M. L., Roeder, T., Krainer, A. R., & Sachidanandam, R. (2006). Comprehensive splice-site analysis using comparative genomics. *Nucleic Acids Research*, 34(14), 3955–3967. <https://doi.org/10.1093/nar/gkl556>
- Shewry, P. R. (2009). Wheat. In *Journal of Experimental Botany*, 60(6), 1537–1553.
<https://doi.org/10.1093/jxb/erp058>
- Simmonds, J. A. (1997). Mitotic activity in wheat shoot apical meristems: Effect of dissection to expose the apical dome. *Plant Science*, 130(2), 217–225.
[https://doi.org/10.1016/S0168-9452\(97\)00206-9](https://doi.org/10.1016/S0168-9452(97)00206-9)
- Simons, K. J., Fellers, J. P., Trick, H. N., Zhang, Z., Tai, Y.-S., Gill, B. S., & Faris, J. D. (2006). Molecular characterization of the major wheat domestication gene Q. *Genetics*, 172(1), 547–555. <https://doi.org/10.1534/genetics.105.044727>

- Singleton, W. R. (1946). Inheritance of indeterminate growth in maize. *Journal of Heredity*, 37, 61–64.
- Siriwitayawan, G., Geneve, R. L., & Bruce, A. (2003). Seed germination of ethylene perception mutants of tomato and Arabidopsis. *Seed Science Research*, 13(4), 303–314. <https://doi.org/10.1079/SSR2003147>
- Skriver, K., Lok Olsen, F., Rogerst, J. C., & Mundy, J. (1991). Cis-acting DNA elements responsive to gibberellin and its antagonist abscisic acid. *Proceedings of the National Academy of Science of the United States of America*, 88(16), 7266–7270. <https://doi.org/10.1073/pnas.88.16.7266>
- Slade, A. J., Fuerstenberg, S. I., Loeffler, D., Steine, M. N., & Facciotti, D. (2005). A reverse genetic, nontransgenic approach to wheat crop improvement by TILLING. *Nature Biotechnology*, 23(1), 75–81. <https://doi.org/10.1038/nbt1043>
- Slade, A. J., McGuire, C., Loeffler, D., Mullenberg, J., Skinner, W., Fazio, G., Holm, A., Brandt, K. M., Steine, M. N., Goodstal, J. F., & Knaufl, V. C. (2012). Development of high amylose wheat through TILLING. *BMC Plant Biology*, 12(1), 1–17. <https://doi.org/10.1186/1471-2229-12-69>
- Slewinski, T. L. (2013). Using evolution as a guide to engineer kranz-type c4 photosynthesis. *Frontiers in Plant Science*, 4, 212. <https://doi.org/10.3389/fpls.2013.00212>
- Smith, I., Greenside, P. G., Natoli, T., Lahr, D. L., Wadden, D., Tirosh, I., Narayan, R., Root, D. E., Golub, T. R., Subramanian, A., & Doench, J. G. (2017). Evaluation of RNAi and CRISPR technologies by large-scale gene expression profiling in the Connectivity Map. *PLoS Biology*, 15(11). <https://doi.org/10.1371/journal.pbio.2003213>
- Snape, J., Butterworth, K., Whitechurch, E., & Worland, A. J. (2001). Waiting for fine times: genetics of flowering time in wheat. *Euphytica*, 119, 185–190.. <https://doi.org/10.1023/A:1017594422176>
- Sparks, C. A., & Doherty, A. (2020). Genetic transformation of common wheat (*Triticum aestivum* L.) using biolistics. *Methods in Molecular Biology*, 2124, 229–250). https://doi.org/10.1007/978-1-0716-0356-7_12
- Spielmeier, W., Ellis, M., Robertson, M., Ali, S., Lenton, J. R., & Chandler, P. M. (2004). Isolation of gibberellin metabolic pathway genes from barley and comparative

- mapping in barley, wheat and rice. *Theoretical and Applied Genetics*, 109(4), 847–855. <https://doi.org/10.1007/s00122-004-1689-6>
- Stellberger, T., Häuser, R., Baiker, A., Pothineni, V. R., Haas, J., & Uetz, P. (2010). Improving the yeast two-hybrid system with permuted fusions proteins: the Varicella Zoster Virus interactome. *Proteome Science*, 8:8. <https://doi.org/10.1186/1477-5956-8-8>
- Suge, H., & Yamada, N. (1965). Flower-promoting effect of gibberellin in winter wheat and barley. *Plant and Cell Physiology*, 6(2), 147–160. <https://doi.org/10.1093/oxfordjournals.pcp.a079090>
- Sun, M. (2018). Starch degradation during and after germination of wheat seeds and its regulation by ethylene. Thesis, University of Manitoba. <http://hdl.handle.net/1993/32690>
- Sun, Q., Li, D. D., Chu, J., Yuan, D. P., Li, S., Zhong, L. J., Han, X., & Xuan, Y. H. (2020). Indeterminate domain proteins regulate rice defense to sheath blight disease. *Rice*, 13(1):15. <https://doi.org/10.1186/s12284-020-0371-1>
- Sun, Q., Li, T. Y., Li, D. D., Wang, Z. Y., Li, S., Li, D. P., Han, X., Liu, J. M., & Xuan, Y. H. (2019). Overexpression of *Loose Plant Architecture 1* increases planting density and resistance to sheath blight disease via activation of *PIN-FORMED 1a* in rice. *Plant Biotechnology Journal*, 17(5), 855–857. <https://doi.org/10.1111/pbi.13072>
- Sun, T., & Gubler, F. (2004). Molecular mechanism of gibberellin signaling in plants. *Annual Review of Plant Biology*, 55(1), 197–223. <https://doi.org/10.1146/annurev.arplant.55.031903.141753>
- Sun, T. P. (2010). Gibberellin signal transduction in stem elongation & leaf growth. In *Plant Hormones: Biosynthesis, Signal Transduction, Action!* (pp. 308–328). Springer Netherlands. https://doi.org/10.1007/978-1-4020-2686-7_15
- Takata, M., Sasaki, M. S., Sonoda, E., Morrison, C., Hashimoto, M., Utsumi, H., Yamaguchi-Iwai, Y., Shinohara, A., & Takeda, S. (1998). Homologous recombination and non-homologous end-joining pathways of DNA double-strand break repair have overlapping roles in the maintenance of chromosomal integrity in vertebrate cells. *The EMBO Journal*, 17(18), 5497–5508. <https://doi.org/10.1093/emboj/17.18.5497>
- Takehara, S., Sakuraba, S., Mikami, B., Yoshida, H., Yoshimura, H., Itoh, A., Endo, M.,

- Watanabe, N., Nagae, T., Matsuoka, M., & Ueguchi-Tanaka, M. (2020). A common allosteric mechanism regulates homeostatic inactivation of auxin and gibberellin. *Nature Communications*, *11*(1), 1–10. <https://doi.org/10.1038/s41467-020-16068-0>
- Talon, M., Koornneef, M., & Zeevaart, J. A. D. (1990). Accumulation of C19-gibberellins in the gibberellin-insensitive dwarf mutant *gai* of *Arabidopsis thaliana* (L.) Heynh. *Planta*, *182*(4), 501–505. <https://doi.org/10.1007/BF02341024>
- Tan-Wilson, A. L., & Wilson, K. A. (2012). Mobilization of seed protein reserves. In *Physiologia Plantarum*, *145*, (1), 140–153. <https://doi.org/10.1111/j.1399-3054.2011.01535.x>
- Tanimoto, M., Reynald, A. E., Ae, T., & Colasanti, J. (2008). Altered gravitropic response, amyloplast sedimentation and circumnutation in the *Arabidopsis shoot gravitropism 5* mutant are associated with reduced starch levels. *Plant Molecular Biology*, *67*, 57–69. <https://doi.org/10.1007/s11103-008-9301-0>
- Tepliyakova, S., Lebedeva, M., Ivanova, N., Horeva, V., Voytsutskaya, N., Kovaleva, O., & Potokina, E. (2017). Impact of the 7-bp deletion in *HvGA20ox2* gene on agronomic important traits in barley (*Hordeum vulgare* L.). *BMC Plant Biology*, *17*(S1), 181. <https://doi.org/10.1186/s12870-017-1121-4>
- Thomas, S. G., Blázquez, M. a., & Alabadí, D. (2016). DELLA proteins: master regulators of gibberellin-responsive growth and development. *Annual Plant Reviews*, *49*, 89–228. <https://doi.org/10.1002/9781119210436.ch7>
- Thomas, S. G., Phillips, A. L., & Hedden, P. (1999). Molecular cloning and functional expression of gibberellin 2-oxidases, multifunctional enzymes involved in gibberellin deactivation. *Proceedings of the National Academy of Sciences of the United States of America*, *96*(8), 4698-4703. <https://doi.org/10.1073/pnas.96.8.4698>
- Thorvaldsdóttir, H., Robinson, J. T., & Mesirov, J. P. (2013). Integrative Genomics Viewer (IGV): High-performance genomics data visualization and exploration. *Briefings in Bioinformatics*, *14*(2), 178–192. <https://doi.org/10.1093/bib/bbs017>
- Tian, C., Wan, P., Sun, S., Li, J., & Chen, M. (2004). Genome-wide analysis of the GRAS gene family in rice and *Arabidopsis*. *Plant Molecular Biology*, *54*(4), 519–532. <https://doi.org/10.1023/B:PLAN.0000038256.89809.57>

- Tong, J., He, R., Tang, X., Li, M., & Yi, T. (2019). RNA-Sequencing analysis reveals critical roles of hormone metabolism and signaling transduction in seed germination of *Andrographis paniculata*. *Journal of Plant Growth Regulation*, *38*(1), 273–282. <https://doi.org/10.1007/s00344-018-9839-2>
- Tonkinson, C. L., Lyndon, R. F., Arnold, G. M., & Lenton, J. R. (1995). Effect of the *Rht3* dwarfing gene on dynamics of cell extension in wheat leaves, and its modification by gibberellic acid and paclobutrazol. *Journal of Experimental Botany*, *46*(9), 1085–1092. <https://doi.org/10.1093/jxb/46.9.1085>
- Tsai, S. Q., Zheng, Z., Nguyen, N. T., Liebers, M., Topkar, V. V., Thapar, V., Wyvekens, N., Khayter, C., lafrate, A. J., Le, L. P., Aryee, M. J., & Joung, J. K. (2015). GUIDE-seq enables genome-wide profiling of off-target cleavage by CRISPR-Cas nucleases. *Nature Biotechnology*, *33*(2), 187–198. <https://doi.org/10.1038/nbt.3117>
- Tsuji, H., Aya, K., Ueguchi-Tanaka, M., Shimada, Y., Nakazono, M., Watanabe, R., Nishizawa, N. K., Gomi, K., Shimada, A., Kitano, H., Ashikari, M., & Matsuoka, M. (2006). GAMYB controls different sets of genes and is differentially regulated by microRNA in aleurone cells and anthers. *Plant Journal*, *47*(3), 427–444. <https://doi.org/10.1111/j.1365-313X.2006.02795.x>
- Tuttle, K. M., Martinez, S. A., Schramm, E. C., Takebayashi, Y., Seo, M., & Steber, C. M. (2015). Grain dormancy loss is associated with changes in ABA and GA sensitivity and hormone accumulation in bread wheat, *Triticum aestivum* (L.). *Seed Science Research*, *25*(2), 179–193. <https://doi.org/10.1017/S0960258515000057>
- Uauy, C., Wulff, B. B., & Dubcovsky, J. (2017). Combining traditional mutagenesis with new high-throughput sequencing and genome editing to reveal hidden variation in polyploid wheat. *Annual Review of Genetics*, *51*(1), 435–454. <https://doi.org/10.1146/annurev-genet-120116-024533>
- Ueguchi-Tanaka, M., Ashikari, M., Nakajima, M., Itoh, H., Katoh, E., Kobayashi, M., Chow, T., Hsing, Y. C., Kitano, H., Yamaguchi, I., & Matsuoka, M. (2005). *GIBBERELLIN INSENSITIVE DWARF1* encodes a soluble receptor for gibberellin. *Nature*, *437*, 693–698. <https://doi.org/10.1038/nature04028>
- Ueguchi-Tanaka, M., Nakajima, M., Motoyuki, A., & Matsuoka, M. (2007). Gibberellin receptor and its role in gibberellin signaling in plants. *Annual Review of Plant*

- Uozu, S., Tanaka-Ueguchi, M., Kitano, H., Hattori, K., & Matsuoka, M. (2000). Characterization of XET-related genes of rice. *Plant Physiology*, 122(3), 853–859. <https://doi.org/10.1104/pp.122.3.853>
- Upadhyay, S. K., Kumar, J., Alok, A., & Tuli, R. (2013). RNA-Guided genome editing for target gene mutations in wheat. *G3: Genes, Genomes, Genetics*, 3(12), 2233–2238. <https://doi.org/10.1534/g3.113.008847>
- Urbanová, T., Tarkowská, D., Novák, O., Hedden, P., & Strnad, M. (2013). Analysis of gibberellins as free acids by ultra performance liquid chromatography-tandem mass spectrometry. *Talanta*, 112, 85–94. <https://doi.org/10.1016/j.talanta.2013.03.068>
- Van De Velde, K., Chandler, P. M., Van Der Straeten, D., & Rohde, A. (2017). Differential coupling of gibberellin responses by *Rht-B1c* suppressor alleles and *Rht-B1b* in wheat highlights a unique role for the DELLA N-terminus in dormancy. *Journal of Experimental Botany*, 68(3), 443–455. <https://doi.org/10.1093/jxb/erw471>
- Van De Velde, K., Ruelens, P., Geuten, K., Rohde, A., & Van Der Straeten, D. (2017). Exploiting DELLA signaling in cereals. *Trends in Plant Science*, 22(10), 880–893. <https://doi.org/10.1016/j.tplants.2017.07.010>
- Van De Velde, K., Thomas, S. G., Heyse, F., Kaspar, R., Van Der Straeten, D., & Rohde, A. (2021). N-terminal truncated RHT-1 proteins generated by translational reinitiation cause semi-dwarfing of wheat Green Revolution alleles. *Molecular Plant*, 14, 679–687. <https://doi.org/10.1016/j.molp.2021.01.002>
- Varty, K., Arreguin, B., Muggenburg, M. I., Mijangos, J. L., And, M., & Trejo, A. (1983). Effect of ethylene on gibberellic acid-induced protease activity in wheat aleurone layers. *New Phytologist*, 94(2), 211–216. <https://doi.org/10.1111/j.1469-8137.1983.tb04494.x>
- Völz, R., Kim, S.-K., Mi, J., Rawat, A. A., Veluchamy, A., Mariappan, K. G., Rayapuram, N., Daviere, J.-M., Achard, P., Blilou, I., Al-Babili, S., Benhamed, M., & Hirt, H. (2019). INDETERMINATE-DOMAIN 4 (IDD4) coordinates immune responses with plant-growth in *Arabidopsis thaliana*. *PLOS Pathogens*, 15(1), e1007499.

<https://doi.org/10.1371/journal.ppat.1007499>

- Wahl, T. I., & O'Rourke, A. D. (1994). The economics of sprout damage in wheat. *Agribusiness*, 10(1), 27–41. [https://doi.org/10.1002/1520-6297\(199401\)10:1<27::AID-AGR2720100105>3.0.CO;2-L](https://doi.org/10.1002/1520-6297(199401)10:1<27::AID-AGR2720100105>3.0.CO;2-L)
- Wang, P., Zhou, G., Cui, K., Li, Z., & Yu, S. (2012). Clustered QTL for source leaf size and yield traits in rice (*Oryza sativa* L.). *Molecular Breeding*, 29(1), 99–113. <https://doi.org/10.1007/s11032-010-9529-7>
- Wang, P., Zhou, G., Yu, H., & Yu, S. (2011). Fine mapping a major QTL for flag leaf size and yield-related traits in rice. *Theoretical and Applied Genetics*, 123(8), 1319–1330. <https://doi.org/10.1007/s00122-011-1669-6>
- Wang, W., Pan, Q., He, F., Akhunova, A., Chao, S., Trick, H., & Akhunov, E. (2018). Transgenerational CRISPR-Cas9 activity facilitates multiplex gene editing in allopolyploid wheat. *The CRISPR Journal*, 1(1), 65–74. <https://doi.org/10.1089/crispr.2017.0010>
- Wang, Xiaomin, Zheng, H., Tang, Q., Mo, W., & Ma, J. (2019). Effects of gibberellic acid application after anthesis on seed vigor of Indica hybrid rice (*Oryza sativa* L.). *Agronomy*, 9(12), 861. <https://doi.org/10.3390/agronomy9120861>
- Wang, Xingyi, Liu, H., Liu, G., Mia, M. S., Siddique, K. H. M., & Yan, G. (2019). Phenotypic and genotypic characterization of near-isogenic lines targeting a major 4BL QTL responsible for pre-harvest sprouting in wheat. *BMC Plant Biology*, 19(1), 348. <https://doi.org/10.1186/s12870-019-1961-1>
- Wang, Yanpeng, Cheng, X., Shan, Q., Zhang, Y., Liu, J., Gao, C., & Qiu, J. L. (2014). Simultaneous editing of three homoeoalleles in hexaploid bread wheat confers heritable resistance to powdery mildew. *Nature Biotechnology*, 32(9), 947–951. <https://doi.org/10.1038/nbt.2969>
- Wang, Youning, Liu, C., Li, K., Sun, F., Hu, H., Li, X., Zhao, Y., Han, C., Zhang, W., Duan, Y., Liu, M., & Li, X. (2007). Arabidopsis EIN2 modulates stress response through abscisic acid response pathway. *Plant Molecular Biology*, 64(6), 633–644. <https://doi.org/10.1007/s11103-007-9182-7>
- Webb, S. E., Appleford, N. E. J., Gaskin, P., & Lenton, J. R. (1998). Gibberellins in internodes and ears of wheat containing different dwarfing alleles. *Phytochemistry*, 47(5), 671–677. <https://doi.org/10.1016/S0031->

- Welch, D., Hassan, H., Blilou, I., Immink, R., Heidstra, R., & Scheres, B. (2007). Arabidopsis JACKDAW and MAGPIE zinc finger proteins delimit asymmetric cell division and stabilize tissue boundaries by restricting SHORT-ROOT action. *Genes & Development*, *21*(17), 2196–2204. <https://doi.org/10.1101/gad.440307>
- Wen, W., Deng, Q., Jia, H., Wei, L., Wei, J., Wan, H., Yang, L., Cao, W., & Ma, Z. (2013). Sequence variations of the partially dominant DELLA gene *Rht-B1c* in wheat and their functional impacts. *Journal of Experimental Botany*, *64*(11), 3299–3312. <https://doi.org/10.1093/jxb/ert183>
- Wilson, Z. A., & Zhang, D.-B. (2009). From Arabidopsis to rice: pathways in pollen development. *Journal of Experimental Botany*, *60*(5), 1479–1492. <https://doi.org/10.1093/jxb/erp095>
- Wray, G. A. (2003). The evolution of transcriptional regulation in eukaryotes. *Molecular Biology and Evolution*, *20*(9), 1377–1419. <https://doi.org/10.1093/molbev/msg140>
- Wu, C., You, C., Li, C., Long, T., Chen, G., Byrne, M. E., & Zhang, Q. (2008). *RID1*, encoding a Cys2/His2-type zinc finger transcription factor, acts as a master switch from vegetative to floral development in rice. *Proceedings of the National Academy of Science of the United States of America*, *105*(35), 12915–12920. <https://doi.org/10.1073/pnas.0806019105>
- Wu, K., Wang, S., Song, W., Zhang, J., Wang, Y., Liu, Q., Yu, J., Ye, Y., Li, S., Chen, J., Zhao, Y., Wang, J., Wu, X., Wang, M., Zhang, Y., Liu, B., Wu, Y., Harberd, N. P., & Fu, X. (2020). Enhanced sustainable green revolution yield via nitrogen-responsive chromatin modulation in rice. *Science*, *367*(6478). <https://doi.org/10.1126/science.aaz2046>
- Wu, X., Tang, D., Li, M., Wang, K., & Cheng, Z. (2013). Loose Plant Architecture1, an INDETERMINATE DOMAIN protein involved in shoot gravitropism, regulates plant architecture in rice. *Plant Physiology*, *161*(1), 317–329. <https://doi.org/10.1104/pp.112.208496>
- Xiang, D., Quilichini, T. D., Liu, Z., Gao, P., Pan, Y., Li, Q., Nilsen, K. T., Venglat, P., Esteban, E., Pasha, A., Wang, Y., Wen, R., Zhang, Z., Hao, Z., Wang, E., Wei, Y., Cuthbert, R., Kochian, L. V., Sharpe, A., ... Datla, R. (2019). The transcriptional

landscape of polyploid wheats and their diploid ancestors during embryogenesis and grain development. *Plant Cell*, 31(12), 2888–2911. <https://doi.org/10.1105/tpc.19.00397>

Xie, K., Minkenberg, B., & Yang, Y. (2015). Boosting CRISPR/Cas9 multiplex editing capability with the endogenous tRNA-processing system. *Proceedings of the National Academy of Sciences of the United States of America*, 112(11), 3570–3575. <https://doi.org/10.1073/pnas.1420294112>

Xiong, F., Yu, X. R., Zhou, L., Wang, F., & Xiong, A. S. (2013). Structural and physiological characterization during wheat pericarp development. *Plant Cell Reports*, 32(8), 1309–1320. <https://doi.org/10.1007/s00299-013-1445-y>

Xu, F., Li, T., Xu, P.-B., Li, L., Du, S.-S., Lian, H.-L., & Yang, H.-Q. (2016). DELLA proteins physically interact with CONSTANS to regulate flowering under long days in Arabidopsis. *FEBS Letters*, 590(4), 541–549. <https://doi.org/10.1002/1873-3468.12076>

Xu, Q., Krishnan, S., Merewitz, E., Xu, J., & Huang, B. (2016). Gibberellin-regulation and genetic variations in leaf elongation for tall fescue in association with differential gene expression controlling cell expansion. *Scientific Reports*, 6(1), 1–12. <https://doi.org/10.1038/srep30258>

Xu, R. F., Li, H., Qin, R. Y., Li, J., Qiu, C. H., Yang, Y. C., Ma, H., Li, L., Wei, P. C., & Yang, J. B. (2015). Generation of inheritable and “transgene clean” targeted genome-modified rice in later generations using the CRISPR/Cas9 system. *Scientific Reports*, 5. <https://doi.org/10.1038/srep11491>

Xuan, Y. H., Kumar, V., Zhu, X. F., Je, B. Il, Kim, C. M., Huang, J., Cho, J. H., Yi, G., & Han, C. deok. (2018). IDD10 is involved in the interaction between NH₄⁺ and auxin signaling in rice roots. *Journal of Plant Biology*, 61(2), 72–79. <https://doi.org/10.1007/s12374-017-0423-2>

Xuan, Y. H., Priatama, R. A., Huang, J., Je, B. Il, Liu, J. M., Park, S. J., Piao, H. L., Son, D. Y., Lee, J. J., Park, S. H., Jung, K. H., Kim, T. H., & Han, C. (2013). Indeterminate domain 10 regulates ammonium-mediated gene expression in rice roots. *New Phytologist*, 197(3), 791–804. <https://doi.org/10.1111/nph.12075>

Yamaguchi, S. (2008). Gibberellin metabolism and its regulation. *Annual Review of Plant Biology*, 59(1), 225–251.

<https://doi.org/10.1146/annurev.arplant.59.032607.092804>

- Yamaguchi, S., Kamiya, Y., & Sun, T. (2001). Distinct cell-specific expression patterns of early and late gibberellin biosynthetic genes during Arabidopsis seed germination. *The Plant Journal*, *28*(4), 443–453. <https://doi.org/10.1046/j.1365-313X.2001.01168.x>
- Yang, D.-L., Yao, J., Mei, C.-S., Tong, X.-H., Zeng, L.-J., Li, Q., Xiao, L.-T., Sun, T., Li, J., Deng, X.-W., Lee, C. M., Thomashow, M. F., Yang, Y., He, Z., & He, S. Y. (2012). Plant hormone jasmonate prioritizes defense over growth by interfering with gibberellin signaling cascade. *Proceedings of the National Academy of Sciences of the United States of America*, *109*(19), E1192. <https://doi.org/10.1073/PNAS.1201616109>
- Yano, K., Aya, K., Hirano, K., Ordonio, R. L., Ueguchi-Tanaka, M., & Matsuoka, M. (2015). Comprehensive gene expression analysis of rice aleurone cells: probing the existence of an alternative gibberellin receptor. *Plant Physiology*, *167*(2), 531–544. <https://doi.org/10.1104/pp.114.247940>
- Yi, G., Neelakandan, A. K., Gontarek, B. C., Vollbrecht, E., Becraft, P. W., & Department, A. (2015). The *naked endosperm* genes encode duplicate INDETERMINATE domain transcription factors required for maize endosperm cell patterning and differentiation. *Plant Physiology*, *167*(2), 443–456. <https://doi.org/10.1104/pp.114.251413>
- Yoshida, H., Hirano, K., Sato, T., Mitsuda, N., Nomoto, M., Maeo, K., Koketsu, E., Mitani, R., Kawamura, M., Ishiguro, S., Tada, Y., Ohme-Takagi, M., Matsuoka, M., & Ueguchi-Tanaka, M. (2014). DELLA protein functions as a transcriptional activator through the DNA binding of the INDETERMINATE DOMAIN family proteins. *Proceedings of the National Academy of Sciences*, *111*(21), 7861–7866. <https://doi.org/10.1073/pnas.1321669111>
- Yoshida, Hideki, & Ueguchi-Tanaka, M. (2014). DELLA and SCL3 balance gibberellin feedback regulation by utilizing INDETERMINATE DOMAIN proteins as transcriptional scaffolds. *Plant Signaling & Behavior*, *9*(9), e29726. <https://doi.org/10.4161/psb.29726>
- Young, T. E., & Gallie, D. R. (2000). Programmed cell death during endosperm development. *Plant Molecular Biology*, *44*(3), 283–301.

<https://doi.org/10.1023/A:1026588408152>

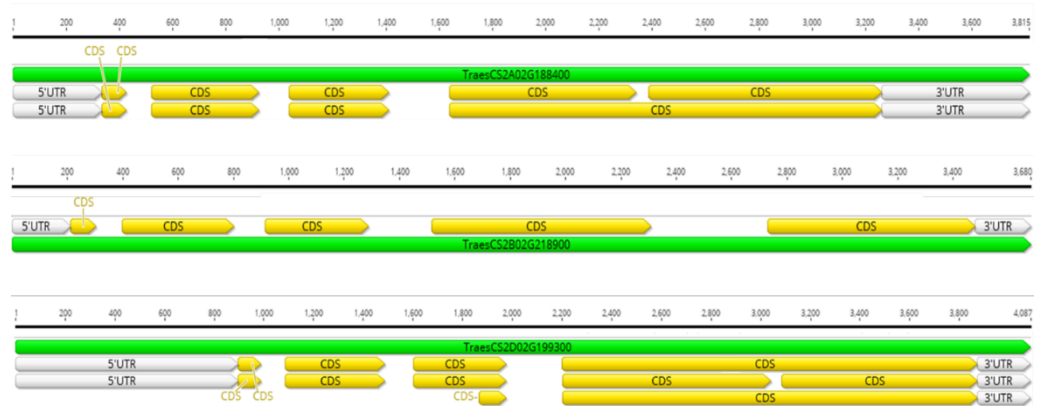
- Young, T. E., Gallie, D. R., & DeMason, D. a. (1997). Ethylene-mediated programmed cell death during maize endosperm development of wild-type and *shrunken2* genotypes. *Plant Physiology*, *115*(2), 737–751. <https://doi.org/10.1093/plphys/115.2.737> [pii]
- Youssefian, S., Kirby, E. J. M., & Gale, M. D. (1992). Pleiotropic effects of the GA-insensitive *Rht* dwarfing genes in wheat. Effects on leaf, stem, ear and floret growth. *Field Crops Research*, *28*(3), 191–210. [https://doi.org/10.1016/0378-4290\(92\)90040-G](https://doi.org/10.1016/0378-4290(92)90040-G)
- Yücel, C. Ö., Baloch, F. S., Hatipoğlu, R., & Özkan, H. (2011). Genetic analysis of preharvest sprouting tolerance in bread wheat (*Triticum aestivum* L. emend. Thell.). *Turkish Journal of Agriculture and Forestry*, *35*(1), 9-22. doi:10.3906/tar-0909-450
- Yue, B., Xue, W. Y., Luo, L. J., & Xing, Y. Z. (2006). QTL analysis for flag leaf characteristics and their relationships with yield and yield traits in rice. *Acta Genetica Sinica*, *33*(9), 824–832. [https://doi.org/10.1016/S0379-4172\(06\)60116-9](https://doi.org/10.1016/S0379-4172(06)60116-9)
- Zanamwe, P. (2019). The potential of ethylene as an alternative to GA3 treatment during malting of barley (*Hordeum vulgare*). *Cereal Research Communications*, *47*(4), 689–700. <https://doi.org/10.1556/0806.47.2019.38>
- Zentella, R., Zhang, Z.-L., Park, M., Thomas, S. G., Endo, A., Murase, K., Fleet, C. M., Jikumaru, Y., Nambara, E., Kamiya, Y., & Sun, T. (2007). Global analysis of della direct targets in early gibberellin signaling in Arabidopsis. *The Plant Cell*, *19*(10), 3037–3057. <https://doi.org/10.1105/tpc.107.054999>
- Zerbino, D. R., Achuthan, P., Akanni, W., Amode, M. R., Barrell, D., Bhai, J., Billis, K., Cummins, C., Gall, A., Girón, C. G., Gil, L., Gordon, L., Haggerty, L., Haskell, E., Hourlier, T., Izuogu, O. G., Janacek, S. H., Juettemann, T., To, J. K., ... Flicek, P. (2018). Ensembl 2018. *Nucleic Acids Research*, *46*(D1), D754–D761. <https://doi.org/10.1093/nar/gkx1098>
- Zetsche, B., Gootenberg, J. S., Abudayyeh, O. O., Slaymaker, I. M., Makarova, K. S., Essletzbichler, P., Volz, S. E., Joung, J., Van Der Oost, J., Regev, A., Koonin, E. V., & Zhang, F. (2015). Cpf1 is a single RNA-guided endonuclease of a Class 2 CRISPR-Cas system. *Cell*, *163*(3), 759–771. <https://doi.org/10.1016/j.cell.2015.09.038>

- Zhang, H., Li, M., He, D., Wang, K., & Yang, P. (2020). Mutations on *ent*-kaurene oxidase 1 encoding gene attenuate its enzyme activity of catalyzing the reaction from *ent*-kaurene to *ent*-kaurenoic acid and lead to delayed germination in rice. *PLoS Genetics*, *16*(1), e1008562. <https://doi.org/10.1371/journal.pgen.1008562>
- Zhang, H., Zhang, J., Wei, P., Zhang, B., Gou, F., Feng, Z., Mao, Y., Yang, L., Zhang, H., Xu, N., & Zhu, J. K. (2014). The CRISPR/Cas9 system produces specific and homozygous targeted gene editing in rice in one generation. *Plant Biotechnology Journal*, *12*(6), 797–807. <https://doi.org/10.1111/pbi.12200>
- Zhang, J., Zhang, H., Botella, J. R., & Zhu, J. K. (2018). Generation of new glutinous rice by CRISPR/Cas9-targeted mutagenesis of the *Waxy* gene in elite rice varieties. In *Journal of Integrative Plant Biology*, *60*(5), 369–375. <https://doi.org/10.1111/jipb.12620>
- Zhang, L., Chen, L., & Yu, D. (2018). Transcription factor WRKY75 interacts with DELLA proteins to affect flowering. *Plant Physiology*, *176*(1), 790–803. <https://doi.org/10.1104/pp.17.00657>
- Zhang, Q., & Li, C. (2017). Comparisons of copy number, genomic structure, and conserved motifs for α -amylase genes from barley, rice, and wheat. *Frontiers in Plant Science*, *8*, 1727. <https://doi.org/10.3389/fpls.2017.01727>
- Zhang, S., Zhang, R., Song, G., Gao, J., Li, W., Han, X., Chen, M., Li, Y., & Li, G. (2018). Targeted mutagenesis using the *Agrobacterium tumefaciens*-mediated CRISPR-Cas9 system in common wheat. *BMC Plant Biology*, *18*(1), 302. <https://doi.org/10.1186/s12870-018-1496-x>
- Zhang, Yi, Li, D., Zhang, D., Zhao, X., Cao, X., Dong, L., Liu, J., Chen, K., Zhang, H., Gao, C., & Wang, D. (2018). Analysis of the functions of *TaGW2* homoeologs in wheat grain weight and protein content traits. *The Plant Journal*, *94*(5), 857–866. <https://doi.org/10.1111/tpj.13903>
- Zhang, Yi, Liang, Z., Zong, Y., Wang, Y., Liu, J., Chen, K., Qiu, J. L., & Gao, C. (2016). Efficient and transgene-free genome editing in wheat through transient expression of CRISPR/Cas9 DNA or RNA. *Nature Communications*, *7*(1), 1–8. <https://doi.org/10.1038/ncomms12617>
- Zhang, Yi, Pribil, M., Palmgren, M., & Gao, C. (2020). A CRISPR way for accelerating improvement of food crops. *Nature Food*, *1*(4), 200–205.

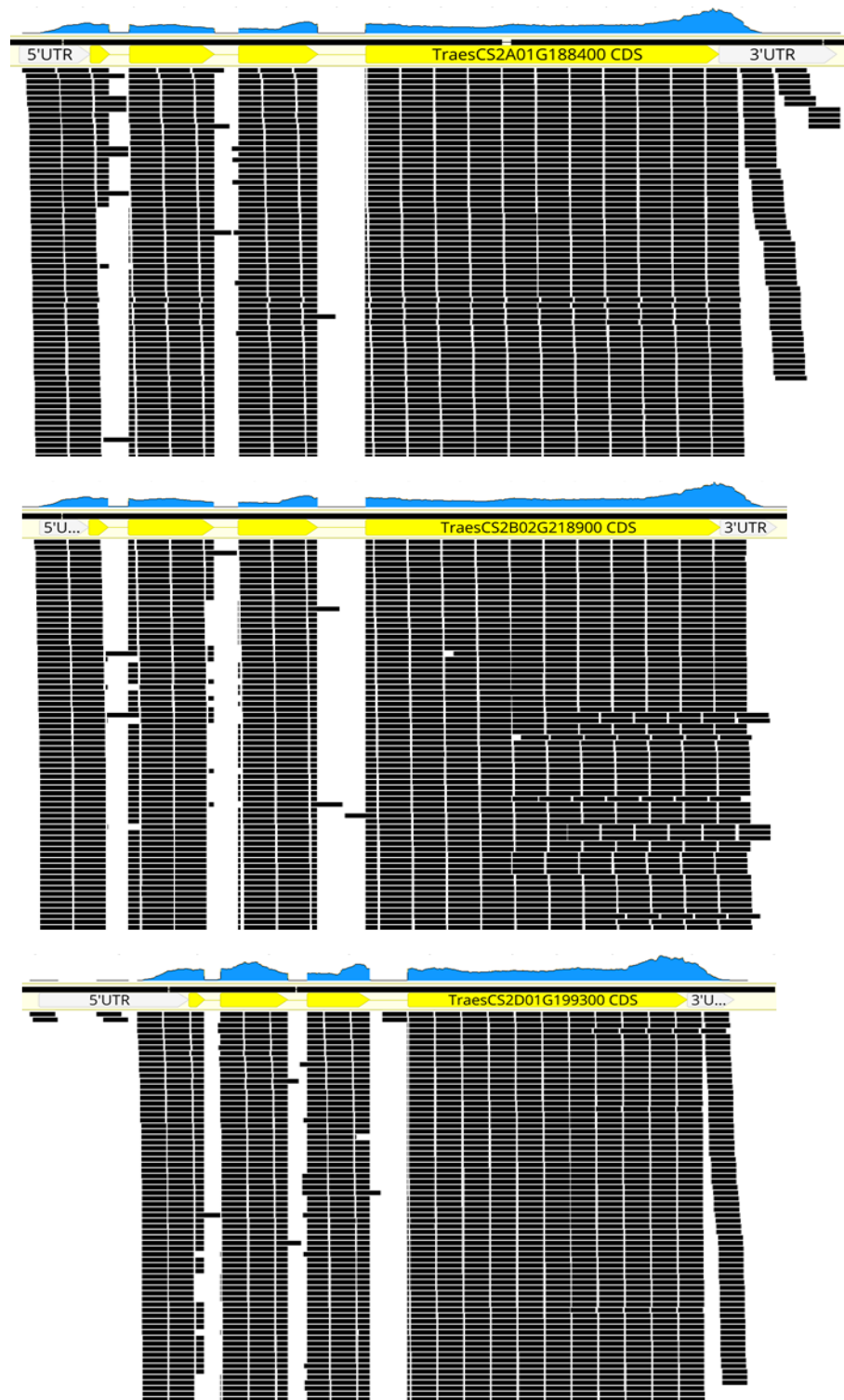
<https://doi.org/10.1038/s43016-020-0051-8>

- Zhang, Yingxiao, Malzahn, A. A., Sretenovic, S., & Qi, Y. (2019). The emerging and uncultivated potential of CRISPR technology in plant science. *Nature Plants*, *5*(8), 778–794. <https://doi.org/10.1038/s41477-019-0461-5>
- Zhang, Yunwei, Bai, Y., Wu, G., Zou, S., Chen, Y., Gao, C., & Tang, D. (2017). Simultaneous modification of three homoeologs of *TaEDR1* by genome editing enhances powdery mildew resistance in wheat. *Plant Journal*, *91*(4), 714–724. <https://doi.org/10.1111/tpj.13599>
- Zhang, Z., Hua, L., Gupta, A., Tricoli, D., Edwards, K. J., Yang, B., & Li, W. (2019). Development of an *Agrobacterium*-delivered CRISPR/Cas9 system for wheat genome editing. *Plant Biotechnology Journal*, *17*(8), 1623–1635. <https://doi.org/10.1111/pbi.13088>
- Zhang, Z. L., Ogawa, M., Fleet, C. M., Zentella, R., Hu, J., Heo, J. O., Lim, J., Kamiya, Y., Yamaguchi, S., & Sun, T. P. (2011). SCARECROW-LIKE 3 promotes gibberellin signaling by antagonizing master growth repressor DELLA in Arabidopsis. *Proceedings of the National Academy of Sciences of the United States of America*, *108*(5), 2160–2165. <https://doi.org/10.1073/pnas.1012232108>
- Zhou, H., Liu, B., Weeks, D. P., Spalding, M. H., & Yang, B. (2014). Large chromosomal deletions and heritable small genetic changes induced by CRISPR/Cas9 in rice. *Nucleic Acids Research*, *42*(17), 10903–10914. <https://doi.org/10.1093/nar/gku806>
- Zhou, X., Zhang, Z. L., Park, J., Tyler, L., Yusuke, J., Qiu, K., Nam, E. A., Lumba, S., Desveaux, D., McCourt, P., Kamiya, Y., & Sun, T. P. (2016). The ERF11 transcription factor promotes internode elongation by activating gibberellin biosynthesis and signaling. *Plant Physiology*, *171*(4), 2760–2770. <https://doi.org/10.1104/pp.16.00154>

APPENDIX



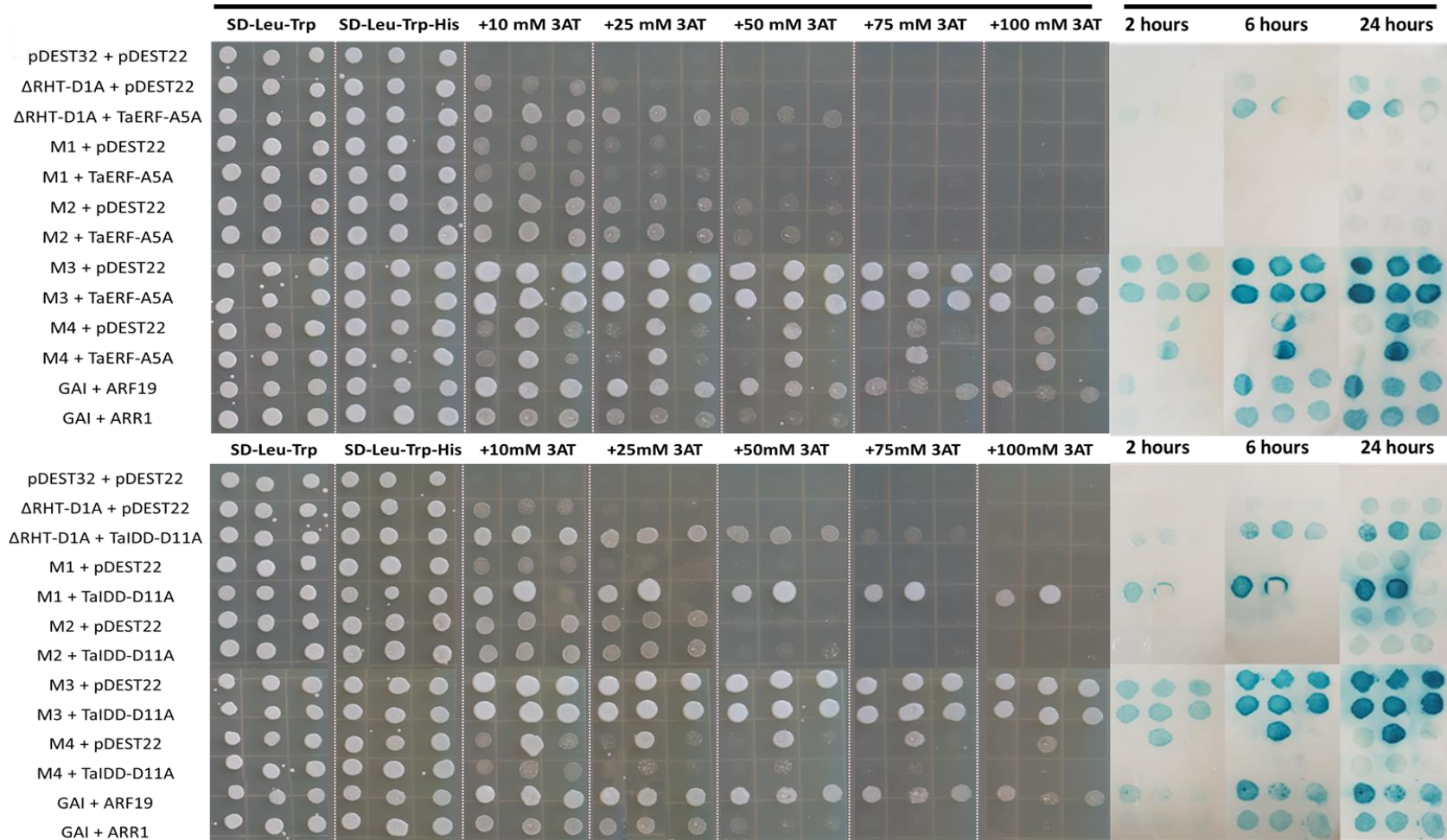
Supplementary Figure 3. 1 The gene models of the three homoeologues of *TaIDD11* gene. In green is the genomic sequence, in yellow the exons and in white the UTRs. The models were annotated using data form Ensemble Plant, *Triticum aestivum* (IWGSC) website. [Accessed on 15th October 2020].



Supplementary Figure 3. 2 Validation of *TaIDD11* gene models by gene transcript data. RNA-Seq reads from crown/leaf/root were mapped to the genomic sequences of three *TaIDD11* homoeologues (cv Chinese spring because in Cadenza sequence, some reads fragments are missing) in Geneious (data provided by Dr Andy Phillips, Rothamsted Research, UK).

Histidine auxotrophy assay

X-gal assay



Supplementary Figure 3. 3 *The yeast two-hybrid (Y2H) experiment to test the interaction between mutated RHT-D1A proteins (M1 - M4) and transcription factors ERF5 and IDD11. Histidine auxotrophy and X-gal reporter gene assays were conducted. Pictures were taken after 48 hours of incubation on the histidine-lacking medium and 24 hours after incubation in the presence of X-gal. GAI with AGF19 - strong positive control, GAI with ARR1 - weak positive control, SD - Sabouraud dextrose broth.*

Supplementary Table 3. 1 Full list of identified interactors grouped into functional categories. Gene accession numbers belong to TGACv1 assembly, as this was the assembly available on Ensemble Plant at the time of the gene identification.

| | Group | Colony # | Accession number (TGACv1) | Function assigned |
|------------------------------|-------------|--|--|---|
| Transcription factors | ERF | 4 | TRIAE_CS42_1BL_TGACv1_031677_AA0118600 | ethylene-responsive transcription factor ABR1-like |
| | | 7 | TRIAE_CS42_2AL_TGACv1_093794_AA0286840 | ethylene-responsive transcription factor ERF105 |
| | | 23 | TRIAE_CS42_6BS_TGACv1_514865_AA1665170 | ethylene-responsive transcription factor 3-like |
| | | 50 | TRIAE_CS42_5AL_TGACv1_375649_AA1225100 | ethylene-responsive transcription factor ERF071 |
| | | 57 | TRIAE_CS42_2DL_TGACv1_162279_AA0562340 | ethylene-responsive transcription factor ERF105 |
| | | 61 | TRIAE_CS42_5AL_TGACv1_374826_AA1209700 | ethylene responsive transcription factor 5a |
| | | 67 | TRIAE_CS42_6AS_TGACv1_486948_AA1566740 | Ethylene-responsive transcription factor 1 |
| | | 70.2 | TRIAE_CS42_3AL_TGACv1_195658_AA0652420 | AP2 domain containing protein |
| | | 108 | TRIAE_CS42_1DL_TGACv1_061734_AA0202680 | ethylene-responsive transcription factor ABR1-like |
| | | 112 | TRIAE_CS42_3B_TGACv1_225151_AA0805500 | AP2 domain containing protein |
| | | 204 | TRIAE_CS42_2DL_TGACv1_159833_AA0543370 | Ethylene-responsive transcription factor ERF113 |
| | | 259 | TRIAE_CS42_1AL_TGACv1_000597_AA0015470 | ethylene-responsive transcription factor ABR1-like |
| | IDD | 9.1 | TRIAE_CS42_2DS_TGACv1_177182_AA0568050 | Zinc finger MAGPIE |
| | | 127 | TRIAE_CS42_2BS_TGACv1_146045_AA0453940 | indeterminate-domain 1-like |
| | | 241 | Not annotated in TGACv1 | indeterminate-domain 1-like |
| | ZF | 11 | TRIAE_CS42_7AS_TGACv1_569870_AA1825950 | B-box zinc finger family protein, putative, expressed |
| | | 216.2 | TRIAE_CS42_7AL_TGACv1_557220_AA1778310 | zinc finger A20 and AN1 domain-containing stress-associated 8 |
| | | 234 | TRIAE_CS42_1BL_TGACv1_032541_AA0131140 | zinc finger CCCH domain-containing 37-like |
| | bHLH | 17 | TRIAE_CS42_5BL_TGACv1_404191_AA1289300 | transcription factor UNE12-like |
| | | 21 | TRIAE_CS42_4BS_TGACv1_330085_AA1105940 | Transcription factor ICE1 |
| 91 | | TRIAE_CS42_2AS_TGACv1_113102_AA0351260 | Transcription factor bHLH47 | |

| | | | | | |
|-------|---------|---------------|--|---|---|
| | | 199 | TRIAE_CS42_1BL_TGACv1_030506_AA0092700 | Transcription factor bHLH87 | |
| | | 211 | TRIAE_CS42_2AS_TGACv1_113707_AA0359670 | Transcription factor bHLH47 | |
| | MYB | 72 | TRIAE_CS42_2AS_TGACv1_112498_AA0339320 | transcription factor MYB30-like | |
| | | 148 | TRIAE_CS42_6BL_TGACv1_501698_AA1620020 | Myb-related 3R-1 | |
| | | 155 | TRIAE_CS42_2AL_TGACv1_092989_AA0268900 | Myb-related Myb4 | |
| | bZIP | 104 | TRIAE_CS42_3B_TGACv1_220594_AA0710320 | bZip type transcription factor 5 | |
| | | 181 | TRIAE_CS42_5DL_TGACv1_433182_AA1404910 | transcription factor RF2a-like | |
| | NAC | 56.2 | TRIAE_CS42_3DL_TGACv1_253070_AA0893220 | NAC domain-containing 83 | |
| | | 252.2 | TRIAE_CS42_1BL_TGACv1_032935_AA0135600 | NAC domain-containing 78 | |
| | Enzymes | E3 Ub ligases | 87 | TRIAE_CS42_4AL_TGACv1_288181_AA0939870 | E3 ubiquitin- ligase SINA 6 |
| | | | 110 | TRIAE_CS42_4AS_TGACv1_307286_AA1019140 | probable BOI-related E3 ubiquitin- ligase 3 |
| | | | 115 | TRIAE_CS42_3AL_TGACv1_196209_AA0658270 | RING finger 115 |
| 144.2 | | | TRIAE_CS42_7DL_TGACv1_604885_AA2002680 | BOI-related E3 ubiquitin- ligase 1 | |
| 152.2 | | | TRIAE_CS42_1DS_TGACv1_081892_AA0263270 | E3 ubiquitin- ligase SINAT3 | |
| 156 | | | TRIAE_CS42_2BL_TGACv1_131298_AA0425600 | probable E3 ubiquitin- ligase HIP1 isoform X2 | |
| 167 | | | TRIAE_CS42_1BL_TGACv1_032451_AA0130070 | E3 ubiquitin ligase BIG BROTHER-related | |
| 169 | | | TRIAE_CS42_7AL_TGACv1_558012_AA1788980 | E3 ubiquitin- ligase SINAT5 | |
| 170 | | | TRIAE_CS42_4AL_TGACv1_290824_AA0989730 | E3 ubiquitin- ligase RBBP6 | |
| 194 | | | TRIAE_CS42_3DS_TGACv1_272288_AA0918460 | E3 ubiquitin- ligase PRT6 | |
| 258 | | | TRIAE_CS42_4DS_TGACv1_361391_AA1166870 | zinc finger CCCH domain-containing 13-like isoform X1 | |
| 263 | | | TRIAE_CS42_3AS_TGACv1_210844_AA0680100 | RING finger 44 | |
| 269 | | | TRIAE_CS42_7DS_TGACv1_622633_AA2042910 | E4 SUMO- ligase PIAL2-like | |
| 185 | | | TRIAE_CS42_5AL_TGACv1_376055_AA1231560 | auxin transport BIG | |

| | | | | |
|--|-----------------------|--------------------|--|--|
| | Alpha amylases | 40.2 | TRIAE_CS42_6BL_TGACv1_501352_AA1616380 | alpha-amylase partial |
| | | 54 | TRIAE_CS42_U_TGACv1_640856_AA2077500 | alpha partial |
| | | 202 | TRIAE_CS42_6DL_TGACv1_526359_AA1680390 | Alpha-amylase type B isozyme |
| | | 233 | TRIAE_CS42_7BL_TGACv1_577011_AA1862720 | alpha partial |
| | | 244 | TRIAE_CS42_6AL_TGACv1_471197_AA1504520 | Alpha-amylase type B isozyme |
| | Kinases | 3 | TRIAE_CS42_2AL_TGACv1_095614_AA0312940 | phosphatidylinositol 3- and 4-kinase family |
| | | 6 | TRIAE_CS42_4AL_TGACv1_290400_AA0985020 | aspartokinase chloroplatic |
| | | 24 | TRIAE_CS42_4BL_TGACv1_321295_AA1058570 | CBL-interacting kinase 31 |
| | | 36 | TRIAE_CS42_7DS_TGACv1_624199_AA2059650 | Serine threonine- kinase CTR1 |
| | | 59 | TRIAE_CS42_4BS_TGACv1_327859_AA1076640 | serine threonine- kinase fray1 isoform X2 |
| | | 99 | TRIAE_CS42_5BL_TGACv1_407072_AA1353020 | G-type lectin S-receptor-like serine threonine- kinase At5g35370 |
| | | 117.2 | TRIAE_CS42_1BL_TGACv1_030788_AA0100770 | probable serine threonine- kinase At4g35230 |
| | | 160 | TRIAE_CS42_2DL_TGACv1_161348_AA0558130 | Serine threonine- kinase SAPK7 |
| | | 177 | TRIAE_CS42_5AL_TGACv1_376012_AA1230750 | FLX-like 3 |
| | | 179.2 | TRIAE_CS42_2AL_TGACv1_093931_AA0289620 | Uridylate kinase |
| | | 231 | TRIAE_CS42_3AS_TGACv1_211087_AA0684800 | Serine threonine- kinase HT1 |
| | | 232 | TRIAE_CS42_5AL_TGACv1_376058_AA1231640 | calcium dependent kinase |
| | | 243 | TRIAE_CS42_7BL_TGACv1_577393_AA1874300 | CDPK-related kinase 3-like |
| | | Dehydrogena | 1 | TRIAE_CS42_3AL_TGACv1_195910_AA0655570 |
| | 9.2 | | TRIAE_CS42_5AL_TGACv1_374729_AA1207680 | NADP-dependent oxidoreductase P1 |
| | 46.2 | | TRIAE_CS42_2BS_TGACv1_146717_AA0471430 | probable acyl- dehydrogenase IBR3 |
| | 95.2 | | TRIAE_CS42_2DL_TGACv1_158363_AA0516660 | Succinate dehydrogenase [ubiquinone] flavo mitochondrial |
| | 122 | | TRIAE_CS42_7DL_TGACv1_604750_AA2001310 | glyceraldehyde-3-phosphate dehydrogenase |

| | | | | | |
|--|--------------|-----------|--|---|------------------------------|
| | | 124 | TRIAE_CS42_6BS_TGACv1_514091_AA1654910 | dihydrolipoyllysine-residue acetyltransferase component 3 of pyruvate dehydrogenase | |
| | | 218 | TRIAE_CS42_7BL_TGACv1_579758_AA1909900 | succinate dehydrogenase subunit mitochondrial | |
| | | 264 | TRIAE_CS42_1AL_TGACv1_000411_AA0011470 | alcohol dehydrogenase ADH3D | |
| | Phosphatases | 41 | TRIAE_CS42_5BS_TGACv1_424020_AA1386070 | probable phosphoinositide phosphatase SAC9 | |
| | | 51 | TRIAE_CS42_7DS_TGACv1_624388_AA2060930 | tyrosine- phosphatase | |
| | | 76 | TRIAE_CS42_2AL_TGACv1_095587_AA0312470 | Soluble inorganic pyrophosphatase | |
| | | 137 | TRIAE_CS42_2BL_TGACv1_130422_AA0411120 | Soluble inorganic pyrophosphatase | |
| | | 195 | TRIAE_CS42_7BS_TGACv1_591944_AA1926280 | probable tyrosine- phosphatase At1g05000 | |
| | | 196 | TRIAE_CS42_3B_TGACv1_221234_AA0734650 | Soluble inorganic pyrophosphatase | |
| | | 198 | TRIAE_CS42_6BL_TGACv1_502250_AA1624010 | soluble inorganic pyrophosphatase | |
| | | Synthases | 5 | TRIAE_CS42_5AL_TGACv1_379781_AA1256830 | citrate glyoxysomal-like |
| | | | 13 | TRIAE_CS42_5DL_TGACv1_435886_AA1456020 | 2-isopropylmalate synthase A |
| | 62 | | TRIAE_CS42_3B_TGACv1_222757_AA0770070 | probable V-type proton ATPase subunit d | |
| | 143 | | TRIAE_CS42_5DL_TGACv1_434037_AA1427680 | citrate glyoxysomal-like | |
| | 261 | | TRIAE_CS42_6AL_TGACv1_470941_AA1499070 | cytosolic glutamine synthetase isoform | |
| | Peptidases | 10.1 | TRIAE_CS42_5BS_TGACv1_423553_AA1379370 | glutathione S-transferase T3-like | |
| | | 35 | TRIAE_CS42_1AL_TGACv1_000490_AA0013370 | protease inhibitor | |
| | | 82.1 | TRIAE_CS42_4BS_TGACv1_328029_AA1081460 | cysteine endopeptidase EP-A | |
| | | 157.1 | TRIAE_CS42_1BL_TGACv1_032601_AA0131900 | type II ase inhibitor family precursor | |
| | | 178 | TRIAE_CS42_3DL_TGACv1_249028_AA0835010 | serine carboxypeptidase 1-like | |
| | | 201.1 | TRIAE_CS42_6AL_TGACv1_471734_AA1513590 | vacuolar-processing enzyme beta-isozyme 1-like | |
| | | 84 | TRIAE_CS42_7DL_TGACv1_602975_AA1973160 | catalase 3 | |
| | | 119 | TRIAE_CS42_7AL_TGACv1_556567_AA1765730 | catalase 3 | |

| | | | | | |
|-------|-----------------------|------------------|--|---|---|
| | Reductases | 32 | TRIAE_CS42_2DL_TGACv1_159647_AA0540920 | non-functional NADPH-dependent codeinone reductase 2-like | |
| | | 45 | TRIAE_CS42_2AS_TGACv1_115171_AA0371320 | B12D isoform X1 | |
| | | 54 | TRIAE_CS42_4AL_TGACv1_289965_AA0979660 | Ferredoxin- chloroplastic | |
| | | 152 | TRIAE_CS42_1DL_TGACv1_061137_AA0186540 | NADH-ubiquinone reductase complex 1 MLRQ subunit | |
| | | 179.1 | TRIAE_CS42_7BL_TGACv1_580707_AA1915150 | NADPH-dependent HC-toxin reductase | |
| | Hydrolases | 16.2 | TRIAE_CS42_5AL_TGACv1_373980_AA1186370 | Glucan endo-1,3-beta-glucosidase 5 | |
| | | 60.2 | TRIAE_CS42_5DS_TGACv1_456904_AA1479740 | general transcriptional corepressor CYC8-like | |
| | | 216.1 | TRIAE_CS42_5AL_TGACv1_375988_AA1230100 | probable polygalacturonase | |
| | Transferases | 118 | TRIAE_CS42_4DL_TGACv1_345108_AA1151720 | 1,4-dihydroxy-2-naphthoate chloroplastic isoform X1 | |
| | | 132.1 | TRIAE_CS42_6BL_TGACv1_499497_AA1584330 | agmatine coumaroyltransferase-2-like | |
| | | 184.1 | TRIAE_CS42_1AL_TGACv1_000880_AA0020950 | glycosyltransferase family 64 C5-like | |
| | | 236 | TRIAE_CS42_1BL_TGACv1_030408_AA0089810 | probable methyltransferase PMT23 | |
| | | 242.2 | TRIAE_CS42_3AL_TGACv1_196342_AA0659660 | aspartate cytoplasmic | |
| | | 267 | TRIAE_CS42_2BS_TGACv1_146590_AA0468870 | Bromodomain and PHD finger-containing 3 | |
| | Endochitinases | 33.1 | TRIAE_CS42_2AL_TGACv1_096368_AA0318950 | Endochitinase PR4 | |
| | | 43.2 | TRIAE_CS42_2DL_TGACv1_158075_AA0508070 | Endochitinase PR4 | |
| | | 208 | TRIAE_CS42_2AL_TGACv1_098187_AA0325770 | Endochitinase PR4 | |
| | Stress | Defensins | 46.1 | TRIAE_CS42_3DL_TGACv1_251714_AA0884080 | no information in the table |
| | | | 65 | TRIAE_CS42_5DL_TGACv1_432979_AA1396560 | DEF2_WHEAT ame: Full=Defensin 2 ame: Full=Gamma-2-purothionin |
| | | | 87 | TRIAE_CS42_5BL_TGACv1_405561_AA1330360 | DEF1_WHEAT ame: Full=Defensin 1 ame: Full=Gamma-1-purothionin |
| 117.1 | | | TRIAE_CS42_5BL_TGACv1_405561_AA1330350 | Defensin 1 | |

| | | | | |
|---------------|------------|--|--|--|
| | | 187 | TRIAE_CS42_5DL_TGACv1_432979_AA1396570 | Defensin 1 |
| | | 246 | TRIAE_CS42_5AL_TGACv1_373959_AA1185390 | Defensin 1 |
| | Heat shock | 16.1 | TRIAE_CS42_1DL_TGACv1_061383_AA0193800 | heat stress transcription factor A-4d-like |
| | | 29 | TRIAE_CS42_3B_TGACv1_222069_AA0756660 | homolog subfamily B member 4 |
| | | 69 | TRIAE_CS42_3DS_TGACv1_272416_AA0920510 | kDa heat-shock |
| | | 106.1 | TRIAE_CS42_3DS_TGACv1_272389_AA0920080 | homolog subfamily B member 4 |
| | | 123 | TRIAE_CS42_7BS_TGACv1_593724_AA1954070 | kDa class I heat shock 1-like |
| Miscellaneous | Ribosomal | 173.2 | TRIAE_CS42_2AS_TGACv1_113688_AA0359360 | 60S ribosomal L19-1 |
| | | 217 | TRIAE_CS42_3DS_TGACv1_272354_AA0919380 | 40S ribosomal S5 |
| | | 262 | TRIAE_CS42_5AL_TGACv1_377277_AA1245540 | 60S ribosomal L23 |
| | 2 | TRIAE_CS42_1DL_TGACv1_062838_AA0220740 | phospholipase A1-II 7-like | |
| | 8.1 | TRIAE_CS42_2DL_TGACv1_161282_AA0557670 | DNA-directed RNA polymerases II and IV subunit 5A-like | |
| | 8.2 | TRIAE_CS42_1BL_TGACv1_030346_AA0087580 | early flowering 3-B1 | |
| | 14 | TRIAE_CS42_5DL_TGACv1_434585_AA1438310 | outer envelope pore chloroplastic | |
| | 15 | TRIAE_CS42_7BS_TGACv1_593824_AA1954620 | probable transcriptional regulator SLK3 isoform X1 | |
| | 19 | TRIAE_CS42_2BS_TGACv1_146333_AA0462840 | rho GTPase-activating 7-like | |
| | 22 | TRIAE_CS42_5BS_TGACv1_423720_AA1382340 | general transcriptional corepressor CYC8-like | |
| | 26 | TRIAE_CS42_2BS_TGACv1_146403_AA0464250 | WW domain-binding 11 | |
| | 27 | TRIAE_CS42_6DS_TGACv1_543118_AA1735680 | Fumarylacetoacetase | |
| | 28 | TRIAE_CS42_5BS_TGACv1_424344_AA1388910 | SEC1 family transport SLY1 | |
| | 31 | TRIAE_CS42_5AL_TGACv1_374424_AA1199840 | ACT domain-containing ACR12 | |
| | 33.2 | TRIAE_CS42_6DS_TGACv1_543041_AA1734490 | SKP1 1A | |
| | 34 | TRIAE_CS42_1AS_TGACv1_020251_AA0076000 | EARLY RESPONSIVE TO DEHYDRATION 15 | |

| | | | | |
|--|--|-------|--|---|
| | | 38 | TRIAE_CS42_7DL_TGACv1_603269_AA1979700 | PAF1 homolog |
| | | 43.1 | TRIAE_CS42_7DS_TGACv1_622972_AA2048030 | AP-1 complex subunit gamma-2-like isoform X1 |
| | | 48.1 | TRIAE_CS42_1BL_TGACv1_031648_AA0117840 | DNA-binding DDB_G0278111 |
| | | 48.2 | TRIAE_CS42_1BL_TGACv1_033706_AA0141480 | EC1_WHEAT ame: Full=EC I II ame: Full=Zinc metallothionein class II |
| | | 52 | TRIAE_CS42_6DL_TGACv1_527960_AA1710240 | clathrin assembly At5g35200 |
| | | 55 | TRIAE_CS42_7DL_TGACv1_602683_AA1965140 | 14 kDa zinc-binding |
| | | 56.1 | TRIAE_CS42_5AS_TGACv1_393516_AA1273500 | pathogenesis-related 5 |
| | | 56.3 | TRIAE_CS42_5AL_TGACv1_375855_AA1228080 | alpha-L-arabinofuranosidase 1-like |
| | | 56.4 | TRIAE_CS42_1AL_TGACv1_002731_AA0044810 | membrane steroid-binding 2-like |
| | | 73 | TRIAE_CS42_6AL_TGACv1_472967_AA1527650 | endoglucanase 7 |
| | | 74 | TRIAE_CS42_4DL_TGACv1_342840_AA1123380 | atherin-like isoform X1 |
| | | 77 | TRIAE_CS42_3DL_TGACv1_251723_AA0884200 | nuclear pore complex NUP62 |
| | | 80 | TRIAE_CS42_3DL_TGACv1_249733_AA0855360 | AF479038_1 holocarboxylase partial |
| | | 81 | TRIAE_CS42_5DL_TGACv1_433802_AA1422480 | Gly d Mal d 3 |
| | | 82.2 | TRIAE_CS42_3B_TGACv1_221518_AA0742720 | 1-interacting 1 |
| | | 83 | TRIAE_CS42_2BS_TGACv1_145940_AA0450160 | Potassium transporter 7 |
| | | 85.2 | TRIAE_CS42_1DL_TGACv1_062951_AA0222040 | cereblon isoform X2 |
| | | 88.1 | TRIAE_CS42_5BL_TGACv1_405570_AA1330640 | EXPORTIN 1A-like |
| | | 88.2 | TRIAE_CS42_1AL_TGACv1_001936_AA0036970 | Thioredoxin H-type |
| | | 107 | TRIAE_CS42_4BS_TGACv1_328465_AA1088260 | heavy-metal-associated domain-containing |
| | | 108.1 | TRIAE_CS42_2BL_TGACv1_129325_AA0378790 | seed specific Bn15D1B |

| | | | | |
|--|--|-------|--|--|
| | | 114 | TRIAE_CS42_4DS_TGACv1_361093_AA1160730 | staphylococcal nuclease domain-containing 1-like |
| | | 116 | TRIAE_CS42_3AS_TGACv1_210768_AA0678510 | mitochondrial glyco |
| | | 121 | TRIAE_CS42_7AS_TGACv1_569962_AA1827770 | RNA-binding 1-like |
| | | 128 | TRIAE_CS42_4DL_TGACv1_343873_AA1140780 | autophagy 9 |
| | | 129 | TRIAE_CS42_3AL_TGACv1_196152_AA0657710 | CASP 5B2 |
| | | 131 | TRIAE_CS42_1DL_TGACv1_061550_AA0198510 | Bowman-Birk type proteinase inhibitor |
| | | 132.2 | TRIAE_CS42_4BS_TGACv1_328661_AA1091800 | Globulin-1 S allele |
| | | 133 | TRIAE_CS42_2AL_TGACv1_093136_AA0272950 | acyl-coenzyme A thioesterase 13-like |
| | | 134.2 | TRIAE_CS42_5AS_TGACv1_393774_AA1275930 | GTP-binding SAR1A |
| | | 135.1 | TRIAE_CS42_2DL_TGACv1_158034_AA0506800 | Aldose 1-epimerase |
| | | 140 | TRIAE_CS42_4DS_TGACv1_362549_AA1180520 | mRNA-decapping enzyme |
| | | 141 | TRIAE_CS42_U_TGACv1_641729_AA2102670 | Thiol protease |
| | | 144.1 | TRIAE_CS42_6DL_TGACv1_527204_AA1700440 | bet1-like SNARE 1-1 |
| | | 147.1 | TRIAE_CS42_7AL_TGACv1_557637_AA1784370 | aminolevulinic acid dehydratase |
| | | 147.2 | TRIAE_CS42_7BS_TGACv1_592370_AA1936790 | polyadenylate-binding - interacting 7 |
| | | 150 | TRIAE_CS42_2BL_TGACv1_130091_AA0403590 | embryonic DC-8 precursor |
| | | 153 | TRIAE_CS42_1DS_TGACv1_080357_AA0246550 | predicted protein, partial |
| | | 154.1 | TRIAE_CS42_4DS_TGACv1_361174_AA1162550 | Globulin-1 S allele |
| | | 154.2 | TRIAE_CS42_3AS_TGACv1_213033_AA0704930 | cell number regulator 8 |
| | | 158 | TRIAE_CS42_7DL_TGACv1_603293_AA1980300 | cytochrome P450 72A13-like |
| | | 165.1 | TRIAE_CS42_5DL_TGACv1_435420_AA1450380 | proton pump-interactor 1-like |
| | | 165.2 | TRIAE_CS42_6BL_TGACv1_499730_AA1590220 | Two-component response regulator ARR2 |

| | | | |
|--|-------|--|--|
| | 166 | TRIAE_CS42_6DL_TGACv1_526363_AA1680760 | furry homolog |
| | 174 | TRIAE_CS42_1BL_TGACv1_031624_AA0117310 | late embryogenesis abundant |
| | 184.2 | TRIAE_CS42_7DL_TGACv1_602886_AA1971130 | DGCR14 isoform X2 |
| | 186 | TRIAE_CS42_6BL_TGACv1_501866_AA1621150 | Ubiquitin-associated protein |
| | 206 | TRIAE_CS42_5AL_TGACv1_374313_AA1196670 | NRT1 PTR FAMILY -like |
| | 210.1 | TRIAE_CS42_U_TGACv1_640781_AA2073960 | glucan endo-1,3-beta-D-glucosidase |
| | 210.2 | TRIAE_CS42_5BL_TGACv1_405530_AA1329550 | probable 6-phosphogluconolactonase chloroplastic |
| | 213 | TRIAE_CS42_5AL_TGACv1_374622_AA1204730 | Actin-depolymerizing factor 4 |
| | 214 | TRIAE_CS42_1AL_TGACv1_000591_AA0015390 | DEHYDRATION-INDUCED 19 |
| | 216.3 | TRIAE_CS42_2AL_TGACv1_096235_AA0318070 | translation initiation factor 5A |
| | 219 | TRIAE_CS42_6AS_TGACv1_487025_AA1567510 | SRC2 homolog |
| | 227 | TRIAE_CS42_3B_TGACv1_222209_AA0759900 | fiber Fb34 |
| | 235 | TRIAE_CS42_3B_TGACv1_221012_AA0726950 | H2B10_ORYSI ame: Full=Histone |
| | 239 | TRIAE_CS42_1AS_TGACv1_019352_AA0065320 | nucleolar MIF4G domain-containing 1 |
| | 248 | TRIAE_CS42_3DL_TGACv1_251058_AA0876850 | eukaryotic peptide chain release factor subunit 1-3 |
| | 249 | TRIAE_CS42_2DS_TGACv1_178157_AA0592020 | Phenylalanine ammonia-lyase |
| | 250 | TRIAE_CS42_7DS_TGACv1_623343_AA2052280 | arginine decarboxylase 1 |
| | 252.1 | TRIAE_CS42_7BL_TGACv1_576990_AA1862100 | Transcription initiation factor IIA subunit 2 |
| | 256.1 | TRIAE_CS42_5DL_TGACv1_435681_AA1453440 | mitochondrial import inner membrane translocase subunit TIM10-like |
| | 257 | TRIAE_CS42_7DS_TGACv1_622470_AA2040240 | probable indole-3-pyruvate monooxygenase YUCCA10 |
| | 260 | TRIAE_CS42_5AL_TGACv1_378065_AA1251030 | Thiol protease aleurain |

| | | | |
|-----------------------------|------|--|-----------------------------------|
| Hypothetical/unknown | 10.2 | TRIAE_CS42_5DL_TGACv1_434877_AA1443000 | hypothetical protein F775_32388 |
| | 37 | TRIAE_CS42_6BL_TGACv1_502543_AA1625350 | predicted protein |
| | 39 | TRIAE_CS42_2BS_TGACv1_146205_AA0458790 | N/A |
| | 40.1 | TRIAE_CS42_3DS_TGACv1_272032_AA0913470 | hypothetical protein F775_43838 |
| | 42 | TRIAE_CS42_6DL_TGACv1_526581_AA1687460 | hypothetical protein TRIUR3_25071 |
| | 44 | TRIAE_CS42_4BL_TGACv1_322093_AA1068460 | hypothetical protein TRIUR3_34830 |
| | 47 | TRIAE_CS42_4DS_TGACv1_361339_AA1165990 | hypothetical protein F775_05934 |
| | 48.3 | TRIAE_CS42_1DL_TGACv1_061133_AA0186370 | predicted protein |
| | 49 | TRIAE_CS42_1DL_TGACv1_064128_AA0232730 | hypothetical protein F775_32018 |
| | 57 | TRIAE_CS42_2BL_TGACv1_132642_AA0438770 | N/A |
| | 60.1 | TRIAE_CS42_3DL_TGACv1_251032_AA0876350 | hypothetical protein F775_31186 |
| | 64 | TRIAE_CS42_4DS_TGACv1_361237_AA1164150 | hypothetical protein F775_32330 |
| | 68 | TRIAE_CS42_6DL_TGACv1_528641_AA1715340 | predicted protein |
| | 70.1 | TRIAE_CS42_1BS_TGACv1_049829_AA0162290 | hypothetical protein F775_31652 |
| | 71 | TRIAE_CS42_5DL_TGACv1_434302_AA1433530 | CCG-binding partial |
| | 79 | TRIAE_CS42_4AL_TGACv1_291899_AA0996960 | hypothetical protein TRIUR3_16524 |
| | 85.1 | TRIAE_CS42_3AS_TGACv1_211563_AA0691540 | hypothetical protein TRIUR3_25651 |
| | 90 | TRIAE_CS42_4BL_TGACv1_321319_AA1058950 | predicted protein |
| | 94 | TRIAE_CS42_4BS_TGACv1_328573_AA1090300 | hypothetical protein TRIUR3_27521 |
| | 95.1 | TRIAE_CS42_5BL_TGACv1_404431_AA1299670 | N/A |
| | 97 | TRIAE_CS42_1AL_TGACv1_000490_AA0013360 | hypothetical protein TRIUR3_06539 |
| | 102 | TRIAE_CS42_6DS_TGACv1_544490_AA1748530 | hypothetical protein F775_20614 |
| | 103 | TRIAE_CS42_5DL_TGACv1_434877_AA1442990 | hypothetical protein F775_32390 |

| | | |
|-------|--|---|
| 105 | TRIAE_CS42_1AL_TGACv1_001869_AA0036120 | hypothetical protein TRIUR3_13994 |
| 106.2 | TRIAE_CS42_3B_TGACv1_221739_AA0748910 | PREDICTED: uncharacterized protein LOC100840710 |
| 125 | TRIAE_CS42_2BL_TGACv1_131531_AA0428900 | hypothetical protein TRIUR3_31155 |
| 134.1 | TRIAE_CS42_4AL_TGACv1_290470_AA0985740 | hypothetical protein TRIUR3_16809 |
| 135.2 | TRIAE_CS42_3AS_TGACv1_212219_AA0698910 | hypothetical protein F775_31135 |
| 139 | TRIAE_CS42_6BS_TGACv1_513883_AA1651350 | hypothetical protein F775_43448 |
| 161 | TRIAE_CS42_1AL_TGACv1_000426_AA0011860 | hypothetical protein TRIUR3_08232 |
| 163 | TRIAE_CS42_5AL_TGACv1_373996_AA1187100 | hypothetical protein TRIUR3_00886 |
| 164 | TRIAE_CS42_3DL_TGACv1_249209_AA0841460 | unnamed protein product |
| 171 | TRIAE_CS42_6BL_TGACv1_499559_AA1586170 | predicted protein |
| 173.1 | TRIAE_CS42_4BL_TGACv1_320932_AA1051970 | hypothetical protein TRIUR3_31004 |
| 182 | TRIAE_CS42_3B_TGACv1_223155_AA0777120 | hypothetical protein BRADI_5g26390 |
| 189 | TRIAE_CS42_2DS_TGACv1_177239_AA0570160 | N/A |
| 190 | TRIAE_CS42_5BL_TGACv1_408838_AA1364620 | hypothetical protein TRIUR3_00886 |
| 201.2 | TRIAE_CS42_1AS_TGACv1_020345_AA0076820 | N/A |
| 203 | TRIAE_CS42_2DL_TGACv1_158074_AA0508000 | N/A |
| 209 | TRIAE_CS42_5AL_TGACv1_375034_AA1214450 | CCG-binding partial |
| 221 | TRIAE_CS42_6AS_TGACv1_485890_AA1553720 | N/A |
| 223 | TRIAE_CS42_6AL_TGACv1_472840_AA1526460 | hypothetical protein TRIUR3_25071 |
| 224 | TRIAE_CS42_1DL_TGACv1_062056_AA0208150 | predicted protein |
| 225 | TRIAE_CS42_1DL_TGACv1_071947_AA0238730 | N/A |
| 226 | TRIAE_CS42_1AL_TGACv1_000426_AA0011860 | hypothetical protein TRIUR3_08232 |
| 230 | TRIAE_CS42_7DS_TGACv1_623113_AA2049710 | hypothetical protein F775_24619 |

| | | | | |
|--|--|-------|--|---------------------------------|
| | | 237 | TRIAE_CS42_7AS_TGACv1_570518_AA1837020 | N/A |
| | | 242.1 | TRIAE_CS42_2BL_TGACv1_130907_AA0419780 | N/A |
| | | 247 | TRIAE_CS42_5BL_TGACv1_405223_AA1322460 | hypothetical protein F775_06510 |
| | | 256.2 | TRIAE_CS42_3B_TGACv1_225360_AA0807520 | unnamed protein product |

Supplementary Table 3. 2 Members of subgroup IX of the ERF family in Arabidopsis and rice.

| Arabidopsis | | | Rice | | |
|-------------|--------------|------------------|------------|--------------|------------------|
| Group name | Generic name | Locus identifier | Group name | Generic name | Locus identifier |
| IXc | AtERF#091 | At4g18450 | IXc | OsERF#083 | Os03g64260 |
| | AtERF#092 | At3g23240 | | OsERF#084 | Os05g49010 |
| | AtERF#093 | At2g31230 | | OsERF#085 | Os05g37640 |
| | AtERF#094 | At1g06160 | | OsERF#086 | Os07g22770 |
| | AtERF#095 | At3g23220 | | OsERF#087 | Os09g39850 |
| | AtERF#096 | At5g43410 | | OsERF#088 | Os03g05590 |
| | AtERF#097 | At1g04370 | | OsERF#089 | Os10g30840 |
| | AtERF#098 | At3g23230 | | OsERF#090 | Os08g44960 |
| IXa | AtERF#099 | At2g44840 | | OsERF#123 | Os09g39810 |
| | AtERF#100 | At4g17500 | | OsERF#128 | Os04g18650 |
| | AtERF#101 | At5g47220 | OsERF#136 | Os07g22730 | |
| IXb | AtERF#102 | At5g47230 | IXa | OsERF#091 | Os02g43790 |
| | AtERF#103 | At4g17490 | | OsERF#092 | Os01g54890 |
| | AtERF#104 | At5g61600 | | OsERF#093 | Os04g46220 |
| | AtERF#105 | At5g51190 | IXb | OsERF#094 | Os04g46250 |
| | AtERF#106 | At5g07580 | | OsERF#095 | Os02g43820 |
| | AtERF#107 | At5g61590 | | OsERF#096 | Os10g41330 |
| | | | OsERF#097 | Os04g46240 | |

Supplementary Table 3. 3 Members of the IDD family in Arabidopsis and rice.

| Arabidopsis | | Rice | |
|--------------|------------------|--------------|------------------|
| Generic name | Locus identifier | Generic name | Locus identifier |
| AtIDD1 | At5g66730 | OslD | Os10g28330 |
| AtIDD2 | At3g50700 | OslDD1 | Os03g10140 |
| AtIDD3 | At1g03840 | OslDD2 | Os01g09850 |
| AtIDD4 | At2g02080 | OslDD3 | Os09g38340 |
| AtIDD5 | At2g02070 | OslDD4 | Os02g45050 |
| AtIDD6 | At1g14580 | OslDD5 | Os07g39310 |
| AtIDD7 | At1g55110 | OslDD6 | Os08g44050 |
| AtIDD8 | At5g44160 | OslDD7 | Os02g31890 |
| AtIDD9 | At3g45260 | OslDD8 | Os01g14010 |
| AtIDD10 | At5g03150 | OslDD9 | Os01g70870 |
| AtIDD11 | At3g13810 | OslDD10 | Os04g47860 |
| AtIDD12 | At4g02670 | OslDD11 | Os01g39110 |
| AtIDD13 | At5g60470 | OslDD12 | Os08g36390 |
| AtIDD14 | At1g68130 | OslDD13 | Os09g27650 |
| AtIDD15 | At2g01940 | OslDD14 | Os03g13400 |
| AtIDD16 | At1g25250 | | |

Supplementary Table 4. 1 Primers used in the experiments summarised in Chapter 4. The sequence in red is the variable part of the primer that allows for sample type recognition during NGS analysis; in the primers used for LIB8437 mutation validation and for genotyping of the TILLING lines by sequencing and by KASP assays, the fragments highlighted in green are the gene-specific sequences.

| Primer name | Primer sequence |
|--|---|
| LIB8437 mutation validation in CAD4-1415 TILLING line | |
| BC1_NGS_BS_FOR | CCATCTCATCCCTGCGTGTCTCCGACTCAGCTAAGGTAAC GATCGCCGCCCAAGAAGAAGAGG |
| BC2_NGS_BS_FOR | CCATCTCATCCCTGCGTGTCTCCGACTCAGTAAGGAGAAC GATCGCCGCCCAAGAAGAAGAGG |
| NGS_CR_BS_REV | CCTCTCTATGGGCAGTCGGTGATGCTCCGCACACGAACCGGTTGGTC |
| TILLING mutations genotyping by sequencing | |
| IDD11-A_FOR | TCGGTACACCATCATCTCTGTTCCCA |
| IDD11-A_REV | ATGAACCTTCCTTGGGGCTGCT |
| IDD11-B_FOR | GGATGCCGCCAATCCGA |
| IDD11-B_REV | GCAAAACCCGAAGCACGCGG |
| IDD11-D_FOR | AGACCACCTCAAGGAAGGTTTCATTGAC |
| IDD11-D_REV | GGGATTGTGTTGAGCTGCTCTCGATA |
| KASP genotyping of TILLING lines | |
| IDD11-B_WT_FAM | GAAGGTGACCAAGTTCATGCTCTCCCCGGGACGCCAGG |
| IDD11-B_MUT_HEX | GAAGGTCGGAGTCAACGGATTCTCCCCGGGACGCCAGA |
| IDD11-B_CR | GCAAAACCCGAAGCACGCGG |
| IDD11-D_WT_FAM | GAAGGTGACCAAGTTCATGCTACACAATCCCGGTTACCCC |
| IDD11-D_MUT_HEX | GAAGGTCGGAGTCAACGGATTACACAATCCCGGTTACCCT |
| IDD11-D_CR | AACCGGAATGTGTTGAGC |
| TaAMY1 expression | |
| TaAMY1-FOR | TGTCAATCAGGACCCGGC |
| TaAMY1-REV | TGATTTGCAGCTTGCTCTCAC |
| Ta2526-FOR | AGAATGGGATGACAAGGAAGA |
| Ta2526-REV | TCCTCCATTGCTGGACA |
| Ta2643-FOR | GCAGATGAGCATGACTCTCGC |
| Ta2643-REV | CCCATGTTAACCAGATGCC |

Supplementary Table 4. 2 Legend for the expression data taken from Ramírez-González et al., (2018). The tissues and developmental stages are assigned a number under which they appear on the graph.

| Number | Sample source |
|---------------|---|
| 1 | Seedling stage:roots:radicle |
| 2 | Seedling stage:leaves/shoots:coleoptile |
| 3 | Seedling stage:leaves/shoots:stem axis |
| 4 | Seedling stage:leaves/shoots:first leaf sheath |
| 5 | Seedling stage:leaves/shoots:first leaf blade |
| 6 | Seedling stage:roots:roots |
| 7 | Seedling stage:leaves/shoots:shoot apical meristem |
| 8 | three leaf stage:leaves/shoots:third leaf blade |
| 9 | three leaf stage:leaves/shoots:third leaf sheath |
| 10 | three leaf stage:roots:roots |
| 11 | three leaf stage:roots:root apical meristem |
| 12 | three leaf stage:roots:axillary roots |
| 13 | fifth leaf stage:leaves/shoots:fifth leaf sheath |
| 14 | fifth leaf stage:leaves/shoots:fifth leaf blade |
| 15 | Tillering stage:leaves/shoots:first leaf sheath |
| 16 | Tillering stage:leaves/shoots:first leaf blade |
| 17 | Tillering stage:leaves/shoots:shoot axis |
| 18 | Tillering stage:leaves/shoots:shoot apical meristem |
| 19 | Tillering stage:roots:roots |
| 20 | Tillering stage:roots:root apical meristem |
| 21 | Flag leaf stage:leaves/shoots:flag leaf blade |
| 22 | Flag leaf stage:leaves/shoots:fifth leaf sheath |
| 23 | Flag leaf stage:leaves/shoots:fifth leaf blade |
| 24 | Flag leaf stage:leaves/shoots:shoot axis |
| 25 | Flag leaf stage:roots:roots |
| 26 | Flag leaf stage:leaves/shoots:flag leaf blade night (-0.25h) 06:45 |
| 27 | Flag leaf stage:leaves/shoots:fifth leaf blade night (-0.25h) 21:45 |
| 28 | Flag leaf stage:leaves/shoots:flag leaf blade night (+0.25h) 07:15 |
| 29 | Flag leaf stage:leaves/shoots:fifth leaf blade night (+0.25h) 22:15 |
| 30 | Full boot:leaves/shoots:leaf ligule |
| 31 | Full boot:leaves/shoots:flag leaf sheath |
| 32 | Full boot:leaves/shoots:flag leaf blade |
| 33 | Full boot:leaves/shoots:shoot axis |
| 34 | Full boot:spike:spike |
| 35 | 30% spike:roots:roots |
| 36 | 30% spike:leaves/shoots:flag leaf sheath |
| 37 | 30% spike:leaves/shoots:flag leaf blade |
| 38 | 30% spike:leaves/shoots:Internode #2 |
| 39 | 30% spike:leaves/shoots:peduncle |
| 40 | 30% spike:spike:spike |

| | |
|----|--|
| 41 | 30% spike:spike:spikelets |
| 42 | Ear emergence:leaves/shoots:flag leaf sheath |
| 43 | Ear emergence:leaves/shoots:flag leaf blade |
| 44 | Ear emergence:leaves/shoots:fifth leaf blade |
| 45 | Ear emergence:leaves/shoots:peduncle |
| 46 | Ear emergence:leaves/shoots:Internode #2 |
| 47 | Ear emergence:spike:awns |
| 48 | Ear emergence:spike:glumes |
| 49 | Ear emergence:spike:lemma |
| 50 | anthesis:spike:anther |
| 51 | anthesis:spike:stigma & ovary |
| 52 | anthesis:leaves/shoots:flag leaf blade night (-0.25h) 06:45 |
| 53 | anthesis:leaves/shoots:fifth leaf blade night (-0.25h) 21:45 |
| 54 | milk grain stage:leaves/shoots:flag leaf sheath |
| 55 | milk grain stage:leaves/shoots:flag leaf blade |
| 56 | milk grain stage:leaves/shoots:shoot axis |
| 57 | milk grain stage:leaves/shoots:fifth leaf blade (senescence) |
| 58 | milk grain stage:leaves/shoots:peduncle |
| 59 | milk grain stage:leaves/shoots:Internode #2 |
| 60 | milk grain stage:spike:awns |
| 61 | milk grain stage:spike:glumes |
| 62 | milk grain stage:spike:lemma |
| 63 | milk grain stage:grain:grain |
| 64 | Dough:leaves/shoots:flag leaf blade (senescence) |
| 65 | Soft dough:grain:grain |
| 66 | Hard dough:grain:grain |
| 67 | Dough:grain:endosperm |
| 68 | Dough:grain:embryo proper |
| 69 | Ripening:grain:grain |
| 70 | Ripening:leaves/shoots:flag leaf blade (senescence) |

Supplementary Table 4. 3 TPMs of DE genes involved in GA biosynthesis and signalling identified in the RNA-seq experiment.

| Gene IDs | Cad.NT.1 | Cad.NT.2 | Cad.NT.3 | Cad.NT.4 | idd.NT.1 | idd.NT.2 | idd.NT.3 | idd.NT.4 | Rht.NT.1 | Rht.NT.2 | Rht.NT.3 | Rht.NT.4 |
|-------------------------------|----------|----------|----------|----------|----------|----------|----------|----------|----------|----------|----------|----------|
| GA3ox2-A: TraesCS3A02G122600 | 0.31 | 0.39 | 0.17 | 0.70 | 1.03 | 1.10 | 1.29 | 0.67 | 0.43 | 0.49 | 0.82 | 0.43 |
| GA3ox2-B: TraesCS3B02G141800 | 2.74 | 2.20 | 2.62 | 2.38 | 3.70 | 4.17 | 4.65 | 3.39 | 3.33 | 2.37 | 2.62 | 2.32 |
| GA3ox2-D: TraesCS3D02G124500 | 2.13 | 1.52 | 1.81 | 2.26 | 4.73 | 3.58 | 4.84 | 4.54 | 3.93 | 2.50 | 3.42 | 1.88 |
| GA20ox1-A: TraesCS4A02G319100 | 0.17 | 0.45 | 0.62 | 0.30 | 0.91 | 1.10 | 1.59 | 1.55 | 1.21 | 1.77 | 1.55 | 1.22 |
| GA20ox1-B: TraesCS5B02G560300 | 0.27 | 0.21 | 0.38 | 0.07 | 1.44 | 0.71 | 0.90 | 1.03 | 0.54 | 0.71 | 0.47 | 0.71 |
| GA20ox2-B: TraesCS3B02G439900 | 1.10 | 0.75 | 1.16 | 1.32 | 0.98 | 0.63 | 1.27 | 1.62 | 0.74 | 0.82 | 1.59 | 0.24 |
| GA2ox10-A: TraesCS1A02G126400 | 5.74 | 5.12 | 4.69 | 3.67 | 2.31 | 2.88 | 3.76 | 2.65 | 2.75 | 2.41 | 2.99 | 2.74 |
| GA2ox10-B: TraesCS1B02G145600 | 1.70 | 2.28 | 2.28 | 1.83 | 1.88 | 1.10 | 1.42 | 1.44 | 1.07 | 1.47 | 0.44 | 1.42 |
| GA2ox10-D: TraesCS1D02G127000 | 1.42 | 1.94 | 1.60 | 1.47 | 1.34 | 1.25 | 1.03 | 1.14 | 0.96 | 1.20 | 0.75 | 1.02 |
| GA2ox3-A: TraesCS3A02G294000 | 1.50 | 1.49 | 0.97 | 0.98 | 1.25 | 1.18 | 1.94 | 0.74 | 0.52 | 0.81 | 1.14 | 0.52 |
| GA2ox3-D: TraesCS3D02G293800 | 1.21 | 1.38 | 0.75 | 1.15 | 0.24 | 0.24 | 0.38 | 0.42 | 0.29 | 0.27 | 0.94 | 0.24 |
| GA2ox7-D: TraesCS3D02G149600 | 1.04 | 0.41 | 0.57 | 0.63 | 0.63 | 0.90 | 0.66 | 0.35 | 0.30 | 0.25 | 0.50 | 0.38 |
| Rht1-A: TraesCS4A02G271000 | 89.00 | 80.78 | 83.76 | 82.73 | 65.27 | 67.44 | 67.16 | 62.39 | 76.73 | 68.74 | 83.83 | 73.85 |
| Rht1-B: TraesCS4B02G043100 | 84.40 | 78.27 | 79.60 | 78.46 | 69.40 | 68.82 | 62.48 | 64.06 | 76.84 | 71.76 | 82.16 | 74.51 |
| Rht1-D: TraesCS4D02G040400 | 70.59 | 61.52 | 63.71 | 66.88 | 53.21 | 52.69 | 50.83 | 57.46 | 105.93 | 103.38 | 106.31 | 103.05 |
| GID1-A: TraesCS1A02G255100 | 10.35 | 9.86 | 8.89 | 9.34 | 16.45 | 19.85 | 16.94 | 12.53 | 13.69 | 11.26 | 14.19 | 21.22 |
| GID1-B: TraesCS1B02G265900 | 10.21 | 8.04 | 7.51 | 8.19 | 15.52 | 15.23 | 16.04 | 14.94 | 14.40 | 11.88 | 12.64 | 14.49 |
| GID1-D: TraesCS1D02G254500 | 8.68 | 10.34 | 7.61 | 9.77 | 15.91 | 17.93 | 16.79 | 15.14 | 15.43 | 11.56 | 15.50 | 17.31 |
| Gene IDs | Cad.GA.1 | Cad.GA.2 | Cad.GA.3 | Cad.GA.4 | idd.GA.1 | idd.GA.2 | idd.GA.3 | idd.GA.4 | Rht.GA.1 | Rht.GA.2 | Rht.GA.3 | Rht.GA.4 |
| GA3ox2-A: TraesCS3A02G122600 | 0.05 | 0.10 | 0.09 | 0.09 | 0.89 | 1.11 | 1.21 | 0.73 | 0.30 | 0.46 | 0.47 | 0.29 |
| GA3ox2-B: TraesCS3B02G141800 | 1.19 | 1.13 | 1.24 | 1.59 | 3.84 | 3.95 | 4.14 | 4.28 | 2.48 | 2.43 | 1.88 | 2.89 |
| GA3ox2-D: TraesCS3D02G124500 | 0.62 | 0.62 | 0.83 | 1.43 | 5.16 | 5.38 | 5.14 | 4.98 | 3.98 | 3.06 | 2.91 | 3.13 |
| GA20ox1-A: TraesCS4A02G319100 | 0.62 | 0.29 | 0.29 | 0.47 | 1.19 | 0.59 | 0.98 | 0.57 | 1.48 | 0.45 | 0.16 | 0.93 |
| GA20ox1-B: TraesCS5B02G560300 | 0.09 | 0.23 | 0.18 | 0.12 | 0.67 | 0.32 | 0.53 | 0.79 | 0.57 | 0.29 | 0.49 | 0.91 |
| GA20ox2-B: TraesCS3B02G439900 | 0.54 | 0.49 | 0.95 | 0.89 | 1.55 | 1.31 | 1.86 | 2.02 | 1.48 | 1.29 | 0.70 | 0.81 |
| GA2ox10-A: TraesCS1A02G126400 | 7.38 | 7.21 | 9.42 | 9.07 | 3.03 | 3.70 | 1.55 | 3.56 | 2.48 | 2.64 | 2.06 | 2.85 |
| GA2ox10-B: TraesCS1B02G145600 | 4.28 | 4.24 | 5.37 | 4.12 | 1.19 | 1.61 | 0.80 | 1.60 | 1.74 | 0.96 | 0.78 | 0.77 |
| GA2ox10-D: TraesCS1D02G127000 | 2.87 | 3.40 | 2.46 | 2.45 | 1.06 | 1.09 | 1.46 | 1.19 | 0.85 | 1.46 | 0.64 | 1.22 |
| GA2ox3-A: TraesCS3A02G294000 | 3.02 | 3.93 | 3.31 | 2.80 | 1.28 | 0.66 | 1.01 | 0.57 | 0.76 | 0.59 | 0.81 | 0.75 |
| GA2ox3-D: TraesCS3D02G293800 | 1.62 | 1.70 | 2.56 | 1.96 | 0.36 | 0.64 | 0.39 | 0.57 | 0.59 | 0.30 | 0.55 | 0.05 |
| GA2ox7-D: TraesCS3D02G149600 | 0.68 | 1.09 | 1.52 | 0.75 | 0.41 | 0.20 | 0.31 | 0.06 | 0.58 | 0.44 | 0.37 | 0.21 |
| Rht1-A: TraesCS4A02G271000 | 101.38 | 98.50 | 113.24 | 108.75 | 67.67 | 63.13 | 78.10 | 75.91 | 88.39 | 74.96 | 87.54 | 76.11 |
| Rht1-B: TraesCS4B02G043100 | 96.99 | 92.12 | 102.61 | 99.83 | 74.87 | 67.54 | 83.18 | 77.17 | 94.18 | 75.14 | 87.68 | 72.09 |
| Rht1-D: TraesCS4D02G040400 | 83.55 | 83.05 | 94.15 | 89.49 | 59.08 | 46.80 | 56.17 | 54.13 | 119.81 | 100.13 | 116.44 | 100.65 |
| GID1-A: TraesCS1A02G255100 | 4.43 | 4.40 | 4.70 | 5.99 | 10.52 | 16.58 | 19.29 | 14.92 | 13.39 | 15.79 | 17.84 | 13.57 |
| GID1-B: TraesCS1B02G265900 | 3.10 | 4.41 | 5.59 | 5.56 | 14.20 | 13.23 | 14.69 | 16.65 | 12.52 | 12.91 | 15.14 | 10.88 |
| GID1-D: TraesCS1D02G254500 | 5.21 | 3.59 | 5.52 | 4.36 | 12.99 | 15.27 | 18.18 | 14.96 | 12.53 | 14.42 | 20.44 | 13.40 |

Supplementary Table 4. 4 Mean TPMs of DE genes involved in GA biosynthesis and signalling identified in the RNA-seq experiment.

| Gene IDs | Cad.NT | Cad.GA | idd.NT | idd.GA | Rht.NT | Rht.GA |
|-------------------------------|--------|--------|--------|--------|--------|--------|
| GA3ox2-A: TraesCS3A02G122600 | 0.39 | 0.08 | 1.02 | 0.99 | 0.54 | 0.38 |
| GA3ox2-B: TraesCS3B02G141800 | 2.48 | 1.29 | 3.98 | 4.05 | 2.66 | 2.42 |
| GA3ox2-D: TraesCS3D02G124500 | 1.93 | 0.88 | 4.42 | 5.16 | 2.93 | 3.27 |
| GA20ox1-A: TraesCS4A02G319100 | 0.39 | 0.42 | 1.29 | 0.83 | 1.44 | 0.75 |
| GA20ox1-B: TraesCS5B02G560300 | 0.23 | 0.16 | 1.02 | 0.58 | 0.61 | 0.56 |
| GA20ox2-B: TraesCS3B02G439900 | 1.08 | 0.72 | 1.13 | 1.69 | 0.85 | 1.07 |
| GA2ox10-A: TraesCS1A02G126400 | 4.81 | 8.27 | 2.90 | 2.96 | 2.72 | 2.51 |
| GA2ox10-B: TraesCS1B02G145600 | 2.02 | 4.50 | 1.46 | 1.30 | 1.10 | 1.07 |
| GA2ox10-D: TraesCS1D02G127000 | 1.61 | 2.80 | 1.19 | 1.20 | 0.98 | 1.04 |
| GA2ox3-A: TraesCS3A02G294000 | 1.23 | 3.26 | 1.28 | 0.88 | 0.75 | 0.73 |
| GA2ox3-D: TraesCS3D02G293800 | 1.12 | 1.96 | 0.32 | 0.49 | 0.44 | 0.37 |
| GA2ox7-D: TraesCS3D02G149600 | 0.66 | 1.01 | 0.63 | 0.24 | 0.36 | 0.40 |
| Rht1-A: TraesCS4A02G271000 | 84.07 | 105.47 | 65.57 | 71.20 | 75.79 | 81.75 |
| Rht1-B: TraesCS4B02G043100 | 80.18 | 97.89 | 66.19 | 75.69 | 76.32 | 82.27 |
| Rht1-D: TraesCS4D02G040400 | 65.67 | 87.56 | 53.55 | 54.04 | 104.67 | 109.26 |
| GID1-A: TraesCS1A02G255100 | 9.61 | 4.88 | 16.44 | 15.33 | 15.09 | 15.15 |
| GID1-B: TraesCS1B02G265900 | 8.49 | 4.66 | 15.43 | 14.69 | 13.36 | 12.86 |
| GID1-D: TraesCS1D02G254500 | 9.10 | 4.67 | 16.44 | 15.35 | 14.95 | 15.20 |

Supplementary Table 5. 1 Primers used in the experiments summarised in Chapter 5. In red is the *Bsa*I restriction site, in green the sequence that aligns to tRNA and gRNA scaffold. NGS primers; in red are the barcodes used for sequencing.

| Primer name | Primer sequence |
|---|--|
| CRISPR/Cas9 polycistronic gene cloning | |
| End- TF | GTGGTCTCCGGCAACAAAGCACCAGTGGTCT |
| gRNA1- REV | TAGGTCTCAACGACGTCACCTGCACCAGCCGGG |
| gRNA1- FOR | GTGGTCTCTCGTCGCAAAAAGTTTCAGAGCTATGCTGGG |
| gRNA2- REV | TAGGTCTCATTCACGTAAGTGGTGCACCAGCCGGG |
| gRNA2- FOR | GTGGTCTCTGAACCTCATATCGTTTCAGAGCTATGCTGGG |
| gRNA3- REV | TAGGTCTCAAAGGGCTCGTTTCAGAGCTATGCTGGG |
| gRNA3- FOR | GTGGTCTCCCTTGGCCGGCAGTTTCAGAGCTATGCTGGG |
| gRNA4- REV | TAGGTCTCACCTCCGAAGTATGCACCAGCCGGG |
| gRNA4- FOR | GTGGTCTCCGAGGTCCTCGACGTTTCAGAGCTATGCTGGG |
| End- SR | GTGCGGTCTCCAAACAAAAAAGCACCAGCTCGGTG |
| Guide and Cas9 plasmids in T0 plants | |
| Os U3-SF2 | CGGCTATCCATAGATCAAAGCTG |
| pRRes-SR2 | CACTATAGGGCGAATTGGAGATGC |
| Ubipr-SF2 | GGATGATGGCATATGCAGCAGC |
| Cas9-SR1 | CACCTTCGCCATCTCGTTGC |
| Initial PCR of T0 plants | |
| ERF5-FOR | GACCTCATCCGCGAGCACC |
| ERF5-REV | CGTCGAGGTGACCCGGAGT |
| NGS genotyping of T0, T1 and T2 plants | |
| ERF5_NGS1-FOR | ACACTCTTCCCTACACGACGCTCTCCGATCTGACCTCATCCGCGAGCACC |
| ERF5_NGS1-REV | GACTGGAGTTCAGACGTGTGCTCTCCGATCTGCCGCTACTTGCCCCA |
| ERF5_NGS2-FOR | TGTAAAACGACGGCCAGTGCCCATGTTCTTCCCGCAGC |
| ERF5_NGS2-REV | CCTCTCTATGGGAGTCGGTGATGCCGCTACTTGCCCCA |
| KASP genotyping of T2 plants | |
| ERF5-A_WT | CCGGCCAAGGGCTCGTT |
| ERF5-A_MUT | CCGGCCAAGGGCTCGT |
| ERF5-A_CF | CCGTCGTCCACGCTGAG |
| ERF5-B_WT | CCGGCCAAGGGCTCGTT |
| ERF5-B_MUT | CCGGCCAAGGGCTCGT |
| ERF5-B_CF | GCGAGCCGTCTCTGTGAT |
| ERF5-D_WT | CCGGCCAAGGGCTCGTT |
| ERF5-D_MUT | CCGGCCAAGGGCTCGT |
| ERF5-D_CF | CCGTCTCTGTGGCTGCA |

Supplementary Table 5. 2 INDELS detected in B3792 T0 plants that were selected for NGS analysis. Plants that showed band shifts after PCR amplification of the fragment encompassing all target sites in three *TaERF5* and three *TaERF5a* genes were chosen for further analysis. Amplicons with barcodes for NGS were sequenced using GENEWIZ Amplicon-EZ service, and the reads mapped to wheat (*Triticum aestivum* cv. Cadenza) genome using BMAP aligner.

| | <i>TaERF5</i> | | <i>TaERF5a</i> | | |
|------|-----------------|--------------|----------------|-----------------|------------|
| R2P1 | sgRNA1 | sgRNA3 | sgRNA1 | sgRNA2 | sgRNA4 |
| A1 | 5 bp DEL | 1 + 3 bp DEL | 3 bp DEL | 11 bp DEL | 2 bp DEL |
| A2 | NO | 96 bp DEL | 3 bp DEL | 148 bp DEL | 2 bp DEL |
| B1 | No reads mapped | | N/A | No reads mapped | |
| B2 | | | | | |
| D1 | NO | 1 bp DEL | | 3 bp DEL | 1 bp DEL |
| D2 | NO | 4 bp DEL | | 3 bp INS | 2 bp DEL |
| D3 | NO | 96 p DEL | | N/A | N/A |
| R3P1 | sgRNA1 | sgRNA3 | | sgRNA1 | sgRNA2 |
| A1 | NO | 5 bp DEL | NO | 173 bp DEL | 6 bp DEL |
| A2 | NO | NO | NO | NO | 7 bp DEL |
| B1 | NO | 1 bp INS | N/A | NO | 173 bp DEL |
| B2 | NO | NO | | NO | 173 bp DEL |
| D1 | NO | NO | | 173 bp DEL | 2 bp DEL |
| D2 | NO | NO | | NO | 3 bp DEL |
| R5P2 | sgRNA1 | sgRNA3 | | sgRNA1 | sgRNA2 |
| A1 | NO | NO | NO | NO | 54 bp DEL |
| A2 | NO | NO | NO | NO | 42 bp DEL |
| B1 | NO | 56 bp DEL | N/A | 2 bp DEL | 6 bp DEL |
| B2 | NO | NO | | 2 bp DEL | 54 bp DEL |
| D1 | No reads mapped | | | No reads mapped | |
| D2 | | | | | |
| R7P1 | sgRNA1 | sgRNA3 | | sgRNA1 | sgRNA2 |
| A1 | NO | NO | NO | 184 bp DEL | 2 bp DEL |
| A2 | NO | NO | NO | 184 bp DEL | 2 bp DEL |
| B1 | NO | 196 bp DEL | N/A | 184 bp DEL | 2 bp DEL |
| B2 | NO | NO | | NO | 6 bp DEL |
| D1 | NO | NO | | 185 bp DEL | 1 bp DEL |
| D2 | NO | NO | | NO | 2 bp DEL |
| R7P2 | sgRNA1 | sgRNA3 | | sgRNA1 | sgRNA2 |
| A1 | NO | NO | NO | 205 bp DEL | 2 bp DEL |
| A2 | NO | NO | NO | NO | 7 bp DEL |
| B1 | NO | NO | N/A | 219 bp DEL | NO |
| B2 | NO | NO | | NO | NO |
| D1 | NO | NO | | 203 bp DEL | 1 bp DEL |
| D2 | NO | NO | | NO | 1 bp INS |

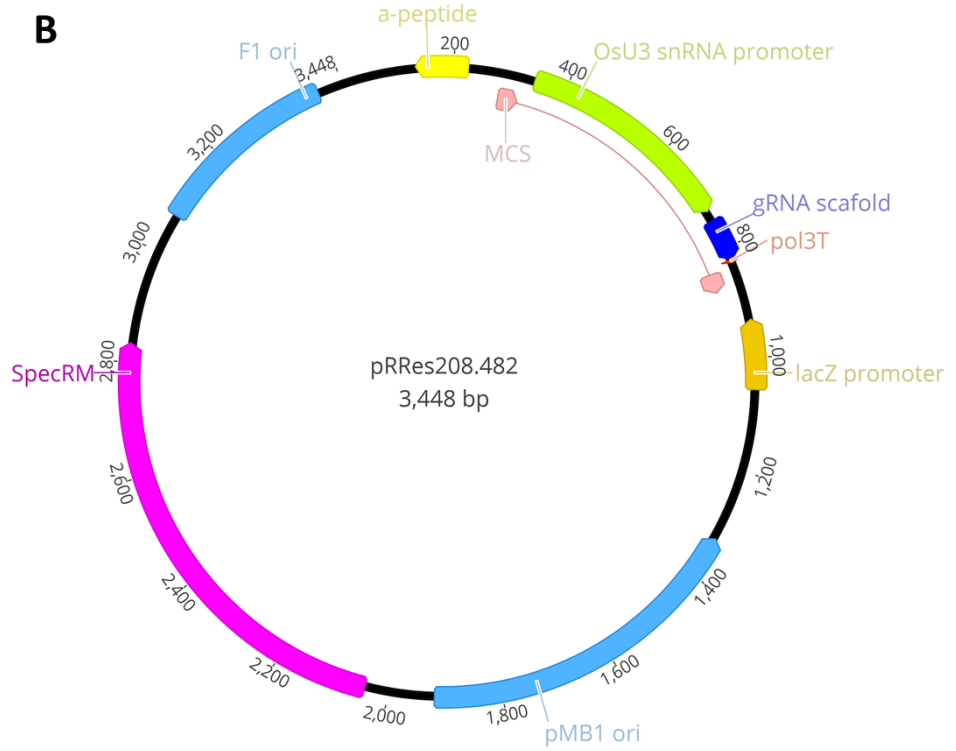
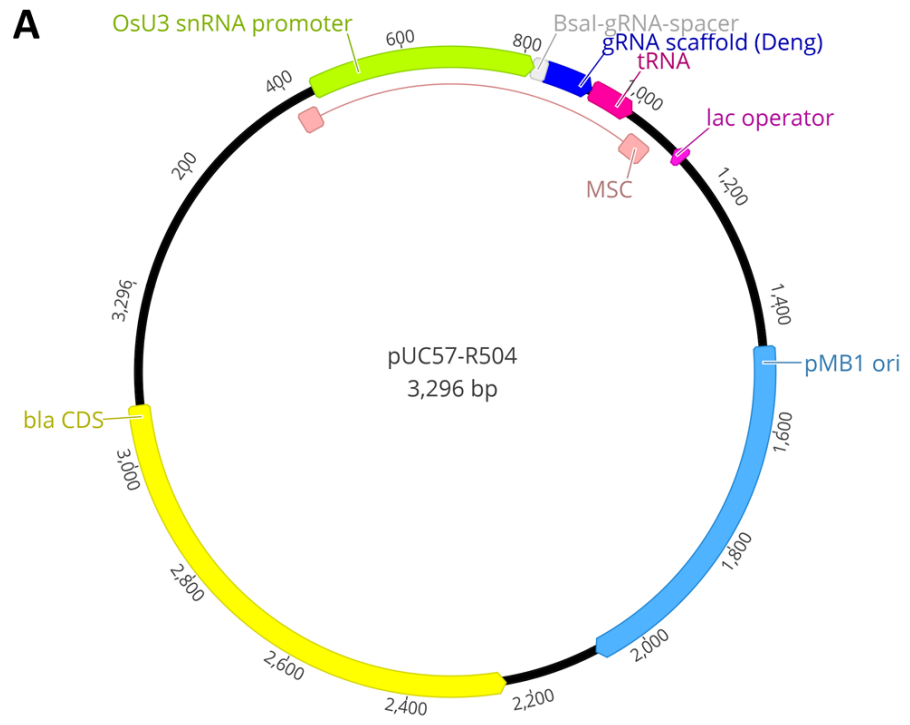
Supplementary Table 5. 3 Segregation of the INDELS in the T1 population. In bold are the plants propagated to the T2 population.

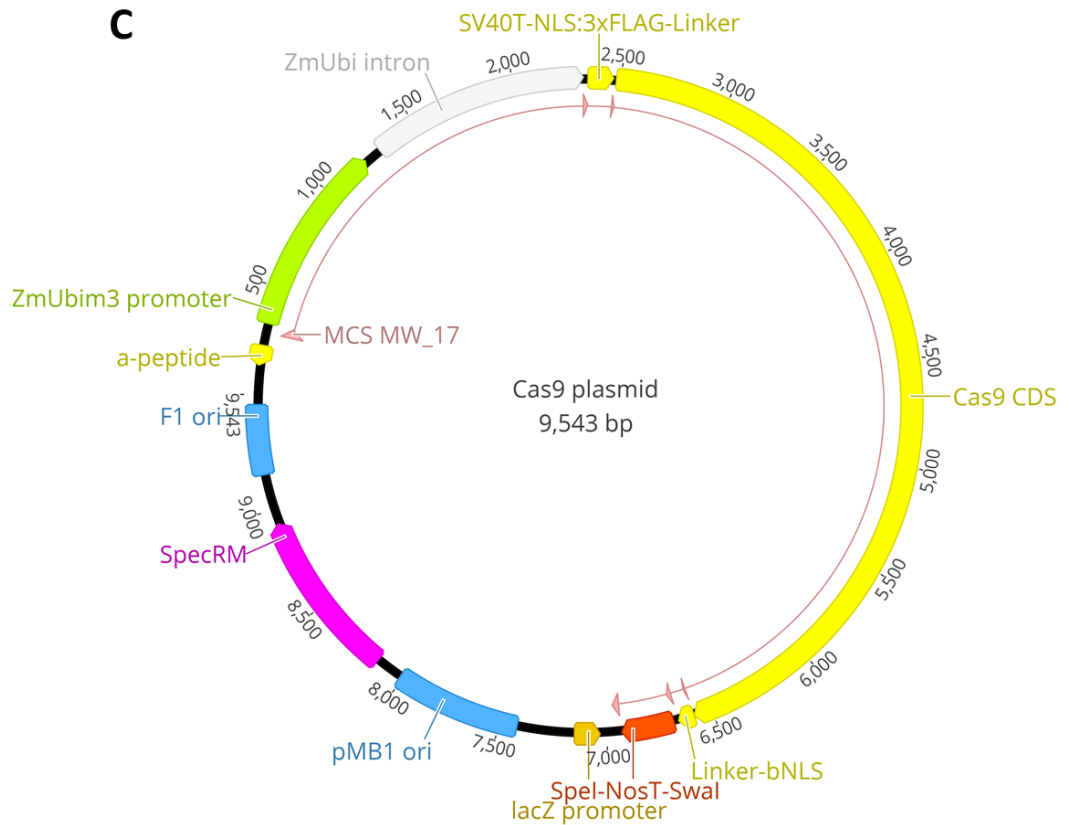
| | TaERF5 | | | TaERF5a | | |
|---|---------------------------|---------------------------|---------------------------|--------------------------------|---|--|
| | A | B | D | A | B | D |
| INDELS in TO progenitor plant  | 1 bp DEL, MON | 1 bp DEL; BI (HOM) | 1 bp DEL; BI (HOM) | 2 bp and 176 bp DELs; BI (HET) | 40 bp and 7 bp DELs or 1 bp INS; BI (HET) | 6 bp with 17 bp DELs or 1 bp DEL; BI (HET) |
| Cad | NO | NO | NO | NO | NO | NO |
| 1 | NO | NO | NO | NO | NO | NO |
| 2 | NO | NO | NO | 176 bp DEL in ~10% reads | NO | NO |
| 3 | 1 bp DEL, MON | 1 bp DEL; BI (HOM) | 1 bp DEL; BI (HOM) | 176 bp and 2 bp DELs; BI (HET) | 40 + 7 bp DEL; BI (HOM) | 6+17 bp and 1 bp DELs; BI (HET) |
| 4 | NO | NO | NO | NO | NO | NO |
| 5 | NO | NO | NO | NO | NO | NO |
| 6 | 1 bp DEL; BI (HOM) | 1 bp DEL; BI (HOM) | 1 bp DEL; BI (HOM) | 2 bp DEL; BI (HOM) | 1 bp INS; BI (HOM) | 6 + 17 bp DEL; BI (HOM) |
| 7 | 1 bp DEL, MON | 1 bp DEL; BI (HOM) | 1 bp DEL; BI (HOM) | 176 bp and 2 bp DELs; BI (HET) | 40 + 7 bp DEL and 1 bp INS; BI (HET) | 1 bp DEL; BI (HOM) |
| 8 | NO | NO | NO | NO | NO | NO |
| 9 | NO | NO | NO | 176 bp DEL in ~14% reads | NO | NO |
| 10 | NO | NO | NO | 176 bp DEL in ~4% reads | NO | NO |
| 11 | NO | NO | NO | NO | NO | 175 bp DEL in ~7% reads |
| 12 | NO | NO | NO | NO | NO | NO |
| 13 | NO | NO | NO | 176 bp DEL in ~3% reads | NO | NO |
| 14 | NO | NO | NO | 176 bp DEL in ~42% reads | NO | NO |
| 15 | NO | NO | NO | 176 bp DEL in ~7% reads | NO | NO |
| 16 | NO | NO | NO | 176 bp DEL in ~5% reads | NO | 175 bp DEL in ~3% reads |
| 17 | 1 bp DEL, MON | 1 bp DEL; BI (HOM) | 1 bp DEL; BI (HOM) | 176 bp and 2 bp DELs; BI (HET) | 1 bp INS; BI (HOM) | 6 + 17 bp DEL; BI (HOM) |
| 18 | 1 bp DEL, MON | 1 bp DEL; BI (HOM) | 1 bp DEL; BI (HOM) | 176 bp and 2 bp DELs; BI (HET) | 40 + 7 bp DEL and 1 bp INS; BI (HET) | 6+17 bp and 1 bp DELs; BI (HET) |
| 19 | NO | NO | NO | NO | NO | 175 bp DEL in ~7% reads |
| 20 | NO | NO | NO | NO | NO | NO |
| 21 | 1 bp DEL; BI (HOM) | 1 bp DEL; BI (HOM) | 1 bp DEL; BI (HOM) | 2 bp DEL; BI (HOM) | 40 + 7 bp DEL; BI (HOM) | 6+17 bp and 1 bp DELs; BI (HET) |
| 22 | NO | 1 bp DEL; BI (HOM) | 1 bp DEL; BI (HOM) | 176 bp DEL; BI (HOM) | 40 + 7 bp DEL and 1 bp INS; BI (HET) | 1bp DEL; BI (HOM) |
| 23 | NO | 1 bp DEL; BI (HOM) | 1 bp DEL; BI (HOM) | 176 bp DEL; BI (HOM) | 40 + 7 bp DEL and 1 bp INS; BI (HET) | 1bp DEL; BI (HOM) |
| 24 | NO | NO | NO | 176 bp DEL in ~21% reads | NO | NO |
| 25 | NO | NO | NO | 176 bp DEL in ~7% reads | NO | NO |
| 26 | NO | 1 bp DEL; BI (HOM) | 1 bp DEL; BI (HOM) | 176 bp DEL; BI (HOM) | 40 + 7 bp DEL and 1 bp INS; BI (HET) | 6 + 17 bp DEL; BI (HOM) |
| 27 | 1 bp DEL, MON | 1 bp DEL; BI (HOM) | 1 bp DEL; BI (HOM) | 176 bp and 2 bp DELs; BI (HET) | 40 + 7 bp DEL; BI (HOM) | 6+17 bp and 1 bp DELs; BI (HET) |
| 28 | NO | NO | NO | 176 bp DEL in ~22% reads | NO | 175 bp DEL in ~8% reads |
| 29 | NO | 1 bp DEL; MON | 1 bp DEL; MON | 176 bp and 2 bp DELs; BI (HET) | 40 + 7 bp; MON | 1 bp DEL; MON |
| 30 | 1 bp DEL, MON | 1 bp DEL; BI (HOM) | 1 bp DEL; BI (HOM) | 176 bp and 2 bp DELs; BI (HET) | 40 + 7 bp DEL; BI (HOM) | 6 + 17 bp DEL; BI (HOM) |

| | | | | | | |
|-----------|---------------------------|---------------------------|---------------------------|--------------------------------|---|---------------------------------|
| 31 | NO | 1 bp DEL; BI (HOM) | 1 bp DEL; BI (HOM) | 176 bp DEL; BI (HOM) | 40 + 7 bp DEL and 1 bp INS; BI (HET) | 6+17 bp and 1 bp DELs; BI (HET) |
| 32 | 1 bp DEL; BI (HOM) | 1 bp DEL; BI (HOM) | 1 bp DEL; BI (HOM) | 2 bp DEL; BI (HOM) | 1 bp INS; BI (HOM) | 6 + 17 bp DEL; BI (HOM) |
| 33 | NO | NO | NO | NO | NO | NO |
| 34 | NO | NO | NO | 176 bp DEL in ~22% reads | NO | NO |
| 35 | NO | NO | NO | 176 bp DEL in ~18% reads | NO | 175 bp DEL in ~6% reads |
| 36 | NO | NO | NO | NO | NO | 175 bp DEL in ~50% reads |
| 37 | 1 bp DEL, MON | 1 bp DEL; BI (HOM) | 1 bp DEL; BI (HOM) | 176 bp and 2 bp DELs; BI (HET) | 1 bp INS; BI (HOM) | 6 and 17 bp DEL; BI (HOM) |
| 38 | NO | NO | NO | 176 bp DEL in ~10% reads | NO | 175 bp DEL in ~14% reads |
| 39 | 1 bp DEL, MON | 1 bp DEL; BI (HOM) | 1 bp DEL; BI (HOM) | 176 bp and 2 bp DELs; BI (HET) | 1 bp INS; BI (HOM) | 6 + 17 bp DEL; BI (HOM) |
| 40 | 1 bp DEL; BI (HOM) | 1 bp DEL; BI (HOM) | 1 bp DEL; BI (HOM) | 2 bp DEL; BI (HOM) | 40 + 7 bp DEL and 1 bp INS; BI (HET) | 6 + 17 bp DEL, BI (HOM) |
| 41 | NO | NO | NO | NO | NO | 175 bp DEL in ~18% reads |
| 42 | NO | NO | NO | NO | NO | 175 bp DEL in ~6% reads |
| 43 | NO | NO | NO | 176 bp DEL in ~10% reads | NO | 175 bp DEL in ~48% reads |
| 44 | NO | NO | NO | NO | NO | 175 bp DEL in ~31% reads |

Supplementary Table 5. 4 Putative off-target sites for the sgRNAs used. Off-targets yielded by *in silico* analysis when screening wheat genome with either the full sequence of sgRNA (20 nt 100% ID) or seed sequence of sgRNA (12 nt immediately upstream of PAM domain; 100% ID) followed by all different PAM domains recognised by Cas9.

| | 20 nt 100% ID | Seed sequence + PAM domain | | | |
|--------|---------------|----------------------------|---------------------------|---------------------------|---------------------------|
| | | AGG | TGG | CGG | GGG |
| sgRNA1 | NO | NO | <i>TraesCS6A02G146300</i> | NO | NO |
| sgRNA2 | NO | <i>TraesCS4A02G230300</i> | <i>TraesCS3A02G118900</i> | <i>TraesCS3D02G302600</i> | NO |
| | | | <i>TraesCS3B02G137900</i> | <i>TraesCSU02G040600</i> | |
| | | | <i>TraesCS3B02G337400</i> | | |
| sgRNA3 | NO | <i>TraesCS1A02G304800</i> | <i>TraesCS2A02G087500</i> | <i>TraesCS1B02G385200</i> | <i>TraesCS2A02G430600</i> |
| | | <i>TraesCS1B02G315600</i> | <i>TraesCS3A02G201700</i> | <i>TraesCS1D02G372400</i> | <i>TraesCS3B02G429900</i> |
| | | | <i>TraesCS5A02G245200</i> | <i>TraesCS1D02G372600</i> | <i>TraesCS3D02G391800</i> |
| | | | <i>TraesCS5D02G251800</i> | <i>TraesCS6B02G293900</i> | |
| | | | <i>TraesCS7A02G249500</i> | | |
| | | | <i>TraesCS7A02G415900</i> | | |
| sgRNA4 | NO | <i>TraesCS7D02G251200</i> | NO | <i>TraesCS5A02G390900</i> | <i>TraesCS4A02G379700</i> |
| | | | | <i>TraesCS5B02G395700</i> | <i>TraesCS6D02G045500</i> |
| | | | | <i>TraesCS5D02G400700</i> | <i>TraesCS7B02G078000</i> |
| | | | | | <i>TraesCS7D02G194900</i> |





Supplementary Figure 5. 1 Maps of plasmids used in the genome editing study.

Supplementary Notes 5. 1 DNA sequences of the plasmids used in the genome editing study.

pUC57-R504

TCGCGCGTTTCGGTGATGACGGTGAAAACCTCTGACACATGCAGCTCCCGGAGACGGTCACAGCTTGTCT
 GTAAGCGGATGCCGGGAGCAGACAAGCCCGTCAGGGCGCGTCAGCGGGTGTGGCGGGTGTCCGGGCTGG
 CTTAACTATGCGGCATCAGAGCAGATTGTACTGAGAGTGCACCATATGCGGTGTGAAATACCGCACAGAT
 GCGTAAGGAGAAAATACCGCATCAGGCGCCATTCGCCATTCAGGCTGCGCAACTGTTGGGAAGGGCGATC
 GGTGCGGGCTCTTCGCTATTACGCCAGCTGGCGAAAGGGGGATGTGCTGCAAGGCGATTAAAGTTGGGTA
 ACGCCAGGGTTTTCCAGTCACGACGTTGTAACACGACGGCCAGTGAATTCGAGCTCGGTACCTCGCGAA
 TGCATCTAGATGTGAAGCTTAAGGAATCTTAAACATACGAACAGATCACTTAAAGTTCTTCTGAAGCAA
 CTTAAAGTTATCAGGCATGCATGGATCTTGGAGGAATCAGATGTGCAGTCAGGACCATAGCACAAAGACA
 GCGTCTTCTACTGGTGTACCAGCAAATGCTGGAAGCCGGGAACACTGGGTACGTTGGAAACCACGTGA
 TGTGAAGAAGTAAGATAAACTGTAGGAGAAAAGCATTTCGTAGTGGGCCATGAAGCCTTTCAGGACATGT
 ATTGCAGTATGGGCCGGCCATTACGCAATTGGACGACAAACAAGACTAGTATTAGTACCACCTCGGCTA
 TCCACATAGATCAAAGCTGATTTAAAAGAGTTGTGCAGATGATCCGTGGCAGGAGACCGAGGTCTCGGTT
 TCAGAGCTATGCTGGGAACAGCATAGCAAGTTGAAATAAGGCTAGTCCGTTATCAACTTGAAAAAGTGGC
 ACCGAGTCGGTGCAACAAAGCACCAGTGGTCTAGTGGTAGAATAGTACCCTGCCACGGTACAGACCCGGG
 TTCGATTCGGCTGGTGCAGAACCTTTCCTAGGAACATCGGATCCCGGGCCCGTTCGACTGCAGAGCCCT
 GCATGCAAGCTTGGCGTAATCATGGTCTAGCTGTTTCTGTGTGAAATGTTATCCGCTCACAAATCCA
 CACAACATACGAGCCGGAAGCATAAAGTGTAAAGCCTGGGGTGCCTAATGAGTGAGCTAACTCACATTAA
 TTGCGTTGCGCTCACTGCCCGCTTTCAGTCGGGAACCTGTCGTGCCAGTGCATTAATGAATCGGCCA

ACGCGCGGGGAGAGGGCGTTTGCCTATTGGGCGCTCTTCCGCTTCTCGCTCACTGACTCGCTGCGCTCG
GTCGTTCCGCTGCGGCGAGCGGTATCAGTCACTCAAAGGCGGTAATACGTTATCCACAGAATCAGGGG
ATAACGCAGGAAAGAATGTGAGCAAAGGCCAGCAAAGGCCAGGAACCGTAAAAAGGCCGCTTGCT
GGCCTTTTTCCATAGGCTCCGCCCCCTGACGAGCATCAGAAAATCGACGCTCAAGTCAAGGTTGGCGA
AACCCGACAGGACTATAAAGATACCAGGGCTTTCCCCCTGGAAAGTCCCTCGTGCGCTCTCCTGTTCCGA
CCCTGCCGCTTACCGGATACCTGTCCGCTTTCTCCCTTCGGGAAGCGTGGCGCTTTCTCATAGCTCAGC
CTGTAGGTATCTCAGTTCGGTGTAGGTCGTTTCGCTCCAAGCTGGGCTGTGTGCACGAACCCCCGTTTCCAG
CCCGACCGCTGCGCTTATCCGGTAACATCGTCTTGAGTCCAACCCGTTAAGACACGACTTATCGCCAC
TGGCAGCAGCCACTGGTAACAGGATTAGCAGAGCGAGGTATGTAGGCGGTGCTACAGAGTTCTTGAAGTG
GTGGCTAACTACGGCTACACTAGAAGAACAGTATTTGGTATCTGCGCTCTGCTGAAGCCAGTTACCTTC
GGAAAAAGAGTTGGTAGCTCTTGATCCGGCAAACAACCACCGCTGGTAGCGGTGGTTTTTTTGGTTGCA
AGCAGCAGATTACGCGCAGAAAAAAGGATCTCAAGAAGATCCTTTGATCTTTTCTACGGGGTCTGACGC
TCAGTGGAAACGAAAACACGTTAAGGGATTTTGGTTCATGAGATTATCAAAAAGGATCTTCCACTAGATC
CTTTTAAATTAATAAATGAAGTTTTAAATCAATCTAAAGTATATATGAGTAACTTGGTCTGACAGTTACC
AATGCTTAATCAGTGAGGCACCTATCTCAGCGATCTGTCTATTTTCGTTCAATAGTTGCTGACTCCC
CGTCGTGATAGATAACTACGATACGGGAGGGCTTACCATCTGGCCCCAGTGTGCAATGATACCGCGAGAC
CCACGCTCACCGGCTCCAGATTTATCAGCAATAAACAGCCAGCCGGAAGGGCCGAGCGCAGAAGTGGTC
CTGCAACTTTATCCGCTCCATCCAGTCTATTAATTGTTGCCGGAAGCTAGAGTAAGTAGTTTCGCCAGT
TAATAGTTTGCACAACGTTGTTGCCATTGCTACAGGCATCGTGGTGTACGCTCGTCTGTTGGTATGGCT
TCATTCAGTCCGTTCCCAACGATCAAGGCGAGTTACATGATCCCCATGTTGTGCAAAAAAGCGGTTA
GCTCCTTCGGTCCCTCCGATCGTTGTCAGAAGTAAGTTGGCCGAGTGTATCACTCATGGTTATGGCAGC
ACTGCATAATTCTTACTGTATGCCATCCGTAAGATGCTTTTCTGTGACTGGTGTAGTACTCAACCAAG
TCATTCGTGAGAATAGTGTATGCGGCGACCGAGTTGCTCTTGGCCGCGTCAATACGGGATAATACCGCGC
CACATAGCAGAACTTTAAAAGTGTCTCATCTTGGAAAACGTTCTTTCGGGGCAGAACTCTCAAGGATCTT
ACCGCTGTTGAGATCCAGTTCGATGTAACCCACTCGTGCACCCAAGTATCTTCAGCATCTTTTACTTTT
ACCAGCGTTTCTGGGTGAGCAAAAACAGGAAGGCAAAATGCCGAAAAAAGGGAATAAGGGCGACACGGA
AATGTTGAATACTCATACTCTTCTTTTCAATATTATGAAGCATTATCAGGGTTATGTCTCATGAG
CGGATACATATTTGAATGTATTTAGAAAAATAAACAAATAGGGGTTCCGCGCACATTTCCCGAAAAAGTG
CCACCTGACGTCTAAGAAACCATTTATTCATGACATTAACCTATAAAAAATAGGCGTATCACGAGGCCCT
TTCGT

pRRes208.482

TAGGGCGCTGGCAAGTGTAGCGGTACGCTGCGCGTAACCACCACACCCGCCGCGCTTAATGC
GCCGCTACAGGGCGCGTCCATTCGCCATTACAGGCTGCGTAACTGTTGGGAAGGGCGATCGGTG
CGGGCTCTTCGCTATTACGCCAGCTGGCGAAAAGGGGGATGTGCTGCAAGGCGATTAAGTTGG
GTAACGCCAGGGTTTTCCAGTACGACGTTGTAACACGACAGCAAGTTGGCCAACACCGGTG
CAATTAACCTCACTAAAGGGAACAAAAGCTGGGCGCGCCGACACGCGTGGCATCGCGCTCTG
TTTTAACAGCTATGACCATGATTACGCCAAGCTTAAGGAATCTTTAAACATACGAACAGATCA
CTTAAAGTTCTTCTGAAGCAACTTAAAGTTATCAGGCATGCATGGATCTTGGAGGAATCAGAT
GTGCAGTACAGGGACCATAGCACAAGACAGGCGTCTTCTACTGGTGTACCAGCAAATGCTGGA
AGCCGGGAACACTGGGTACGTTGGAACCACGTGATGTGAAGAAGTAAGATAAACTGTAGGAG
AAAAGCATTTCGTAGTGGGCCATGAAGCCTTTTCAGGACATGTATTGCAGTATGGGCCGGCCCA
TTACGCAATTGGACGACAACAAAGACTAGTATTAGTACCACCTCGGCTATCCACATAGATCAA
AGCTGATTTAAAAGAGTTGTGCAGATGATCCGTGGCAGGAGACCGAGGTTCTCGGTTTTAGAGC
TAGAAATAGCAAGTTAAAATAAGGCTAGTCCGTTATCAACTTGA AAAAGTGGCACCGAGTCCG
TGCTTTTTTGTTTTAGCTAGTGCATTTAAATCCTTAATTAACCTGCAGGCATCTCCAATTCG
CCATATAGTGAGTCGTATTACACCGGTGAGGCTGCGTAATCATGGTCATAGCTGTTTCCCTGT
GTGAAATTGTTATCCGCTCACAATTCACACAACATACGAGCCGGAAGCATAAAGTGTAAAGC
CTGGGGTGCCTAATGAGTGAAGTCACTCACTAATTAATGCGTTGCGCTCACTGCCCGCTTTCCA
GTCGGGAAACCTGTGCGTCCAGCTGCATTAATGAATCGGCCAACGCGGGGAGAGGCGGTTTT
GCGTATTGGGCGCTCTTCCGCTTCCCTCGCTCACTGACTCGCTGCGCTCGGTCGTTCCGCTGCG
GCGAGCGGTATCAGCTCACTCAAAGGCGGTAATACGGTTATCCACAGAATCAGGGGATAACGC
AGGAAAGAACATGTGAGCAAAAAGGCCAGCAAAAAGGCCAGGAACCGTAAAAAGGCCGCTTGCT
GGCCTTTTTCCATAGGCTCCGCCCCCTGACGAGCATCAGAAAATCGACGCTCAAGTCAAG
GTGGCGAAACCCGACAGGACTATAAAGATACCAGGCGTTTCCCCCTGGAAAGTCCCTCGTGGC
CTCTCCTGTTCCGACCTGCGCTTACCGGATACCTGTCCGCTTTCTCCCTTCGGGAAGCGT
GGCGCTTTCTCATAGCTCAGCTGTAGGTATCTCAGTTCGGTGTAGGTCGTTTCGCTCCAAGCT
GGGCTGTGTGCACGAACCCCCGTTTACGCCGACCGCTGCGCTTATCCGGTAACATATCGTCT
TGAGTCCAACCCGTTAAGACACGACTTATCGCCACTGGCAGCAGCCACTGGTAACAGGATTAG
CAGAGCGAGGTATGTAGGCGGTGCTACAGAGTTCTTGAAGTGGTGGCCTAACTACGGCTACAC
TAGAAGAACAGTATTTGGTATCTGCGCTCTGCTGAAGCCAGTTACCTTCGGAAAAAGAGTTGG

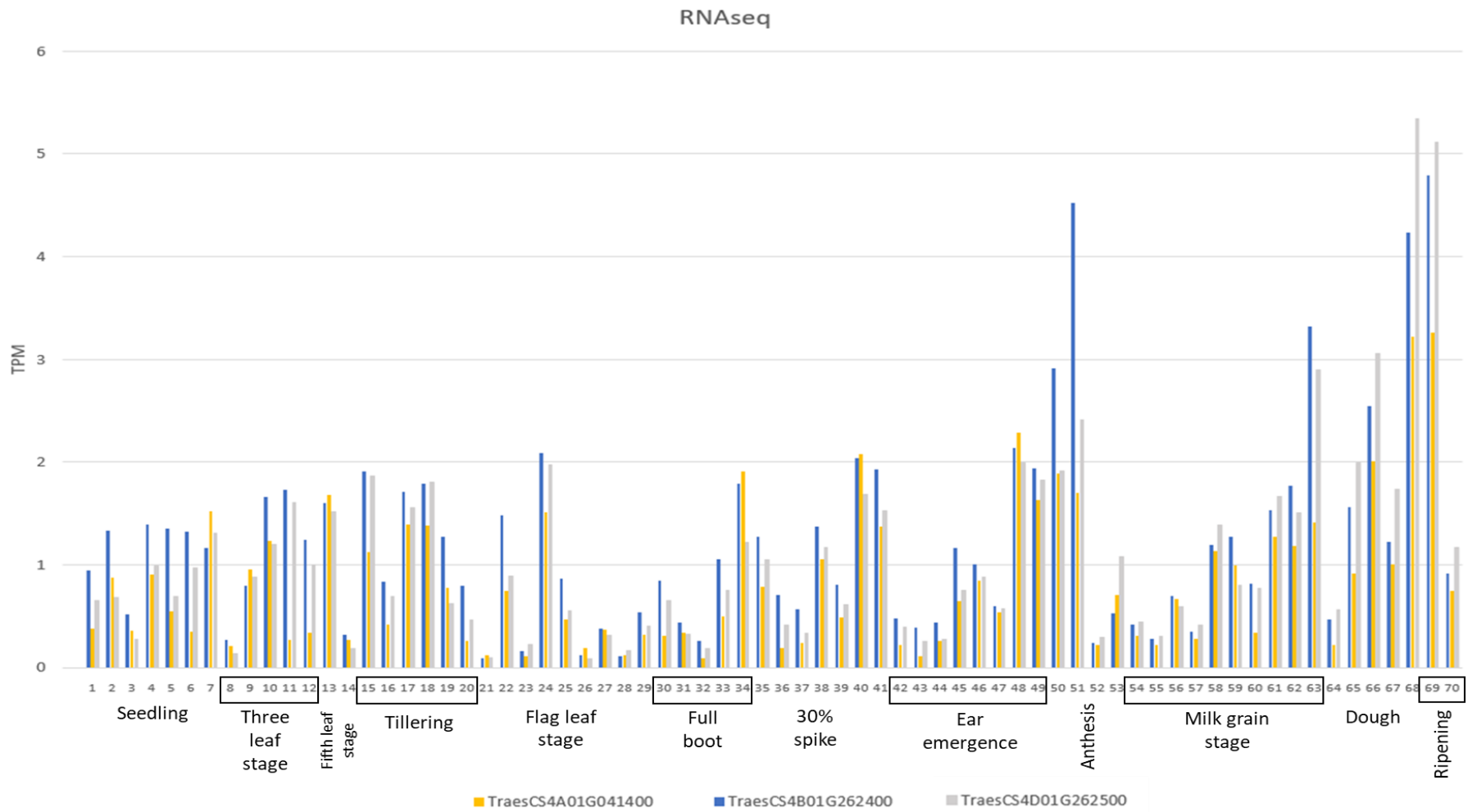
TAGCTCTTGATCCGGCAAACAAACCACCGCTGGTAGCGGTGGTTTTTTTTGTTTTGCAAGCAGCA
GATTACGCGCAGAAAAAAGGATCTCAAGAAGATCCTTTGATCTTTTCTACGGGGTCTGACGC
TCAGTGAACGAAAACTCACGTTAAGGGATTTTGGTCATGTGACAATAACCTGATAAAATGCT
TCAATAATATTGAAAAAGGACCTAGTATGAGGGAAAGCGGTGATCGCCGAAGTATCGACTCAAC
TATCAGAGGTAGTTGGCGTCATCGAGCGCCATCTCGAACCGACGTTGCTGGCCGTACATTTGT
ACGGCTCCGCAGTGGATGGCGGCTGAAGCCACACAGTGATATTGATTTGCTGGTTACGGTGA
CCGTAAGGCTTGATGAAACAACCGGGGAGCTTTGATCAACGACCTTTTGGAACTTCGGCTT
CCCCTGGAGAGAGCGAGATTCTCCGCGCTGTAGAAGTCACCATTTGTTGTGCACGACGACATCA
TTCCGTGGCGTTATCCAGCTAAGCGGAACTGCAATTTGGAGAATGGCAGCGCAATGACATTC
TTGCAGGTATCTTCGAGCCAGCCAGATCGACATGATCTGGCTATCTTGCTGACAAAAAGCAA
GAGAACATAGCGTTGCCTTGGTAGGTCAGCGGCGAGGAACTCTTTGATCCGGTTCCCTGAAC
AGGATCTATTTGAGGCGCTAAATGAAACCTTAACGCTATGGAACCTCGCCGCCGACTGGGCTG
GCGATGAGCGAAATGTAGTGCTTACGTTGTCCCGCATTTGGTACAGCGCAGTAACCGGCAAAA
TCGCGCCGAAGGATGTGCTGCGGACTGGGCAATGGAGCGCCTGCCGGCCAGTATCAGCCCG
TCATACTTGAAGCTAGACAGGCTTATCTTGGACAAGAAGAAGATCGCTTGGCTCGCGCGCAG
ATCAGTTGGAAGAATTTGTCCACTACGTGAAAAGCGAGATCACCAAGGTAGTCGGCAAATAAG
TCAGGACCTTGTGACACCAAGTTTACTCATATATACTTTAGATTGATTTAAAACCTCATTTTT
AATTTAAAAGGATCTAGGTGAAGATCCTTTTTGATAATCACATGAGCGGATACATATTTGAAT
GTATTTAGAAAAATAAACAAATAGGGTTCCGCGCACATTTCCCGGAAAAGTGCCACCTGATG
CGGTGTGAAATACCGCACAGATGCGTAAGGAGAAAAATACCGCATCAGGAAATGTAAGCGTTA
ATATTTTGTAAAATTCGCGTTAAATTTTTGTAAAATCAGCTCATTTTTTTAACCAATAGGCCG
AAATCGGCAAAAATCCCTTATAAATCAAAAAGATAGACCGAGATAGGGTTGAGTGTGTTCCAG
TTTGGAAACAAGAGTCCACTATTAAGAACGTGGACTCCAACGTCAAAGGGCGAAAAACCGTCT
ATCAGGGCGATGGCCACTACGTGAACCATCACCTAATCAAGTTTTTTGGGGTTCGAGGTGCC
GTAAAGCACTAAATCGGAACCTAAAGGGAGCCCCCGATTTAGAGCTTGACGGGAAAAGCCGG
CGAACGTGGCGAGAAAAGGAAGGGAAAGAAAGCGAAAAGGAGCGGGGCGC

Cas9 plasmid

TAGGGCGCTGGCAAGTGTAGCGGTACGCTGCGCGTAACCACCACACCCGCCGCGCTTAATGC
GCCGCTACAGGGCGCGTCCATTCGCCATTCAGGCTGCGTAACTGTTGGGAAGGGCGATCGGTG
CGGGCCTCTTCGCTATTACGCCAGCTGGCGAAAGGGGATGTGCTGCAAGGCGATTAAGTTGG
GTAACGCCAGGGTTTTCCAGTCACGACGTTGTAACACGACAGCAAGTTGGCCAACACCGGTG
CAATTAACCCCTCACTAAAGGGAACAAAAGCTGGGCGCGCCGACACGCGTGCATCGCGCTCTG
TTTTAAACGCCCATCGCTGACCCGGTCTGCCCCCTCTCTAGAGATAATGAGCATTGCATGTCTA
AGTTATAAAAAATTACCACATATTTTTTTTTGTACACTTGTGTTGAAGTGCAGTTTATCTATCT
TTATACATATATTTAACTTTACTCTACGAATAATATAATCTATAGTACTACAATAATATCAG
TGTTTTAGAGAATCATATAAATGAACAGTTAGACATGGTCTAAAGGACAATTGAGTATTTTGA
CAACAGGACTCTACAGTTTTATCTTTTAGTGTGCATGTGTTCTCCTTTTTTTTTTGC AAATAG
CTTCACCTATATAATACTTCATCCATTTTATTAGTACATCCATTTAGGGTTTAGGGTTAATGG
TTTTTTATAGACTAATTTTTTTTAGTACATCTATTTTATTCTATTTTAGCCTCTAAATTAAGAAA
ACTAAAACCTCTATTTTAGTTTTTTTATTTAATAATTTAGATATAAAATAGAATAAAATAAAGT
GACTAAAATTAACAAATACCCTTTTAAGAAATTAAAAAAATAAGGAAACATTTTTCTTGT
TCGAGTAGATAATGCCAGCCTGTTAAACGCCGTCGACGAGTCTAACGGACACCAACCAGCGAA
CCAGCAGCGTCGCGTCGGGCAAGCGAAGCAGACGGCACGGCATCTCTGTGCTGCCCTCTGGA
CCCCTCTCGAGAGTTCCGCTCCACCGTTGGACTTGTCCGCTGTCCGCATCCAGAAATGCGTG
GCGGAGCGGCAGACGTGAGCCGGCACGGCAGGCGGCTCCTCCTCCTCTCACGGCACCGGCAG
CTACGGGGGATTCCTTTCCACCGCTCCTTCGCTTTCCCTCCTCGCCCGCGTAATAAATAG
ACACCCCTCCACACCCCTCTTTCCCAACCTCGTGTGTTTCGGAGCGCACACACACACAACCA
GATCGATCTCCCCAAATCCACCCGTCGGCACCTCCGCTTCAAGGTACGCCGCTCGTCTCCC
CCCCCCCCCTCTCTACCTTCTCTAGATCGGCGTTCCGGTCCATGATTAGGGCCCGGTAGTTC
TACTTCTGTTTATGTTTGTGTTAGATCCGTTGTTGTTAGATCCGTTGCTGCTAGCGTTTCGTA
CACGGATGCGACCTGTACGTGACACGTTCTGATTGCTAACTTGCCAGTGTCTCTTTGGG
GAATCCTGGGATGGCTCTAGCCGTTCCGACAGCGGATCGATTTTCATGCATGATTTTTTTTTGT
TTCGTTGCATAGGGTTGGTTTGCCTTTTCTTTTATTTCAATATATGCCGTGCACCTGTTTTG
TCGGGTCTCTTTTCTGCTTTTTTTGCTTGGTTGTGATGATGTGGTCTGGTTGGGCGGTC
GTTCTAGATCGGAGTAGAATTAATTTCTGTTCAAACCTACCTGGTGGATTTATTAATTTTGGAT
CTGTATGTGTGTCATACATATTCATAGTTACGAATTGAAGATGATGGATGGAATATCGAT
CTAGGATAGGTATACATGTTGATGCGGGTTTTACTGATGCATATACAGAGATGCTTTTTGTTT
GCTTGGTTGTGATGATGTGGTGTGGTTGGGCGGTCGTTCAATCGTTCTAGATCGGAGTAGAAT

ACTGTTTCAAACCTACCTGGTGTATTTATTAATTTTGGAACTGTATGTGTGTGCATACATCTT
CATAGTTACGAGTTTAAGATGGATGGAAATATCGATCTAGGATAGGTATAACATGTTGATGTGG
GTTTTACTGATGCATATACATGATGGCATATGCAGCATCTATTCATATGCTCTAACCTTGAGT
ACCTATCTATTATAATAAACAAGTATGTTTTATAATTAATTTTGATCTTGATATACTTGGATGA
TGGCATATGCAGCAGCTATATGTGGATTTTTTTTTAGCCCTGCCCTTCATACGCTATTTATTTGCT
TGGTACTGTTTCTTTTGTGCGATGCTCACCTGTTGTTTGGTGTACTTGTGCAGGTGCGCCGG
GCGAATTCGGGACGTCCATGGCACC GAAGAAGAGCGCAAAGTGGCCACGTGATGGACTATA
AGGACCACGATGGGACTACAAGGACCATGACATTGACTATAAGGATGACGACGATAAGAACG
CCCAGAGCGGGCCAGCGTCATGGACAAGAAGTACAGCATCGGCCTGGACATCGGGACCAACA
GCGTGGGGTGGGCGGTTATCACGGACGAGTACAAGGTGCCAAGCAAGAAGTTCAAGGTGCTGG
GCAACACCGACCCCACTCCATCAAGAAGAACCCTCATCGGAGCCCTCCTTCGACAGCGGGC
AAACGGCTGAGGCTACCAGGCTCAAGAGGACCGTAGGCGCAGGTACACCCGAGGAAGAACA
GGATCTGCTACCTCCAAGAAATCTTCAGCAACGAGATGGCGAAGGTGGACGACTCCTTCTTCC
ACCGCTGGAGGAGAGCTTCCCTCGTCGAGGAAGATAAGAAGCACGAGAGGCACCCAATCTTCG
GCAACATCGTGGACGAGGTGCCTACCACGAGAAGTACCCAACCATCTACCACCTGAGGAAGA
AGCTCGTGGACAGCACCGACAAGGCCGACCTCCGCTGATCTACCTCGCCCTGGCCACATGA
TTAAGTTTCAGGGCCACTTCCCTGATCGAGGGCGACCTCAACCAGACAACCTCGACGTGGACA
AGCTGTTTCATCCAACCTCGTCCAGACCTACAACCAACTCTTCGAGGAGAACCCAATCAACGCTT
CCGGCGTGGACGCTAAGGCTATCCTGAGCGCCAGGCTCTCCAAGTCCCGCAGGCTGGAGAACC
TGATCGCCAGCTCCCAGGCGAGAAGAAGACGGCTGTTTCGGCAACCTCATCGCTCTCTCCC
TGGGCTCACCCCAAACCTCAAGAGCAACTTCGACCTCGCTGAGGACGCCAAGCTGCAACTCA
GCAAGGACACCTACGACGACGACCTCGACAACCTCCTGGCCAGATCGGCGACCAATACGCCG
ACCTGTTCCCTCGCCGCAAGAACCTGTCCGACGCCATCCTCCTGAGCGACATCCTCCGCGTGA
ACACCGAGATCACCAAGGCCCACTCTCCGCCAGCATGATCAAACGCTACGACGAGCACCACC
AGGACCTGACCTCCTGAAGGCCCTGGTCAGGCAACAGCTCCCAGAGAAGTACAAGGAAATCT
TCTTCGACCAGTCCAAGAACGGCTACGCTGGCTACATCGACGGCGGAGCGAGCCAAGAGGAGT
TCTACAAGTTTCATCAAGCCAATCCTGGAGAAGATGGACGGCACCGAGGAGCTGCTGGTGAAGC
TCAACAGGGAGGACCTCCTGAGGAAGCAGCGCACCCTTCGACAACGGCTCCCAACCAAAA
TCCACCTCGGCGAGCTGCACGCTATCCTCCGACGGCAAGAGGACTTCTACCCATTCCTCAAGG
ACAACAGGGAGAAGATCGAGAAGATCCTGACCTTCCGCATCCCATACTACGTGGGGCCACTCG
CCAGGGGCAACTCCCGCTTCGCTTGGATGACCCGCAAGAGCGAGGAAACGATCACCCCGTGGGA
ACTTCGAGGAAGTGGTGGACAAGGGCGCTTCCGCTCAGAGCTTCATCGAGAGGATGACCAACT
TCGACAAGAACCTGCCAAACGAGAAGGTGCTCCCAAAGCACAGCTCCTGTACGAATACTTCA
CCGTCTACAACGAGCTGACCAAGGTGAAGTATGTGACCGAGGGCATGAGGAAACCAGCCTTCC
TGTCCGGCGAGCAGAAGAAGGCCATCGTGGACCTCCTGTTCAAGACCAACAGGAAGGTGACCG
TCAAGCAACTCAAGGAAGATTACTTCAAGAAGATCGAGTCTTCGACTCCGTGGAGATCAGCG
GCGTCGAGGACAGGTTCAACGCCAGCTCGGCACCTACCACGACCTCCTGAAGATCATCAAGG
ACAAGGACTTCTGGACAACGAGGAGAACGAGGACATCCTGGAGGACATCGTGTGACCCCTCA
CCCTGTTTCGAGGACAGGGAGATGATCGAGGAGCGCCTCAAGACCTACGCCACCTCTTCGACG
ACAAAGTTATGAAGCAACTGAAGCGCAGGGCGCTACACCGGCTGGGGCAGGCTGTCCCGCAAGC
TCATCAACGGCATCCGCGACAAGCAGTCCGGCAAGACCATCCTCGACTTCTGAAGAGCGACG
GCTTCGCCAACAGGAACCTTCATGCAACTGATCCACGACGACTCCCTCACCTTCAAGGAAGATA
TTCAGAAGGCTCAAGTCTCCGGCCAGGGCGACAGCTGCACGAGCACATCGCTAACCTCGCTG
GCTCCCCAGCCATCAAGAAGGGCATCCTGCAAACCGTGAAGTCTGTTGACGAGCTGGTGAAGG
TCATGGGCAGGCACAAGCCAGAGAACATCGTCAATCGAGATGGCCCGGAGAACCAAAACCCAC
AGAAGGGCCAAAAGAACAGCAGGGAGCGCATGAAGCGCATCGAGGAAGGCATCAAGGAGCTGG
GCTCCCAAATCCTCAAGGAGCACCCAGTTCGAGAACACCCAACTCCAGAACGAGAAGCTTACC
TGTAACCTCCAGAACGGCAGGGATATGTATGTGGACCAAGAGCTGGACATCAACCGCCTCA
GCGACTACGACGTGGACCACATCGTCCCACAGTCTTCTTGAAGGACGACAGCATCGACAACA
AGGTGCTCACCAGGTCCGACAAGAACCGGGCAAGTCCGACAACGTCCCAAGCGAGGAAGTGG
TCAAGAAGATGAAGAACTACTGGAGGCAGCTCCTGAACGCCAAGCTCATCAACCAAGGAAGT
TCGACAACCTCACCAAGGCTGAGCGCGGGCCTCAGCGAGCTGGACAAGGCGGGCTTCATCA
AGAGGCAGCTCGTGGAAAACCGCAAATCACCAAGCACGTGCCCCAAATCCTCGACTCCCGCA
TGAACACCAAGTACGACGAGAACGACAAGCTGATTAGGGAGGTGAAGTTCATCACCTGAAGT
CCAAGCTCGTGGAGCAGTTCAGGAAGGACTTCCAGTTCACAAGGTCCGCGAGATCAACAACCT
ACCACCACGCCCACGACGCTTACCTCAACGCTGTGGTGGGCACCGCCCTCATCAAGAAGTACC
CAAAGCTGGAGTCCGAGTTCGTGTACGGCGACTACAAGGTGTACGACGTTTCGCAAGATGATCG
CCAAGAGCGAGCAAGAGATCGGCAAGGCCACCGCCAAAATACTTCTTCTACTCCAACATTAATGA
ACTTCTTCAAGACCGAGATCACCTGGCTAACGGCGAGATCAGGAAGCGCCACTCATCGAAA
CGAACGGCGAGACTGGCGAGATCGTGTGGGACAAGGGCAGGGACTTCGCCACCGTCCGCAAGG
TCCTCTCCATGCCACAGGTGAACATCGTCAAGAAAACCGAGGTCCAGACCGGGCTTCTCCA

AGGAGAGCATCCTGCCAAAGAGGAACTCCGACAAGCTCATCGCCC GCAAGAAGGACTGGGACC
CAAAGAAGTACGGCGGATTTCGACTCCCCAACCGTGGCCTACAGCGTCTGGTGGTCGCCAAGG
TGGAGAAGGGCAAGTCCAAGAAGCTCAAGAGCGTCAAGGAGCTGCTGGGCATCACCATCATGG
AGAGGAGCAGCTTCGAGAAGAACCCAATCGACTTCTGGAGGCCAAGGGCTACAAGGAAGTGA
AGAAGGACCTGATTATCAAGCTCCCAAAGTATTCCTCTTCGAGCTGGAGAACGGCAGGAAGC
GCATGTTGGCTTCCGCTGGCGAGCTGCAAAAAGGGCAACGAGCTGGCCCTGCCATCCAAGTATG
TGAACTTCTCTACCTGGCCTCCCACTACGAGAAGCTCAAGGGCAGCCCAGAGGACAACGAGC
AAAAGCAGCTGTTTCGTCGAGCAGCACAAGCACTACCTCGACGAGATCATCGAGCAAATCTCCG
AGTTCTCCAAGCGCGTGATCCTCGCCGACGCCAACCTGGACAAGGTCTCAGCGCCTACAACA
AGCACAGGGACAAGCCAATCCGCGAGCAGGCCGAGAACATCATCCACCTTTCACCCTGACCA
ACCTCGGGCGCTCCAGCGCCTTCAAATACTTCGACACCACCATCGACAGGAAACGCTACACCT
CCACCAAGGAAGTGTCTCGACGCCACCTCATCCATCAAAGCATCACCGGGCTCTACGAAACGA
GAATCGACCTGTCACAACTGGGCGGCACAGTTCTCTAAACGCCACCAGCGGGAAGCGCGTGC
CTAAGGAGGCCGGAGCCGGGACCGACAAGAAGAAAGTAACTTAGCGGCCGCATGATAT
CACTAGTGTTCAAAATTTGGCAATAAAGTTTCTTAAGATTGAATCCTGTTGCCGGTCTTGCG
ATGATTATCATATAATTTCTGTTGAATTACGTTAAGCATGTAATAATTAACATGTAATGCATG
ACGTTATTTATGAGATGGGTTTTATGATTAGAGTCCC GCAATTATAACATTTAATACGCGATA
GAAAACAAAATATAGCGCGCAAAC TAGGATAAATATCGCGCGCGGTGTCATCTATGTTACTG
CTAGTCGATTTAAATCCTTAATTAACCTGCAGGCATCTCAAATTCGCCCTATAGTGAGTCTG
ATTACACCGGTGAGGCCTGCGTAATCATGGTCATAGCTGTTTCTGTGTGAAATTTGTTATCCG
CTCACAATTCACACAACATACGAGCCGGAAGCATAAAGTGTAAGCCTGGGGTGCCTAATGA
GTGAGCTAACTCACATTAATTGCGTTGCGCTCACTGCCCGCTTTCAGTCGGGAAACCTGTCTG
TGCCAGCTGCATTAATGAATCGGCCAACCGCGCGGGGAGAGGCGGTTTGCCTATTGGGCGCTCT
TCCGCTTCTCGCTCACTGACTCGCTGCGCTCGGTTCGTTTCGGCTGCGGCGAGCGGTATCAGCT
CACTCAAAGGCGGTAATACGGTTATCCACAGAATCAGGGGATAACGCAGGAAAGAACATGTGA
GCAAAAGGCCAGCAAAAGGCCAGGAACCGTAAAAAGGCCGCGTTGCTGGCGTTTTTCCATAGG
CTCCGCCCCCTGACGAGCATCACAAAAATCGACGCTCAAGTCAGAGGTGGCGAAACCCGACA
GGACTATAAAGATACCAGGCGTTTTCCCTTGAAGCTCCCTCGTGCCTCTCTTCCGATC
CTGCCGCTTACC GGATAACCTGTCCGCTTCTCCCTTCGGGAAGCGTGGCGCTTTTCTCATAGC
TCACGCTGTAGGTATCTCAGTTCGGTGTAGGTCGTTTCGCTCCAAGCTGGGCTGTGTGCACGAA
CCCCCGTTT CAGCCGACCGCTGCGCCTTATCCGGTAACTATCGTCTTGAGTCCAACCCGGTA
AGACACGACTTATCGCCACTGGCAGCAGCCACTGGTAACAGGATTAGCAGAGCGAGGTATGTA
GGCGGTGTACAGAGTTCTTGAAGTGGTGGCTAACTACGGCTACACTAGAAGAACAGTATTT
GGTATCTGCGCTCTGCTGAAGCCAGTTACCTTCGGAAAAAGAGTTGGTAGCTCTTGATCCGGC
AAACAAACCACCGCTGGTAGCGGTGGTTTTTTTTGTTTGC AAGCAGCAGATTACGCGCAGAAAA
AAAGGATCTCAAGAAGATCCTTTGATCTTTTCTACGGGTCTGACGCTCAGTGAACGAAAAAC
TCACGTTAAGGGATTTTGGTCATGTGACAATAACCTGATAAATGCTTCAATAATATTGAAAA
AGGACCTAGTATGAGGGAAGCGGTGATCGCCGAAGTATCGACTCAACTATCAGAGGTAGTTGG
CGTCATCGAGCGCCATCTCGAACCGACGTTGCTGGCCGTACATTTGTACGGCTCCGCAGTGGA
TGGCGGCTGAAGCCACACAGTGATATTGATTTGCTGGTTACGGTGACCGTAAGGCTTGATGA
AACAACGGCGGAGCTTTGATCAACGACCTTTTGGAAACTTCGGCTTCCCTGGAGAGAGCGA
GATTCTCCGCGCTGTAGAAGTACCATTGTTGTGCACGACGACATCATTCCTGGCGTTATCC
AGCTAAGCGGCAACTGCAATTTGGAGAATGGCAGCGCAATGACATTCCTGCAGGTATCTTCGA
GCCAGCCACGATCGACATTGATCTGGCTATCTTGCTGACAAAAGCAAGAGAACATAGCGTTGC
CTTGGTAGGTCCAGCGCGGAGGAACCTTTGATCCGGTTCTGACAGGATCTATTTGAGGC
GCTAAATGAAACCTTAACGCTATGGAACCTCGCCGCCCCGACTGGGCTGGCGATGAGCGAAATGT
AGTGCTTACGTTGTCCCGCATTTGGTACAGCGCAGTAACCGGCAAAATCGCGCCGAAGGATGT
CGCTGCCGACTGGGCAATGGAGCGCCTGCCGGCCAGTATCAGCCCGTCATACTTGAAGCTAG
ACAGGCTTATCTTGGACAAGAAGAAGATCGCTTGGCCTCGCGCGCAGATCAGTTGGAAGAATT
TGTCCACTACGTGAAAGGCGAGATCACCAAGGTAGTCGGCAAATAAGTCAGGACCTTGT CAGA
CCAAGTTTACTCATATATACTTTAGATTGATTTAAAACTTCATTTTTAATTTAAAAGGATCTA
GGTGAAGATCCTTTTTGATAATCATATGAGCGGATACATATTTGAATGTATTTAGAAAAATAA
ACAAATAGGGGTTCCGCGCACATTTCCCGAAAAAGTGCCACCTGATGCGGTGTGAAATACCGC
ACAGATGCGTAAGGAGAAAAATACCGCATCAGGAAATGTAAGCGTTAATATTTTGTAAAATT
CGCGTTAAATTTTTGTTAAATCAGCTCATTTTTTAACCAATAGGCCGAAATCGGCAAAATCCC
TTATAAATCAAAGAATAGACCGAGATAGGGTTGAGTGTGTTCCAGTTTGGAAACAAGAGTCC
ACTATTAAGAACGTGGACTCCAACGTCAAAGGGCGAAAAACCGTCTATCAGGGCGATGGCCC
ACTACGTGAACCATCACCTAATCAAGTTTTTTGGGGTCGAGGTGCCGTAAGCACTAAATCG
GAACCCTAAAGGGAGCCCCGATTTAGAGCTTGACGGGGAAAGCCGGCGAACGTGGCGAGAAA
GGAAGGGAAGAAAGCGAAAGGAGCGGGCGC



Supplementary Figure 6. 1 *Relative expression of the three homoeologues of TaIDD12 gene. The gene was found in the same clade as TaIDD11 and Arabidopsis ENY and GAF1. The expression was measured in wheat variety Chinese Spring and is presented in TPMs (transcripts per million). Data for 70 samples taken from different tissues at various developmental stages are presented. The developmental stages can be grouped: seedling (1-7), three leaf (8-12), fifth leaf (13-14), tillering (15-20), flag leaf (21-29), full boot (30-34), 30% spike (35-41), ear emergence (42-49), anthesis (50-53), milk grain (54-63), dough grain (64-68) and ripening (69-70) (refer to Appendix, Table 3 for full details). Data taken from Ramírez-González et al., 2018.*